

THE UNIVERSITY OF CHICAGO

ASYMMETRIC TOTAL SYNTHESSES OF THE FONTONAMIDES VIA FORMANILIDE-
DIRECTED PALLADIUM-CATALYZED C-H FUNCTIONALIZATION AND SYNTHETIC
STUDIES TOWARDS (+)-WELWITINDOLINONE A

A DISSERTATION SUBMITTED TO
THE FACULTY OF THE DIVISION OF THE PHYSICAL SCIENCES
IN CANDIDACY FOR THE DEGREE OF
DOCTOR OF PHILOSOPHY

DEPARTMENT OF CHEMISTRY

BY

NATHANIEL D. DURFEE

CHICAGO, ILLINOIS

AUGUST 2023

*Dedicated to My Family,
Thank You for All Your Unending Support*

TABLE OF CONTENTS

LIST OF SCHEMES.....	vi
LIST OF TABLES.....	xii
LIST OF FIGURES	xiii
LIST OF ABBREVIATIONS.....	xxii
Acknowledgements.....	xxvi
Abstract.....	xxx
Chapter 1: Introduction to the Hapalindoles and Total Synthesis Efforts Towards Oxidized	
Members of the Hapalindole Family	1
Preface.....	1
1.1 Hapalindole Natural Products	2
1.1A: Isolation, Biological activity, and Structure	2
1.1B Biosynthesis of the hapalonamides and welwitindolinones.....	4
1.1C Previous Synthetic Approaches towards the Hapalonamides	10
1.1D Previous Synthetic Approaches Towards Welwitindolinone A.....	15
1.2 Retrosynthetic Analysis of the Fontonamides	20
1.2A Strategy Design.....	20
1.2B The Use of Anilides as Directing Groups for C-H Activation.....	21
1.3 Retrosynthetic Analysis of Welwitindolinone A	24
1.3A Strategy Design.....	24
1.3B Transition Metal-Catalyzed Alkenylation and Arylation of indolinones.....	25
Chapter 2: Total Synthesis of (-)-Dechlorofontonamide	31
2.1 Studies on the Friedel-Crafts Fragment Coupling	31

2.2 Studies on the Palladium-Mediated Cyclization.....	40
2.2.A Exploration of Direct Carbonylative Cyclization	40
2.2.B Two Step Cyclization Proceeding Through the Carboxylic Acid.....	45
2.2.C Two Step Cyclization Proceeding Through the Aldehyde.....	47
Chapter 3: Total synthesis of (-)-fontonamide and (±)-13-hydroxy dechlorofontonamide	53
3.1 Synthesis of the oxygenated D-ring.....	53
3.2 Studies on the formation of the enol triflate	70
3.3 Completion of the Synthesis of (-)-Fontonamide	74
3.4 Synthesis and Structural Revision of 13-Hydroxy Dechlorofontonamide	81
3.5 Conclusion	85
Chapter 4: Synthetic Studies Toward Welwitindolinone A	87
4.1 Retrosynthetic Analysis and Model studies.....	87
4.2 Synthesis of the Fully-Decorated Indolinone Precursor	94
4.3 Investigation of the Palladium-Mediated Cyclization and Further Steps	101
4.4 Conclusion	106
Chapter 5: Development of Novel 1-Alkoxy-1-amino-1,3-butadienes for the Diels-Alder	
Reaction	107
5.1 Background on 1,1-Diactivated Dienes	107
5.2 First and Second Generation Syntheses of the Oxazolidine-Fused Butadiene	111
5.3 Scope of the Diels-Alder Reactions of the Oxazolidine-Fused Butadiene	114
5.3A: Diels-Alder Reactions	114
5.3B: Hetero-Diels-Alder Reactions	117

5.4 Kinetics Analysis of the Oxazolidine-Fused Butadiene and Other Highly-Reactive Dienes	118
5.5 Conclusion	121
Chapter 6: Experimental Procedures and Characterization Data	122
6.1 General Information.....	122
6.2 Experimental Details and Characterization Data for Chapter 2.....	124
6.3 Experimental Details and Characterization Data for Chapter 3.....	142
6.4 Experimental Details and Characterization Data for Chapter 4.....	167
6.5 Experimental Details and Characterization Data for Chapter 5.....	193
Chapter 7: Selected ¹H, ¹³C, ¹⁹F, and 2D NMR Spectra	219

LIST OF SCHEMES

Scheme 1.1 Moore's proposed routes to (a) the dechlorinated and (b) chlorinated tricyclic hapalindoles. Cyclization gives the (c) tetracyclic hapalindoles and (d) fischerindoles	5
Scheme 1.2 Sherman's updated route to the tetracyclic hapalindoles and fischerindoles	6
Scheme 1.3 (a) Oxygen and light degrades hapalindole A to hapalonamide A, fontonamide and anhydrohapaloxindole A. (b) Moore's proposed pathway for the oxidations.	7
Scheme 1.4 (a) Moore's original proposed pathway to the welwitindolinones. (b) Baran's updated proposed pathway	9
Scheme 1.5 Li's synthesis of hapalindole Q and 12-epi-hapalindole Q isonitrile	11
Scheme 1.6 Li's synthesis of hapalonamide H.....	12
Scheme 1.7 Maji's synthesis of hapalindole H and formal synthesis of hapalondamide H.....	13
Scheme 1.8 Natsume's seminal syntheses of hapalindole J and M.....	14
Scheme 1.9 Baran's protecting-group-free syntheses of fischerindole I and welwitindolinone A	17
Scheme 1.10 Wood's synthesis of welwitindolinone A	19
Scheme 1.11. Retrosynthetic analysis of the fontonamides	20
Scheme 1.12. Tremont's proposed mechanisms for the ortho alkylation of acetanilide.....	21
Scheme 1.13 A selective substrate scope for van Leeuwen's catalytic ortho olefination of anilides	22
Scheme 1.14 Transformations possible via transition metal-mediated ortho C-H activation of anilides	23

Scheme 1.15. Retrosynthetic analysis of welwitindolinone A	25
Scheme 1.16. (a) Buchwald's initial report on arylation of ketone enolate. (b) Hartwig extends the reaction to secondary amides. (c) Intramolecular arylation of secondary amides. (d) Sequential intra-molecular and intermolecular diarylation of N-methyl acetanilide	26
Scheme 1.17. (a) Huang demonstrates that free N-H indolinones can be selectively alkenylated at the C-3 position. (b) Buchwald shows that free N-H indoles can be orthogonally arylated at the C-3 or N-1 position. (c) Buchwald demonstrates an asymmetric arylation and alkenylation of N-methyl indolinones.	27
Scheme 1.18. (a) The first example of cyclobutene-forming intramolecular vinylation of an enolate. (b) The reaction selects for the four-membered ring rather than the five-membered ring. (c) The first intramolecular alkenylation of an oxindole by Taenzler and Rawal	29
Scheme 1.19. Palladium-mediated alkenylative cyclobutene formation in Dong's synthesis of phainanoid A. (a) on a model substrate. (b) on a late stage substrate within the total synthesis...	30
Scheme 2.1. Retrosynthetic analysis of the fontonamides	31
Scheme 2.2. First and second generation synthesis of the lower fragment.....	32
Scheme 2.3. First generation synthesis of the upper fragment.....	33
Scheme 2.4. Issues with the first generation synthesis.....	36
Scheme 2.5. (a) Second generation asymmetric synthesis of the upper fragment. (b) Racemic route to the same compound	37
Scheme 2.6. Friedel-Crafts reaction and attempts to install the vinyl triflate	39
Scheme 2.7. Proposed catalytic cycle for the desired direct carbonylation	41
Scheme 2.8. Addition of nucleophiles to the carbonylation reaction in order to trap the acyl palladium intermediate.....	44

Scheme 2.9. (a) Refluxing with SOCl ₂ gives an unexpected selectivity for the desired ortho compound, possibly proceeding through the indicated intermediate. (b) Other conditions failed to selectively give the ortho compound.	45
Scheme 2.10. Li's proposed catalytic mechanism for the ortho directed C-H activation and acylation.....	46
Scheme 2.11. Palladium-mediated cyclization reaction from the aldehyde successfully gives the desired compound as the sole isolated product.....	47
Scheme 2.12. Control experiments on the palladium-mediated cyclization	48
Scheme 2.13 Postulated mechanism for the palladium-mediated cyclization proceeding through an oxidative addition into the aldehyde C-H bond	49
Scheme 2.14 Chen's proposed mechanism for palladium-mediated coupling of aryl iodonium's with ortho-hydroxy benzaldehydes.....	50
Scheme 2.15. (a) final steps to the natural product. (b) The C-15 epimer of the natural product is substantially slower to form.....	51
Scheme 2.16. Complete total synthesis of (-)-dechlorofontonamide	52
Scheme 3.1. Retrosynthetic analysis of fontonamide and 13-hydroxy dechlorofontonamide.....	53
Scheme 3.2. (a) Frejd's synthesis of ketone 3.10 . (b) The Rawal group's use of a derivative of 3.10 for the synthesis of welwitindolinone B	54
Scheme 3.3. Natsume's synthesis of ketone 3.19 and use in the synthesis of hapalindole O	55
Scheme 3.4. Based on results from Natsume and Rawal, a cis relationship is necessary between the protected alcohol and vinyl group.	56
Scheme 3.5. Issues with adapting (a) Rawal/Frejd's and (b) Natsume's routes to give the cis ketone required for the synthesis	57

Scheme 3.6. Retrosynthesis of ketone 3.24-c	57
Scheme 3.7. Asymmetric and racemic Diels-Alder reactions and attempted alkynylation of the aldehyde 3.31	58
Scheme 3.8. Hydride-based reduction of the eneone to the gamma-acetoxy ketone proves difficult. Deacetylation and reduction with Red-Al is successful.	62
Scheme 3.9. (a) Kishi shows that alcohols can direct reduction of allyl-alcohol epoxides with Red-Al. (b) Koide uses Red-Al to reduce gamma hydroxy alkynoic esters selectively.....	63
Scheme 3.10. Analysis of the Friedel-Crafts reaction with various protecting groups on the alcohol.	65
Scheme 3.11. (a) Yin uses NaBH ₄ and NiCl ₂ to perform a 1,4-reduction of 2-siloxy dienes (b) Application of Yin's conditions on our system	66
Scheme 3.12. Analysis of different silane-promoted eneone reduction conditions (a) Using Lipshutz's "hot" Stryker's reagent. (b) Using Karstedt's catalyst. (b) Using Wilkinson's catalyst and a silylative or desilylative workup	68
Scheme 3.13. Failed and successful routes to the enol triflate.....	72
Scheme 3.14. Carbonylation and cyclization followed by de-acetylation	75
Scheme 3.15. (a) Undesired rearrangement of the trans vinyl/alcohol in Rawal's synthesis of welwitindolinone B. (b) Desired chlorination of the cis vinyl/alcohol in Rawal's synthesis of ambiguine G.	75
Scheme 3.16. Rearrangement of alcohol 3.24-d in Favorskii-like reaction.....	76
Scheme 3.17. Analysis of different leaving groups for the attempted chlorination reaction	77
Scheme 3.18. Use of different nucleophile sources for the chlorination and iodination reactions	78

Scheme 3.19. Failed Mitsunobu reaction and successful oxidation/reduction.....	81
Scheme 3.20. Complete total synthesis of (-)-fontonamide and 13-hydroxy dechlorofontonamide	85
Scheme 4.1. Retrosynthetic analysis of welwitindolinone A.....	87
Scheme 4.2 (a) Huang’s palladative coupling of an enol triflate and an unprotected 3-methyl indolinone. (b) Taenzler’s successful model study on a N-methyl indole (c) A model compound employed by Dong in the synthesis of Phainanoid A (d) the desired free N-H model compound to test.....	89
Scheme 4.3 Synthesis of the Tosyl-protected model ketone.....	90
Scheme 4.4 Successful triflation and unsuccessful de-protection of the tosyl ketone.....	91
Scheme 4.5 Synthesis of the Boc-protected model ketone.....	91
Scheme 4.6 Failed and successful conditions for removing the Boc.....	92
Scheme 4.7 Oxidation to the model indolinone and successful palladium-mediated cyclization.	93
Scheme 4.8 Friedel-Crafts reaction on the real system.....	94
Scheme 4.9 Funk, as well as Bhat and Rawal, found that C-carboxylation was not possible with this relative stereochemistry.....	95
Scheme 4.10 Stereo inversion and switching of the protecting group from Tosyl to Boc.....	97
Scheme 4.11 Triflation, deprotection, and oxidation to the indolinone.....	99
Scheme 4.12 Triflation, deprotection, and oxidation to the indolinone.....	101
Scheme 4.13 Two possible pathways for formation of 4.46	102
Scheme 4.14 Huang’s reaction of ketone enolates with a vinyl triflate and a vinylogous carboxyl triflate.....	103

Scheme 4.15 Three possible routes to avoid the undesired O-cyclization (a) reduction of the ester. (b) silylation of the indole. (c) transformation of the ester to a formamide	104
Scheme 4.16 Proposed endgame following the successful cyclization	105
Scheme 5.1. Activated butadienes for Diels-Alder reactions.....	108
Scheme 5.2 First generation synthesis of diene 5.13	111
Scheme 5.3 Second generation synthesis of oxazolinium salt 5.18	112
Scheme 5.4 Modified synthesis of diene 5.13	113

LIST OF TABLES

Table 2.1. Conditions for the optimization of the Friedel-Crafts reaction	34
Table 2.2. Failed conditions for the direct carbonylative cyclization	43
Table 3.1. Investigation of vinylation conditions.....	59
Table 3.2. Optimization of the allylic oxidation to eneone 3.29	60
Table 3.3. Optimization of chlorination conditions	79
Table 3.4. Largest discrepancies in NMR shifts between the synthetic sample of 13-hydroxy dechlorofontonamide and the original isolated compound, as well as a comparison to natural and synthetic fontonamide.....	84
Table 4.1. Optimization of C-carboxylation conditions.....	98
Table 5.1. Percent recovery of diene 5.13 under various aqueous wash conditions.....	113
Table 5.2 Substrate scope of the Diels-Alder reaction between diene 5.13 and various common dienophiles	115
Table 5.3 Substrate scope of the Diels-Alder reaction between diene 5.13 and various nitrostyrenes and nitroalkenes	116
Table 5.4 Substrate scope for the hetero-Diels-Alder reaction between diene 5.13 and various aldehydes.....	118
Table 5.5 Rate constants for Diels-Alder reactions of some highly-reactive dienes	119
Table 6.1 Comparison of the NMR of the synthetic compound with the reported shifts by Orjala, 2012, as well as the reported shifts from the isolation of fontonamide, Moore 1988, and our synthetic sample of fontonamide.	166
Table 6.2 Rate constants for the some highly-reactive dienes at different temperatures.....	216
Table 6.3 Kinetic information of diene 5.1 and 5.13	217

LIST OF FIGURES

Figure 1.1 Building blocks of the hapalindoles and structures of the subfamilies.	3
Figure 1.2 The members of the hapalonamide subfamily.....	10
Figure 1.3 The members of the welwitindolinone subfamily	16
Figure 3.1 Steric hindrance from the acetate-protected alcohol slows deprotonation of the alpha hydrogen by bulky amide bases	71
Figure 3.2 (a) Predicted 3d structure of ketone 3.81 . (b) The angle of approach from above the plane of the ketone is blocked by two methyl groups.....	82
Figure 4.1 Steric hindrance from the TBS-protected alcohol precludes C-carboxylation.....	96
Figure 5.1 Arrhenius plots and activation parameters for the reaction of dienes 1 and 10 with diethyl fumarate in toluene; [diene] ₀ = 0.2 M, [dienophile] ₀ = 0.6 M. Rate constants for 1 measured at 50, 60, and 70 °C. Rate constants for 10 measured at 40, 50, and 60 °C	120
Figure 6.1 The concentrations of the products of the three reactions were measured over time.	215
Figure 6.2 Protons indicated in red were used to measure the concentrations of products	216
Figure 6.3 Extrapolated Arrhenius Plots of the Diels-Alder reactions of dienes 5.1 and 5.13 with diethyl fumarate in toluene.	218
Figure 7.1 ¹ H NMR Spectrum of 2.3 (500 MHz, CDCl ₃)	220
Figure 7.2 ¹³ C NMR Spectrum of 2.3 (125 MHz, CDCl ₃)	221
Figure 7.3 ¹ H NMR Spectrum of 2.6 (500 MHz, CDCl ₃)	222
Figure 7.4 ¹³ C NMR Spectrum of 2.6 (125 MHz, CDCl ₃)	223
Figure 7.5 ¹ H NMR Spectrum of 2.7 (500 MHz, CDCl ₃)	224
Figure 7.6 ¹³ C NMR Spectrum of 2.7 (125 MHz, CDCl ₃)	225

Figure 7.7 ^1H NMR Spectrum of 2.17 (500 MHz, CDCl_3)	226
Figure 7.8 ^{13}C NMR Spectrum of 2.17 (125 MHz, CDCl_3)	227
Figure 7.9 ^1H NMR Spectrum of 2.18 (500 MHz, CDCl_3)	228
Figure 7.10 ^{13}C NMR Spectrum of 2.18 (125 MHz, CDCl_3)	229
Figure 7.11 ^1H NMR Spectrum of 2.19 (500 MHz, CDCl_3)	230
Figure 7.12 ^{13}C NMR Spectrum of 2.19 (125 MHz, CDCl_3)	231
Figure 7.13 ^1H NMR Spectrum of 2.21 (500 MHz, CDCl_3)	232
Figure 7.14 ^{13}C NMR Spectrum of 2.21 (125 MHz, CDCl_3)	233
Figure 7.15 ^1H NMR Spectrum of 2.22 (500 MHz, CDCl_3)	234
Figure 7.16 ^{13}C NMR Spectrum of 2.22 (125 MHz, CDCl_3)	235
Figure 7.17 ^1H NMR Spectrum of SI.1 (500 MHz, CDCl_3)	236
Figure 7.18 ^{13}C NMR Spectrum of SI.1 (125 MHz, CDCl_3)	237
Figure 7.19 ^{19}F NMR Spectrum of SI.1 (500 MHz, CDCl_3)	238
Figure 7.20 ^1H NMR Spectrum of 2.26 (500 MHz, CDCl_3)	239
Figure 7.21 ^{13}C NMR Spectrum of 2.26 (125 MHz, CDCl_3)	240
Figure 7.22 ^{19}F NMR Spectrum of 2.26 (500 MHz, CDCl_3)	241
Figure 7.23 ^1H NMR Spectrum of 2.28 (500 MHz, CDCl_3)	242
Figure 7.24 ^{13}C NMR Spectrum of 2.28 (125 MHz, CDCl_3)	243
Figure 7.25 ^1H NMR Spectrum of 2.33 (500 MHz, CDCl_3)	244
Figure 7.26 ^{13}C NMR Spectrum of 2.33 (125 MHz, CDCl_3)	245
Figure 7.27 ^1H NMR Spectrum of 2.27 (500 MHz, CDCl_3)	246
Figure 7.28 ^{13}C NMR Spectrum of 2.27 (125 MHz, CDCl_3)	247
Figure 7.29 ^1H NMR Spectrum of 2.35 (500 MHz, CDCl_3)	248

Figure 7.30 ^1H NMR Spectrum of 2.41 (500 MHz, CDCl_3)	249
Figure 7.31 ^{13}C NMR Spectrum of 2.41 (125 MHz, CDCl_3)	250
Figure 7.32 ^1H NMR Spectrum of dechlorofontonamide (500 MHz, CDCl_3).....	251
Figure 7.33 ^{13}C NMR Spectrum of dechlorofontonamide (125 MHz, CDCl_3).....	252
Figure 7.34 ^1H NMR Spectrum of 3.32 (500 MHz, CDCl_3)	253
Figure 7.35 ^{13}C NMR Spectrum of 3.32 (125 MHz, CDCl_3)	254
Figure 7.36 ^1H NMR Spectrum of 3.31 (500 MHz, CDCl_3)	255
Figure 7.37 ^{13}C NMR Spectrum of 3.31 (125 MHz, CDCl_3)	256
Figure 7.38 ^1H NMR Spectrum of 3.30 (500 MHz, CDCl_3)	257
Figure 7.39 ^{13}C NMR Spectrum of 3.30 (125 MHz, CDCl_3)	258
Figure 7.40 ^1H NMR Spectrum of 3.29 (500 MHz, CDCl_3)	259
Figure 7.41 ^{13}C NMR Spectrum of 3.29 (125 MHz, CDCl_3)	260
Figure 7.42 ^1H NMR Spectrum of 3.24-d (500 MHz, CDCl_3).....	261
Figure 7.43 ^{13}C NMR Spectrum of 3.24-d (125 MHz, CDCl_3).....	262
Figure 7.44 ^1H NMR Spectrum of 3.24-a (500 MHz, CDCl_3).....	263
Figure 7.45 ^{13}C NMR Spectrum of 3.24-a (125 MHz, CDCl_3).....	264
Figure 7.46 ^1H NMR Spectrum of 3.46-a (500 MHz, CDCl_3).....	265
Figure 7.47 ^{13}C NMR Spectrum of 3.46-a (125 MHz, CDCl_3).....	266
Figure 7.48 ^1H NMR Spectrum of 3.48 (500 MHz, CDCl_3)	267
Figure 7.49 ^{13}C NMR Spectrum of 3.48 (125 MHz, CDCl_3)	268
Figure 7.50 ^1H NMR Spectrum of 3.24-c (500 MHz, CDCl_3)	269
Figure 7.51 ^{13}C NMR Spectrum of 3.24-c (125 MHz, CDCl_3).....	270
Figure 7.52 ^1H NMR Spectrum of 3.46-c (500 MHz, CDCl_3).....	271

Figure 7.53 ^{13}C NMR Spectrum of 3.46-c (125 MHz, CDCl_3).....	272
Figure 7.54 ^1H NMR Spectrum of 3.47-c (500 MHz, CDCl_3).....	273
Figure 7.55 ^{13}C NMR Spectrum of 3.47-c (125 MHz, CDCl_3).....	274
Figure 7.56 ^1H NMR Spectrum of 3.61 (500 MHz, CDCl_3).....	275
Figure 7.57 ^{13}C NMR Spectrum of 3.61 (125 MHz, CDCl_3).....	276
Figure 7.58 ^1H NMR Spectrum of 3.63 (500 MHz, CDCl_3).....	277
Figure 7.59 ^{13}C NMR Spectrum of 3.63 (125 MHz, CDCl_3).....	278
Figure 7.60 ^{19}F NMR Spectrum of 3.63 (500 MHz, CDCl_3).....	279
Figure 7.61 ^1H NMR Spectrum of 3.60 (500 MHz, CDCl_3).....	280
Figure 7.62 ^{13}C NMR Spectrum of 3.60 (125 MHz, CDCl_3).....	281
Figure 7.63 ^{19}F NMR Spectrum of 3.60 (500 MHz, CDCl_3).....	282
Figure 7.64 ^1H NMR Spectrum of 3.64 (500 MHz, CDCl_3).....	283
Figure 7.65 ^{13}C NMR Spectrum of 3.64 (125 MHz, CDCl_3).....	284
Figure 7.66 ^1H NMR Spectrum of 3.65 (500 MHz, CDCl_3).....	285
Figure 7.67 ^{13}C NMR Spectrum of 3.64 (125 MHz, CDCl_3).....	286
Figure 7.68 ^1H NMR Spectrum of 3.66 (500 MHz, CDCl_3).....	287
Figure 7.69 ^{13}C NMR Spectrum of 3.66 (125 MHz, CDCl_3).....	288
Figure 7.70 ^1H NMR Spectrum of 3.75 (500 MHz, CDCl_3).....	289
Figure 7.71 ^{13}C NMR Spectrum of 3.75 (125 MHz, CDCl_3).....	290
Figure 7.72 HSQC Spectrum of 3.75 (500 MHz, CDCl_3).....	291
Figure 7.73 ^1H NMR Spectrum of 3.78 (500 MHz, CDCl_3).....	292
Figure 7.74 ^1H NMR Spectrum of fontonamide (500 MHz, CDCl_3).....	293
Figure 7.75 ^{13}C NMR Spectrum of fontonamide (125 MHz, CDCl_3).....	294

Figure 7.76 ^1H NMR Spectrum of 3.81 (500 MHz, CDCl_3)	295
Figure 7.77 ^{13}C NMR Spectrum of 3.81 (125 MHz, CDCl_3)	296
Figure 7.78 ^1H NMR Spectrum of 13-Hydroxy dechlorofontonamide (500 MHz, CDCl_3) ...	297
Figure 7.79 ^{13}C NMR Spectrum of 13-Hydroxy dechlorofontonamide (125 MHz, CDCl_3) ..	298
Figure 7.80 NOESY Spectrum of 13-Hydroxy dechlorofontonamide (500 MHz, CDCl_3)	299
Figure 7.81 ^1H NMR Spectrum of 4.11 (500 MHz, CDCl_3)	300
Figure 7.82 ^{13}C NMR Spectrum of 4.11 (125 MHz, CDCl_3)	301
Figure 7.83 ^1H NMR Spectrum of 4.12 (500 MHz, CDCl_3)	302
Figure 7.84 ^{13}C NMR Spectrum of 4.12 (125 MHz, CDCl_3)	303
Figure 7.85 ^1H NMR Spectrum of 4.27 (500 MHz, CDCl_3)	304
Figure 7.86 ^1H NMR Spectrum of 4.14 (500 MHz, CDCl_3)	305
Figure 7.87 ^{13}C NMR Spectrum of 4.14 (125 MHz, CDCl_3)	306
Figure 7.88 ^1H NMR Spectrum of 4.15 (500 MHz, CDCl_3)	307
Figure 7.89 ^{13}C NMR Spectrum of 4.15 (125 MHz, CDCl_3)	308
Figure 7.90 ^1H NMR Spectrum of 4.17 (500 MHz, CDCl_3)	309
Figure 7.91 ^{13}C NMR Spectrum of 4.17 (125 MHz, CDCl_3)	310
Figure 7.92 ^{19}F NMR Spectrum of 4.17 (500 MHz, CDCl_3)	311
Figure 7.93 ^1H NMR Spectrum of 4.18 (500 MHz, CDCl_3)	312
Figure 7.94 ^{13}C NMR Spectrum of 4.18 (125 MHz, CDCl_3)	313
Figure 7.95 ^1H NMR Spectrum of 4.20 (500 MHz, CDCl_3)	314
Figure 7.96 ^{13}C NMR Spectrum of 4.20 (125 MHz, CDCl_3)	315
Figure 7.97 ^1H NMR Spectrum of 4.21 (500 MHz, CDCl_3)	316
Figure 7.98 ^{13}C NMR Spectrum of 4.21 (125 MHz, CDCl_3)	317

Figure 7.99 ^1H NMR Spectrum of 4.22 (500 MHz, CDCl_3)	318
Figure 7.100 ^{13}C NMR Spectrum of 4.21 (125 MHz, CDCl_3)	319
Figure 7.101 ^1H NMR Spectrum of 4.22 (500 MHz, CDCl_3)	320
Figure 7.102 ^{13}C NMR Spectrum of 4.22 (125 MHz, CDCl_3)	321
Figure 7.103 ^1H NMR Spectrum of 4.24 (500 MHz, CDCl_3)	322
Figure 7.104 ^{13}C NMR Spectrum of 4.24 (125 MHz, CDCl_3)	323
Figure 7.105 ^{19}F NMR Spectrum of 4.24 (500 MHz, CDCl_3)	324
Figure 7.106 ^1H NMR Spectrum of 4.19 (500 MHz, CDCl_3)	325
Figure 7.107 ^{13}C NMR Spectrum of 4.19 (125 MHz, CDCl_3)	326
Figure 7.108 ^{19}F NMR Spectrum of 4.19 (500 MHz, CDCl_3)	327
Figure 7.109 ^1H NMR Spectrum of 4.8 (500 MHz, CDCl_3)	328
Figure 7.110 ^{13}C NMR Spectrum of 4.8 (125 MHz, CDCl_3)	329
Figure 7.111 ^{19}F NMR Spectrum of 4.8 (500 MHz, CDCl_3)	330
Figure 7.112 ^1H NMR Spectrum of 4.9 (500 MHz, CDCl_3)	331
Figure 7.113 ^1H NMR Spectrum of 4.26 (500 MHz, CDCl_3)	332
Figure 7.114 ^{13}C NMR Spectrum of 4.26 (125 MHz, CDCl_3)	333
Figure 7.115 ^1H NMR Spectrum of 4.35 (500 MHz, CDCl_3)	334
Figure 7.116 ^{13}C NMR Spectrum of 4.35 (125 MHz, CDCl_3)	335
Figure 7.117 HSQC Spectrum of 4.35 (500 MHz, CDCl_3)	336
Figure 7.118 ^1H NMR Spectrum of 4.36 (500 MHz, CDCl_3)	337
Figure 7.119 ^{13}C NMR Spectrum of 4.36 (125 MHz, CDCl_3)	338
Figure 7.120 ^1H NMR Spectrum of SI.2 (500 MHz, CDCl_3)	339
Figure 7.121 ^{13}C NMR Spectrum of 4.37 (125 MHz, CDCl_3)	340

Figure 7.122 ^1H NMR Spectrum of 4.37 (500 MHz, CDCl_3)	341
Figure 7.123 ^{13}C NMR Spectrum of 4.37 (125 MHz, CDCl_3)	342
Figure 7.124 ^1H NMR Spectrum of 4.40 (500 MHz, CDCl_3)	343
Figure 7.125 ^{13}C NMR Spectrum of 4.40 (125 MHz, CDCl_3)	344
Figure 7.126 ^1H NMR Spectrum of 4.41 (500 MHz, CDCl_3)	345
Figure 7.127 ^{19}F NMR Spectrum of 4.41 (500 MHz, CDCl_3)	346
Figure 7.128 ^1H NMR Spectrum of 4.42 (500 MHz, CDCl_3)	347
Figure 7.129 ^{13}C NMR Spectrum of 4.42 (125 MHz, CDCl_3)	348
Figure 7.130 ^1H NMR Spectrum of 4.43 (500 MHz, CDCl_3)	349
Figure 7.131 ^{13}C NMR Spectrum of 4.43 (125 MHz, CDCl_3)	350
Figure 7.132 ^{19}F NMR Spectrum of 4.43 (500 MHz, CDCl_3)	351
Figure 7.133 ^1H NMR Spectrum of 4.43 (500 MHz, CDCl_3)	352
Figure 7.134 ^{13}C NMR Spectrum of 4.44 (125 MHz, CDCl_3)	353
Figure 7.135 ^{19}F NMR Spectrum of 4.44 (500 MHz, CDCl_3)	354
Figure 7.136 ^1H NMR Spectrum of 5.17 (500 MHz, CDCl_3)	355
Figure 7.137 ^{13}C NMR Spectrum of 5.17 (125 MHz, CDCl_3)	356
Figure 7.138 ^1H NMR Spectrum of 5.18 (500 MHz, CDCl_3)	357
Figure 7.139 ^{13}C NMR Spectrum of 5.18 (125 MHz, CDCl_3)	358
Figure 7.140 ^1H NMR Spectrum of 5.13 (500 MHz, CDCl_3)	359
Figure 7.141 ^{13}C NMR Spectrum of 5.13 (125 MHz, CDCl_3)	360
Figure 7.142 ^1H NMR Spectrum of 5.20 (500 MHz, CDCl_3)	361
Figure 7.143 ^{13}C NMR Spectrum of 5.20 (125 MHz, CDCl_3)	362
Figure 7.144 ^1H NMR Spectrum of 5.23a (500 MHz, CDCl_3)	363

Figure 7.145 ^{13}C NMR Spectrum of 5.23a (125 MHz, CDCl_3)	364
Figure 7.146 ^1H NMR Spectrum of 5.23b (500 MHz, CDCl_3)	365
Figure 7.147 ^{13}C NMR Spectrum of 5.23b (125 MHz, CDCl_3)	366
Figure 7.148 ^1H NMR Spectrum of 5.23c (500 MHz, CDCl_3)	367
Figure 7.149 ^{13}C NMR Spectrum of 5.23c (125 MHz, CDCl_3)	368
Figure 7.150 ^1H NMR Spectrum of 5.23d (500 MHz, CDCl_3)	369
Figure 7.151 ^{13}C NMR Spectrum of 5.23d (125 MHz, CDCl_3)	370
Figure 7.152 ^1H NMR Spectrum of 5.23f (500 MHz, CDCl_3)	371
Figure 7.153 ^{13}C NMR Spectrum of 5.23f (125 MHz, CDCl_3)	372
Figure 7.154 ^1H NMR Spectrum of 5.23g (500 MHz, CDCl_3)	373
Figure 7.155 ^{13}C NMR Spectrum of 5.23g (125 MHz, CDCl_3)	374
Figure 7.156 ^1H NMR Spectrum of 5.23h (500 MHz, CDCl_3)	375
Figure 7.157 ^{13}C NMR Spectrum of 5.23h (125 MHz, CDCl_3)	376
Figure 7.158 ^1H NMR Spectrum of 5.26a (500 MHz, CDCl_3)	377
Figure 7.159 ^{13}C NMR Spectrum of 5.26a (125 MHz, CDCl_3)	378
Figure 7.160 ^1H NMR Spectrum of 5.26b (500 MHz, CDCl_3)	379
Figure 7.161 ^{13}C NMR Spectrum of 5.26b (125 MHz, CDCl_3)	380
Figure 7.162 ^1H NMR Spectrum of 5.26c (500 MHz, CDCl_3)	381
Figure 7.163 ^{13}C NMR Spectrum of 5.26c (125 MHz, CDCl_3)	382
Figure 7.164 ^1H NMR Spectrum of 5.26d (500 MHz, CDCl_3)	383
Figure 7.165 ^{13}C NMR Spectrum of 5.26d (125 MHz, CDCl_3)	384
Figure 7.166 ^1H NMR Spectrum of 5.26e (500 MHz, CDCl_3)	385
Figure 7.167 ^{13}C NMR Spectrum of 5.26e (125 MHz, CDCl_3)	386

Figure 7.168 ^1H NMR Spectrum of 5.26f (500 MHz, CDCl_3).....	387
Figure 7.169 ^{13}C NMR Spectrum of 5.26f (125 MHz, CDCl_3).....	388
Figure 7.170 ^1H NMR Spectrum of 5.26g (500 MHz, CDCl_3).....	389
Figure 7.171 ^{13}C NMR Spectrum of 5.26g (125 MHz, CDCl_3).....	390
Figure 7.172 ^1H NMR Spectrum of 5.26h (500 MHz, CDCl_3).....	391
Figure 7.173 ^{13}C NMR Spectrum of 5.26h (125 MHz, CDCl_3).....	392
Figure 7.174 ^1H NMR Spectrum of 5.26i (500 MHz, CDCl_3).....	393
Figure 7.175 ^{13}C NMR Spectrum of 5.26i (125 MHz, CDCl_3).....	394
Figure 7.176 ^1H NMR Spectrum of 5.29a (500 MHz, CDCl_3).....	395
Figure 7.177 ^{13}C NMR Spectrum of 5.29a (125 MHz, CDCl_3).....	396
Figure 7.178 ^1H NMR Spectrum of 5.29b (500 MHz, CDCl_3).....	397
Figure 7.179 ^{13}C NMR Spectrum of 5.29b (125 MHz, CDCl_3).....	398
Figure 7.180 ^1H NMR Spectrum of 5.29c (500 MHz, CDCl_3).....	399
Figure 7.181 ^{13}C NMR Spectrum of 5.29c (125 MHz, CDCl_3).....	400
Figure 7.182 ^1H NMR Spectrum of 5.29d (500 MHz, CDCl_3).....	401
Figure 7.183 ^{13}C NMR Spectrum of 5.29d (125 MHz, CDCl_3).....	402
Figure 7.184 ^1H NMR Spectrum of 5.29e (500 MHz, CDCl_3).....	403
Figure 7.185 ^{13}C NMR Spectrum of 5.29e (125 MHz, CDCl_3).....	404
Figure 7.186 ^1H NMR Spectrum of 5.29f (500 MHz, CDCl_3).....	405
Figure 7.187 ^{13}C NMR Spectrum of 5.29f (125 MHz, CDCl_3).....	406

LIST OF ABBREVIATIONS

AIBN = azobisisobutyronitrile

Ac = acetyl

AcOH = acetic acid

ATP = adenosine triphosphate

9-BBN = 9-borabicyclo(3.3.1)nonane

Bn = benzyl

Boc = *tert*-butyloxycarbonyl

Bs = benzenesulfonyl

Bu = butyl

Bz = benzoyl

c = concentration

CAN = ceric ammonium nitrate

Cbz = benzyloxycarbonyl

CDI = 1,1'-carbonyldiimidazole

Cp = cyclopentadienyl

Cp* = 1,2,3,4,5-pentamethylcyclopentadienyl

cod = 1,5-cyclooctadiene

COSY = correlation spectroscopy

m-CPBA = *meta*-chloroperoxybenzoic acid

CSA = camphorsulfonic acid

DCE = 1,2-dichloroethane

DEG = diethylene glycol

DFT = density-functional theory

DIAD = diisopropyl azodicarboxylate

DIBAL-H = diisobutylaluminum hydride

(4-)DMAP = 4-dimethylaminopyridine

DMF = dimethylformamide

DMP = Dess-Martin periodinane

DMPU = 1,3-Dimethyl-3,4,5,6-tetrahydro-2-pyrimidinone

DMSO = dimethyl sulfoxide

DPPA = diphenylphosphoryl azide

2,6-DTBP = 2,6-di-*tert*-butylpyridine

dr = diastereomeric ratio

ee = enantiomeric excess

eq. = equivalents

ESI = electrospray ionization

Et = ethyl

h = hours

h ν = light

HMDS = bis(trimethylsilyl)amine

HMPA = hexamethylphosphoramide

HRMS = high resolution mass spectrometry

HSQC = heteronuclear single-quantum correlation spectroscopy

Hz = Hertz

IR = infrared

LDA = lithium diisopropylamide

Me = methyl

MeCN = acetonitrile

MOM = methoxymethyl

Ms = methanesulfonyl

MVK = methyl vinyl ketone

NBS = *N*-bromosuccinimide

NCS = *N*-chlorosuccinimide

NMO = *N*-methylmorpholine *N*-oxide

NMR = nuclear magnetic resonance

NOE = nuclear Overhauser effect

Oct = octanoate

Ph = phenyl

PhH = benzene

PhMe = toluene

Piv = pivaloyl

PMB = *para*-methoxybenzyl

PPTS = pyridinium *para*-toluenesulfonate

Pr = propyl

pyr = pyridine

R_f = retention factor

sp. = species

TBAF = tetra-*n*-butylammonium fluoride

TBDPS = *tert*-butyldiphenylsilyl

TBS = *tert*-butyldimethylsilyl

TES = triethylsilyl

Tf = trifluoromethanesulfonyl

THF = tetrahydrofuran

THP = tetrahydropyranyl

TIPS = triisopropylsilyl

TLC = thin-layer chromatography

TMDSO = 1,1,3,3-tetramethyldisiloxane

TMP = 2,2,6,6-tetramethylpiperidine

TMS = trimethylsilyl

TPAP = tetrapropylammonium perruthenate

Tr = trityl

Troc = 2,2,2-trichloroethoxycarbonyl

TS = transition state

Ts = *para*-toluenesulfonyl

p-TsOH = *para*-toluenesulfonic acid

ACKNOWLEDGEMENTS

I would first like to thank Professor Rawal for all the mentorship he has given me over the previous five years. I came into this lab having never worked in an organic chemistry lab, Professor Rawal always made sure that his door was open and that he was available for any question, no matter how big or small. Professor Rawal was always willing to dive into problems we were facing, and through our weekly group meetings helped to foster a sense of camaraderie that helped us all to become better chemists as we collectively worked to overcome the groups hurdles. It is clear that Professor Rawal's commitment to research and teaching is genuine, and I will always look back on my time in this lab, and the science that we did, with fondness and gratitude.

I would also like to thank the other members of my committee, Professors Snyder and Levin. Both served on my candidacy committees as well, and as such, I have spent the better part of four years turning to them for advice and assistance with various problems. Professor Snyder also taught the organic synthesis course my first year, which, while being the most information-dense class I have ever taken, helped me reaffirm that I was in the right place and played a large role in me becoming the organic chemist I am today. Professor Levin is the most energetic and optimistic chemist I have ever met, and simply being across the hall from him was enough to inspire me to work harder and find more interesting solutions to my problems. In addition to these two professors, I also have to extend my gratitude to Professor Dong, who similarly was always willing to offer suggestions and answer questions. Professor Dong also invited the Rawal group to the Dong group literature meetings, which exposed me to a whole world of chemistry

that I had never learned, and which played a large role in my ultimate route towards my natural products.

I also need to thank the other members of the Rawal group for being such fantastic coworkers these last five years. Bowei Hu was the first member of the lab that I met, and helped teach me everything I know about synthesis, from how to run a column to how to use reaxys, and a million more things. He always had interesting questions and insightful suggestions, and I couldn't have asked for a better labmate my first three years. Ferdinand Taenzler was an exceptionally hard worker, and his habit of asking questions in group meeting helped me to learn to look at my chemistry in new ways. Although his lab notebooks left something to be desired, he was always an enormous help, and his background work on the welwitindolinones helped pave the way for me to accomplish as much as I did. Kyle Cassaidy was another brilliant chemist, and one of the most meticulous people I have ever met. I wish I had stolen more of his good habits before he graduated, but he always inspired me to try something difficult that just might work. He also had the most beautiful presentation slides, which makes me feel bad every time I compare his to my own.

Additionally, I need to thank Jirapon Sae-Jew for being a delightful bay-mate over these last few years, as well as for volunteering to help finish the fontonamide project for publications. Sudhakar Athe joined in my third year, and together we worked on a entirely novel project for the group developing fluorescent probes for a Covid project. He is a smart, hardworking chemist, and I am glad we got to work on such an interesting project together. Daler Baidilov was one of the most helpful members of the lab in my last year, not only for his great suggestions on how to finish my syntheses, but also for his invaluable feedback in putting together my thesis and presentations. Finally, all other members of the lab that I have overlapped with, including Yun-

Jeong Shin, Li Li, Yoko Hasegawa, Peter Ryfell, and William Zhao, have made my time in lab more fun and interesting, and all of their assistance and companionship has been much appreciated.

I of course also need to thank my family for all of their support, both over the last five years and in the 21 years prior. My parents David Durfee and Melanie Dexter are two of the smartest people I know, and always gave me all the support to succeed without ever pushing me beyond my comfort zone. My brothers Sebastian and Josiah have also been fantastic supporters, intellectual sparring partners, and two of my best friends. My grandmother Doris Dexter is another brilliant woman who gave me far more praise than I ever deserved, and I have spent my life in pursuit of actualizing her view of me. I never met her husband, my grandfather David Dexter, but his memory as a brilliant scientist and loving family man has inspired me from the beginning, and I don't think I would have started down this path without something of him in me. My other grandparents, Horton and Jean, were equally kind, brilliant, and well rounded people, and it is certainly only an accident of fate that I ended up a chemist rather than following in Jean's footsteps to pursue mathematics.

I briefly need to thank all of my friends, both at Middlebury for undergrad, and here at UChicago. At Middlebury I was able to surround myself with driven, interesting, and varied people, joining the track team, the a cappella group Stuck in the Middle, and finding friends in classrooms and the lab. A liberal arts education is an amazing experience, and I will forever be grateful for the people I met there. I'm similarly grateful for all the friends I have made at UChicago, from my roommates at 5491 and Shoreland, the members of the recruitment committee, team beer, and all the other random acquaintances and friendships I have built.

Nobody can do science all the time, and its those in-between times that made UChicago so special.

Finally, last but certainly not least, I need to extend a thank you to my undergraduate advisor, Sunhee Choi. The tiger mother I never had, Sunhee always had the highest expectations for all of her students. From the moment I met her, in my first chemistry class my first day of school, she taught me and all of her students that we were expected to perform at our highest levels, and she made sure to give us all of the tools necessary to do that. I have also never met a person more interested in scientific discovery, and her passion for our research inspired me and every member of our lab to do more and work harder. Sunhee is also one of the best cooks I have ever met, and anyone who has met me knows how important great food is to winning my admiration. Sunhee inspired me to be a chemistry major, she inspired me to go to graduate school, and she will always inspire me to be the best in anything I do, and I will forever be grateful for her guidance and support through the last nine years of my life.

ABSTRACT

Using a novel route that takes advantage of the directing ability of the natural formanilide directing group, the first total synthesis of two members of the hapalonamide family, (-)-fontonamide and (-)-dechlorofontonamide, are reported herein. The syntheses are highly convergent, coupling the A ring formanilide fragment and the D ring highly-decorated-cyclohexanone fragment through a Friedel-Crafts reaction and an ortho-directed C-H functionalization. Both syntheses have been rendered asymmetric. A third member of the hapalonamide family, 13-hydroxy dechlorofontonamide, was also synthesized, however it was determined upon its synthesis that the original isolation paper had misassigned the isolated compound, which was in actuality fontonamide. This thesis also describes the synthetic effort undertaken towards welwitindolinone A, with the goal of using a novel intramolecular palladium-mediated alkenylation to create the core cyclobutene ring of the compound. This reaction was successful in model studies, but ultimately failed on the fully-decorated molecule. Finally, this thesis describes the successful development of a novel 1,1-disubstituted diene for use in the Diels-Alder reaction. The novel diene allows access to 6-substituted and 6,6-disubstituted cyclohexenones and 6-substituted 5,6-dihydropyran-2-ones. The synthesis of the diene is highly scalable and operationally facile, and kinetics experiments show the reactivity of the diene is high compared to other highly active dienes.

Chapter 1: Introduction to the Hapalindoles and Total Synthesis Efforts Towards Oxidized Members of the Hapalindole Family

Preface

This majority of this thesis will focus on the total synthesis of three molecules from the hapalonamide subfamily of the hapalindole family of natural products, namely; (-)-fontonamide, (-)-dechlorofontonamide, and (\pm)-13-hydroxy dechlorofontonamide; as well as synthetic studies towards a 4th member from the broader hapalindole family, (+)-welwitindolinone A. The beginning of this chapter will serve as a brief introduction to the family, including the biosynthesis of the various subfamilies, as well as an overview of previous syntheses of the hapalonamides and welwitindolinone A. The end of the chapter will discuss our retrosynthetic analysis of the fontonamides and welwitindolinone A, as well as present some background information on the key steps proposed. The second and third chapter will detail the synthetic efforts taken in the total synthesis of the fontonamides, while the fourth chapter will be focused on the synthetic studies performed towards the synthesis of welwitindolinone A. Finally, chapter five will focus on a separate project: the development of a vinyl ketene equivalent diene for use in synthesizing 6,6-disubstituted cyclohexenones through the Diels-Alder reaction.

1.1 Hapalindole Natural Products

1.1A: Isolation, Biological activity, and Structure

The hapalindoles are a wide family of indole alkaloid natural products derived from blue-green algae. Interest in the family can be traced back to initial reports in 1969 that *Hapalosiphon fontinalis*, a blue-green algae found in the Marshall Islands, produced a substance that strongly inhibited the growth of other algae. In 1984, Richard Moore and coworkers isolated the first two members of the family, hapalindoles A and B, and proposed that they may be responsible for this activity.¹ Substantial biological activities of other algal species drove continued interest in the family, and in the following four decades, nearly 100 members of the family have been isolated and characterized.² These compounds have shown a wide range of diverse biological activities: in addition to showing anti-algal behavior, certain compounds also show anti-biotic, anti-fungal, and anti-tumor activities, as well as the rare ability to overcome multi-drug resistance.

In addition to demonstrating a diverse range of activity across the biological spectrum, the broader family is also structurally diverse. Members of the family all contain a highly-functionalized six-membered D ring decorated with a methyl and vinyl quaternary center para to an exocyclic isopropyl unit, as well as the eponymous indole core (Figure 1.1). However, these two basic building blocks can be assembled in a wide variety of ways, leading to a multitude of subfamilies with distinct ring structures. The most common structural type, and the first isolated, belongs to the hapalindoles. These molecules are defined by the presence of a direct connection between the C-3 position on the indole and C-10 on the D ring, as well as an optional closure

¹ Moore, R. E.; Cheuk, C.; Patterson, G. M. L. *J. Am. Chem. Soc.* **1984**, *106* (21), 6456–6457

² Bhat, V.; Dave, A.; MacKay, J. A.; Rawal, V. H. In *The Alkaloids: Chemistry and Biology*; Knölker, H.-J., Ed.; Chemistry and Biology; Academic Press, 2014; Vol. 73, pp 65–160.

between the C-5 position on the indole and the exocyclic isopropyl unit of the D ring. These connections give the tri- and tetra-cyclic hapalindoles respectively. Adding an isoprene unit at the C-2 position leads to the ambiguines, which can be left open to give the tetracyclic ambiguines or cyclized onto the D ring a C-11 to give the pentacyclic ambiguines. The next largest subfamily is the fischerindoles. As with the hapalindoles, a direct connection can be observed between the C-3 position of the indole and C-10 on D ring. However, for this family the exocyclic isopropyl unit cyclizes onto the C-2 position of the indole rather than C-5, giving a five membered C ring.

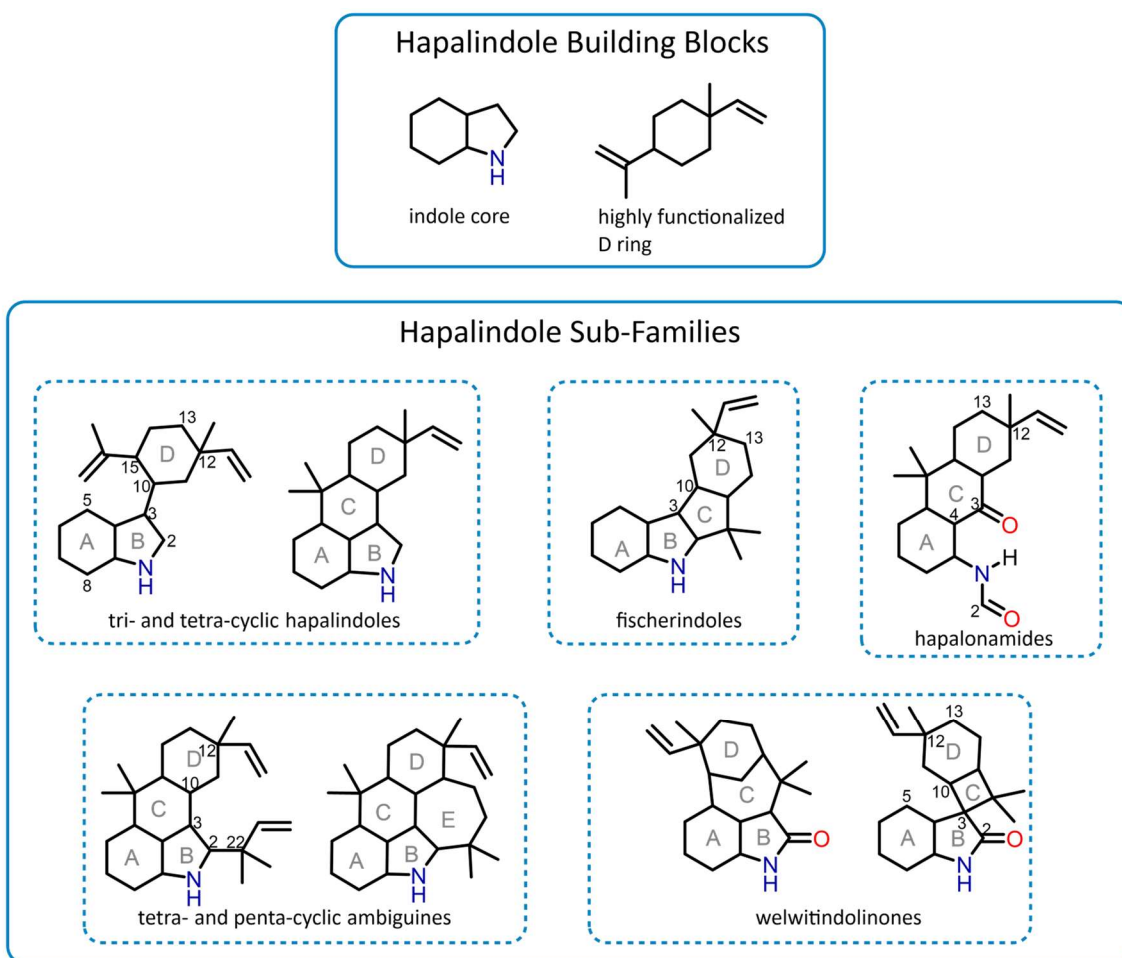
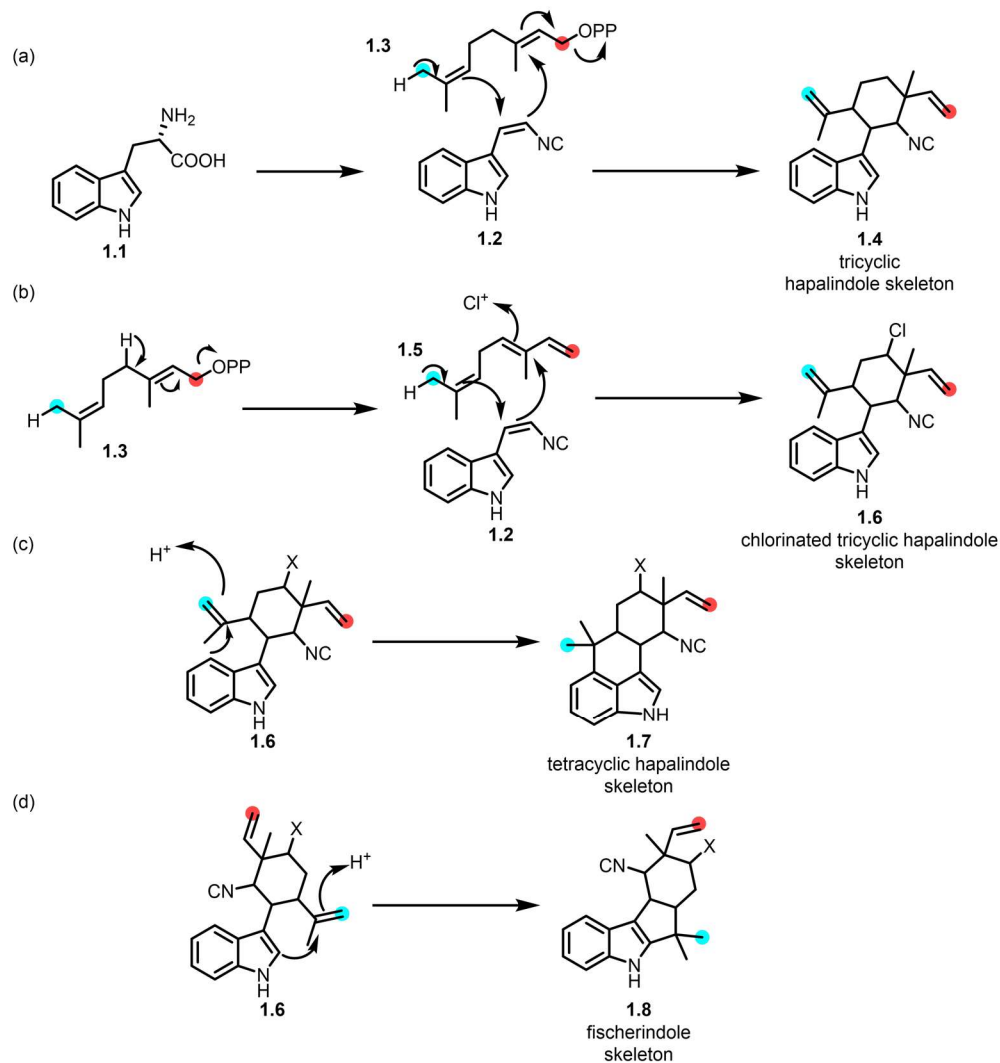


Figure 1.1 Building blocks of the hapalindoles and structures of the subfamilies.

All three of these subfamilies contain members exhibiting varying levels of oxidation, primarily on the D ring, where approximately half of the family is chlorinated at the C-13 position. However, many members of the larger family contain oxidation of the indole core as well. The welwitindolinones are a relatively small subfamily, but due to the interesting structures and unique biological activities of its members, the subfamily has seen significant synthetic interest. As the name suggests, the indole core has been oxidized to a 2-indolinone. Additionally, while the C-3 position of the indole is substituted, it is connected to the exocyclic isopropyl unit of the D ring rather than the D ring itself. For three members of the family, C-10 on the D ring is then connected to the C-5 position on the indole, giving a bridged structure; for welwitindolinone A, C-10 is cyclized onto the C-3 position, giving a quaternary center and cyclobutyl ring. One other oxidized subfamily of note is the hapalonamides. These compounds share the same connectivity as the hapalindoles but have had the indole ring oxidatively cleaved along the C-2 to C-3 double bond, giving a formamide group and a ketone. Notably, this subfamily contains the only members of the hapalindole family that do not have the full indole core. Although a brief discussion of the hapalindoles and fischerindoles is necessary to understand the structure and synthesis of the welwitindolinones and hapalonamides, the bulk of the remainder of this thesis will be concerned with these more highly oxidized compounds.

1.1B Biosynthesis of the hapalonamides and welwitindolinones

From the beginning, the structural similarities of the various members of the broader hapalindole family suggested to Moore from the beginning that a common biosynthetic origin was likely. Moore noted in the original isolation paper that the metabolites appeared to arise from the fusion of a tryptophan and monoterpene unit and in 1994 proposed the identity of this monoterpene unit to be geranyl pyrophosphate (GPP) (**1.3**). The route proposed by Moore in 1994 begins with

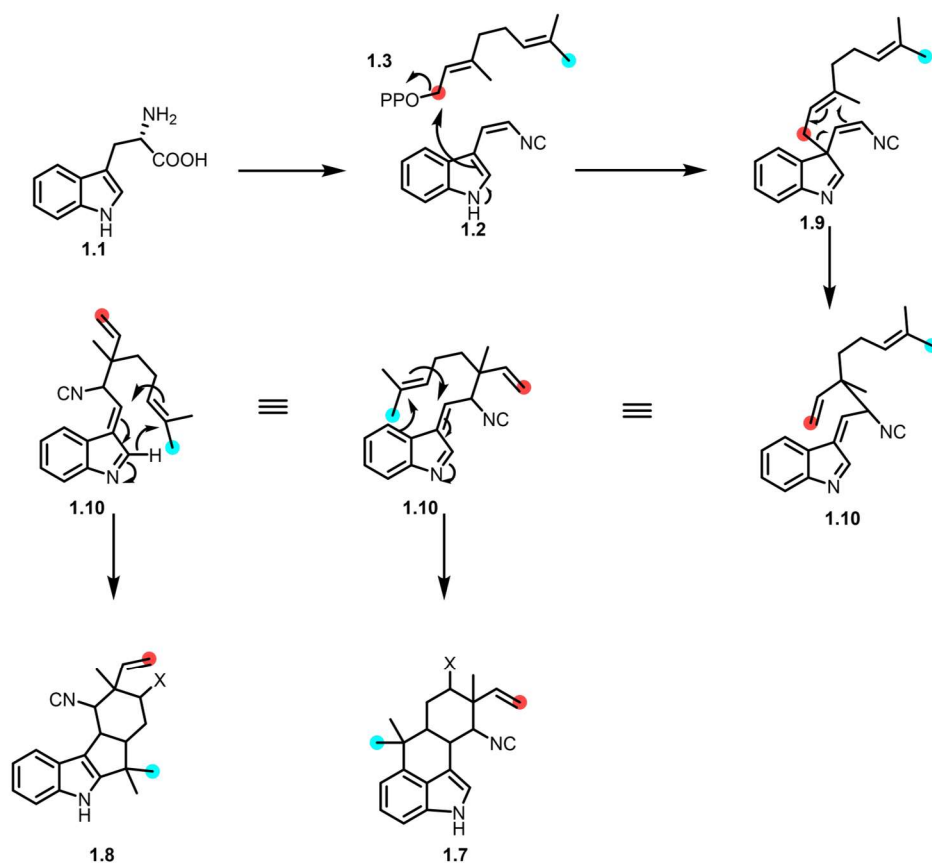


Scheme 1.1 Moore's proposed routes to (a) the dechlorinated and (b) chlorinated tricyclic hapalindoles. Cyclization gives the (c) tetracyclic hapalindoles and (d) fischerindoles

conversion of tryptophan to *cis*-indole isonitrile **1.2** (Scheme 1.1). He hypothesized that a direct cyclization of the isonitrile compound with GPP would lead to the dechlorinated half of the family (**1.4**), while a chloronium ion-mediated cyclization would give rise to the chlorinated members (**1.6**). In both cases, this cyclization would lead to compounds structurally similar to the tricyclic hapalindoles. From here, he proposed that an acid-mediated Friedel-Crafts-type cyclization at either the C-5 or C-2 positions of the indole would lead to the tetracyclic hapalindoles (**1.7**) or fischerindoles (**1.8**), respectively. Acid mediated cyclization of tricyclic hapalindoles to

fischerindoles has been demonstrated in the lab, but cyclization to the tetracyclic hapalindoles is only possible when the C-2 position is blocked.³

This route was generally accepted, and in 2014, Xinyu Liu and coworkers reported substantial supporting evidence when they, for the first time, characterized the gene cluster responsible for the biosynthesis of both the indole isonitrile and GPP in *F. Ambigua*.¹ However, three years later, David Sherman and coworkers, while searching for the enzyme responsible for the cyclization, found that this process was unlikely to occur in a single step.⁴ Sherman found that two enzymes

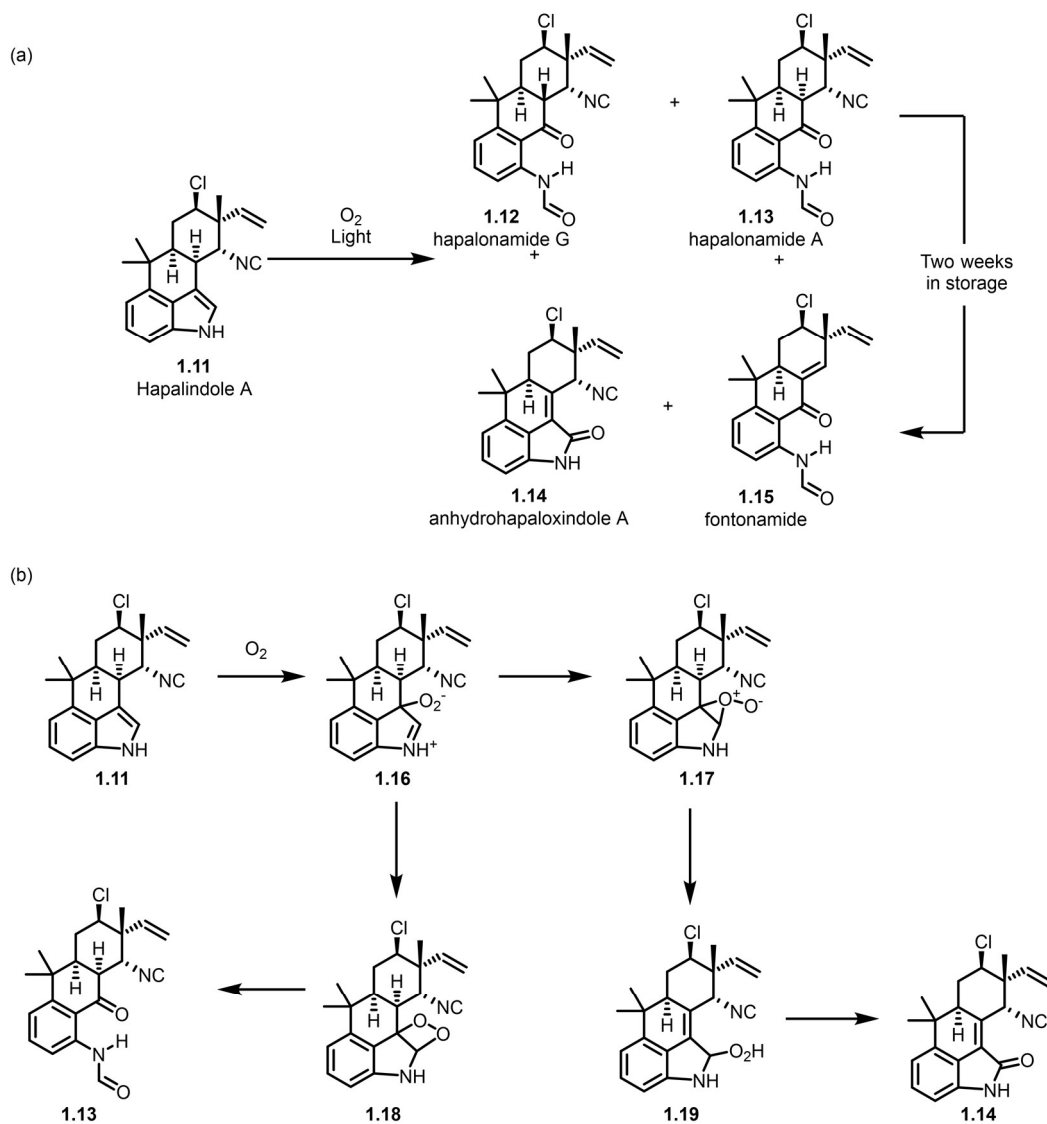


Scheme 1.2 Sherman's updated route to the tetracyclic hapalindoles and fischerindoles

³ Baran, P. S.; Richter, J. M. *J. Am. Chem. Soc.* **2005**, *127* (44), 15394–15396

⁴ Li, S.; Lowell, A. N.; Newmister, S. A.; Yu, F.; Williams, R. M.; Sherman, D. H. *Nat. Chem. Biol.* **2017**, *13* (5), 467–469

were responsible for this process—the first, a prenyltransferase, attached the GPP unit to the indole unit at the C-3 position to give a structure like **1.9**, while the second, a cyclase, catalyzed a cope rearrangement and subsequent Friedel-Crafts cascade to form in one step the tetracyclic hapalindoles or fischerindoles (Scheme 1.2).



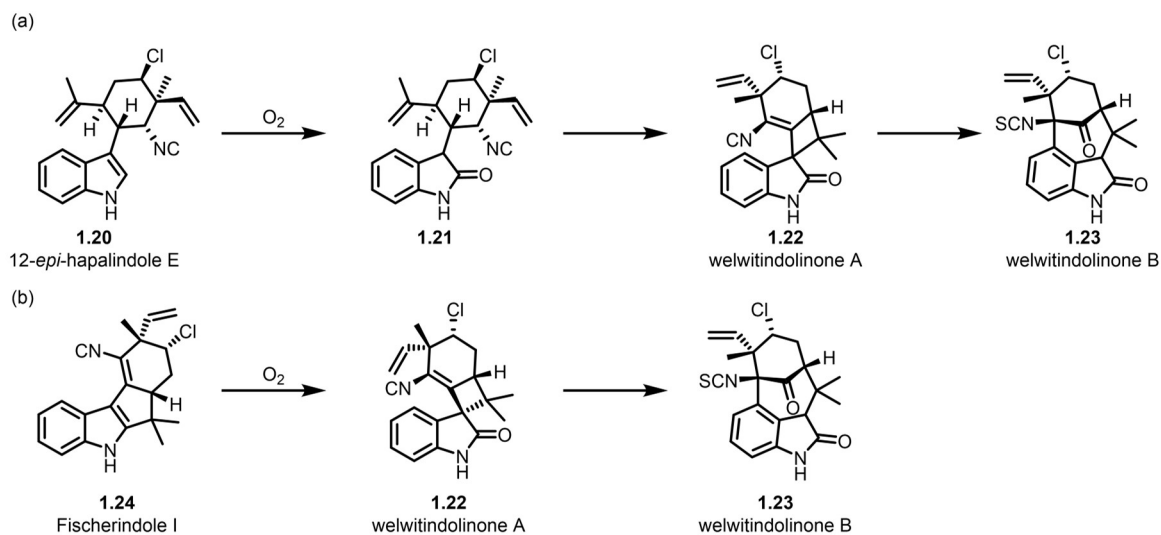
Scheme 1.3 (a) Oxygen and light degrades hapalindole A to hapalonamide A, fontonamide and anhydrohapaloxindole A. (b) Moore's proposed pathway for the oxidations.

Many of the other members of the hapalindole family arise directly from the oxidation of the hapalindoles and fisherindoles. The hapalonamides, first discovered by Moore in 1987 with the isolation of fontonamide, are a prime example of this.⁵ As previously discussed, the hapalonamides are the only members of the family that do not contain an intact indole ring, instead possessing a formamide group and a benzylic ketone. In the isolation paper, Moore demonstrated that the oxidative cleavage of the C-2 to C-3 indole double bond was achievable via a singlet oxygen-mediated oxidation. Subjecting hapalindole A to singlet oxygen conditions led to a mixture of products including fontonamide, anhydrohapaloxindole A, and others. Moore suggested a reasonable chemical mechanism for this, but the enzymes responsible has yet to be positively identified (Scheme 1.3).

While the proposed biological synthesis of the the hapalonamides is fairly un-controversial, the origin of the welwitindolinones is less well understood. Two different pathways have been proposed. The first route, proposed by Moore along with the isolation of welwitindolinone A, B, and C in 1994, suggests that the subfamily is accessed by oxidation of tricyclic hapalindole 12-*epi*-hapalindole E isonitrile.⁶ Oxidation gives oxindole **1.21**, which then cyclizes to give welwitindolinone A. From here, Moore proposed, further oxidation would lead to cleavage of the original C-3 to D ring bond, and rearrangements to give the remaining members of the welwitindolinone subfamily, i.e. **1.23**. Conversely, Baran proposed in 2005 that Welwitindolinone A was instead formed by the oxidation and subsequent ring contraction of Fischerindole I. Baran

⁵ (a) Original isolation paper: Moore, R. E.; Yang, X. Q. G.; Patterson, G. M. L. *J. Org. Chem.* **1987**, *52* (17), 3773–3777. Isolation of other members of the family: (b) Moore, R. E.; Yang, X. G.; Patterson, G. M. L.; Bonjouklian, R.; Smitka, T. A. *Phytochemistry* **1989**, *28* (5), 1565–1567. (c) Kim, H.; Lantvit, D.; Hwang, C. H.; Kroll, D. J.; Swanson, S. M.; Franzblau, S. G.; Orjala, J. *Bioorg. Med. Chem.* **2012**, *20* (17), 5290–5295

⁶ Stratmann, K.; Moore, R. E.; Bonjouklian, R.; Deeter, J. B.; Patterson, G. M. L.; Shaffer, S.; Smith, C. D.; Smitka, T. A. *J. Am. Chem. Soc.* **1994**, *116* (22), 9935–9942



Scheme 1.4 (a) Moore's original proposed pathway to the welwitindolinones. (b) Baran's updated proposed pathway

went on to demonstrate that this first step was feasible (*vide infra*) and it is now broadly accepted as the likely biosynthetic route to welwitindolinone A. However, the conversion of welwitindolinone A to the other welwitindolinones has not been demonstrated. Additionally, as with the hapalonamides, the enzymes responsible for the oxidation remain unknown, although recent work has identified multiple oxygenases of unknown function that may be responsible.^{7,8}

⁷ Hohlman, R. M.; Sherman, D. H. *Nat. Prod. Rep.* **2021**, *38* (9), 1567–1588

⁸ Newmister, S. A.; Li, S.; Garcia-Borràs, M.; Sanders, J. N.; Yang, S.; Lowell, A. N.; Yu, F.; Smith, J. L.; Williams, R. M.; Houk, K. N.; Sherman, D. H. *Nat. Chem. Biol.* **2018**, *14* (4), 345–351

1.1C Previous Synthetic Approaches towards the Hapalonamides

Included within the hapalonamide subfamily are six natural products—hapalonamides H (**1.25**), G, and V, as well as the three fontonamides (See Figure 1.2). In 1987, in the same paper announcing their initial discovery, Moore also demonstrated the first semi-synthesis of a hapalonamide.⁵ Subjection of hapalindole A (**1.11**) to oxidation using rose bengal and oxygen in methanol led to the formation of a number of oxidized products, including fontonamide (**1.15**), anhydrohapaloxindole A (**1.14**), and the non-natural product hapalonamide A (**1.13**). Interestingly, over the course of two weeks of storage, the isonitrile group of hapalonamide A was eliminated, giving clean conversion to fontonamide (*vide infra*). Despite this early result and the significant amount of synthetic interest in the broader family, it would not be until 2014 that a true total synthesis would be completed.

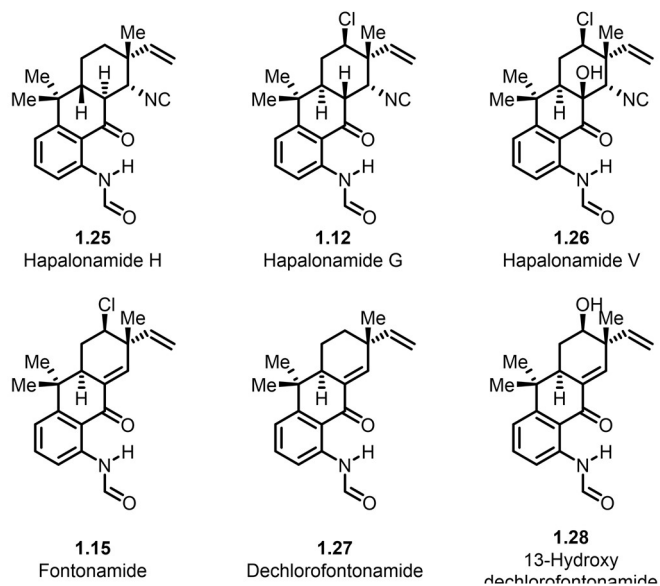
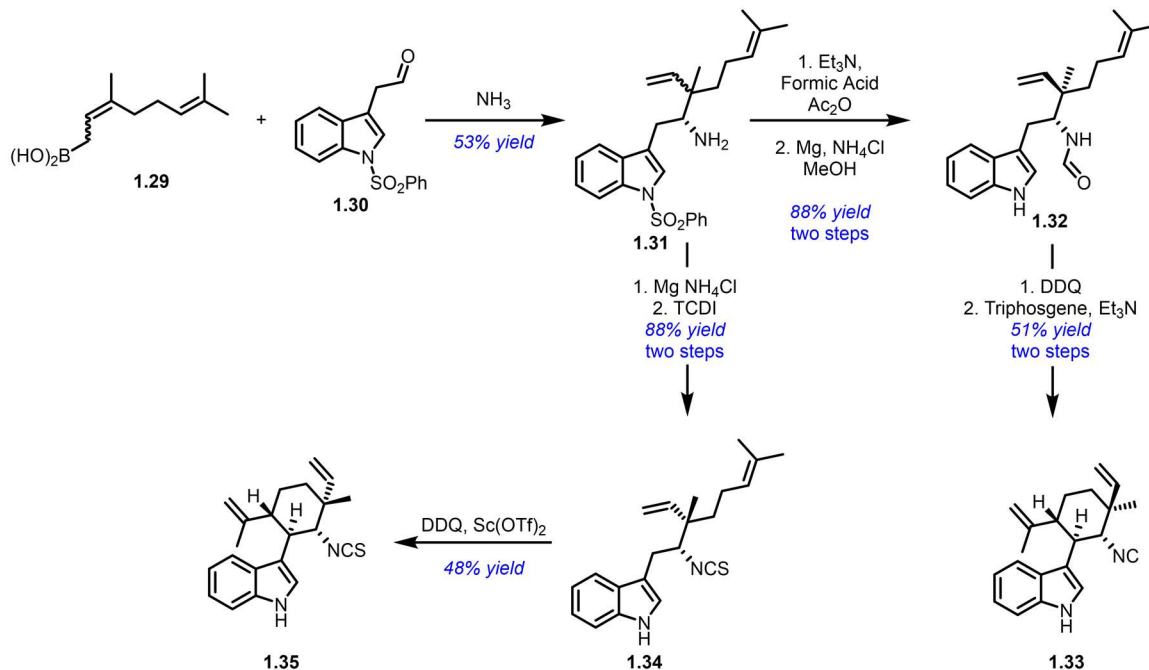


Figure 1.2 The members of the hapalonamide subfamily

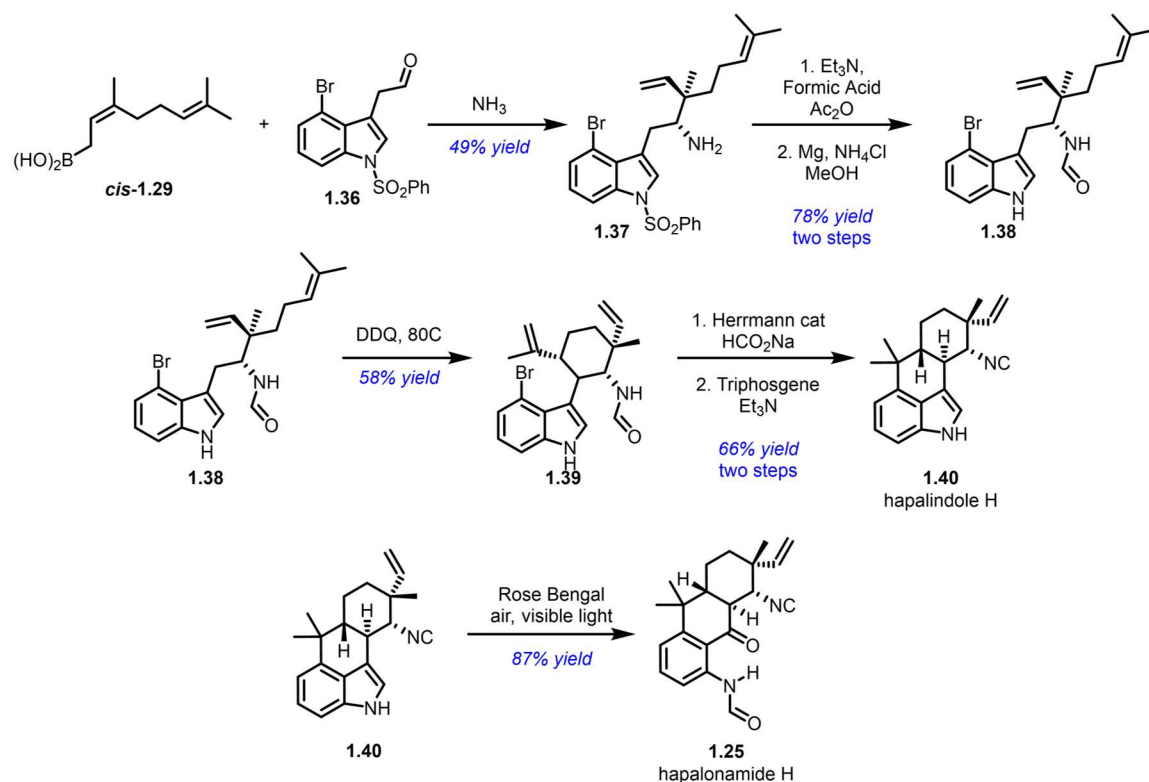


Scheme 1.5 Li's synthesis of hapalindole Q and 12-*epi*-hapalindole Q isonitrile

That year, Li and coworkers reported a broadly successful route to multiple tri- and tetracyclic hapalindoles, as well as members of the fischerindole subfamily.⁹ Their route takes advantage of an DDQ-promoted oxidative cyclization to form the D ring in a single step. The strategy begins with the coupling of indole aldehyde **1.30** with *cis*- or *trans*-geranyl boronate **1.29** in the presence of ammonia. The resulting amine **1.31** is then converted to an isothiocyanate using TCDI (1,1'-thiocarbonyldiimidazole), giving **1.32**, or to formamide **1.34** with formic acetic anhydride. Oxidative cyclization occurs in the presence of DDQ to give the tricyclic natural products hapalindole Q and 12-*epi*-hapalindole Q isonitrile, respectively, as racemic mixtures (Scheme 1.5). In order to access the tetracyclic hapalindole skeleton, the same process is performed using an indole that has been pre-decorated with a bromine at the C-4 position (Scheme 1.6). After the oxidative cyclization to give the tricyclic structure is completed, reductive Heck annulation is

⁹ Lu, Z.; Yang, M.; Chen, P.; Xiong, X.; Li, A. *Angew. Chem. Int. Ed.* **2014**, *53* (50), 13840–13844

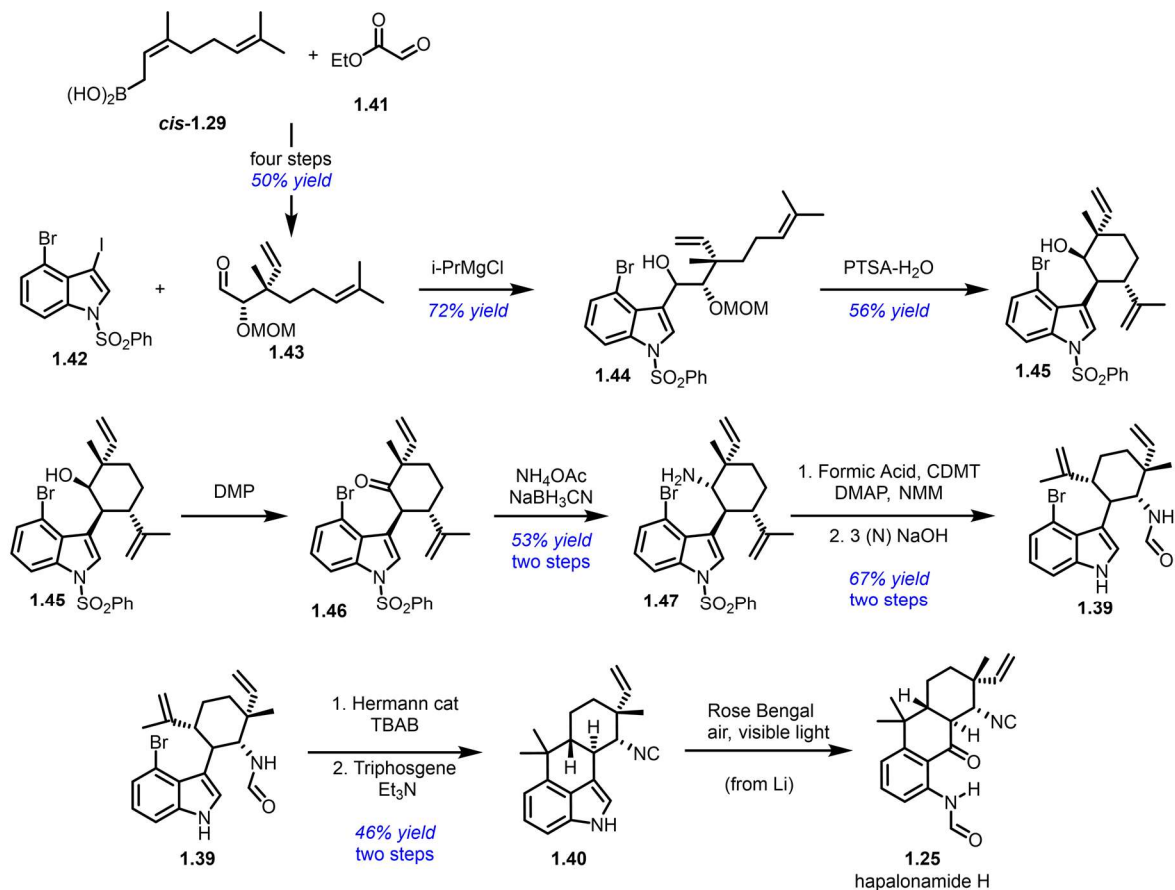
performed using Herrmann's catalyst to give the tetracyclic hapalindole H. From here, Li showed that careful oxidation of hapalindole H using rose bengal and air under visible light would lead in high yield to racemate hapalonamide H.



Scheme 1.6 Li's synthesis of hapalonamide H

A similar strategy was exploited in 2018 by Maji and coworkers, who used *cis*-geranyl boronate, ethyl glyoxylate, and tosyl indole to assemble intermediate **1.44**.¹⁰ Subjecting the benzylic alcohol to strong acid was enough to prompt the cyclization, giving the tricyclic hapalindole skeleton **1.45** as a single diastereomer. Late stage conversion of the alcohol to isonitrile or isothiocyanate produced hapalindoles C, D, and Q, as well as 12-*epi*-hapalindole Q isonitrile. Again, it was necessary to begin with the pre-decorated 4-bromo indole in order to access the tetracyclic skeleton. Hapalindole H was assembled from the same intermediate **XX** by

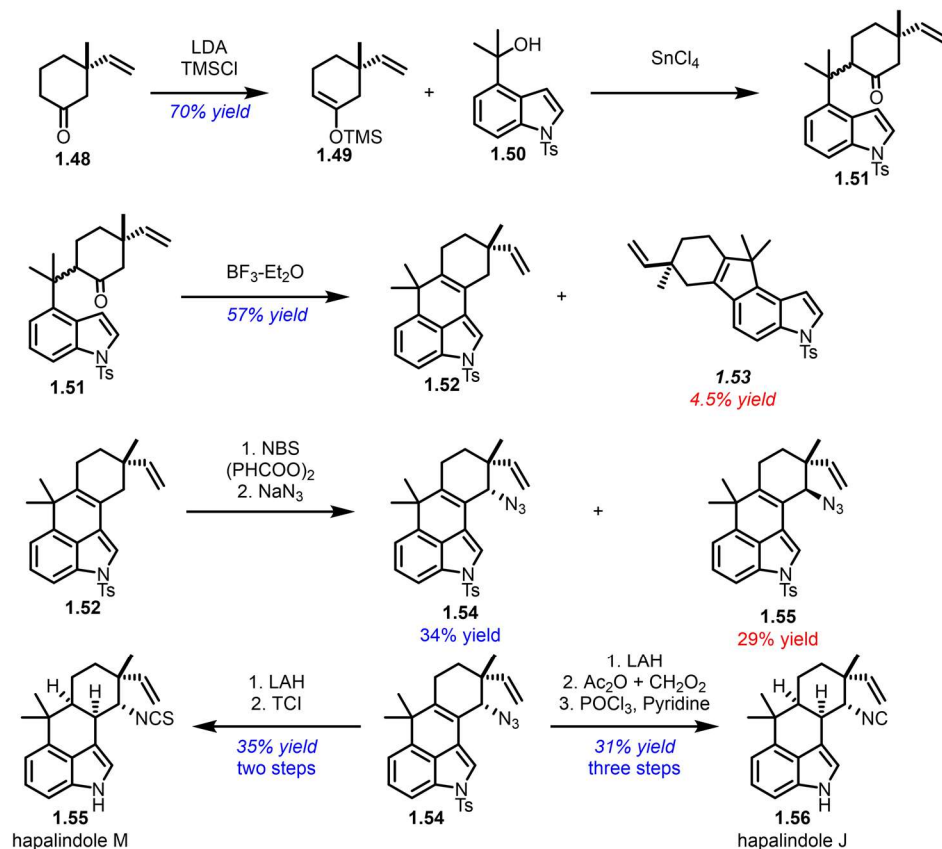
¹⁰ Sahu, S.; Das, B.; Maji, M. S. *Org. Lett.* **2018**, *20* (20), 6485–6489



Scheme 1.7 Maji's synthesis of hapalindole H and formal synthesis of hapalondamide H

reductive Heck annulation and dehydration. Maji did not perform the final oxidative cleavage step required to produce hapalondamide H, so this represented a formal synthesis of the racemic natural product.

In that vein, a number of other syntheses of hapalindoles could be viewed as formal syntheses of natural and non-natural hapalondamides. A full dissection of these syntheses is outside the scope of this thesis, but interested readers can find a more in-depth discussion in Bhat and Rawal's 2014



Scheme 1.8 Natsume's seminal syntheses of hapalindole J and M

alkaloids chapter.² However, a brief discussion of Natsume and coworker's seminal syntheses of hapalindoles J, M, U, and H is necessary. In June 1990, just 3 years after their initial isolation, Natsume published a series of three papers demonstrating the total synthesis of these four natural products.¹¹ The route relied on the coupling of the D ring with the indole through the use of a series of Friedel-Crafts reactions. However, unlike in the biosynthetic pathway, wherein the exocyclic isopropylene unit is protonated to instigate the Friedel-Crafts, Natsume used a tertiary benzylic

¹¹ (a) Muratake, H.; Natsume, M. *Tetrahedron* **1990**, *46* (18), 6331–6342. (b) Muratake, H.; Natsume, M. *Tetrahedron* **1990**, *46* (18), 6343–6350. (c) Muratake, H.; Kumagami, H.; Natsume, M. *Tetrahedron* **1990**, *46* (18), 6351–6360

alcohol at the C-4 position of the indole as the source of the electrophilic partner and a silyl enol ether as the nucleophilic partner. Adding in a stoichiometric amount of Lewis acid promoted the Friedel-Crafts coupling, giving the ketone **1.51** as an isolable product. Subsequent addition of BF₃-Et₂O prompted a second Friedel-Crafts reaction, giving the tetracyclic hapalindole skeleton **1.52**. Finishing the synthesis of the natural products from here involved simple oxidation and reduction steps along with functional group interconversions.

1.1D Previous Synthetic Approaches Towards Welwitindolinone A

The welwitindolinone subfamily is divided into four groups distinguished by oxidation state on the upper ring: welwitindolinone A, B, C, and D. Welwitindolinone A (**1.22**) and D (**1.59**) are both unique, while there exist multiple natural products under the welwitindolinone B and C headings, distinguished by various small structural differences (See Figure 1.3) Due to the unique structures and rare biological properties of the welwitindolinones, there has been significant synthetic interest in the welwitindolinones since they were first discovered in 1994. The Rawal,¹² Garg,¹³ Wood,¹⁴ and Baran¹⁵ labs have all contributed to tackling the syntheses of these difficult

¹² (a) Reyes, J. R.; Xu, J.; Kobayashi, K.; Bhat, V.; Rawal, V. H. *Angew. Chem. Int. Ed.* **2017**, *56* (33), 9962–9966. (b) Allan, K. M.; Kobayashi, K.; Rawal, V. H. *J. Am. Chem. Soc.* **2012**, *134* (3), 1392–1395. (c) Bhat, V.; Allan, K. M.; Rawal, V. H. *J. Am. Chem. Soc.* **2011**, *133* (15), 5798–5801.

¹³ (a) Weires, N. A.; Styduhar, E. D.; Baker, E. L.; Garg, N. K. *J. Am. Chem. Soc.* **2014**, *136* (42), 14710–14713. (b) Styduhar, E. D.; Hutters, A. D.; Weires, N. A.; Garg, N. K. *Angew. Chem. Int. Ed.* **2013**, *52* (47), 12422–12425. (c) Hutters, A. D.; Styduhar, E. D.; Garg, N. K. *Angew. Chem. Int. Ed.* **2012**, *51* (16), 3758–3765. (d) Quasdorf, K. W.; Hutters, A. D.; Lodewyk, M. W.; Tantillo, D. J.; Garg, N. K. *J. Am. Chem. Soc.* **2012**, *134* (3), 1396–1399.

¹⁴ (a) Reisman, S. E.; Ready, J. M.; Weiss, M. M.; Hasuoka, A.; Hirata, M.; Tamaki, K.; Ovaska, T. V.; Smith, C. J.; Wood, J. L. *J. Am. Chem. Soc.* **2008**, *130* (6), 2087–2100. (b) Reisman, S. E.; Ready, J. M.; Hasuoka, A.; Smith, C. J.; Wood, J. L. *J. Am. Chem. Soc.* **2006**, *128* (5), 1448–1449.

¹⁵ (a) Baran, P. S.; Richter, J. M. *J. Am. Chem. Soc.* **2005**, *127* (44), 15394–15396. (b) Baran, P. S.; Maimone, T. J.; Richter, J. M. *Nature* **2007**, *446* (7134), 404–408

compounds, and each welwitindolinone type has succumbed to total synthesis. The syntheses of welwitindolinones B, C, and D have been recently summarized, and interested readers are directed to Rawal's alkaloid chapter.² This section will focus on the synthetic efforts towards welwitindolinone A.

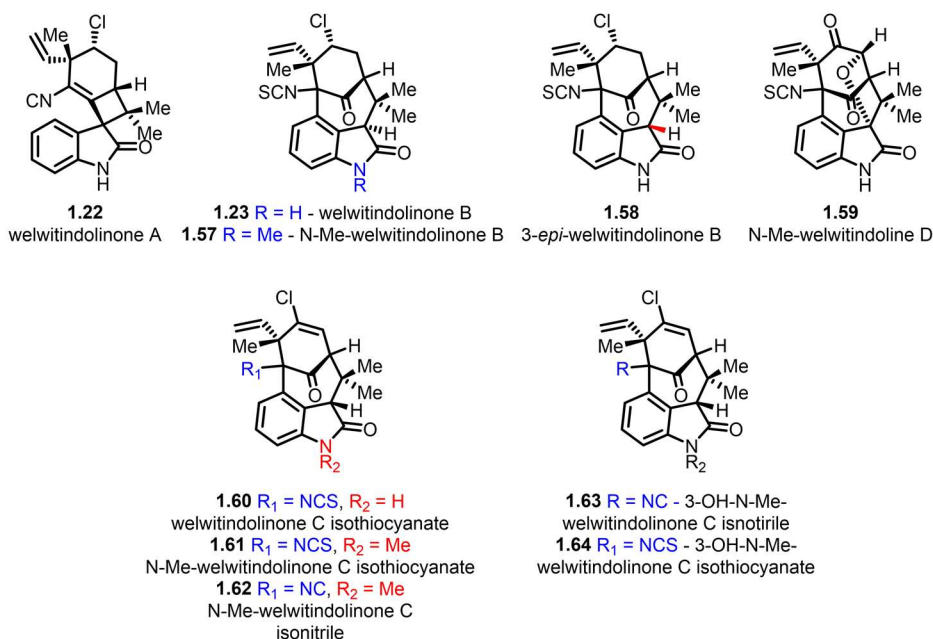
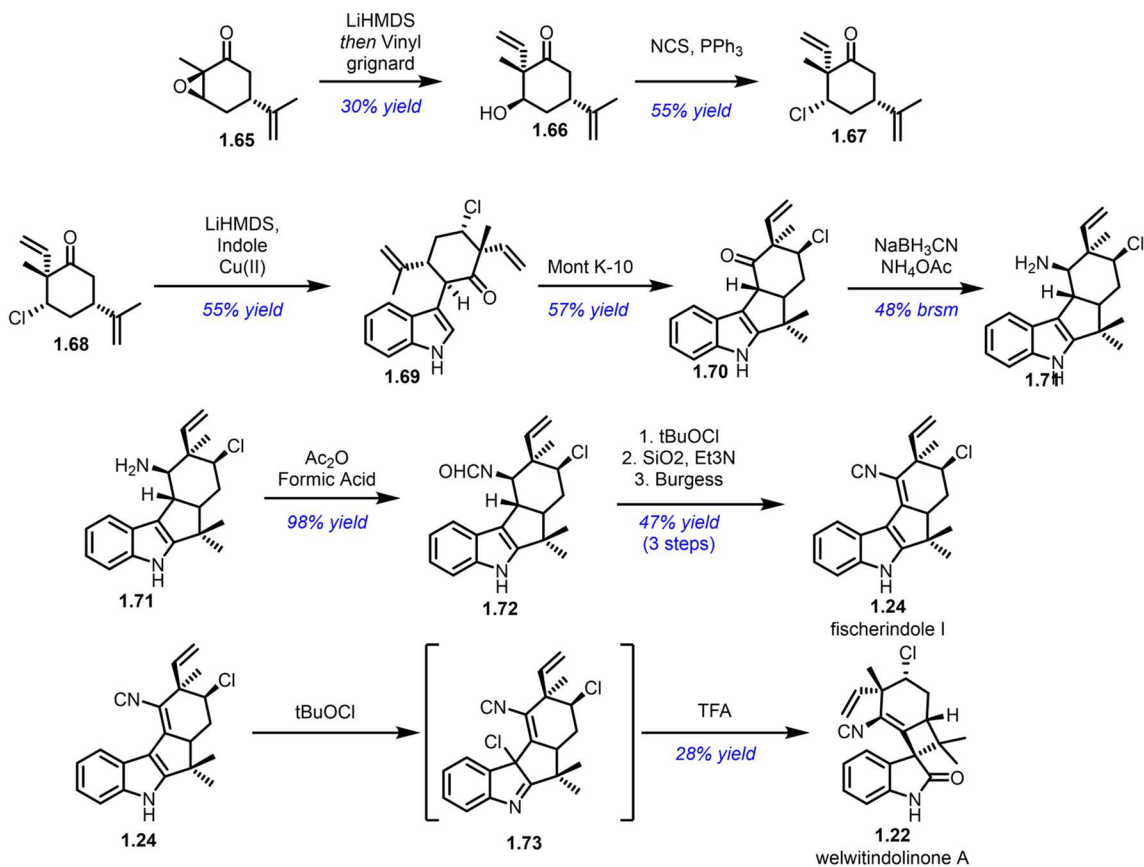


Figure 1.3 The members of the welwitindolinone subfamily

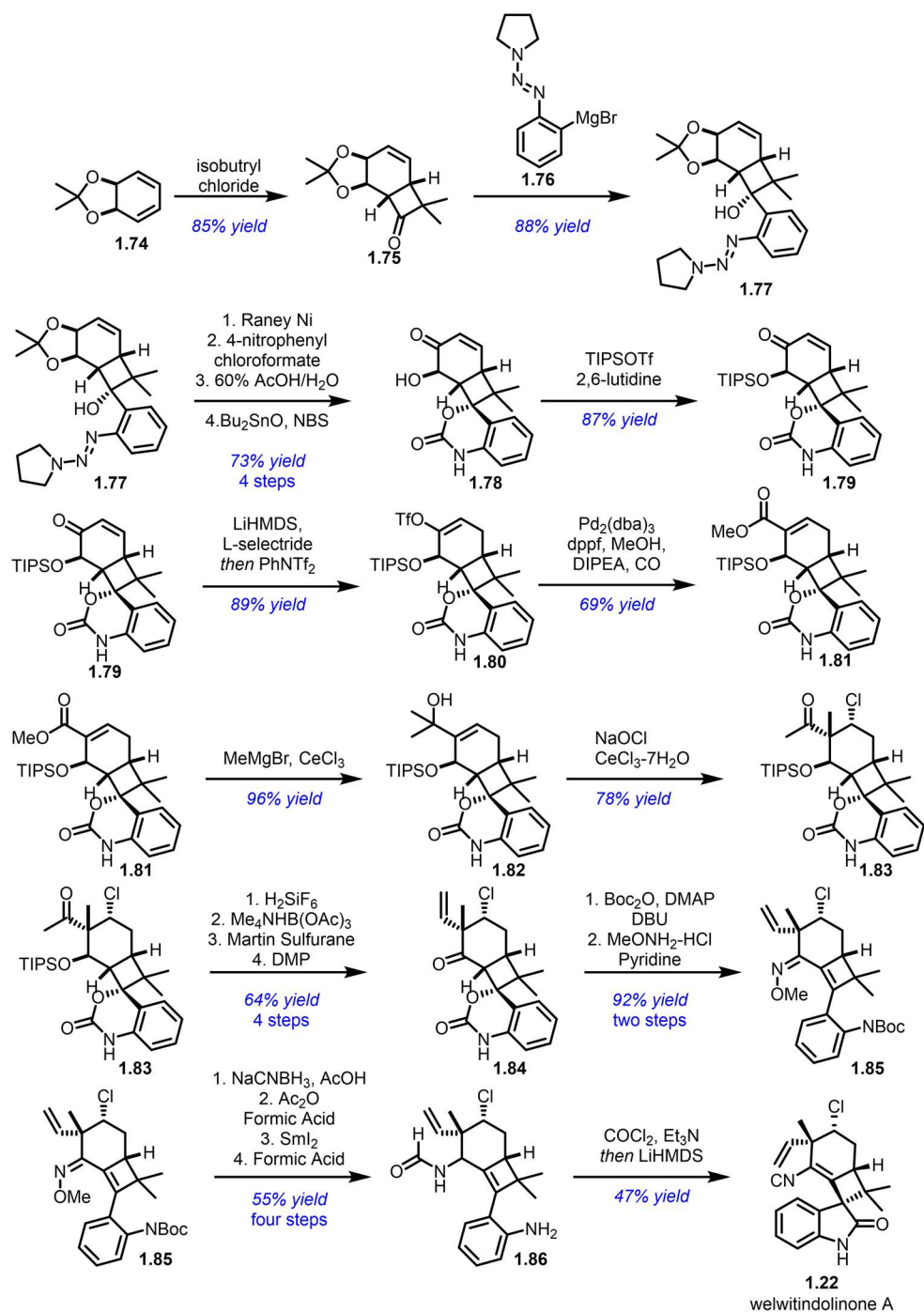
Welwitindolinone A, which was isolated from *Hapalosiphon welwitschia* along with welwitindolinones B and C, is the only member of the family to have a four-membered C ring, located at a spirocyclic quaternary center at the C-3 position of the indolinone ring. As previously discussed, the compound is hypothesized to be the biosynthetic precursor to the other members of the subfamily and was the first to succumb to total synthesis. In 2005, Baran published an impressive total synthesis of (-)-fischerindole I and (+)-welwitindolinone A that followed Baran's proposed biosynthetic oxidative rearrangement (*vide supra*).¹⁵ The route began with *R*-carvone as a chiral pool molecule. In two steps carvone oxide was converted to cyclohexanone **1.67**, which



Scheme 1.9 Baran's protecting-group-free syntheses of fischerindole I and welwitindolinone A

possesses all of the functionality of the final compounds except for the isonitrile unit. Oxidative coupling with free indole gives the tricyclic hapalindole structure, and a simple Lewis acid-mediated Friedel-Crafts reaction gives the fischerindole skeleton **1.70**. From here, simple functional group and oxidation state transformations serve to give the natural product (-)-fischerindole I (**1.24**) as a single enantiomer. Treatment of this compound with tert-butyl hypochlorite gives the chlorinated compound **1.73**, which upon treatment with acid undergoes a ring contraction to give (+)-welwitindolinone A. Two years later Baran disclosed an updated procedure that used XeF₂ to prompt the same reaction without the need for acid.

Just three months after Baran's initial publication, the Wood lab published a racemic total synthesis of welwitindolinone A.¹⁵⁴ Unlike Baran, who decided to create the central cyclobutyl ring last, Wood and coworkers decided to construct this ring first and build the molecule outwards from the core. The synthesis begins with the symmetric acetal **XX**, which undergoes a highly regioselective [2+2] cycloaddition with dimethyl ketene to form the cyclobutyl ring. Grignard addition of a triazene-protected aniline into the new ketone added the majority of the remaining atoms that would make up the indole rings. Reductive triflation of the enone followed by palladium catalyzed carbonylation gave ester **XX**. The ester was converted into the tertiary alcohol **XX**, and a clever chloronium-mediated rearrangement installed the C-12 quaternary center and the C-15 chloride in remarkably high yield and diastereoselectivity. Simple chemical modifications then gave the ketone **XX**. In the end game of the synthesis, the ketone underwent reductive amination and amide formation alongside Boc deprotection to give formamide **XX**. Dehydration with phosgene transformed the formamide to an isonitrile and at the same time converted the aniline to an isocyanate. Treatment with a strong base was enough to initiate the cyclization of the cyclobutyl ring onto the isocyanate, closing up the indolinone ring and completing the total synthesis of racemic welwitindolinone A.

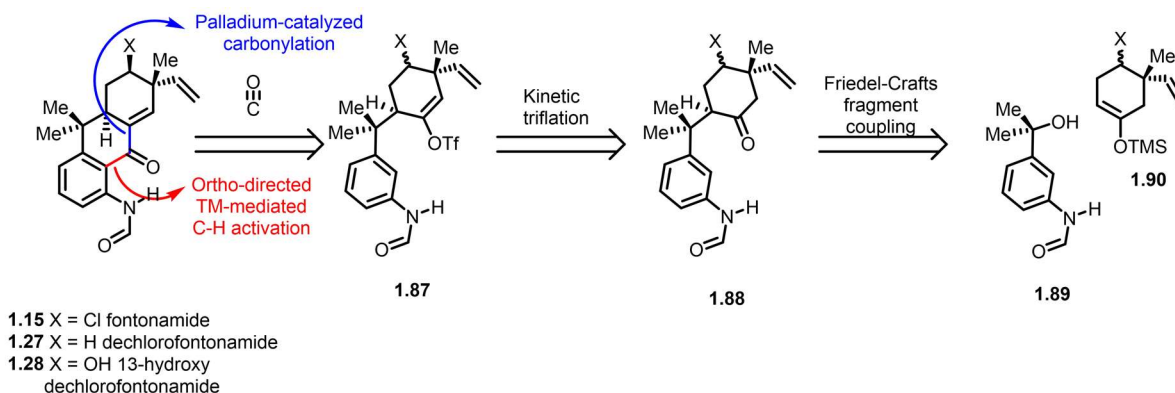


Scheme 1.10 Wood's synthesis of welwitindolinone A

1.2 Retrosynthetic Analysis of the Fontonamides

1.2A Strategy Design

The fontonamides, namely fontonamide (**1.15**), dechlorofontonamide (**1.27**), and 13-hydroxy dechlorofontonamide (**1.28**), are three members of the hapalonamide subfamily defined by the lack of an isonitrile or isothiocyanate unit at the C-11 position. Instead, this unit has been eliminated, giving an alpha-beta unsaturated ketone. In designing a route to these natural products, we wanted to take advantage of their two unique structural characteristics—the presence of a double bond on the D ring, and the formamide moiety on the A ring. Anilides are known to be strong directing groups for transition metal-mediated C-H activations.¹⁶ We therefore envisioned that the bond between the carbonyl at C-9 and the phenyl ring would be formed by one such directed C-H activation using palladium. We also looked at cutting the bond on the other side of the carbonyl, connecting the ketone to the D ring. We envisioned forming this bond by the carbonylation of an enol triflate like **1.87**, again catalyzed by palladium or some other transition metal. This enol triflate should be readily formed from the ketone **1.88** through kinetic triflation. The ketone, in turn, could be readily prepared through a variation of Natsume's Friedel-Crafts reaction, using an



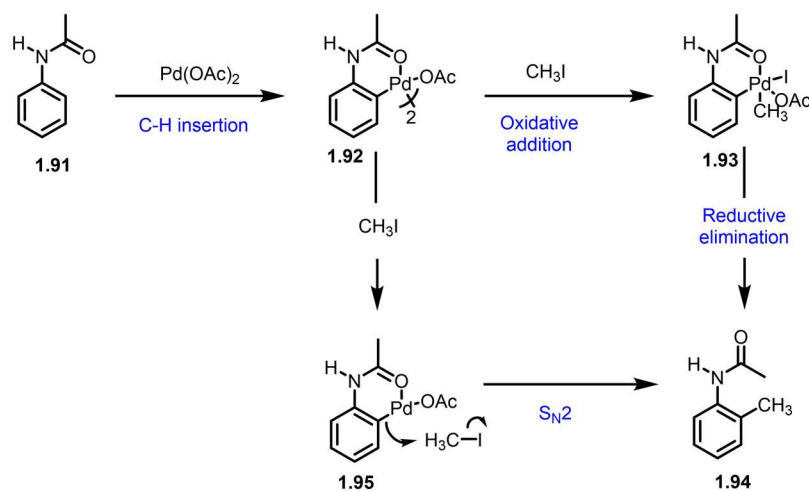
Scheme 1.11. Retrosynthetic analysis of the fontonamides

¹⁶ Tomberg, A.; Muratore, M. É.; Johansson, M. J.; Terstiege, I.; Sköld, C.; Norrby, P.-O. *iScience* **2019**, *20*, 373–391.

anilide version of the benzylic alcohol rather than the indole version employed by Natsume.¹² This route would allow us to couple the two halves of the molecule with all of the functionality already in place on both the upper and lower rings, giving a truly convergent synthesis.

1.2B The Use of Anilides as Directing Groups for C-H Activation

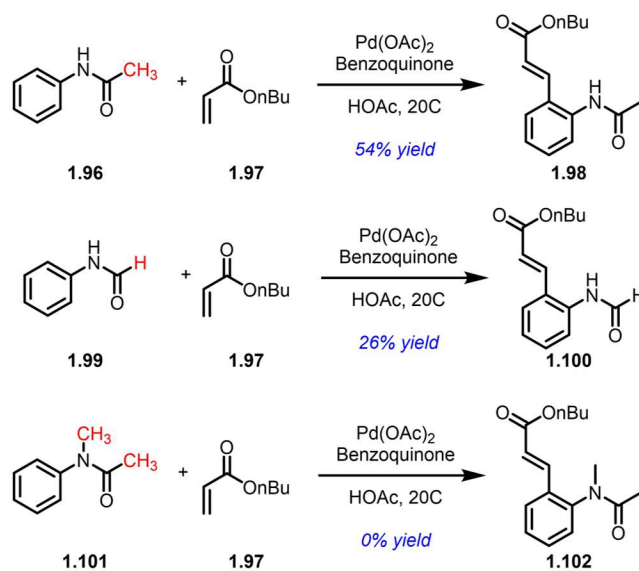
As C-H activation has seen a surge in popularity over the recent decades, the number of directing groups that have been investigated has also grown. Alcohols, amines, carboxylic acids, heterocycles, and their derivatives have all seen successful use as highly selective directing groups. Additionally, transient and *in situ* generated directing groups such as imines and oximes have shown to have strong directing powers.¹⁷ One powerful group that has been given increasing attention in recent years is the amide group. Interestingly, amides, or more specifically anilides, are able to direct to phenyl rings on both the C- and N- sides where applicable, although directing onto an ortho position on the N-side is strongly preferred.¹⁶



Scheme 1.12. Tremont's proposed mechanisms for the ortho alkylation of acetanilide

¹⁷ Chen, Z.; Wang, B.; Zhang, J.; Yu, W.; Liu, Z.; Zhang, Y. *Org. Chem. Front.* **2015**, 2 (9), 1107–1295

Anilides were first used as ortho directing groups in 1984, when Tremont and coworkers used stoichiometric palladium acetate and methyl iodide to methylate anilides selectively at the ortho position.¹⁸ The reaction was tolerant of electron-donating and electron-withdrawing functional groups, and demonstrated, where applicable, high regioselectivity for the less hindered C-H bond. The first catalytic reaction employing an anilide as an ortho directing group was accomplished in 2002 by van Leeuwen and coworkers.¹⁹⁵ Van Leeuwen accomplished the highly selective ortho olefination of a wide variety of acetanilides using palladium acetate and benzoquinone as an oxidant. Interestingly, the reaction worked reasonably well with formanilide, but it failed to give any product with N-methyl acetanilide. Since then, palladium catalysis has been utilized to perform

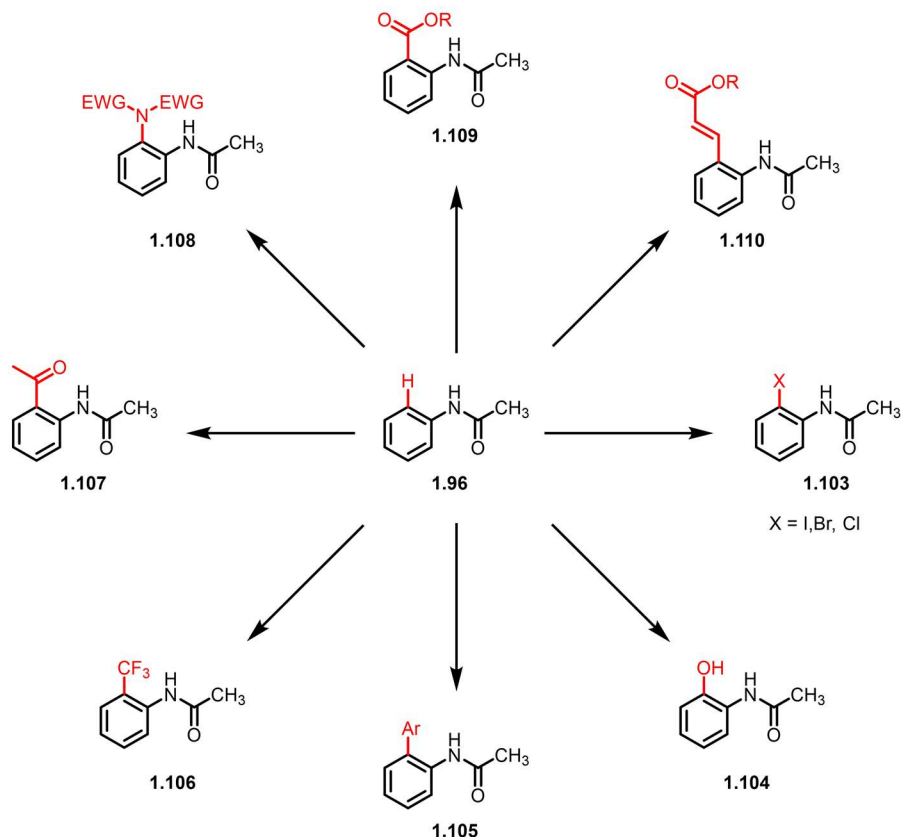


Scheme 1.13 A selective substrate scope for van Leeuwen's catalytic ortho olefination of anilides

¹⁸ Tremont, S. J.; Rahman, H. U. *J. Am. Chem. Soc.* **1984**, *106* (19), 5759–5760

¹⁹ Boele, M. D. K.; van Strijdonck, G. P. F.; de Vries, A. H. M.; Kamer, P. C. J.; de Vries, J. G.; van Leeuwen, P. W. N. M. *J. Am. Chem. Soc.* **2002**, *124* (8), 1586–1587

a myriad of ortho-directed C-H activations on anilides, including ortho-acylation,²⁰ carboxylation,²¹ arylation,²² amination and amidation,²³ halogenation,²⁴ hydroxylation,²⁵ and



Scheme 1.14 Transformations possible via transition metal-mediated ortho C-H activation of anilides

²⁰ (a) Wu, Y.; Li, B.; Mao, F.; Li, X.; Kwong, F. Y. *Org. Lett.* **2011**, *13* (12), 3258–3261. (b) Li, C.; Wang, L.; Li, P.; Zhou, W. *Chem. – Eur. J.* **2011**, *17* (37), 10208–10212. (c) Chan, C.-W.; Zhou, Z.; Yu, W.-Y. *Adv. Synth. Catal.* **2011**, *353* (16), 2999–3006

²¹ (a) Giri, R.; Lam, J. K.; Yu, J.-Q. *J. Am. Chem. Soc.* **2010**, *132* (2), 686–693. (b) Wang, S.; Yang, Z.; Liu, J.; Xie, K.; Wang, A.; Chen, X.; Tan, Z. *Chem. Commun.* **2012**, *48* (79), 9924–9926

²² (a) Shabashov, D.; Daugulis, O. *J. Org. Chem.* **2007**, *72* (20), 7720–7725. (b) Brasche, G.; García-Fortanet, Jorge; Buchwald, S. L. *Org. Lett.* **2008**, *10* (11), 2207–2210.

²³ (a) Ng, K.-H.; Chan, A. S. C.; Yu, W.-Y. *J. Am. Chem. Soc.* **2010**, *132* (37), 12862–12864. (b) Sun, K.; Li, Y.; Xiong, T.; Zhang, J.; Zhang, Q. *J. Am. Chem. Soc.* **2011**, *133* (6), 1694–1697

²⁴ (a) Wan, X.; Ma, Z.; Li, B.; Zhang, K.; Cao, S.; Zhang, S.; Shi, Z. *J. Am. Chem. Soc.* **2006**, *128* (23), 7416–7417. (b) Wang, X.-C.; Hu, Y.; Bonacorsi, S.; Hong, Y.; Burrell, R.; Yu, J.-Q. *J. Am. Chem. Soc.* **2013**, *135* (28), 10326–10329.

²⁵ Jiang, T.-S.; Wang, G.-W. *J. Org. Chem.* **2012**, *77* (21), 9504–9509.

trifluoromethylation.²⁶ Anilides have also seen use as directing groups in combination with other transition metals, including copper, rhodium, ruthenium, iridium, and cobalt. For a full overview on the use of anilide and other nitrogen-based directing groups, readers are directed to Zhang's recent comprehensive review.¹⁸ Although anilides have been found to be weaker directing groups than pyridines, oximes, and imines, they are stronger than esters and sulfates, as well as some other more exotic directing groups.¹⁶ Formanilides have been shown to be less efficient directing group than acetanilides or benzanilides, as evidenced by the lower yield van Leeuwen saw with formanilides. However, we expected that the intramolecular nature of our proposed cyclization, along with the Thorpe-Ingold effect arising from the benzylic quaternary center, would overcome this potential difficulty. Importantly, no intramolecular C-H activations have been reported with anilides, which increased the interest in exploring this approach.

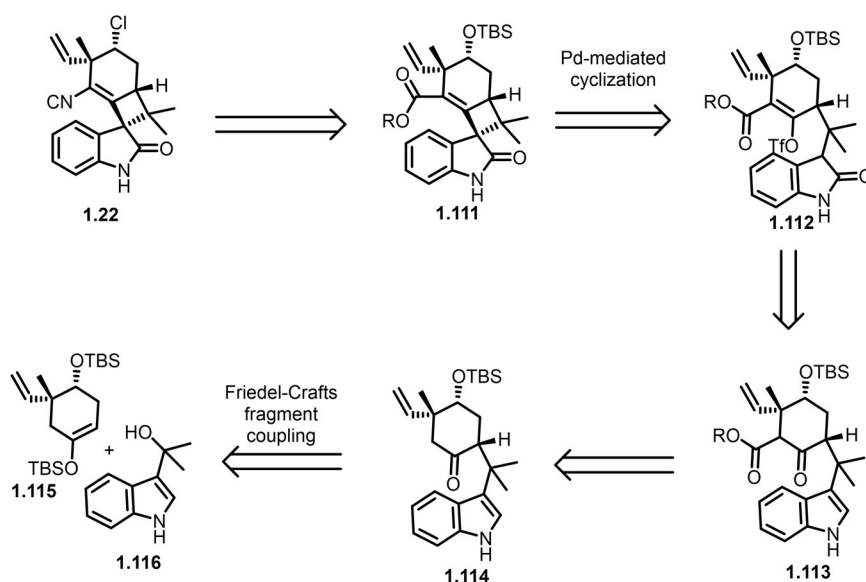
1.3 Retrosynthetic Analysis of Welwitindolinone A

1.3A Strategy Design

In addition to the fontonamides, the synthesis of welwitindolinone A was also investigated in the course of the dissertation research. Welwitindolinone A is the only member of the welwitindolinone subfamily and, indeed, of the whole hapalindole family, which includes a four-membered C ring. While all members of the family include the quaternary center substitution at the C-3 position, welwitindolinone A is the only one to have the second substitution also at C-3. This connection means that the D-ring is directly attached to a potentially nucleophilic carbon. Welwitindolinone A's unique connectivity will become the basis for our approach to its synthesis. Tracing the natural product back through some functional group transformations, we arrive at

²⁶ Zhang, L.-S.; Chen, K.; Chen, G.; Li, B.-J.; Luo, S.; Guo, Q.-Y.; Wei, J.-B.; Shi, Z.-J. *Org. Lett.* **2013**, *15* (1), 10–13

tetracycle **1.111**. This compound is set up perfectly to be formed through a palladium-catalyzed alkenylation reaction, coupling an enol triflate like **1.112** on the D ring with the enolate of the indolinone. This enol triflate would arise from ketone **1.113**, which would be accessible through a similar route as that employed in Rawal's synthesis of welwitindolinones B and C, coupling a silyl enol ether like **1.115** and a tertiary benzylic alcohol such as **1.116** through a Friedel-Crafts reaction.¹³

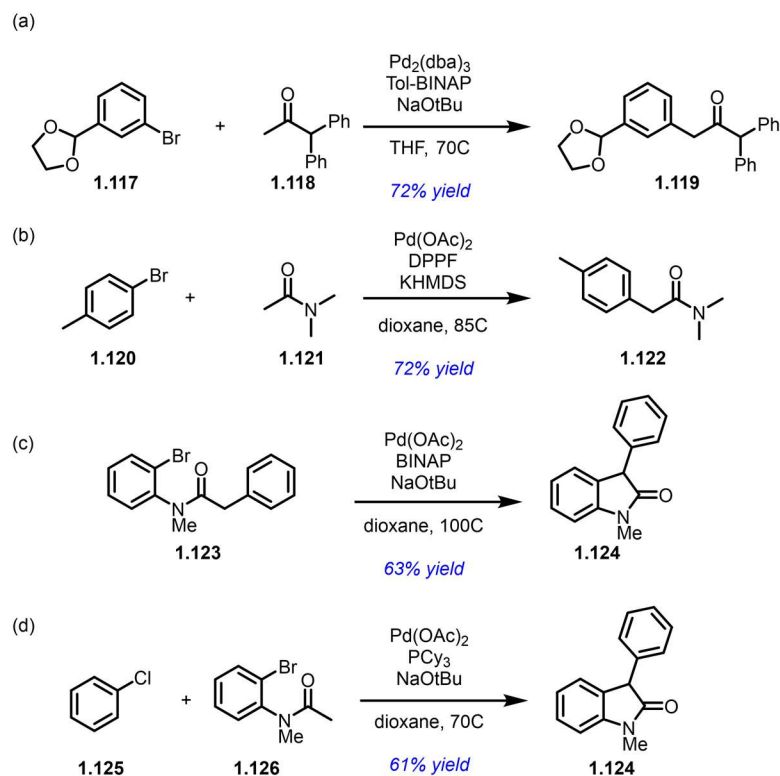


Scheme 1.15. Retrosynthetic analysis of welwitindolinone A

1.3B Transition Metal-Catalyzed Alkenylation and Arylation of indolinones

3-Substituted and 3,3-disubstituted indolinones are a common structural motif in natural products, being seen in over 1000 natural products isolated to date.²⁷ While a smaller number of compounds contain an aryl- or alkenyl- substituent at this position, the number is not insignificant. This motif has in turn inspired a number of reactions meant to create such compounds. One such

²⁷ As determined by a structure search on Reaxys July 6th 2023.



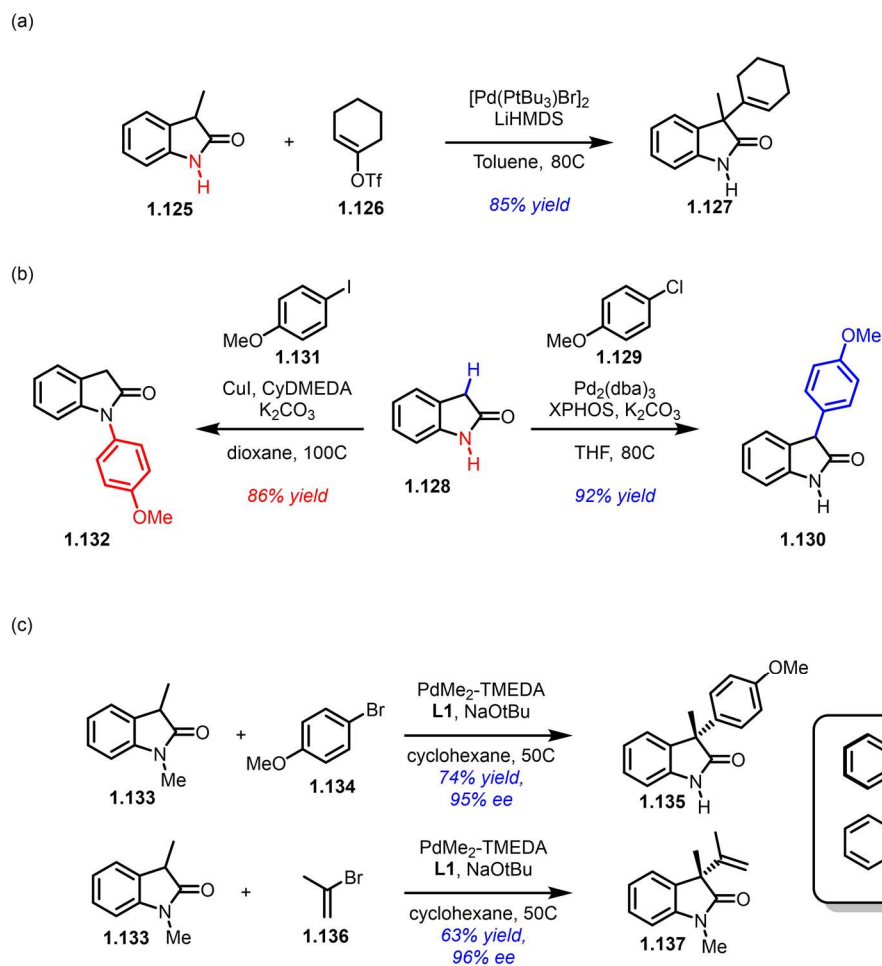
Scheme 1.16. (a) Buchwald's initial report on arylation of ketone enolate. (b) Hartwig extends the reaction to secondary amides. (c) Intramolecular arylation of secondary amides. (d) Sequential intra-molecular and intermolecular diarylation of N-methyl acetanilide

reaction, which takes advantage of the ease with which indolinones are deprotonated, is the transition metal-catalyzed alkenylation and arylation of these enolates.

The palladium catalyzed arylation of enolates was first reported in 1997 by Buchwald and coworkers, who used $\text{Pd}_2(\text{dba})_2$ with a BINAP ligand and sodium tert-butoxide as a strong base with which to couple aryl bromides and ketones in good yield (Scheme 1.16a).²⁸ In 1998, Hartwig and coworkers extended this reaction to secondary amides by using a stronger base, with KHMDS giving the best yields (Scheme 1.16b).²⁹ Hartwig also showed that such reactions could be run

²⁸ Palucki, M.; Buchwald, S. L. *J. Am. Chem. Soc.* **1997**, *119* (45), 11108–11109

²⁹ Shaughnessy, K. H.; Hamann, B. C.; Hartwig, J. F. *J. Org. Chem.* **1998**, *63* (19), 6546–6553



Scheme 1.17. (a) Huang demonstrates that free N-H indolinones can be selectively alkenylated at the C-3 position. (b) Buchwald shows that free N-H indoles can be orthogonally arylated at the C-3 or N-1 position. (c) Buchwald demonstrates an asymmetric arylation and alkenylation of N-methyl indolinones.

intramolecularly, most interestingly by using the reaction to form 3-substituted and 3,3-disubstituted indolinones from N-(2-bromophenyl)-N-methyl anilides such as **1.123** (Scheme 1.16c). Three years later, Hartwig demonstrated that these indolinones could also act as a substrate for this reaction and combined an intra-molecular arylation with an inter-molecular arylation. In one example, the group reacted N-(2-bromophenyl)-N-methyl acetanilide **1.126** and a wide variety

of aryl chlorides, along with Pd(OAc)₂, PCy₃ as a ligand, and sodium tert-butoxide as a base, to form 3-arylated indolinones such as **1.124** in good yield (Scheme 1.16d).³⁰

At this point, all of these reactions required either a ketone or a secondary amide due to the competing reactivity of a deprotonated primary amide N-H. However, in 2007, Huang and coworkers showcased that 3-methyl indolinone could be used as a coupling partner with a wide variety of vinyl bromide and vinyl triflates, using [Pd(P-tBu₃)Br]₂ as the palladium source and LiHMDS as a strong base (Scheme 1.17a).³¹ Possibly due to the lower pK_a of the hydrogen on the 3-position of an indolinone compared to a normal amide, no reaction at the nitrogen was observed. The following year, 2008, Buchwald confirmed that this was true, demonstrating that while typical primary lactams were arylated at the nitrogen, indolinones could be arylated at the C position with high selectivity using Pd₂(dba)₃, XPhos, and a weak base K₂CO₃.³² In the same paper, Buchwald also showed that N-arylation of indolinones is possible using copper iodide and a diamine catalyst. This selectivity is likely caused by the copper first coordinating with the indole nitrogen, then undergoing an oxidative insertion into the aryl-halide bond (Scheme 1.17b). Finally, in 2009, Buchwald reported an asymmetric arylation of N-methyl indolinones using a “chiral-at-phosphorous” amino-binap derivative.³³ The reaction arylated the indolinones with high yield and good ee and was also successful at effecting the asymmetric vinylation (Scheme 1.17c).

It is important to note that the majority of these reactions have been intermolecular, while our proposed strategy calls for an intramolecular cyclization. The formation of 5-, 6-, and 7- membered

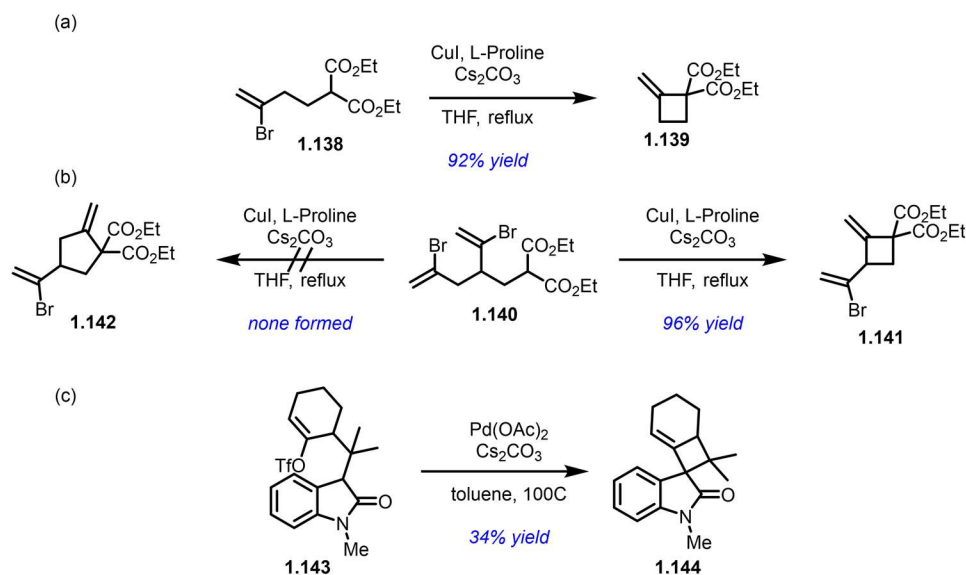
³⁰ Lee, S.; Hartwig, J. F. *J. Org. Chem.* **2001**, *66* (10), 3402–3415

³¹ Huang, J.; Bunel, E.; Faul, M. M. *Org. Lett.* **2007**, *9* (21), 4343–4346

³² Altman, R. A.; Hyde, A. M.; Huang, X.; Buchwald, S. L. *J. Am. Chem. Soc.* **2008**, *130* (29), 9613–9620.

³³ Taylor, A. M.; Altman, R. A.; Buchwald, S. L. *J. Am. Chem. Soc.* **2009**, *131* (29), 9900–9901

rings through such intramolecular reactions is well known, although to date the substrate scope explored does not include indolinones.³⁴ That said, the creation of cyclobutene rings through these types of reactions has been less successful, with, until recently, the only successful example being a 2008 paper from Li and coworkers. The group used copper iodide and a proline catalyst to cyclize diethyl 2-(3-bromobut-3-enyl)malonate (**1.138**), giving the desired cyclobutene **1.139** in good yield (Scheme 1.18a).³⁵ Interestingly, this reaction led preferentially to the cyclobutene (**1.141**) over the cyclopentane (**1.142**) on applicable substrates, indicating the possibility of an atypical mechanism (Scheme 1.18b). The first intramolecular alkenylation of an oxindole was carried out in 2015 by Ferdinand Taenzler, a former member of the Rawal group, who used an N-methyl oxindole to evaluate the feasibility of the key step in the synthesis of welwitindolinone A.³⁶ The Thorpe-Ingold effect of the gem-dimethyl group was believed to be assisting the otherwise difficult



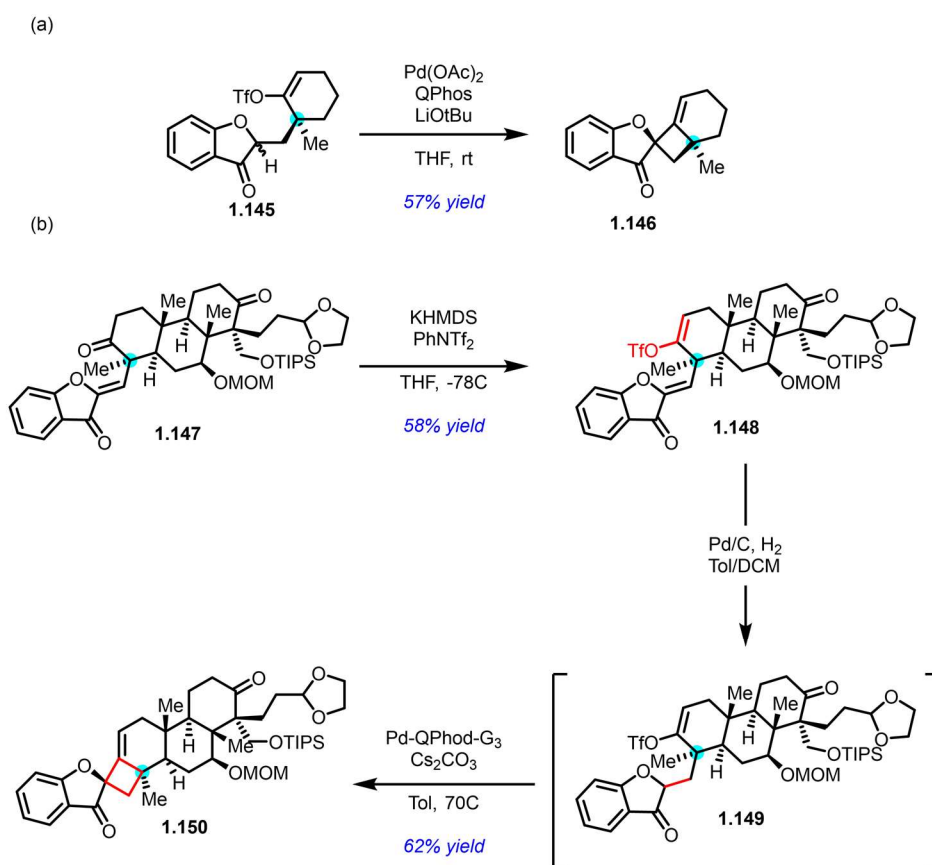
Scheme 1.18. (a) The first example of cyclobutene-forming intramolecular vinylation of an enolate. (b) The reaction selects for the four-membered ring rather than the five-membered ring. (c) The first intramolecular alkenylation of an oxindole by Taenzler and Rawal

³⁴ Ankner, T.; Cosner, C. C.; Helquist, P. *Chem. – Eur. J.* **2013**, *19* (6), 1858–1871

³⁵ Sun, K.; Li, Y.; Xiong, T.; Zhang, J.; Zhang, Q. *J. Am. Chem. Soc.* **2011**, *133* (6), 1694–1697.

³⁶ Taenzler, F; PhD. *Unpublished work*

cyclization (Scheme 1.18c). More recently, however, the Dong group recently published an elegant synthesis of *phainanoid A* that used Pd(OAc)₂ and QPhos to effect the cyclization of **1.148** to **1.149**, giving the desired compound in a reasonably high 62% yield (Scheme 1.19).³⁷ It is important to note that, while a different enolate the Dong group's molecule also contained a quaternary center on the resulting ring, again indicating that the Thorpe-Ingold effect played some role in driving the reaction to completion. As our proposed intermediate will also contain a quaternary center, so we should be able to take advantage of the Thorpe-Ingold effect as well.



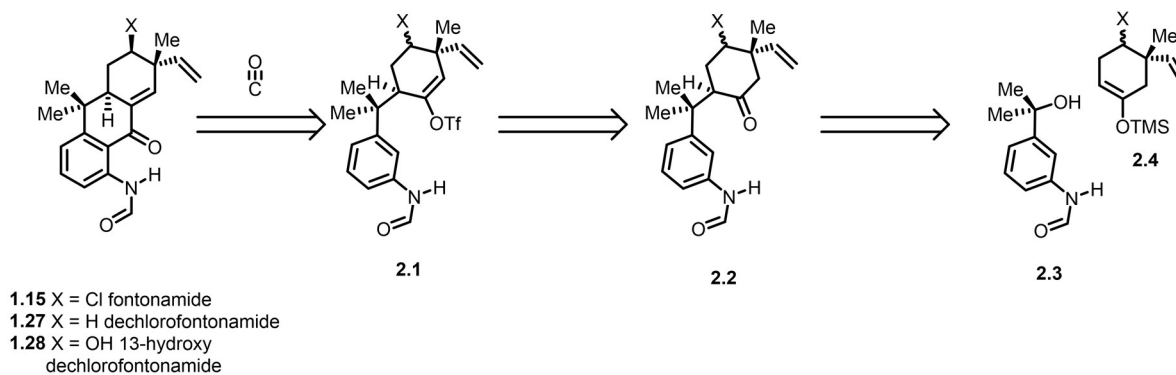
Scheme 1.19. Palladium-mediated alkenylative cyclobutene formation in Dong's synthesis of *phainanoid A*. (a) on a model substrate. (b) on a late stage substrate within the total synthesis

³⁷ (a) Xie, J.; Zheng, Z.; Liu, X.; Zhang, N.; Choi, S.; He, C.; Dong, G. *J. Am. Chem. Soc.* **2023**.
 (b) Xie, J.; Liu, X.; Zhang, N.; Choi, S.; Dong, G. *J. Am. Chem. Soc.* **2021**, *143* (46), 19311–19316, (c) Xie, J.; Wang, J.; Dong, G. *Org. Lett.* **2017**, *19* (11), 3017–3020.

Chapter 2: Total Synthesis of (-)-Dechlorofontonamide

2.1 Studies on the Friedel-Crafts Fragment Coupling

Our proposed route to the fontonamide family of natural products involved the coupling of two fragments, the A and D rings, by way of two key C-C bond forming steps, a Friedel-Crafts-type reaction and a carbonylative C-H activation and cyclization (Scheme 2.1). The proposed Friedel-Crafts reaction would couple a tertiary benzylic alcohol with a silyl enol ether. Such Friedel-Crafts reactions have been used in the synthesis of multiple members of the hapalindole family, including the syntheses of hapalindoles H, J, M, and U by Natsume and the syntheses of welwitindolinones B, C, and D by Rawal (*vide supra*).^{1,2} However, for all of these syntheses, the

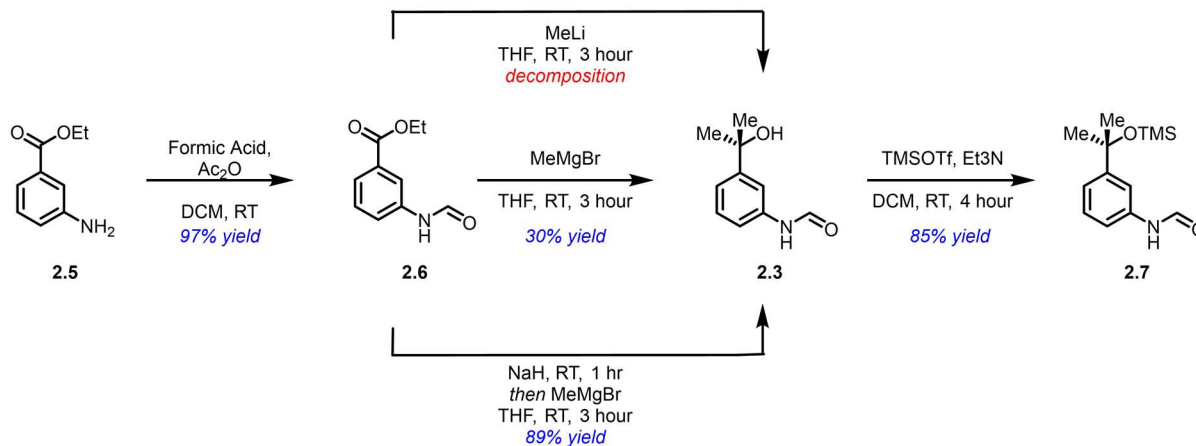


Scheme 2.1. Retrosynthetic analysis of the fontonamides

alcohol utilized was positioned benzylic to an indole unit. For the purposes of the present synthesis,

¹ (a) Muratake, H.; Natsume, M. *Tetrahedron* **1990**, *46* (18), 6331–6342. (b) Muratake, H.; Natsume, M. *Tetrahedron* **1990**, *46* (18), 6343–6350. (c) Muratake, H.; Kumagami, H.; Natsume, M. *Tetrahedron* **1990**, *46* (18), 6351–6360

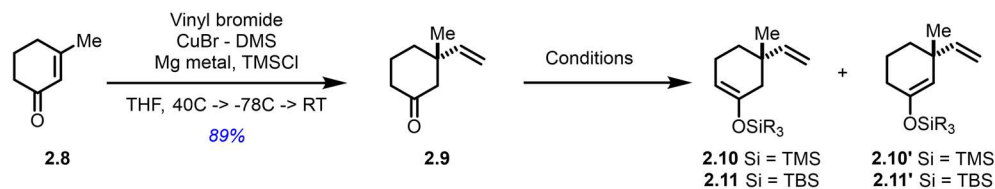
² (a) Bhat, V.; Allan, K. M.; Rawal, V. H. *J. Am. Chem. Soc.* **2011**, *133* (15), 5798–5801. (b) Allan, K. M.; Kobayashi, K.; Rawal, V. H. *J. Am. Chem. Soc.* **2012**, *134* (3), 1392–1395.



Scheme 2.2. First and second generation synthesis of the lower fragment

the tertiary alcohol required would ideally be benzylic to a phenyl ring containing an anilide moiety. However, as this species could function as a Lewis base and would be a considerably less electron rich aryl unit than an indole, there were a number of possible issues that warranted consideration.

Synthesis of the lower fragment began with installation of the formyl unit onto ethyl 3-aminobenzoate, which was accomplished using a mixed anhydride generated in situ from formic acid and acetic anhydride. Formanilide **2.6** was then reacted with methyl Grignard to generate the necessary tertiary alcohol. However, alcohol **2.3** was formed in low yield, giving ~30% conversion even when further equivalents of Grignard were added. As the reaction progressed, it would quickly turn turbid, and soon after, non-crystalline solids would rapidly crash out of solution. This led us to suspect that the di-anionic intermediate was poorly soluble, perhaps exacerbated by the di-cationic magnesium counterion. Switching to methyl lithium led to decomposition of the starting material as methyl was added to the formanilide, and boc-protection of the formanilide to remove the troublesome proton led to de-formylation upon addition of methyl Grignard. However,



Base	Silyl Triflate	Yield	Ratio D:U ^a
LDA	TMSCl	96%	2.5:1
Et ₃ N	TMSOTf	93%	18:1
Et ₃ N	TBSOTf	97%	22:1
DIPEA	TMSOTf	95%	>25:1
DIPEA	TBSOTf	92%	>25:1

^a desired(**2.10** or **2.11**) to undesired (**2.10'** or **2.11'**)

Scheme 2.3. First generation synthesis of the upper fragment

we were able to avoid the insolubility through prior deprotonation of the anilide with sodium hydride. Addition of a single equivalent of sodium hydride proved sufficient, leading to formation of the desired alcohol **2.3** in 89% yield.

Thankfully, the synthesis of the upper fragment proved more straightforward. Vinyl Grignard was produced from bromoethylene, and its cuprate was made *in situ* by exposure to copper iodide-dimethyl sulfide complex. The cuprate was then added to 3-methyl-2-cyclohexeneone (**2.8**), with the resulting enolate trapped *in situ* with TMSCl to avoid further reaction and then hydrolyzed upon workup to give the desired ketone **2.9**. While classical kinetic enolate formation gave the desired silyl enol ether **2.10** as a 2.5:1 mixture of regioisomers, simple soft enolization conditions using TMSOTf and triethyl amine proved fruitful, giving a much-improved 18:1 mixture of regioisomers in high yield. The same process was carried out using TBSOTf to give the equivalent TBS enol ether **2.11** in a slightly improved 20:1 mixture of regioisomers. Switching to DIPEA as the base gave comparable yields and improved the ratio to greater than 25:1 for both **2.10** and **2.11**.



Silyl Enol Ether (eq) ^a	Benzylic Alcohol	Lewis Acid (eq)	Temperature	Yield 2.12 (d.r. D:U) ^f	Yield 2.13
2.10 (3 eq)	2.3	TMSOTf (3 eq)	-78°C	0%	100%
2.10 (3 eq)	2.3	TiCl ₄ (3 eq)	-78°C	0%	0%
2.10 (3 eq)	2.3	TiCl ₄ (3 eq)	-40°C	~10% (nd)	20%
2.10 (3 eq)	2.3	TiCl ₄ (3 eq)	RT	31% (2:1)	50%
2.10 (3 eq)	2.7	TiCl ₄ (3 eq)	-78°C	35% (4:1)	nd
2.11 (3 eq)	2.7	TiCl ₄ (3 eq)	-78°C	43% (4:1)	nd
2.11 (3 eq)	2.7	SnCl ₄ (3 eq)	-78°C	60% (4:1)	nd
2.11 (1.5 eq)	2.7	SnCl ₄ (3 eq)	-78°C	35% (4:1)	nd
2.11 (5 eq)	2.7	SnCl ₄ (3 eq)	-78°C	63% (4:1)	nd
2.11 (3 eq)	2.7	SnCl ₄ (1.5 eq)	-78°C	28% (4:1)	nd
2.11 (3 eq) ^b	2.7	SnCl ₄ (3 eq)	-78°C	32% (4:1)	nd
2.11 (3 eq) ^c	2.7	SnCl ₄ (3 eq)	-78°C	43% (4:1)	nd
2.11 (3 eq) ^d	2.7	SnCl ₄ (3 eq)	-78°C	58% (4:1)	nd
2.11 (3 eq) ^e	2.7	SnCl ₄ (3 eq)	-78°C	61% (4:1)	nd

^a DCM used as a solvent unless otherwise stated

^b Reaction run in THF

^c Reaction run in Et₂O

^d Reaction run in 10:1 DCM:MeNO₂

^e Reaction run in 5:1 DCM:MeNO₂

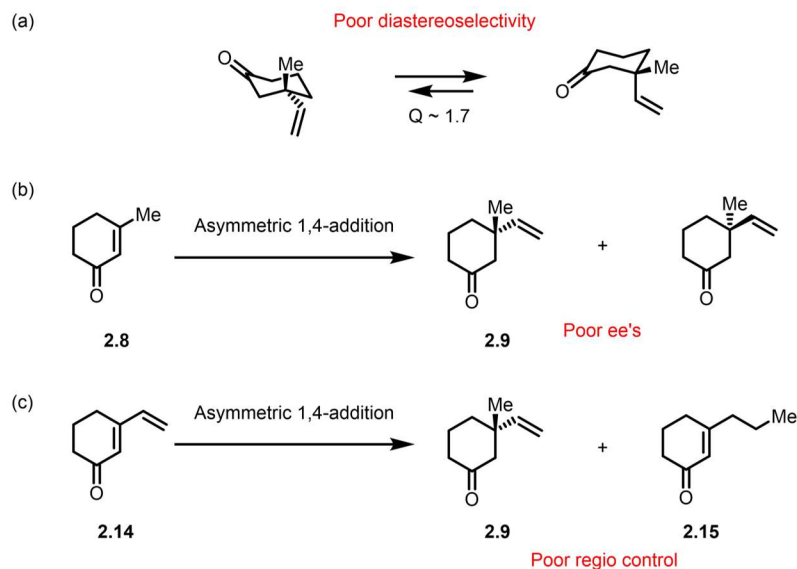
^f Desired – α-H, undesired – β-H

Table 2.1. Conditions for the optimization of the Friedel-Crafts reaction

With the two fragments in hand, we began to investigate the Friedel-Crafts reaction to couple them together. Disappointingly, the use of TMS triflate as the Lewis acid, the conditions utilized by Rawal and coworkers in the synthesis of the welwitindolinones, proved unsuccessful. (Table 2.1), giving only the dehydration product **2.13**. Switching to metal-based Lewis acids was more fruitful. Using three equivalents of TiCl₄ and three equivalents of the TMS silyl enol ether gave no reaction at -78 °C, but by running the reaction at -40 °C, a small amount of product was formed, and at RT the yield of **2.12** was 31%, a 2:1 mixture of diastereomers. However, as the temperature was increased, so too was the amount of elimination product formed. We reason that

the low yield was due to rapid hydrolysis of the silyl enol ether, possibly accelerated by the HCl generated through the reaction between the benzylic alcohol and TiCl_4 . In order to avoid this issue, TMS-protected benzylic alcohol **2.7** was prepared via the reaction of the alcohol **2.3** with triethylamine and TMSOTf. This gave the added benefit of the reaction temperature to be lowered, as the TMS ether was substantially more soluble than the benzylic alcohol. This was expected to slow hydrolysis as well as increase diastereoselectivity. At -78°C , the reaction between the TMS protected benzylic silyl ether and the TMS enol ether **2.10** proceeded in 35% yield with an improved 4:1 diastereomeric ratio, increasing to 43% when the TMS enol ether was replaced with a TBS enol ether **2.11**. We believe this is due to slower hydrolysis of the TBS enol ether compared to the TMS, allowing more productive bond formation. The yield was finally increased to 60% by using the weaker Lewis acid SnCl_4 . Lowering the equivalents of the silyl enol ether led to lower yield, but no significant increase in yield was observed by increasing the equivalents beyond three. Similarly, three equivalents of Lewis acid proved necessary, but further equivalents led to significantly decreased yield. At least in the case of the metal-based Lewis acids, we believe this is due to a single equivalent being tied up by the anilide moiety, necessitating a larger excess than is used in similar reactions elsewhere. Multiple solvents, including THF, Et_2O , and DCM/NO_2 , were also screened; however, DCM proved to give the highest yield.

Overall, our worries about the lower reactivity of our benzylic alcohol compared to the indole benzylic alcohols used elsewhere proved somewhat valid, although this lower reactivity could be alleviated by adjusting the temperature and equivalents. The Lewis basicity of the anilide was less of an issue than we had predicted, and a simple corresponding increase in Lewis acid equivalents was sufficient to overcome this issue.

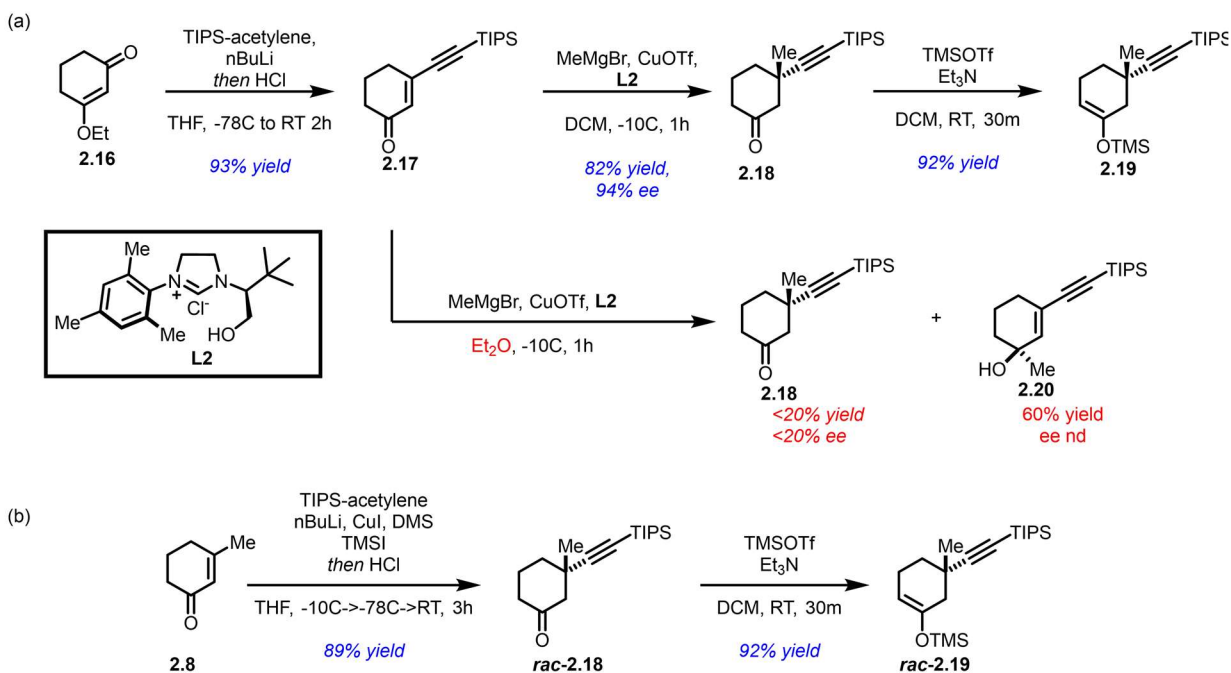


Scheme 2.4. Issues with the first generation synthesis

Although the yield for the Friedel-Crafts reaction had been increased to a reasonable level, there remained an issue with the diastereoselectivity. Even when the reaction was run at $-78\text{ }^{\circ}\text{C}$, the highest diastereoselectivity observed was 4:1. While the selectivity is modest, it is remarkably high when one considers the small difference in the steric bulk of the two substituents at the quaternary center (Scheme 2.4a). Published A values for a methyl substituent are approximately 1.7 kcal/mol, while a vinyl substituent has an A value of 1.4 kcal/mol.³ In order to increase the diastereoselectivity in favor of the desired product, a much smaller group would need to replace the vinyl group. Another issue with the long-term viability of this initial route was the inability to render it asymmetric. As the absolute stereochemistry of this quaternary center is crucial in setting the remaining stereochemistry in the molecule, a stereospecific route to the upper fragment would be necessary. Unfortunately, there did not appear to be any way to access **2.9** through any direct, stereospecific routes. Due to the small steric bulk of the methyl group, asymmetric conjugate

³ Eliel, E. L. *J. Org. Chem.* **1981**, *46*, 1959

additions of vinyl groups to 3-methyl-2-cyclohexeneone give ee values of less than 20% (Scheme 2.4b), and the poly conjugated nature of 3-vinyl-2-cyclohexeneone makes selective 1,4-addition of a methyl group unfeasible (Scheme 2.4c).^{4,5}



Scheme 2.5. (a) Second generation asymmetric synthesis of the upper fragment. (b) Racemic route to the same compound

Thankfully, both of these problems can be solved with a single alteration – replacing the vinyl group with a silyl alkyne substituent, specifically a TIPS-alkyne, to give ketone **2.18**. In 2012, Alexakis and coworkers published a route to the asymmetric addition of Grignards to poly-conjugated diene-one and ene-yne-one systems using NHC-Copper catalysts.⁶ The large steric bulk of the TIPS group served to block the 1,6-addition of the various cuprates, giving the 1,4 products selectively and with high ee (>90%). As the alkyne group has a significantly smaller A value than

⁴ Müller, D.; Alexakis, A. *Chem. – Eur. J.* **2013**, *19* (45), 15226–15239

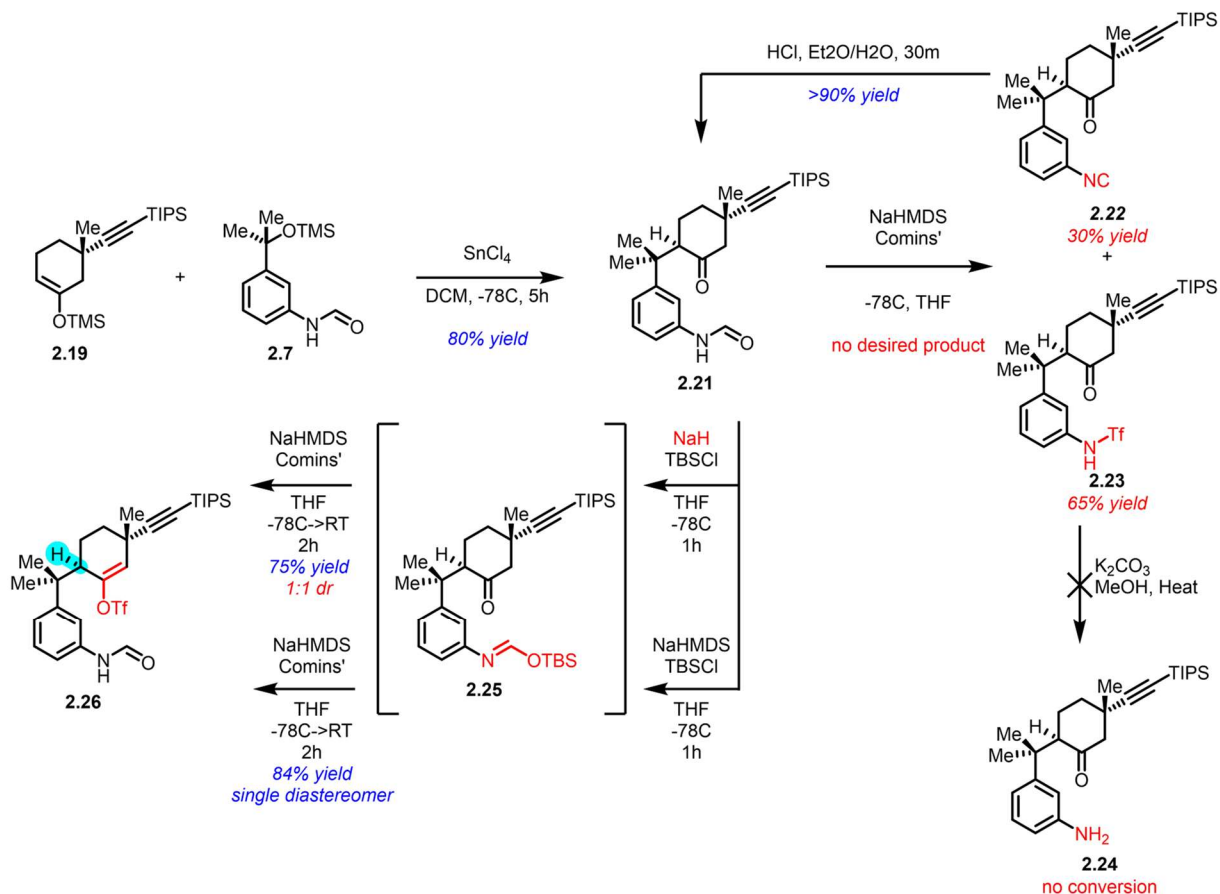
⁵ Näf, F.; Degen, P.; Ohloff, G. *Helv. Chim. Acta* **1972**, *55* (1), 82–85.

⁶ Tissot, M.; Poggiali, D.; Hénon, H.; Müller, D.; Guénee, L.; Mauduit, M.; Alexakis, A. *Chem. – Eur. J.* **2012**, *18* (28), 8731–8747.

a vinyl group at 0.4 kcal/mol, this approach was expected to also greatly increase the diastereoselectivity of the subsequent Friedel-Crafts reaction.

Following a route adapted from Alexakis' published procedure, we prepared ene-yn-one **2.17** from 3-ethoxy-2-cyclohexeneone in high yield, and methylation proceeded smoothly to give the desired ketone **2.18** in 82% yield with 94% ee. Notably, this reaction must be run in DCM, and we found that it was crucial to completely remove all ethereal solvents from the Grignard prior to the addition of the NHC catalyst, copper, and substrate. If the entirety of the ethereal solvent is not removed, either by vacuum or by blowing off with a nitrogen gas stream, the racemic 1,2- and 1,4-additions of the Grignard will dominate, giving **2.20** and **rac-2.18**, respectively. However, if the Grignard reagent is rendered much less soluble by replacing the ethereal solvent with DCM, the vast majority of the organometallic species in solution will be the NHC-linked cuprate, allowing the asymmetric addition to continue unaffected.

The same ketone could also be made in a non-asymmetric fashion through a process analogous to the addition of the vinyl group to 3-methyl-2-cyclohexeneone. The resulting ketone was then subjected to the same silyl enol ether-forming conditions used previously, giving the TMS silyl enol ether **2.19** in high yield as a >20:1 mixture of regioisomers. By using the Friedel-Crafts conditions identified as optimal for the vinyl-containing substrate, ketone **2.21** was formed in 80% yield and as a single diastereomer, confirming our hypothesis that this modification would solve the diastereomer issues.



Scheme 2.6. Friedel-Crafts reaction and attempts to install the vinyl triflate

After the Friedel-Crafts reaction, the final step prior to investigating the carbonylation was the formation of the enol triflate. However, standard conditions using NaHMDS and Comins' reagent gave none of the desired compound **2.26**. Instead, what was isolated was a ~2:1 mixture of N-triflated and deformylated product **2.23** and the isonitrile **2.22**, arising from O-triflation and subsequent elimination. While **2.22** could be hydrolyzed *in situ* back to the starting ketone **2.21**, the nitrogen-sulfur bond in **2.23** proved difficult to break. Interestingly, when other formamides such as **2.6** were subjected to the same conditions, the sole compound former was the isonitrile, suggesting that some intramolecular chelation between the formamide and the upper ring ketone

with the counterion was blocking the O-triflation. Unfortunately, neither LiHMDS nor KHMDS were successful in reversing this selectivity.

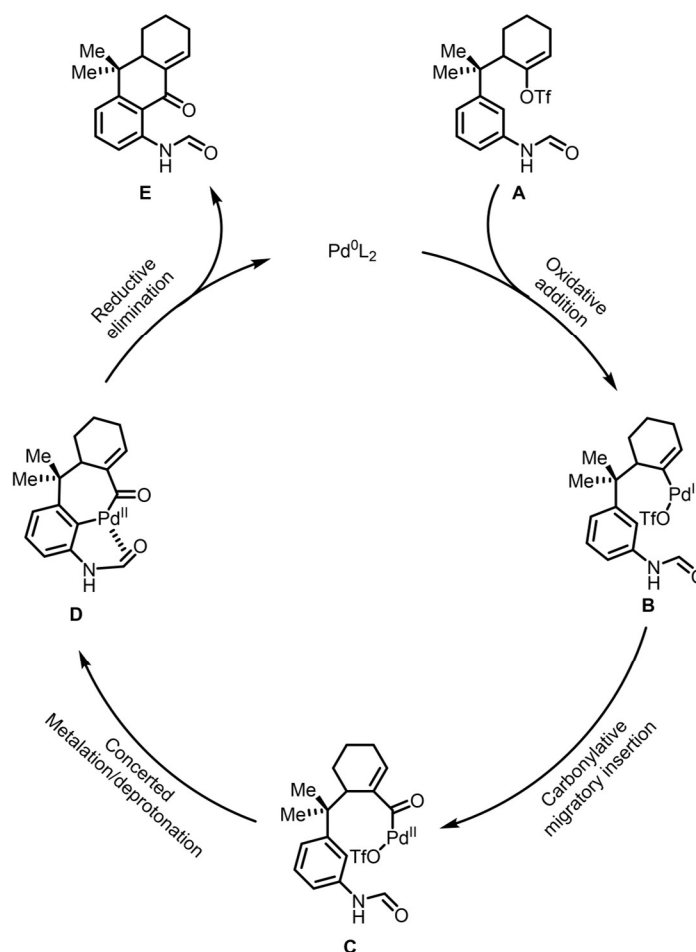
In order to circumvent this issue, we decided to employ an *in situ* protecting group. Taking inspiration from our successful overcoming of the Grignard solubility issue, sodium hydride was used to deprotonate the anilide, and TBSCl was added as an electrophile to block the ability of the anilide to triflate. The reaction was monitored by NMR, and after complete conversion of the anilide to triflate. The reaction was monitored by NMR, and after complete conversion of the anilide to the protected silyl imidate **2.25**, NaHMDS was added to deprotonate the ketone. The reaction was then warmed to RT and Comins' reagent was added. The silyl-protected anilide was de-protected spontaneously during a mildly acidic workup, affording the desired enol triflate **2.26** in high yield. These conditions sometimes led to a decay of the d.r., but using NaHMDS for both the initial and second deprotonation overcame this complication.

2.2 Studies on the Palladium-Mediated Cyclization

2.2.A Exploration of Direct Carbonylative Cyclization

With the enol triflate in hand, we were ready to begin exploring various routes for the palladium mediated carbonylation and subsequent cyclization. Our initial idea had been to perform this process in a single transformation. Palladium would undergo an oxidative addition into the enol triflate **A** to give **B**, then migratory insertion of a carbon monoxide unit would give an acyl palladium intermediate **C** that would be intercepted by the aryl ring of the anilide, with the anilide directing the palladium towards the ortho position. Concerted metalation and deprotonation (CMD) would give the palladacycle **D**, and subsequent reductive elimination would give the desired compound **E** and return the catalyst. Larock and coworkers had employed a similar process

in their synthesis of fluoren-9-ones in 2002, and in 2018 Arndtsen and coworkers used AgOTf to promote the intramolecular carbonylative coupling of aryl iodides with a wide variety of arene- and heteroarene- C-H bonds, although this process likely proceeds through a Friedel-Crafts mechanism.^{7,8} We were concerned that the published work had no examples wherein a 6-membered ring was successfully formed through Pd-catalyzed carbonylative cyclization, ostensibly due to the greater difficulty of accessing the required 7-membered ring palladacyclic



Scheme 2.7. Proposed catalytic cycle for the desired direct carbonylation

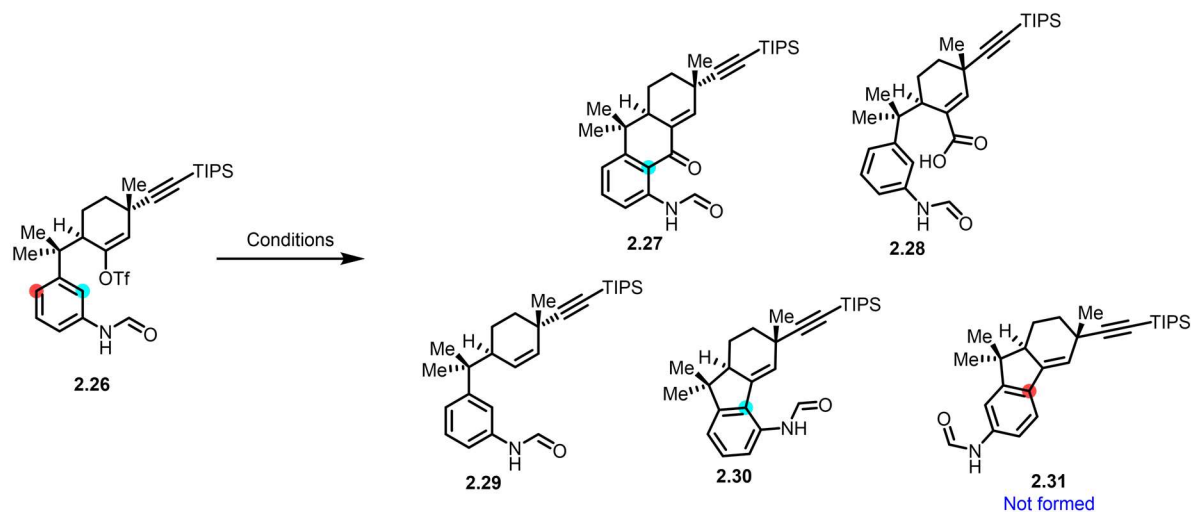
⁷ Campo, M. A.; Larock, R. C. *J. Org. Chem.* **2002**, *67* (16), 5616–5620

⁸ Garrison Kinney, R.; Tjutris, J.; Torres, G. M.; Liu, N. J.; Kulkarni, O.; Arndtsen, B. A. *Nat. Chem.* **2018**, *10* (2), 193–199

intermediate. On the other hand, we were hopeful that the desired cyclization would be possible in our system since the Thorpe-Ingolde effect provided by the benzylic quaternary center would help to drive the reaction towards completion.

Initially, Larock's conditions were employed, using PCy₃ as a ligand and CsOPiv as the base in DMF. However, none of the desired cyclized product **2.27** was observed. Instead, the starting material was converted primarily to the acid **2.28**, along with a mixture of other minor products that were assigned as the reduced compound **2.29** and the non-carbonylated cyclized compound **2.30**. Interestingly, none of the non-carbonylated, para-cyclized compound **2.31** was isolated, indicating that the palladium may have successfully promoted the desired ortho-selectivity, albeit to afford the cyclization product that had not incorporated the required carbonyl group. Repeating the reaction with added molecular sieves lowered the amount of acid formed, but still gave none of the desired compound. We then switched to rigorously dried DMAc, but this similarly gave no cyclization, only a messy reaction mixture—the same as was seen with benzene. A variety of inorganic bases with different counter ions were examined; however, all gave the acid **2.28** in low to medium yields with no desired compound. Using Et₃N as a base slowed the reaction considerably and, as expected from Larock's findings, gave none of the desired compound. Using Arndtsen's trick of adding AgOTf to promote the reaction also proved fruitless, still giving the acid as the primary isolated product. A number of phosphine ligands were screened, including bulky (PtBu₃), electron rich (PCy₃), and electron poor (P(furyl)₃) ligands, with none of the desired cyclization seen (Table 2.2).

As the oxidative addition and the carbonylative migratory insertion steps both took place smoothly, as evidenced by the formation of the acid, we believed that the issue must be with the ability of intermediate **C** to undergo the CMD reaction, either due to the weak nucleophilicity of the arene ring or the steric strain of the palladacycle intermediate **D**. One obvious solution to this issue would be to install an organo metallic component on the lower fragment, allowing the



Palladium Source ^{a,b}	Ligand ^b	Base	Solvent	Additive	CO Pressure	Yield 2.27	Yield 2.28	Yield of 2.29, 2.30
Pd(OAc) ₂	PCy ₃	CsOPiv	DMF	None	Balloon	0%	48%	10%, 10%
Pd(OAc) ₂	PCy ₃	CsOPiv	DMF	Mol Sieves 4Å	Balloon	0%	35%	nd
Pd(OAc) ₂	PCy ₃	CsOPiv	DMAC	None	Balloon	0%	<10%	nd
Pd(OAc) ₂	PCy ₃	CsOPiv	Benzene	None	Balloon	0%	<10%	nd
Pd(OAc) ₂	PCy ₃	CsOPiv	Benzene	None	10 Atm	0%	30%	nd
Pd(OAc) ₂	PCy ₃	NaOAc	DMF	None	Balloon	0%	40%	nd
Pd(OAc) ₂	PCy ₃	KOAc	DMF	None	Balloon	0%	35%	nd
Pd(OAc) ₂	PCy ₃	K ₂ CO ₃	DMF	None	Balloon	0%	40%	nd
Pd(OAc) ₂	PCy ₃	Et ₃ N	DMF	None	Balloon	0%	<10%	nd
Pd(OAc) ₂	PCy ₃	CsOAc	DMF	AgOTf	Balloon	0%	48%	nd
Pd(PPh ₃) ₄	None	CsOAc	DMF	None	Balloon	0%	28%	nd
Pd(OAc) ₂	P(Furyl) ₃	CsOAc	DMF	None	Balloon	0%	35%	nd

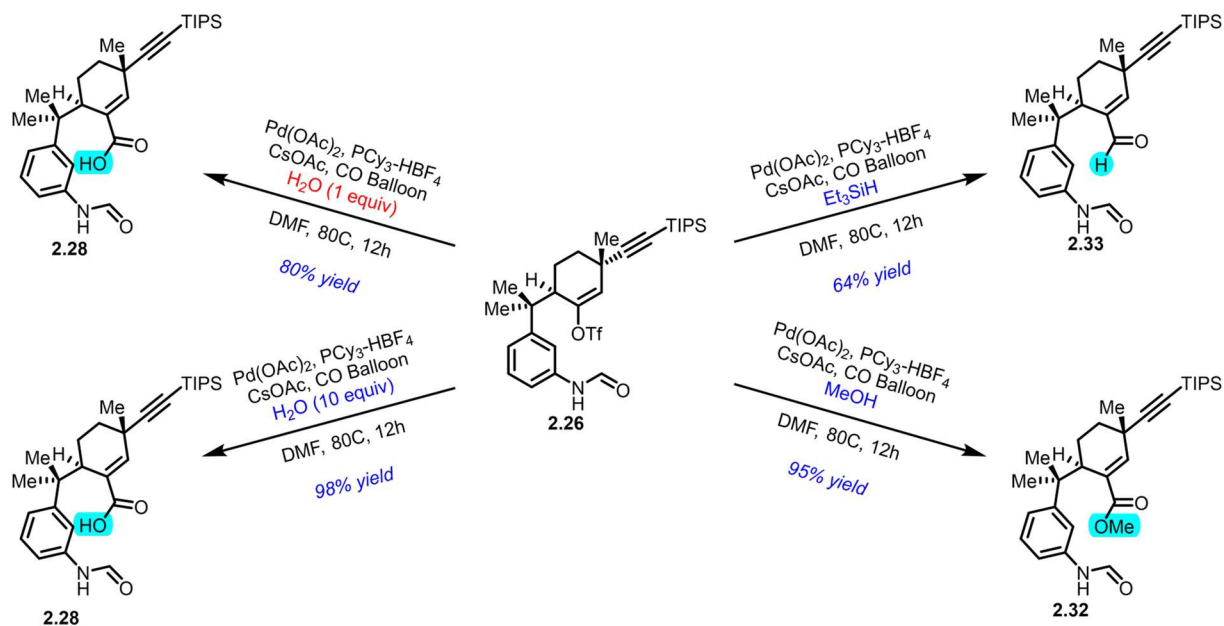
^aAll reactions run at 80°C for 12 hours

^b10% Loading

^c20% loading

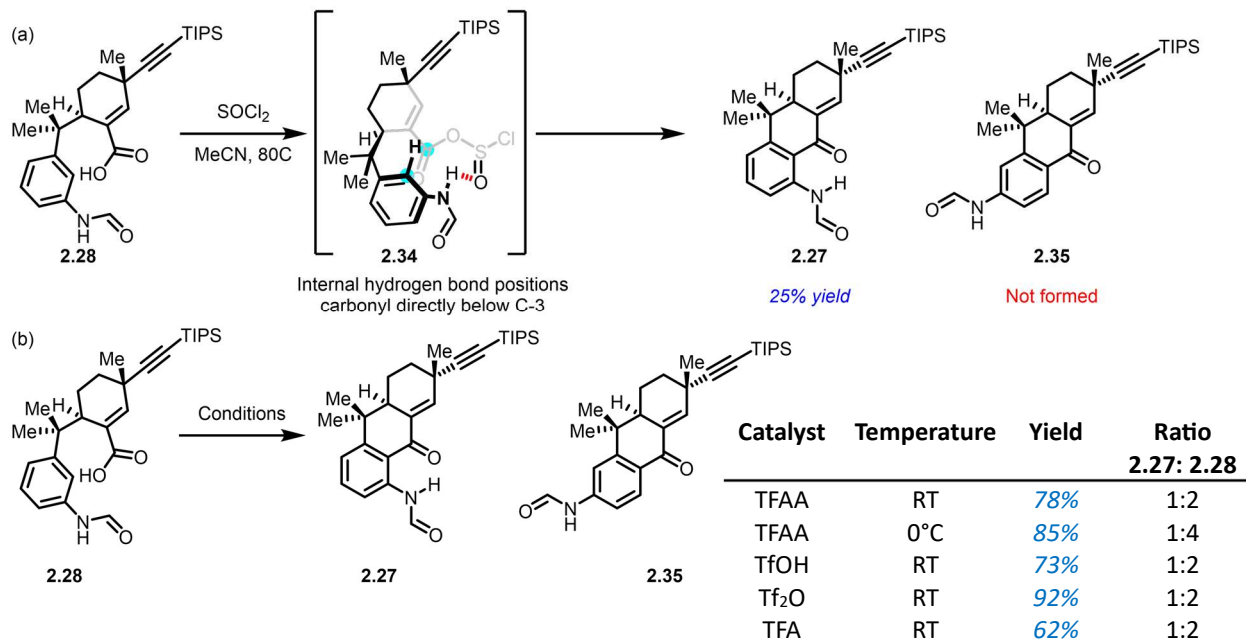
Table 2.2. Failed conditions for the direct carbonylative cyclization

reaction to take place through a more classical carbonylative cross-coupling mechanism.⁹ However, this route was undesirable for a few reasons, including the length it would add to the synthesis, the operational difficulty caused by the high CO pressures required in the literature for such reactions, and the fact that it would negate the unique ability of the anilide to act as a directing group. So, given that this direct carbonylative cyclization appeared to be unworkable, we decided to identify what other nucleophiles could be beneficially added to the acyl palladium intermediate C. We first turned to water, as we already knew that acid **2.28** was easy to form. By adding a single equivalent of water to the reaction mixture, we could increase the yield of **2.28** to >80%, and upon adding ten equivalents, the reaction became effectively quantitative. Methanol was similarly a



Scheme 2.8. Addition of nucleophiles to the carbonylation reaction in order to trap the acyl palladium intermediate

⁹ Stille, J. K. *Pure Appl. Chem.* **1985**, 57 (12), 1771–1780.



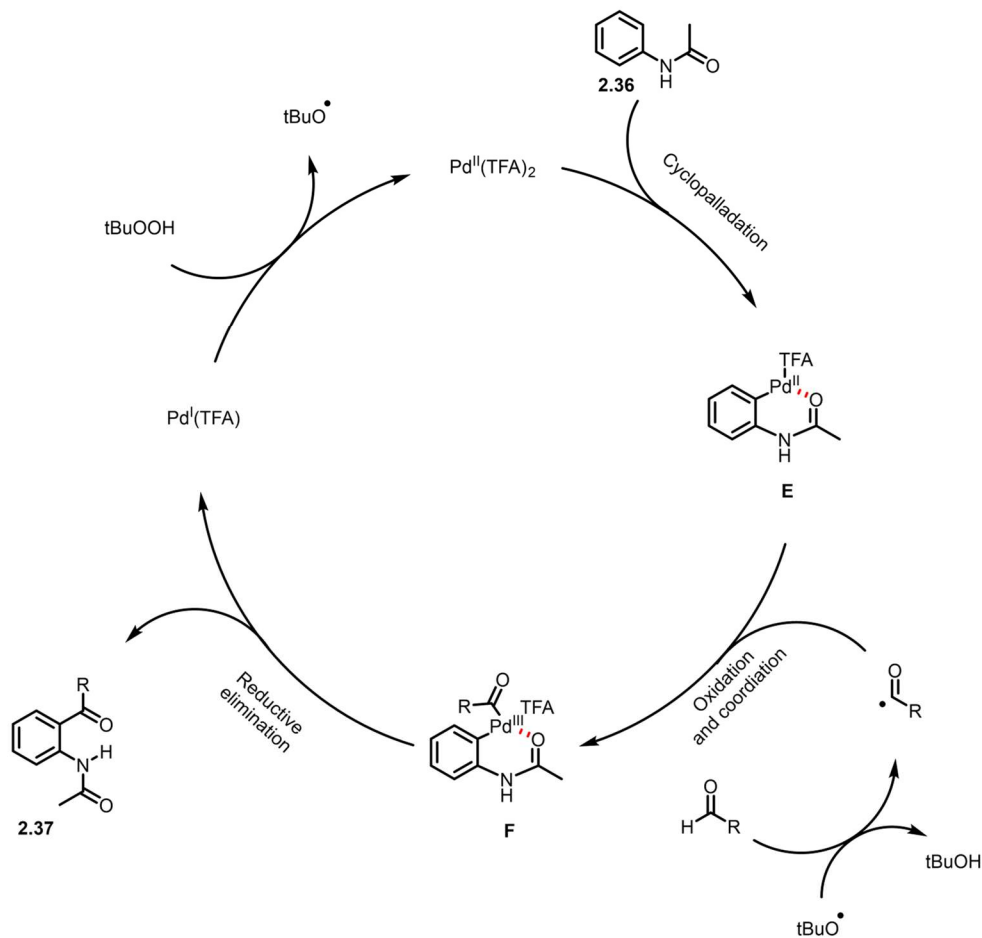
Scheme 2.9. (a) Refluxing with SOCl_2 gives an unexpected selectivity for the desired ortho compound, possibly proceeding through the indicated intermediate. (b) Other conditions failed to selectively give the ortho compound.

potent nucleophile, and we were able to form the methyl ester **2.32** in high yields. Triethyl silane served as a good source of hydride, and the aldehyde **2.33** was accessible in moderate yields, although the reduced compound **2.29** was also formed in low yields.¹⁰

2.2.B Two Step Cyclization Proceeding Through the Carboxylic Acid

With a reliable route to the acid, we decided to investigate ways to perform this cyclization. The acid was exposed to SOCl_2 in refluxing acetonitrile with the intention of forming the acid halide—however, this instead caused the direct cyclization to give the ultimately desired ketone **2.27**, albeit in low yields and amid multiple other products. Notably, however, the reaction did not

¹⁰ Behenna, D. C.; Stockdill, J. L.; Stoltz, B. M. *Angew. Chem. Int. Ed.* **2007**, 46 (22), 4077–4080.



Scheme 2.10. Li's proposed catalytic mechanism for the ortho directed C-H activation and acylation¹³

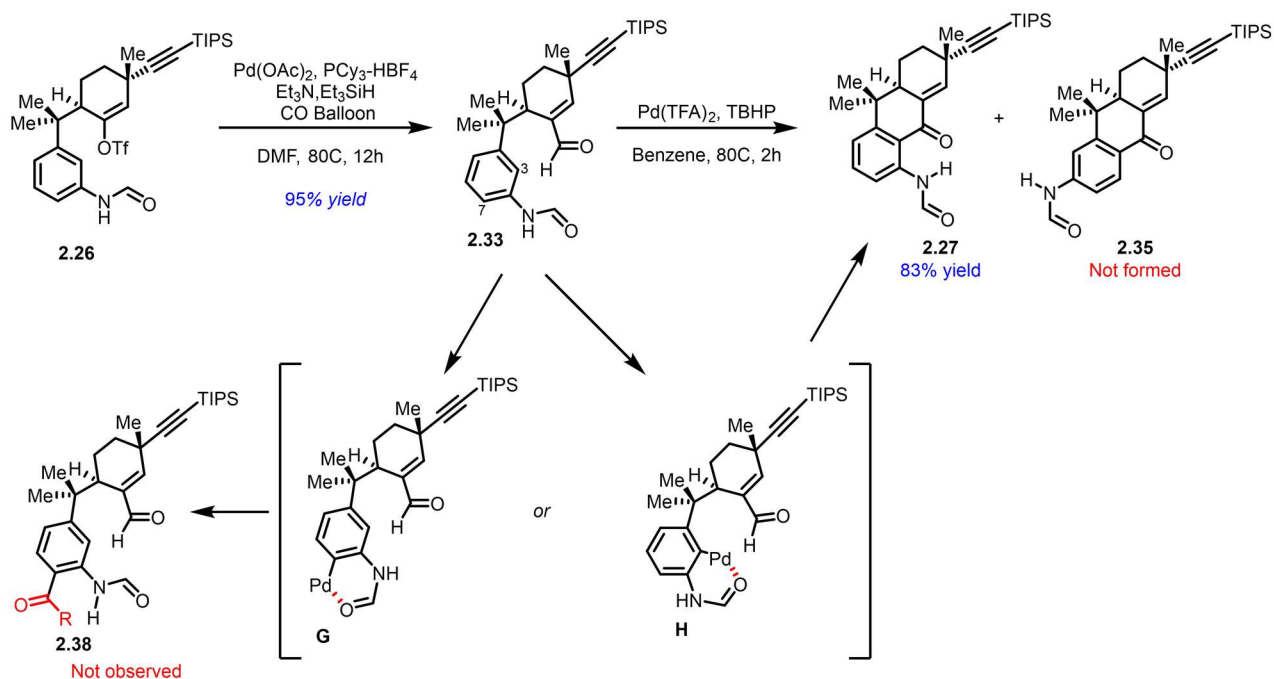
appear to produce any of the alternative cyclization product **2.35**, which would form by cyclization at the less-hindered position para- to the anilide. The reason for this remains unclear; however, intramolecular direction from the anilide could be playing a role, as in scheme 2.9. Unfortunately, other cyclization conditions, while primarily giving higher yields, also gave product mixtures more closely matching what is expected for Friedel-Crafts reactions onto anilides, with the para-cyclization dominating.¹¹ Trifluoro acetic anhydride gave a 2:1 ratio of para- to ortho- cyclization

¹¹ Kobayashi, S.; Komoto, I.; Matsuo, J. *Adv. Synth. Catal.* **2001**, *343* (1), 71–74.

when run at room temperature, which increased to a 4:1 ratio when run in an ice bath. Triflic acid, triflic anhydride, and trifluoroacetic acid all gave similar results, with the para-cyclization far exceeding the desired ortho cyclization.

2.2.C Two Step Cyclization Proceeding Through the Aldehyde

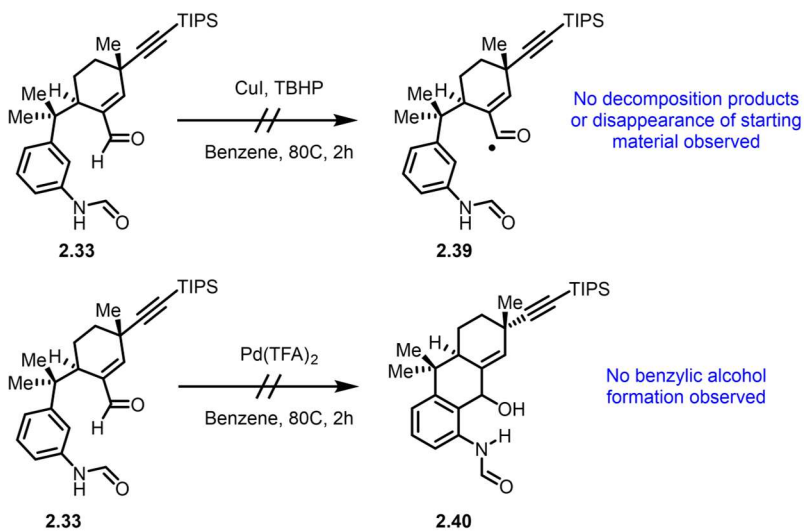
We expected the same to happen were we to attempt a Friedel-Crafts cyclization with methyl ester **2.32**. However, the aldehyde **2.33** provided access to a different potential pathway, one that could potentially take advantage of the directing ability of the anilide. In 2011, Kwong and coworkers had showed that Pd(TFA)₂ in the presence of TBHP could be used to oxidatively couple aldehydes and acetanilides selectively at the ortho position.¹² That same year, a report from



Scheme 2.11. Palladium-mediated cyclization reaction from the aldehyde successfully gives the desired compound as the sole isolated product

¹² Wu, Y.; Li, B.; Mao, F.; Li, X.; Kwong, F. Y. *Org. Lett.* **2011**, *13* (12), 3258–3261.

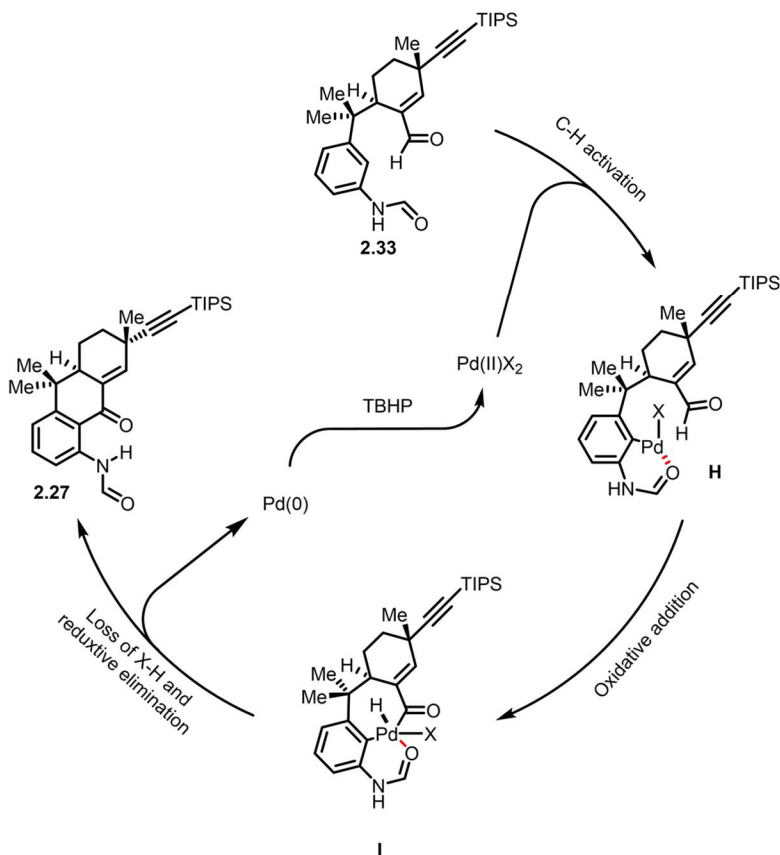
Li and coworkers confirmed the broad scope of the conditions and proposed that the mechanism proceeded through a ortho-directed cyclopalladation to give a species like **E**.¹³ This is followed by oxidative coupling of the aldehyde and palladium to give intermediate **F**, after which reductive elimination gives the desired product. Although the specific nature of the palladium intermediates has not been explored, this mechanism would suggest that the reductive intermediate gives a palladium(I) species that is then oxidized by TBHP to return the palladium(II) active catalyst. At the same time, the tert-butanol radical formed carries out the oxidation of the aldehyde. Kwong reported that the reactivity was conserved for phenyl- and isopropyl-substituted anilides, but neither paper reported on any formanilide-containing substrates. Although formanilides are known to be weaker directing groups than acetanilides, we hoped that the intramolecular nature of the reaction would promote the cyclization, with the Thorpe-Ingolde effect again providing a driving force forward.¹⁴



Scheme 2.12. Control experiments on the palladium-mediated cyclization

¹³ Li, C.; Wang, L.; Li, P.; Zhou, W. *Chem. – Eur. J.* **2011**, *17* (37), 10208–10212

¹⁴ Tomberg, A.; Muratore, M. É.; Johansson, M. J.; Terstiege, I.; Sköld, C.; Norrby, P.-O. *iScience* **2019**, *20*, 373–391.

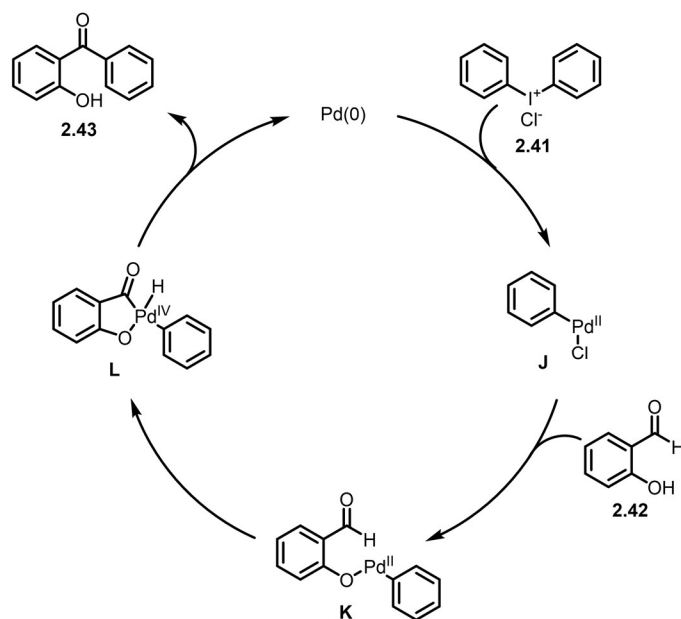


Scheme 2.13 Postulated mechanism for the palladium-mediated cyclization proceeding through an oxidative addition into the aldehyde C-H bond

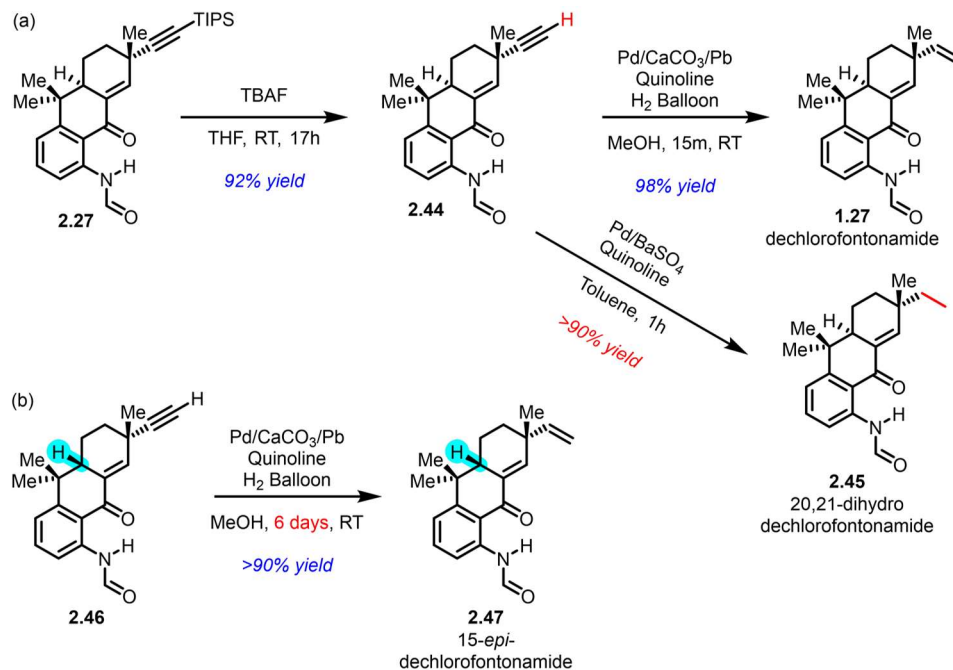
By changing the base from to Et₃N, we were able to access aldehyde **2.33** from the enol triflate **2.26** in 95% yield, and using Kwong's conditions, we were able to produce the desired compound **2.27** in good yields. Notably, neither the para-cyclized product **2.35** nor any dimerized or polymerized products of the form **2.38** were formed. This confirms that the reaction is indeed proceeding through a directed palladium intermediate and also indicates that the formation of this palladacycle may be reversible, as palladated intermediate **G**, formed by palladation at the other ortho position (on C-7), would likely be preferred kinetically over intermediated **H** by virtue of the decreased steric interference, as seen in Kwong and Li's scopes. This also suggests that Li's proposed mechanism may not be entirely correct, as any free aldehyde radical produced, as

proposed by them, would likely be intercepted by **2.38**, and no compound was observed that could have arisen from undesired decomposition of the radical. Alternatively, the aldehyde may be acting as a second directing group to promote formation of **H** over **G**.

To test whether the TBHP was sufficient to produce the acyl radical, the reaction was run without any added Pd(TFA)₂, instead using CuI to produce the tert-butoxyl radical. As predicted, on the time scale of the palladium-catalyzed reaction no decomposition of starting material was observed, indicating that TBHP alone was not sufficient to oxidize the aldehyde. While this does not necessarily overrule Li's proposed mechanism, it suggests that it may not be so simple. One other possibility was that Pd(TFA)₂ was acting as a catalytic Lewis acid to promote the Friedel-Crafts reaction, and that TBHP was acting to promote the subsequent oxidation of the benzylic alcohol to the ketone. However, when the reaction was run without TBHP, none of the proposed benzylic alcohol **2.40** was formed, confirming that a Friedel-Crafts reaction was not the first step.



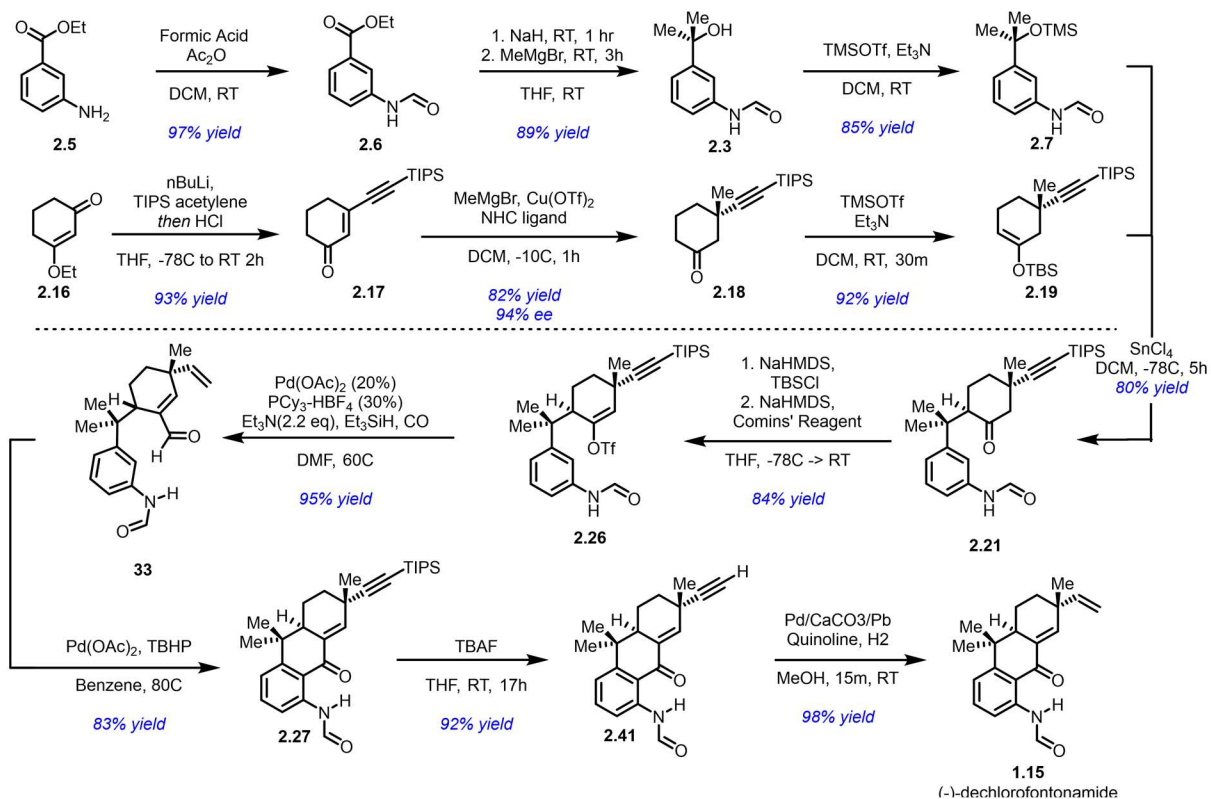
Scheme 2.14 Chen's proposed mechanism for palladium-mediated coupling of aryl iodonium's with ortho-hydroxy benzaldehydes



Scheme 2.15. (a) final steps to the natural product. (b) The C-15 epimer of the natural product is substantially slower to form

One other possible mechanism is that, following the insertion of the palladium into the C-H bond to make **H**, the palladium could undergo an oxidative addition into the C-H bond of the aldehyde, giving intermediate **I** (Scheme 2.13). This would be followed by the loss of trifluoroacetic acid and a subsequent reductive elimination to form the C-C bond. The resulting Pd(0) species would then be re-oxidized to Pd(II) with TBHP.¹⁵ A similar mechanism was invoked by Chen and coworkers to explain their palladium-catalyzed arylation of ortho-hydroxy benzaldehydes (Scheme 2.14) While further study is warranted, this mechanism would explain the high selectivity observed, and suggests that other oxidants beyond TBHP may be of use in promoting such reactions.

¹⁵ Xia, M.; Chen, Z. *Synth. Commun.* **2000**, *30* (3), 531–536



Scheme 2.16. Complete total synthesis of (-)-dechlorofontonamide

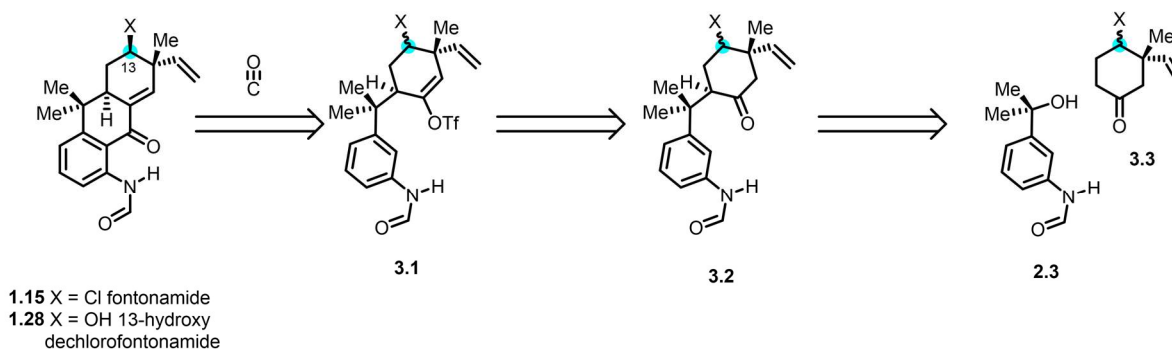
Completion of the synthesis then required only the conversion of the alkyne substituent on the D ring to the vinyl group. Excess TBAF served to cleanly remove the TIPS group, giving alkyne **2.41**. Hydrogenation of the alkyne was accomplished using a highly-poisoned palladium catalyst (Pd/CaCO₃/Pb with quinoline in MeOH), rapidly giving the natural product **1.27** in 98% yield. The highly poisoned nature of the catalyst was necessary to give the desired compound, as overreduction to the non-natural product 20,21-dihydro dechlorofontonamide (**2.42**) was rapidly formed when the more active catalyst Pd/BaSO₄ was used with toluene as a solvent. Interestingly, when the C-15 epimer (**2.43**), prepared through an analogous route, was exposed to the successful conditions, the reduction was considerably slower, giving the final compound and non-natural product 15-*epi*-dechlorofontonamide cleanly only after 6 days of reaction. In summary, the first asymmetric synthesis of dechlorofontonamide was completed in 9 steps from commercially available starting material with an overall yield of 33%.

Chapter 3: Total synthesis of (-)-fontonamide and (±)-13-hydroxy dechlorofontonamide

3.1 Synthesis of the oxygenated D-ring

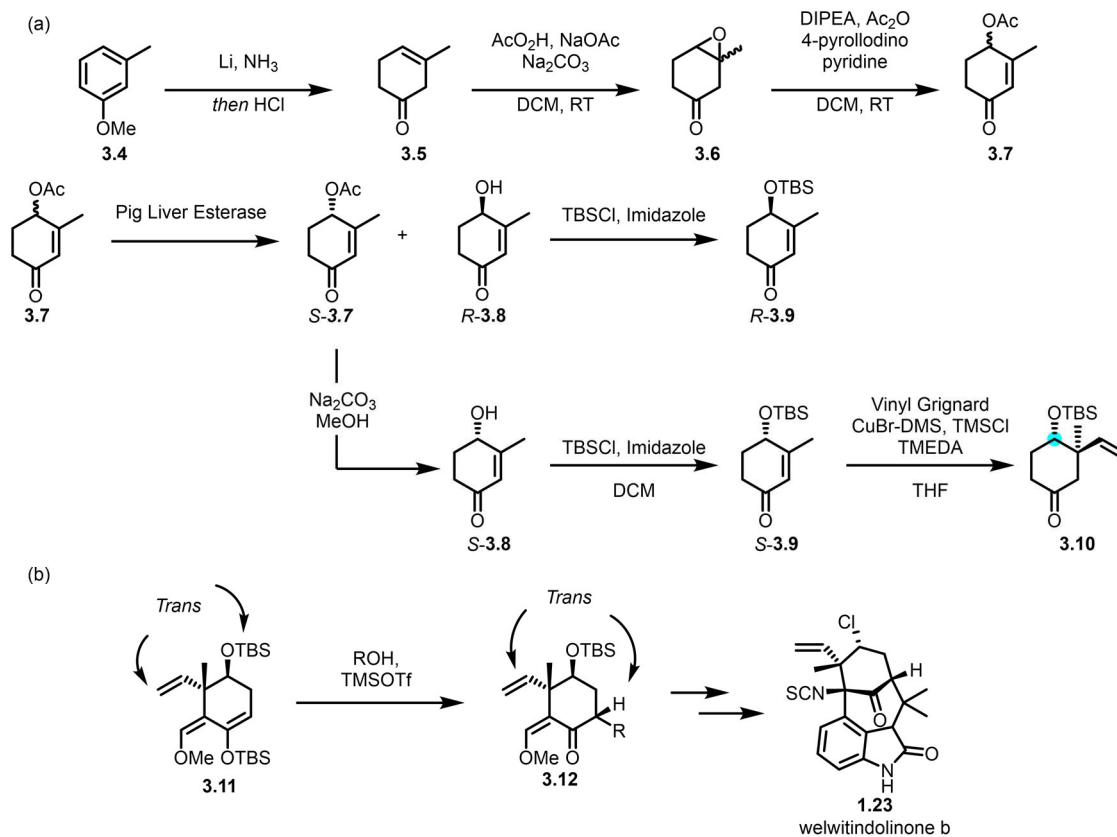
Having completed the first total synthesis of dechlorofontonamide completed, we set our sites on its chlorinated and hydroxylated cousins, fontonamide and 13-hydroxy dechlorofontonamide, respectively. Given the success enjoyed with the palladium-mediated, anilide-directed acylation/cyclization reaction, as well as the simplicity of the convergent strategy, we aimed to pursue a similar route for some related natural products. As the retrosynthetic analysis suggests (scheme 3.1), this would require access to a ketone such as **3.3**, with the 4-position (what will end up the C-13 carbon in the natural product) carrying a chlorine or protected alcohol.

The Rawal Group had utilized a similar ketone, **3.10** in their syntheses of welwitindolinones B, C, and D.¹ The ketone, which exhibits a *trans* relationship between the TBS-



Scheme 3.1. Retrosynthetic analysis of fontonamide and 13-hydroxy dechlorofontonamide

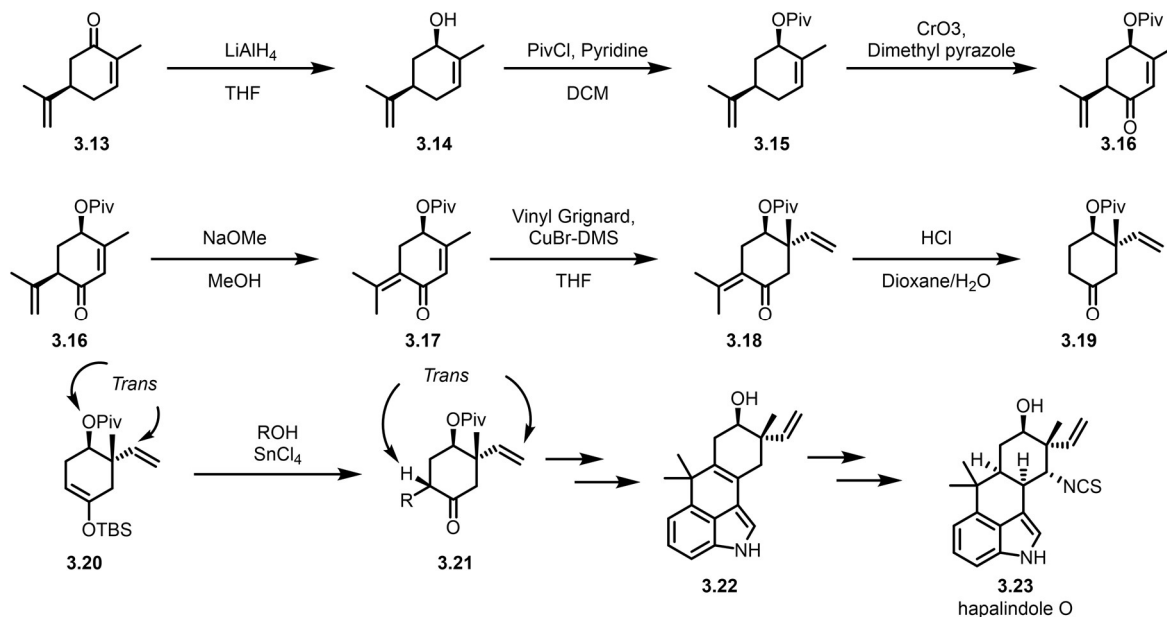
¹ (a) Allan, K. M.; Kobayashi, K.; Rawal, V. H. *J. Am. Chem. Soc.* **2012**, *134* (3), 1392–1395. (b) Bhat, V.; Allan, K. M.; Rawal, V. H. *J. Am. Chem. Soc.* **2011**, *133* (15), 5798–5801. (c) Reyes, J. R.; Xu, J.; Kobayashi, K.; Bhat, V.; Rawal, V. H. *Angew. Chem. Int. Ed.* **2017**, *56* (33), 9962–9966.



Scheme 3.2. (a) Frejd's synthesis of ketone **3.10**. (b) The Rawal group's use of a derivative of **3.10** for the synthesis of welwitindolinone B

protected alcohol and the vinyl group, was made following a route first developed by Frejd in 1991 (Scheme 3.2).² Birch reduction and hydrolysis of 3-methyl anisole gives ketone **3.5**. Epoxidation and subsequent tandem elimination/acetylation gives the gamma-acetoxy enone **3.7**. Unfortunately, this sequence was difficult to render asymmetric, so the enantiomers were resolved through pig liver esterase de-acetylation. The desired enantiomer *S*-**3.7** remains acetylated, so it is deacetylated to give alcohol *S*-**3.8**, which is then protected with a TBS group to give *S*-**3.9**. Vinyl cuprate addition gives the desired ketone **3.10**, and trapping of the enolate with Zaiya's reagent gives ketone **3.11**. The diastereoselectivity of the reaction is driven by the steric bulk of the TBS

² Polla, M.; Frejd, T. *Tetrahedron* **1991**, *47* (30), 5883–5894.



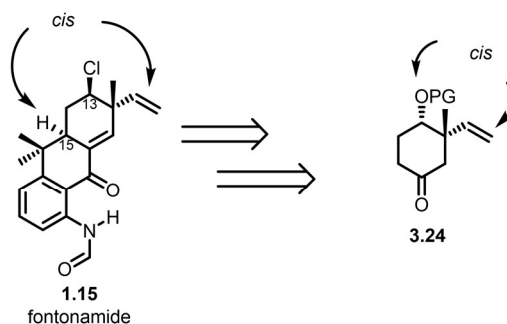
Scheme 3.3. Natsume's synthesis of ketone **3.19** and use in the synthesis of hapalindole O

ether, giving rise to the *trans* relationship between the TBS ether and the vinyl group as mentioned above. Unfortunately, this same steric bulk meant that this ketone route, while highly scalable and well-tested, would not work for the present syntheses. The stereocenter at C-15 is set during the Friedel-Crafts reaction and is controlled by the stereocenter at C-13, the carbon that bears the TBS ether. The relative stereochemistry at C-15 of the fontonamides is opposite that seen in the welwitindolinones, and the undesired stereocenter is therefore the expected major product in this reaction.

Natsume and coworkers, in their enantiospecific synthesis of hapalindole O, used a similar ketone **3.19**, which also exhibited a *trans* relationship between the pivaloyl protected alcohol and the vinyl group.³ This ketone was made in 6 steps from carvone, and the *trans* relationship again arises from the addition of a vinyl cuprate to the enone **3.17**. As in Rawal's welwitindolinone

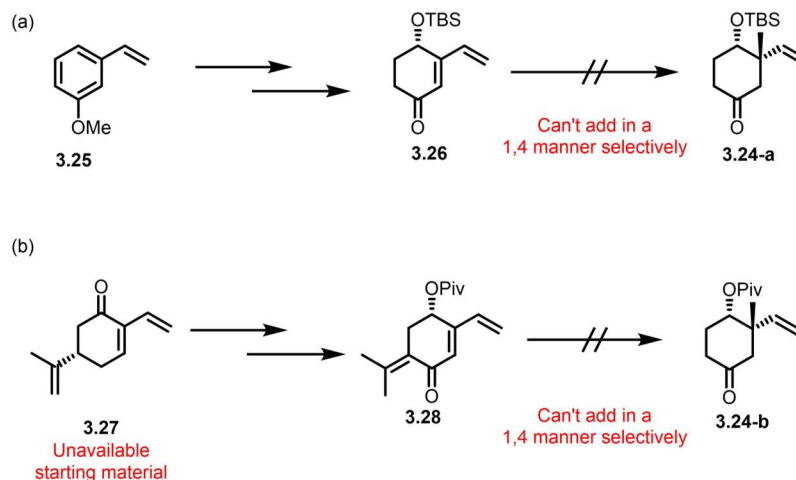
³ Sakagami, M.; Muratake, H.; Natsume, M. *Chem. Pharm. Bull. (Tokyo)* **1994**, *42* (7), 1393–1398

syntheses, the product of the Friedel-Crafts reaction contains the opposite relative stereochemistry at the C-15 position from that now needed. Natsume then opted to oblate the stereochemistry and install the proper diastereomer at a later stage (Scheme 3.3).



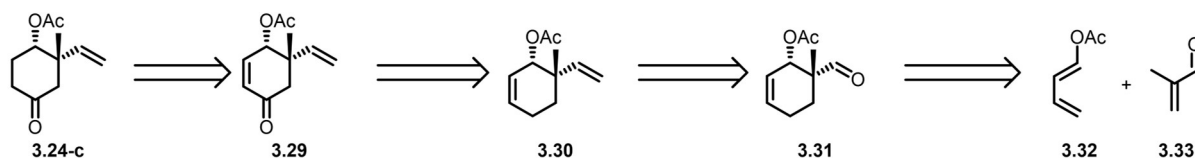
Scheme 3.4. Based on results from Natsume and Rawal, a *cis* relationship is necessary between the protected alcohol and vinyl group.

Based on these results, the ketone needed for the current route must exhibit the opposite relative stereochemistry at the eventual C-13 position from that employed by Rawal and Natsume, i.e. ketone **3.24**. Unfortunately, this also means that a new route would need to be developed, as neither Rawal/Frejd's nor Natsume's could be modified for present purpose. For the same reasons discussed in Chapter 2, the conjugate addition of a methyl nucleophile to the poly-unsaturated ketone **3.26** that could arise from a route similar to Rawal's would be difficult to control. The same issue would be present in trying to adapt Natsumes route; additionally, because Natsume's route relies on the availability of the starting material carvone, changing the relative stereochemistry within would be difficult (See Scheme 3.4).



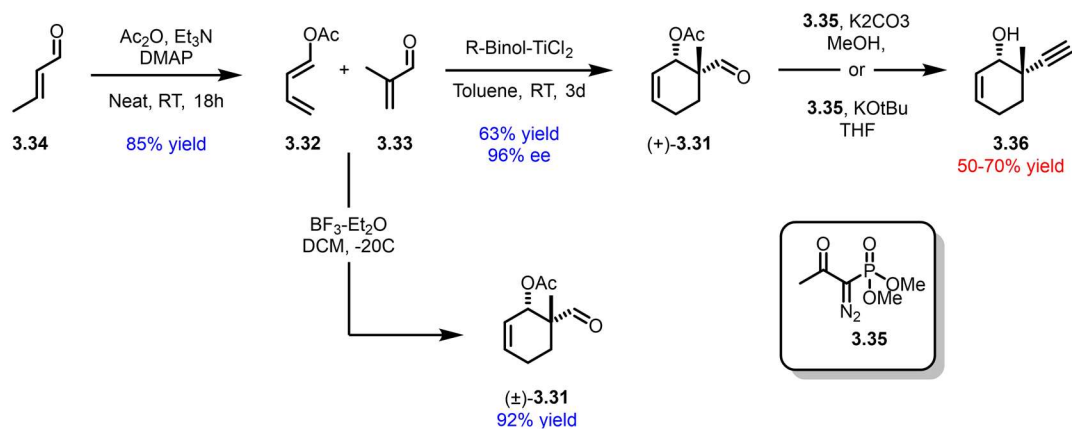
Scheme 3.5. Issues with adapting (a) Rawal/Frejd's and (b) Natsume's routes to give the *cis* ketone required for the synthesis

Instead, a drastically different route to **3.24** was conceived. As shown in the retrosynthesis in scheme 3.4, the final compound would be obtained through 1,4-reduction of enone **3.29**, which would in turn arise from the allylic oxidation of allylic acetate **3.30**. This can be traced back through simple vinylation of aldehyde **3.31**, which can be readily assembled through a Diels-Alder reaction between 1-acetoxy-1,3-butadiene **3.32** and methacrolein, **3.33**. Importantly, Mikami rendered this reaction asymmetric in 1994 using a Binol-Titanium Lewis acid catalyst, allowing us ready access to the enantiomerically enriched substrate with no additional steps or enzymatic resolution and without needing a chiral starting molecule.⁴



Scheme 3.6. Retrosynthesis of ketone **3.24-c**

⁴ Mikami, K.; Motoyama, Y.; Terada, M. *J. Am. Chem. Soc.* **1994**, *116* (7), 2812–2820.



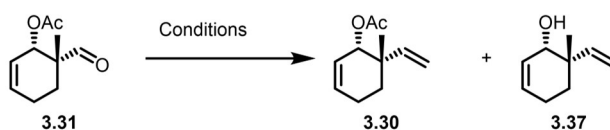
Scheme 3.7. Asymmetric and racemic Diels-Alder reactions and attempted alkylation of the aldehyde **3.31**

Diene **3.32** can be rapidly produced from crotonaldehyde simply by stirring neat with Et_3N , Ac_2O , and catalytic DMAP, or is commercially available for $<\$10/\text{g}$. This reaction was high yielding and highly scalable, allowing the preparation the diene on a 1 mole (70g) scale with no drop in yield. The chiral Diels-Alder reaction proceeded smoothly using Mikami's conditions, and the racemic reaction was also easily performed using $\text{BF}_3\text{-Et}_2\text{O}$ as a catalyst at -20°C . With cycloadduct **3.31** in hand, we began to look at conditions for the one-carbon homologation. Initially, we explored using the aldehyde to install an alkyne, which could be hydrogenated after the Friedel-Crafts reaction. The alkyne was expected to afford increased diastereoselectivity during the Friedel-Crafts reaction, as was observed during the synthesis of dechlorofontonamide (Chapter 2). However, installation of the alkyne proved difficult. We first used the typical conditions for the Bestmann-Ohira modification to Seyferth-Gilbert homologation.⁵ The Bestmann-Ohira reagent was stirred with aldehyde **3.31** along with excess K_2CO_3 in methanol. Unfortunately, the major product was alcohol **3.36**, resulting from hydrolysis of the acetate competing with formation of the

⁵ (a) Ohira, S. *Synth. Commun.* **1989**, *19* (3–4), 561–564., (b) Müller, S.; Liepold, B.; Roth, G. J.; Bestmann, H. J. *Synlett* **1996**, *1996* (06), 521–522

alkyne. Switching the base to KOEt and subsequently KOtBu and the solvent to THF helped to slow the hydrolysis, but **3.36** remained the major product.⁶

We then decided to explore methods to produce the vinyl directly from the aldehyde, with the hope that the steric bulk at the four position would be sufficient to dictate the diastereoselectivity of the reaction. Petasis' reagent worked well on a small scale, but on larger scales, the yield dropped considerably.⁷ Tebbe's reagent showed similar issues and was slightly lower yielding.⁸ Standard Wittig olefination conditions in THF led to similar issues as were observed with the Bestmann-Ohira reagent, with hydrolysis of the acetate, likely due to KOH, outcompeting the olefination. However, a simple switch to pre-formation of the ylide using Et₂O as a solvent, followed by addition of the ylide to the substrate, led to clean conversion to the desired



Conditions	Scale	Yield	
		3.30	3.37
Petasis' Reagent	0.2 mmol	65%	nd
Petasis Reagent	2 mmol	42%	nd
Tebbe's Reagent	0.2 mmol	58%	nd
Tebbe's Reagent	2 mmol	37%	nd
KOtBu/PPh ₃ MeBr ^a	0.2 mmol	63%	30%
KOtBu/PPh ₃ MeBr ^b	0.2 mmol	71%	20%
KOtBu/PPh ₃ MeBr ^c	0.2 mmol	89%	0%
KOtBu/PPh ₃ MeBr ^c	2 mmol	87%	0%
KOtBu/PPh ₃ MeBr ^c	20 mmol	83%	0%

^a THF used as a solvent

^b Et₂O used as a solvent

^c Et₂O used as a solvent, reverse addition

Table 3.1. Investigation of vinylation conditions

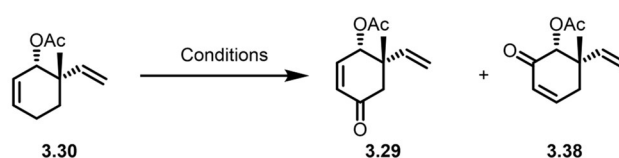
⁶ Cassaidy, K. J.; Rawal, V. H. *J. Am. Chem. Soc.* **2021**, *143* (40), 16394–16400.

⁷ Petasis, N. A.; Bzowej, E. I. *J. Am. Chem. Soc.* **1990**, *112* (17), 6392–6394.

⁸ (a) Tebbe, F. N.; Parshall, G. W.; Reddy, G. S. *J. Am. Chem. Soc.* **1978**, *100* (11), 3611–3613.
 (b) Pine, S. H.; Pettit, R. J.; Geib, G. D.; Cruz, S. G.; Gallego, C. H.; Tijerina, T.; Pine, R. D. *J. Org. Chem.* **1985**, *50* (8), 1212–1216.

compound. Pleasingly, this reaction was highly scalable, and purification was achieved with a simple filtration through a silica plug.

The next challenge was to perform the allylic oxidation to give eneone **3.29**. While allylic oxidations are well precedented, the substrate at hand posed a special challenge due to the presence of the allylic acetate, the oxidation of which was expected to be problematic. Natsume had performed a similar oxidation in his enantiospecific synthesis of hapalindole O, using chromium trioxide and 3,4-dimethyl pyrazole to oxidize pivalate-protected limonen-6-ol (**3.15**) to the corresponding eneone **3.16** (Scheme 3.3).³ However, we wanted to use a less-toxic and ideally a bulkier reagent in order to selectively oxidize at the less-hindered position. In 2005, Doyle showed that rhodium tetracaprolactam would catalyze the oxidation of benzylic methylenes to their corresponding ketones using TBHP as an oxidant, demonstrating remarkable selectivity even in



Catalyst	Temperature	Solvent	Additive	Yield
Rh ₂ (Cap) ₄ (0.5%) ^a	60°C	DCM	None	59%
CrO ₃ (10%) ^a	0°C	DCM	None	35%
Fe(OTf) ₂ (10%) ^a	RT	EtCN	None	0%
Fe(OTf) ₂ (10%) ^a	RT	EtCN	1,10-phen	40%
CuI (1%) ^a	50°C	MeCN	None	70%
CuI (1%) ^b	50°C	MeCN	None	52%
RuCl₃ (1%)^a	RT	DCM	None	78%
RuCl ₃ (0.1%) ^b	RT	DCM	None	71%
RuCl ₃ (1%) ^c	RT	DCM	None	73%

^a 1 mmol scale

^b 10 mmol scale

^c 100 mmol

Table 3.2. Optimization of the allylic oxidation to eneone **3.29**

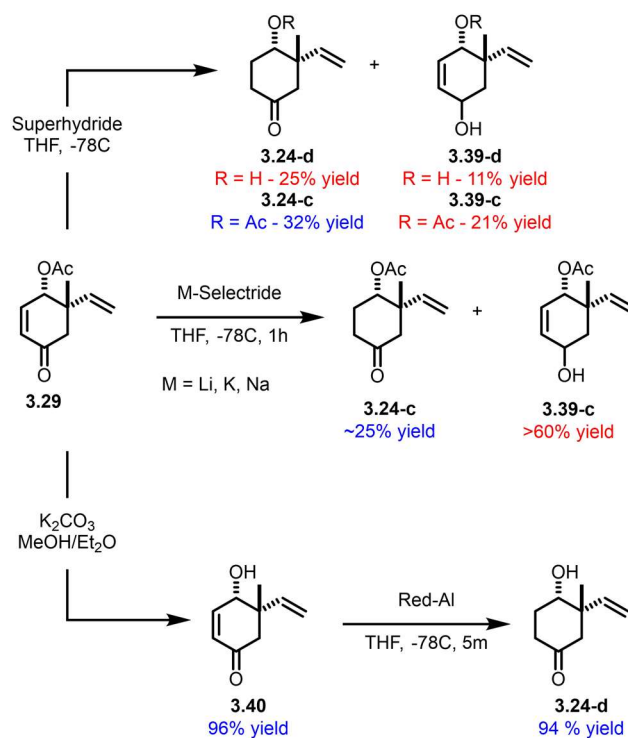
the presence of benzylic acetates.⁹ Following Doyle's conditions, we found this reaction to be highly successful, giving the desired eneone **3.29** in 59% yield (91% brsm), with the only byproduct being eneone **3.38**, formed in 5% yield. However, while the reaction worked well, the high cost of the catalyst (greater than \$1000/g) prompted us to look for other catalysts that could perform the same function. Inspired by Natsume, we initially investigated the use of CrO₃ as a potential catalyst. Unfortunately, the reaction required high catalyst loadings, and the yields were considerably lower than observed with Doyle's rhodium catalyst. A small solvent screen failed to increase the yields, so we turned our sights to iron triflate, which our lab and others had found to be useful for a variety of oxidations.^{1,10} Interestingly, while a mixture of iron triflate and TBHP failed to give any significant amounts of the desired compound even after sustained heating, simple addition of 1,10-phenanthroline as a ligand greatly increased the reactivity, giving greater than 40% yield. More predictable reactivity was observed with catalytic copper iodide, which has seen considerable use in allylic oxidations of steroids.¹¹ With just 1% loading, we were able to obtain up to 70% yield of the desired compound. However, the reaction was considerably slower, requiring sustained heating for two or three days. Additionally, the yield dropped considerably upon scaling the reaction from one to ten mmol. Finally, inspired by Maimone's synthesis of (-)-6-epi-ophiobolin N, we investigated the use of ruthenium trichloride.¹² Pleasingly, this worked quite well. With as low as 0.1% loading we were able to achieve conversions higher than 70%,

⁹ (a) Catino, A. J.; Forslund, R. E.; Doyle, M. P. *J. Am. Chem. Soc.* **2004**, *126* (42), 13622–13623. (b) Catino, A. J.; Nichols, J. M.; Choi, H.; Gottipamula, S.; Doyle, M. P. *Org. Lett.* **2005**, *7* (23), 5167–5170

¹⁰ Nishikawa, Y.; Yamamoto, H. *J. Am. Chem. Soc.* **2011**, *133* (22), 8432–8435.

¹¹ (a) Salvador, J. A. R.; Sáe Melo, M. L.; Campos Neves, A. S. *Tetrahedron Lett.* **1997**, *38* (1), 119–122. (b) Arsenou, E. S.; Koutsourea, A. I.; Fousteris, M. A.; Nikolaropoulos, S. S. *Steroids* **2003**, *68* (5), 407–414

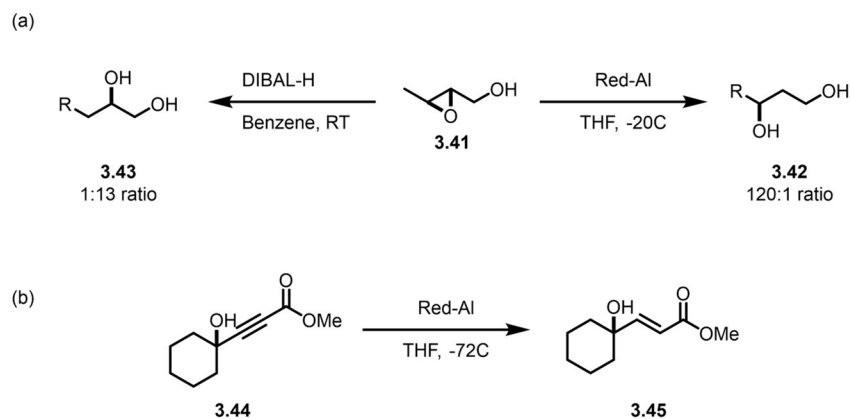
¹² Brill, Z. G.; Grover, H. K.; Maimone, T. J. *Science* **2016**, *352* (6289), 1078–1082.



Scheme 3.8. Hydride-based reduction of the eneone to the gamma-acetoxy ketone proves difficult. Deacetylation and reduction with Red-Al is successful.

with no drop upon scaling. Notably, we were able to scale the reaction up to 100 mmol in a single pass, giving 73% yield.

The final challenge for the synthesis of the D ring was to reduce the eneone to the ketone. However, this proved more difficult than we had initially predicted. The first reductant we examined was L-selectride. While it did give some of the desired ketone **3.24-c**, the primary product was allylic alcohol **3.39-c**, arising from the 1,2-reduction. Switching to K-selectride and Na-selectride gave similar results, likely due to the acetate blocking the approach of the reducing reagent at the beta position. The less bulky reducing reagent superhydride (LiHBEt₃) gave more of the 1,4-reduction but also led to deacetylation, making the resulting product mixture much messier.



Scheme 3.9. (a) Kishi shows that alcohols can direct reduction of allyl-alcohol epoxides with Red-Al. (b) Koide uses Red-Al to reduce gamma hydroxy alkynoic esters selectively

While not the result we were hoping for, it did give us an idea – using the alcohol as a tether could allow for selective 1,4-reduction. Gamma and delta alcohols have been used as directing groups for 1,4-reductions using LAH.¹³ However, these reactions are highly sensitive and prone to overreduction due to the four equivalents of hydride available for each equivalent of reductant added. Based on this, we decided to attempt the reduction using Red-Al, a reducing agent with only two hydrides. In 1982, Kishi showed that Red-Al could be used to selectively open allyl-alcohol epoxides such as **3.41** to 1,3-diols (**3.42**), giving the opposite selectivity of single hydride reducing agents like DIBAL-H which gave the 1,2-diol like **3.43** preferentially (Scheme 3.9a).¹⁴ The first hydride serves to rapidly deprotonate the alcohol, whereupon the aluminum coordinates to the resulting alkoxide. As the aluminum is tethered to the alcohol, the subsequent reduction can only occur at the adjacent position, as the hydride is unable to reach the further carbon. In 2004, Koide and coworkers showed that Red-Al, for similar reasons, is able to reduce gamma-hydroxy alkynoic esters to the corresponding gamma-hydroxy alkenoic esters in a trans-selective fashion

¹³ Overman, L. E.; Ricca, D. J.; Tran, V. D. *J. Am. Chem. Soc.* **1993**, *115* (5), 2042–2044.

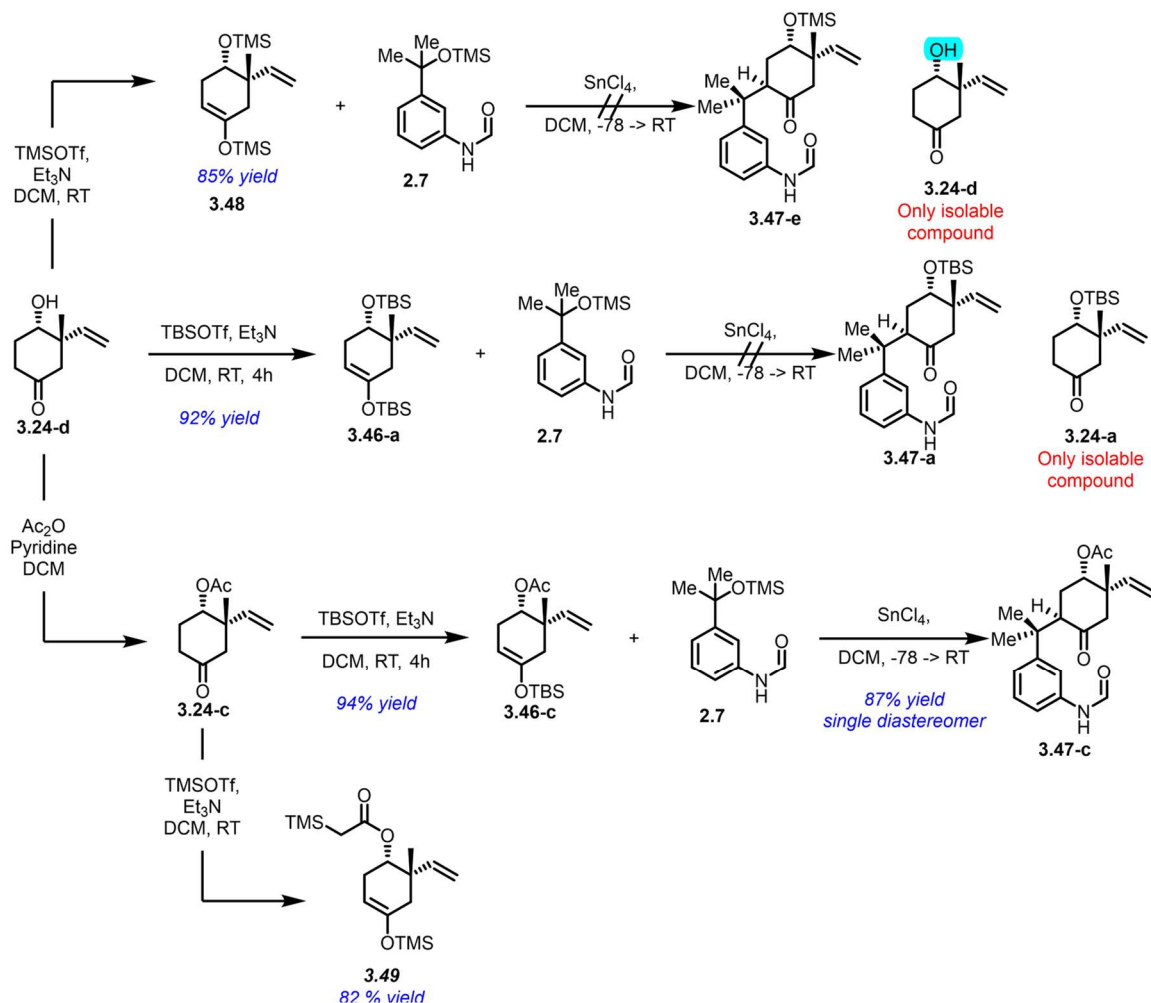
¹⁴ Finan, J. M.; Kishi, Y. *Tetrahedron Lett.* **1982**, *23* (27), 2719–2722

(Scheme 3.9b).¹⁵ Here, the coordination to the alcohol precludes 1,2-reduction due to the distance. In both cases, no over-reduction is observed, and, in fact, the reactions proceed cleanly and rapidly at temperatures far lower than what is often necessary for equivalent LAH reductions. Although Koide showed that the reduction of gamma-hydroxy alkenoic esters to the corresponding fully saturated ester also proceeded cleanly, the corresponding reaction with gamma-hydroxy alpha,beta-unsaturated enones remains uninvestigated.

In order to test this reaction, we needed to obtain the de-acetylated alcohol **3.40**. Based on our results while accidentally forming the deacetylated alkyne **3.36**, we knew that K₂CO₃ in methanol provided a reliable method for rapidly hydrolyzing the ester. However, on this substrate, the desired compound was obtained in only 20% yield, the remainder of the mass balance most likely having been lost to polymerization. The reaction was slowed by diluting the methanol with Et₂O, which thankfully lead to a dramatic decrease in the presumed polymerization, thereby increasing the yield of the desired alcohol **3.40** to greater than 90%. With the alcohol in hand, we were able to examine the Red-Al reduction. The substrate was dissolved in THF and cooled to -78°C, whereupon a slight excess of Red-Al was added. Remarkably, after only 5 minutes, the reduction was finished, with a complete selectivity for the desired ketone **3.24-d**. Although outside of the scope of this thesis, this impressive selectivity is notable and warrants further investigation.

After obtaining ketone **3.24-d**, the final steps necessary before attempting the Friedel-Crafts reaction were to re-protect the alcohol and install the silyl enol ether. We opted to do this in a single step by protecting the alcohol as a TBS silyl ether. The silylation was carried out uneventfully by treating the ketone in DCM with TBSOTf and triethyl amine. The silyl enol ether

¹⁵ Meta, C. T.; Koide, K. *Org. Lett.* **2004**, 6 (11), 1785–1787.

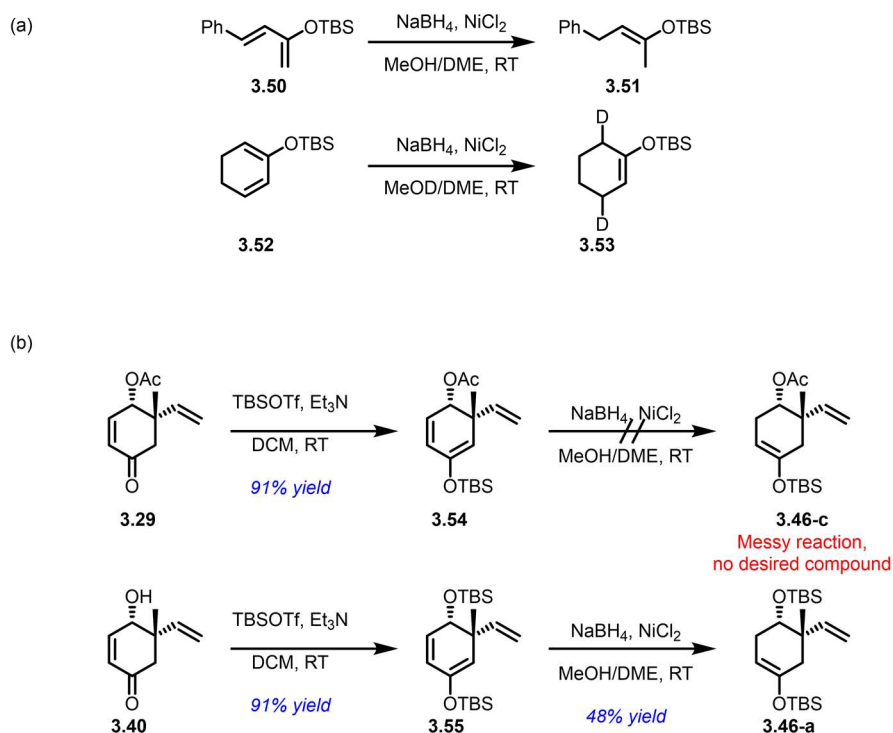


Scheme 3.10. Analysis of the Friedel-Crafts reaction with various protecting groups on the alcohol.

formed within 30 minutes, and after three hours the disilylated product **3.46-a** was isolated cleanly as a single regioisomer. Unfortunately, subjecting this compound to the optimized Friedel-Crafts conditions, using SnCl₄ and benzylic silyl ether **2.7** (Chapter 2.1), gave none of the desired product. Instead, the TBS-protected ketone **3.24-a** was the only product, with the benzylic silyl ether having completely decomposed. The outcome was the same when run with TiCl₄ as the Lewis acid, as well as when benzylic alcohol **2.3** was used as the electrophilic partner. Thinking that the bulk of the TBS was somehow at fault, the bis-TMS silyl enol ether **3.48** was also prepared via the same

protocol. Unfortunately, this substrate fared no better, and the only compound isolated was **3.24-d**, which had undergone cleavage of both TMS groups.

With the silyl-protected alcohols seeming to not work for the Friedel-Crafts reaction, we decided to look at other potential protecting groups. The obvious first choice was acetylation, so the acetate was reinstalled using acetic anhydride and pyridine, giving ketone **3.24-c** in good yield. Silylation with TBSOTf proceeded cleanly to give silyl enol ether **3.46-c** as a single regioisomer. Surprisingly, the same reaction, when run with excess TMSOTf, gave silyl enol ether **3.49**, which had been silylated on the acetate alpha carbon. This interesting reaction does not appear to have been reported in the literature, but it was not pursued further. The Friedel-Crafts reaction between **3.46-c** and **2.7** was performed using the standard conditions. While no reaction was observed overnight at -78°C , warming the reaction to room temperature over the course of twelve hours led



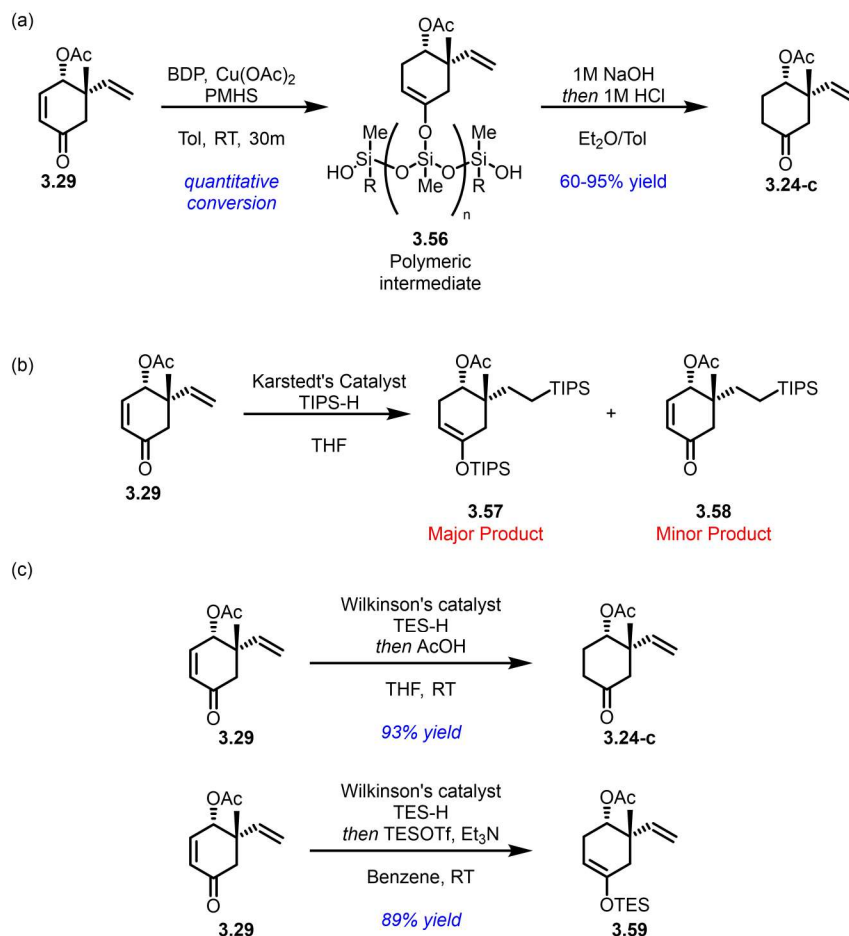
to the desired compound **3.47-c** in a fantastic 87% yield. Notably, only a single diastereomer was observed, although there was some decay if care was not taken during workup. This surpassed expectations based on A values and results seen during the synthesis of the welwitindolinones. It also served to put to rest the worries about having to replace the vinyl group with an alkyne in order to increase selectivity, and suggested that there may be some extra intramolecular interaction between the anilide and acetate that facilitates the reaction.

Having found the acetate to be a good choice of protecting group, we decided to return to the issue of the conjugate reduction with the goal of avoiding the step-intensive and circuitous removal and reinstallation of the acetate. Knowing that aluminum- or boron-based hydride reagents were unlikely to be successful, we instead looked to less-traditional ways to enact the reduction, either to the ketone or to a silyl enol ether directly.

One approach that seemed promising was to do, in essence, a 1,4-reduction of diene **3.19**. In 2011, the Yin lab reported a unique procedure that allowed such electron rich siloxy dienes to be reduced to the internal silyl enol ether by using catalytic NiCl₂ and sodium borohydride in methanol.¹⁶ To test this on our system, we prepared **3.54** from ketone **3.29** using standard silylation conditions in good yield. Unfortunately, subjection of **3.54** to Yin's reported conditions led to a messy reaction that yielded none of the desired product. This outcome was somewhat expected, given that Yin had reported the same conditions to be effective at removing allylic acetoxy groups. However, when the same reaction was performed on diene **3.55**, prepared by di-silylation of allylic alcohol **3.40**, silyl enol ether **3.46-a** was formed in moderate yield, along with some unidentified

¹⁶ Yin, B.-L.; Cai, C.-B.; Lai, J.-Q.; Zhang, Z.-R.; Huang, L.; Xu, L.-W.; Jiang, H.-F. *Adv. Synth. Catal.* **2011**, 353 (18), 3319–3324

side products. While this outcome is worth noting, we knew this product **3.46-a** was not going to be of use for the synthesis (*vide supra*), so the reaction was not optimized further.



Scheme 3.12. Analysis of different silane-promoted enone reduction conditions (a) Using Lipshutz's "hot" Stryker's reagent. (b) Using Karstedt's catalyst. (b) Using Wilkinson's catalyst and a silylative or desilylative workup

A slightly more typical approach to conjugate reduction is to use copper hydrides. While Stryker's reagent is known to have difficulty with more sterically hindered substrates, Lipshutz and coworkers reported a "hot" Stryker's reagent that was able to reduce highly hindered substrates with remarkable selectivity for the 1,4-reduction and with far lower catalyst loadings.¹⁷ The reaction uses bis-diphenyl phosphino benzene (BDP) as a ligand and copper acetate as the catalyst,

¹⁷ Baker, B. A.; Bošković, Ž. V.; Lipshutz, B. H. *Org. Lett.* **2008**, *10* (2), 289–292.

with the copper hydride generated and regenerated in situ from PMHS. Subjection of eneone **3.29** to Lipshutz's conditions indeed led to rapid reduction, even with catalyst loadings as low as 0.1%. Unfortunately, the workup of the reaction proved difficult, especially on scaleup. The polymeric silyl enol ether **3.56** that is formed during the reaction needs to be cleaved using strong base or acid, which led to some decomposition of the acetate. In addition, the reaction was not reliable: on larger scales, the reaction would sometimes fail, with no product being observed and the copper catalyst crashing out of solution. We attributed this to the PMHS used, as the failure tended to occur when using older bottles or PMHS of larger polymer size. However, on one such occasion using a large polymer, workup with 1M sodium hydroxide solution led to immediate and complete formation of the desired compound, leading us to suspect that some sort of activation of the PMHS was necessary to kick-start the reaction. Lipshutz had reported that added tert-butanol would accelerate the reaction, which may be playing a similar role. Unfortunately, this trick could similarly not be reliably reproduced, so we again decided to look for conditions that would allow for scalable and reproducible success without the difficult workup that this reaction posed.

Next, we turned to transition metal-promoted hydrosilylation conditions that could allow for direct access to the silyl enol ether. One possible catalyst for the reduction is Karstedt's catalyst. In a 1994 publication, Johnson showed that Karstedt's catalyst could be used for hydrosilylation of eneones to give TIPS silyl enol ethers, while being tolerant of allylic acetates.¹⁸ Unfortunately, although perhaps unsurprisingly, the hydrosilylation of the enone was outcompeted by the hydrosilylation of the vinyl group, leading to formation of **3.57** as the main product when run with an excess of silane. Another potentially useful catalyst was Wilkinson's catalyst, which was shown

¹⁸ Johnson, C. R.; Raheja, R. K. *J. Org. Chem.* **1994**, *59* (9), 2287–2288.

by Ojima to be highly selective for the 1,4-reduction of α,β -unsaturated ketones and aldehydes.¹⁹ Subjecting ketone **3.29** to Ojimas conditions (1% catalyst in THF at 50 °C) unfortunately led to decomposition. Fortunately the situation was improved by simply running the reaction at room temperature which led to a 1:1 mixture of TES silyl enol ether **3.59** and the ketone **3.24-c**. Workup with acetic acid converted the mixture to solely **3.24-c**. Alternatively, when the reaction was run in toluene, addition of triethyl amine and TESOTf enabled the formation and isolation of **3.59** as a single product. Ultimately, we chose to use the acid workup, as the TES silyl enol ether performed worse on the Friedel-Crafts reaction than did the TBS silyl enol ether.

3.2 Studies on the formation of the enol triflate

With a reliable and scalable route to the necessary D ring fragment and a working Friedel-Crafts reaction, we were now ready to move forward with the synthesis. Following the strategy from our synthesis of dechlorofontonamide (Chapter 2), the next step was to install the enol triflate. In that synthesis, we had employed an *in situ* protecting group strategy wherein the formanilide was converted into a silyl formimidate using NaHMDS and TBSCl. Then, in the same pot, the upper ring was deprotonated and triflated before hydrolysis led to a return of the formanilide. Unfortunately, when **3.47-c** was subjected to the same conditions, none of the desired product was formed. While monitoring the reaction by NMR, it was observed that the silyl formimidate formed rapidly, but subsequent addition of NaHMDS evidently failed to deprotonate the upper ring. This outcome can be attributed to the axial nature of the acetate group, which could block the approach of a bulky base to the axial alpha hydrogen that must be deprotonated to form the enolate (Figure 3.1).

¹⁹ Ojima, I.; Kogure, T. *Organometallics* **1982**, *1* (10), 1390–1399

In order to solve this problem, we decided to remove the complication of the formamide group and *in situ* protection by protecting the formamide with a Boc group. Simple stirring of **3.47-c** with Boc anhydride and DMAP led to complete formation of Boc anilide **3.61**. With this substrate in hand, we began to investigate possible routes to the enol triflate **3.60**. Knowing that deprotonation of the ketone was difficult, we first decided to look at “soft” enol triflate forming conditions, namely triflic anhydride and an amine base in DCM. While the initial worry was that this would lead to formation of only the undesired thermodynamically-favored enol triflate, it turns out there was a bigger issue: addition of the triflic anhydride led to rapid decomposition of both the Boc anilide and the acetate groups. A short screen of other solvents and bases confirmed that this was not going to be a viable route, with all procedures leading only to complete destruction of the starting material.

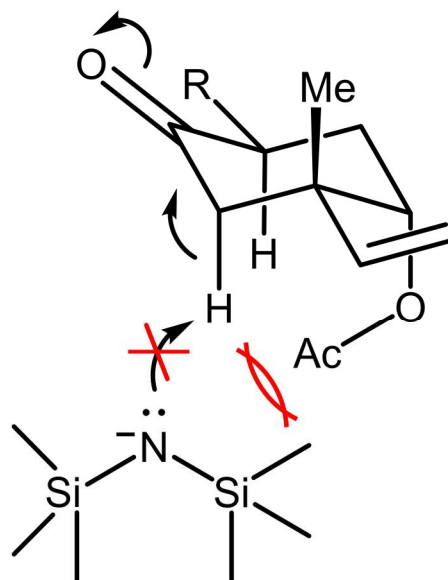
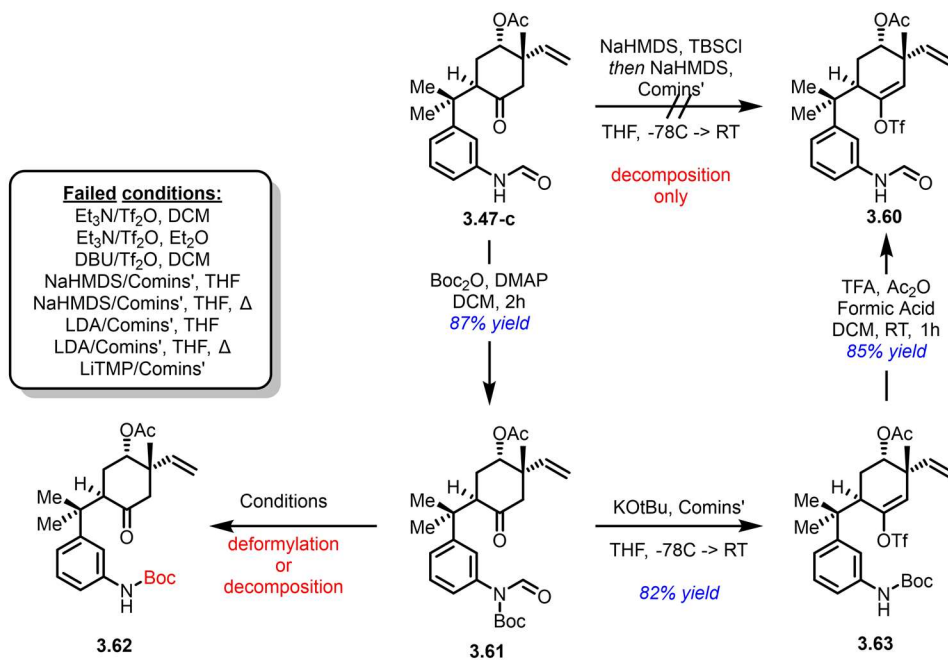


Figure 3.1 Steric hindrance from the acetate-protected alcohol slows deprotonation of the alpha hydrogen by bulky amide bases



Scheme 3.13. Failed and successful routes to the enol triflate

Returning to the classic enol triflate formation conditions, we began to look into ways to increase the amount of enolate formed. The first thing tried was heating the reaction. NaHMDS was added at low temperatures, and the reaction was then heated to 50 °C for one hour before the reaction was cooled back to zero and Comin's reagent was added. Unfortunately, the only new product observed was the de-formylated Boc aniline **3.62**. Careful monitoring of the reaction indicated that deformylation occurs rapidly upon addition of the base, even at temperatures as low as -40 °C. Considering that this deformylation consumes one equivalent of the base, the reaction was repeated with two equivalents of NaHMDS. Unfortunately, the desired compound was still not produced. Extended heating with two equivalents of base led to deprotection of the acetate, likely through deprotonation-mediated ketene formation.

The complications observed during attempts to form the required triflate using HMDS bases motivated the examination of stronger bases, in particular LDA. Miraculously, when the

reaction was performed on a 0.1 mmol scale with two equivalents of LDA, allowing the reaction to warm to 0 °C prior to the addition of Comin's reagent, the desired compound was formed in high yield. Unfortunately, when the reaction was scaled up to 1 mmol, the yield dropped to less than 10%, with only other isolable product being the deformedylated **3.62**, in less than 25% recovery. Puzzlingly, the yield remained low even when the reaction was reformed on a small scale. All manipulatable variables (solvent, concentration, temperature, equivalents, and freshness and origin of reagents) were systematically examined, but it was not possible to replicate the initial result. In order to check if the enolate was actually being formed, the reaction was allowed to stir at room temperature for one hour, then was quenched with D₂O. As expected, none of the deuterated compound was observed, indicating that the intended initial deprotonation had never occurred, presumably due to the steric interference of the co-axial acetate group. In an attempt to overcome this problem, we also examined the use of LiTMP, which is known to be uniquely effective with some sterically hindered substrates.²⁰ However, the result was the same as when using LDA, with **3.62** being the only product formed.

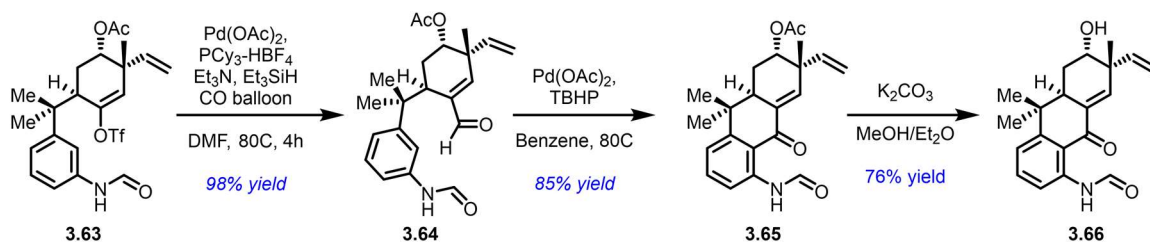
With neither the weak amine bases or bulky amide bases proving to be of use, it seemed necessary to use a base in the middle—something that would be strong enough to form the enolate, while still being less bulky than LDA and LiTMP. We settled on KOtBu, which, although recognized as a bulky base, is expected to exhibit significantly less steric interaction with the acetate group, as the singular alkyl chain can be rotated away from the ring. We also believed that the lower pK_a of the base would have the added benefit of minimizing deprotonation of the acetate, thereby lowering ketene-mediated decomposition. Thankfully, this intuition proved fruitful, and

²⁰ Two examples where reaction with LiTMP cleanly gave products that were inaccessible using LDA (a) Shiner, C. S.; Berks, A. H.; Fisher, A. M. *J. Am. Chem. Soc.* **1988**, *110* (3), 957–958 (b) Smith, A. B.; Richmond, R. E. *J. Org. Chem.* **1981**, *46* (23), 4814–4816.

simple stirring of Boc-anilide **3.61** with excess K_{Ot}Bu at -78 °C for one hour led to complete formation of the enolate, as evidenced by D₂O quenching. Addition of Comins' along with the base at -78 °C, and allowing the reaction to warm to room temperature slowly, afforded **3.63** cleanly and in remarkably high yield. As was observed with the amide bases, the product was still mostly deformylated. Happily, we were able to restore the formyl group and remove the Boc group in one step by reacting the product with *in situ*-generated mixed formic acetic anhydride followed by TFA, giving enol triflate **3.60** in good yield.

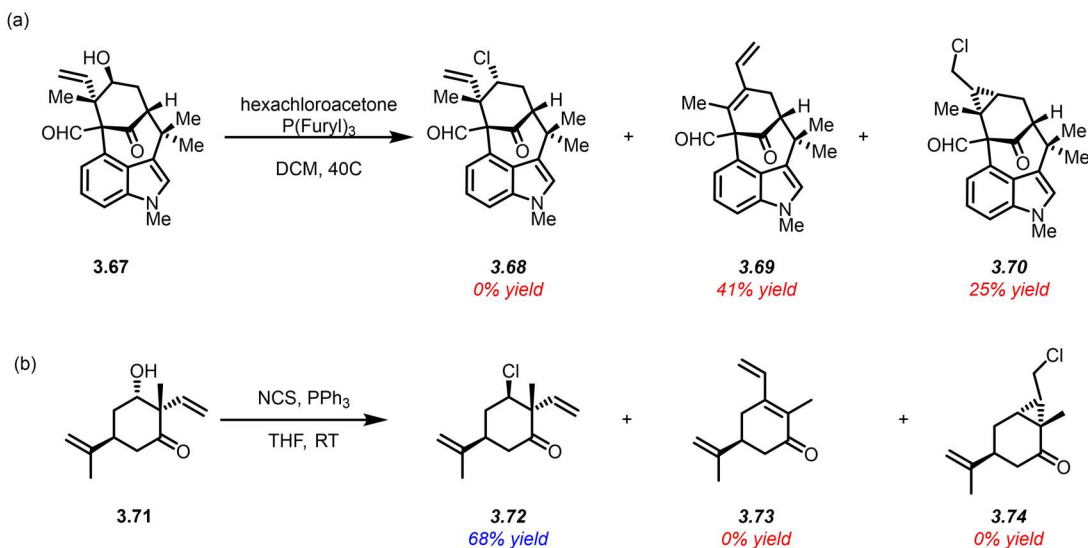
3.3 Completion of the Synthesis of (-)-Fontonamide

With a reliable and scalable route to enol triflate **3.60** in place, we were now poised to enter the end game of the synthesis. Using the same chemistry developed for the synthesis of dechlorofontonamide, the carbonylation of enol triflate proceeded smoothly, giving aldehyde **3.64** in high yield. The next step, palladium mediated cyclization, was lower yielding, with a large amount of a side product that was tentatively assigned to be epoxidized at the vinyl group, the equivalent of which hadn't been observed in the previous synthesis due to the absence of the vinyl at this stage. However, by switching the catalyst from Pd(TFA)₂ to Pd(OAc)₂ and carefully monitoring the progress of the reaction, it was possible to avoid the formation of the side product and obtain the cyclized **3.65** in good yield as a single compound. Again, it is notable that this cyclization occurs solely intramolecularly at the position ortho to the anilide, with no observable para-cyclization or polymerization products. De-acetylation to give **3.66** was conducted using K₂CO₃ in 10% methanol/90% ether in order to avoid de-formylation.



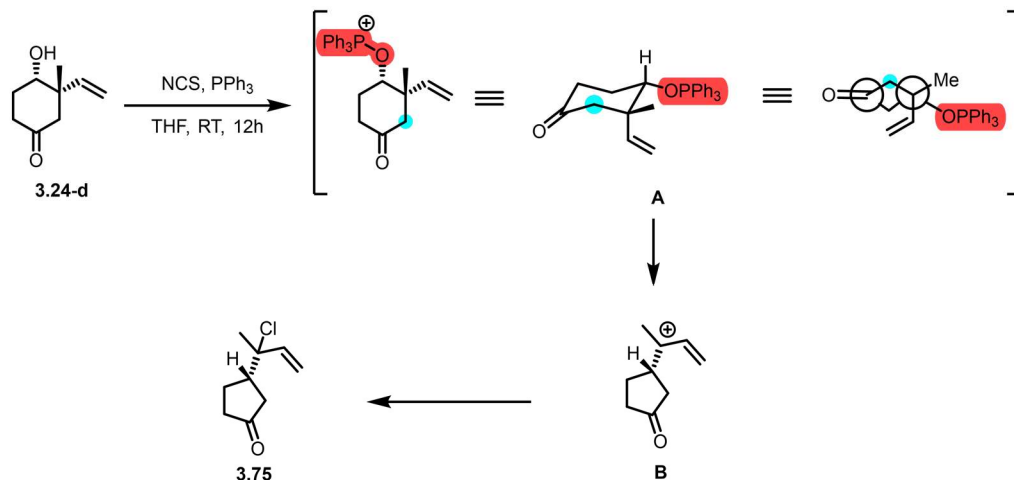
Scheme 3.14. Carbonylation and cyclization followed by de-acetylation

The final step required to transform **3.66** to fontonamide is a stereoinvertive chlorination at the C-13 position. This step had proven difficult in the lab's syntheses of the welwitindolinones, with typical conditions leading to rearrangements. Efforts by Bhat and Rawal had found that the difficulty was due in part to interference from the vinyl group in alcohol **3.67**, which stabilized the fleeting carbocation intermediate through anchimeric assistance, thereby allowing the formation of rearrangement products **3.69** and **3.70**.^{1,21} Hydrogenation or hydro-silylation of the double bond, both of which removed this cyclization potential, allowed formation of the chloride. Interestingly, en route to ambigune G, Hu and Rawal found that a similar stereoinvertive chlorination on alcohol



Scheme 3.15. (a) Undesired rearrangement of the trans vinyl/alcohol in Rawal's synthesis of welwitindolinone B. (b) Desired chlorination of the cis vinyl/alcohol in Rawal's synthesis of ambigune G.

²¹ Bhat, V.; Rawal, V. H. *Chem. Commun.* **2011**, 47 (34), 9705–9707.

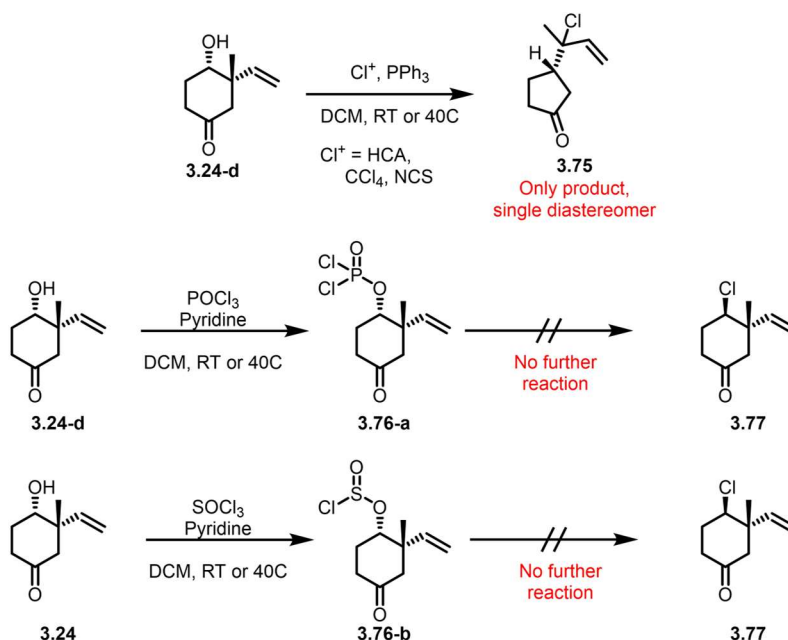


Scheme 3.16. Rearrangement of alcohol **3.24-d** in Favorskii-like reaction

3.71 worked well.²² Mixing **3.71** with PPh₃ and NCS gave chloride **3.72** in good yield, with no formation of the internally cyclized product. While both examples involved a hydroxyl group adjacent to a quaternary center bearing a vinyl substituent, they differed in the relative stereochemistry of the hydroxy group and the vinyl – in the welwitindolinone substrate the two were *trans*, while in the substrate used for the ambiguline synthesis the two were *cis*. We hypothesized that the cyclization occurred through an intra-molecular S_N2-type mechanism, which required the *trans* relationship. As the hydroxy group in **3.65** is *cis* to the vinyl, we predicted the cyclization would not be an issue.

However, before subjecting the precious late-stage material to possibly destructive chlorination conditions, it was important to first confirm the hypothesis on a simpler substrate. As alcohol **3.24-d** was already accessible, it represented an ideal place to start. Thus, alcohol **3.24-d** was subjected to the same conditions used by Hu and Rawal for the synthesis of **3.72**. Surprisingly,

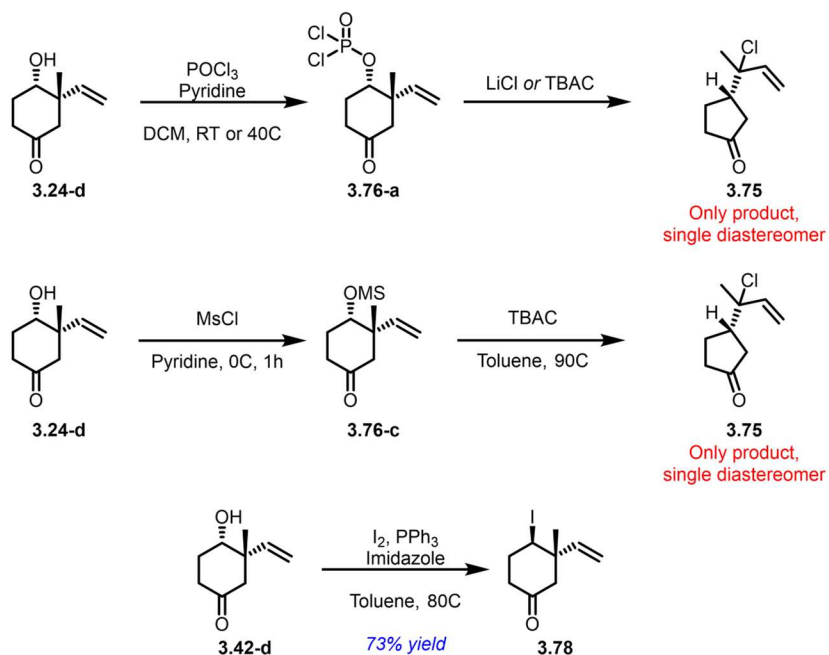
²² Hu, L.; Rawal, V. H. *J. Am. Chem. Soc.* **2021**, *143* (29), 10872–10875.



Scheme 3.17. Analysis of different leaving groups for the attempted chlorination reaction

neither the vinyl cyclization product nor the desired chloride **3.77** was formed – instead, the major product was chloride **3.75**, which had gone through a ring contractive-rearrangement to give the stabilized tertiary and allylic carbocation **B** followed by chlorination (Scheme 3.16). This was surprising, especially given the structural similarity between **3.24-d** and Hu’s **3.71**, but the result can be understood by considering the chair conformation and Newman structures of the activated intermediate **A**. The carbon adjacent to the ketone is situated antiperiplanar from the oxyphosphonium leaving group, allowing easy rearrangement in a Favorskii-like manner to give the stabilized carbocation. Such rearrangement was not possible in Hu’s substrate, explaining the different outcome.

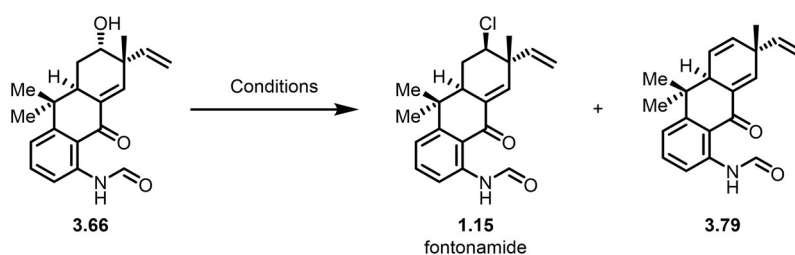
Other typical chlorination procedures also failed to give the desired compound. Initial studies were focused on other conditions that used PPh_3 along with an alternative chloronium source such as CCl_4 or hexachloroacetone (HCA). Unfortunately, these conditions invariably led



Scheme 3.18. Use of different nucleophile sources for the chlorination and iodination reactions to formation of **3.75**. In order to avoid this undesired cyclization, two possibilities were considered; namely, increasing the strength of the nucleophile, and decreasing the leaving group ability, both of which should move the reaction in the desired direction. Starting with the latter, **3.24d** was treated with POCl_3 and pyridine. This led to rapid formation of the intermediate **3.76-a**, as determined by NMR monitoring. However, no further reaction was seen, even upon extended heating. The same trend was observed with SOCl_2 – rapid formation of the intermediate **3.76-b**, but no further reaction. This implied that the weakness of the chloride nucleophile was responsible for the lack of chlorination. While the raw nucleophilicity of the chloride anion couldn't be increased, it was possible to increase its concentration, which was done by adding LiCl or tetra-butyl ammonium chloride (TBAC) to the reactions. Unfortunately, mixing either of these chloride sources with **3.24-d** and POCl_3 once again led to no reaction beyond the formation of **3.76-a**. Finally, we synthesized mesylate **3.76-c** as an intermediate strength electrophile and heated it with

tetra-butyl ammonium chloride. Unfortunately, no reaction was observed at room temperature, and extended heating led solely to the formation of **3.75**. To confirm that the low nucleophilicity of the chloride anion was at fault, **3.24-d** was subjected to stereoinvertive iodinating conditions. **3.24-d** was heated with I₂, PPh₃, and imidazole, and iodide **3.78** was isolated in good yield, supporting the notion that the failure to form **3.77** was due primarily to the chloride anion.

While none of these reactions succeeded in giving us the desired chloride **3.77**, these results were also not entirely bad. Our main hypothesis, that the *cis* relationship between the hydroxy and vinyl group would avoid the internal cyclization, did appear to be valid. Additionally, the hydroxy in **3.66** was expected to sit in a pseudo-axial arrangement, which should allow easier displacement by the chloride. Finally, as the stereoelectronics of **3.66** preclude the ring-contraction, we were hopeful that the chlorination would be more successful.



Phosphine	Chloronium	Solvent ^a	Additive	Temp	Yield A	Yield B
PPh ₃	NCS	THF	None	RT	0%	100%
P(furyl) ₃	HCA	DCM	None	40°C	16%	84%
PPh ₃	HCA	DCM	None	40°C	12%	88%
PPh ₃	HCA	toluene	None	40°C	0%	0%
P(furyl) ₃	HCA	toluene	None	40°C	25%	75%
P(furyl) ₃	HCA	hexane	None	40°C	0%	0%
P(furyl) ₃	HCA	toluene ^b	None	40°C	35%	65%
P(furyl) ₃	HCA	toluene ^b	LiCl	40°C	0%	0%
P(furyl) ₃	HCA	toluene ^b	TBAC	40°C	0%	0%

^a Unless otherwise indicated, reactions run at 0.05 M concentration

^b Run at 0.2 M concentration

Table 3.3. Optimization of chlorination conditions

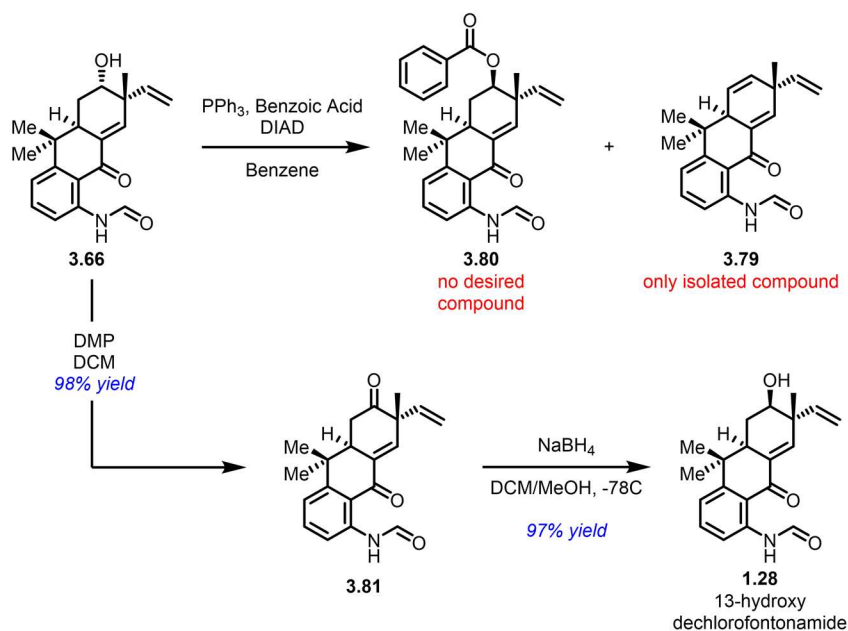
The first conditions we tried were those employed by Hu during the synthesis of ambiguine G; PPh₃ and NCS in THF. Unfortunately, these conditions led cleanly to the formation of a new

type of undesired compound, the elimination product **3.79**. The reaction was then attempted using P(Furyl)₃ and HCA in DCM, which were the conditions employed by Bhat en route to welwitindolinone B. While **3.79** was still the major product, a small amount of the desired chloride, i.e. the natural product fontonamide, was formed, with an approximately 5:1 ratio of products, or a 16% yield. We then looked for ways to slow down the elimination, which was believed to take place through an E1 mechanism due to the lack of a strong base in the system. As phenyl groups are less electron withdrawing, the oxophosphonium of PPh₃ is expected to be a weaker leaving group. However, the product mix was approximately the same, although considerably slower. We then looked at solvents, deciding to switch to toluene in order to destabilize any possible carbocation intermediate. No reaction was observed when using PPh₃, due to the intermediate oxophosphonium being insoluble. However, with P(furyl)₃, the reaction proceeded cleanly, and gave the desired compound in a higher ratio of 3:1, up to a 25% yield. Unfortunately taking this one step further and using hexane led to no reaction, again likely due to insolubility of one of the intermediates. Given that the chlorinative inversion is a bimolecular reaction, it stood to reason that increasing the concentration of the chloride anion would lead to more of the desired compound. We attempted to increase the concentration of the chloride anion further by adding in LiCl and TBAC; however, both surprisingly completely shut down reactivity, giving only starting material even after sustained heating. We also looked at increasing the concentration of the reaction as a whole. Increasing the concentration from 0.05M to 0.2M led to a modest increase in yield up

to 35%, with the residual mass balance being the elimination product **3.79**. Although this result could likely be optimized higher, we decided to focus our attention and remaining material on the completion of the synthesis of 13-hydroxy dechlorofontonamide. In summary, this represents the first synthesis of fontonamide, accomplished in 13 steps from commercially available starting material, with an overall yield of 6.5%. As we have also identified a method for obtaining the starting material in an enantioenriched form, this can also be considered a formal asymmetric synthesis of (-)-fontonamide.

3.4 Synthesis and Structural Revision of 13-Hydroxy Dechlorofontonamide

With alcohol **3.66** in hand, the last step to 13-hydroxy dechlorofontonamide was an inversion of the C-13 alcohol. This was first attempted through a Mitsunobu reaction, and **3.66** was exposed to DIAD and triphenyl phosphine along with benzoic acid. Unfortunately, as with the initial chlorination procedures, this led only to formation of the elimination product **3.79**. The



Scheme 3.19. Failed Mitsunobu reaction and successful oxidation/reduction

reaction was then re-run using para-nitro benzoic acid, which is known to increase the yield of Mitsunobu reactions on highly sterically hindered substrates.²³ However the result was the same—only slow conversion to **3.79**.

Given the difficulty encountered when attempting to optimize this reaction for the chlorinative stereoinversion, we decided to try a different route. Structural analysis of ketone **3.81** suggested that the methyl at C-12 and one of the two methyls on C-16 would both be pointing axially (Figure 3.2). This would hinder the approach of a nucleophile, and therefore should cause

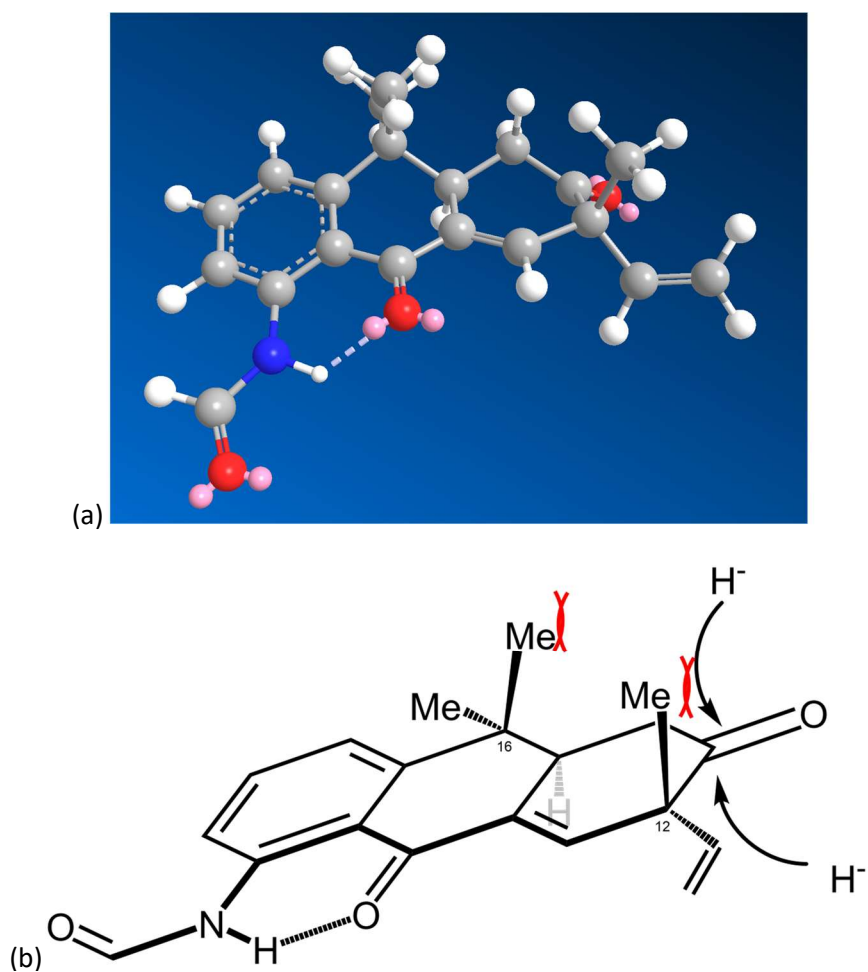


Figure 3.2. (a) Predicted 3d structure of ketone **3.81**. (b) The angle of approach from above the plane of the ketone is blocked by two methyl groups.

²³ Martin, S. F.; Dodge, J. A. *Tetrahedron Lett.* **1991**, 32 (26), 3017–3020

reduction to occur from the bottom face. To test this hypothesis, we first oxidized alcohol **3.66** with DMP, giving ketone **3.81** cleanly and in high yield.²⁴ The ketone was then dissolved in 1:1 DCM:MeOH and exposed to NaBH₄ at -78°C, following Ward's procedure for selective reduction of ketones in the presence of eneones.²⁵ After only 15 minutes the reaction was complete, and the product was isolated as a single diastereomer. However, while the isolated compound was distinct from alcohol **3.66**, it did not match the NMR shifts for 13-hydroxy dechlorofontonamide reported by Orjala and coworkers in their isolation paper in 2012.²⁶ A full spectroscopic analysis of the new product confirmed that we had made the desired compound **1.28**, suggesting that the reported structure for 13-hydroxy dechlorofontonamide may be incorrect. Notably, the hydrogen at C-13 in our samples had a chemical shift of 3.84 ppm for both alcohol **3.66** and **1.28**, while the same hydrogen was reported at 4.05 ppm for 13-hydroxy dechlorofontonamide, and 4.07 ppm for fontonamide. We had found it the proton to be at 4.08 ppm in our synthetic sample of fontonamide. Chemical shifts at C-14, C-19, and C-21 also showed significant discrepancies between our results and those reported by Orjala (Table 3.4). This prompted us to compare the other reported chemical shifts for 13-hydroxy dechlorofontonamide and fontonamide, as reported by Moore in 1987.²⁷ In every instance, the hydrogen chemical shifts were within 0.03 ppm, and, even more strikingly, every carbon shift was within 0.5 ppm (See Chapter 6 for a full comparison). Further, the coupling constants are nearly identical where reported. We therefore propose that the compound isolated by Orjala in 2012 was misidentified as containing a hydroxy, and was actually fontonamide. The

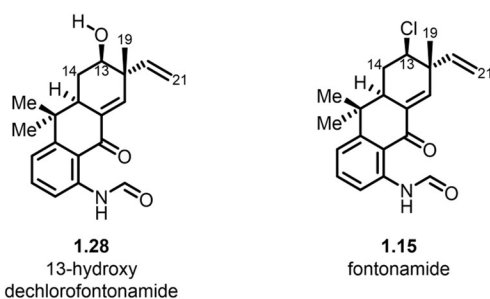
²⁴ Reisman, S. E.; Ready, J. M.; Weiss, M. M.; Hasuoka, A.; Hirata, M.; Tamaki, K.; Ovaska, T. V.; Smith, C. J.; Wood, J. L. *J. Am. Chem. Soc.* **2008**, *130* (6), 2087–2100.

²⁵ Ward, D. E.; Rhee, C. K.; Zoghaib, W. M. *Tetrahedron Lett.* **1988**, *29* (5), 517–520.

²⁶ Kim, H.; Lantvit, D.; Hwang, C. H.; Kroll, D. J.; Swanson, S. M.; Franzblau, S. G.; Orjala, J. *Bioorg. Med. Chem.* **2012**, *20* (17), 5290–5295

²⁷ Moore, R. E.; Yang, X. Q. G.; Patterson, G. M. L. *J. Org. Chem.* **1987**, *52* (17), 3773–3777.

original assignment was based in part on the lack of a chlorine in the parent ion of the compounds mass spectrum. However, electron spray ionization mass spectrometry conditions are known to be able to cleave carbon-chlorine bonds through alpha cleavage, and it is possible that dechlorination and subsequent hydroxylation occurred during the mass measurement.²⁸ While the compound we made, 13-hydroxy dechlorofontonamide, appears not to be a natural product, its synthesis reaffirms the usefulness of total synthesis as a means for structural confirmation, and provides access to a novel compound that may bear some biological properties.



Carbon #	13-hydroxy this work		"13-hydroxy" Orjala, 2012		Fontonamide Moore, 1988		Fontonamide this work	
	C	H	C	H	C	H	C	H
C13	72.6	3.84	64.8	4.05	64.59	4.071	64.67	4.08
C13-OH		1.69		1.56 ^a				
C14	29.7	2.11	30.8	2.32	30.85	2.336	30.92	2.3 ⁵
		1.83		2.09		2.098		2.11
C19	17.5	1.24	19.9	1.35	19.75	1.31	19.81	1.32
C21	115.5	5.3	115.1	5.20	115.07	5.22	115.17	5.23
		5.27		5.18		5.19		5.20

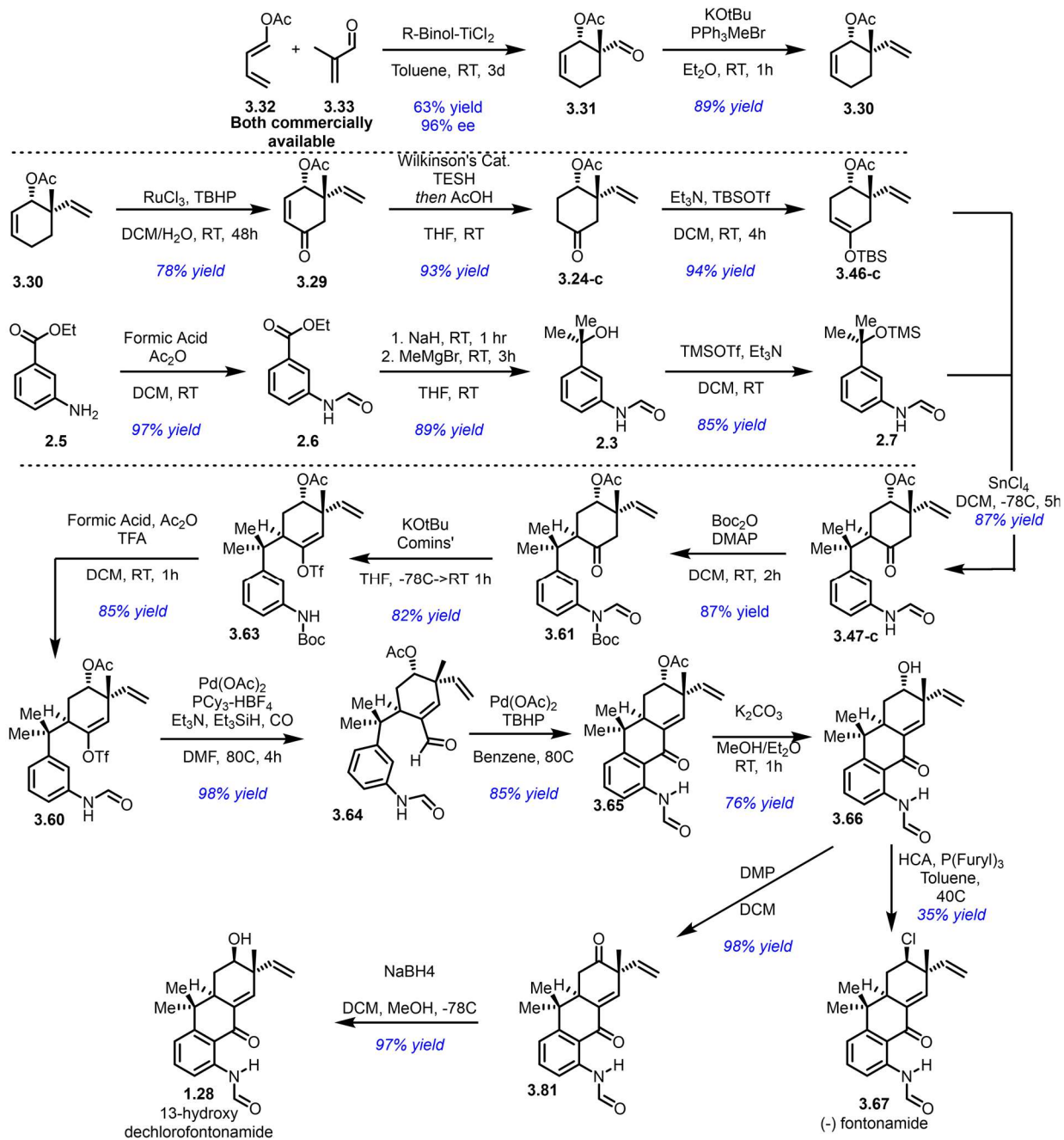
^aThis peak likely corresponds to water in the sample

Table 3.4. Largest discrepancies in NMR shifts between the synthetic sample of 13-hydroxy dechlorofontonamide and the original isolated compound, as well as a comparison to natural and synthetic fontonamide

²⁸ In our hands the parent ion of the chlorinated compound **3.75** was entirely dechlorinated under ESI conditions. Others have seen similar phenomena, including the formation of $[M-Cl+O]^-$ ions. (a) Mass, S. Joanne, MS; Thesis, Dalhousie University, Canada.

3.5 Conclusion

In summary, we have reported the first total synthesis of natural product fontonamide and the first total synthesis and structural revision of 13-hydroxy dechlorofontonamide, which was



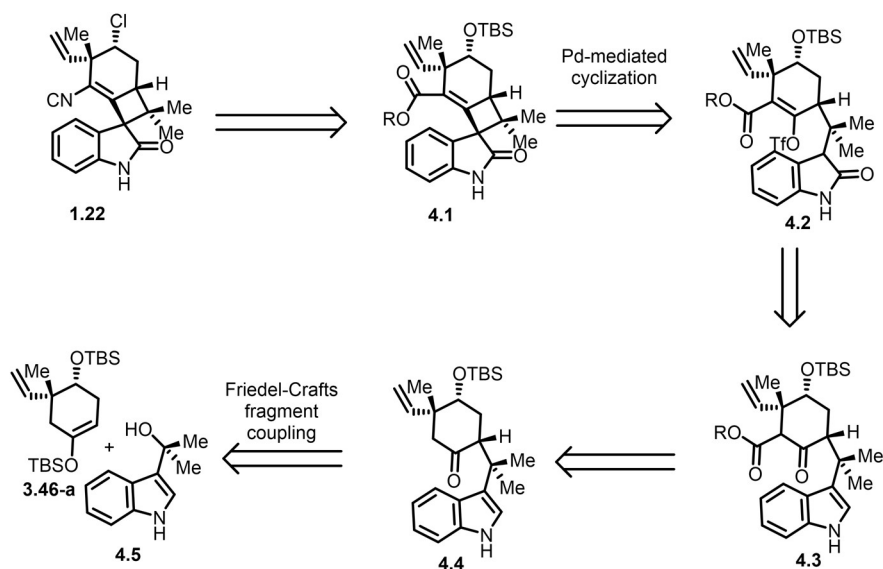
Scheme 3.20. Complete total synthesis of (-)-fontonamide and 13-hydroxy dechlorofontonamide

reported to be a natural product, but appears to have been mis-identified. The former was completed in 13 steps and 6.5% overall yield, while the latter was accomplished in 14 steps and an overall yield of 17.7%. The two compounds were accessed through a common intermediate along a pathway that took advantage of the directing ability of the natural formamide to accomplish a novel intramolecular C-H activation and acylation. While the two compounds were formed as racemates, certain intermediates were synthesized with high ee, allowing access to the enantioenriched final compounds if desired and designating the former route a formal synthesis of (-)-fontonamide.

Chapter 4: Synthetic Studies Toward Welwitindolinone A

4.1 Retrosynthetic Analysis and Model studies

The chemical synthesis of welwitindolinone A was also investigated during the course of the doctoral studies. Isolated in 1988 along with welwitindolinones B and C, welwitindolinone A possesses an intricate skeleton wherein an oxindole is fused to a cyclobutane ring through a spiro linkage. The pursuit of this natural product was of special interest, since the cyclohexene ring within it is analogous to that in fontonamide, and to which a novel, scalable route was developed. (Cf., ketone 3.24-c).¹ Importantly, the double bond on the ring lends itself to a similar strategy to that which had been employed for the synthesis of fontonamide, namely triflate formation and subsequent palladium chemistry. By tracing the molecule back through a late stage introduction of the isonitrile and a stereoretentive chlorination, tetracycle **4.1** is identified as a precursor. Unlike



Scheme 4.1. Retrosynthetic analysis of welwitindolinone A

¹ Stratmann, K.; Moore, R. E.; Bonjouklian, R.; Deeter, J. B.; Patterson, G. M. L.; Shaffer, S.; Smith, C. D.; Smitka, T. A. *J. Am. Chem. Soc.* **1994**, *116* (22), 9935–9942

in fontonamide, the key cyclization would involve a palladium-mediated intramolecular enolate vinylation reaction from the triflate **4.2** to afford the spiro-fused cyclobutane unit, arguably the most challenging part of the molecule. The required triflate would arise from the ketone **4.3**, which could arise from a Friedel-Crafts reaction between benzylic alcohol **4.4** and silyl enol ether **3.46-a**, akin to what was performed in the synthesis of the fontonamides and what Rawal and coworkers had utilized for the synthesis of other members of the welwitindolinone family.²

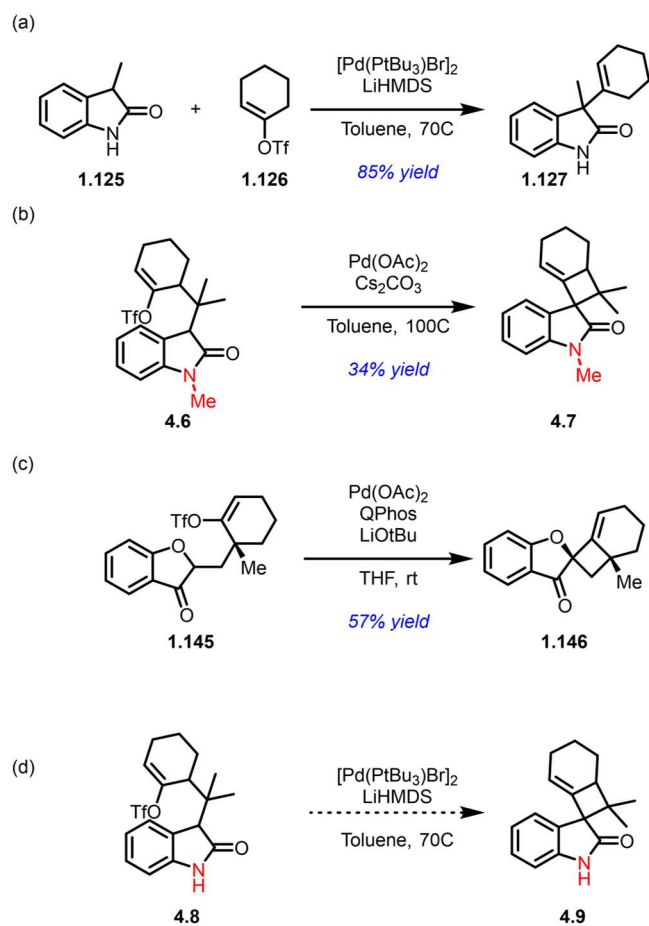
An early example of palladium-mediated alkenylation of an oxindole was accomplished by Huang and coworkers in 2007.³ 3-Methyl oxindole **1.125** was combined with enol triflate **1.126** in the presence of a strong base and catalytic palladium to give the desired compound **1.127** in high yield (Scheme 4.2a). The first intramolecular alkenylation of an oxindole was performed in 2015 by Ferdinand Taenzler, a former member of the Rawal group, who carried out preliminary model studies to evaluate the key step of the above strategy to welwitindolinone A (Scheme 4.2b). The success of the cyclization, although modest yielding, demonstrated the feasibility of the key step in the strategy. The Thorpe-Ingold effect of the gem-dimethyl group was believed to be assisting the otherwise difficult cyclization. More recently, in their elegant total synthesis of phainanoid A, Dong and coworkers successfully formed cyclobutane **1.144** through an intramolecular palladium-mediated vinylation of ketone **4.143** (Scheme 4.2b).⁴ The enolate in this example is of a different type, but their success also illustrates that the cyclobutane is accessible through a palladium-mediated cyclization. Here, too, it is likely that cyclobutene ring formation in **1.144** is being facilitated by the Thorpe-Ingold effect (See chapter 1 for more detail).

² Allan, K. M.; Kobayashi, K.; Rawal, V. H. *J. Am. Chem. Soc.* **2012**, *134* (3), 1392–1395.

³ Huang, J.; Bunel, E.; Faul, M. M. *Org. Lett.* **2007**, *9* (21), 4343–4346.

⁴ Xie, J.; Zheng, Z.; Liu, X.; Zhang, N.; Choi, S.; He, C.; Dong, G. *J. Am. Chem. Soc.* **2023**

Before moving forward with the synthesis of welwitindolinone A, the plan was to examine further the key Pd-catalyzed cyclization reaction on model compounds with an unmethylated oxindole N (scheme 4.2d) or one possessing a removable blocking group. In preparation for the tosyl protected cyclization-precursor, 3-acetyl indole **4.10** was tosylated using sodium hydride and tosyl chloride to afford tosyl indole **4.11** in quantitative yield. Subsequent addition of methyl Grignard gave the tertiary benzylic alcohol **4.12** in high yield. The nucleophilic coupling partner,

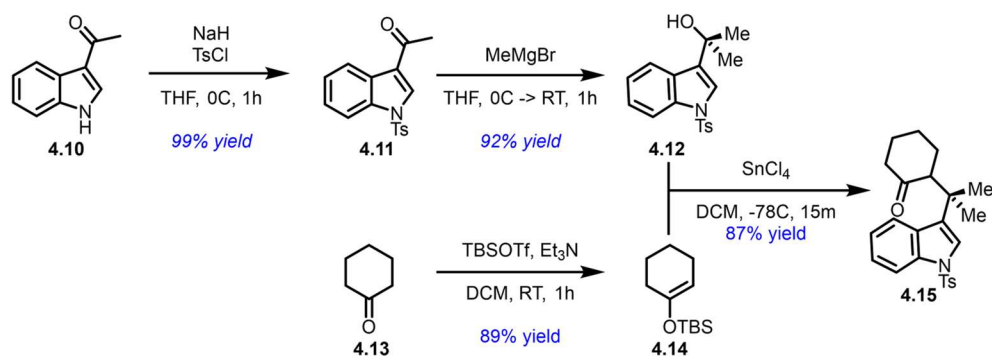


Scheme 4.2 (a) Huang's palladative coupling of an enol triflate and an unprotected 3-methyl indolinone. (b) Taenzler's successful model study on a N-methyl indole (c) A model compound employed by Dong in the synthesis of Phainanoid A (d) the desired free N-H model compound to test

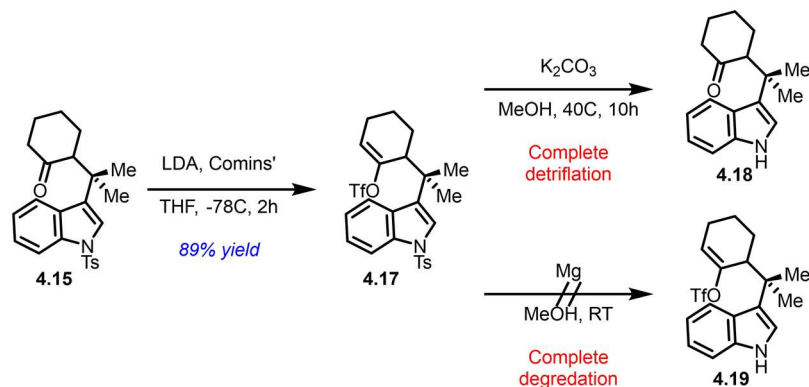
silyl enol ether **4.14**, was made in good yield from cyclohexanone using standard silylation conditions. The two were reacted together using the Friedel-Crafts conditions identified in Chapter

2, giving ketone **4.15** in excellent yield. Unlike the reaction between **3.46-c** and the anilide benzylic alcohol used for the synthesis of the fontonamides (Chapter 3), the coupling reaction was rapidly completed at $-78\text{ }^{\circ}\text{C}$, giving **4.15** in 87% yield within 15 minutes.

The triflate **4.17** was then formed in good yield using LDA and Comins' reagent. However, the subsequent de-tosylation reaction proved difficult. Reductive conditions using magnesium metal in methanol led to complete decomposition, and basic conditions using K_2CO_3 in methanol led to competitive de-triflation, giving ketone **4.18** as the major product. Based on these results, we decided to prepare the Boc-protected indole. Indole **4.10** was protected using Boc anhydride and DMAP, and the resulting compound **4.20** was reacted with methyl Grignard to give tertiary benzylic alcohol **4.21**. Both reactions proceeded cleanly and in high yield, although the glassy nature of **4.21** made its purification difficult. The Friedel-Crafts reaction again proceeded rapidly to give ketone **4.22**, albeit in slightly lower yield, with a significant amount of the dimerized indole **4.23** being formed as a side product. This side product is rapidly formed when **4.21** is exposed to SnCl_4 alone, suggesting that adding additional equivalents of silyl enol ether such **4.14** would be

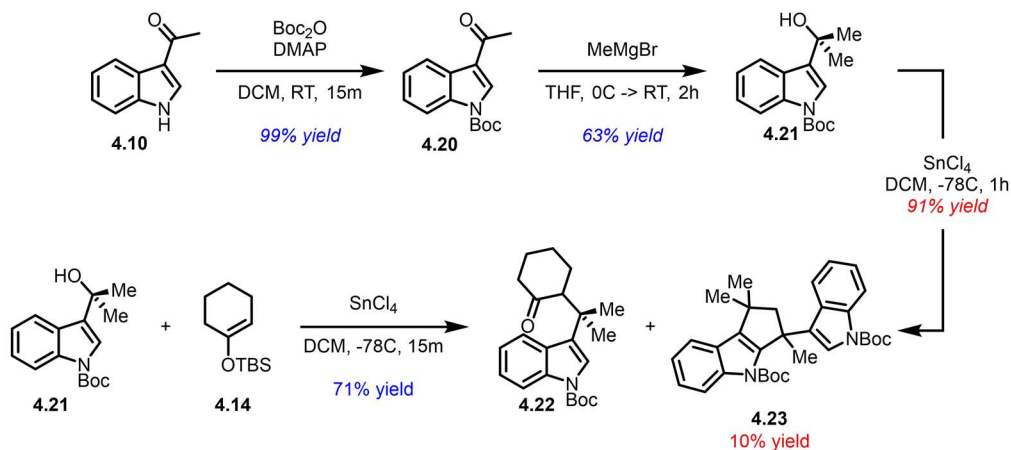


Scheme 4.3 Synthesis of the Tosyl-protected model ketone



Scheme 4.4 Successful triflation and unsuccessful de-protection of the tosyl ketone

beneficial to avoiding this side product. Ketone **4.22** was then reacted with LDA and Comins' to give the desired enol triflate **4.24** in high yield. However, the removal of the Boc group again proved tricky. Base-mediated cleavage, while requiring less harsh conditions than the desotylation, lead to significant amounts of de-triflation to give ketone **4.18**. Acidic conditions were similarly fruitless, leading to rapid dimerization to some unidentified novel product immediately upon removal of the Boc group. Luckily, thermolytic cleavage of the Boc group was successful. Using Rawal and Cava's conditions, **4.24** was heated to 180°C under high vacuum, giving the desired compound **4.19** cleanly within 5 minutes.⁵ Provided the reaction vessel was kept entirely

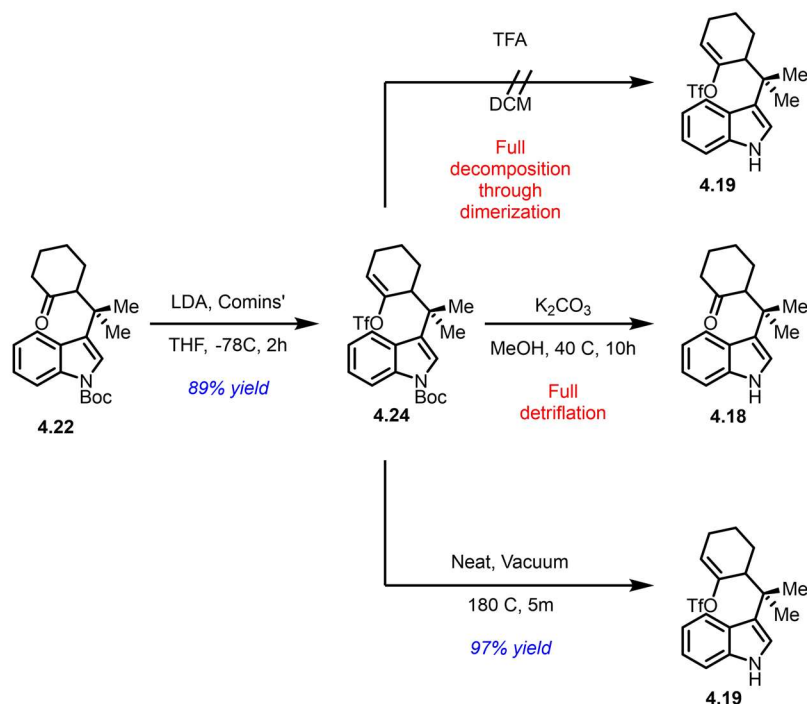


Scheme 4.5 Synthesis of the Boc-protected model ketone

⁵ Rawal, V. H.; Cava, M. P. *Tetrahedron Lett.* **1985**, 26 (50), 6141–6142

oxygen free, no side products were observed. However, instantaneous decomposition occurred if the heated reaction vessel was exposed to air, so care must be taken when setting up and taking down the reaction.

Having developed a route to the free indole, the attention was then directed to oxidation of the indole to the oxindole. The Rawal lab has used multiple oxidation conditions in their syntheses of the welwitindolinones, and it is noteworthy that conditions that work well for some substrates completely fail on others. In that vein, no desired product was observed when exposing indole **4.19** to either magnesium monoperoxyphthalate (MMPP) or $\text{Fe}(\text{OTf})_2$ and peracetic acid, conditions that had been used successfully in the synthesis of welwitindolinones B and C.^{6,7} However, when



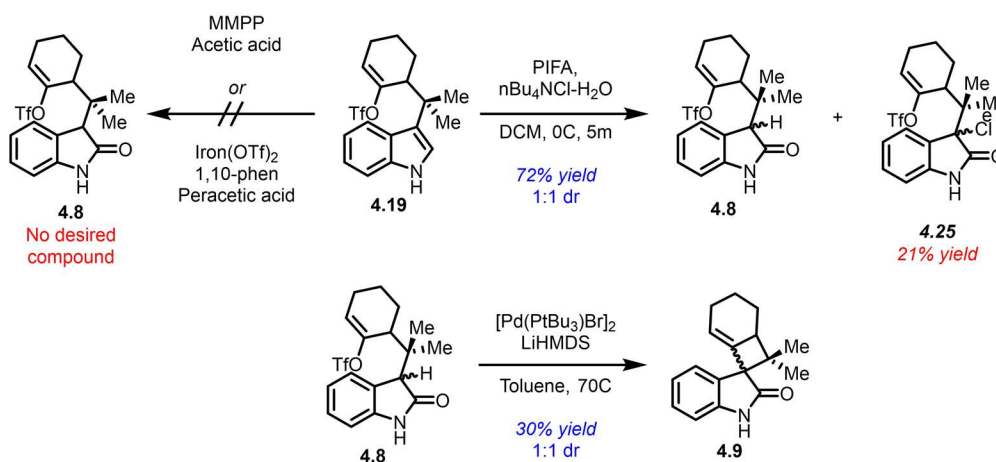
Scheme 4.6 Failed and successful conditions for removing the Boc

⁶ (a) Bhat, V.; Allan, K. M.; Rawal, V. H. *J. Am. Chem. Soc.* **2011**, *133* (15), 5798–5801. (b) Bhat, V.; Rawal, V. H. *Chem. Commun.* **2011**, 47 (34), 9705–9707.

⁷ Reyes, J. R.; Xu, J.; Kobayashi, K.; Bhat, V.; Rawal, V. H. *Angew. Chem. Int. Ed.* **2017**, *56*

indole **4.19** was exposed to PIFA in the presence of tetrabutyl ammonium chloride mono-hydrate (TBAC-H₂O) in DCM, following a procedure published by the Ma and Shao labs, the desired indolinone **4.8** was rapidly formed as a 1:1 mixture of diastereomers, albeit with some of the over-oxidized 3-chloro oxindole **4.25** as a side product.⁸

With the oxindole **4.8** in hand, we were then positioned to test the proposed cyclization. Using Huang's conditions, **4.8** was exposed to catalytic [Pd(P-tBu₃)Br]₂ and LiHMDS in toluene at 60°C. Although the reaction proceeded more slowly and had a lower yield than that in Huang's report, the starting material was converted cleanly to the desired compound **4.9**, which was formed as a 1:1 mixture of diastereomers. With this successful proof of the viability of the strategy, the attention was next directed towards the construction of the fully decorated system.

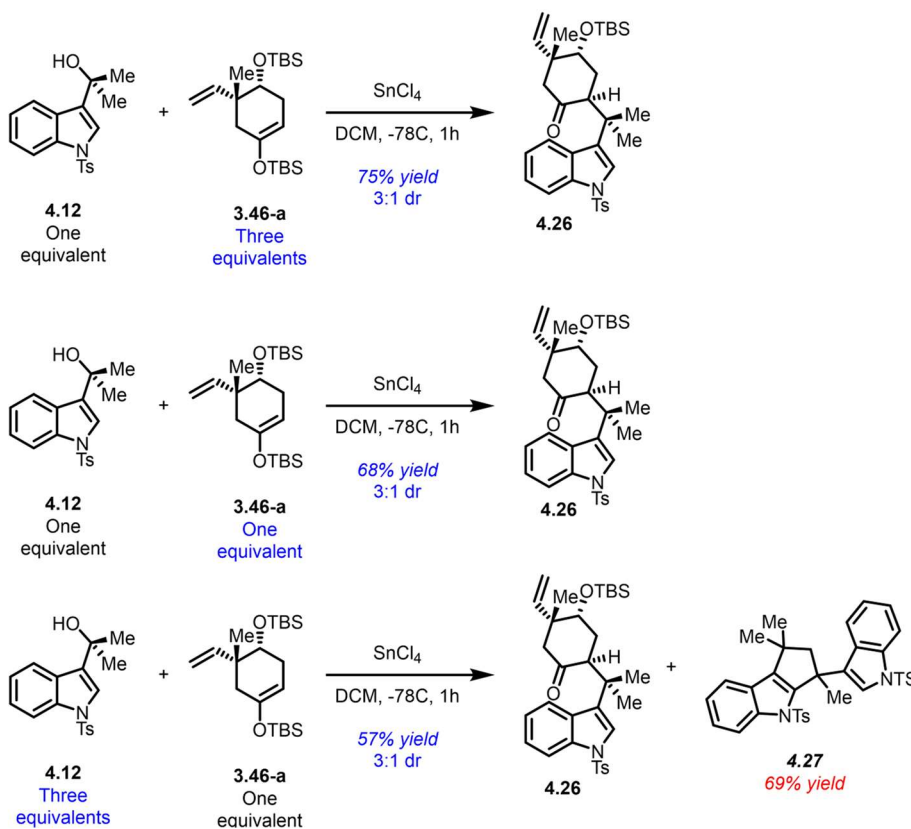


Scheme 4.7 Oxidation to the model indolinone and successful palladium-mediated cyclization

⁸ Liang, P.; Zhao, H.; Zhou, T.; Zeng, K.; Jiao, W.; Pan, Y.; Liu, Y.; Fang, D.; Ma, X.; Shao, H. *Adv. Synth. Catal.* **2021**, *363* (14), 3532–3538

4.2 Synthesis of the Fully-Decorated Indolinone Precursor

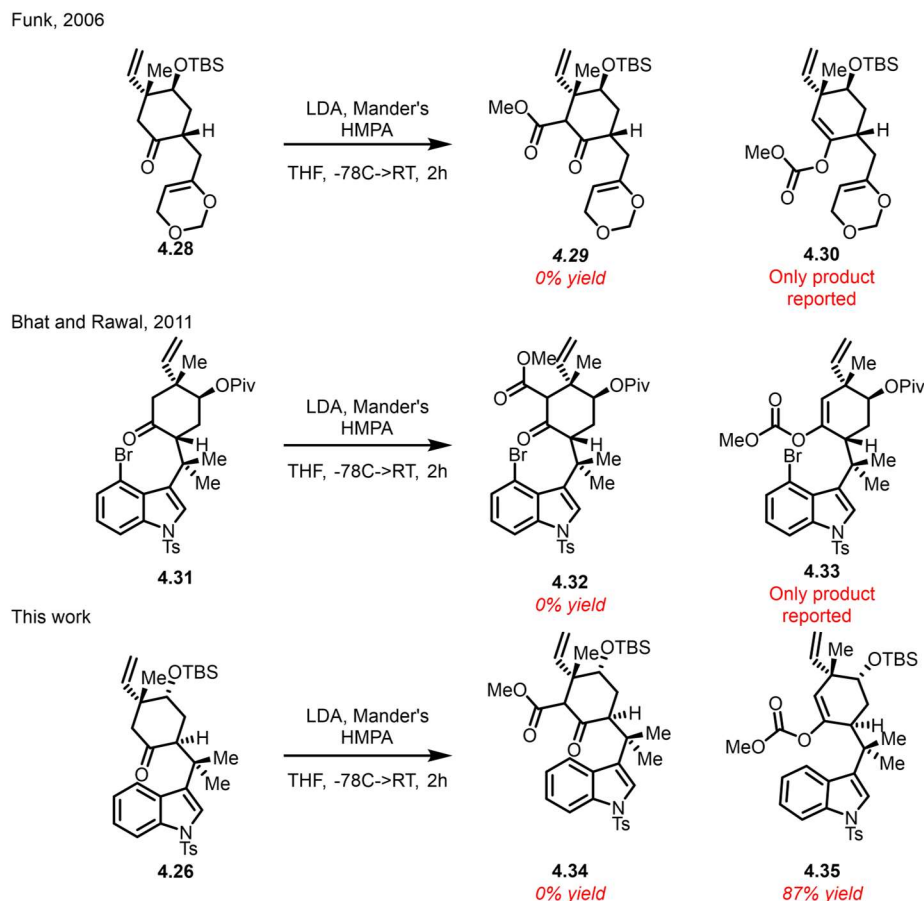
Because of the difficulties the acetate protecting group had posed in the synthesis of fontonamide, we decided to use the TBS protected silyl enol ether **3.24-a** as the precursor to the upper ring (See chapter 3). Although this compound had given no desired product in the Friedel-Crafts reaction with anilide **2.7**, a similarly sterically hindered silyl enol ether had been successfully employed in Rawal's synthesis of welwitindolinone B.⁶ As the tosyl protected indole alcohol **4.12** appeared to be a superior coupling partner, it was reacted with **3.24-a** at -78 °C to give **4.26**. The yield was not quite as good as it had been when the reaction was run with the less-hindered **4.14** as a coupling partner, but it was overall a smooth reaction, and proceeded much more rapidly than had the reactions with the anilide. Given that **3.46-a** was the more difficult



Scheme 4.8 Friedel-Crafts reaction on the real system

material to make, the reaction was then examined using fewer equivalents of it. Pleasingly, the yield dropped only slightly when **3.46-a** was used as only a single equivalent. Additionally, it was possible to run the reaction with **3.46-a** as the limiting reagent and with **4.12** in excess; although the yield was lower, the conversion percentage of **3.46-a** to **4.26** was substantially higher, reducing the need for multiple passthroughs of the same material. The major side product, as expected, was **4.27**, the dimerized indole.

It is worth noting that the diastereoselectivity of the reaction was not nearly as good as that seen in the synthesis of fontonamide. While in that case the product had been obtained in greater



Scheme 4.9 Funk, as well as Bhat and Rawal, found that C-carboxylation was not possible with this relative stereochemistry

than 20:1 dr, here we observed closer to 3:1, lending further credence to the hypothesis that an additional intramolecular force may be facilitating the Friedel-Crafts reaction between benzylic silyl ether **2.7** and silyl enol ether **3.46-c**. The dr of the reaction is of secondary importance however, as the major C-15 diastereomer obtained, that with an α -H, was the opposite of that present in the natural product. This result was not unexpected, as the observed major diastereomer was predicted by the relative A values of the substituents. However, it did necessitate an epimerization of the C-15 carbon. This epimerization would prove to be crucial for the success of the next step, the installation of a carboxyl group at the C-11 carbon. In 2006, while working on the total synthesis of welwitindolinone C, Funk and coworkers found that the carboxylation of a similar compound, ketone **4.28**, invariably led to the O-carboxylated product **4.30**.⁹¹ Five years later, also while working on the total synthesis of the welwitindolinones, Vikram Bhat encountered the same phenomenon while attempting to carboxylate ketone **4.31**—sole formation of the O-

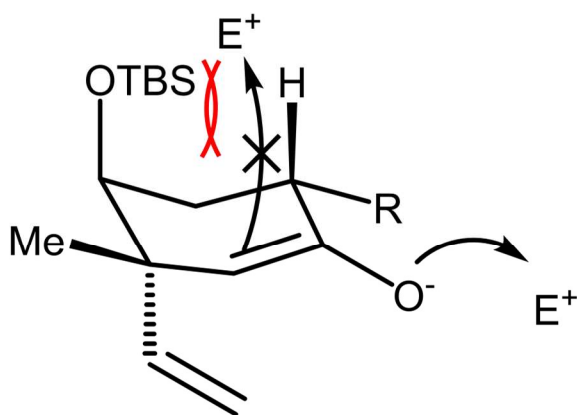
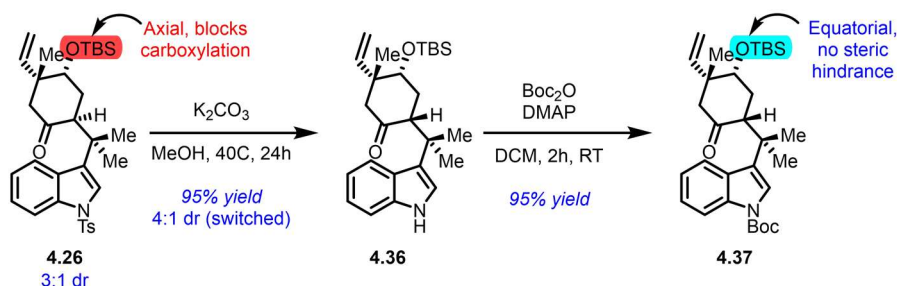


Figure 4.1 Steric hindrance from the TBS-protected alcohol precludes C-carboxylation

⁹ (a) Greshock, T. J.; Funk, R. L. *Org. Lett.* **2006**, *8* (12), 2643–2645. (b) Greshock, T.J. PhD., Thesis, The Pennsylvania State University, United States

carboxylated compound **4.33**.¹⁰ Similarly, when **4.26** was subjected to standard C-carboxylation conditions (LDA, HMPA, and Mander's reagent in THF), only formation of enol carboxylate **4.35** was observed.

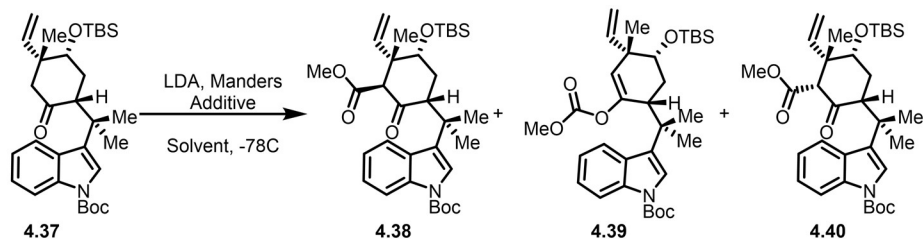
In all three cases, the more-hindered alpha carbon contains a large substituent that is equatorially locked. In addition, in all three cases, this substituent is trans to the bulky protected alcohol at the 4-position of the ring, forcing this alcohol into a pseudo axial arrangement. When the ketone is deprotonated, the axial approach of the electrophile is then blocked by this bulky group, precluding reaction at the carbon (Figure 4.1). As the oxygen is pointed away from the steric hindrance, O-carboxylation then proceeds rapidly and exclusively. While this steric bulk blocks the desired reaction from occurring, it should also allow easy epimerization of the compound, as C-15 epimerization will allow the TBS ether to sit in the more stable equatorial position. To that end, **4.26**, as a mixture of diastereomers, was subjected to epimerization using K_2CO_3 in methanol at high temperatures. This gave good conversion to the desired diastereomer and simultaneously removed the tosyl group, giving ketone **4.36**. Given the successful experience with thermolytic deprotection of the indole on the model system, we took advantage of this



Scheme 4.10 Stereoinversion and switching of the protecting group from Tosyl to Boc

¹⁰ Bhat, V. Ph.D., Thesis, The University of Chicago, United States

concurrent deprotection to install a boc protecting group. Reaction **4.36** with Boc anhydride and DMAP gave ketone **4.37** in good yield.



Solvent	Additive	Yield 4.38	Yield 4.39	Yield 4.40
THF	HMPA	15%	85%	nd
THF	None	20%	75%	nd
Et ₂ O	None	25%	70%	nd
1:1 Et ₂ O:Tol	None	50%	45%	nd
Tol ^a	None	60%	30%	10%
1:1 Tol:Hex	None	60%	30%	nd
Hex	None	0%	0%	0%
Tol ^b	None	0%	30%	70%

^a Quenched at -78°C

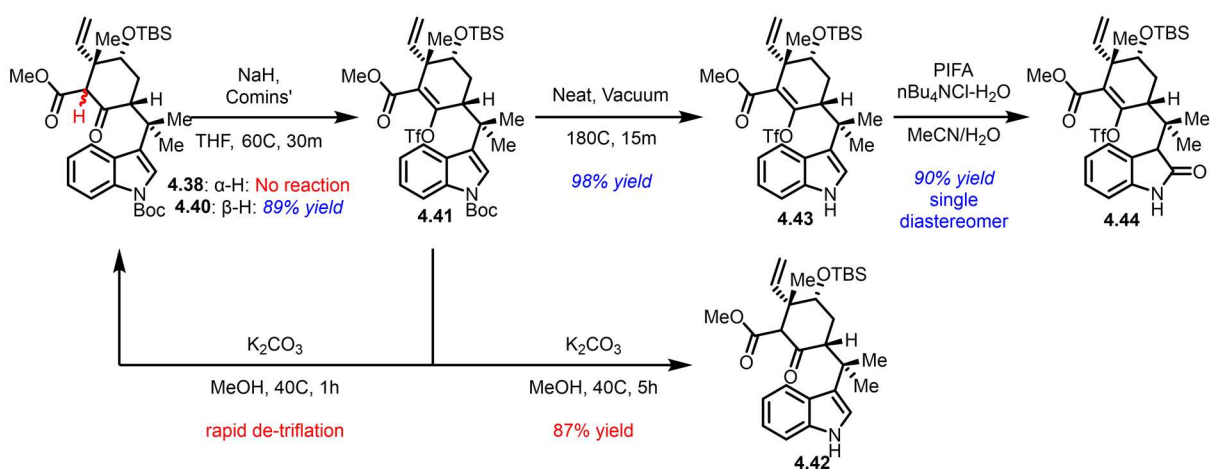
^b Quenched at room temperature after 5 hours

Table 4.1. Optimization of C-carboxylation conditions

Ketone **4.37** was then subjected to the same carboxylation procedure, using LDA to deprotonate then trapping with Mander's reagent in the presence of HMPA. While the major product, in about 85% yield, was the O-carboxylated compound **4.39**, we were pleased to see that the desired C-carboxylated compound was formed in approximately 15% yield as a separable mixture of diastereomers **4.38** and **4.40**. Interestingly, while the reaction with ketone **4.26** had required warming to room temperature in order to proceed, **4.37** was fully reacted within 15 minutes at -78°C. Because HMPA is added in order to increase reactivity by tying up the lithium counterion, which appeared not to be necessary, we hoped that by removing it, the oxygen on the enolate would be blocked, leading to an increase in selectivity for the C position. Indeed, the selectivity was marginally increased, giving the desired compound in 20% yield, with **4.39** as the remaining 80%. In order to further increase the coordination of lithium to the oxygen, a range of

less coordinating solvents were explored. Running the reaction in diethyl ether gave the C-carboxylated product in a slightly higher 25% yield. However, running in a 1:1 mixture of diethyl ether and toluene gave pushed this up to a 50% yield. Moving to an all toluene mixture moved this ratio even further in the desired direction, giving the C-carboxylated compound in 70% yield. Unfortunately it was not possible to further improve the reaction: running the reaction in hexane provided no product, likely due to poor solubility, and a 1:1 mixture of toluene and hexane gave the product in the same 70% yield. While the reaction gave a mixture of diastereomers when quenched at -78°C , with the large majority being **4.38**, allowing it to stir at room temperature for 5 hours prior to quenching led to the sole formation of **4.40**, which was assigned as having both alpha hydrogens sitting in the axial position, with the TBS protected alcohol, the benzylic quaternary center, and the new carboxyl all sitting equatorially.

This beta keto ester was then transformed into the corresponding enol triflate using sodium hydride and Comins' reagent. Surprisingly, this reaction did not go at room temperature, but upon heating to 60°C afforded the desired enol triflate **4.41** in quantitative yield. Interestingly, the same

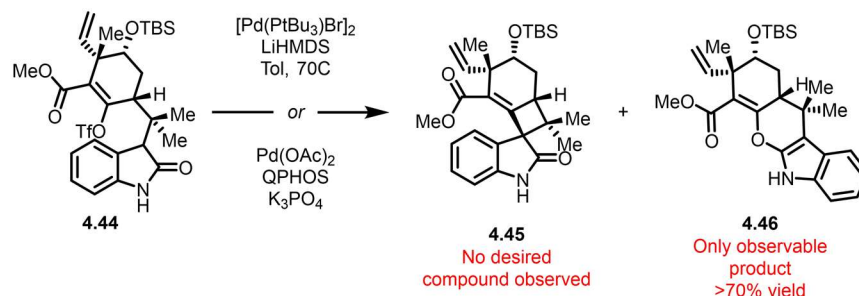


Scheme 4.11 Triflation, deprotection, and oxidation to the indolinone

conditions cause no reaction at all with the opposite diastereomer **4.38**, possibly due to the equatorial nature of the alpha proton, which would make it difficult to deprotonate due to stereoelectronic reasons. Because of this realization, the carboxylation reaction was always allowed to complete equilibration prior to quenching. With the enol triflate in hand, the next task was to remove the Boc group. As with the model substrate, acidic removal of the Boc group lead to decomposition and dimerization. Additionally, basic conditions lead to rapid de-triflation, returning ketone **4.42** after completion of the reaction. The speed of this de-triflation is likely due to the fact that the triflate can be viewed as a vinylogous carboxyl triflate. Thankfully, the same thermolytic conditions employed on the model substrate worked well—heating at 180°C under vacuum lead to complete conversion to the desired free indole **4.43** within 10 minutes. Strangely, but fitting with the lab's prior experiences, the indole oxidation did not proceed at 0 °C or at room temperature. One hypothesis to understand the poor oxidation was that the low water concentration in the solvent (DCM) did not allow formation of the active oxidant. Indeed, addition of extra water helped improve the reaction somewhat, giving the desired compound **4.44** in 20% yield. Happily, switching to acetonitrile, a water-miscible solvent, increased the yield dramatically to 90%, giving **4.44** as a single diastereomer of undetermined stereochemistry.

4.3 Investigation of the Palladium-Mediated Cyclization and Further Steps

With the indolinone precursor in hand, the stage was set to test the pivotal cyclization reaction. Using the conditions optimized by Huang and demonstrated on our model system, triflate **4.44** was reacted with NaHMDS in the presence of $[\text{Pd}(\text{P}-t\text{Bu}_3)\text{Br}]_2$. Pleasingly, **4.44** was rapidly transformed into a new compound; however, upon workup we found that the new compound arose from cyclization onto the oxygen of the enolate rather than the carbon, giving tetracycle **4.46**. The reaction was repeated using the conditions Dong and coworkers had found worked best in their synthesis of phainanoid A, using $\text{Pd}(\text{OAc})_2$ and QPhos as a ligand along with K_3PO_4 , a weaker base. However, the sole isolable product was again **4.46**.

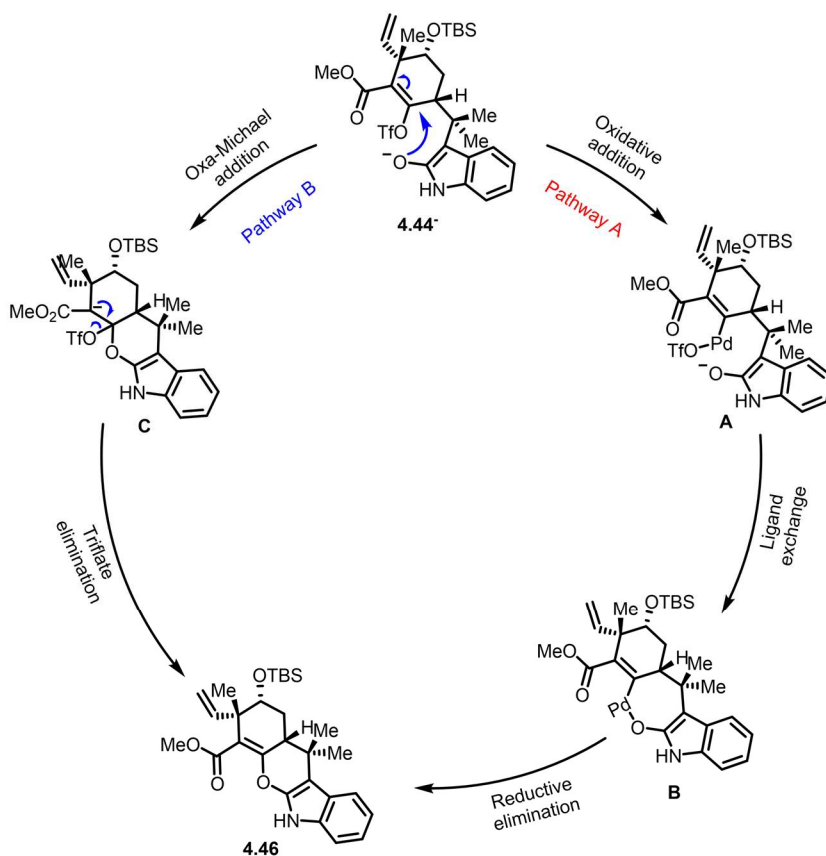


Scheme 4.12 Triflation, deprotection, and oxidation to the indolinone

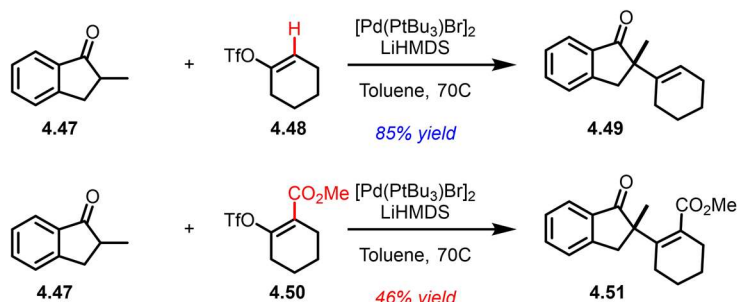
We could imagine two ways that this undesired compound would form. The first, Pathway A, would be initiated by an oxidative addition of palladium into the carbon-triflate bond, as desired, to give intermediate **A** (Scheme 4.12). The palladium would then undergo a ligand exchange, replacing the triflate with the enolate oxygen to give palladacycle **B**. This would then undergo a reductive elimination to give tetracycle **4.46**. While reasonable, this pathway seems unlikely for multiple reasons. Primarily, no product arising from O- attack on the palladium intermediate was reported by Huang. Indeed, Huang reported that there was no reactivity at either the oxygen or the nitrogen when run intermolecularly, suggesting that the preferred reaction site is the carbon (See

Chapter 1). Additionally, the palladacycle intermediates that would be formed by reaction at the carbon and oxygen have 5- and 7-membered rings respectively, so the thermodynamic driving force for the C-O bond formation arising from ring strain should be minimal.

The second possibility, Pathway B, is that the oxygen of the enolate is reacting at the triflate site directly, prior to insertion of the palladium into the carbon-triflate bond. As discussed above, because of the conjugated ester the enol triflate may also be thought of as a vinylogous carboxyl triflate, which would make the carbon much more electrophilic than the carbon in a typical enol triflate. Just as basic methanol conditions lead to much faster de-triflation on **4.41** than in the model system **4.24**, the attack of the enolate onto the triflate should be much faster in the real system than



Scheme 4.13 Two possible pathways for formation of **4.46**

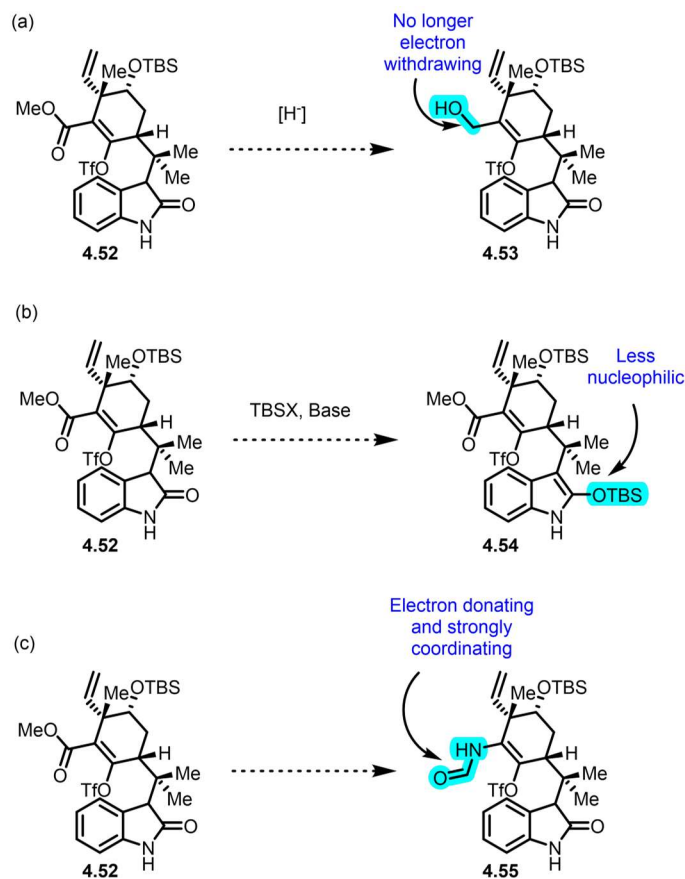


Scheme 4.14 Huang's reaction of ketone enolates with a vinyl triflate and a vinylogous carboxyl triflate

the model. Such an attack would give intermediate **C** (Scheme 4.12), which would then readily eliminate the triflate to give **4.46**. Huang's lab did not react any indolinone substrates with vinylogous carboxyl triflate, however, they did react ketone **4.47** with vinylogous carboxyl triflate **4.50** as well as the simple enol triflate **4.48**.³ While the latter reaction performed well, giving the product **4.49** in 85% yield, the former reaction was far less successful, giving the desired compound **4.51** in only 48% yield. Although Huang did not discuss this outcome further, it is possible that the cause of the loss in yield is the undesired reaction on the oxygen. It is also worth noting that **4.50** is the only substrate Huang does not report reacting with the indolinone, suggesting that that reaction may have failed. While Huang did see some desired compound in the reaction between **4.47** and **4.50**, the intramolecular nature of the proposed oxa-Michael cyclization in our system would be expected to greatly increase its rate relative to the desired palladium insertion.

If Pathway B is the origin of **4.46**, there are a few tactics that could help to avoid this undesired reactivity. The first, and most direct, would be to remove the EWG by reducing the ester to the primary alcohol, giving **4.53**.¹¹ This should substantially limit the ability of the oxygen to

¹¹ This was accomplished on a similar compound by Liang and coworkers. Hsu, D.-S.; Liang, S.-P. *J. Org. Chem.* **2020**, *85* (2), 1270–1278.



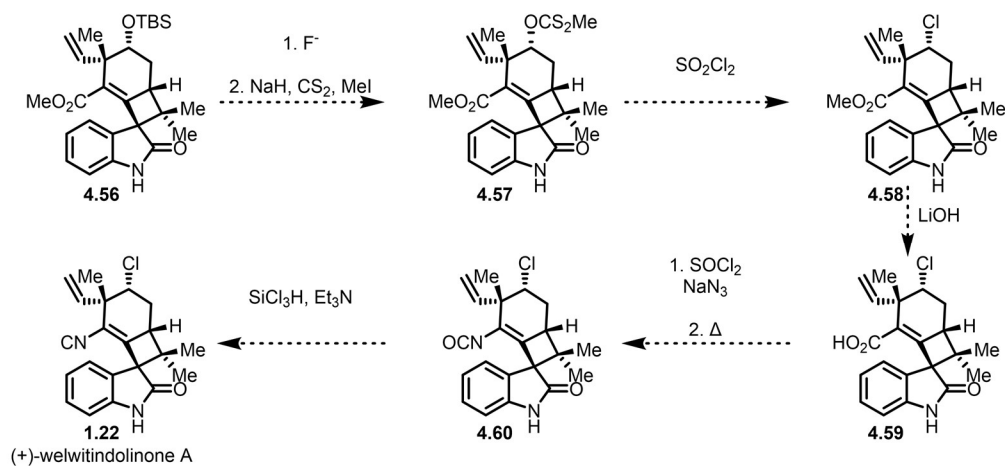
Scheme 4.15 Three possible routes to avoid the undesired O-cyclization (a) reduction of the ester. (b) silylation of the indole. (c) transformation of the ester to a formamide

attack prior to formation of the palladated intermediate, thereby avoiding this undesired reaction. Alternatively, the oxa-Michael reaction could be slowed by reducing the nucleophilicity of the oxygen. This could be achieved through silylation to give silyloxy indole **4.54**.¹² Although this would likely slow down the reaction with the palladated intermediate, it should limit the ability of the undesired cyclization reaction to occur. Finally, prior to the cyclization reaction the ester could be replaced with a formamide, either directly or by prior installation of a nitrogen, to give **4.55**, which

¹² The silylation of a molecule of similar complexity was achieved by Nicolaou and coworkers. Nicolaou, K. C.; Hao, J.; Reddy, M. V.; Rao, P. B.; Rassias, G.; Snyder, S. A.; Huang, X.; Chen, D. Y.-K.; Brenzovich, W. E.; Giuseppone, N.; Giannakakou, P.; O'Brate, A. *J. Am. Chem. Soc.* **2004**, *126* (40), 12897–12906

contains an electron rich enol triflate rather than an electron deficient one. This approach is the most risky, however, as electron rich enol triflates are much slower to undergo oxidative addition with palladium, although the coordinating nature of the formamide may help. Additionally, the route to **4.55** is unclear and indirect, making this route more prone to failure.

Regardless of the approach chosen, the end game of the natural product should be straightforward. TBS removal and stereo-retentive conversion of the resulting alcohol to the chlorine should be possible, either through classical conditions or by first forming a xanthate ester like **4.57**, which can be converted to the chlorine **4.58** stereo-retentively using sulfuryl chloride.¹³ The ester, or primary alcohol, can then be converted to the carboxylic acid **4.59**. Conversion of **4.59** to acyl azide **4.60** will then allow a Curtius rearrangement to the isocyanate **4.60**. This can finally be reduced to the isonitrile **1.22** using trichlorosilane and triethyl amine, thereby giving the natural product.¹⁴



Scheme 4.16 Proposed endgame following the successful cyclization

¹³ Kozikowski, A. P.; Lee, J. *Tetrahedron Lett.* **1988**, 29 (25), 3053–3056.

¹⁴ Baldwin, J. E.; Bottaro, J. C.; Riordan, P. D.; Derome, A. E. *J. Chem. Soc. Chem. Commun.* **1982**, No. 16, 942–943

4.4 Conclusion

While the synthesis remains incomplete, significant progress has been made towards the final compound. The synthesis takes advantage of a novel route to the D ring that provides the opposite relative stereochemistry at the C-13 position, and takes advantage of this fact to complete a here-to-fore unachieved C-carboxylation. This novel approach also allows access to the D ring through an asymmetric route, allowing this synthesis, when completed, to be the first asymmetric synthesis of a welwitindolinone. In the near term, attention should be focused on achieving the palladium-mediated cyclization, with the end game of the synthesis expected to be relatively straightforward. Overall, this synthesis has provided a platform for exploring exciting new chemistry, and when completed should be a concise and direct route to the natural product.

Chapter 5: Development of Novel 1-Alkoxy-1-amino-1,3-butadienes for the Diels-Alder Reaction

5.1 Background on 1,1-Diactivated Dienes

Since its initial discovery in 1928, the Diels-Alder reaction has come to be known as one of the most important reactions in organic synthesis.¹ The reaction, which couples a 4-membered diene with a 2-membered dienophile, allows the simultaneous formation of two carbon-carbon or carbon-hetero atom bonds, as well as a new 6-membered ring. The reaction also tends to proceed with remarkable diastereo- and regio-selectivity, giving up to four new stereocenters. Since the initial discovery, a number of highly-active, electron-rich dienes have been developed, allowing reaction with less-activated dienophiles, as well as the development of asymmetric versions of the reaction. It should be noted that many of the results summarized in this chapter have been reported in a publication. Portions of the chapter were adapted from that publication.²

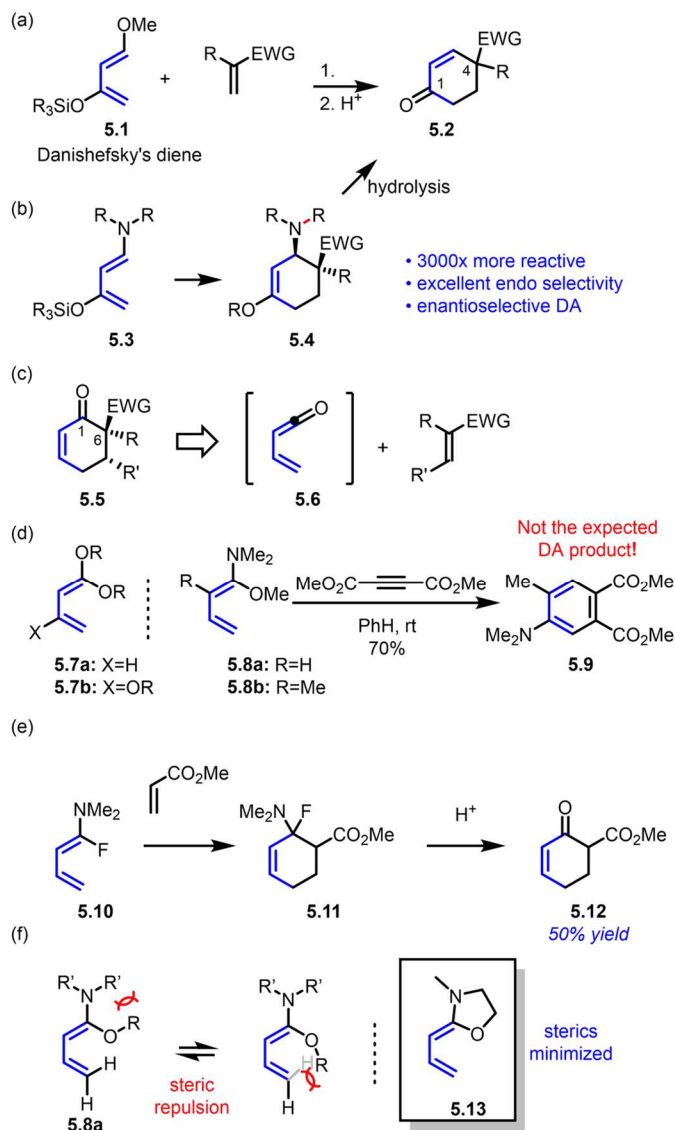
One of these highly-active dienes, 1-methoxy-3-siloxy-butadiene, also known as Danishefsky's diene, (**5.1**) is interesting for its ability to form eneones upon hydrolysis of the cycloadduct (Scheme 5.1a).³ Research in the Rawal lab extended this activity through the development of 1-amino-3-siloxy-butadienes (**5.3**), which, because of the introduction of a more

¹ Oppolzer, W. In *Comprehensive Organic Synthesis*; Pergamon Press: New York, 1991; Vol. 5, pp 315–400

² This chapter is adapted from the following publication. Some of the work in the publication was performed by Dr. Pavel Elkin, however all reactions reported in this chapter were either originally run by me or checked by me in advance of the publication. (a) Elkin, P. K.; Durfee, N. D.; Rawal, V. H. *Org. Lett.* **2021**, 23 (14), 5288–5293. (b) Elkin, P., PhD., Thesis, The University of Chicago, United States

³ (a) Danishefsky, S. *Acc. Chem. Res.* **1981**, 14 (12), 400–406. (b) Hiraoka, S.; Harada, S.; Nishida, A. *J. Org. Chem.* **2010**, 75 (11), 3871–3874

electron-donating nitrogen, are even further activated.⁴ The reactions with these dienes achieve excellent endo selectivity and can be rendered asymmetric through the use of chiral cobalt or chromium salen complexes or hydrogen bonding catalysis (Scheme 5.1b).⁵



Scheme 5.1. Activated butadienes for Diels-Alder reactions

⁴ (a) Kozmin, S. A.; Rawal, V. H. *J. Org. Chem.* **1997**, *62* (16), 5252–5253. (b) Kozmin, S. A.; Rawal, V. H. *J. Am. Chem. Soc.* **1999**, *121* (41), 9562–9573

⁵ (a) Huang, Y.; Iwama, T.; Rawal, V. H. *J. Am. Chem. Soc.* **2002**, *124* (21), 5950–5951. (b) Huang, Y.; Unni, A. K.; Thadani, A. N.; Rawal, V. H. *Nature* **2003**, *424* (6945), 146–146.

While 4,4-disubstituted eneones are readily available through the Diels-Alder reactions of these dienes, to date there has been no report of a diene that is able to access 6,6-disubstituted eneones (**5.5**). 6,6-disubstituted eneones are a common moiety in both natural products and pharmaceuticals, as well as their synthetic intermediates, so a direct route to their synthesis would be highly valuable.⁶ Retrosynthetic analysis of such eneones suggests that the necessary diene would need to take the form of vinyl ketene or some masked equivalent, i.e. a 1,1-diaactivated butadiene (Scheme 5.1c). Several examples of such butadienes exist in the literature, and many have been examined in cycloaddition reactions. One example, published by Sustmann in 1996, used 1,1-dimethoxybutadiene (**5.7a**), prepared from methyl crotonate.⁷ While this diene reacted reasonably well with highly electron-deficient dienophiles such as dimethyl 2,3-dicyanomaleate, the reactions with common dienophiles such as methyl acrylate and the intermediate-strength dimethyl maleate all failed to give the desired product, returning instead polymeric materials. Brassard's diene (**5.7b**), which carries an extra oxidation at the 3-position of the diene, has been more successful, giving the desired products in good yield when used in hetero Diels-Alder reactions.⁸ Its usefulness in Diels-Alder reactions is, however, limited, with the scope of dienophiles being restricted to quinones and other doubly-activated dienophiles.⁹ Additionally, because the diene carries an extra oxidation, the products are necessarily overoxidized, giving, upon hydrolysis, vinylogous esters rather than the more-useful eneone subunit. Similar results

⁶ The 6,6-disubstituted cyclohexanone motif, or its further modified derivative, is found in numerous natural products, including the previously discussed fontonamides and welwitindolinones, as well as platencin, cyanthiwigin B, acutifolone A, and lycopoclavamine A. A recent synthesis of (+)-psoracorylifol F and other members of the family proceeded through a similar cyclohexanone. Chen, X.-W.; Hou, Z.-C.; Chen, C.; Zhang, L.-H.; Chen, M.-E.; Zhang, F.-M. *Chem. Sci.* **2023**, *14* (21), 5699–5704

⁷ Sustmann, R.; Tappanchai, S.; Bandmann, H. *J. Am. Chem. Soc.* **1996**, *118* (50), 12555–12561.

⁸ Banville, J.; Brassard, P. *J. Chem. Soc. Perkin 1* **1976**, No. 17, 1852–1856

⁹ Caron, B.; Brassard, P. *Tetrahedron* **1991**, *47* (25), 4287–4298.

were seen when 1,1-dithio-butadienes were used, with the dienes only reacting successfully with the most activated dienophiles.¹⁰

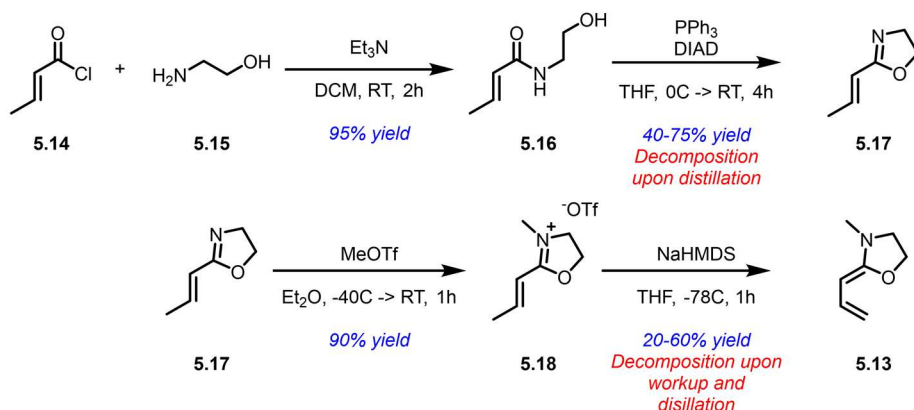
One final example is the 1-dimethylamino-1-methoxy-butadiene (**5.8**), which Ghosez first reported attempting to use for cycloadditions in 1979.¹¹ The diene, which is expected to be even more active than the 1,1-dialkoxy dienes, completely failed to give the expected products on reaction with typical dienophiles. In the majority of cases the reaction failed to proceed, while reaction of methylated **5.8b** with dimethyl acetylenedicarboxylate gave only a product “with a substitution pattern incompatible with the normal Diels–Alder pathway”. However, the reaction between 1-amino-1-fluoro-butadiene, a less active diene, and methacrylate proceeded relatively cleanly, if in low yield. We reasoned that the drastic difference in reactivity between the two dienes arose from the difference in steric hindrance posed by the two non-amino substituents, with the substantially smaller but less activating fluoride allowing the diene to access an *s-cis* conformation that the large methoxy prohibited. We reasoned that one way to overcome this steric issue would be to connect the oxygen and nitrogen substituents, giving an oxazolidine-fused butadiene. This would minimize steric clashes between the alkoxy substituent and hydrogens at the far end of the diene, and would allow for successful cycloaddition with a wide variety of dienophiles.

¹⁰ Ross Kelly, T.; Goerner, R. N.; Gillard, J. W.; Prazak, B. K. *Tetrahedron Lett.* **1976**, *17* (43), 3869–3872.

¹¹ Gillard, M.; T’Kint, C.; Sonveaux, E.; Ghosez, L. *J. Am. Chem. Soc.* **1979**, *101* (19), 5837–5839

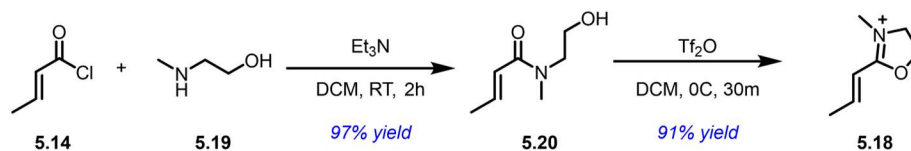
5.2 First and Second Generation Syntheses of the Oxazolidine-Fused Butadiene

Our initial route to the butadiene was based on a route developed by Pavel Elkin from the Rawal group, which started with crotonyl chloride, and followed Woolaston's route to an α,β -unsaturated oxazoline.¹² Crotonyl chloride was combined with ethanolamine, giving the desired amide **5.16** in high yield. Cyclization of the alcohol onto the carbonyl was achieved through dehydration using PPh_3 and DIAD, to give the oxazoline **5.17** in reasonable yield. Purification however proved difficult, as the compound was unstable to column chromatography and rapidly polymerized when heated during distillation. The oxazoline was then combined with methyl triflate to give the oxazolinium salt **5.18** in good yield. The solvent was exchanged, and NaHMDS was added to deprotonate oxazolinium, giving the desired diene **5.13** in good conversion. Here too, however, the purification was difficult: as observed with the previously identified 1-amino-3-siloxy-butadienes, the diene was unstable to even the mildest of acidic workup, and decomposed readily on silica and under oxygen. Workup was carried out by dilution with hexanes and filtration



Scheme 5.2 First generation synthesis of diene **5.13**

¹² Robertson, J.; Chovatia, P. T.; Fowler, T. G.; Withey, J. M.; Woollaston, D. J. *Org. Biomol. Chem.* **2009**, 8 (1), 226–233

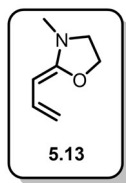


Scheme 5.3 Second generation synthesis of oxazolinium salt **5.18**

through a packed Celite plug followed by distillation; however, the diene again decomposed quickly under the high temperatures, limiting the recovered material.

Although **5.13** was available through this route, the procedure has some issues and was difficult to scale up past 1 mmol. We returned to the beginning, with the goal of developing a route that was highly scalable and avoided difficult purifications such as high temperature distillations. Combining crotonyl chloride with N-methyl ethanolamine promoted amide formation, affording the secondary amide in high yield. Taking inspiration from Ghosez's route to the 1-alkoxy-1-amino butadienes, triflic anhydride was then added to the amide, which underwent spontaneous cyclization to the oxazolinium salt. The salt was purified by dissolving it in acetone then slowly adding the solution to rapidly stirring diethyl ether, which caused the pure salt to precipitate out as feathery white crystals, formed in high yield. The crystalline salt was stable at room temperature and under air for extended periods of time, making it an ideal intermediate for storage.

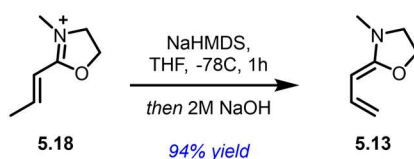
The above procedure nicely circumvented the difficulties associated with purifying the oxazoline intermediate, but there was still a need for a reliable method to convert the oxazolinium to the desired diene. We began by analyzing the stability of the diene under different aqueous conditions. A solution of the diene in 1:1 THF/Et₂O was mixed for 20 seconds with various aqueous solutions, and the recovery of the diene was monitored by NMR. While the diene rapidly decomposed under acidic and even neutral conditions, it showed surprising stability to more basic media. Washing with 1M NaOH lead to 73% recovery, while washing with 2M NaOH saw a



Aqueous Wash	Solvent	% Recovery
		5.18
1M HCl	1:1 THF:Et ₂ O	0%
NaPH ₂ O ₄ /Na ₂ PHO ₄ Buffer (pH7)	1:1 THF:Et ₂ O	65%
H ₂ O	1:1 THF:Et ₂ O	72%
1M NaOH	1:1 THF:Et ₂ O	76%
2M NaOH	1:1 THF:Et ₂ O	87%
5M NaOH	1:1 THF:Et ₂ O	84%
10M NaOH	1:1 THF:Et ₂ O	75%
2M NaOH	1:3 THF:Et ₂ O	92%

Table 5.1. Percent recovery of diene **5.13** under various aqueous wash conditions

recovery of 87%, which could be increased above 90% by increasing the solvent ratio of Et₂O to THF in the diene solution. These studies suggested that a base workup would allow higher recovery of the diene, while also removing polar non-volatiles from the solution. The oxazolinium was deprotonated with a slight excess of NaHMDS, and, after the reaction was complete by NMR, 2M NaOH was added, giving a crude mixture of the desired diene and some (<20%) residual HMDS. The HMDS was removed under high vacuum with minimal heating, giving the pure diene in a remarkable 88% yield. This route was operationally superior, requiring no columns or distillation to access the diene, and was also highly scalable. We were able to make 15 grams of the oxazolinium salt and 4 grams of the diene in a single pass, with no loss in yield. With a scalable route to the diene in hand, we were now ready to investigate its reactivity.



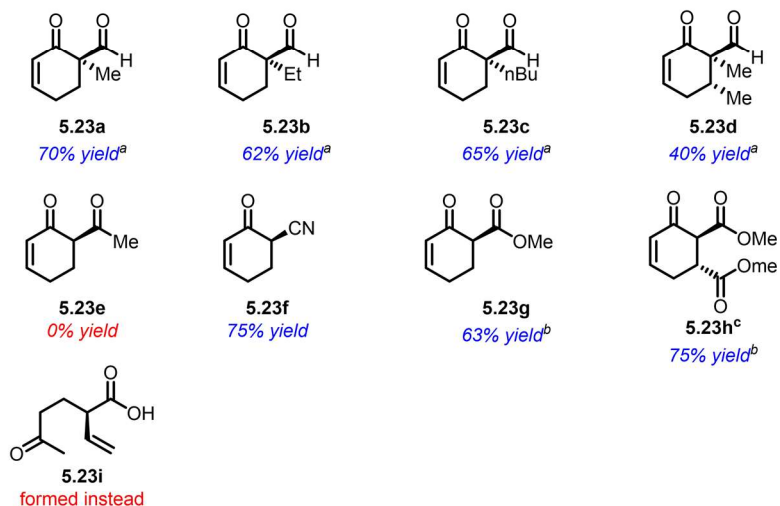
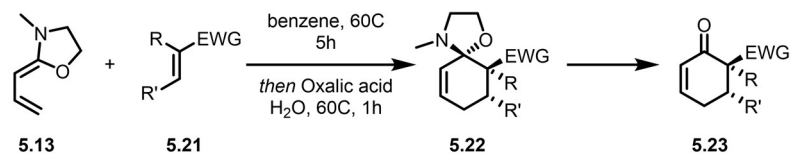
Scheme 5.4 Modified synthesis of diene **5.13**

5.3 Scope of the Diels-Alder Reactions of the Oxazolidine-Fused Butadiene

5.3A: Diels-Alder Reactions

In order to assess the cycloaddition capability of the new diene, we initially combined the diene with methacrolein in toluene at 60 °C for two hours. NMR monitoring indicated the diene was fully consumed, giving a 3:1 mixture of the Diels-Alder and hetero-Diels-Alder cycloadducts. Switching the solvent to benzene somewhat improved the ratio in favor of the Diels-Alder product, and running the reaction in a sealed tube to avoid loss of methacrolein increased the ratio to 4:1. The observed cycloadduct could not be isolated directly, but in-situ hydrolysis with oxalic acid and water lead to clean formation of the desired 6,6-disubstituted cyclohexeneone.

The scope of the Diels-Alder reaction with a variety of common dienophiles was investigated next. As expected, ethacrolein and n-butyl-acrolein both performed similarly to methacrolein, giving the desired cycloadducts in good yield. The more sterically-hindered tiglic aldehyde also reacted cleanly, albeit in slightly lower yield, giving the trisubstituted cyclohexanone. Reactions with acrylonitrile, methyl acrylate, and methyl maleate all proceeded smoothly, giving the resulting eneones in good yields, although the cycloadducts of methyl acrylate and methyl maleate were both isolated as a mixture of keto and enol forms. Unfortunately, the reaction of the diene with methyl vinyl ketone did not proceed, giving instead, upon hydrolysis, the Michael addition product.



^a Diels-Alder reaction run in a sealed tube

^b Isolated as a mixture of keto-enol forms

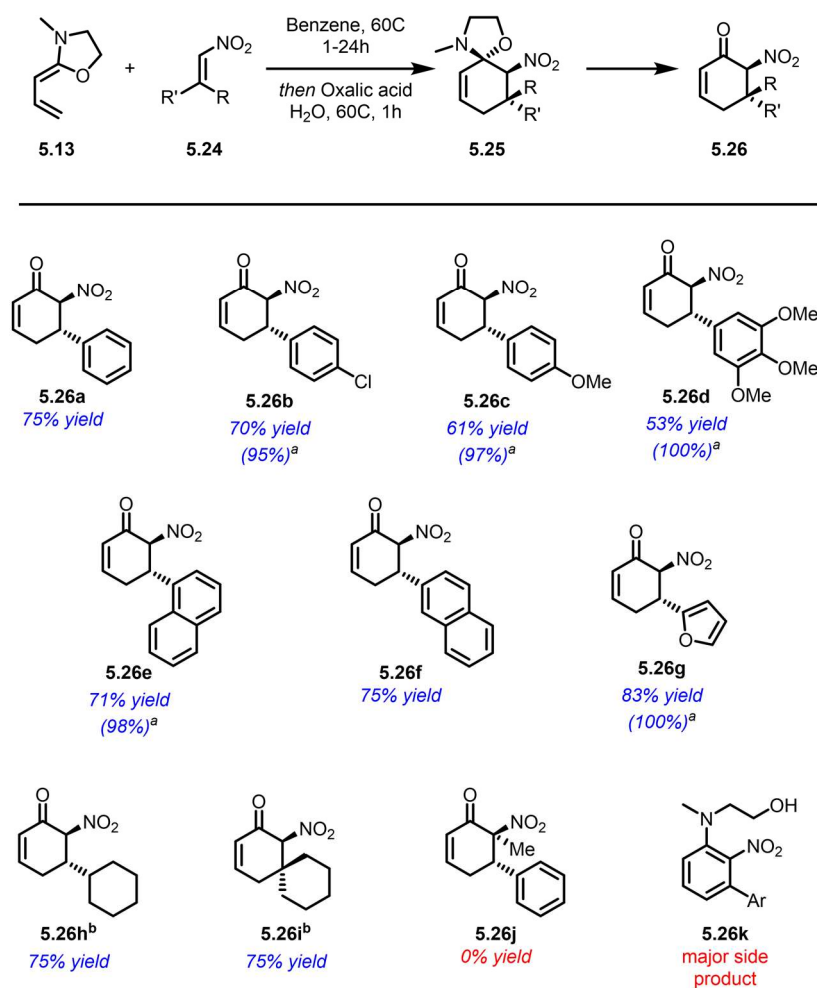
^c Data obtained by Pavel Elkin²

Table 5.2 Substrate scope of the Diels-Alder reaction between diene **5.13** and various common dienophiles

Next we investigated nitrosyrenes as possible dienophiles. Whereas nitroethylene is reported to react at room temperature with highly active dienes like cyclopentadiene, the DA reaction of β -arylnitroethylenes is reported to require higher temperatures or special activation modes.^{13,15,16} With diene **5.13**, however, the Diels-Alder adducts were formed rapidly and in high yield, typically giving full conversion to the cycloadduct within one hour. The reaction tolerated both electron donating and electron withdrawing substituents on the aryl ring, as well as bulkier naphthalene rings and hetero-aryls. Unfortunately, the hydrolysis of these compounds was trickier,

¹³ (a) Martinez, A. R.; Iglesias, G. Y. M. *J. Chem. Res. Synop.* **1998**, 0 (4), 169–169. (b) Some dienes give apparent DA products, although they likely proceed by a stepwise process: Hosokawa, S.; Matsushita, K.; Tokimatsu, S.; Toriumi, T.; Suzuki, Y.; Tatsuta, K. *Tetrahedron Lett.* **2010**, 51 (42), 5532–5536

with the major side product being **5.26k**, which arises through the partial hydrolysis and subsequent oxidation of the cycloadduct, suggesting that the workup would fare better if run in a strictly oxygen-free environment. The reaction also proceeded well using alkyl-substituted nitroalkenes, giving **5.36h** and **5.36i** in good yields after workup. The successful use of a 2,2-disubstituted nitroalkene, to give the quaternary carbon-containing spiro-fused cyclohexanone **5.26i** is noteworthy. Unfortunately, 1-alkyl nitrosyrenes proved unreactive under the conditions,



^a Percentages in parentheses refer to the NMR yield of the cycloadduct **5.25**

^b Data obtained by Pavel Elkin²

Table 5.3 Substrate scope of the Diels-Alder reaction between diene **5.13** and various nitrostyrenes and nitroalkenes

likely due to the increased steric bulk. Regardless, the present method offers a simple route to various 6-nitrocyclohexenones, the chemistry of which appears to have been scarcely investigated.¹⁴

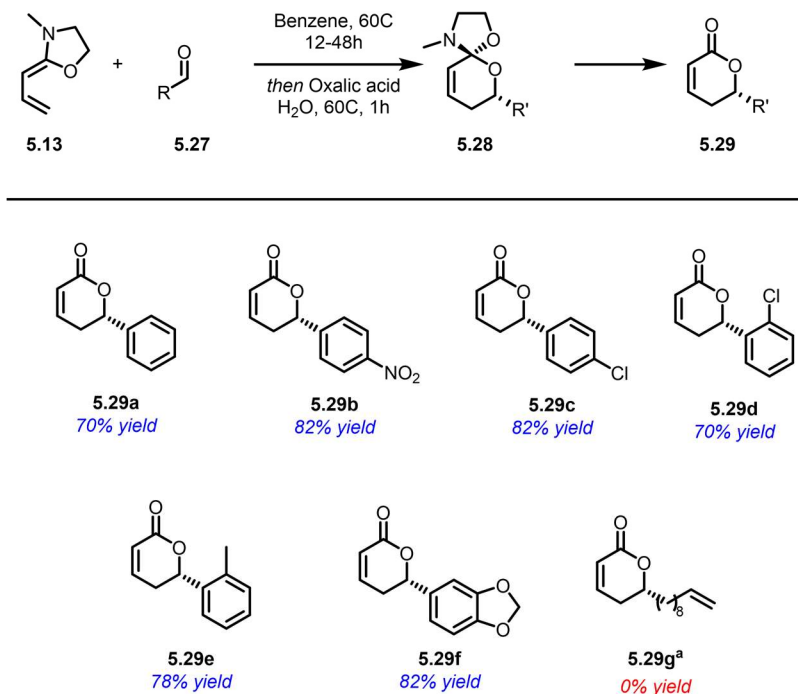
5.3B: Hetero-Diels-Alder Reactions

Based on the observation that the hetero-Diels-Alder proceeded competitively when using methacrolein, we next examined the reaction of diene **5.13** with other aldehydes, which would provide a simple and direct route to 6-substituted dihydro-2-pyrones. This subunit is found in many bioactive natural products and has been the subject of much synthesis work.¹⁵ We first carried out the reaction of the diene with benzaldehyde under our standard conditions, and were delighted to observe the clean formation of the cycloadduct by NMR. As before, the cycloadduct could not be isolated directly, but hydrolysis with oxalic acid in water once again lead to formation of the desired compound in 70% yield.

Given the simplicity of the procedure, we then looked at the reaction of the diene with some other common aldehydes. The reaction was well tolerated with both electron-rich and electron-poor benzaldehydes. Ortho substitution did lead to a small drop in yield, and 2,6-disubstituted benzaldehydes were unreactive under the standard conditions, again likely due to the

¹⁴ Ballini, R.; Petrini, M. *Arkivoc* **2008**, 2009 (9), 195–223

¹⁵ Tietze, L. F.; Ketschau, G. Hetero Diels-Alder Reactions in Organic Chemistry. In *Stereoselective Heterocyclic Synthesis I. Topics in Current Chemistry*; Springer: Berlin, 1997; Vol. 189, pp 1– 120 and references therein



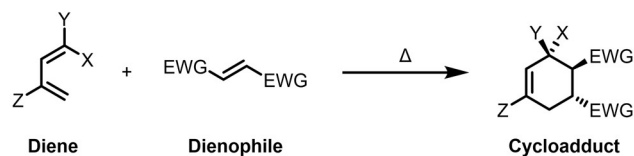
^a data obtained by Pavel Elkin²

Table 5.4 Substrate scope for the hetero-Diels-Alder reaction between diene **5.13** and various aldehydes

steric hindrance from the additional substituents pose. No reaction was observed when aliphatic aldehydes were subjected to the standard conditions.

5.4 Kinetics Analysis of the Oxazolidinone-Fused Butadiene and Other Highly-Reactive Dienes

The breadth of facile reactions observed with the new diene motivated us to benchmark its reactivity against other highly reactive dienes, such as Danishefsky's diene (**5.1**), 1-amino-3-siloxybutadiene (**5.3**), and its carbamate derivative (**5.30**). Diethyl fumarate was chosen as a coupling partner due to its high reactivity and the complete conversion observed in its crude NMR reaction with the new diene. The kinetic measurements were carried out at 60 °C in C₆D₆, and the product concentrations were monitored by ¹H NMR. The second-order rate constant for the reaction between diene **5.13** and diethyl fumarate in benzene was determined as $2.6 \times 10^{-4} \text{M}^{-1} \text{s}^{-1}$



Entry	Diene	Dienophile	Temperature (°C)	k_2 ($\text{m}^{-1}\text{s}^{-1}$)	Relative rate
1 ^a			60	2.6×10^{-4}	7.1
2 ^a			60	4.1×10^{-5}	1.1
3 ^{b,c}			17	3.6×10^{-6}	0.1
4 ^a			60	3.5×10^{-5}	1.0
5 ^{a,b}			17	1.5×10^{-3}	42.8
6 ^{a,b}			17	2.0×10^{-3}	57.1
7 ^{b,d}			60	2.0×10^{-2}	571.4
8 ^{b,c}			17	1.2×10^{-2}	342.9

^a Run in C6D6

^b Values from Kozmin et al¹⁶

^c Run in CDCl₃

^d Run in Tol-d₈

Table 5.5 Rate constants for Diels-Alder reactions of some highly-reactive dienes

(Table 5.5). For diene **5.1** and carbamate diene **5.30**, the rate constants are $4.11 \times 10^{-5} \text{ M}^{-1}\text{s}^{-1}$ and $3.5 \times 10^{-5} \text{ M}^{-1}\text{s}^{-1}$, respectively. Also listed are the reported rate constants for the reaction between the 1-amino-3-siloxy diene **5.3** and diethyl fumarate at 17 °C and with methacrolein at 17 and 60 °C, some of which were obtained by Sergei Kozmin from the Rawal lab.¹⁶¹⁸ The results show that whereas Danishefsky's diene **5.1** and carbamate diene **5.30** react with diethyl fumarate at approximately the same rate, diene **5.13** reacts nearly seven times faster. All three dienes reacted two to three times faster in chloroform than benzene. Interestingly, although dienes **5.3** and **5.13** have similar heteroatom substituents, the latter is considerably less reactive, likely due to the steric hindrance from the cis-oriented oxygen.

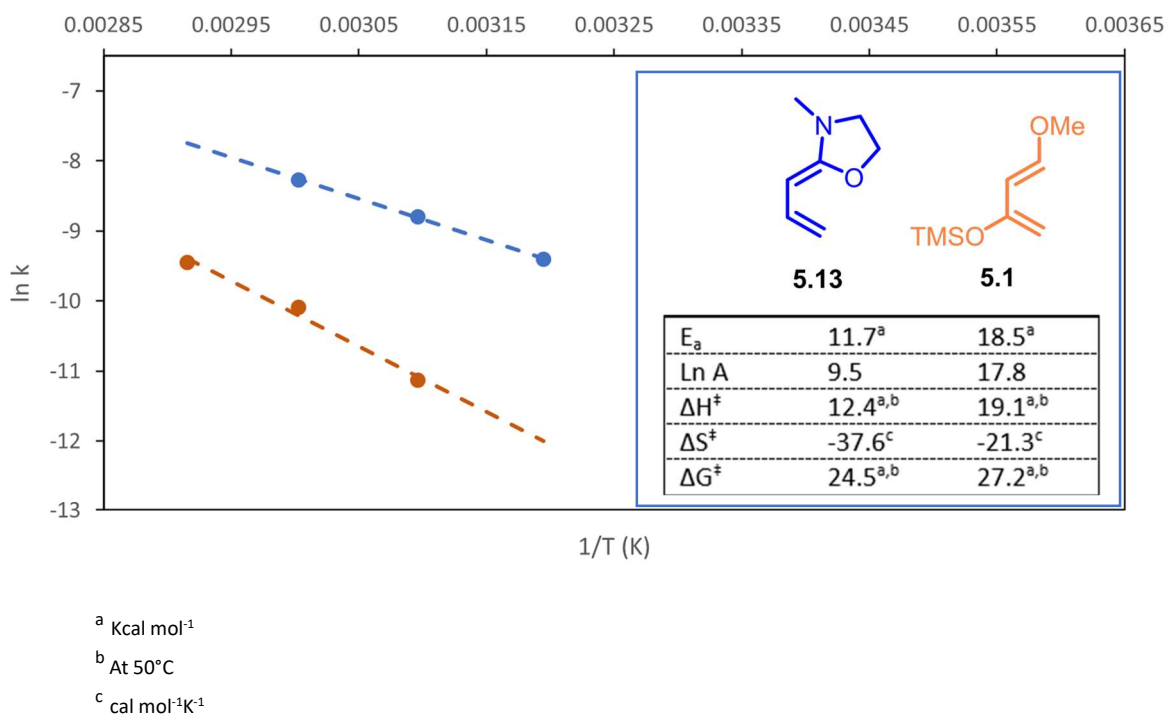


Figure 5.1 Arrhenius plots and activation parameters for the reaction of dienes **1** and **10** with diethyl fumarate in toluene; [diene]₀ = 0.2 M, [dienophile]₀ = 0.6 M. Rate constants for **1** measured at 50, 60, and 70 °C. Rate constants for **10** measured at 40, 50, and 60 °C

¹⁶ Kozmin, S. A.; Green, M. T.; Rawal, V. H. *J. Org. Chem.* **1999**, *64* (21), 8045–8047.

To gain further insight into the relative reactivities of the dienes, we determined the activation parameters for the DA reactions of diethyl fumarate with dienes **5.13** and **5.1** (Figure 5.1). As expected, the activation energy (E_a) for the reaction with Danishefsky's diene **5.1** was found to be substantially larger than that with diene **5.13**. Danishefsky's diene **5.1** also has a much higher $\ln A$, indicating the higher steric effects observed by the novel diene **5.13**. Arrhenius plots extrapolated from the kinetic data indicate a much larger difference in the relative reactivities of dienes **5.1** and **5.13** at room temperature. Interestingly, above 140 °C, diene **5.1** is predicted to react faster with diethyl fumarate than diene **5.13**, both as a result of this mismatch of steric and electronic effects.

5.5 Conclusion

As the previously described results demonstrate, 1-amino-1-oxobutadienes such as **5.13** represent an important addition to the family of reactive, heteroatom-substituted dienes. The parent diene can be synthesized in one step from a stable triflate salt precursor, and it can be prepared on a multigram scale, requiring no column or distillation. The new diene undergoes Diels-Alder reactions with a broad range of dienophiles to afford, after in situ hydrolysis, a variety of 6- and 6,6-disubstituted 2-cyclohexenones, which should prove to be versatile building blocks for the synthesis of complex molecules. The hetero-Diels-Alder reactions of the parent diene with aldehydes give direct access to 6-substituted 5,6-dihydro-2-pyrones. Kinetics experiments indicate that the new diene, despite its added steric interactions, is significantly more reactive than other highly active dienes such as Danishefsky's diene **5.1**, especially at lower temperatures. Further expansion of the chemistry of these dienes, especially the development of enantioselective Diels-Alder or hetero-Diels-Alder reactions or reactions with other heterodienophiles, is expected to greatly enhance their usefulness in chemical synthesis.

Chapter 6 Experimental Procedures and Characterization Data

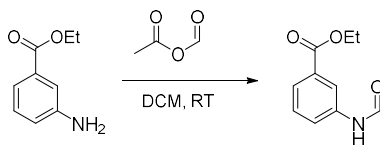
6.1 General Information

All reactions were performed in oven-dried (>12 h at 150 °C) and/or flame-dried glassware equipped with a Teflon-coated magnetic stir bar under an atmosphere of nitrogen which had been pre-dried by passage through a Drierite column ($\text{CaSO}_4 \geq 98\% + \text{CoCl}_2 < 2\%$) unless otherwise specified. Reaction solvents dichloromethane (CH_2Cl_2 ; unstabilized HPLC grade), tetrahydrofuran (THF; HPLC grade), toluene (PhMe; ACS grade), and diethyl ether (Et_2O ; ACS grade, stabilized with BHT) were dried by passage through an activated alumina column purification system (Innovative Technology Inc. Pure-Solv™). Anhydrous methanol (MeOH), ethanol (EtOH), 2-propanol (*i*-PrOH), *N,N*-dimethyl acetamide (DMAC), and benzene (PhH) were purchased from Sigma-Aldrich and used as received. Anhydrous acetonitrile (MeCN) and *N,N*-dimethylformamide (DMF) was purchased from ACROS Organics and used as received. Commercially obtained reagents were used as received, unless stated otherwise. Ambient temperature refers to 20 – 24 °C. Higher than ambient temperature was maintained using pre-heated oil baths. Lower temperatures were maintained using a cooling bath of acetone/dry ice (–78 °C), water/ice (0 °C), or NESLAB CB-80 Cryobath for all other temperatures in between. All reaction temperatures refer to external bath temperatures monitored using a thermometer, unless otherwise stated.

Thin-layer chromatography (TLC) was performed using EMD Millipore silica gel 60 Å plates and visualization was achieved with either UV fluorescence quenching (254 nm), potassium permanganate stain (KMnO_4) with heat, *p*-anisaldehyde stain, or Seebach's stain ($\text{Ce}(\text{SO}_4)_2$) in

phosphomolybdic acid) with heat. Flash column chromatography was performed on SiliCycle SiliaFlash P60 (40-63 μm particle size) using ACS grade solvents purchased from Fisher Scientific. Nuclear magnetic resonance (NMR) data were acquired on either a 600 MHz Bruker Avance-III-HD nanobay spectrometer equipped with a BBFO SmartProbe or a 500 MHz Bruker Avance-III-HD nanobay spectrometer equipped with a BBFO SmartProbe or a 500 MHz Bruker Avance-III-HD spectrometer equipped with a BBO Probe, using Topspin 3.6.2. ^1H NMR spectra were calibrated from internal standard (TMS: δ 0.0 ppm) or solvent (CD_3OD : δ 3.31 ppm; CD_3CN : δ 1.94 ppm; $\text{DMSO}-d_6$: δ 2.50 ppm) resonance and ^{13}C NMR spectra from solvent (CDCl_3 : δ 77.16 ppm, CD_3OD : δ 49.00 ppm) resonance. Chemical shifts (δ) are reported in parts per million (ppm) relative to the residual solvent resonance and coupling constants (J) are reported in hertz (Hz). NMR peak pattern abbreviations are as follows: s = singlet, d = doublet, t = triplet, q = quartet, pent = pentet, sept = septet, dd = doublet of doublets, dt = doublet of triplets, td = triplet of doublets, tt = triplet of triplets, qd = quarter of doublets, ddd = doublet of doublet of doublets, ddt = doublet of doublet of triplets, tdd = triplet of doublet of doublets, m = multiplet, br = broad (i.e., signal is broadened), app = apparent (i.e., signal appears as). Most ^1H and ^{13}C are corroborated by 2-D experiments (e.g., COSY, HSQC). High-resolution mass spectral (HRMS) analysis was measured on Agilent Technologies 6224 TOF LC/MS using electrospray ionization (ESI) at the University of Chicago Mass Spectroscopy Core Facility. Optical rotations were measured on a Jasco DIP-1000 polarimeter using a 100 mm-path-length cell, $c = \text{g}/100 \text{ mL}$. Infrared (IR) spectra were recorded on a Thermo Scientific Nicolet iS50 FT-IR spectrometer and are reported as a frequency of absorption (cm^{-1}). Chiral high-performance liquid chromatography (HPLC) analysis was performed using an Agilent analytical chromatography system with a commercial Chiralcel® column (OD-H) equipped with a guard.

6.2 Experimental Details and Characterization Data for Chapter 2



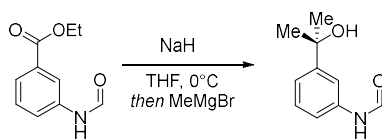
Anilide 2.6. To a 250 mL round-bottomed flask equipped with a stir bar was added formic acid (4.5 mL, 120 mmol, 4 equiv.) and acetic anhydride (3.6 mL, 38 mmol, 1.25 equiv.). After stirring for 10 minutes at room temperature, ethyl 3-aminobenzoate (4.5 g, 30 mmol, 1 equiv.) in 90 mL DCM was added. After 12 further hours of stirring, the reaction was quenched by the addition of 50 mL of concentrated NaHCO_3 and stirred for one hour. Further solid NaHCO_3 was added until evolution of CO_2 ceased. The reaction was partitioned with H_2O and DCM, and the aqueous layer was further extracted two times with 50 mL DCM. The combined organic layers were dried with MgSO_4 and concentrated under reduced pressure, giving a pale orange solid (5.7g, 29.4 mmol, 97% yield) pure by NMR.

$R_f = 0.3$ (40:60 EtOAc:hexanes)

$^1\text{H NMR}$ (500 MHz, CDCl_3) δ 2.52 (dt, $J = 13.7, 2.1$ Hz, 1H), 2.39 (dddd, $J = 10.4, 9.3, 6.3, 4.3$ Hz, 1H), 2.30 – 2.23 (m, 1H), 2.23 – 2.10 (m, 2H), 2.02 – 1.88 (m, 2H), 1.68 – 1.61 (m, 1H), 1.36 (s, 3H), 1.20 – 0.86 (m, 21H).

$^{13}\text{C NMR}$ (126 MHz, CDCl_3) δ 208.83, 112.13, 83.05, 54.21, 40.42, 37.73, 36.95, 29.49, 22.78, 18.55, 11.09.

HRMS Calculated for $\text{C}_{10}\text{H}_{11}\text{NO}_3$ [$\text{M}+\text{H}^+$]:193.0739 Found: 193.0721.



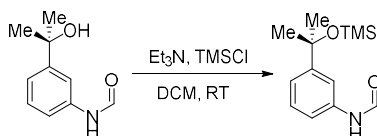
Alcohol 2.3. A 2L round-bottomed flask equipped with a magnetic stir bar was charged with NaH (60% by weight, 4g, 100 mmol, 1.1 equiv.) and THF (450 mL) and cooled to 0 °C with an ice bath. Anilide **2.6** (17.4 g, 90 mmol, 1 equiv.) was added in one portion. The reaction was stirred at 0 °C for 60 minutes. Methylmagnesium bromide (3 M in THF, 100 mL, 300 mmol, 3 equiv.) was then added dropwise over 5 min while vigorously stirring. After 90 minutes, the reaction was diluted with 400 mL Et₂O, slowly quenched with 200 mL of saturated NH₄Cl and allowed to warm to ambient temperature. The reaction mixture was partitioned between H₂O and Et₂O, and the aqueous layer was then extracted three times with 200 mL Et₂O. The combined organic layers were dried with MgSO₄ and concentrated under reduced pressure. While the desired product was crystalline, crystallization proved difficult. Instead, flash chromatography (50:50 EtOAc:hexanes) was used, giving alcohol **2.3** (14.3 g, 80 mmol, 89% yield) as a yellow crystal. Alternatively, the crude material could be used for the following step with no apparent decrease in yield.

$R_f = 0.25$ (50:50 EtOAc:hexanes)

¹H NMR (500 MHz, CDCl₃) δ 8.84 (d, $J = 11.4$ Hz, 0.5H), 8.59 (d, $J = 11.3$ Hz, 0.5H), 8.46 (s, 0.5H), 8.23 (d, $J = 1.9$ Hz, 0.5H), 7.66 (t, $J = 2.0$ Hz, 0.5H), 7.50 (dt, $J = 7.9, 1.6$ Hz, 0.5H), 7.30 – 7.19 (m, 2H), 7.16 (dt, $J = 7.9, 1.4$ Hz, 0.5H), 6.96 – 6.90 (m, 0.5H), 3.38 (s, 0.5H), 3.22 (s, 0.5H), 1.54 (d, $J = 14.4$ Hz, 6H).

^{13}C NMR (126 MHz, CDCl_3) δ 163.14, 159.87, 151.42, 150.44, 136.96, 136.73, 129.44, 128.87, 121.55, 121.03, 118.56, 116.74, 116.42, 115.38, 72.50, 72.37, 31.67, 31.59.

HRMS Calculated for $\text{C}_{10}\text{H}_{13}\text{NO}_2$ [$\text{M}+\text{H}^+$]:179.0946. Found: 179.0881.



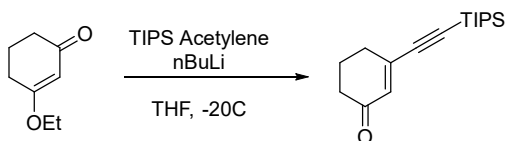
Silyl Ether 2.7. A 1L round-bottomed flask equipped with a magnetic stir bar was charged with alcohol **2.3** (14.3 g, 80 mmol, 1 equiv), Et_3N (13.8 mL, 100 mmol, 1.25 equiv) and DCM (600 mL) at RT. TMSOTf (16.2 mL, 90 mmol, 1.125 equiv) was added dropwise. The reaction was stirred at room temperature for 120 minutes. The reaction was then slowly quenched with 100 mL of saturated NaHCO_3 . The reaction mixture was partitioned between H_2O and DCM , and the aqueous layer was then extracted three times with 200 mL DCM . The combined organic layers were dried with MgSO_4 and concentrated under reduced pressure. The crude material was purified by flash chromatography (30:70 EtOAc :hexanes) giving silyl ether **2.7** (17 g, 68 mmol, 85% yield) as a dark yellow oil.

R_f = 0.40 (30:70 EtOAc :hexanes)

^1H NMR (500 MHz, CDCl_3) δ 8.71 (d, J = 11.5 Hz, 0.5H), 8.41 (d, J = 1.9 Hz, 0.5H), 7.63 (d, J = 9.9 Hz, 0.5H), 7.57 (t, J = 2.0 Hz, 0.5H), 7.52 (ddd, J = 7.9, 2.3, 1.1 Hz, 0.5H), 7.31 (td, J = 7.9, 6.5 Hz, 0.5H), 7.26 – 7.23 (m, 1H), 7.23 – 7.20 (m, 1H), 6.95 (ddd, J = 7.8, 2.3, 1.1 Hz, 0.5H), 1.59 (s, 6H), 0.14 (d, J = 4.9 Hz, 9H).

^{13}C NMR (126 MHz, CDCl_3) δ 162.28, 158.76, 152.54, 151.53, 136.50, 136.22, 129.33, 128.73, 121.73, 121.27, 118.03, 116.77, 116.31, 115.67, 75.14, 75.05, 32.41, 32.39, 2.43.

HRMS Calculated for $\text{C}_{13}\text{H}_{21}\text{NO}_2\text{Si}$ $[\text{M}+\text{H}]^+$: 251.1342. Found: 251.1361.



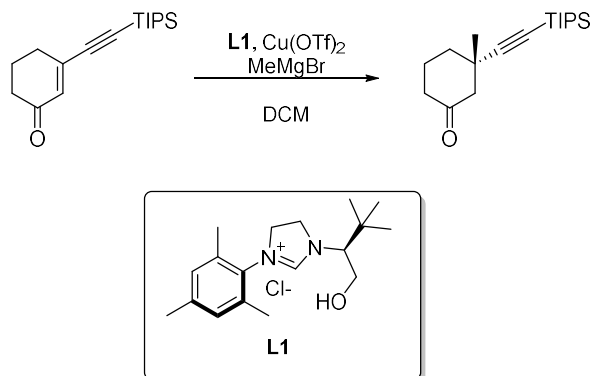
Ene-yne-one 2.17 A 100 mL round-bottomed flask was charged with TIPS acetylene (4.5 mL, 20 mmol, 2 equiv) and THF (15 mL). The reaction was cooled to -78°C in a dry ice/acetone bath and $n\text{BuLi}$ (1.6M in THF/Hexanes, 11.25 mL, 18 mmol, 1.8 equiv) was added. The reaction was stirred for 1 hour at -78°C . 3-ethoxycyclohex-2-en-1-one (1.4 g, 10 mmol, 1 equiv.) was added, and the reaction was allowed to warm to 0°C . After 1 hour, the reaction was quenched with 1M HCl (20 mL) and stirred vigorously for a further 2 hours. The reaction was then diluted with Et_2O and partitioned between Et_2O and H_2O . The aqueous layer was then extracted twice with Et_2O . The combined organic layers were dried with MgSO_4 , and the solvent was removed under reduced pressure. The crude was then re-dissolved in DCM and stirred over SiO_2 for 1 hour. The DCM was then removed under reduced pressure, and the SiO_2 was then applied to the top of a column. The crude was then purified by flash chromatography (10% EtOAc :90% Hexanes) giving ene-yne-one **2.17** (2,567 mg, 9.3 mmol, 93% yield) as a colorless oil.

R_f = 0.30 (10:90 EtOAc :hexanes)

^1H NMR (500 MHz, CDCl_3) δ 6.24 (s, 1H), 2.47 (td, J = 6.0, 1.8 Hz, 3H), 2.45 – 2.36 (m, 3H), 2.04 (ddt, J = 8.8, 7.6, 5.0 Hz, 3H), 1.16 – 1.02 (m, 21H)

^{13}C NMR (126 MHz, CDCl_3) δ 198.92, 143.30, 133.01, 105.65, 94.75, 37.33, 30.55, 22.56, 18.56, 18.46, 11.13, 11.02.

HRMS Calculated for $\text{C}_{17}\text{H}_{28}\text{OSi}$ $[\text{M}+\text{H}]^+$: 276.1909. Found: 276.184.



(+) - **Ketone 2.18**. A 100 mL round-bottomed flask was charged with MeMgBr (2.26 mL, 3M in Et_2O , 6.8 mmol, 2 equiv). The ethereal solvent was blown off with dry nitrogen and replaced with xx mL DCM . This process was repeated three times. After the final time, the solid was further dried under house vacuum for 10 minutes. $\text{Cu}(\text{OTf})_2$ (75 mg, 0.21 mmol, 0.06 equiv) and ligand **L1** (100 mg, 0.31 mmol, 0.09 equiv) were combined in 10 mL dry DCM . The solution was added to the Grignard to give a grey suspension. The solution was cooled to -20°C . Ene-yne-one **2.17** (946 mg, 3.4 mmol, 1 equiv) was added as a 0.1M solution, and the reaction was stirred for 2 hours. After the reaction completed, the reaction was quenched with concentrated NH_4Cl and partitioned between Et_2O and H_2O . The aqueous layer was then extracted twice with Et_2O . The combined organic layers were dried with MgSO_4 , and the solvent was removed under reduced

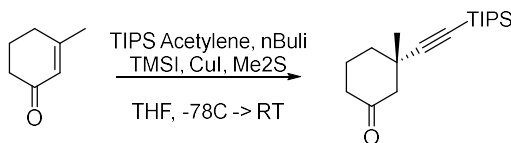
pressure. The crude was purified by flash chromatography (10% EtOAc:90% Hexanes) giving ketone (+)-**2.18** (814 mg, 2.79 mmol, 82% yield) as a colorless oil in 94% ee.

$R_f = 0.25$ (10:90 EtOAc:hexanes)

$^1\text{H NMR}$ (500 MHz, CDCl_3) δ 2.52 (dt, $J = 13.7, 2.1$ Hz, 1H), 2.39 (dddd, $J = 10.4, 9.3, 6.3, 4.3$ Hz, 1H), 2.30 – 2.23 (m, 1H), 2.23 – 2.10 (m, 2H), 2.02 – 1.88 (m, 2H), 1.68 – 1.61 (m, 1H), 1.36 (s, 3H), 1.20 – 0.86 (m, 21H).

$^{13}\text{C NMR}$ (126 MHz, CDCl_3) δ 208.83, 112.13, 83.05, 54.21, 40.42, 37.73, 36.95, 29.49, 22.78, 18.55, 11.09.

HRMS Calculated for $\text{C}_{18}\text{H}_{32}\text{OS}$ $i[\text{M}+\text{H}]^+$: 292.2222. Found: 292.2097.



(+) - **Ketone 2.18**. A 500 mL round-bottomed flask was charged with TIPS-acetylene (8.2 g, 45 mmol, 1.5 equiv) and THF (180 mL). The flask was cooled to -10 °C, and nBuLi (26.2 mL, 1.6M in hexanes, 42 mmol, 1.4 equiv) was added dropwise. The reaction was stirred for 30 minutes, then CuI (9.1 g, 48 mmol, 1.6 equiv) and Me₂S (3.1 mL, 42 mmol, 1.4 equiv) were added in one portion. The reaction was cooled to -20 °C for one hour, then further cooled to -78 °C, at which point the reaction had turned green. Once cooled, TMSI (6.4 mL, 45 mmol, 1.5 equiv) was added, and the reaction was stirred for 10 minutes. 3-methyl-2-cyclohexenone (3.4 mL, 3.3 g, 30 mmol, 1 equiv) was added neat, and the reaction was stirred at -78 °C for one further hour. The reaction was then quenched at -78 °C with 250 mL of concentrated NH₄Cl, then allowed to warm to RT and a further 50 mL of 1M HCl was added. The reaction was then filtered through celite, partitioned between

Et₂O and H₂O, and the organic layer was washed once with Na₂S₂O₃. The aqueous layer was then extracted three times with Et₂O. The combined organic layers were dried with MgSO₄, and the solvent was removed under reduced pressure. The crude was purified by flash chromatography (10% EtOAc:90% Hexanes) giving racemic ketone **2.18** (7.8 g, 26.7 mmol, 89% yield) as a colorless oil.

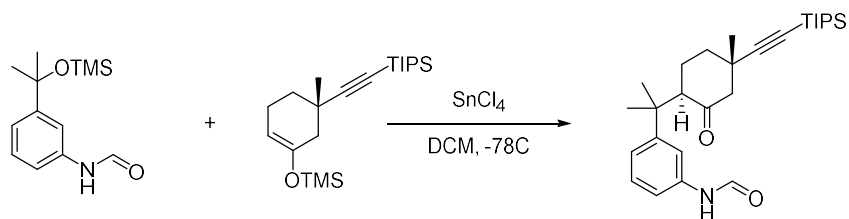
Spectral data identical to those reported above for the chiral compound.



Enol ether 2.19. A 25 mL round-bottomed flask was charged with Ketone **2.18** (527 mg, 1.8 mmol, 1 equiv), Et₃N (0.37 mL, 2.7 mmol, 1.5 equiv) and DCM (5mL). TMSOTf (0.40 mL, 2.2 mmol, 1.25 equiv) was added slowly. The reaction was stirred at room temperature for 4 hours. The reaction was then quenched with xx mL of concentrated NaHCO₃. The reaction was portioned between DCM and H₂O. The aqueous layer was extracted twice with DCM. The combined organic layers were dried with MgSO₄, and the solvent was removed under reduced pressure. The crude material was purified by flash chromatography (5% EtOAc:95%hexanes) giving enol ether **2.19** (611 mg, 1.66 mmol, 92% yield) as a colorless oil. *R_f* = 0.7 (10:90 EtOAc:hexanes)

¹H NMR (500 MHz, CDCl₃) δ 4.87 (ddd, *J* = 5.0, 3.0, 1.4 Hz, 1H), 2.43 – 2.25 (m, 1H), 2.22 – 2.14 (m, 1H), 2.08 – 1.97 (m, 2H), 1.73 – 1.63 (m, 1H), 1.41 – 1.32 (m, 1H), 1.27 (s, 3H), 1.12 – 0.95 (m, 21H), 0.25 – 0.15 (m, 9H).

^{13}C NMR (126 MHz, CDCl_3) δ 148.08, 115.35, 103.39, 77.27, 77.02, 76.76, 43.10, 34.73, 32.06, 28.78, 21.74, 18.65, 18.58, 11.25, 11.23, 0.38.



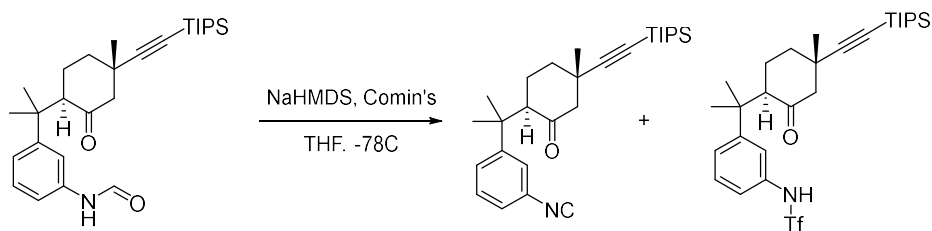
Ketone 2.21. A 100 mL round-bottomed flask was charged with silyl enol ether **2.19** (1350 mg, 3.7 mmol, 3 equiv), Silyl ether **2.7** (308 mg, 1.23 mmol, 1 equiv) and DCM (20 mL). The reaction was cooled to -78°C in an acetone/dry ice bath. SnCl_4 (0.31 mL, 3.7 mmol, 3 equiv) was added slowly. The reaction was stirred at -78°C for 3 hours. The reaction was slowly quenched with xxx mL of saturated NaHCO_3 while stirring rapidly. The mixture was diluted with water and filtered through a celite plug. The filter cake was then washed with 20 mL DCM . The filtrate was then partitioned between H_2O and DCM , and the aqueous layer was then extracted three times with DCM . The combined organic layers were dried with MgSO_4 and concentrated under reduced pressure. The crude material was purified by flash chromatography (30% EtOAc :70% hexanes) to give ketone **2.21** (446 mg, 0.98 mmol, 80% yield) as a colorless oil.

$R_f = 0.15$ (30:70 EtOAc :hexanes)

^1H NMR (500 MHz, CDCl_3) δ 8.68 (d, $J = 11.5$ Hz, 0.5H), 8.41 (d, $J = 1.8$ Hz, 0.5H), 7.53 (t, $J = 2.0$ Hz, 0.5H), 7.49 – 7.37 (m, 0.5H), 7.35 – 7.29 (m, 1H), 7.20 (ddd, $J = 7.9, 1.8, 0.9$ Hz, 0.5H), 7.18 – 7.12 (m, 0.5H), 7.10 (s, 0.5H), 7.03 (t, $J = 2.1$ Hz, 0.5H), 6.99 – 6.89 (m, 0.5H), 2.93 – 2.69 (m, 1H), 2.65 (dd, $J = 12.8, 2.8$ Hz, 1H), 2.28 (ddd, $J = 13.1, 4.1, 1.9$ Hz, 1H), 2.08 – 1.96 (m, 1H), 1.93 – 1.72 (m, 1.5H), 1.66 (ddd, $J = 13.9, 9.6, 5.0$ Hz, 1.5H), 1.47 (s, 3H), 1.40 (d, $J = 6.3$ Hz, 3H), 1.19 (d, $J = 4.3$ Hz, 3H), 1.11 – 1.00 (m, 21H).

^{13}C NMR (126 MHz, CDCl_3) δ 209.06, 208.68, 162.56, 158.93, 151.63, 150.62, 136.76, 136.41, 129.36, 128.74, 122.97, 122.37, 117.65, 117.45, 117.07, 116.26, 114.77, 114.67, 80.35, 80.26, 58.88, 58.86, 55.32, 39.37, 39.33, 37.76, 37.69, 36.32, 36.27, 26.47, 26.07, 25.47, 25.40, 24.82, 24.57, 24.54, 24.45, 18.60, 11.12.

HRMS Calculated for $\text{C}_{28}\text{H}_{43}\text{NO}_2\text{Si}$ $[\text{M}+\text{H}]^+$: 453.3063. Found: 453.306.



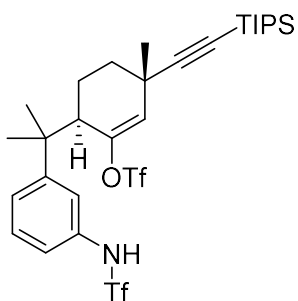
Isonitrile 2.22 and N-triflamide 2.23. A 10 mL round-bottomed flask was charged with Ketone **2.21** (44 mg, 0.1 mmol, 1 equiv) and THF (0.5mL). The reaction was cooled to $-78\text{ }^\circ\text{C}$, and NaHMDS (0.2 mL, 1M in THF, 0.2 mmol, 2 equiv) was added. The reaction was stirred at $-78\text{ }^\circ\text{C}$ for 30 minutes, and Comin's (102 mg, 0.3 mmol, 3equiv) was added as a solid in a single portion. The reaction was stirred for a further 30 minutes at $-78\text{ }^\circ\text{C}$, at which point it was quenched at $-78\text{ }^\circ\text{C}$ with concentrated NH_4Cl . The mixture was diluted with Et_2O and then partitioned between H_2O and Et_2O , and the aqueous layer was then extracted three times with Et_2O . The combined organic layers were dried with MgSO_4 and concentrated under reduced pressure. The crude material was purified by flash chromatography (30% EtOAc :70% hexanes) to give isonitrile **2.23** (13 mg, 0.03 mmol, 30% yield) as a dark brown oil and N-triflamide **2.23** (xx g, xx mmol, 65% yield) as a red-orange solid.

Data for Isonitrile 2.22

$R_f = 0.6$ (30:70 EtOAc :hexanes)

¹H NMR (500 MHz, CDCl₃) δ 7.38 (ddd, *J* = 8.1, 2.0, 1.1 Hz, 1H), 7.34 (t, *J* = 1.9 Hz, 1H), 7.31 (t, *J* = 7.9 Hz, 1H), 7.22 – 7.16 (m, 1H), 2.72 (dd, *J* = 11.9, 5.6 Hz, 1H), 2.62 (d, *J* = 13.2 Hz, 1H), 2.27 (dd, *J* = 13.2, 2.1 Hz, 1H), 2.03 (td, *J* = 12.9, 4.2 Hz, 1H), 1.87 – 1.73 (m, 2H), 1.63 (td, *J* = 12.7, 3.7 Hz, 1H), 1.44 (s, 3H), 1.36 (s, 3H), 1.17 (s, 3H).

¹³C NMR (101 MHz, CDCl₃) δ 208.24, 151.55, 129.00, 127.00, 124.15, 123.66, 114.63, 58.75, 55.25, 39.28, 37.75, 36.19, 25.56, 25.32, 25.09, 24.45, 18.60, 11.13, -0.00.



SI.1

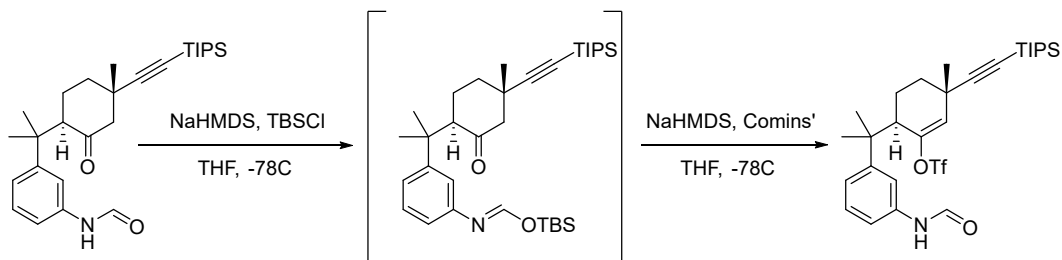
Data for bis-triflated triflimide SI.1

R_f = 0.35 (30:70 EtOAc:hexanes)

¹H NMR (500 MHz, CDCl₃) δ 7.37 (t, *J* = 7.9 Hz, 1H), 7.31 (d, *J* = 8.2 Hz, 1H), 7.25 (s, 1H), 7.16 (d, *J* = 8.0 Hz, 1H), 5.83 (s, 1H), 2.84 (dd, *J* = 6.9, 4.2 Hz, 1H), 1.94 – 1.78 (m, 1H), 1.61 (dd, *J* = 11.3, 5.2 Hz, 2H), 1.49 (s, 3H), 1.42 (s, 3H), 1.18 (s, 3H), 1.03 (d, *J* = 5.1 Hz, 21H).

¹³C NMR (126 MHz, CDCl₃) δ 160.06, 150.45, 149.51, 134.07, 130.53, 129.44, 129.29, 129.17, 128.36, 128.04, 127.69, 127.28, 125.49, 124.91, 121.70, 121.21, 119.75, 118.56, 117.20, 112.06, 81.42, 60.86, 47.10, 41.30, 41.15, 33.80, 33.52, 33.37, 33.18, 28.77, 28.38, 27.59, 27.39, 23.53, 21.02, 18.57, 18.54, 18.44, 14.04, 11.15, 11.05.

¹⁹F NMR (470 MHz, CDCl₃) δ -73.11, -74.00.



Enol triflate 2.26. A 25 mL round-bottomed flask was charged with Ketone **2.26** (440 mg, 1.01 mmol, 1 equiv) and THF (5 mL). The reaction was cooled to $-78\text{ }^{\circ}\text{C}$ in an acetone/dry ice bath, and NaHMDS (0.98 mL, 1M in THF, 0.98 mmol, 0.98 equiv) was added. The reaction was stirred at $-78\text{ }^{\circ}\text{C}$ for 30 minutes, and TBSCl (151 mg, 1.01 mmol, 1 equiv) was added as a solid in a single portion. The reaction was stirred for a further 1 hour at $-78\text{ }^{\circ}\text{C}$, or until monitoring by NMR indicated that the starting ketone had been completely converted to silylated amide **2.AT**. Further NaHMDS (2.2 mL, 1M in THF, 2.2 mmol, 2.2 equiv) was added, and the reaction was stirred at $-78\text{ }^{\circ}\text{C}$ for one hour, after which Comins (1,037 mg, 3.03 mmol, 3 equiv) was added as a solid. The reaction was allowed to warm to $0\text{ }^{\circ}\text{C}$, and stirred at that temperature for a further 1 hour, at which point it was quenched with concentrated NH_4Cl . The mixture was diluted with Et_2O and then partitioned between H_2O and Et_2O , and the aqueous layer was then extracted three times with xxx mL Et_2O . The combined organic layers were dried with MgSO_4 and concentrated under reduced pressure. The crude material was purified by flash chromatography (30% EtOAc :70% hexanes) to give enol triflate **2.26** (496 mg, 0.85 mmol, 84% yield) as a colorless oil.

$R_f = 0.20$ (30:70 EtOAc :hexanes)

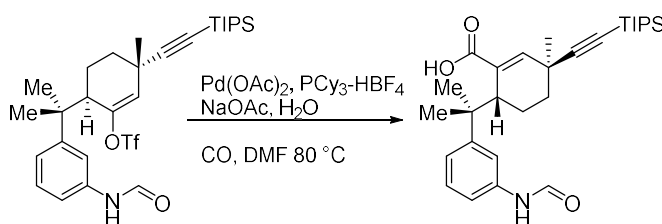
$^1\text{H NMR}$ (500 MHz, CDCl_3) δ 8.69 (d, $J = 11.5\text{ Hz}$, 0.5H), 8.41 (d, $J = 1.8\text{ Hz}$, 0.5H), 7.82 (d, $J = 11.4\text{ Hz}$, 0.5H), 7.49 (d, $J = 7.7\text{ Hz}$, 1H), 7.32 (dt, $J = 12.8, 7.9\text{ Hz}$, 1H), 7.25 (s, 0.5H), 7.19 (d, $J = 7.9\text{ Hz}$, 0.5H), 7.13 (d, $J = 7.9\text{ Hz}$, 0.5H), 7.07 – 6.96 (m, 1H), 5.84 (s, 1H), 3.03 – 2.74 (m,

1H), 1.99 – 1.76 (m, 1H), 1.69 – 1.62 (m, 2H), 1.66 – 1.55 (m, 1H), 1.48 (d, $J = 3.3$ Hz, 3H), 1.41 (s, 3H), 1.21 (d, $J = 12.0$ Hz, 3H), 1.13 – 0.94 (m, 21H).

^{13}C NMR (126 MHz, CDCl_3) δ 162.56, 158.93, 150.73, 150.56, 149.99, 148.86, 136.86, 136.57, 129.61, 128.95, 127.90, 127.81, 123.49, 122.87, 117.92, 117.35, 116.78, 81.46, 47.01, 41.17, 41.09, 33.61, 33.56, 33.53, 29.02, 28.29, 27.75, 27.32, 26.96, 23.69, 23.58, 18.62, 18.60, 18.49, 18.47, 11.17, 11.06.

^{19}F NMR (470 MHz, CDCl_3) δ -72.98, -73.09.

HRMS Calculated for $\text{C}_{29}\text{H}_{42}\text{F}_3\text{NO}_4\text{SSi}$ $[\text{M}+\text{H}]^+$: 585.2556. Found: 585.263.



Carboxylic Acid 2.28. A 100 mL round-bottomed flask was charged with $\text{Pd}(\text{OAc})_2$ (10 mg, 0.046 mmol, 0.2 equiv), $\text{PCy}_3\text{-HBF}_4$ (25 mg, 0.069 mmol, 0.3 equiv), and NaOAc (41 mg, 0.5 mmol, 2.3 equiv). The atmosphere was removed with vacuum and replaced with nitrogen three times. A solution of enol triflate **2.26** (140 mg, 0.23 mmol, 1 equiv) in DMF (3 mL) was added. The atmosphere was again removed with vacuum, and refilled with CO three times. Following the third removal a balloon filled with CO was attached. H_2O (41 mg, 0.09 mL, 2.3 mmol, 10 equiv) was added, and the reaction was heated to 100°C . After stirring for 18 hours, the reaction was diluted with ether and washed with water. The reaction was partitioned between Et_2O and water. The aqueous layer was then extracted four times with Et_2O . The combined organic layers were dried over MgSO_4 and concentrated under reduced pressure. The crude material was purified by flash

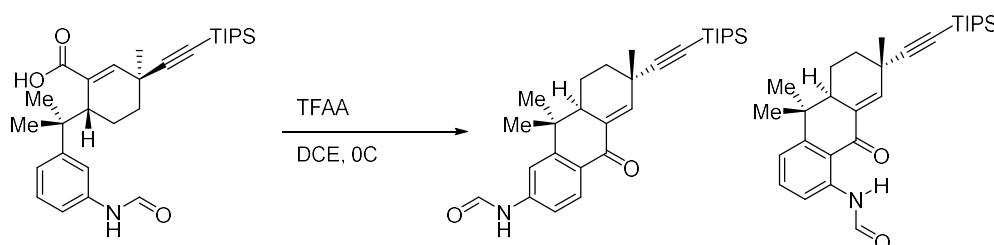
chromatography (5% MeOH:95% DCM) giving carboxylic acid **2.A28** (108 mg, 0.23 mmol, 98% yield) as a pale yellow amorphous solid.

$R_f = 0.4$ (5:95 MeOH:DCM)

$^1\text{H NMR}$ (500 MHz, CDCl_3) δ 9.77 (s, 0.66H), 8.69 (d, $J = 11.2$ Hz, 0.66H), 7.26 (dd, $J = 7.9, 2.7$ Hz, 1H), 7.19 (d, $J = 8.1$ Hz, 1H), 7.15 (d, $J = 2.1$ Hz, 1H), 6.94 (d, $J = 7.8$ Hz, 1H), 6.70 (s, 1H), 3.10 (d, $J = 6.3$ Hz, 1H), 1.91 – 1.67 (m, 5H), 1.42 (s, 4H), 1.38 (d, $J = 2.5$ Hz, 4H), 1.33 (s, 3H), 1.11 – 0.95 (m, 29H).

$^{13}\text{C NMR}$ (101 MHz, CDCl_3) δ 173.90, 163.67, 159.10, 151.11, 144.06, 136.50, 136.35, 131.60, 131.50, 129.12, 123.58, 118.70, 118.00, 117.06, 115.32, 113.17, 81.05, 42.33, 42.24, 41.90, 33.89, 33.11, 29.71, 28.25, 27.87, 27.01, 22.34, 18.59, 18.58, 11.14, 0.00.

HRMS Calculated for $\text{C}_{29}\text{H}_{43}\text{NO}_3\text{Si}$ $[\text{M}+\text{H}]^+$: 481.3012. Found: 481.3005.



Para-Cyclized Ketone 2.35. A 3 mL scintillation vial was charged with carboxylic acid **2.28** (28 mg, 0.06 mmol, 1 equiv) and DCE (0.2 mL). The vial was chilled to 0°C with an ice bath, and trifluoroacetic anhydride (25 mg, 0.12 mmol, 2 equiv) was added. The reaction was stirred for two hours, then diluted with DCM and quenched with concentrated NaHCO_3 . The reaction was partitioned between water and DCM. The aqueous layer was then extracted three times with DCM. The combined organic layers were dried over MgSO_4 and concentrated under reduced pressure. The crude material was purified by flash chromatography (10-40% EtOAc:90-60%Hexanes)

giving of para-cyclized ketone **2.35** (21 mg, 0.046 mmol, 76% yield) and ortho-cyclized ketone **2.27** (5 mg, 0.011 mmol, 18% yield), each as pale yellow amorphous solid.

Data for para-cyclized ketone 2.35

$R_f = 0.2$ (30:70 EtOAc:hexanes)

$^1\text{H NMR}$ (500 MHz, CDCl_3) δ 8.88 (d, $J = 11.2$ Hz, 0.5H), 8.47 (d, $J = 1.6$ Hz, 1H), 8.11 (d, $J = 8.2$ Hz, 0.5H), 8.08 (d, $J = 8.4$ Hz, 1H), 7.89 (d, $J = 2.1$ Hz, 0.5H), 7.75 (d, $J = 11.2$ Hz, 0.5H), 7.41 – 7.36 (m, 1H), 7.25 – 7.20 (m, 1H), 7.11 – 7.05 (m, 1H), 2.78 – 2.56 (m, 1H), 2.05 – 1.88 (m, 3H), 1.76 – 1.64 (m, 1H), 1.50 (d, $J = 4.0$ Hz, 3H), 1.43 (d, $J = 2.1$ Hz, 3H), 1.15 – 0.96 (m, 24H).

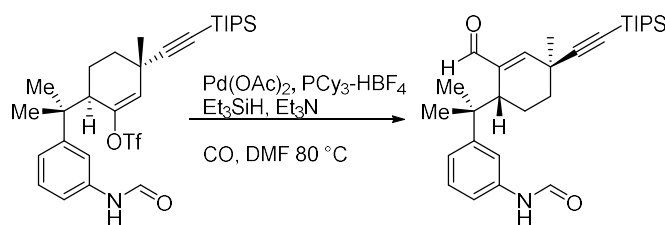
Data for orth-cyclized ketone 2.27 (matches results below)

$R_f = 0.6$ (30:70 EtOAc:hexanes)

$^1\text{H NMR}$ (500 MHz, CDCl_3) δ 12.02 (s, 1H), 8.62 (d, $J = 8.4$ Hz, 1H), 8.52 (d, $J = 1.9$ Hz, 1H), 7.54 (t, $J = 8.1$ Hz, 1H), 7.24 (t, $J = 1.8$ Hz, 2H), 2.63 (dq, $J = 8.1, 2.8$ Hz, 1H), 2.00 (d, $J = 11.3$ Hz, 3H), 1.97 – 1.84 (m, 1H), 1.49 (s, 3H), 1.46 – 1.42 (m, 3H), 1.18 – 1.05 (m, 21H), 1.03 (s, 3H).

$^{13}\text{C NMR}$ (101 MHz, CDCl_3) δ 189.97, 159.89, 154.27, 144.14, 140.65, 134.95, 133.90, 119.62, 118.91, 118.20, 113.60, 80.73, 42.75, 37.67, 34.71, 33.06, 27.73, 25.85, 24.36, 19.82, 18.64, 11.17, -0.00.

HRMS Calculated for $\text{C}_{29}\text{H}_{41}\text{NO}_2\text{Si}$ $[\text{M}+\text{H}]^+$: 463.2907. Found: 463.2839.



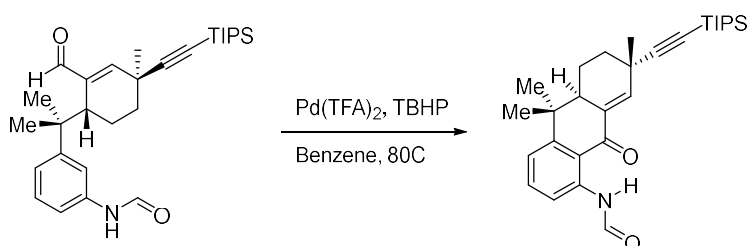
Aldehyde 2.33. A 10 mL round-bottomed flask was charged with Pd(OAc)₂ (7 mg, 0.03 mmol, 0.15 equiv.) and PCy₃-HBF₄ (22 mg, 0.06 mmol, 0.3 equiv.). The atmosphere was removed with vacuum and replaced with nitrogen three times. Et₃N (42 mg, 0.06 mL, 0.42 mmol, 2.3 equiv.), and a solution of enol triflate **2.26** (100 mg, 0.17 mmol, 1 equiv.) in DMF (1.5 mL) were added. The atmosphere was again removed with vacuum, and refilled with CO three times. Following the third removal a balloon filled with CO was attached. Et₃SiH (0.05 mL, 0.34 mmol, 2 equiv.) was added to the reaction, and the reaction was heated to 80 °C. After stirring for 18 hours, the reaction was diluted with ether and washed with water. The reaction was partitioned between Et₂O and water. The aqueous layer was then extracted two times with Et₂O. The combined organic layers were dried over MgSO₄ and concentrated under reduced pressure. The crude material was purified by flash chromatography (30% EtOAc:70% hexanes) giving aldehyde **2.33** (75 mg, 0.16 mmol, 95% yield) as a pale yellow amorphous solid.

$R_f = 0.25$ (30:70 EtOAc:hexanes)

¹H NMR (500 MHz, CDCl₃) δ 9.47 (d, $J = 4.6$ Hz, 1H), 8.70 (d, $J = 11.4$ Hz, 0.5H), 8.40 (d, $J = 1.8$ Hz, 0.5H), 8.14 (d, $J = 11.5$ Hz, 0.5H), 7.54 – 7.43 (m, 1.5H), 7.37 – 7.23 (m, 1.5H), 7.19 (d, $J = 8.0$ Hz, 0.5H), 7.12 (d, $J = 7.9$ Hz, 0.5H), 7.03 (t, $J = 2.1$ Hz, 0.5H), 6.98 (dd, $J = 7.9, 2.1$ Hz, 0.5H), 6.62 (d, $J = 7.3$ Hz, 1H), 3.04 (dt, $J = 8.5, 3.2$ Hz, 1H), 1.66 (m, 3H), 1.37 (s, 3H), 1.30 (d, $J = 3.9$ Hz, 3H), 1.28 – 1.21 (m, 3H), 1.09 (p, $J = 4.2$ Hz, 3H), 1.00 (d, $J = 4.4$ Hz, 21H).

^{13}C NMR (126 MHz, CDCl_3) δ 194.44, 194.19, 162.53, 158.93, 154.42, 154.20, 150.45, 149.37, 140.87, 140.83, 136.79, 136.47, 129.33, 128.70, 123.85, 123.22, 118.38, 117.72, 117.68, 116.43, 112.33, 112.07, 82.21, 81.96, 77.30, 77.04, 76.79, 42.04, 39.77, 39.62, 33.83, 33.81, 33.77, 33.71, 30.02, 29.94, 29.71, 28.09, 27.92, 27.74, 27.67, 22.43, 18.66, 18.60, 18.56, 18.54, 11.19, 11.09.

HRMS Calculated for $\text{C}_{29}\text{H}_{43}\text{NO}_2\text{Si}$ $[\text{M}+\text{H}]^+$: 465.3063. Found: 465.3053.



Ortho-cyclized ketone 2.27. A 5 mL round-bottomed flask was charged with $\text{Pd}(\text{TFA})_2$ (1 mg, 0.004 mmol, 0.2 equiv.), Aldehyde **2.33** (9 mg, 0.02 mmol, 1 equiv) and benzene (0.5 mL). TBHP (0.01 mL, 70% by weight, 0.08 mmol, 4 equiv) was added and the reaction was warmed to 80 °C. The reaction was stirred for one hour, then diluted with Et_2O and quenched with conc Na_2SO_3 . The reaction was partitioned between water and Et_2O . The aqueous layer was then extracted three times with Et_2O . The combined organic layers were dried over MgSO_4 and concentrated under reduced pressure. The crude material was purified by flash chromatography (20% EtOAc :80%Hexanes) giving ketone **2.27** (7.7 mg, 0.017 mmol, 83% yield) as a pale yellow amorphous solid.

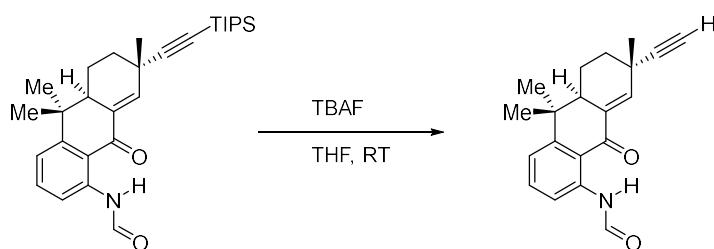
R_f = 0.6 (30:70 EtOAc :hexanes)

^1H NMR (500 MHz, CDCl_3) δ 12.02 (s, 1H), 8.62 (d, J = 8.4 Hz, 1H), 8.52 (d, J = 1.9 Hz, 1H), 7.54 (t, J = 8.1 Hz, 1H), 7.24 (t, J = 1.8 Hz, 2H), 2.63 (dq, J = 8.1, 2.8 Hz, 1H), 2.00 (d, J = 11.3

Hz, 3H), 1.97 – 1.84 (m, 1H), 1.49 (s, 3H), 1.46 – 1.42 (m, 3H), 1.18 – 1.05 (m, 21H), 1.03 (s, 3H).

^{13}C NMR (101 MHz, CDCl_3) δ 189.97, 159.89, 154.27, 144.14, 140.65, 134.95, 133.90, 119.62, 118.91, 118.20, 113.60, 80.73, 42.75, 37.67, 34.71, 33.06, 27.73, 25.85, 24.36, 19.82, 18.64, 11.17, -0.00.

HRMS Calculated for $\text{C}_{29}\text{H}_{41}\text{NO}_2\text{Si}$ $[\text{M}+\text{H}]^+$: 463.2907. Found: 463.2839.



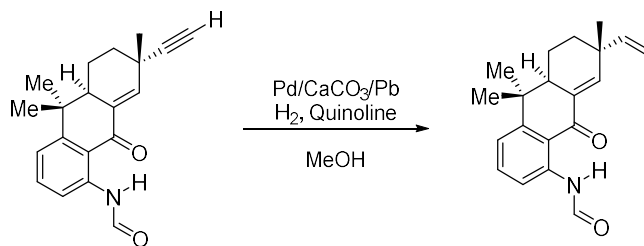
Ketone 2.44. A 5 mL round-bottomed flask was charged with ketone **2.27** (8 mg, 0.017 mmol, 1 equiv) and THF(0.8 mL). TBAF (0.039 mL, 1M in THF, 0.034 mmol, 2 equiv) was added and the reaction was stirred for two hours. Following complete consumption of starting material the reaction was then diluted with Et_2O and quenched with conc NH_4Cl . The reaction was partitioned between water and Et_2O . The aqueous layer was then extracted three times with Et_2O . The combined organic layers were dried over MgSO_4 and concentrated under reduced pressure. The crude material was purified by flash chromatography (20% EtOAc :80%hexanes) giving ketone **2.44** (4.7 mg, 0.015 mmol, 92% yield) as a pale yellow amorphous solid.

R_f = 0.2 (20:80 EtOAc :hexanes)

^1H NMR (500 MHz, CDCl_3) δ 11.97 (s, 1H), 8.60 (d, J = 8.4 Hz, 1H), 8.49 (s, 1H), 7.52 (t, J = 8.1 Hz, 1H), 7.23 – 7.19 (m, 2H), 2.61 (ddd, J = 10.5, 5.4, 2.5 Hz, 1H), 2.22 (s, 1H), 2.03 – 1.94

(m, 2H), 1.89 (dd, $J = 13.5, 10.3$ Hz, 1H), 1.66 – 1.58 (m, 1H), 1.47 (s, 3H), 1.43 (d, $J = 1.5$ Hz, 3H), 1.01 (s, 3H).

^{13}C NMR (126 MHz, CDCl_3) δ 189.78, 159.85, 154.25, 143.42, 140.70, 135.08, 134.41, 119.67, 118.93, 118.06, 89.40, 68.89, 42.82, 37.67, 34.35, 31.97, 27.20, 25.87, 24.35, 19.70, 0.01.



Dechlorofontonamide 1.27. A 5 mL round-bottomed flask was charged with ketone **2.44** (4.7 mg, 0.015 mmol, 1 equiv), Pd/CaCO₃ poisoned with lead (1mg, 5% by weight, 0.05 equiv), quinoline (5 mg, 0.039 mmol, 2 equiv) and MeOH (0.5 mL). The atmosphere was removed by vacuum and replace three times with H₂ gas. After the final time, a balloon filled with H₂ was attached. The reaction was stirred for 15 minutes. Note that this reaction is very rapid and prone to over-reduction, and as such requires careful monitoring by TLC every 5 minutes. Monitoring required removal of the H₂ through vacuum and replacing with N₂ to halt the reaction. After the TLC plate had been developed the atmosphere was again replace three times through subsequent evacuation and refill from an H₂ balloon, and the balloon was attached after the third evacuation. After the reaction was complete the crude material was diluted with Et₂O and filtered through celite. The filter cake was washed with Et₂O and the combined organic layers were concentrated under reduced pressure. The crude material was purified by preparative thin layer chromatography (20% EtOAc:80%Hexanes) giving (-)-dechlorofontonamide (4.4 mg, 0.014 mmol, 98% yield) as a pale yellow amorphous solid.

$R_f = 0.25$ (20:80 EtOAc:hexanes)

^1H NMR (500 MHz, CDCl_3) δ 12.02 (s, 1H), 8.58 (d, $J = 8.4$ Hz, 1H), 8.49 (d, $J = 1.9$ Hz, 1H), 7.52 (t, $J = 8.1$ Hz, 1H), 7.22 (d, $J = 8.0$ Hz, 1H), 7.19 – 7.14 (m, 1H), 5.88 (dd, $J = 17.5, 10.6$ Hz, 1H), 5.07 (d, $J = 17.5$ Hz, 1H), 5.04 (d, $J = 10.6$ Hz, 1H), 2.58 (ddd, $J = 10.0, 5.7, 2.5$ Hz, 1H), 2.04 – 1.94 (m, 1H), 1.82 – 1.63 (m, 2H), 1.62 – 1.55 (m, 1H), 1.48 (s, 3H), 1.21 (s, 3H), 1.04 (s, 3H). A

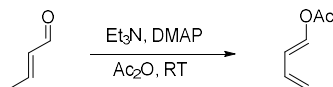
^{13}C NMR (126 MHz, CDCl_3) δ 190.01, 159.84, 154.46, 146.70, 146.16, 140.63, 134.87, 134.57, 119.58, 118.90, 118.28, 112.19, 43.31, 38.92, 37.73, 33.39, 30.33, 25.82, 25.39, 24.42, 20.27, 0.00.

HRMS Calculated for $\text{C}_{20}\text{H}_{23}\text{NO}_2$ $[\text{M}+\text{H}]^+$: 309.1729. Found: 309.1753.

$[\alpha]_D^{20} = -92$ (CHCl_3 , c 0.01)

All data matches published data for the natural product.

6.3 Experimental Details and Characterization Data for Chapter 3



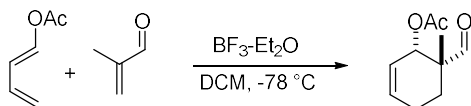
Diene 3.32. A 1 L round-bottomed flask was charged with crotonaldehyde (28 g, 32 mL, 400 mmol, 1 equiv.), triethylamine (80 g, 112 mL, 800 mmol, 2 equiv.), and Ac₂O (82 g, 78 mL, 800 mmol, 2 equiv.). DMAP (5 g, 40 mmol, 0.1 equiv.) was added and the reaction was run neat at ambient temperature. After 18 hours, the reaction was quenched with 16 mL MeOH (1 equiv.) and then diluted with 500 mL Et₂O and 500 mL H₂O. The aqueous layer was then extracted twice with Et₂O. The combined organic layers were dried with MgSO₄, and the solvent was removed under reduced pressure, leaving diene **3.32** (38.1 g, 340 mmol, 85% yield) as a colorless oil essentially

pure by NMR. Note that the diene is volatile so low temperature rotovap is necessary. This volatility is the source of decreased yield.

$R_f = 0.7$ (10:90 EtOAc:hexanes)

$^1\text{H NMR}$ (500 MHz, CDCl_3) δ 7.48 – 7.34 (m, 1H, trans), 7.06 (ddt, $J = 6.5, 1.9, 1.0$ Hz, 0.15H, cis), 6.77 – 6.58 (m, 0.15H, Cis), 6.36 – 6.16 (m, 1H, trans), 6.14 – 5.94 (m, 1H, trans), 5.51 (ddt, $J = 11.0, 6.4, 0.9$ Hz, 0.15H, cis), 5.35 – 5.14 (m, 1.15H, cis and trans), 5.14 – 5.02 (m, 1.15H, cis and trans), 2.23 (s, 0.45H, cis), 2.15 (d, $J = 1.1$ Hz, 3H, trans).

$^{13}\text{C NMR}$ (126 MHz, CDCl_3) δ 167.84, 138.69, 131.68, 117.28, 116.05, 20.69.

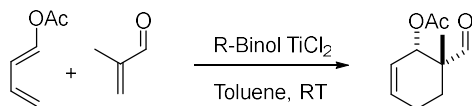


Racemic Aldehyde 3.31. A 1 L round-bottomed flask was charged with diene 3.32 (29 g, 260 mmol, 1 equiv.), methacrolein (32.1 mL, 27.3 g, 390 mmol, 1.5 equiv.) and DCM (260 mL) and was cooled to -78°C . $\text{BF}_3 \cdot \text{Et}_2\text{O}$ (3.21 mL, 26 mmol, 0.1 equiv.) was added dropwise and the reaction was allowed to warm to -20°C . After 4 hours, the reaction was quenched with 250 mL concentrated NaHCO_3 . The reaction was partitioned between DCM and H_2O . The aqueous layer was then extracted twice with DCM. The combined organic layers were dried with MgSO_4 , and the solvent was removed under reduced pressure. The essentially pure crude material was purified by flash chromatography (20% EtOAc:80%Hexanes) giving racemic aldehyde **3.31** (43.5 g, 239 mmol, 92% yield) as a colorless oil. Alternatively, the crude material could be used for the following step with no loss in yield.

$R_f = 0.2$ (10:90 EtOAc:hexanes)

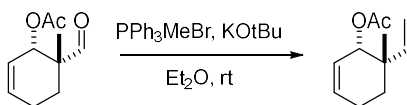
¹H NMR (500 MHz, CDCl₃) δ 9.70 (s, 1H), 5.98 (dddd, *J* = 10.0, 4.1, 3.2, 1.2 Hz, 1H), 5.79 (ddt, *J* = 10.0, 3.8, 2.2 Hz, 1H), 5.30 (ddt, *J* = 3.9, 1.9, 0.9 Hz, 1H), 2.31 – 2.18 (m, 1H), 2.16 – 2.07 (m, 1H), 2.06 (s, 3H), 2.01 (ddd, *J* = 13.7, 7.5, 6.2 Hz, 1H), 1.76 – 1.57 (m, 1H), 1.09 (s, 3H).

¹³C NMR (126 MHz, CDCl₃) δ 204.15, 170.54, 132.42, 123.78, 71.98, 47.72, 25.78, 22.07, 21.01, 17.87.



(+)-Aldehyde 3.31. A 20 mL sealed tube was charged with diene **3.32** (179 mg, 1.6 mmol, 1 equiv.), methacrolein (0.12 mL, 140 mg, 2 mmol, 1.25 equiv.), R-Binol-TiCl₂ and toluene (4mL). The reaction was sealed under nitrogen and allowed to react for 3 days. After 3 days, the reaction was diluted with 4 mL Et₂O quenched with 4 mL concentrated NaHCO₃. The reaction was partitioned between Et₂O and H₂O. The aqueous layer was then extracted twice with Et₂O. The combined organic layers were dried with MgSO₄, and the solvent was removed under reduced pressure. The essentially pure crude material was purified by flash chromatography (20% EtOAc:80%Hexanes) giving (+)-**3.31** (182 mg, 1 mmol, 63% yield) as a colorless oil.

Spectral data matches that for the racemic compound above.



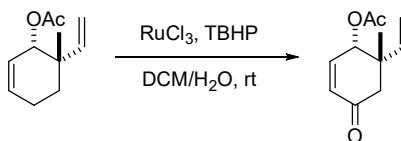
Acetate 3.3. A 1 L round-bottomed flask was charged with PPh₃MeBr (50.5 g, 150 mmol, 1.5 equiv) and Et₂O (500 mL). KOTBu (22.9 g, 200 mmol, 2 equiv) was added, and the reaction was

stirred vigorously for 1 hour. After 1 hour the stirring was stopped. A second round-bottomed flask was charged with aldehyde **3.31** (18.2 g, 100 mmol, 1 equiv.) and Et₂O (200 mL). After the remaining solid in the first flask had settled, the liquid phase was transferred to the second flask via a cannula. After the entirety of the liquid had been transferred, the reaction was stirred for a further 30 minutes. The reaction was then quenched with 300 mL concentrated NH₄Cl. The reaction was portioned between Et₂O and H₂O. The aqueous layer was then extracted twice with Et₂O. The combined organic layers were dried with MgSO₄, and the solvent was removed under reduced pressure. The crude material was purified by vacuum filtration through silica using 5% EtOAc:95%hexanes as a mobile phase, giving acetate **3.3** (14.9 g, 83 mmol, 83% yield) as a colorless oil.

$R_f = 0.6$ (10:90 EtOAc:hexanes)

¹H NMR (500 MHz, CDCl₃) δ 6.04 – 5.94 (m, 1H), 5.97 – 5.81 (m, 1H), 5.65 (ddt, $J = 10.0, 4.3, 2.3$ Hz, 1H), 5.17 – 4.97 (m, 3H), 2.29 – 2.14 (m, 1H), 2.13 – 2.00 (m, 1H), 2.06 (s, 3H), 1.81 (ddd, $J = 13.5, 7.5, 6.1$ Hz, 1H), 1.65 – 1.48 (m, 1H), 1.06 (s, 3H).

¹³C NMR (126 MHz, CDCl₃) δ 170.86, 143.02, 131.26, 124.85, 112.76, 74.03, 38.62, 29.73, 22.87, 22.72, 21.23.



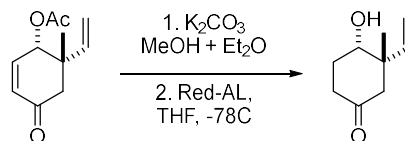
Eneone 3.29. A 500 mL round-bottomed flask was charged with acetate **3.3** (7.2 g, 40 mmol, 1 equiv), RuCl₃·3H₂O (80 mg, 0.4 mmol, 0.01 equiv), DCM (150mL) and H₂O (15 mL). TBHP (5.1

mL, 70% by weight, 40 g, 240 mmol, 1 equiv) was added. Further TBHP (31 mL, 70% by weight, 21.6 g, 240 mmol, 6 equiv) was added by syringe pump over the course of 24 hours. Following the complete addition of TBHP the reaction was stirred for a further 24 hours. The reaction was then quenched with 200 mL 5% Na₂SO₃. The reaction was portioned between DCM and H₂O. The aqueous layer was then extracted twice with DCM. The combined organic layers were dried with MgSO₄, and the solvent and residual *tert*-butanol was removed under reduced pressure. The crude material was purified by flash chromatography (10% EtOAc:90%hexanes) giving eneone **3.29** (5.7 g, 29.2 mmol, 72% yield) as a colorless oil.

$R_f = 0.15$ (10:90 EtOAc:hexanes)

¹H NMR (500 MHz, CDCl₃) δ 6.67 (dd, $J = 10.2, 2.9$ Hz, 1H), 6.06 (ddd, $J = 10.2, 1.9, 0.9$ Hz, 1H), 5.96 (dd, $J = 17.6, 11.0$ Hz, 1H), 5.60 – 5.52 (m, 1H), 5.16 (d, $J = 11.0$ Hz, 1H), 5.08 (d, $J = 17.6$ Hz, 1H), 2.75 (dd, $J = 16.4, 0.9$ Hz, 1H), 2.43 (d, $J = 16.4$ Hz, 1H), 2.16 (s, 3H), 1.19 (s, 3H).
¹³C NMR (126 MHz, CDCl₃) δ 197.59, 170.48, 145.93, 139.51, 130.51, 115.24, 77.28, 77.03, 76.77, 74.37, 47.00, 43.98, 25.17, 20.89.

HRMS Calculated for C₁₁H₁₄O₃ [M+H]⁺: 194.0943. Found: 194.0906.



Ketone 3.24-d. A 1L round-bottomed flask was charged with eneone **3.29** (3.2 g, 16.5 mmol, 1equiv), K₂CO₃ (4.6 g, 33 mmol, 2 equiv), Et₂O (360 mL), and MeOH (60 mL). The reaction was stirred for 6 hours, then quenched with 50 mL 1M HCl and stirred until bubbling ceased. The reaction was portioned between Et₂O and H₂O. The aqueous layer was extracted twice with Et₂O.

The combined organic layers were dried with MgSO₄, and the solvent was removed under reduced pressure. The crude ketone **3.40** (2.4 g, 15.79 mmol, 96% yield) was used immediately for the next step

$R_f = 0.25$ (30:70 EtOAc:hexanes)

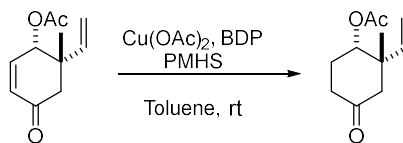
A 1L round-bottomed flask was then charged with ketone **3.40** (2.4 g, 15.79 mmol, 1 equiv) and THF (300 mL). The reaction was cooled to -78°C, and Red-Al (6.7 mL, 60% by weight in Toluene, 4.0 g, 20 mmol, 1.25 equiv) was then added slowly, and the reaction was stirred at -78°C for 15 minutes. **Caution** – the reaction creates a significant amount of H₂ gas at this stage. After 15 minutes, when bubbling ceased, the reaction was diluted with 300 mL Et₂O and 300 mL of concentrated Rochelle's salt was added – note be aw. he reaction was portioned between Et₂O and H₂O. The aqueous layer was extracted twice with Et₂O. The combined organic layers were dried with MgSO₄, and the solvent was removed under reduced pressure. The crude material was purified by flash chromatography (30% EtOAc:70%hexanes) giving ketone **3.24-d** (2.3 g, 14.8 mmol, 94% yield) as a colorless oil.

$R_f = 0.25$ (30:70 EtOAc:hexanes)

¹H NMR (500 MHz, CDCl₃) δ 5.88 (dd, $J = 17.6, 10.9$ Hz, 1H), 5.27 (dd, $J = 10.9, 0.8$ Hz, 1H), 5.13 (d, $J = 17.6$ Hz, 1H), 3.74 (t, $J = 4.4$ Hz, 1H), 2.82 – 2.75 (m, 1H), 2.63 (dtd, $J = 14.6, 8.3, 1.4$ Hz, 1H), 2.28 (dtd, $J = 14.7, 5.6, 1.9$ Hz, 1H), 2.17 – 2.09 (m, 1H), 2.06 (ddd, $J = 8.7, 5.5, 4.4$ Hz, 2H), 1.87 (s, 1H), 1.08 (s, 3H).

¹³C NMR (126 MHz, CDCl₃) δ 210.89, 142.29, 115.67, 72.16, 46.56, 46.06, 36.56, 28.44, 24.37, -0.00.

HRMS Calculated for C₉H₁₄O₂ [M+H]⁺: 154.0994. Found: 154.0958.



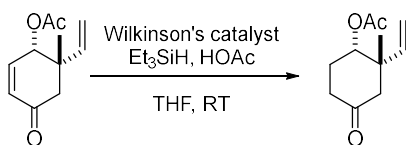
Ketone 3.24-c. A 250 mL pear-shaped flask was charged with $\text{Cu}(\text{OAc})_2$ (197 mg, 1 mmol, 0.05 equiv), BDP (220 mg, 0.5 mmol, 0.025 equiv) and toluene (70 mL). The liquid was bubbled with nitrogen for 15 minutes. PMHS (4.8 mL, 80 mmol, 5 equiv) was added, and the reaction was stirred for 1 hour or until the reaction turned dark yellow. Stirring was then stopped, and the residual solid was allowed to settle. A 250 mL round-bottomed flask was charged with enone **3.29** (3.9 g, 20 mmol, 1 equiv) and toluene (30 mL). The liquid from the first flask was added, and the reaction was stirred for 1 hour or until the reaction was complete. The reaction was quenched with 50 mL of 1M NaOH and vigorously stirred. The reaction was portioned between toluene and H_2O . The aqueous layer was extracted twice with Et_2O mL. The combined organic layers were then washed once with 1M HCl, and the acid layer was then extracted one time with Et_2O mL. The combined organic layers were dried with MgSO_4 , and the solvent was removed under reduced pressure. The crude material was purified by flash chromatography (10% EtOAc:90%hexanes) giving ketone **3.24-c** (2.7 g, 14 mmol, 70% yield) as a colorless oil.

$R_f = 0.15$ (10:90 EtOAc:hexanes)

$^1\text{H NMR}$ (500 MHz, CDCl_3) δ 5.88 (dd, $J = 17.6, 10.9$ Hz, 1H), 5.14 (dd, $J = 10.9, 0.7$ Hz, 1H), 5.05 (dd, $J = 17.6, 0.7$ Hz, 1H), 5.06 – 5.03 (m, 1H), 2.75 (dd, $J = 14.4, 1.8$ Hz, 1H), 2.61 – 2.44 (m, 1H), 2.36 (dddd, $J = 15.0, 7.5, 6.0, 1.6$ Hz, 1H), 2.25 (ddd, $J = 14.4, 1.7, 0.7$ Hz, 1H), 2.12 (s, 2H), 2.13 – 1.95 (m, 3H), 1.09 (s, 3H).

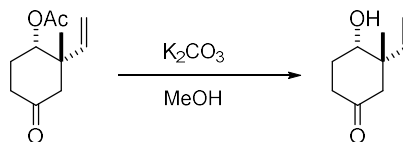
^{13}C NMR (126 MHz, CDCl_3) δ 209.36, 170.38, 141.37, 114.62, 74.75, 48.00, 44.21, 37.26, 26.57, 24.90, 21.13.

HRMS Calculated for $\text{C}_{11}\text{H}_{16}\text{O}_3$ $[\text{M}+\text{H}]^+$: 196.1099. Found: 196.1107.



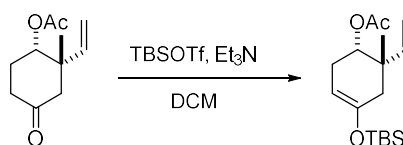
Ketone 3.24-c alternate route. A 50 mL pear-shaped flask was charged with Wilkinson's catalyst (240 mg, 0.2 mmol, 0.04 equiv), Et_3SiH (1.7 mL, 10.4 mmol, 2 equiv), eneone **3.29** (1g, 5.2 mmol, 1 equiv), and THF (10 mL). The reaction was stirred for 3 hours, then acetic acid (3.0 mL, 52 mmol, 10 equiv) was added and the reaction was stirred for a further one hour at RT. The reaction was then diluted with 20 mL Et_2O and quenched with 10 mL NaHCO_3 . The reaction was portioned between Et_2O and H_2O . The aqueous layer was extracted twice with Et_2O mL. The combined organic layers were dried with MgSO_4 , and the solvent was removed under reduced pressure. The crude material was purified by flash chromatography (10% EtOAc :90%hexanes) giving ketone **3.24-c** (947 mg, 4.8 mmol, 93% yield) as a colorless oil.

Spectral data identical to that obtained above.



Alcohol 3.S alternate route. A 50 mL round-bottomed flask was charged with Ketone **3.24-c** (196 mg, 1 mmol, 1 equiv), K_2CO_3 (548 mg, 4 mmol, 4 equiv) and MeOH (10 mL). The reaction was stirred at room temperature for 8 hours. The reaction was then diluted with 10 mL Et_2O , cooled to $0^\circ C$ and quenched with 10 mL of 1M HCl. The reaction was partitioned between Et_2O and H_2O . The aqueous layer was extracted twice with Et_2O . The combined organic layers were dried with $MgSO_4$, and the solvent was removed under reduced pressure. The crude material was purified by flash chromatography (50% EtOAc:50%hexanes) giving ketone **3.24-d** (148 mg, 0.96 mmol, 96% yield) as a colorless oil.

Spectral data identical to above.



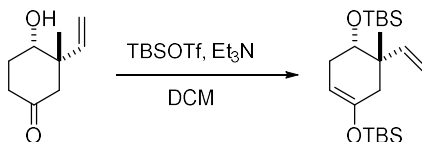
Enol ether 3.46-c. A 250 mL round-bottomed flask was charged with Ketone **3.24-c** (1.2 g, 6 mmol, 1 equiv), Et_3N (1.7 mL, 12 mmol, 2 equiv) and DCM (100 mL). TBSOTf (2 mL, 9 mmol, 1.5 equiv) was added slowly. The reaction was stirred at room temperature for 4 hours. The reaction was then quenched with 100 mL of concentrated $NaHCO_3$. The reaction was partitioned between DCM and H_2O . The aqueous layer was extracted twice with DCM. The combined organic layers were dried with $MgSO_4$, and the solvent was removed under reduced pressure. The crude

material was purified by flash chromatography (5% EtOAc:95%hexanes) giving enol ether **3.AW** (1.7 g, 5.64 mmol, 94% yield) as a colorless oil.

$R_f = 0.6$ (5:95 EtOAc:hexanes)

$^1\text{H NMR}$ (500 MHz, CDCl_3) δ 5.96 – 5.85 (m, 1H), 5.11 – 5.03 (m, 2H), 4.81 (t, $J = 5.1$ Hz, 1H), 4.71 (tt, $J = 3.8, 1.3$ Hz, 1H), 2.38 (dddd, $J = 17.2, 6.4, 4.0, 1.9$ Hz, 1H), 2.32 (dq, $J = 17.0, 1.8$ Hz, 1H), 2.12 (dddt, $J = 17.2, 5.6, 3.8, 1.9$ Hz, 1H), 1.93 (dq, $J = 17.0, 1.7$ Hz, 1H), 1.06 (s, 3H), 0.95 (s, 9H), 0.16 (d, $J = 1.5$ Hz, 6H).

$^{13}\text{C NMR}$ (126 MHz, CDCl_3) δ 170.82, 148.69, 142.56, 113.05, 99.39, 74.32, 39.72, 38.52, 27.12, 25.69, 25.67, 23.51, 21.21, 18.04, -4.36, -4.39.

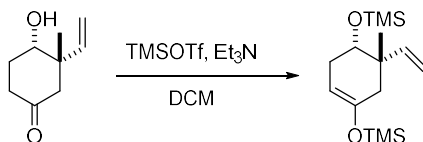


Enol ether 3.46-a. A 50 mL round-bottomed flask was charged with Alcohol **3.24-d** (180 mg, 1.2 mmol, 1 equiv), Et_3N (0.56 mL, 4 mmol, 3.3 equiv) and DCM (10 mL). TBSOTf (0.67 mL, 3mmol, 2.5 equiv) was added slowly. The reaction was stirred at room temperature for 10 hours. The reaction was then quenched with 5 mL of concentrated NaHCO_3 . The reaction was partitioned between DCM and H_2O . The aqueous layer was extracted twice with DCM. The combined organic layers were dried with MgSO_4 , and the solvent was removed under reduced pressure. The crude material was purified by flash chromatography (2% EtOAc:98%hexanes) giving enol ether **3.46-a** (421 mg, 1.1 mmol, 92% yield) as a colorless oil.

$R_f = 0.8$ (5:95 EtOAc:hexanes)

¹H NMR (500 MHz, CDCl₃) δ 6.00 (dd, *J* = 17.6, 11.0 Hz, 1H), 5.18 – 4.86 (m, 2H), 4.86 – 4.58 (m, 1H), 3.53 (dd, *J* = 7.0, 4.8 Hz, 1H), 2.30 – 2.12 (m, 2H), 2.08 – 1.95 (m, 1H), 1.90 (dq, *J* = 15.7, 1.6 Hz, 1H), 1.03 (s, 3H), 0.94 (s, 9H), 0.90 (s, 9H), 0.15 (d, *J* = 1.7 Hz, 6H), 0.05 (d, *J* = 1.7 Hz, 6H).

¹³C NMR (126 MHz, CDCl₃) δ 148.66, 143.17, 112.18, 100.10, 73.87, 41.48, 39.16, 30.97, 25.87, 25.85, 25.73, 25.70, 24.42, 18.08, 18.02, 0.01, -4.15, -4.28, -4.43, -4.87.

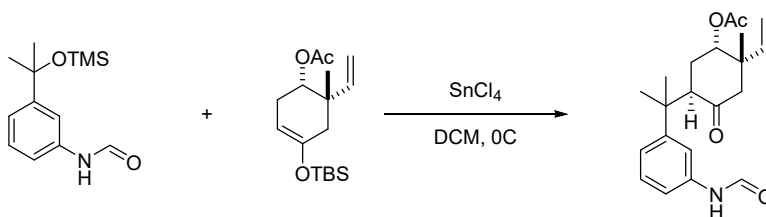


Enol ether 3.48. A 50 mL round-bottomed flask was charged with Alcohol **3.24-d** (180 mg, 1.2 mmol, 1 equiv), Et₃N (0.56 mL, 4 mmol, 3.3 equiv) and DCM (10 mL). TMSOTf (0.54 mL, 3 mmol, 2.5 equiv) was added slowly. The reaction was stirred at room temperature for 10 hours. The reaction was then quenched with 5 mL of concentrated NaHCO₃. The reaction was partitioned between DCM and H₂O. The aqueous layer was extracted twice with DCM. The combined organic layers were dried with MgSO₄, and the solvent was removed under reduced pressure. The crude material was purified by flash chromatography (0.1%Et₃N:2% EtOAc:98%hexanes) giving enol ether **3.46-a** (304 mg, 1.02 mmol, 85% yield) as a colorless oil.

R_f = 0.7 (5:95 EtOAc:hexanes)

¹H NMR (500 MHz, CDCl₃) δ 6.05 – 5.84 (m, 1H), 5.11 – 4.88 (m, 2H), 4.71 – 4.60 (m, 1H), 3.51 (dd, *J* = 7.4, 4.9 Hz, 1H), 2.22 – 2.10 (m, 2H), 1.98 (ddtd, *J* = 16.6, 7.6, 3.1, 1.8 Hz, 1H), 1.89 (ddt, *J* = 17.3, 3.5, 1.9 Hz, 1H), 1.00 (s, 3H), 0.18 (s, 9H), 0.09 (s, 9H).

^{13}C NMR (126 MHz, CDCl_3) δ 148.41, 142.61, 112.41, 100.40, 73.86, 41.20, 39.56, 31.60, 30.95, 24.39, 22.66, 14.11, 0.34, 0.31.



Ketone . A 250 mL round-bottomed flask was charged with Enol ether **3.AW** (1.53 g, 5 mmol, 3 equiv), Silyl ether **2.7** (0.43 g, 1.7 mmol, 1 equiv) and DCM (150 mL). The reaction was cooled to 0°C in an ice bath. SnCl_4 (0.6 mL, 5 mmol, 3 equiv) was added slowly. The reaction was stirred for 18 hours and allowed to warm to RT. The reaction was slowly quenched with 30 mL of saturated NaHCO_3 while stirring rapidly. The mixture was diluted with water and filtered through a celite plug. The filter cake was then washed with 30 mL DCM. The filtrate was then partitioned between H_2O and DCM, and the aqueous layer was then extracted three times with 50 mL DCM. The combined organic layers were dried with MgSO_4 and concentrated under reduced pressure. The crude material was purified by flash chromatography (30% EtOAc :70% hexanes) to give ketone **3.47-c** (528 mg, 1.48 mmol, 87% yield) as a colorless oil.

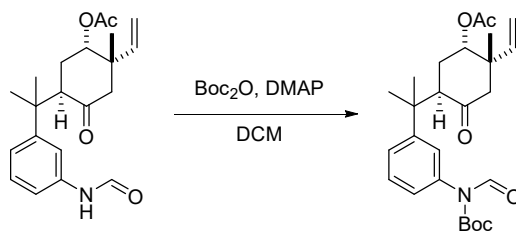
$R_f = 0.4$ (30:70 EtOAc :hexanes)

^1H NMR (500 MHz, CDCl_3) δ 8.68 (d, $J = 11.4$ Hz, 0.5H), 8.35 (d, $J = 1.9$ Hz, 0.5H), 8.24 (d, $J = 11.4$ Hz, 0.5H), 7.67 (t, $J = 2.0$ Hz, 0.5H), 7.62 (s, 0.5H), 7.32 – 7.27 (m, 1H), 7.25 (t, $J = 7.8$ Hz, 0.5H), 7.16 (ddd, $J = 8.1, 1.9, 0.9$ Hz, 0.5H), 7.09 (dt, $J = 7.9, 1.5$ Hz, 0.5H), 7.06 (t, $J = 2.0$ Hz, 0.5H), 6.94 (ddd, $J = 7.8, 2.2, 0.9$ Hz, 0.5H), 5.77 (ddd, $J = 17.5, 10.8, 1.3$ Hz, 1H), 5.03 (ddd, $J = 10.8, 5.2, 0.7$ Hz, 1H), 4.97 – 4.91 (d, 17.5 Hz, 1H), 4.95 – 4.87 (m, 1H), 3.06 (ddd, $J = 15.5,$

12.3, 6.0 Hz, 1H), 2.84 (dd, $J = 12.9, 8.6$ Hz, 1H), 2.07 (d, $J = 4.5$ Hz, 3H), 2.09 – 1.98 (m, 1H), 1.98 – 1.77 (m, 3H), 1.48 (d, $J = 2.2$ Hz, 3H), 1.40 (d, $J = 8.4$ Hz, 3H), 0.98 (d, $J = 4.0$ Hz, 3H).

^{13}C NMR (126 MHz, CDCl_3) δ 209.83, 209.43, 170.23, 170.05, 162.38, 158.79, 151.32, 150.36, 142.70, 142.61, 136.86, 136.41, 129.41, 128.74, 122.78, 122.05, 117.62, 117.41, 117.11, 116.55, 113.23, 113.15, 73.94, 73.89, 53.50, 53.45, 48.84, 48.71, 45.54, 45.51, 38.96, 38.84, 29.70, 26.85, 26.20, 26.05, 23.63, 21.14, 21.10.

HRMS Calculated for $\text{C}_{21}\text{H}_{27}\text{NO}_4$ $[\text{M}+\text{H}]^+$: 357.194. Found: 357.1889.

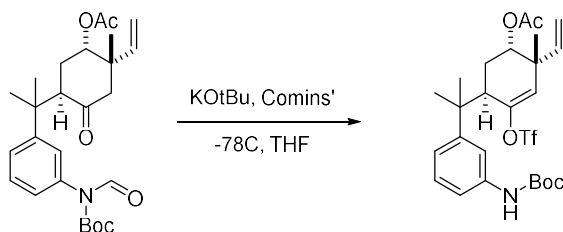


Boc Anilide 3.61. A 25 mL round-bottomed flask was charged with ketone **3.47-c** (357 mg, 1 mmol, 1 equiv), Boc_2O (327 mg, 1.5 mmol, 1.5 equiv), DMAP (12 mg, 0.1 mmol, 0.1 equiv) and DCM (5 mL). The reaction was stirred at room temperature for 8 hours. Following complete conversion of starting material, the reaction quenched with 3 mL of saturated NaHCO_3 . The reaction was then partitioned between H_2O and DCM, and the aqueous layer was then extracted three times with DCM. The combined organic layers were dried with MgSO_4 and concentrated under reduced pressure. The crude material was purified by flash chromatography (40% EtOAc:60% hexanes) to give Boc anilide **3.61** (397 mg, 0.87 mmol, 87% yield) as a colorless oil. Note that although the product will move in lower polarity solvents, a high polarity is required to avoid the compound streaking.

$R_f = 0.8$ (40:60 EtOAc:hexanes)

$^1\text{H NMR}$ (500 MHz, CDCl_3) δ 9.41 (s, 1H), 7.40 – 7.31 (m, 2H), 7.08 (t, $J = 1.8$ Hz, 1H), 6.95 (dt, $J = 6.9, 2.0$ Hz, 1H), 5.76 (dd, $J = 17.4, 10.8$ Hz, 1H), 5.01 (dd, $J = 10.8, 0.8$ Hz, 1H), 4.94 – 4.87 (m, 2H), 3.00 (dd, $J = 12.6, 5.8$ Hz, 1H), 2.82 (d, $J = 12.7$ Hz, 1H), 2.05 (m, $J = 3.1$ Hz, 4H), 1.88 (ddd, $J = 15.2, 12.6, 2.8$ Hz, 1H), 1.48 (s, 9H), 1.47 (s, 3H), 1.44 (s, 3H), 0.97 (s, 3H).

$^{13}\text{C NMR}$ (126 MHz, CDCl_3) δ 209.52, 169.94, 162.78, 152.38, 149.97, 142.81, 134.42, 128.58, 126.00, 125.72, 125.57, 125.36, 113.00, 84.31, 73.57, 53.56, 48.70, 45.65, 38.89, 29.80, 27.94, 27.93, 23.58, 21.06.



Boc Triflate 3.63. A 25 mL round-bottomed flask was charged with Boc anilide **3.61** (400 mg, 0.87 mmol, 1 equiv) and THF (15 mL). The reaction was cooled to -78 °C. A solution of KOtBu (4.4 mL, 1M in THF, 4.4 mmol, 5 equiv) was added. Immediately, Comins' (890 mg, 2.61 mmol, 3 equiv) was added as a solid in one portion. The reaction was stirred at -78 °C for 2 hours, then warmed to 0 °C. After reaching 0 °C, the reaction was diluted with 20 mL Et_2O and quenched with 10 mL of concentrated NH_4Cl . The reaction was then partitioned between H_2O and Et_2O , and the aqueous layer was then extracted three times with Et_2O . The combined organic layers were dried with MgSO_4 and concentrated under reduced pressure. The crude material was purified by flash chromatography (20% EtOAc:80% hexanes) to give Boc triflate **3.63** (400 mg, 0.71 mmol, 82% yield) as a colorless oil.

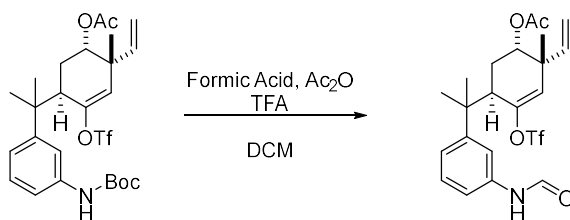
$R_f = 0.3$ (20:80 EtOAc:hexanes)

$^1\text{H NMR}$ (500 MHz, CDCl_3) δ 7.40 (s, 1H), 7.34 – 7.23 (m, 1H), 7.22 (d, $J = 2.1$ Hz, 1H), 7.04 (d, $J = 7.9$ Hz, 1H), 6.54 (s, 1H), 5.73 – 5.66 (q, $J = 10.7$ Hz, 17.5 Hz, 1H), 5.65 (s, 1H), 5.17 (d, $J = 10.7$ Hz, 1H), 5.09 (d, $J = 17.5$ Hz, 1H), 4.79 – 4.58 (m, 1H), 2.90 (t, $J = 5.8$ Hz, 1H), 1.99 (s, 3H), 1.62 – 1.51 (m, 9H), 1.52 – 1.50 (m, 3H), 1.49 (s, 3H), 1.03 (s, 3H).

$^{13}\text{C NMR}$ (126 MHz, CDCl_3) δ 170.42, 152.79, 149.62, 147.90, 140.29, 138.35, 128.87, 126.46, 121.13, 116.27, 73.09, 47.39, 42.75, 41.41, 31.60, 29.36, 28.36, 27.99, 26.34, 24.92, 22.66, 21.05, 14.13.

$^{19}\text{F NMR}$ (470 MHz, CDCl_3) δ -73.66.

HRMS Calculated for $\text{C}_{26}\text{H}_{34}\text{F}_3\text{NO}_7\text{S}$ $[\text{M}+\text{H}]^+$: 561.2008. Found: 561.1888.



Formanilide Triflate 3.60. A 25 mL round-bottomed flask was charged with formic acid (3.5 mL, 92 mmol, 115 equiv) and acetic anhydride (1.3 mL, 14 mmol, 17.5 equiv). The reaction was stirred for 10 minutes. A solution of Boc triflate **3.63** (449 mg, 0.8 mmol, 1 equiv) in DCM (2 mL) was added. The reaction was stirred for five minutes, then TFA (1.2 mL, 16 mmol, 20 equiv) was added. The reaction was stirred at RT for further 15 minutes, then was diluted with 10 mL DCM and carefully quenched with concentrated NaHCO_3 while stirring rapidly. **Caution:** Lots of CO_2 is generated, be very slow. The reaction was then partitioned between H_2O and DCM, and the

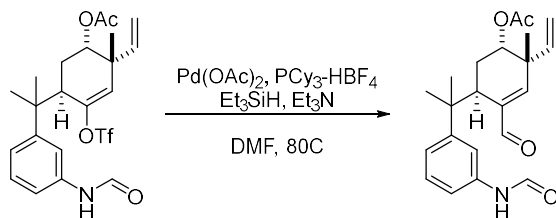
aqueous layer was extracted three times with DCM. The combined organic layers were dried with MgSO_4 and concentrated under reduced pressure. The crude material was purified by flash chromatography (40% EtOAc:60% hexanes) to give formanilide triflate **3.60** (332mg, 0.68 mmol, 85% yield) as a colorless oil.

$R_f = 0.45$ (40:60 EtOAc:hexanes)

$^1\text{H NMR}$ (500 MHz, CDCl_3) δ 8.70 (d, $J = 11.5$ Hz, 0.5H), 8.42 (d, $J = 1.8$ Hz, 0.5H), 7.64 (d, $J = 8.0$ Hz, 0.5H), 7.54 – 7.49 (m, 0.5H), 7.41 (t, $J = 2.0$ Hz, 0.5H), 7.34 (q, $J = 7.7$ Hz, 1H), 7.22 (d, $J = 7.9$ Hz, 0.5H), 7.18 – 7.14 (m, 0.5H), 7.12 (t, $J = 2.1$ Hz, 0.5H), 6.99 (d, $J = 8.4$ Hz, 0.5H), 5.70 (ddd, $J = 17.6, 10.7, 2.6$ Hz, 1H), 5.62 (s, 1H), 5.18 (dd, $J = 10.7, 4.7$ Hz, 1H), 5.09 (d, $J = 17.6$ Hz, 1H), 4.64 – 4.42 (m, 1H), 2.87 (dt, $J = 7.0, 4.1$ Hz, 1H), 2.00 (s, 3H), 1.85 – 1.65 (m, 2H), 1.54 (d, $J = 1.6$ Hz, 3H), 1.52 (s, 3H), 1.01 (d, $J = 4.9$ Hz, 3H).

$^{13}\text{C NMR}$ (101 MHz, CDCl_3) δ 170.59, 170.49, 162.33, 158.85, 149.38, 149.24, 148.93, 147.82, 140.09, 139.97, 136.77, 136.60, 129.47, 128.97, 126.84, 126.67, 123.72, 123.05, 118.57, 118.47, 118.28, 117.14, 116.59, 116.49, 73.20, 73.11, 42.63, 42.59, 41.41, 29.71, 28.96, 28.50, 27.89, 27.77, 27.37, 26.96, 24.82, 21.08, 21.03, 1.02, 0.00.

$^{19}\text{F NMR}$ (471 MHz, CDCl_3) δ -73.63, -73.68.



Aldehyde 3.64. A 25 mL round-bottomed flask was charged with Pd(OAc)₂ (36 mg, 0.16 mmol, 0.2 equiv.) and PCy₃-HBF₄ (118g, 0.32 mmol, 0.3 equiv.). The atmosphere was removed with vacuum and replaced with nitrogen three times. Formanilide triflate **3.60** (391 mg, 0.8 mmol, 1 equiv.) in DMF (8 mL) was added, followed by Et₃N (0.28 mL, 2 mmol, 2.25 equiv.). The atmosphere was again removed with vacuum, and refilled with CO three times. Following the third removal a balloon filled with CO was attached. Et₃SiH (0.26 mL, 1.6 mmol, 2 equiv.) was added to the reaction, and the reaction was heated to 80 °C. After stirring for 6 hours, the reaction was diluted with ether and washed with water. The reaction was partitioned between Et₂O and water. The aqueous layer was then extracted two times with Et₂O. The combined organic layers were dried over MgSO₄ and concentrated under reduced pressure. The crude material was purified by flash chromatography (40% EtOAc:60% Hexanes) giving aldehyde **3.64** (289 mg, 0.78 mmol, 98% yield) as a pale yellow amorphous solid.

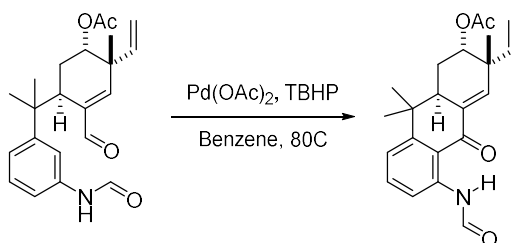
$R_f = 0.4$ (40:60 EtOAc:hexanes)

¹H NMR (500 MHz, CDCl₃) δ 9.52 (d, $J = 10.5$ Hz, 1H), 8.71 (d, $J = 11.5$ Hz, 0.5H), 8.41 (d, $J = 1.8$ Hz, 0.5H), 7.76 – 7.60 (m, 0.5H), 7.58 (d, $J = 11.6$ Hz, 0.5H), 7.41 (t, $J = 2.1$ Hz, 0.5H), 7.31 (ddd, $J = 13.5, 8.6, 4.7$ Hz, 1H), 7.21 – 7.18 (m, 0.5H), 7.17 (t, $J = 2.0$ Hz, 0.5H), 7.13 (ddd, $J = 7.9, 1.9, 1.0$ Hz, 0.5H), 6.38 (d, $J = 8.4$ Hz, 1H), 5.72 (ddd, $J = 17.6, 10.7, 1.5$ Hz, 1H), 5.25 – 5.08 (m, 1H), 4.83 (dd, $J = 17.5, 0.9$ Hz, 1H), 4.65 (ddd, $J = 16.7, 12.4, 3.9$ Hz, 1H), 3.19 (dd, $J = 6.7,$

2.2 Hz, 1H), 2.00 (d, $J = 3.7$ Hz, 3H), 1.84 – 1.73 (m, 1H), 1.58 – 1.44 (m, 1H), 1.43 (s, 3H), 1.39 (d, $J = 5.0$ Hz, 3H), 1.08 (d, $J = 8.4$ Hz, 3H).

^{13}C NMR (126 MHz, CDCl_3) δ 192.98, 192.82, 170.70, 170.55, 162.41, 158.89, 154.55, 154.15, 149.44, 148.31, 141.46, 139.75, 139.63, 136.62, 136.53, 129.15, 128.70, 124.20, 123.60, 119.15, 118.82, 118.56, 116.97, 116.08, 115.96, 74.82, 74.66, 42.95, 42.93, 42.51, 42.40, 42.33, 42.23, 29.63, 29.50, 27.95, 27.85, 26.95, 26.89, 23.28, 23.25, 21.15, 21.07, 0.01.

HRMS Calculated for $\text{C}_{22}\text{H}_{27}\text{NO}_4$ $[\text{M}+\text{H}]^+$: 369.194. Found: 369.188.

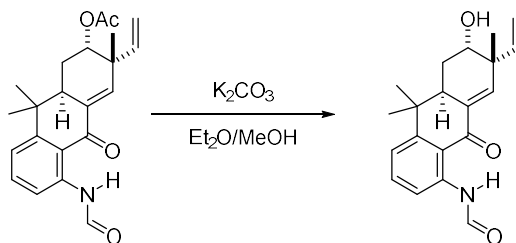


Ketone 3.65. A 25 mL round-bottomed flask was charged with $\text{Pd}(\text{OAc})_2$ (17 mg, 0.075 mmol, 0.2 equiv.), Aldehyde **3.64** (140 mg, 0.38 mmol, 1 equiv) and Benzene (5 mL). TBHP (0.1 mL, 70% by weight, 0.76 mmol, 2 equiv) was added and the reaction was warmed to 80 °C. The reaction was stirred for one hour, then diluted with Et_2O and quenched with conc Na_2SO_3 . The reaction was partitioned between water and Et_2O . The aqueous layer was then extracted three times with Et_2O . The combined organic layers were dried over MgSO_4 and concentrated under reduced pressure. The crude material was purified by flash chromatography (20% EtOAc :80% Hexanes) giving ketone **3.65** (118 mg, 0.32mmol, 85% yield) as a pale yellow amorphous solid.

$R_f = 0.2$ (15:85 EtOAc :hexanes)

¹H NMR (500 MHz, CDCl₃) δ 12.06 (s, 1H), 8.64 (d, J = 8.4 Hz, 1H), 8.54 (s, 1H), 7.56 (t, J = 8.1 Hz, 1H), 7.26 (d, J = 8.3 Hz, 2H), 5.84 (dd, J = 17.6, 10.7 Hz, 1H), 5.18 (d, J = 10.7 Hz, 1H), 5.15 (s, 1H), 5.12 (d, J = 17.8 Hz, 1H), 2.83 (ddd, J = 9.6, 6.1, 2.6 Hz, 1H), 2.20 – 2.10 (m, 1H), 1.97 (s, 3H), 1.96 (s, 1H), 1.48 (s, 3H), 1.28 (s, 3H), 1.10 (s, 3H).

¹³C NMR (126 MHz, CDCl₃) δ 189.32, 170.53, 159.85, 154.25, 143.05, 140.98, 140.87, 135.10, 134.68, 119.80, 119.09, 115.21, 72.91, 42.63, 39.00, 37.57, 29.71, 25.95, 25.84, 24.67, 24.45, 21.20.

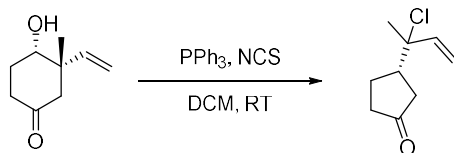


Alcohol 3.66. A 10 mL round-bottomed flask was charged with Ketone **3.65** (110 mg, 0.3 mmol, 1 equiv.), Et₂O (1.5 mL) and MeOH (1.5 mL). K₂CO₃ (82 mg, 0.6 mmol, 2 eq) was added and the reaction was stirred at RT for one hour. After complete conversion the reaction was diluted with 5 Et₂O and quenched with 2 mL 1M HCl. The reaction was partitioned between water and Et₂O. The aqueous layer was then extracted three times with Et₂O. The combined organic layers were dried over MgSO₄ and concentrated under reduced pressure. The crude material was purified by flash chromatography (50% EtOAc:50% Hexanes) giving ketone **3.66** (74 mg, 0.23 mmol, 76% yield) as a pale yellow amorphous solid. The compound crystallized slowly out of Et₂O to give small colorless diamond shaped crystals.

$R_f = 0.3$ (50:50 EtOAc:hexanes)

¹H NMR (500 MHz, CDCl₃) δ 12.07 (s, 1H), 8.63 (d, *J* = 8.3 Hz, 1H), 8.53 (d, *J* = 1.9 Hz, 1H), 7.55 (t, *J* = 8.1 Hz, 1H), 7.27 – 7.23 (m, 2H), 5.91 (dd, *J* = 17.7, 10.7 Hz, 1H), 5.40 (dd, *J* = 10.6, 0.9 Hz, 1H), 5.26 (dd, *J* = 17.6, 0.9 Hz, 1H), 2.96 (ddd, *J* = 10.7, 5.9, 2.7 Hz, 1H), 2.24 (ddd, *J* = 14.0, 6.0, 4.4 Hz, 1H), 1.89 (t, *J* = 12.3 Hz, 1H), 1.81 (s, 1H), 1.50 (s, 3H), 1.27 (s, 3H), 1.08 (s, 3H).

¹³C NMR (126 MHz, CDCl₃) δ 189.40, 159.83, 154.57, 142.37, 141.82, 140.86, 135.39, 135.03, 119.62, 119.00, 118.07, 117.77, 70.21, 44.63, 38.19, 37.42, 31.94, 29.72, 29.38, 26.18, 26.09, 25.91, 24.38, 22.71, 14.13.

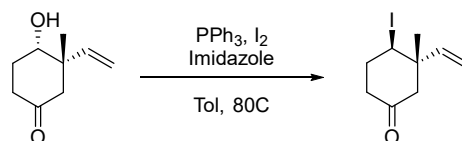


Ketone 3.75. A 10 mL round-bottomed flask was charged with PPh₃ (79 mg, 0.3 mmol, 1.5 equiv) and DCM (1 mL). The flask was wrapped in foil to exclude light, and NCD (38 mg, 0.3 mmol, 1.5 equiv) was added. The reaction was stirred at RT for 30 minutes, then a solution of alcohol **3.24-d** (31 mg, 0.2 mmol, 1 equiv) in DCM (1 mL) was added. The reaction was stirred for 17 hours, then quenched with 1 mL concentrated NaHCO₃. The reaction was partitioned between H₂O and DCM. The aqueous layer was then extracted three times with DCM. The combined organic layers were dried over MgSO₄ and concentrated under reduced pressure. The crude material was purified by preparative TLC (10% EtOAc:90% Hexanes) giving ketone **3.75** (23 mg, 0.134 mmol, 67% yield) as a colorless liquid.

R_f = 0.3 (10:90 EtOAc:hexanes)

¹H NMR (500 MHz, CDCl₃) δ 5.99 (dd, *J* = 17.0, 10.7 Hz, 1H), 5.35 (d, *J* = 17.0 Hz, 1H), 5.19 (d, *J* = 10.7 Hz, 1H), 2.53 (tt, *J* = 11.0, 5.4 Hz, 1H), 2.48 – 2.32 (m, 2H), 2.31 – 2.14 (m, 4H), 1.73 (s, 3H).

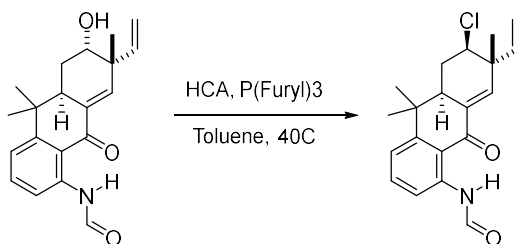
¹³C NMR (126 MHz, CDCl₃) δ 217.54, 141.23, 114.74, 73.80, 48.56, 41.09, 38.59, 27.58, 24.57, 1.03.



Ketone 3.78. A 10 mL round-bottomed flask was charged with alcohol **3.24-d** (15 mg, 0.1 mmol, 1 equiv), PPh₃ (105 mg, 0.4 mmol, 4equiv), Imidazole (28 mg, 0.4 mmol, 4 equiv), and toluene (3 mL). I₂ (75 mg, 0.3 mmol, 3 equiv) was added, and the reaction was heated to 80 °C for 1 hour. After one hour the reaction was quenched with 3 mL concentrated NaHCO₃. The reaction was partitioned between H₂O and toluene. The aqueous layer was then extracted three times with Et₂O. The combined organic layers were dried over MgSO₄ and concentrated under reduced pressure. The crude material was purified by preparative TLC (10% EtOAc:90% Hexanes) giving ketone **3.78** (19 mg, 0.073mmol, 73% yield) as a colorless liquid. Note that the product is volatile, and will come off in the rotovap upon extended heating with high vacuum.

R_f = 0.3 (10:90 EtOAc:hexanes)

¹H NMR (600 MHz, CDCl₃) δ 5.76 (dd, *J* = 17.5, 10.8 Hz, 1H), 5.17 (d, *J* = 10.8 Hz, 1H), 5.11 (d, *J* = 17.4 Hz, 1H), 4.56 – 4.51 (m, 1H), 2.72 – 2.62 (m, 1H), 2.59 (d, *J* = 15.2 Hz, 1H), 2.56 – 2.50 (m, 1H), 2.44 (ddt, *J* = 13.6, 8.9, 4.1 Hz, 1H), 2.42 – 2.34 (m, 1H), 2.34 – 2.28 (m, 1H), 1.22 (d, *J* = 1.0 Hz, 3H).



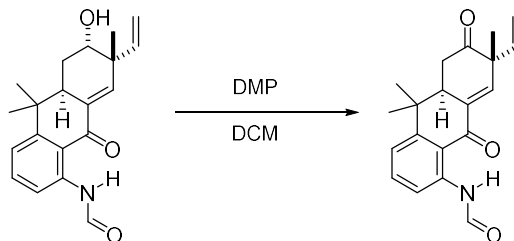
Fontonamide 1.15. A 2 mL scintillation vial was charged with alcohol **3.66** (6 mg, 0.02 mmol, 1 equiv.), P(Furyl)₃ (7.2 mg, 0.03 mmol, 1.5 eq), and toluene (0.1 mL). Hexachloro acetone (0.02 mL, 0.12 mmol, 6 equiv) was added and the reaction was warmed to 40 °C. After complete conversion the reaction was diluted with 2 mL Et₂O and quenched with 1 mL concentrated NaHCO₃. The reaction was partitioned between water and Et₂O. The aqueous layer was then extracted three times with Et₂O. The combined organic layers were dried over MgSO₄ and concentrated under reduced pressure. The crude material was purified by preparative TLC (10% EtOAc:90% Hexanes) giving fontonamide (2.4 mg, 0.007 mmol, 35% yield) as a pale yellow amorphous solid.

$R_f = 0.15$ (10:90 EtOAc:hexanes)

¹H NMR (600 MHz, CDCl₃) δ 11.96 (s, 1H), 8.61 (d, $J = 8.5$ Hz, 1H), 8.50 (s, 1H), 7.54 (t, $J = 8.2$ Hz, 1H), 7.21 (d, $J = 7.8$ Hz, 1H), 7.13 (d, $J = 2.5$ Hz, 1H), 5.95 (dd, $J = 17.5, 10.6$ Hz, 1H), 5.23 (d, $J = 10.6$ Hz, 1H) 5.20(d, $J = 17.5$ Hz, 1H), 4.08 (dd, $J = 12.9, 3.4$ Hz, 1H), 2.85 (s, 1H), 2.35 (d, $J = 7.5$ Hz, 1H), 2.22 (d, $J = 7.8$ Hz, 1H), 2.11 (q, $J = 12.3$ Hz, 1H), 1.48 (s, 2H), 1.32 (s, 3H), 1.07 (s, 3H).

^{13}C NMR (151 MHz, CDCl_3) δ 188.54, 159.83, 153.76, 144.81, 142.91, 140.95, 135.38, 134.75, 133.64, 119.89, 118.92, 115.17, 64.67, 44.51, 44.09, 37.81, 30.92, 25.75, 24.32, 19.81.

All data matches the published data for the natural product (See below)

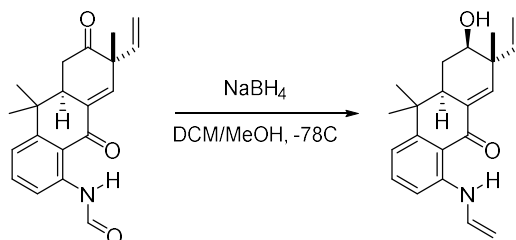


Ketone 3.81. A 10 mL round-bottomed flask was charged with alcohol **3.66** (10 mg, 0.03 mmol, 1 equiv.) and DCM (0.6 mL). DMP (32 mg, 0.075, 2.5 equiv) was added. The reaction was stirred for 2 hours at room temperature. After complete conversion by TLC, the reaction was diluted with 3 mL DCM, and quenched with 3 mL $\text{Na}_2\text{S}_2\text{O}_3$ and stirred until both layers were clear. The reaction was partitioned between water and DCM. The aqueous layer was then extracted three times with DCM. The combined organic layers were dried over MgSO_4 and concentrated under reduced pressure. The crude material was purified by preparative TLC (20% EtOAc:80% Hexanes) giving ketone **3.81** (9.5 mg, 0.029 mmol, 98% yield) as a pale yellow amorphous solid.

$R_f = 0.2$ (15:85 EtOAc:hexanes)

^1H NMR (500 MHz, CDCl_3) δ 11.92 (s, 1H), 8.65 (d, $J = 8.4$ Hz, 1H), 8.54 (s, 1H), 7.58 (t, $J = 8.3$ Hz, 1H), 7.25 (d, $J = 8.0$ Hz, 1H), 7.09 (s, 1H), 5.93 (dd, $J = 17.5, 10.4$ Hz, 1H), 5.24 (d, $J = 10.4$ Hz, 1H), 5.14 (d, $J = 17.5$ Hz, 1H), 3.14 (t, $J = 7.8$ Hz, 1H), 2.81 (dd, $J = 15.2, 6.1$ Hz, 1H), 2.72 (dd, $J = 15.1, 9.0$ Hz, 1H), 1.48 (s, 3H), 1.47 (s, 3H), 1.12 (s, 3H).

^{13}C NMR (126 MHz, CDCl_3) δ 210.47, 189.23, 159.86, 153.20, 143.06, 140.81, 138.73, 135.68, 135.61, 119.94, 119.52, 117.83, 116.24, 51.77, 43.84, 38.21, 36.83, 25.93, 24.62.



13-hydroxy dechlorofontonamide 1.28. A 5 mL round-bottomed flask was charged with ketone **3.81** (3 mg, 0.01 mmol, 1 equiv), DCM (0.25 mL), MeOH (0.25 mL). The reaction was cooled to -78°C , and NaBH_4 (2 mg, 0.05 mmol, 5 equiv). The reaction was stirred for 45 minutes at -78°C , then quenched with acetone (0.1 mL) and allowed to warm to RT. The reaction was diluted with 1 mL DCM, and 1 mL concentrated NaHCO_3 was added. The reaction was partitioned between water and DCM. The aqueous layer was then extracted three times with DCM. The combined organic layers were dried over MgSO_4 and concentrated under reduced pressure, giving 13-hydroxy dechlorofontonamide (3.15 mg, 0.0097 mmol, 97% yield) as a pale yellow glassy solid.

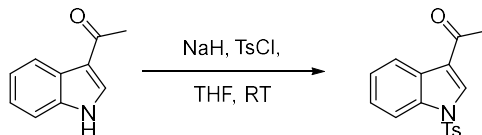
^1H NMR (500 MHz, CDCl_3) δ 12.03 (s, 1H), 8.62 (d, $J = 8.4$ Hz, 1H), 8.51 (s, 1H), 7.55 (t, $J = 8.2$ Hz, 1H), 7.24 (d, $J = 7.7$ Hz, 1H), 7.07 (s, 1H), 5.92 (dd, $J = 17.5, 10.7$ Hz, 1H), 5.30 (d, $J = 17.9$ Hz, 2H), 5.31 – 5.23 (d, $J = 1.8$ Hz, 1H), 3.84 (d, $J = 12.2$ Hz, 1H), 2.87 (s, 1H), 2.11 (d, $J = 12.6$ Hz, 1H), 1.83 (q, $J = 12.0$ Hz, 1H), 1.70 (s, 1H), 1.50 (s, 3H), 1.24 (s, 3H), 1.09 (s, 3H).

^{13}C NMR (126 MHz, CDCl_3) δ 189.58, 159.83, 154.17, 145.28, 143.27, 140.88, 135.19, 134.01, 119.76, 118.98, 117.92, 115.50, 72.66, 53.42, 44.24, 43.90, 37.76, 29.71, 27.89, 25.79, 24.39, 17.47.

Table 6.1 Comparison of the NMR of the synthetic compound with the reported shifts by Orjala, 2012, as well as the reported shifts from the isolation of fontonamide, Moore 1988, and our synthetic sample of fontonamide.

Carbon #	13-hydroxy this work		"13-hydroxy" Orjala, 2012		Fontonamide Moore, 1988		Fontonamide this work	
	C	H	C	H	C	H	C	H
N1		12.03		11.67		11.96		11.96
C2	159.8	8.51	159.9	8.47	159.75	8.48	159.8	8.50
C3	189.5		188.9		188.97		188.54	
C4	134.0		133.6		134.76		134.75	
C5	119.0	7.24	118.8	7.19	118.85	7.2	118.92	7.21
C6	135.2	7.55	135.3	7.51	135.27	7.53	135.38	7.54
C7	119.7	8.62	119.3	8.59	119.78	8.60	119.89	8.61
C8	140.9		140.8		140.83		140.95	
C9	134.0				133.54		133.64	
C10	154.2		153.7		153.68		153.76	
C11	145.3	7.07	144.5	7.1	144.70	7.113	144.81	7.13
C12	43.9		44		44.01		44.09	
C13	72.6	3.84	64.8	4.05	64.59	4.071	64.67	4.08
C13-OH		1.69		1.56				
C14	29.7	2.11	30.8	2.32	30.85	2.336	30.92	2.35
		1.83		2.09		2.098		2.11
C15	44.2	2.87	44.2	2.82	44.43	2.838	44.51	2.85
C16	37.8		37.8		37.74		37.81	
C17	25.8	1.09	25.4	1.04	25.68	1.06	25.72	1.07
C18	24.4	1.50	24.2	1.44	24.25	1.47	24.32	1.48
C19	17.5	1.24	19.9	1.35	19.75	1.31	19.81	1.32
C20	143.3	5.92	142.9	5.92	142.81	5.94	142.9	5.95
C21	115.5	5.3	115.1	5.20	115.07	5.22	115.17	5.23
		5.27		5.18		5.19		5.20

6.4 Experimental Details and Characterization Data for Chapter 4



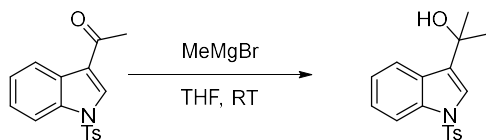
Tosyl Indole 4.11. A 25 mL round-bottomed flask was charged with NaH (250 mg, 60% by weight, 6.3 mmol, 1 equiv) and THF (5 mL). The solution was cooled to 0°C using an ice bath and 3-acetyl indole (1000mg, 6.3 mmol, 1 equiv.) was added as a solid in three portions. The ice bath was removed, and the solution was allowed to stir at room temperature for 30 minutes. TsCL (1.2 g, 6.3 mmol, 1 equiv) was added as a solid in one portion. The reaction was allowed to stir at RT for one hour. The reaction was then diluted with Et₂O and quenched with conc NH₄Cl. The reaction was partitioned between Et₂O and H₂O. The aqueous layer was then extracted two times with Et₂O. The combined organic layers were dried over MgSO₄ and concentrated under reduced pressure, giving tosyl indole **4.11** (1.95 g, 6.2 mmol, 99% yield) as a white solid.

$R_f = 0.2$ (15:85 EtOAc:hexanes)

¹H NMR (500 MHz, CDCl₃) δ 8.39 – 8.32 (m, 1H), 8.23 (s, 1H), 7.99 – 7.92 (m, 1H), 7.90 – 7.82 (m, 2H), 7.44 – 7.33 (m, 2H), 7.34 – 7.29 (m, 2H), 7.28 (s, 1H), 2.59 (s, 3H), 2.39 (s, 3H).

¹³C NMR (126 MHz, CDCl₃) δ 193.47, 145.95, 134.92, 134.56, 132.20, 130.26, 127.53, 127.15, 125.74, 124.84, 123.14, 121.62, 113.06, 27.81, 21.66.

HRMS Calculated for C₁₇H₁₅NO₃S [M+H]⁺: 313.0773. Found: 313.0705.



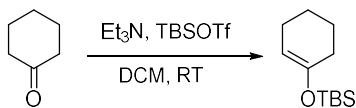
Alcohol 4.12. A 100 mL round-bottomed flask was charged with tosyl indole **4.11** (2.23 g, 7.1 mmol, 1 equiv) and THF (25 mL). MeMgBr (2.6 mL, 3M in Et₂O, 7.8 mmol, 1.1 equiv) was added dropwise. The reaction was allowed to stir at RT for one hour. The reaction was then diluted with Et₂O and quenched with conc NH₄Cl. The reaction was partitioned between Et₂O and H₂O. The aqueous layer was then extracted two times with Et₂O. The combined organic layers were dried over MgSO₄ and concentrated under reduced pressure. The crude material was purified by flash chromatography (40%EtOAc:60%Hexanes) giving tosyl indole **4.12** (2.15 g, 6.5 mmol, 92% yield) as an off-white solid.

$R_f = 0.3$ (40:60 EtOAc:hexanes)

¹H NMR (600 MHz, CDCl₃) δ 8.01 (d, $J = 8.3$ Hz, 1H), 7.84 (d, $J = 8.0$ Hz, 1H), 7.80 (d, $J = 8.1$ Hz, 2H), 7.48 (s, 1H), 7.34 (t, $J = 7.8$ Hz, 1H), 7.26 (d, $J = 8.3$ Hz, 3H), 2.38 (s, 3H), 1.71 (s, 6H).

¹³C NMR (151 MHz, CDCl₃) δ 144.94, 135.82, 135.33, 130.37, 129.91, 128.60, 126.87, 124.52, 123.00, 121.83, 121.33, 113.70, 70.07, 30.52, 21.58.

HRMS Calculated for C₁₈H₁₉NO₃S [M+H]⁺: 329.1086. Found: 329.1065.

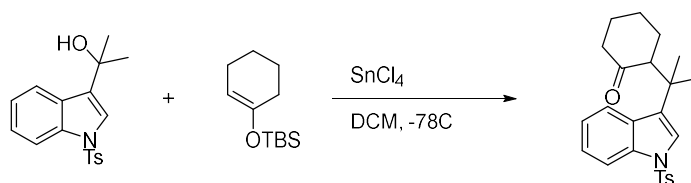


Silyl Enol Ether 4.14. A 500 mL round-bottomed flask equipped with a magnetic stir bar was charged with cyclohexanone (4.9 g, 50 mmol, 1 equiv.), Triethylamine (13.9 mL, 100 mmol, 2 equiv.), and DCM (125mL). TBSOTf (17.2 mL, 75 mmol, 1.5 equiv) was added in one portion, and the reaction was let stir at ambient temperature. After 30 min, the reaction was slowly quenched with 100 mL of saturated NaHCO₃. The reaction mixture was partitioned between H₂O and DCM, and the aqueous layer was then extracted two times with DCM. The combined organic layers were dried with MgSO₄ and concentrated under reduced pressure. The crude material was purified by passage through a silica plug (10:90 EtOAc:hexanes) to afford silyl enol ether **4.14** (9.4g, 44.5 mmol, 89% yield) as a colorless oil.

$R_f = 0.7$ (10:90 EtOAc:hexanes)

¹H NMR (500 MHz, CDCl₃) δ 4.91 – 4.86 (m, 1H), 2.06 – 1.97 (m, 4H), 1.71 – 1.63 (m, 2H), 1.56 – 1.48 (m, 2H), 0.93 (s, 9H), 0.14 (s, 6H).

¹³C NMR (126 MHz, CDCl₃) δ 150.50, 104.35, 29.89, 25.72, 25.71, 23.83, 23.17, 22.37, 18.02, -4.38.



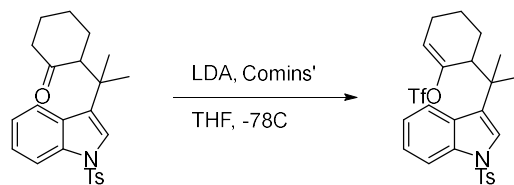
Ketone 4.15. A 500 mL round-bottomed flask was charged with silyl enol **4.14** (1.76 g, 8.2 mmol, 2 equiv), Alcohol **4.12** (1.35g, 4.1 mmol, 1 equiv) and DCM (150 mL). The reaction was cooled to $-78\text{ }^{\circ}\text{C}$ in an acetone/dry ice bath. SnCl_4 (1 mL, 8.2 mmol, 2 equiv) was added slowly. The reaction was stirred at -78°C for 30 minutes. The reaction was slowly quenched with 100 mL of saturated NaHCO_3 while stirring rapidly. The mixture was diluted with water and filtered through a celite plug. The filter cake was then washed with 50 mL DCM. The filtrate was then partitioned between H_2O and DCM, and the aqueous layer was then extracted three times with mL DCM. The combined organic layers were dried with MgSO_4 and concentrated under reduced pressure. The crude material was purified by flash chromatography (30% EtOAc:70% hexanes) to give ketone **4.15** (1.46 g, 3.6 mmol, 87% yield) as an off-white solid.

$R_f = 0.4$ (20:80 EtOAc:hexanes)

$^1\text{H NMR}$ (500 MHz, CDCl_3) δ 8.00 (d, $J = 8.3$ Hz, 1H), 7.76 – 7.71 (m, 2H), 7.65 (d, $J = 8.0$ Hz, 1H), 7.33 (s, 1H), 7.26 (t, 1H), 7.21 (t, $J = 8.2$ Hz, 3H), 3.00 (dd, $J = 11.8, 5.0$ Hz, 1H), 2.35 (s, 3H), 2.39 – 2.24 (m, 3H), 2.02 (d, $J = 13.2$ Hz, 1H), 1.88 (p, $J = 6.3$ Hz, 2H), 1.76 – 1.61 (m, 1H), 1.59 (s, 3H), 1.51 (s, 3H).

$^{13}\text{C NMR}$ (126 MHz, CDCl_3) δ 211.32, 144.72, 136.15, 135.06, 131.39, 129.73, 129.14, 126.68, 124.15, 123.15, 122.85, 121.58, 114.15, 56.69, 44.04, 41.90, 36.94, 30.25, 28.29, 27.00, 26.06, 25.81, 23.09, 21.37.

HRMS Calculated for $\text{C}_{24}\text{H}_{27}\text{NO}_3\text{S}$ $[\text{M}+\text{H}]^+$: 409.1712. Found: 409.1824.



Enol Triflate 4.17. A 25 mL round bottom flask was charged with ketone **4.15** (409 mg, 1 mmol, 1 equiv) and THF (5 mL). The reaction was cooled to -78°C in an acetone/dry ice bath. LDA (1.1 mL, 1M in THF/Hexanes, 1.1 mmol, 1.1 equiv). The reaction was stirred for 30 minutes, then Comin's (682 mg, 2 mmol, 2 equiv) was added a solid in one portion. The reaction was allowed to warm to RT, then diluted with 10 mL Et₂O and quenched with 10 5 mL concentrated NH₄Cl. The reaction mixture was partitioned between H₂O and Et₂O, and the aqueous layer was then extracted two times with Et₂O. The combined organic layers were dried with MgSO₄ and concentrated under reduced pressure. The crude material was purified by flash chromatography (20:80 EtOAc:hexanes) to afford enol triflate **4.17** (481 mg, 0.89 mmol, 89% yield) as an off-white solid.

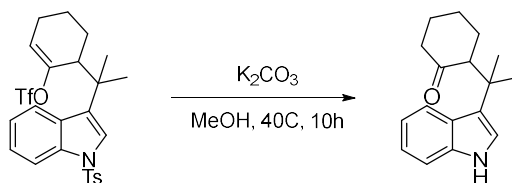
$R_f = 0.45$ (20:80 EtOAc:Hexanes)

¹H NMR (500 MHz, CDCl₃) δ 8.02 (d, $J = 8.3$ Hz, 1H), 7.79 – 7.72 (m, 2H), 7.67 (d, $J = 8.0$ Hz, 1H), 7.35 – 7.30 (m, 1H), 7.30 – 7.24 (m, 1H), 7.24 (s, 1H), 5.97 (dd, $J = 5.7, 3.2$ Hz, 1H), 3.25 (t, $J = 6.5$ Hz, 1H), 2.36 (s, 2H), 2.26 – 1.99 (m, 2H), 1.61 (s, 3H), 1.43 (s, 3H), 1.39 – 1.18 (m, 4H).

¹³C NMR (126 MHz, CDCl₃) δ 151.14, 144.83, 136.08, 135.20, 130.90, 129.76, 129.18, 126.78, 124.51, 123.02, 122.65, 122.19, 121.49, 119.78, 117.23, 114.07, 44.69, 38.51, 31.60, 28.81, 27.31, 24.33, 22.67, 21.53, 20.36, 14.13.

¹⁹F NMR (471 MHz, CDCl₃) δ -73.47.

HRMS Calculated for C₂₅H₂₆F₃NO₅S₂ [M+H]⁺: 541.1204. Found: 541.1113.

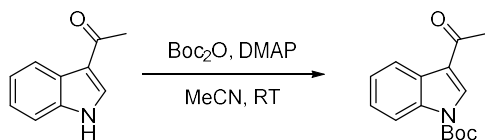


Enol Triflate 4.18. A 10 mL round bottom flask was charged with enol triflate **4.17** (108 mg, 0.2 mmol, 1 equiv) and MeOH (2 mL). K_2CO_3 (110 mg, 0.8 mmol, 4 equiv) was added, and the reaction was heated to 40°C. The reaction was stirred for 10 hours, then diluted with 3 mL Et_2O and quenched with 2 mL 1M HCl. The reaction was partitioned between Et_2O and H_2O . The aqueous layer was then extracted two times with Et_2O . The combined organic layers were dried over $MgSO_4$ and concentrated under reduced pressure. The crude reaction was purified by flash chromatography (20% EtOAc:80% hexanes) to give ketone **4.18** (42 mg, 0.164 mmol, 82% yield) as a colorless oil.

$R_f = 0.40$ (20:80 EtOAc:Hexanes)

1H NMR (500 MHz, $CDCl_3$) δ 7.95 (s, 1H), 7.77 (d, $J = 8.0$ Hz, 1H), 7.39 (d, $J = 8.1$ Hz, 1H), 7.19 (t, $J = 7.6$ Hz, 1H), 7.14 – 7.07 (m, 1H), 6.99 (d, $J = 2.4$ Hz, 1H), 3.19 – 3.13 (m, 1H), 2.42 – 2.28 (m, 1H), 2.07 (s, 1H), 1.81 (s, 1H), 1.75 (s, 1H), 1.66 (s, 3H), 1.55 (s, 3H).

^{13}C NMR (126 MHz, $CDCl_3$) δ 212.83, 137.23, 125.41, 125.29, 121.45, 121.16, 121.01, 118.87, 111.46, 57.88, 44.34, 36.79, 30.62, 28.60, 26.95, 26.10, 23.24, 0.01.

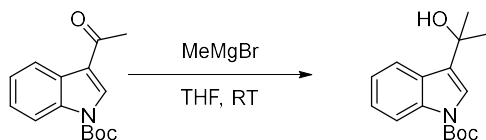


Boc Indole 4.20. A 50 mL round-bottomed flask was charged with 3-acetyl indole (1000 mg, 6.3 mmol, 1 equiv.), Boc_2O (2 g, 9.45 mmol, 1.5 equiv), and MeCN (15 mL). DMAP (77 mg, 0.63 mmol, 0.1 equiv) was added as a solid, causing the reaction to begin to bubble. The reaction was allowed to stir at RT for 30 minutes. The reaction was then diluted with 15 Et_2O and quenched with 10 mL concentrated NH_4Cl . The reaction was partitioned between Et_2O and H_2O . The aqueous layer was then extracted two times with Et_2O . The combined organic layers were dried over MgSO_4 and concentrated under reduced pressure, giving Boc indole **4.20** (1.62 g, 6.2 mmol, 99% yield) as a white solid.

$R_f = 0.3$ (15:85 EtOAc:hexanes)

$^1\text{H NMR}$ (600 MHz, CDCl_3) δ 8.40 (dd, $J = 7.5, 1.7$ Hz, 1H), 8.25 (s, 1H), 8.14 (d, $J = 8.0$ Hz, 1H), 7.39 (tt, $J = 7.9, 6.2$ Hz, 2H), 2.60 (s, 3H), 1.74 (s, 9H).

$^{13}\text{C NMR}$ (151 MHz, CDCl_3) δ 193.94, 149.19, 135.56, 132.41, 127.40, 125.50, 124.40, 122.73, 120.67, 114.96, 85.43, 28.14, 27.74.



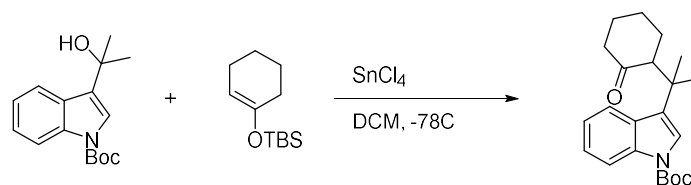
Alcohol 4.21. A 100 mL round-bottomed flask was charged with tosyl indole **4.20** (1 g, 4 mmol, 1 equiv) and THF (15 mL). MeMgBr (1.67 mL, 3M in Et₂O, 5 mmol, 1.25 equiv) was added dropwise. The reaction was allowed to stir at RT for one hour. The reaction was then diluted with Et₂O and quenched with conc NH₄Cl. The reaction was partitioned between Et₂O and H₂O. The aqueous layer was then extracted two times with Et₂O. The combined organic layers were dried over MgSO₄ and concentrated under reduced pressure. The crude material was purified by flash chromatography (40%EtOAc:60%Hexanes) giving Boc indole **4.21** (6.93 g, 2.52 mmol, 63% yield) as a colorless glass.

$R_f = 0.3$ (40:60 EtOAc:hexanes)

¹H NMR (500 MHz, CDCl₃) δ 8.28 – 8.06 (m, 1H), 7.87 (d, $J = 7.9$ Hz, 1H), 7.50 (s, 1H), 7.34 (ddd, $J = 8.4, 7.2, 1.3$ Hz, 1H), 7.26 (d, $J = 7.0$ Hz, 1H), 1.74 (s, 6H), 1.70 (s, 9H).

¹³C NMR (151 MHz, CDCl₃) δ 128.62, 124.24, 122.42, 121.33, 121.05, 115.38, 70.10, 30.51, 28.24, 28.18, 28.11.

HRMS Calculated for C₁₆H₂₁NO₃ [M+H]⁺: 275.1521. Found: 275.1572.



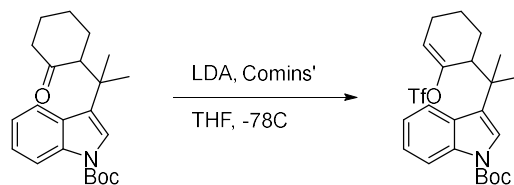
Ketone 4.22. A 50 mL round-bottomed flask was charged with silyl enol **4.14** (248 mg, 2 mmol, 2 equiv), Alcohol **4.21** (271 mg, 1 mmol, 1 equiv) and DCM (10 mL). The reaction was cooled to $-78\text{ }^{\circ}\text{C}$ in an acetone/dry ice bath. SnCl_4 (0.24 mL, 2 mmol, 2 equiv) was added slowly. The reaction was stirred at -78°C for 30 minutes. The reaction was slowly quenched with 100 mL of saturated NaHCO_3 while stirring rapidly. The mixture was diluted with water and filtered through a celite plug. The filter cake was then washed with 10 mL DCM. The filtrate was then partitioned between H_2O and DCM, and the aqueous layer was then extracted three times with mL DCM. The combined organic layers were dried with MgSO_4 and concentrated under reduced pressure. The crude material was purified by flash chromatography (30% EtOAc:70% hexanes) to give ketone **4.22** (252 mg, 0.71 mmol, 71% yield) as an off-white solid.

$R_f = 0.4$ (20:80 EtOAc:hexanes)

$^1\text{H NMR}$ (500 MHz, CDCl_3) δ 8.19 (s, 1H), 7.70 (d, $J = 7.9$ Hz, 1H), 7.34 (s, 1H), 7.30 (t, $J = 7.8$ Hz, 1H), 7.22 (t, $J = 7.6$ Hz, 1H), 3.31 – 2.73 (m, 1H), 2.57 – 2.22 (m, 3H), 2.10 – 1.99 (m, 1H), 1.69 (s, 10H), 1.63 (s, 3H), 1.53 (s, 3H).

$^{13}\text{C NMR}$ (126 MHz, CDCl_3) δ 212.13, 129.13, 129.04, 128.70, 128.23, 123.79, 122.45, 121.99, 121.08, 115.63, 56.98, 44.25, 36.86, 30.53, 28.44, 28.25, 26.33, 26.01, 22.84.

HRMS Calculated for $\text{C}_{22}\text{H}_{29}\text{NO}_3$ $[\text{M}+\text{H}]^+$: 355.2147. Found: 355.2145.



Enol Triflate 4.24. A 50 mL round bottom flask was charged with ketone **4.22** (355 mg, 1 mmol, 1 equiv) and THF (10 mL). The reaction was cooled to -78°C in an acetone/dry ice bath. LDA (2.4 mL, 0.5M in THF/Hexanes, 1.2 mmol, 1.2 equiv). The reaction was stirred for 30 minutes, then Comin's (682 mg, 2 mmol, 2 equiv) was added a solid in one portion. The reaction was allowed to warm to RT, then diluted with 10 mL Et₂O and quenched with 10 5 mL concentrated NH₄Cl. The reaction mixture was partitioned between H₂O and Et₂O, and the aqueous layer was then extracted two times with Et₂O. The combined organic layers were dried with MgSO₄ and concentrated under reduced pressure. The crude material was purified by flash chromatography (20:80 EtOAc:hexanes) to afford enol triflate **4.24** (481 mg, 0.89 mmol, 89% yield) as an colorless highly viscous oil.

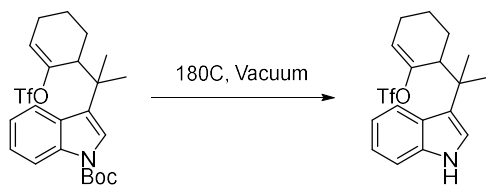
$R_f = 0.45$ (15:85 EtOAc:hexanes)

¹H NMR (500 MHz, CDCl₃) δ 8.43 – 7.98 (m, 1H), 7.72 (d, $J = 7.9$ Hz, 1H), 7.37 (s, 1H), 7.36 – 7.31 (m, 1H), 7.29 – 7.23 (m, 1H), 5.99 (dd, $J = 5.7, 3.1$ Hz, 1H), 3.36 (dq, $J = 7.0, 3.5$ Hz, 1H), 2.28 – 2.04 (m, 2H), 1.71 (s, 10H), 1.66 (s, 3H), 1.62 – 1.48 (m, 2H), 1.45 (s, 3H).

¹³C NMR (126 MHz, CDCl₃) δ 151.50, 128.84, 128.82, 124.13, 123.80, 122.42, 122.30, 122.01, 121.74, 121.04, 119.84, 117.28, 115.65, 115.55, 44.75, 38.32, 28.80, 28.23, 27.46, 24.43, 24.19, 20.55.

¹⁹F NMR (470 MHz, CDCl₃) δ -73.52.

HRMS Calculated for C₂₃H₂₈F₃NO₅S [M+H]⁺: 487.164. Found: 487.155.



Indole 4.19. A 25 mL round-bottomed flask was charged with enol triflate **4.24** (974 mg, 2 mmol, 1 equiv) as a neat solid. The flask was placed under vacuum (4 mmHg) and heated to 180 °C. The solid quickly melted and after about 90 seconds began to bubble. Over the next 5 minutes the liquid turned from colorless to pale brown to light purple/brown and bubbling ceased. The reaction was cooled back to RT prior to releasing the vacuum, giving indole **4.19** (750.8 g, 1.94 mmol, 97% yield) as a purple/brown solid.

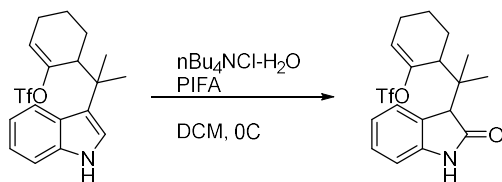
$R_f = 0.35$ (15:85 EtOAc:hexanes)

$^1\text{H NMR}$ (500 MHz, CDCl_3) δ 7.95 (s, 1H), 7.77 (d, $J = 8.0$ Hz, 1H), 7.39 (dd, $J = 8.2, 1.2$ Hz, 1H), 7.21 (ddd, $J = 8.2, 7.0, 1.1$ Hz, 1H), 7.12 (ddd, $J = 8.1, 7.1, 1.1$ Hz, 1H), 6.96 (d, $J = 2.5$ Hz, 1H), 5.95 (td, $J = 3.8, 1.9$ Hz, 1H), 3.34 (s, 1H), 2.20 – 2.04 (m, 2H), 1.66 (s, 3H), 1.45 (s, 3H).

$^{13}\text{C NMR}$ (126 MHz, CDCl_3) δ 152.06, 137.20, 125.63, 124.88, 122.03, 121.83, 120.96, 120.34, 119.18, 117.28, 111.35, 45.37, 38.33, 29.23, 27.47, 24.85, 24.49, 20.46, 0.00.

$^{19}\text{F NMR}$ (470 MHz, CDCl_3) δ -73.54.

HRMS Calculated for $\text{C}_{18}\text{H}_{20}\text{F}_3\text{NO}_3\text{S}$ $[\text{M}+\text{H}]^+$: 387.1116. Found: 387.1069.



Indolinone 4.8. A 25 mL round-bottomed flask was charged with indole **4.19** (445 mg, 1 mmol, 1 equiv) and $n\text{Bu}_4\text{NCl}\cdot\text{H}_2\text{O}$ (309 mg, 1.05 mmol, 1.05 equiv), and DCM (6 mL). The reaction was cooled to 0 °C with an ice bath. PIFA (451 mg, 1.05 mmol, 1.05 equiv) was added as a solid in three portions. The reaction was stirred at 0°C for 5 minutes then quenched with 3 mL H_2O . The reaction was partitioned into DCM and H_2O . The aqueous layer was then extracted two times with DCM. The combined organic layers were dried over MgSO_4 and concentrated under reduced pressure. The crude reaction was purified by flash chromatography (10% EtOAc:90% hexanes) to give indolinone **4.8** as a 1:1 inseparable mixture of diastereomers (290 mg, 0.72 mmol, 72% combined yield) as white solids.

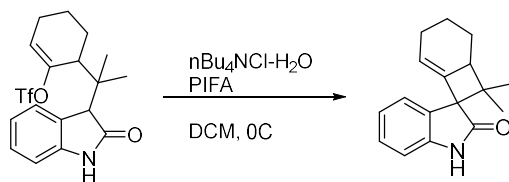
$R_f = 0.2$ (25:75 EtOAc:hexanes)

$^1\text{H NMR}$ (500 MHz, CDCl_3) δ 7.49 (s, 1H), 7.33 (d, $J = 7.6$ Hz, 1H), 7.25 (td, $J = 7.6, 2.5$ Hz, 1H), 7.08 – 6.97 (m, 1H), 6.86 (d, $J = 7.8$ Hz, 1H), 6.03 (ddd, $J = 9.2, 5.7, 3.0$ Hz, 1H), 3.77 (s, 0.5H), 3.72 – 3.66 (m, 0.5H), 3.62 (s, 0.5H), 3.49 (t, $J = 7.0$ Hz, 0.5H), 2.37 – 2.12 (m, 2.5H), 2.09 – 1.95 (m, 0.5H), 1.94 – 1.72 (m, 2H), 1.26 (s, 1.5H), 1.16 (s, 1.5H), 1.03 (s, 1.5H), 1.01 (s, 1.5H).

$^{13}\text{C NMR}$ (126 MHz, CDCl_3) δ 178.05, 177.32, 151.78, 151.40, 142.01, 141.75, 128.18, 128.11, 127.51, 126.49, 126.27, 122.85, 121.90, 121.82, 109.27, 109.25, 52.84, 51.79, 43.50, 42.03, 40.79, 40.28, 26.73, 26.62, 24.48, 24.35, 23.63, 23.48, 22.46, 21.09, 20.82, 20.47, 0.00.

$^{19}\text{F NMR}$ (470 MHz, CDCl_3) δ -73.84, -73.97.

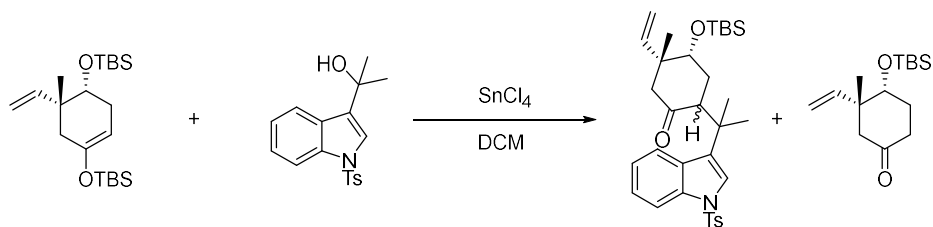
HRMS Calculated for $\text{C}_{18}\text{H}_{20}\text{F}_3\text{NO}_4\text{S}$ $[\text{M}+\text{H}]^+$: 403.1065. Found: 402.1013.



Indolinone 4.9. A 5 mL round-bottomed flask was charged with indole **4.8** (20 mg, 0.05 mmol, 1 equiv), [Pd(PtBu₃)Br]₂ (7.8 mg, 0.01 mmol, 0.2 equiv), and toluene (0.5 mL). The atmosphere was removed by vacuum and replaced three times with argon. LiHMDS (0.1 mL, 1 M in THF, 0.1 mmol, 2 equiv) was added, and the atmosphere was again replaced three times with Argon. The reaction was then heated in an oil bath to 60°C for one hour. The reaction was diluted with 2 mL Et₂O and quenched with 2 mL NaHCO₃. The reaction was partitioned into Et₂O and H₂O. The aqueous layer was then extracted two times with Et₂O. The combined organic layers were dried over MgSO₄ and concentrated under reduced pressure. The crude reaction was purified by preparative chromatography (10% EtOAc:90% hexanes) to give indolinone **4.9** as a 1:1 separable mixture of diastereomers (3.8 mg, 0.015 mmol, 30% combined yield) as white solids.

$R_f = 0.15$ (25:75 EtOAc:hexanes)

¹H NMR (500 MHz, CDCl₃) δ 7.31 (d, $J = 8.2$ Hz, 1H), 7.14 – 6.98 (m, 2H), 6.82 (d, $J = 7.8$ Hz, 1H), 5.00 – 4.95 (m, 1H), 3.37 (d, $J = 6.2$ Hz, 1H), 2.21 – 2.10 (m, 1H), 1.92 (d, $J = 13.6$ Hz, 1H), 1.84 (dt, $J = 10.0, 4.9$ Hz, 1H), 1.45 (s, 3H), 1.02 (s, 3H).



Ketone 4.26. A 500 mL round-bottomed flask was charged with Enol ether **3.46-a** (2.1 g, 5.4 mmol, 1 equiv), Alcohol **2.3** (3.3 g, 10.8 mmol, 2 equiv) and DCM (100 mL). The reaction was cooled to $-78\text{ }^{\circ}\text{C}$ in an acetone/dry ice bath. SnCl_4 (1 mL, 8.1 mmol, 1.5 equiv) was added slowly. The reaction was stirred at $-78\text{ }^{\circ}\text{C}$ for 30 minutes. The reaction was slowly quenched with 50 mL of saturated NaHCO_3 while stirring rapidly. The mixture was diluted with water and filtered through a celite plug. The filter cake was then washed with 50 mL DCM. The filtrate was then partitioned between H_2O and DCM, and the aqueous layer was then extracted three times with DCM. The combined organic layers were dried with MgSO_4 and concentrated under reduced pressure. The crude material was purified by flash chromatography (30% EtOAc:70% hexanes) to give ketone **4.26** (1.78g, 3.1 mmol, 57% yield, 87% brsm), a colorless oil, as a 3:1 mixture of diastereomers along with recovered ketone **3.24-a** (506 mg, 1.89 mmol, 35% yield) as a colorless oil.

Ketone 4.26

$R_f = 0.5$ (20:80 EtOAc:hexanes)

$^1\text{H NMR}$ (500 MHz, CDCl_3) δ 7.98 (dt, $J = 8.3, 0.9$ Hz, 1H), 7.75 (d, $J = 8.4$ Hz, 2H), 7.63 (dt, $J = 8.1, 1.0$ Hz, 1H), 7.33 (s, 1H), 7.29 – 7.24 (m, 1H), 7.22 (dt, $J = 8.5, 1.4$ Hz, 2H), 7.17 (ddd, $J =$

8.1, 7.2, 1.1 Hz, 1H), 5.86 (dd, $J = 17.5, 10.8$ Hz, 1H), 4.97 (dd, $J = 10.8, 1.0$ Hz, 1H), 4.88 (dd, $J = 17.5, 1.0$ Hz, 1H), 3.48 (d, $J = 3.2$ Hz, 1H), 3.42 (dd, $J = 12.8, 5.8$ Hz, 1H), 2.88 (d, $J = 12.6$ Hz, 1H), 2.35 (s, 3H), 1.90 (dd, $J = 12.6, 1.3$ Hz, 1H), 1.88 – 1.76 (m, 1H), 1.66 (s, 3H), 1.50 (s, 3H), 0.92 (s, 3H), 0.75 (s, 9H), -0.15 (s, 3H), -0.80 (s, 3H).

^{13}C NMR (126 MHz, CDCl_3) δ 210.84, 144.83, 144.62, 136.09, 135.25, 131.16, 129.75, 129.09, 126.83, 124.17, 122.94, 122.83, 121.86, 114.06, 112.01, 73.36, 49.16, 48.52, 47.16, 36.28, 33.15, 25.92, 22.50, 21.54, 17.93, -5.17, -5.22.

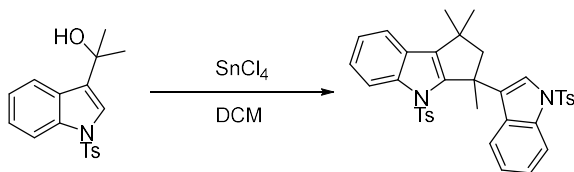
HRMS Calculated for $\text{C}_{33}\text{H}_{45}\text{NO}_4\text{Si}$ $[\text{M}+\text{H}]^+$: 579.2839. Found: 579.2711.

Ketone 3.24-a

$R_f = 0.6$ (20:80 EtOAc:hexanes)

^1H NMR (500 MHz, CDCl_3) δ 5.95 (dd, $J = 17.7, 10.9$ Hz, 1H), 5.05 (d, $J = 10.8$ Hz, 1H), 4.96 (d, $J = 17.8$ Hz, 1H), 3.70 (dd, $J = 6.4, 2.9$ Hz, 1H), 2.76 (d, $J = 13.8$ Hz, 1H), 2.60 – 2.49 (m, 1H), 2.28 – 2.17 (m, 1H), 2.08 (dd, $J = 13.9, 1.7$ Hz, 1H), 1.97 (dtdd, $J = 9.8, 5.5, 3.1, 1.2$ Hz, 1H), 1.93 – 1.81 (m, 1H), 1.01 (s, 3H), 0.96 (s, 9H), 0.09 (s, 6H).

^{13}C NMR (126 MHz, CDCl_3) δ 211.01, 143.34, 113.21, 74.16, 74.13, 47.69, 45.86, 36.92, 30.12, 25.82, 24.52, 18.07, -4.32, -4.56, -4.79.

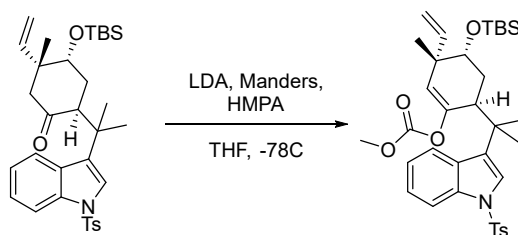


Indole Dimer 4.27. A 25 mL round-bottomed flask was charged Alcohol **2.3** (61 mg, 0.16 mmol, 1 equiv) and DCM (4 mL). The reaction was cooled to -20 °C in an acetone/dry ice bath. SnCl_4

(0.04 mL, 0.32 mmol, 2 equiv) was added slowly. The reaction was stirred at -78°C for 30 minutes. The reaction was slowly quenched with 50 mL of saturated NaHCO_3 while stirring rapidly. The mixture was diluted with water and filtered through a celite plug. The filter cake was then washed with 5 mL DCM. The filtrate was then partitioned between H_2O and DCM, and the aqueous layer was then extracted three times with DCM. The combined organic layers were dried with MgSO_4 and concentrated under reduced pressure. The crude material was purified by flash chromatography (30% EtOAc:70% hexanes) to give indole Dimer **4.27** (46 mg, 0.074 mmol, 93% yield, 87% brsm), a white crystalline solid.

$R_f = 0.4$ (20:80 EtOAc:hexanes)

$^1\text{H NMR}$ (500 MHz, CDCl_3) δ 8.12 – 8.04 (m, 1H), 7.93 (d, $J = 8.4$ Hz, 1H), 7.90 – 7.85 (m, 2H), 7.63 (s, 1H), 7.61 – 7.57 (m, 1H), 7.35 – 7.29 (m, 2H), 7.14 (dd, $J = 7.7, 1.1$ Hz, 3H), 6.81 (d, $J = 7.9$ Hz, 1H), 6.67 (ddd, $J = 8.1, 7.2, 1.0$ Hz, 1H), 6.53 (d, $J = 8.3$ Hz, 2H), 6.32 (d, $J = 8.1$ Hz, 2H), 2.90 (d, $J = 13.5$ Hz, 1H), 2.36 (d, $J = 13.5$ Hz, 1H), 2.17 (s, 3H), 2.10 (d, $J = 3.2$ Hz, 6H), 1.55 (s, 3H), 1.51 (s, 3H).



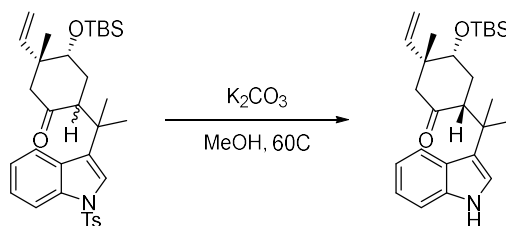
Enol Carboxylate 4.40. A 50 mL round-bottomed flask was charged with tosyl indole **4.26** (127 mg, 0.2 mmol, 1 equiv) and THF (2 mL). The reaction was cooled to -78°C with an acetone/dry ice bath. LDA (0.3 mL, 1M in THF, 0.3 mmol, 1.5 equiv) was added and the reaction was allowed to warm to 0°C over one hour. The reaction was then cooled back to -78°C and HMPA (0.07 mL,

0.4 mmol, 2 equiv) was added, followed by Mander's reagent (0.032 mL, 0.4 mmol, 2 equiv) was added in a single portion. The ice bath was then removed and the reaction was allowed to warm to room temperature. The reaction was then diluted with Et₂O and quenched with conc NH₄Cl slowly (**Important note** – Cyanide gas is generated during this process – make sure to keep nitrogen blowing over the reaction). The reaction was partitioned between Et₂O and H₂O. The aqueous layer was then extracted two times with Et₂O. The combined organic layers were dried over MgSO₄ and concentrated under reduced pressure. The crude reaction was purified by flash chromatography (20% EtOAc:80% hexanes) to give enol carboxylate **4.35** (110 mg, 0.174 mmol, 87% yield) as a white solid.

$R_f = 0.4$ (10:90 EtOAc:hexanes)

¹H NMR (500 MHz, CDCl₃) δ 7.96 (d, $J = 8.3$ Hz, 1H), 7.80 (d, $J = 8.2$ Hz, 2H), 7.64 (d, $J = 8.0$ Hz, 1H), 7.34 (s, 1H), 7.25 (d, $J = 8.2$ Hz, 2H), 7.19 (t, $J = 7.6$ Hz, 1H), 5.91 – 5.69 (m, 1H), 5.23 (s, 1H), 5.12 – 5.05 (m, 2H), 3.63 (dd, $J = 13.3, 3.3$ Hz, 1H), 3.44 – 3.39 (m, 1H), 3.37 (s, 2H), 2.36 (d, $J = 9.5$ Hz, 3H), 1.73 – 1.64 (m, 1H), 1.51 (s, 3H), 1.45 (d, $J = 2.0$ Hz, 3H), 1.11 (s, 2H), 0.86 (s, 9H), 0.01 (s, 3H), -0.15 (s, 3H).

¹³C NMR (101 MHz, CDCl₃) δ 153.78, 148.33, 142.34, 131.64, 129.75, 129.06, 126.97, 124.18, 123.97, 122.61, 122.13, 121.92, 113.67, 77.33, 77.22, 73.26, 54.56, 43.53, 42.19, 38.14, 29.71, 25.77, 25.62, 21.56, 17.96, 0.00, -4.11, -4.92.



Ketone 4.36. A 250 mL round-bottomed flask was charged with ketone **4.26** as a 3:1 diastereomeric mixture (3.7g, 6.3 mmol, 1 equiv) and MeOH (30 mL). K_2CO_3 (4.4 g, 31.5 mmol, 5 eq) was added, and the reaction flask was affixed with a reflux condenser and heated to 60 °C. The reaction was stirred for 2 days, then cooled to room temperature and diluted with 50 mL Et_2O . 50 mL of 1M HCl was added to quench the reaction and the reaction was partitioned between Et_2O and H_2O . The aqueous layer was then extracted three times with Et_2O . The combined organic layers were dried with $MgSO_4$ and concentrated under reduced pressure. The crude material was purified by flash chromatography (30% EtOAc:70% hexanes) to give ketone **4.36** as the major diastereomer (2 g, 4.8 mmol, 76% yield) as an off-white solid, and the minor diastereomer **SI.2** (500 mg, 1.2 mmol, 19% yield)

Ketone 4.36

$R_f = 0.5$ (20:80 EtOAc:hexanes)

1H NMR (500 MHz, $CDCl_3$) δ 7.95 (s, 1H), 7.72 (d, $J = 8.0$ Hz, 1H), 7.37 (d, $J = 8.1$ Hz, 1H), 7.21 – 7.14 (m, 1H), 7.09 (ddd, $J = 8.1, 7.0, 1.1$ Hz, 1H), 6.95 (d, $J = 2.5$ Hz, 1H), 5.91 (dd, $J = 17.9, 11.2$ Hz, 1H), 5.15 – 5.04 (m, 2H), 3.64 (dd, $J = 11.2, 3.9$ Hz, 1H), 3.08 (dd, $J = 13.6, 5.0$ Hz, 1H), 2.53 (d, $J = 14.5$ Hz, 1H), 2.27 (d, $J = 14.5$ Hz, 1H), 1.68 (s, 3H), 1.51 (m, 1H), 1.48 (s, 3H), 1.39 (dt, $J = 12.8, 4.4$ Hz, 1H), 1.06 (s, 3H), 0.20 (s, 3H), -0.47 (s, 3H).

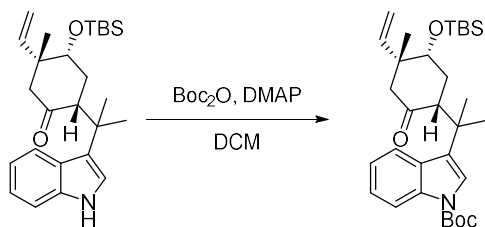
^{13}C NMR (126 MHz, CDCl_3) δ 189.57, 140.52, 137.32, 125.23, 121.61, 120.83, 120.51, 118.97, 115.10, 111.45, 54.57, 51.06, 46.27, 36.66, 33.83, 31.60, 27.17, 27.02, 25.64, 22.67, 22.23, 17.90, -4.95, -5.34.

Ketone SI.2

R_f = 0.4 (20:80 EtOAc:hexanes)

^1H NMR (500 MHz, CDCl_3) δ 7.91 (s, 1H), 7.74 (d, J = 8.0 Hz, 1H), 7.43 – 7.31 (m, 1H), 7.16 (ddd, J = 8.2, 7.0, 1.1 Hz, 1H), 7.05 (ddd, J = 8.2, 7.1, 1.1 Hz, 1H), 6.97 (d, J = 2.4 Hz, 1H), 5.89 (dd, J = 17.5, 10.8 Hz, 1H), 4.97 (dd, J = 10.8, 1.1 Hz, 1H), 4.89 (dd, J = 17.5, 1.1 Hz, 1H), 3.57 – 3.50 (m, 2H), 2.93 (d, J = 12.5 Hz, 1H), 1.90 (dd, J = 12.4, 1.4 Hz, 1H), 1.90 – 1.82 (m, 1H), 1.72 (s, 3H), 1.52 (s, 3H), 0.93 (s, 3H), 0.81 (s, 9H), -0.10 (s, 3H), -0.55 (s, 3H).

^{13}C NMR (126 MHz, CDCl_3) δ 212.20, 145.03, 137.28, 125.45, 124.91, 121.40, 121.29, 120.98, 119.06, 111.87, 111.38, 73.63, 50.54, 48.83, 47.40, 36.06, 34.71, 34.56, 33.41, 31.63, 29.10, 26.58, 26.02, 25.71, 25.32, 23.54, 22.70, 22.60, 20.74, 18.03, 14.16, -4.90, -5.12.



Boc Indole 4.37. A 250 mL round-bottomed flask was charged with ketone **4.36** (620 mg, 1.45 mmol, 1 equiv), Boc_2O (436 mg, 2 mmol, 1.38 equiv) and DCM (50 mL). DMAP (17 mg, 0.15 mmol, 0.1 eq) was added and the reaction was stirred for 17 hours at room temperature. After complete conversion, the reaction was diluted with hexanes, and applied directly to the top of a

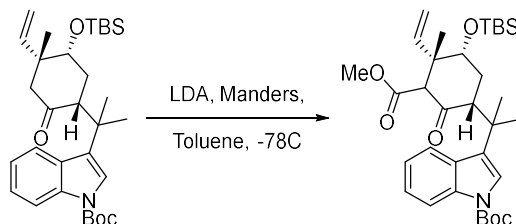
column. The crude reaction was purified by flash chromatography (10% EtOAc:90% hexanes) to boc indole **4.37** (723 mg, 1.38 mmol, 95% yield) as a white solid.

R_f = 0.55 (20:80 EtOAc:hexanes)

$^1\text{H NMR}$ (500 MHz, CDCl_3) δ 8.20 (s, 1H), 7.66 (d, J = 7.9 Hz, 1H), 7.35 – 7.25 (m, 2H), 7.25 – 7.17 (m, 1H), 5.91 (dd, J = 18.0, 11.2 Hz, 1H), 5.13 (d, J = 11.1 Hz, 1H), 5.10 – 5.03 (m, 1H), 3.64 (dd, J = 11.2, 3.8 Hz, 1H), 3.03 (dd, J = 13.5, 5.1 Hz, 1H), 2.55 (d, J = 14.6 Hz, 1H), 2.25 (d, J = 14.5 Hz, 1H), 1.68 (s, 9H), 1.66 (s, 3H), 1.47 (s, 3H), 1.06 (s, 3H), -0.16 (s, 3H), -0.41 (s, 3H).

$^{13}\text{C NMR}$ (126 MHz, CDCl_3) δ 208.50, 149.77, 140.40, 129.04, 128.48, 123.98, 122.28, 122.06, 120.60, 115.70, 115.22, 83.41, 77.12, 53.81, 50.93, 46.13, 36.73, 33.85, 28.22, 27.12, 26.22, 25.61, 22.17, 17.94, -5.01, -5.20.

HRMS Calculated for $\text{C}_{31}\text{H}_{47}\text{NO}_4\text{Si}$ $[\text{M}+\text{H}]^+$: 525.3274. Found: 525.3168.



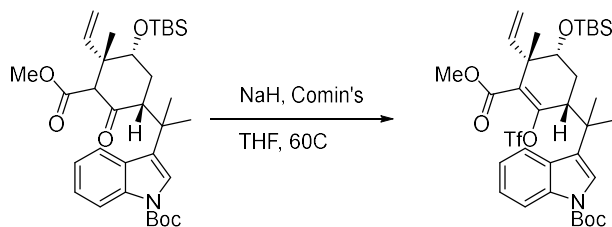
Beta-Keto Ester 4.40. A 50 mL round-bottomed flask was charged with boc indole **4.37** (735 mg, 1.4 mmol, 1 equiv) and Toluene (14 mL). The reaction was cooled to -78°C with an acetone/dry ice bath. LDA (2.1 mL, 1M in THF, 2.1 mmol, 1.5 equiv) was added and the reaction was allowed to warm to -20°C over one hour. The reaction was then cooled back to -78°C and Mander's reagent (0.18 mL, 2.3 mmol, 1.64 equiv) was added in a single portion. The ice bath was then

removed and the reaction was allowed to warm to room temperature. After reaching room temperature, the reaction was stirred for a further 18 hours. The reaction was then diluted with Et₂O and quenched with conc NH₄Cl slowly (**Important note** – Cyanide gas is generated during this process – make sure to keep nitrogen blowing over the reaction). The reaction was partitioned between Et₂O and H₂O. The aqueous layer was then extracted two times with Et₂O. The combined organic layers were dried over MgSO₄ and concentrated under reduced pressure to give a 10:1 mixture of diastereomers. The crude reaction was purified by flash chromatography (10% EtOAc:90% hexanes) to give the major diastereomer, beta-keto ester **4.40** (571 mg, 0.98 mmol, 70% yield) as an off-white amorphous solid.

$R_f = 0.15$ (20:80 EtOAc:hexanes)

¹H NMR (500 MHz, CDCl₃) δ 8.21 (s, 1H), 7.67 (d, $J = 8.0$ Hz, 1H), 7.37 – 7.28 (m, 2H), 7.23 (t, $J = 7.1$ Hz, 1H), 5.84 (dd, $J = 17.3, 11.1$ Hz, 1H), 5.26 (d, $J = 11.2$ Hz, 1H), 5.16 – 5.09 (m, 1H), 3.73 (s, 3H), 3.61 (dd, $J = 11.3, 4.2$ Hz, 1H), 3.38 (s, 1H), 3.20 (dd, $J = 13.6, 5.6$ Hz, 1H), 1.68 (s, 9H), 1.58 (s, 3H), 1.53 (s, 3H), 1.15 (s, 3H), 0.70 (s, 9H), -0.16 (s, 3H), -0.41 (s, 3H).

¹³C NMR (126 MHz, CDCl₃) δ 203.67, 168.00, 149.70, 135.86, 128.39, 128.24, 124.11, 122.49, 122.17, 120.44, 117.38, 115.75, 83.53, 76.54, 66.07, 53.89, 51.74, 48.91, 36.89, 34.02, 30.33, 28.21, 26.19, 25.70, 25.65, 25.58, 22.71, 17.97, 0.00, -4.91, -5.17.



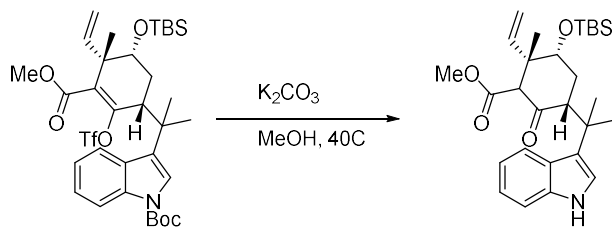
Vinylogous carboxyl triflate 4.41. A 50 mL round-bottomed flask was charged with beta-keto ester **4.40** (120 mg, 0.2 mmol, 1 equiv) and THF (8 mL). NaH (24 mg, 60% by weight, 1 mmol, 5 equiv) was added and the reaction was heated to 60 °C for 30 minutes. The reaction was then cooled back to room temperature, and Comin's reagent (170 mg, 0.5 mmol, 2.5 equiv) was added as a solid in a single portion. The reaction was then warmed back to 60 °C for a further thirty minutes. After conversion had completed, the reaction was cooled back to room temperature, diluted with Et₂O, and quenched with conc NH₄Cl. The reaction was partitioned between Et₂O and H₂O. The aqueous layer was then extracted two times with Et₂O. The combined organic layers were dried over MgSO₄ and concentrated under reduced pressure. The crude reaction was purified by flash chromatography (10% EtOAc:90% hexanes) to give enol triflate **4.41** (127 mg, 0.178 mmol, 89% yield) as a white solid.

$R_f = 0.5$ (20:80 EtOAc:hexanes)

¹H NMR (500 MHz, CDCl₃) δ 8.14 (s, 1H), 7.64 (d, $J = 7.9$ Hz, 1H), 7.38 – 7.29 (m, 2H), 7.27 – 7.21 (m, 1H), 5.83 (dd, $J = 17.8, 10.9$ Hz, 1H), 5.40 – 5.05 (m, 2H), 3.80 (s, 3H), 3.49 (dd, $J = 10.6, 7.5$ Hz, 1H), 3.43 (dd, $J = 12.2, 3.4$ Hz, 1H), 1.71 (s, 9H), 1.68 (s, 3H), 1.44 (s, 3H), 1.33 (s, 3H), 0.70 (s, 9H), -0.10 (s, 3H), -0.37 (s, 3H).

¹⁹F NMR (471 MHz, CDCl₃) δ -73.46.

HRMS Calculated for C₃₄H₄₈F₃NO₈SSi [M+H]⁺: 715.2822. Found: 715.2693.

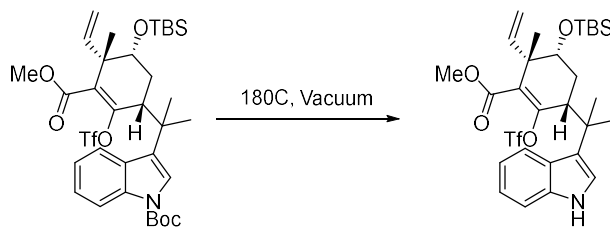


Ketone 4.42. A 25 mL round-bottomed flask was charged with enol triflate **4.41** (20 mg, 0.028 mmol, 1 equiv) and MeOH (1 mL). K_2CO_3 (15 mg, 0.112 mmol, 4 equiv) was added, and the reaction was heated to 40°C. The reaction was stirred for 3 hours, then diluted with 3 mL Et_2O and quenched with 0.2 mL 1M HCl. The reaction was partitioned between Et_2O and H_2O . The aqueous layer was then extracted two times with Et_2O . The combined organic layers were dried over $MgSO_4$ and concentrated under reduced pressure. The crude reaction was purified by preparative TLC (20% $EtOAc$:80% hexanes) to give ketone **4.42** (11.8 mg, 0.024 mmol, 87% yield) as a white solid.

R_f = 0.15 (30:70 $EtOAc$:hexanes)

1H NMR (500 MHz, $CDCl_3$) δ 8.05 (s, 1H), 7.73 (d, J = 8.1 Hz, 1H), 7.41 – 7.34 (m, 1H), 7.18 (q, J = 7.9 Hz, 1H), 7.11 (t, J = 7.6 Hz, 1H), 6.97 (d, J = 2.4 Hz, 1H), 5.86 (dd, J = 17.4, 11.2 Hz, 1H), 5.26 (dd, J = 11.1, 1.4 Hz, 1H), 5.16 – 5.08 (m, 1H), 3.73 (s, 3H), 3.61 (dd, J = 11.3, 4.1 Hz, 1H), 3.42 (s, 1H), 3.27 (dd, J = 13.5, 5.7 Hz, 1H), 1.71 (s, 3H), 1.55 (s, 3H), 1.16 (s, 3H), 0.71 (s, 9H), -0.19 (s, 3H), -0.47 (s, 3H).

^{13}C NMR (126 MHz, $CDCl_3$) δ 204.33, 168.19, 137.32, 136.02, 125.00, 124.48, 121.70, 121.07, 120.32, 119.07, 117.19, 111.58, 76.70, 66.13, 54.71, 51.71, 49.04, 36.83, 34.68, 34.01, 31.61, 29.08, 27.00, 25.70, 25.61, 25.30, 22.72, 22.68, 22.06, 20.72, 17.93, 14.15, 11.46, -4.83, -5.30.



Vinylogous Carboxyl Triflate 4.41. A 25 mL round-bottomed flask was charged with enol triflate **4.41** (20 mg, 0.028 mmol, 1 equiv) as a neat solid. The flask was placed under vacuum (4 mmHg) and warmed to 180 °C. The solid quickly melted and after about 90 seconds began to bubble. Over the next 5 minutes the liquid turned from colorless to pale brown to light purple/brown and bubbling ceased. The reaction was cooled back to RT, giving indole **4.43** (16 mg, .0266 mmol, 98% yield) as a purple/brown solid.

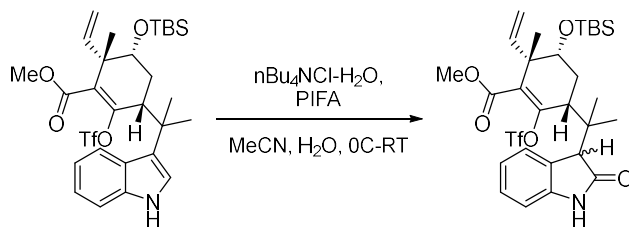
$R_f = 0.5$ (15:85 EtOAc:hexanes)

$^1\text{H NMR}$ (500 MHz, CDCl_3) δ 7.99 – 7.87 (m, 1H), 7.70 (d, $J = 8.0$ Hz, 1H), 7.37 (d, $J = 8.1$ Hz, 1H), 7.20 (t, $J = 7.6$ Hz, 1H), 7.11 (t, $J = 7.5$ Hz, 1H), 6.93 (d, $J = 2.5$ Hz, 1H), 5.78 (dd, $J = 17.7$, 11.0 Hz, 1H), 5.19 – 5.11 (m, 2H), 3.79 (s, 3H), 3.48 (dd, $J = 10.5$, 7.6 Hz, 1H), 3.43 (dd, $J = 12.3$, 3.6 Hz, 1H), 1.72 (s, 3H), 1.45 (s, 3H), 1.32 (s, 3H), 0.70 (s, 9H), -0.12 (s, 3H), -0.39 (s, 3H).

$^{13}\text{C NMR}$ (126 MHz, CDCl_3) δ 165.03, 151.43, 139.64, 137.08, 131.99, 125.47, 124.06, 122.00, 120.40, 120.10, 119.43, 116.86, 111.34, 74.36, 52.13, 48.28, 45.80, 39.55, 32.67, 29.72, 29.02, 28.23, 25.62, 24.33, 24.17, 17.89, -4.68, -5.13.

$^{19}\text{F NMR}$ (470 MHz, CDCl_3) δ -73.43.

HRMS Calculated for $\text{C}_{29}\text{H}_{40}\text{F}_3\text{NO}_6\text{Si}$ $[\text{M}+\text{H}]^+$: 615.2298. Found: 615.2197.



Indolinone 4.44. A 10 mL round-bottomed flask was charged with vinyllogous carboxyl triflate **4.43** (10 mg, 0.016 mmol, 1 equiv) and $n\text{Bu}_4\text{NCl}\cdot\text{H}_2\text{O}$ (4.7 mg, 0.016 mmol, 1 equiv), MeCN (0.15 mL) and H_2O (0.5 mL). The reaction was cooled to 0 °C with an ice bath. PIFA (6.9 mg, 0.016 mmol, 1 equiv) was added as a solid in one portion. The reaction was allowed to warm to room temperature over one hour, then stirred at room temperature for a further three hours. The reaction was then diluted with Et_2O and H_2O , and partitioned into Et_2O and H_2O . The aqueous layer was then extracted two times with Et_2O . The combined organic layers were dried over MgSO_4 and concentrated under reduced pressure. The crude reaction was purified by flash chromatography (10% EtOAc :90% hexanes) to give indolinone **4.44** as a single diastereomer (9 mg, 0.0144 mmol, 90% yield) as a white solid.

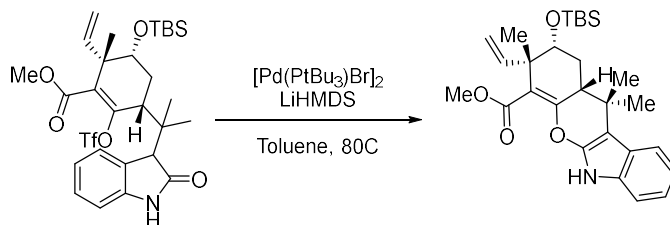
$R_f = 0.3$ (20:80 EtOAc :hexanes)

$^1\text{H NMR}$ (500 MHz, CDCl_3) δ 7.59 (s, 1H), 7.31 (s, 1H), 7.25 (t, $J = 7.8$ Hz, 1H), 7.02 (dd, $J = 8.3, 7.1$ Hz, 1H), 6.85 (d, $J = 7.8$ Hz, 1H), 5.99 (dd, $J = 17.8, 10.9$ Hz, 1H), 5.35 – 5.26 (m, 2H), 3.80 (s, 3H), 3.70 – 3.62 (m, 2H), 3.52 (s, 1H), 2.42 – 2.34 (m, 0H), 1.81 (td, $J = 12.2, 9.9$ Hz, 1H), 1.37 (s, 3H), 1.30 (s, 3H), 0.99 (s, 3H), 0.93 (s, 9H), 0.15 (s, 3H), 0.13 (s, 3H).

$^{13}\text{C NMR}$ (126 MHz, CDCl_3) δ 176.99, 165.09, 150.29, 142.00, 139.38, 133.42, 128.32, 127.11, 126.49, 121.91, 119.43, 117.28, 109.34, 74.27, 52.17, 51.40, 48.15, 44.12, 42.05, 32.01, 25.83, 24.36, 22.79, 18.04, -4.08, -5.01.

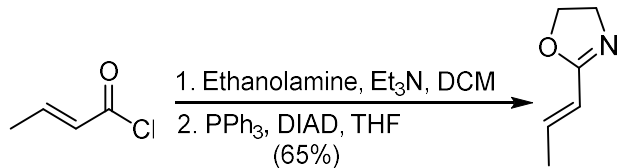
^{19}F NMR (470 MHz, CDCl_3) δ -73.52.

HRMS Calculated for $\text{C}_{29}\text{H}_{40}\text{F}_3\text{NO}_7\text{SSi}$ $[\text{M}+\text{H}]^+$: 631.2247. Found: 631.2132.



Tetracycle 4.46. A 5 mL round-bottomed flask was charged with indolinone **4.44** (5 mg, 0.008 mmol, 1 equiv), $[\text{Pd}(\text{PtBu}_3)\text{Br}]_2$ (1.7 mg, 0.0016 mmol, 0.2 equiv), and toluene (0.2 mL). The atmosphere was removed by vacuum and replaced three times with argon. LiHMDS (0.02 mL, 1 M in THF, 0.02 mmol, 2 equiv) was added, and the atmosphere was again replaced three times with Argon. The reaction was then heated in an oil bath to 60°C for one hour. The reaction was diluted with 2 mL Et_2O and quenched with 2 mL NaHCO_3 . The reaction was partitioned into Et_2O and H_2O . The aqueous layer was then extracted two times with Et_2O . The combined organic layers were dried over MgSO_4 and concentrated under reduced pressure. The crude reaction was purified by preparative chromatography (10% EtOAc :90% hexanes) to give tetracycle **4.9** (2.7 mg, 0.0056 mmol, 70% yield).

6.5 Experimental Details and Characterization Data for Chapter 5



5.17

(E)-2-(prop-1-en-1-yl)-4,5-dihydrooxazole (5.17): A 50 mL recovery flask equipped with a Teflon-coated magnetic stir bar was charged with DCM (20 mL) and crotonyl chloride (2.08 g, 20 mmol, 1 equiv). The resulting solution was cooled to 0 °C by means of an ice-water bath, and a solution of ethanolamine (2.68 g, 44 mmol, 2.2 equiv) in DCM (5 mL) was added dropwise over 20 min. The resulting slurry was allowed to warm to room temperature and stirred at ambient temperature. After 1 hour the slurry was filtered through Celite and the filtrate washed with aq. NaHCO₃ (2x30 mL). The organic phase was separated, dried over Na₂SO₄, and concentrated under reduced pressure to provide crude amide **5.16** (data not given) as an essentially pure liquid, based on ¹H NMR.

The crude amide was then redissolved in THF (4 mL), and treated with PPh₃ (6.0 g, 21 mmol, 1.05 equiv). The mixture was cooled to 0 °C by means of ice-water bath and diisopropyl azodicarboxylate (4.1 mL, 21 mmol, 1.05 equiv) was added dropwise. The resulting dark-red solution was stirred at 0 °C for 15 min, the cold bath was removed, and the mixture was stirred at ambient temperature for 1 hour. The reaction mixture was diluted with Et₂O (30 mL) and placed in a -20 °C freezer for 8 h, during which significant amounts of white precipitate of triphenylphosphine oxide formed. The slurry was filtered through a pad of Celite[®], and the filter cake was washed with 1:1 hexanes:Et₂O mixture. The filtrate was concentrated under the reduced pressure. The resulting slurry was redissolved in 1:1 hexanes:Et₂O (30 mL), filtered through a pad

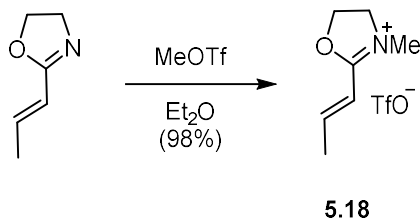
of Celite®, and the solvent evaporated under the reduced pressure. The residue was distilled under reduced pressure in short path distillation to provide the desired oxazoline **5.17** as a colorless oil (1.44g, 13 mmol, 65% yield). Bp = ca. 25 °C at 0.5 torr.

¹H NMR (500 MHz, CDCl₃): δ 6.59 (dq, *J* = 15.8, 7.0 Hz, 1H), 6.01 (d, *J* = 15.8 Hz, 1H), 4.26 (dd, *J* = 14.0, 4.9 Hz, 2H), 3.90 (dd, *J* = 14.0, 4.9 Hz, 2H), 1.87 (d, *J* = 7.0 Hz, 3H).

¹³C NMR (125 MHz, CDCl₃): δ 138.8, 119.0, 66.9, 54.6, 18.2;

IR(Neat film): 3412, 1674, 1644, 1613, 1482, 1444, 1378, 1368, 1000 cm⁻¹;

HRMS (ES) calcd for C₆H₁₀NO [M+H]⁺: 112.0762, found 112.0803



(E)-3-methyl-2-(prop-1-en-1-yl)-4,5-dihydrooxazol-3-ium trifluoromethanesulfonate (5.18)

A 50 mL recovery flask equipped with a Teflon-coated magnetic stir bar was charged with Et₂O (10 mL) and oxazoline **5.17** (1.11g, 10 mmol, 1 equiv). The resulting solution was cooled to -40°C, and MeOTf (1.2 mL, 11 mmol, 1.1 equiv) was added dropwise over 20 min. The resulting slurry was warmed to room temperature and stirred at ambient temperature for 1 h, during which a white crystalline precipitate formed. After 1 hour the solvent was decanted, and the crystals were dried under reduced pressure to provide corresponding triflate salt **5.18** in 98% yield (2.69g), which proved to be essentially pure by ¹H NMR.

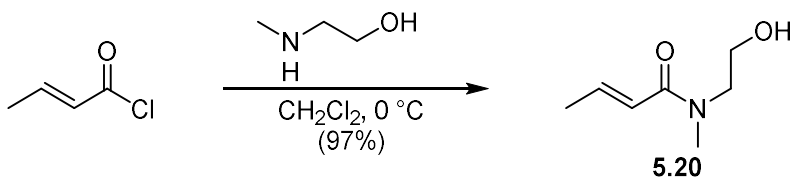
mp = 79-80 °C.

¹H NMR (500 MHz, CDCl₃): δ 7.41 (dq, *J* = 14.0, 7.0 Hz, 1H), 6.34 (d, *J* = 14.0 Hz, 1H), 5.00 (t, *J* = 9.8 Hz, 2H), 4.38 (t, *J* = 9.8 Hz, 2H), 3.46 (s, 3H), 2.14 (dd, *J* = 7.0, 1.5 Hz, 4H).

¹³C NMR (125 MHz, CDCl₃): δ 157.1, 110.3, 70.5, 52.5, 33.9, 19.8;

IR (neat film): 3079, 2956, 1675, 1629, 1481, 1449, 1265, 1156, 1033, 971 cm⁻¹.

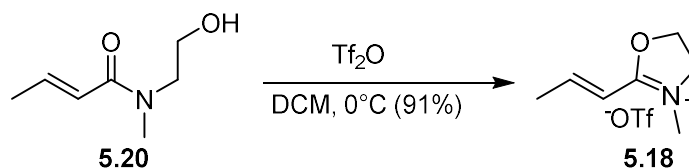
HRMS (ES) calcd for C₇H₁₂NO⁺ [M]⁺: 126.0913, found 126.0910



(E)-N-(2-hydroxyethyl)-N-methylbut-2-enamide (5.20) A 1000 mL round-bottom flask equipped with a Teflon-coated magnetic stir bar was charged with DCM (100 mL) and crotonoyl chloride (10.4 g, 100 mmol, 1 equiv). Resulting solution was cooled to 0°C by means of ice water bath, and a solution of methyl-ethanolamine (16.1 mL, 200 mmol, 2 equiv) in DCM (50 mL) was added dropwise over 10 min. Resulting slurry was allowed to warm to room temperature and stirred at ambient temperature. After 1 hour the reaction was diluted with 250 mL of Et₂O, which caused the ethanolanionium salt to leave solution as a thick oil. The oil was removed by filtration through Celite®, and the filtrate was concentrated under reduced pressure to give crude amide **5.20** (13.8 g, 97%) as a 2:1 mixture of rotamers, essentially pure based on ¹H NMR. Over time the oil turned from clear to yellow, with no apparent loss of purity by NMR. **¹H NMR** (500 MHz, CDCl₃) δ 6.93 (dd, *J* = 14.8, 7.4 Hz, 1H), 6.46 – 6.16 (d, *J* = 15.0, 1H), 3.98 – 3.40 (m, 5H), 3.13 (s, 3H), 1.97 – 1.85 (m, 3H).

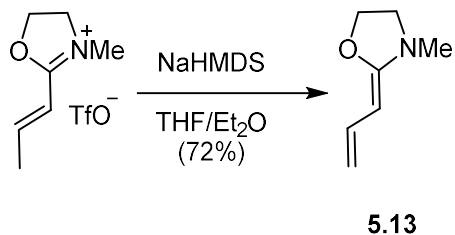
¹³C NMR (126 MHz, CDCl₃) δ 168.7 (Major), 142.7 (Major), 141.5 (Minor), 121.9 (Minor), 121.5 (Major), 61.8 (Major), 60.3 (Minor), 51.9 (Major), 36.8 (Major), 34.3 (Minor), 18.3 (Major).

HRMS (ES) calcd for $C_7H_{13}NO_2$ $[M]^+$: 143.0946, found 143.0945.



(E)-3-methyl-2-(prop-1-en-1-yl)-4,5-dihydrooxazol-3-ium trifluoromethanesulfonate (5.18)

alternative route The crude amide **5.20** was re-dissolved in 400 mL dry DCM and cooled to $0^\circ C$ by means of ice water bath. Triflic anhydride (16.3 mL, 97 mmol, 1 equiv) was added to the solution dropwise, after which the ice water bath was removed, and the mixture was stirred at ambient temperature for 15 minutes. During this time the solution turned from clear to dark red. Following complete conversion by TLC, the solution was concentrated under reduced pressure, then re-dissolved in 10 mL dry acetone. This new solution was slowly added to rapidly stirring Et_2O (300 mL). Crystals of **5.18** rapidly formed, and the solution was cooled to $0^\circ C$ for 15 minutes. The feathery tan crystals were isolated by filtration and washed 2 times with 30 mL cold Et_2O , giving a final yield of 24.3 g (91%). The crystals are lightly hygroscopic, but appear to be completely stable over extended periods open to the atmosphere. Spectroscopic data identical to above.



(Z)-2-allylidene-3-methyloxazolidine (5.13). Triflate salt **15** (6.9 g, 25 mmol, 1 equiv) was suspended in 75 mL of dry Et₂O in a flame dried 250 mL round-bottomed flask. The resulting slurry was cooled to -78°C using a dry ice bath. NaHMDS (27.5 mmol, 1M in THF, 27.5 mL, 1.1 equiv) was added over 20 minutes using a syringe pump, and the reaction was stirred for 2 hours at -78°C. After conversion was complete by NMR, the reaction was stopped by addition of 50 mL of 2M NaOH in H₂O. The organic layer was removed and the aqueous layer was washed 3 times with 50 mL of a 1:1 mixture Et₂O:hexanes. The combined organic layers were dried with MgSO₄, and the solvent was removed under reduced pressure. Excess hexamethyldisilazane was removed by drying under high vacuum at RT, leaving **10** as a pure, lightly yellow oil in 84% yield (2.6g).

¹H NMR (500 MHz, CDCl₃): δ 6.59 (dt, *J* = 17.0, 10.6 Hz, 1H), 4.71 (dd, *J* = 17.0, 2.3 Hz, 1H), 4.43 (dd, *J* = 10.4, 2.3 Hz, 1H), 4.27 – 4.26 (m, 1H), 4.26 – 4.19 (m, 2H), 3.31 (t, *J* = 9.0 Hz, 2H), 2.71 (s, 3H).

¹³C NMR (125 MHz, CDCl₃): δ 132.1, 102.6, 74.2, 65.3, 50.8, 33.3.;

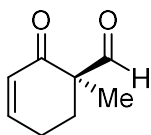
IR(Neat film): 3423, 1635, 1489, 1408, 1266, 1162, 1051 cm⁻¹;

HRMS (ES) calcd for C₇H₁₂NO [M+H]⁺: 126.0919, found 126.0916

**General procedure for the one-pot Diels-Alder reaction between oxazolidine
butadienes and dienophiles and subsequent hydrolysis of the cycloadduct (General
procedure A)**

To a flame-dried 1 dram vial, equipped with a magnetic stir bar and charged with Ar, were added dry benzene (1 mL), followed by corresponding dienophile (0.3 mmol) and diene (0.2 mmol). Resulting solution was heated to 60°C until full conversion of the diene (monitored by ¹H NMR,

typically for 8-16 hours), at which point the mixture was diluted with water (1 mL), and oxalic acid (135 mg, 7.5 equiv) was added to the mixture. Resulting heterogeneous mixture was stirred extensively at 60°C over 6 h, cooled to room temperature and diluted with EtOAc (6 mL). The organic layer was decanted, aqueous layer was washed with EtOAc (2x6 mL), combined organic layers were washed with NaHCO₃ (aq.) (2x4 mL), dried over Na₂SO₄ and concentrated under reduced pressure. The residue was purified by column chromatography (SiO₂, 10-50% EtOAc/hexanes) to afford corresponding cyclohexenones.



5.23a

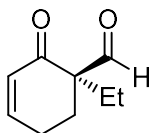
1-methyl-2-oxocyclohex-3-ene-1-carbaldehyde (5.23a). The reaction was performed according to General Procedure A, using diene **5.13** and methacrolein as reaction partners, in a sealed tube. The title compound was obtained as a colorless oil in 70% yield (19 mg) after column chromatography (30% EtOAc/70% Hexanes).

¹H NMR (500 MHz, CDCl₃): δ 9.62 (s, 1H), 7.01 (dt, *J* = 10.1, 4.3 Hz, 1H), 6.27 – 5.94 (m, 1H), 2.62 – 2.46 (m, 1H), 2.44 – 2.24 (m, 2H), 1.96 – 1.73 (m, 1H), 1.32 (s, 3H).

¹³C NMR (125 MHz, CDCl₃): δ 200.4, 150.6, 128.9, 37.2, 29.7, 29.0, 22.9, 17.9;

IR (neat film): 3313, 2924, 1731, 1437, 1375, 1260, 1109, 1022 cm⁻¹.

HRMS (ES) calcd for C₈H₁₁O₂ [M+H]⁺: 139.0759, found 139.0732



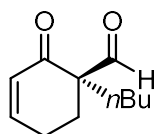
5.23b

1-ethyl-2-oxocyclohex-3-ene-1-carbaldehyde (5.23b). The reaction was performed according to General Procedure A, using diene **5.13** and 2-methylenebutanal as reaction partners in a sealed tube. The title compound was obtained as a colorless oil in 62% yield (19 mg) after column chromatography (30% EtOAc/70% Hexanes).

¹H NMR (400 MHz, CDCl₃) δ 9.63 (d, J = 0.8 Hz, 1H), 6.99 (dt, J = 10.1, 4.0 Hz, 1H), 6.02 (dt, J = 10.1, 2.0 Hz, 1H), 2.58 – 2.36 (m, 2H), 2.29 (ddd, J = 13.9, 6.4, 5.3 Hz, 1H), 1.98 – 1.81 (m, 3H), 0.86 (t, J = 7.5 Hz, 4H).

¹³C NMR (125 MHz, CDCl₃): δ 201.3, 197.7, 150.8, 129.2, 61.4, 24.9, 24.8, 22.8, 8.3,

HRMS (ES) calcd for C₉H₁₂O₂: 152.0837, found 152.0818.



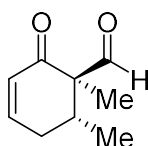
5.23c

1-butyl-2-oxocyclohex-3-ene-1-carbaldehyde (5.23c). The reaction was performed according to General Procedure A, using diene **5.13** and 2-methylenehexanal as reaction partners. The title compound was obtained as a colorless oil in 65% yield (23 mg) after column chromatography (30% EtOAc/70% Hexanes).

¹H NMR (500 MHz, CDCl₃): δ 9.65 (s, 1H), 7.02 – 6.95 (m, 1H), 6.02 (d, *J* = 10.1 Hz, 1H), 2.57 – 2.45 (m, 1H), 2.44 – 2.33 (m, 1H), 2.33 – 2.26 (m, 1H), 2.01 – 1.92 (m, 1H), 1.87 – 1.79 (m, 2H), 1.40 – 1.07 (m, 6H), 0.89 (t, *J* = 7.2 Hz, 3H).

¹³C NMR (125 MHz, CDCl₃): δ. 201.3, 150.6, 129.1, 31.6, 29.2, 26.0, 25.4, 25.0, 23.0, 22.9, 13.8.;

HRMS (ES) calcd for C₁₁H₁₇O₂ [M+H]⁺: 181.1228, found 181.1215



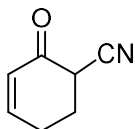
5.23d

1,6-dimethyl-2-oxocyclohex-3-ene-1-carbaldehyde (5.23d). The reaction was performed according to General Procedure A, using diene **5.13** and tiglic aldehyde as reaction partners in a sealed tube. The title compound was obtained as a colorless oil in 40% yield (12 mg) after column chromatography (30% EtOAc/70% Hexanes).

¹H NMR (400 MHz, CDCl₃) δ 9.53 (s, 1H), 6.98 (ddd, *J* = 10.2, 5.3, 3.2 Hz, 1H), 6.05 (ddd, *J* = 10.1, 2.6, 1.5 Hz, 1H), 2.73 – 2.60 (m, 1H), 2.59 – 2.46 (m, 1H), 2.29 – 2.13 (m, 1H), 1.18 (s, 3H), 0.93 (d, *J* = 6.9 Hz, 3H).

¹³C NMR (101 MHz, CDCl₃) δ 200.4, 180.7, 149.7, 128.2, 77.2, 32.2, 30.9, 15.2, 10.9.

HRMS (ES) calcd for C₉H₁₂O₂ [M]⁺: 152.0837, found 152.0838.



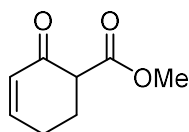
5.23f

2-oxocyclohex-3-ene-1-carbonitrile (5.23f). The reaction was performed according to General Procedure A, using diene **5.13** and acrylonitrile as reaction partners. The title compound was obtained as a colorless oil in 75% yield (18 mg) after column chromatography (30% EtOAc/70% Hexanes).

¹H NMR (500 MHz, CDCl₃): δ 7.09 (dddd, *J* = 10.2, 4.8, 3.2, 0.9 Hz, 1H), 6.15 (dt, *J* = 10.5, 2.0 Hz, 1H), 3.56 (dd, *J* = 11.1, 4.4 Hz, 1H), 2.67 – 2.56 (m, 1H), 2.48 (qdd, *J* = 9.3, 6.8, 3.8 Hz, 2H), 2.41 – 2.30 (m, 1H).

¹³C NMR (125 MHz, CDCl₃): δ. 188.0, 151.0, 128.1, 39.6, 26.9, 24.4.;

HRMS (ES) calcd for C₇H₇NO [M]⁺: 121.0528, found 121.0515



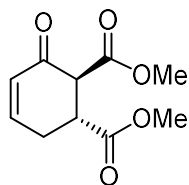
5.23g

Methyl 2-oxocyclohex-3-ene-1-carboxylate (5.23g). The reaction was performed according to General Procedure A, using diene **5.13** and methyl acrylate as reaction partners. The title compound was obtained as a colorless oil in 63% yield (19 mg) as a 6:1 keto:enol mixture after column chromatography (30% EtOAc/70% Hexanes).

¹H NMR (500 MHz, CDCl₃): δ 7.05 – 6.97 (m, 1H), 6.08 (dt, *J* = 10.2, 2.0 Hz, 1H), 3.76 (s, 3H), 3.48 – 3.39 (m, 1H), 2.46 – 2.33 (m, 3H), 2.28 – 2.07 (m, 1H).

^{13}C NMR (125 MHz, CDCl_3): δ . 193.9, 170.5, 150.8, 129.1, 53.3, 52.4, 25.6, 24.3;

HRMS (ES) calcd for $\text{C}_8\text{H}_9\text{O}_3$ $[\text{M}]^+$: 153.0551, found 153.0568



5.23h

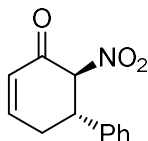
Dimethyl 3-oxocyclohex-4-ene-1,2-dicarboxylate (5.23h). The reaction was performed according to General Procedure A, using diene **5.13** and dimethyl fumarate as reaction partners. The title compound was obtained as a colorless oil in 72% yield (30 mg) as a 4:1 keto:enol mixture after column chromatography (30% EtOAc/70% Hexanes).

^1H NMR (500 MHz, CDCl_3): δ 6.97 (ddd, $J = 10.1, 5.4, 2.9$ Hz, 1H), 6.12 (ddd, $J = 10.1, 2.7, 1.5$ Hz, 1H), 3.81 (s, 3H), 3.77 (d, $J = 9.8$ Hz, 2H), 3.73 (s, 3H), 3.71 (d, $J = 2.5$ Hz, 2H), 3.51 (ddd, $J = 11.4, 10.1, 5.3$ Hz, 1H), 2.85 (dtd, $J = 19.1, 5.3, 1.5$ Hz, 1H), 2.58 (ddt, $J = 19.2, 10.1, 2.8$ Hz, 1H).

^{13}C NMR (125 MHz, CDCl_3): δ . 192.2, 172.5, 169.6, 149.4, 147.7, 129.1, 128.5, 55.1, 53.8, 52.7, 52.6, 52.6, 52.4, 42.1, 41.2, 27.7, 25.7;

IR (neat film): 2917, 2849, 1734, 1684, 1559, 1540, 1457 cm^{-1} .

HRMS (ES) calcd for $\text{C}_{10}\text{H}_{12}\text{O}_5$ $[\text{M}]^+$: 212.0685, found 212.0692



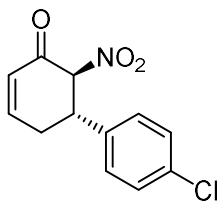
5.26a

2-nitro-1,6-dihydro-[1,1'-biphenyl]-3(2H)-one (5.26a). The reaction was performed according to General Procedure A, using diene **5.13** and β -nitrostyrene as reaction partners. The title compound was obtained as a yellowish solid in 75% yield (32 mg) after column chromatography (30% EtOAc/70% Hexanes).

$^1\text{H NMR}$ (500 MHz, CDCl_3): δ 7.36 (tt, $J = 8.1, 1.8$ Hz, 2H), 7.33 – 7.27 (m, 3H), 7.19 – 7.12 (m, 1H), 6.28 (ddd, $J = 10.1, 2.8, 1.0$ Hz, 1H), 5.64 (d, $J = 13.5$ Hz, 1H), 4.03 (ddd, $J = 13.5, 11.2, 5.3$ Hz, 1H), 2.86 (dtd, $J = 19.5, 5.6, 1.1$ Hz, 1H), 2.81 – 2.77 (m, 1H).

$^{13}\text{C NMR}$ (125 MHz, CDCl_3): δ 150.2, 129.3, 128.5, 127.9, 127.1, 94.5, 45.5, 33.6;

HRMS (ES) calcd for $\text{C}_{12}\text{H}_{11}\text{NO}_3$ $[\text{M}]^+$: 217.0738, found 217.0705



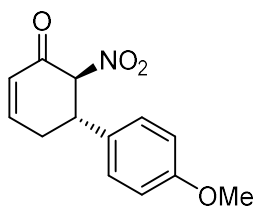
5.26b

4'-chloro-2-nitro-1,6-dihydro-[1,1'-biphenyl]-3(2H)-one (5.26b). The reaction was performed according to General Procedure A, using diene **5.13** and (E)-1-chloro-4-(2-nitrovinyl)benzene as reaction partners. The title compound was obtained as a yellowish solid in 70% yield (35 mg) after column chromatography (30% EtOAc/70% Hexanes).

¹H NMR (500 MHz, CDCl₃) δ 7.38 – 7.33 (m, 1H), 7.26 – 7.22 (m, 1H), 7.19 – 7.13 (m, 0H), 6.30 (ddd, J = 10.2, 2.9, 1.1 Hz, 0H), 5.58 (d, J = 13.4 Hz, 0H), 4.03 (ddd, J = 13.4, 11.2, 5.3 Hz, 1H), 2.91 – 2.81 (m, 0H), 2.80 – 2.69 (m, 0H).

¹³C NMR (101 MHz, CDCl₃) δ 186.3, 150.1, 135.8, 134.5, 129.5, 128.5, 128.0, 94.3, 44.9, 33.4.

HRMS (ES) calcd for C₁₂H₁₀ClNO₃ [M]⁺: 252.0427, found 252.0440



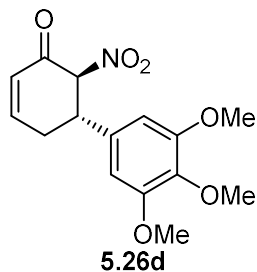
5.26c

4'-methoxy-2-nitro-1,6-dihydro-[1,1'-biphenyl]-3(2H)-one (5.26c). The reaction was performed according to General Procedure A, using diene **5.13** and (E)-1,2,3-trimethoxy-5-(2-nitrovinyl)benzene as reaction partners. The title compound was obtained as a yellow solid in 61% yield (31 mg) after column chromatography (30% EtOAc/70% Hexanes).

¹H NMR (400 MHz, CDCl₃) δ 7.25 – 7.18 (m, 2H), 7.18 – 7.09 (m, 1H), 6.93 – 6.78 (m, 2H), 6.27 (ddd, J = 10.0, 2.8, 1.1 Hz, 1H), 5.56 (d, J = 13.5 Hz, 1H), 3.97 (ddd, J = 13.4, 11.0, 5.5 Hz, 1H), 3.79 (s, 2H), 2.90 – 2.66 (m, 2H).

¹³C NMR (101 MHz, CDCl₃) δ 186.8, 159.5, 150.5, 129.4, 128.2, 127.9, 114.6, 94.9, 55.3, 44.9, 33.7.

HRMS (ES) calcd for C₁₃H₁₃NO₄ [M]⁺: 247.0845, found 247.0855

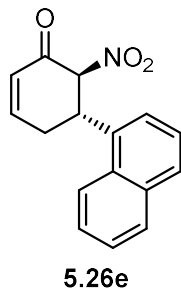


3',4',5'-trimethoxy-2-nitro-1,6-dihydro-[1,1'-biphenyl]-3(2H)-one (5.26d). The reaction was performed according to General Procedure A, using diene **5.13** and (E)-1,2,3-trimethoxy-5-(2-nitrovinyl)benzene as reaction partners. The title compound was obtained as a yellow solid in 53% yield (33 mg) after column chromatography (30% EtOAc/70% Hexanes).

¹H NMR (400 MHz, CDCl₃) δ 7.17 (ddd, J = 10.2, 5.8, 2.3 Hz, 1H), 6.49 (s, 2H), 6.30 (ddd, J = 10.0, 2.9, 1.0 Hz, 1H), 5.64 (d, J = 13.5 Hz, 1H), 4.18 – 3.91 (m, 1H), 3.87 (s, 6H), 3.84 (s, 3H), 2.96 – 2.85 (m, 1H), 2.84 – 2.69 (m, 1H).

¹³C NMR (101 MHz, CDCl₃) δ 186.6, 150.3, 138.0, 133.0, 127.8, 104.2, 94.5, 60.8, 56.2, 45.8, 33.7.

HRMS (ES) calcd for C₁₅H₁₇NO₆ [M]⁺: 307.1056, found 307.1045.



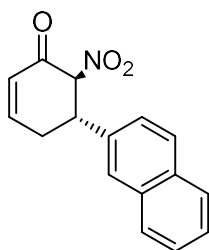
5-(naphthalen-1-yl)-6-nitrocyclohex-2-en-1-one (5.26e). The reaction was performed according to General Procedure A, using diene **5.13** and (E)-1-(2-nitrovinyl)naphthalene as reaction partners.

The title compound was obtained as a brown solid in 71% yield (39 mg) after column chromatography (30% EtOAc/70% Hexanes).

¹H NMR (400 MHz, CDCl₃) δ 8.12 (d, J = 8.5 Hz, 1H), 7.89 (dd, J = 8.0, 1.5 Hz, 1H), 7.81 (dd, J = 6.6, 2.8 Hz, 1H), 7.64 – 7.37 (m, 4H), 7.18 (ddd, J = 10.1, 5.8, 2.3 Hz, 1H), 6.35 (ddd, J = 10.1, 2.9, 1.1 Hz, 1H), 5.96 (d, J = 13.2 Hz, 1H), 5.00 (s, 1H), 3.11 – 2.99 (m, 1H), 2.85 – 2.56 (m, 1H).

¹³C NMR (126 MHz, CDCl₃) δ 187.2, 158.5, 150.4, 134.3, 130.9, 129.3, 128.9, 127.91, 127.0, 126.2, 125.4, 122.7, 122.0, 93.4, 60.4, 34.0;

HRMS (ES) calcd for C₁₆H₁₃NO₃ [M+H]⁺: 268.0973, found 268.0960



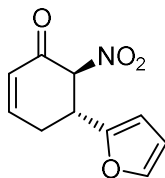
5.26f

5-(naphthalen-2-yl)-6-nitrocyclohex-2-en-1-one (5.26f). The reaction was performed according to General Procedure A, using diene **5.13** and (E)-2-(2-nitrovinyl)naphthalene as reaction partners. The title compound was obtained as a yellow solid in 75% yield (40 mg) after column chromatography (30% EtOAc/70% Hexanes).

¹H NMR (500 MHz, CDCl₃) δ 7.96 – 7.79 (m, 3H), 7.75 (d, J = 1.9 Hz, 1H), 7.61 – 7.46 (m, 2H), 7.41 (dd, J = 8.4, 2.0 Hz, 1H), 7.23 – 7.15 (m, 1H), 6.32 (ddd, J = 10.1, 2.7, 1.3 Hz, 1H), 5.77 (d, J = 13.5 Hz, 1H), 4.21 (ddd, J = 13.5, 10.6, 6.0 Hz, 1H), 3.13 – 2.65 (m, 3H).

^{13}C NMR (101 MHz, CDCl_3) δ 186.7, 150.4, 134.7, 133.4, 133.1, 129.3, 127.9, 127.9, 127.8, 126.7, 126.7, 126.6, 124.2, 94.4, 45.7, 33.6.

HRMS (ES) calcd for $\text{C}_{16}\text{H}_{13}\text{NO}_3$ $[\text{M}]^+$: 268.0973, found 268.0950



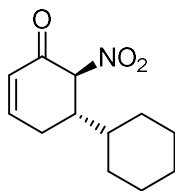
5.26g

5-(furan-2-yl)-6-nitrocyclohex-2-en-1-one (5.26g). The reaction was performed according to General Procedure A, using diene **5.13** and (E)-2-(2-nitrovinyl)furan as reaction partners. The title compound was obtained as a yellow solid in 83% yield (34 mg) after column chromatography (30% EtOAc/70% Hexanes).

^1H NMR (500 MHz, CDCl_3) δ 7.38 (d, $J = 1.9$ Hz, 1H), 7.16 (ddd, $J = 10.1, 5.2, 3.1$ Hz, 1H), 6.32 (dd, $J = 3.3, 1.9$ Hz, 1H), 6.30 – 6.24 (m, 1H), 6.22 (d, $J = 3.3$ Hz, 1H), 5.56 (d, $J = 12.9$ Hz, 1H), 4.19 (ddd, $J = 12.9, 9.7, 6.6$ Hz, 1H), 2.99 – 2.84 (m, 2H).

^{13}C NMR (126 MHz, CDCl_3) δ 186.0, 150.3, 150.1, 142.8, 127.9, 110.6, 107.9, 92.6, 38.9, 30.2;

HRMS (ES) calcd for $\text{C}_{10}\text{H}_{10}\text{NO}_4$ $[\text{M}+\text{H}]^+$: 208.0609, found 208.0635



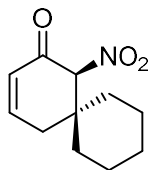
5.26h

2-nitro-[1,1'-bi(cyclohexan)]-4-en-3-one (5.26h). The reaction was performed according to General Procedure A, using diene **5.13** and (E)-(2-nitrovinyl)cyclohexane as reaction partners. The title compound was obtained as a yellow solid in 90% yield (40 mg) after column chromatography (30% EtOAc/70% Hexanes).

¹H NMR (500 MHz, CDCl₃): δ 7.13 (ddd, *J* = 9.7, 6.0, 2.3 Hz, 1H), 6.17 (dd, *J* = 10.0, 1.9 Hz, 1H), 5.31 (d, *J* = 13.2 Hz, 1H), 2.88 – 2.78 (m, 1H), 2.59 (dt, *J* = 19.3, 5.4 Hz, 1H), 2.37 (ddt, *J* = 19.3, 11.1, 2.6 Hz, 1H), 1.84 – 1.75 (m, 3H), 1.70 (d, *J* = 12.2 Hz, 3H), 1.60 – 1.53 (m, 1H), 1.39 (ddd, *J* = 11.9, 7.4, 3.0 Hz, 2H), 1.34 – 1.04 (m, 9H).

¹³C NMR (125 MHz, CDCl₃): δ. 151.2, 127.6, 92.9, 44.1, 38.2, 30.6, 26.8, 26.5, 26.3, 26.2, 25.7.;

HRMS (ES) calcd for C₁₂H₁₇NO₃ [M+H]⁺: 224.1286, found 224.1260



5.26i

1-nitrospiro[5.5]undec-3-en-2-one (5.26i). The reaction was performed according to General Procedure A, using diene **5.13** and (E)-(2-nitrovinyl)cyclohexane as reaction partners. The title

compound was obtained as a yellow solid in 78% yield (32 mg) after column chromatography (30% EtOAc/70% Hexanes).

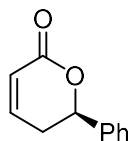
$^1\text{H NMR}$ (500 MHz, CDCl_3): δ 7.07 (ddd, $J = 10.2, 5.4, 3.1$ Hz, 1H), 6.27 – 6.15 (m, 1H), 5.03 (s, 1H), 2.68 (dt, $J = 19.6, 2.8$ Hz, 1H), 2.42 (dd, $J = 19.6, 4.6$ Hz, 1H), 1.64 (ddd, $J = 13.8, 8.6, 3.4$ Hz, 2H), 1.61 – 1.39 (m, 10H).

$^{13}\text{C NMR}$ (125 MHz, CDCl_3): δ . 150.4, 127.0, 40.2, 33.4, 32.8, 25.4, 21.1, 20.8;

HRMS (ES) calcd for $\text{C}_{11}\text{H}_{16}\text{NO}_3$ $[\text{M}+\text{H}]^+$: 210.1130, found 210.1168

General procedure for the one-pot Hetero Diels-Alder reaction between (Z)-2-allylidene-3-methyloxazolidine (10) and aldehydes and subsequent hydrolysis of the cycloadduct (General procedure B)

To a flame-dried 1 dram vial, equipped with a magnetic stir bar and charged with Ar, were added dry toluene (1 mL), followed by diene **5.13** (25 mg, 0.2 mmol). The corresponding aldehyde was washed over Na_2CO_3 , then added to the reaction (0.3 mmol). Resulting solution was heated to 60°C until full conversion of the diene (monitored by $^1\text{H NMR}$, typically for 16-24 hours), at which point the mixture was diluted with water (1 mL), and oxalic acid (135 mg, 7.5 equiv) was added to the mixture. Resulting heterogeneous mixture was stirred extensively at 60°C over 6 h, cooled to room temperature and diluted with EtOAc (6 mL). The organic layer was decanted, aqueous layer was washed with EtOAc (2x6 mL), combined organic layers were washed with NaHCO_3 (aq.) (2x4 mL), dried over Na_2SO_4 and concentrated under reduced pressure. The residue was purified by column chromatography (SiO_2 , 10-50% EtOAc/hexanes) to afford corresponding cyclohexenones.



5.29a

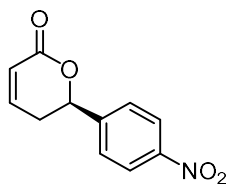
6-phenyl-5,6-dihydro-2H-pyran-2-one (5.29a). The reaction was performed according to General Procedure B, using benzaldehyde as reaction partner. The title compound was obtained as a yellow solid in 70% yield (24 mg) after column chromatography (30% EtOAc/70% Hexanes).

¹H NMR (500 MHz, CDCl₃): 7.47 – 7.32 (m, 4H), 6.98 (ddd, *J* = 9.6, 5.6, 2.8 Hz, 1H), 6.22 – 6.09 (m, 1H), 5.46 (dd, *J* = 11.3, 4.6 Hz, 1H), 2.76 – 2.49 (m, 2H).

¹³C NMR (126 MHz, CDCl₃) δ 144.7, 138.5, 128.7, 128.6, 126.0, 121.8, 79.2, 31.7.

IR (neat film): 3853, 3743, 2361, 2336, 1773, 1717, 1699, 1684, 1652, 1635, 1575, 1558, 1521, 1506, 1456 cm⁻¹.

HRMS (ES) calcd for C₁₁H₁₁O₂ [M+H]⁺: 175.0759, found 175.0740



5.29b

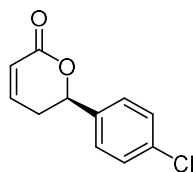
6-(4-nitrophenyl)-5,6-dihydro-2H-pyran-2-one (5.29b). The reaction was performed according to General Procedure B, using 4-nitrobenzaldehyde as reaction partner. The title compound was

obtained as a yellow solid in 82% yield (35 mg) after column chromatography (30% EtOAc/70% Hexanes).

$^1\text{H NMR}$ (500 MHz, CDCl_3): 8.29 (d, $J = 8.7$ Hz, 2H), 7.64 (d, $J = 8.9$ Hz, 2H), 7.02 (ddd, $J = 9.6, 5.9, 2.5$ Hz, 1H), 6.28 – 6.11 (m, 1H), 5.60 (dd, $J = 11.8, 4.3$ Hz, 1H), 2.82 – 2.53 (m, 2H).

$^{13}\text{C NMR}$ (126 MHz, CDCl_3) δ 145.4, 144.2, 126.7, 124.0, 121.9, 77.8, 31.5.

HRMS (ES) calcd for $\text{C}_{11}\text{H}_{10}\text{NO}_4$ $[\text{M}+\text{H}]^+$: 220.0609, found 220.0618



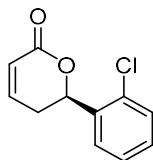
5.29c

6-(4-chlorophenyl)-5,6-dihydro-2H-pyran-2-one (5.29c). The reaction was performed according to General Procedure B, using 4-chlorobenzaldehyde as reaction partner. The title compound was obtained as a yellow solid in 82% yield (34 mg) after column chromatography (30% EtOAc/70% Hexanes).

$^1\text{H NMR}$ (500 MHz, CDCl_3) δ 7.43 – 7.33 (m, 4H), 7.03 – 6.94 (m, 1H), 6.16 (dt, $J = 9.8, 1.8$ Hz, 1H), 5.45 (dd, $J = 9.3, 6.7$ Hz, 1H), 2.70 – 2.57 (m, 2H).

$^{13}\text{C NMR}$ (101 MHz, CDCl_3) δ 163.8, 144.7, 137.0, 134.5, 128.9, 127.4, 121.7, 78.5, 31.6.

HRMS (ES) calcd for $\text{C}_{11}\text{H}_{10}\text{ClO}_2$ $[\text{M}+\text{H}]^+$: 209.0369, found 209.0360



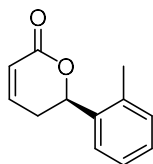
5.29d

6-(2-chlorophenyl)-5,6-dihydro-2H-pyran-2-one (5.29d). The reaction was performed according to General Procedure B, using 4-chlorobenzaldehyde as reaction partner. The title compound was obtained as a yellow solid in 70% yield (34 mg) after column chromatography (30% EtOAc/70% Hexanes).

¹H NMR (500 MHz, CDCl₃) δ 7.68 (dd, J = 7.8, 1.7 Hz, 1H), 7.43 – 7.34 (m, 2H), 7.34 – 7.26 (m, 1H), 7.01 (ddd, J = 9.8, 6.2, 2.2 Hz, 1H), 6.18 (ddd, J = 9.7, 2.8, 0.9 Hz, 1H), 5.86 (dd, J = 12.2, 3.8 Hz, 1H), 2.88 – 2.78 (m, 1H), 2.54 – 2.43 (m, 1H).

¹³C NMR (126 MHz, CDCl₃) δ 163.9, 145.0, 136.4, 131.3, 129.6, 127.6, 127.4, 121.5, 76.1, 30.3.

HRMS (ES) calcd for C₁₁H₁₀ClO₂ [M+H]⁺: 209.0369, found 209.0360



5.29e

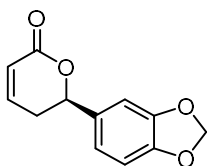
6-(o-tolyl)-5,6-dihydro-2H-pyran-2-one (5.29e). The reaction was performed according to General Procedure B, using 2-methylbenzaldehyde as reaction partner. The title compound was obtained as a yellow solid in 78% yield (29 mg) after column chromatography (30% EtOAc/70% Hexanes).

¹H NMR (500 MHz, CDCl₃): 7.29 (d, *J* = 7.6 Hz, 2H), 7.18 (t, *J* = 8.3 Hz, 2H), 7.02 – 6.90 (m, 1H), 6.15 (ddd, *J* = 9.8, 2.5, 1.1 Hz, 1H), 5.43 (dd, *J* = 11.2, 4.8 Hz, 1H), 2.68 – 2.60 (m, 2H), 2.38 (s, 3H).

¹³C NMR (126 MHz, CDCl₃) δ 144.9, 129.4, 128.55, 126.7, 123.1, 121.7, 79.3, 31.7, 21.5.

IR (neat film): 3744, 2916, 2360, 1718, 1653, 1558, 1506, 1457, 1382, 1241, 1063 cm⁻¹.

HRMS (ES) calcd for C₁₂H₁₃O₂ [M+H]⁺: 189.0916, found 189.0965



5.29f

6-(benzo[d][1,3]dioxol-5-yl)-5,6-dihydro-2H-pyran-2-one (5.29f). The reaction was performed according to General Procedure B, using piperonal as reaction partner. The reaction was slow, taking 6 days at 60°C. The title compound was obtained as a yellow solid in 82% yield (37 mg) after column chromatography (30% EtOAc/70% Hexanes).

¹H NMR (500 MHz, CDCl₃) δ 6.98 (ddd, *J* = 9.7, 6.0, 2.4 Hz, 1H), 6.96 – 6.78 (m, 3H), 6.15 (ddd, *J* = 9.8, 2.7, 1.0 Hz, 1H), 6.02 – 5.99 (m, 2H), 5.38 (dd, *J* = 11.9, 4.1 Hz, 1H), 2.72 – 2.53 (m, 2H).

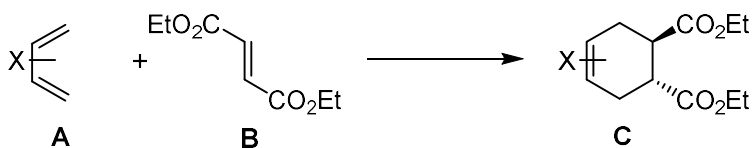
¹³C NMR (126 MHz, CDCl₃) δ 164.1, 148.0, 147.9, 144.8, 132.3, 121.7, 120.0, 108.3, 106.8, 101.3, 79.2, 31.7.

HRMS (ES) calcd for C₁₂H₁₁O₄ [M+H]⁺: 219.0657, found 219.0642.

Kinetic experiments

General Procedure.

To an oven-dried NMR tube was added a solution of diene (0.2 mmol) and tri-methoxybenzene (0.066 mmol, used as a standard) in 1 mL C₆D₆ or CDCl₃. The atmosphere was flushed with nitrogen and the tube was closed. A single scan was taken at the reaction temperature, then the tube was removed from the NMR. The contents of the tube were combined with diethyl fumarate (0.6 mmol) and returned to the tube. The atmosphere was again flushed with nitrogen, and the tube was sealed and returned to the NMR. The tube was heated to the reaction temperature and spun to induce mixing, and a single scan was taken every 5 minutes for 2 hours.



The concentration of diene, diethyl fumarate, and product were measured over time (See Figure 6.1). The initial concentrations of diene and diethyl fumarate were designated $[A]_0$ and $[B]_0$ respectively, and the concentration of product was designated $[C]_t$. For the irreversible reaction of the type listed above:

$$\frac{d[C]}{dt} = -\frac{d[B]}{dt} = k[A][B]$$

Solving this second order reaction in terms of $[A]_0$ and $[B]_0$ gives us the time-dependent concentration of **B** and **C**, as follows.

$$[B]_t = \frac{([A]_0 - [B]_0)[B]_0}{[A]_0 e^{k([A]_0 - [B]_0)t} - [B]_0}$$

$$[C]_t = [B]_0 - \frac{([A]_0 - [B]_0)[B]_0}{[A]_0 e^{k([A]_0 - [B]_0)t} - [B]_0}$$

Although in theory these two equations should lead to the same k values, the presence or absence of side reactions can lead to slight deviations. We opted to use the product concentration, that is $[C]$ in order to minimize these effects. Protons were chosen to avoid overlap with other signals in the NMR spectrum and were as indicated below.

Figure 6.1: The concentrations of the products of the three reactions were measured over time.

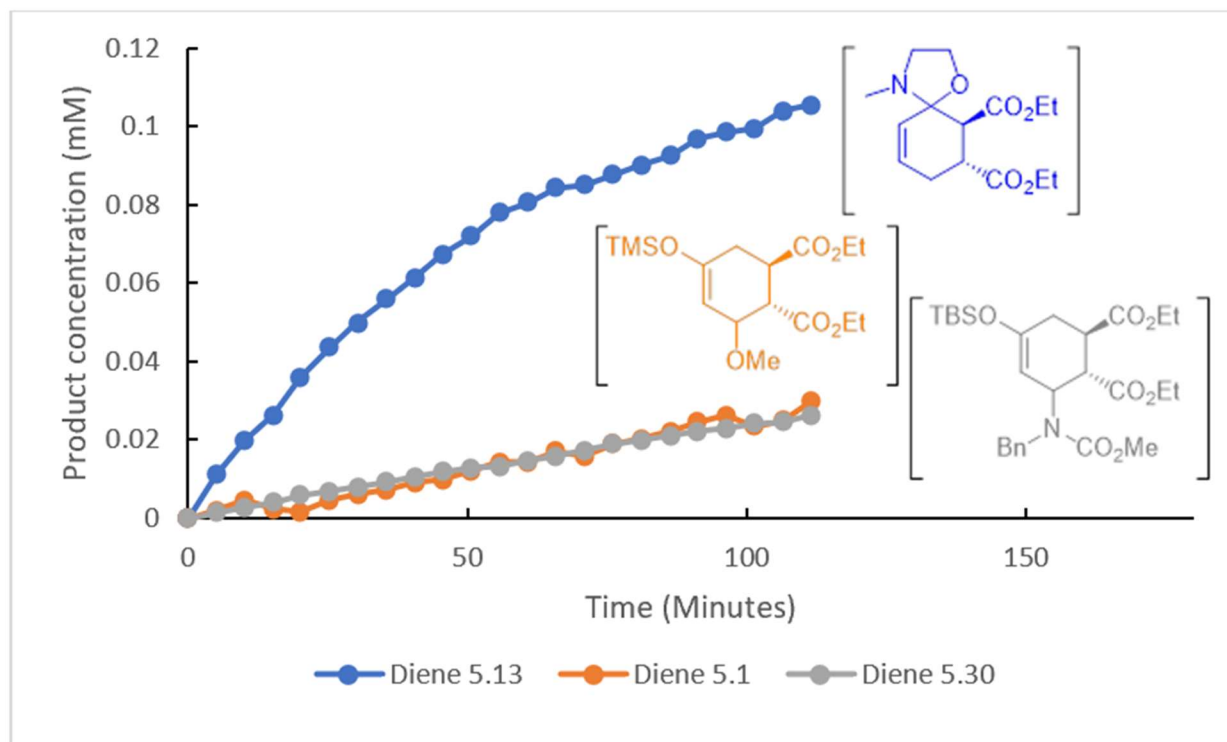
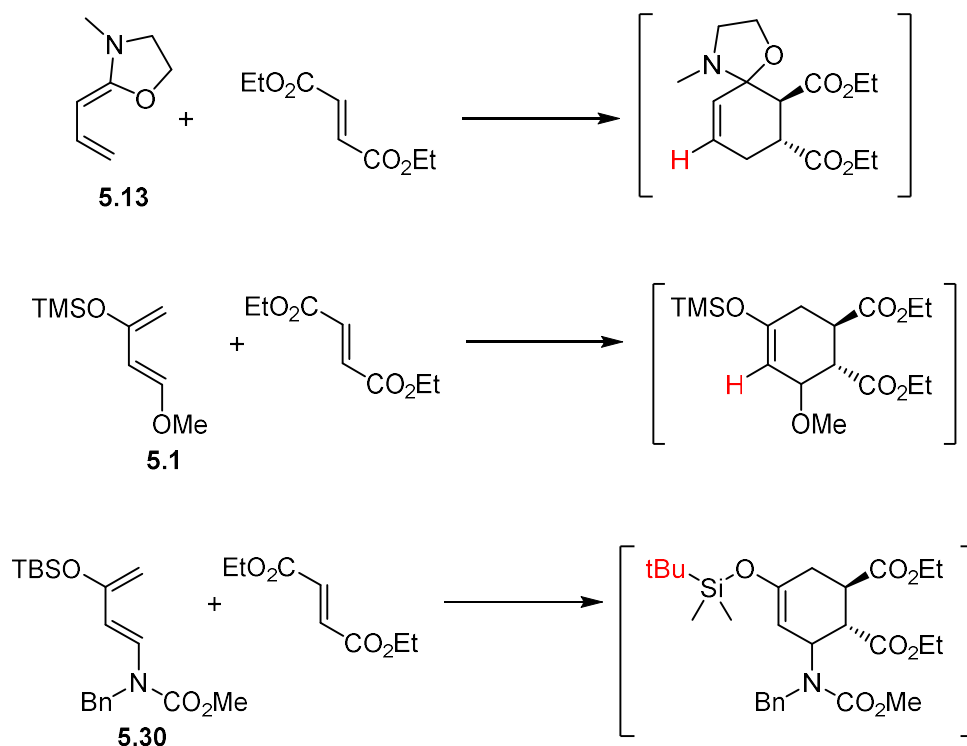


Figure 6.2: Protons indicated in red were used to measure the concentrations of products



The equation above was fit to the data obtained, giving the second order rate constant k (Table 6.2).

Table 6.2 Rate constants for the some highly-reactive dienes at different temperatures

Diene	Solvent	Temperature (°C)	k ($\text{mol}^{-1} \text{s}^{-1}$)
5.30	C_6D_6	60	3.5×10^{-5}
5.30	CDCl_3	60	7.8×10^{-5}
5.1	C_6D_6	50	1.5×10^{-5}
5.1	C_6D_6	60	4.1×10^{-5}
5.1	CDCl_3	60	7.7×10^{-5}
5.1	C_6D_6	70	7.8×10^{-5}

Table 6.2 continuation

5.13	C ₆ D ₆	40	8.3 x 10 ⁻⁵
5.13	C ₆ D ₆	50	1.5 x 10 ⁻⁴
5.13	C ₆ D ₆	60	2.6 x 10 ⁻⁴
5.13	CDCl ₃	60	5.0 x 10 ⁻⁴

To obtain the activation energy (E_a) and frequency factor ($\ln A$) of the reactions of dienes **5.1** and **5.13** with diethyl fumarate, the natural log of the rate ($\ln k$) was plotted against the inverse of the temperature. A linear fit gives $\ln A$ as the interception, and E_a as the slope multiplied by the gas constant. ΔG^\ddagger was calculated from the k values at 50 °C, and ΔH^\ddagger was derived from the slope of the plot $\ln(k/T)$ vs $1/T$. ΔS^\ddagger was then obtained from the relationship $\Delta G^\ddagger = \Delta H^\ddagger - T\Delta S^\ddagger$ at 50°C (Table 6.3).

Table 6.3 Kinetic information of diene **5.1** and **5.13**

(a) Measured in kcal mol⁻¹. (b) Measured in cal mol⁻¹ K⁻¹.

<i>Diene</i>	<i>ln A</i>	<i>E_a^a</i>	<i>ΔG[‡]</i>	<i>ΔH^{‡a}</i>	<i>ΔS^{‡b}</i>
5.1	17.	18.5	27.	19.1	-21.3
	8		2		
5.13	9.5	11.7	24.	12.4	-37.6

5

The derived values for $\ln A$ and E_a were used to create an extrapolated Arrhenius' plot over a larger temperature range (Figure 6.3). This indicates that the rate difference between the two dienes is

expected to increase as temperatures decrease. While at 60°C the rate difference is approximately 7x, this difference would increase to 50x at 7°C. Conversely, as the temperature goes up to 140 °C the rate difference would disappear. Above 140°C, diene **5.1** is expected to react faster.

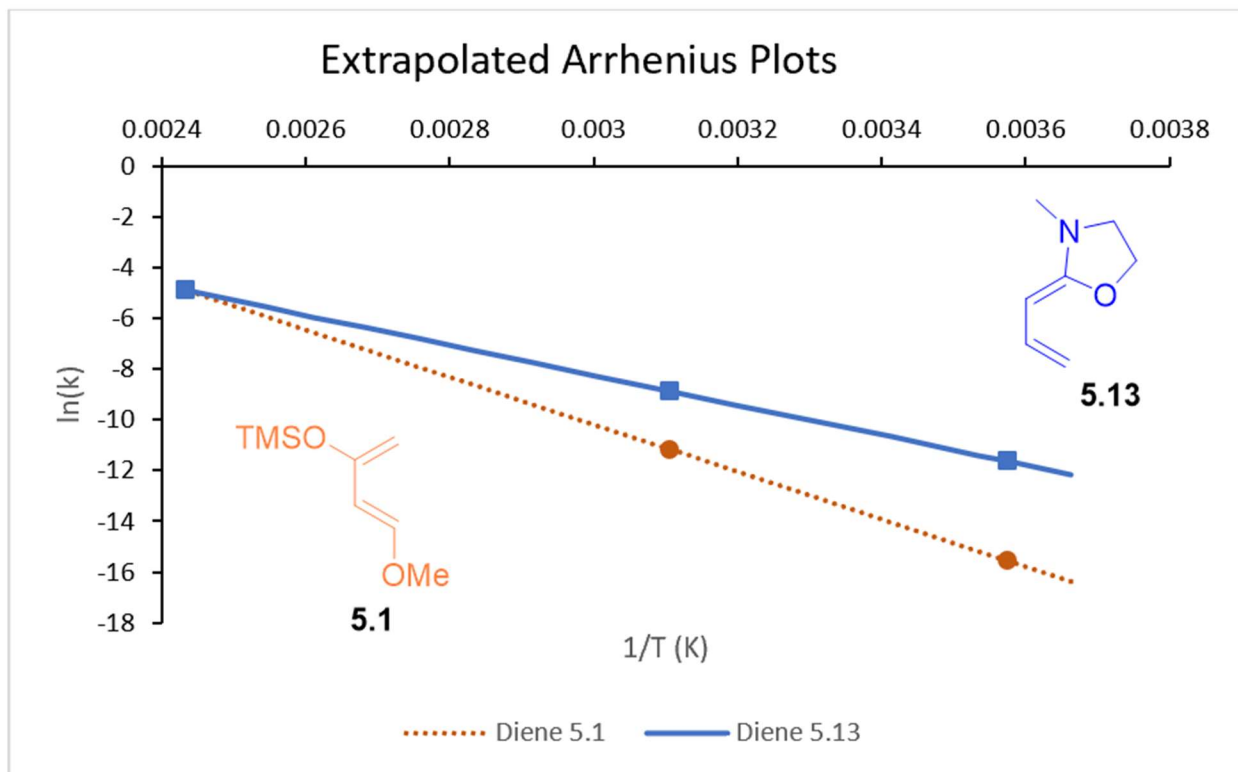


Figure 6.3: Extrapolated Arrhenius Plots of the Diels-Alder reactions of dienes **1** and **10** with diethyl fumarate in toluene.

Chapter 7: Selected ^1H , ^{13}C , ^{19}F , and 2D NMR Spectra

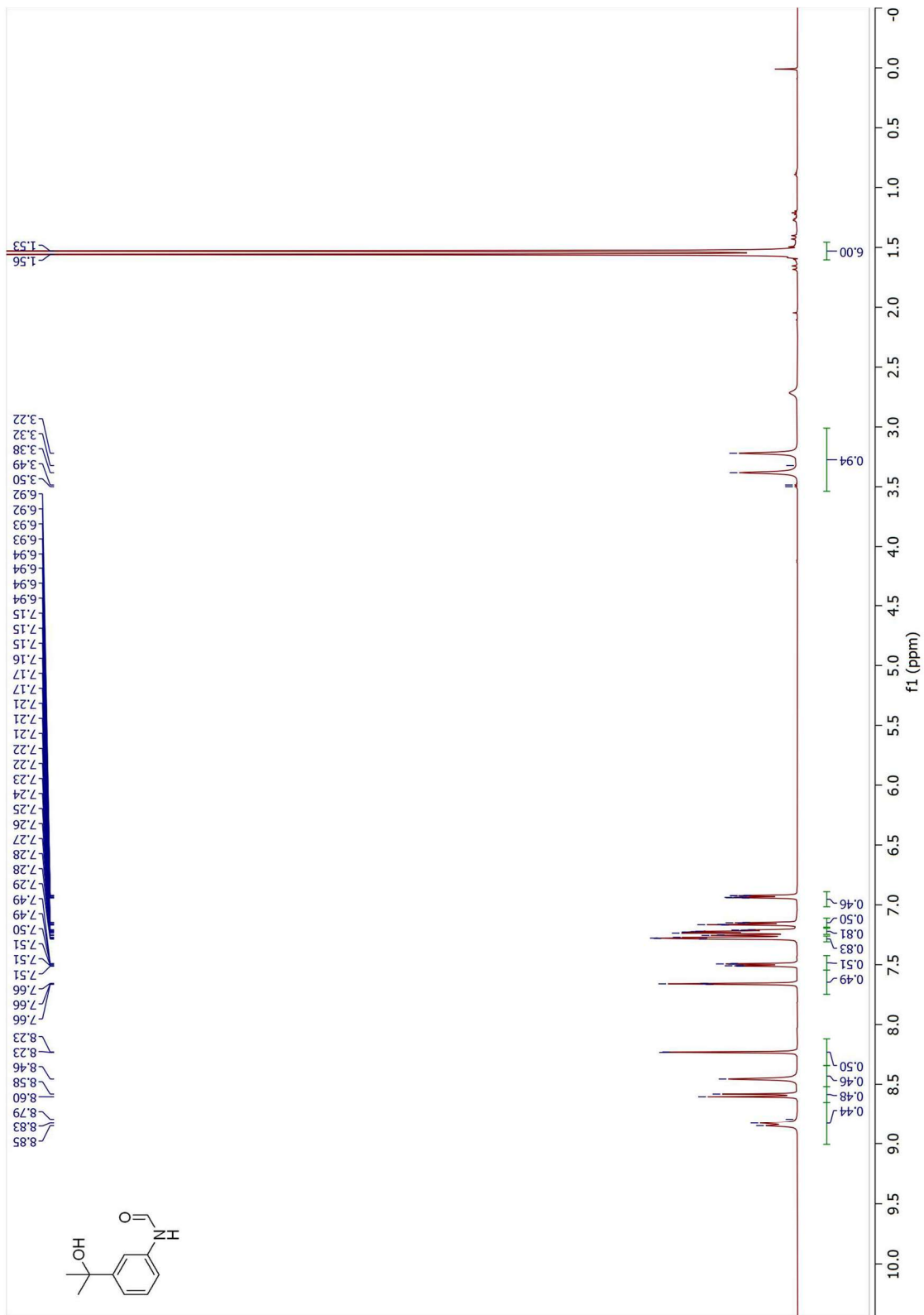


Figure 7.1 ^1H NMR Spectrum of 2.3 (500 MHz, CDCl_3)

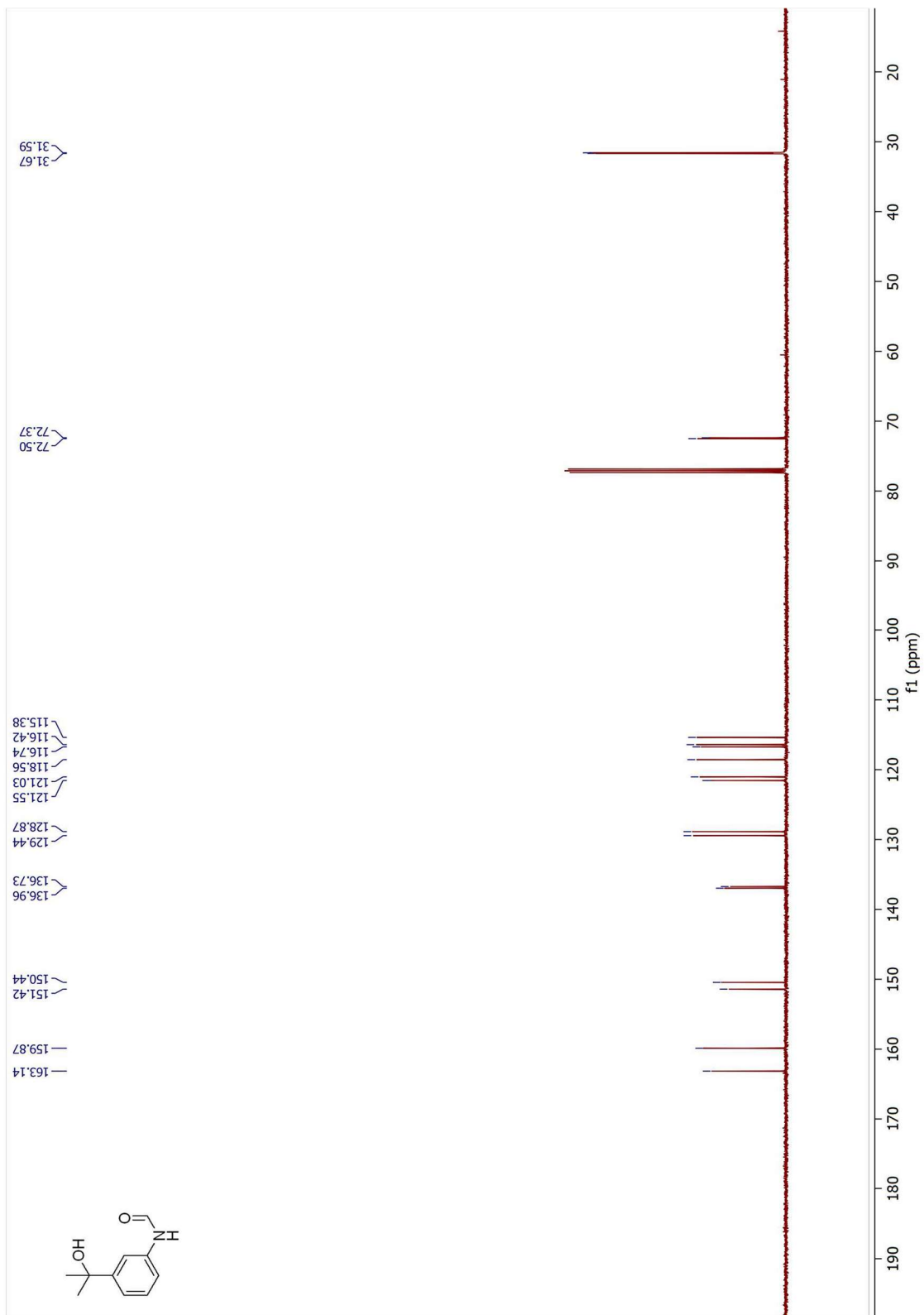


Figure 7.2 ^{13}C NMR Spectrum of **2.3** (125 MHz, CDCl_3)

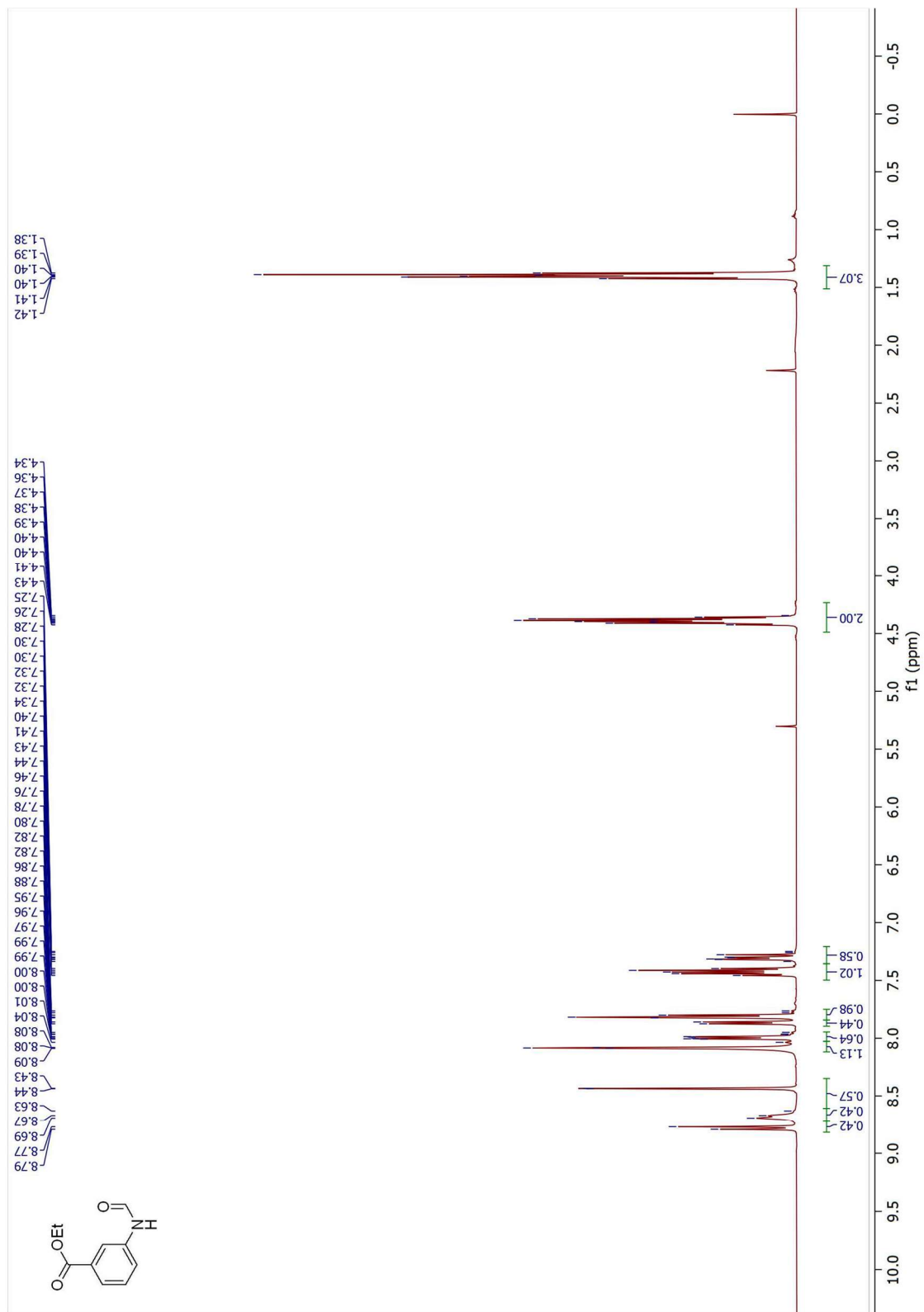


Figure 7.3 ^1H NMR Spectrum of **2.6** (500 MHz, CDCl_3)

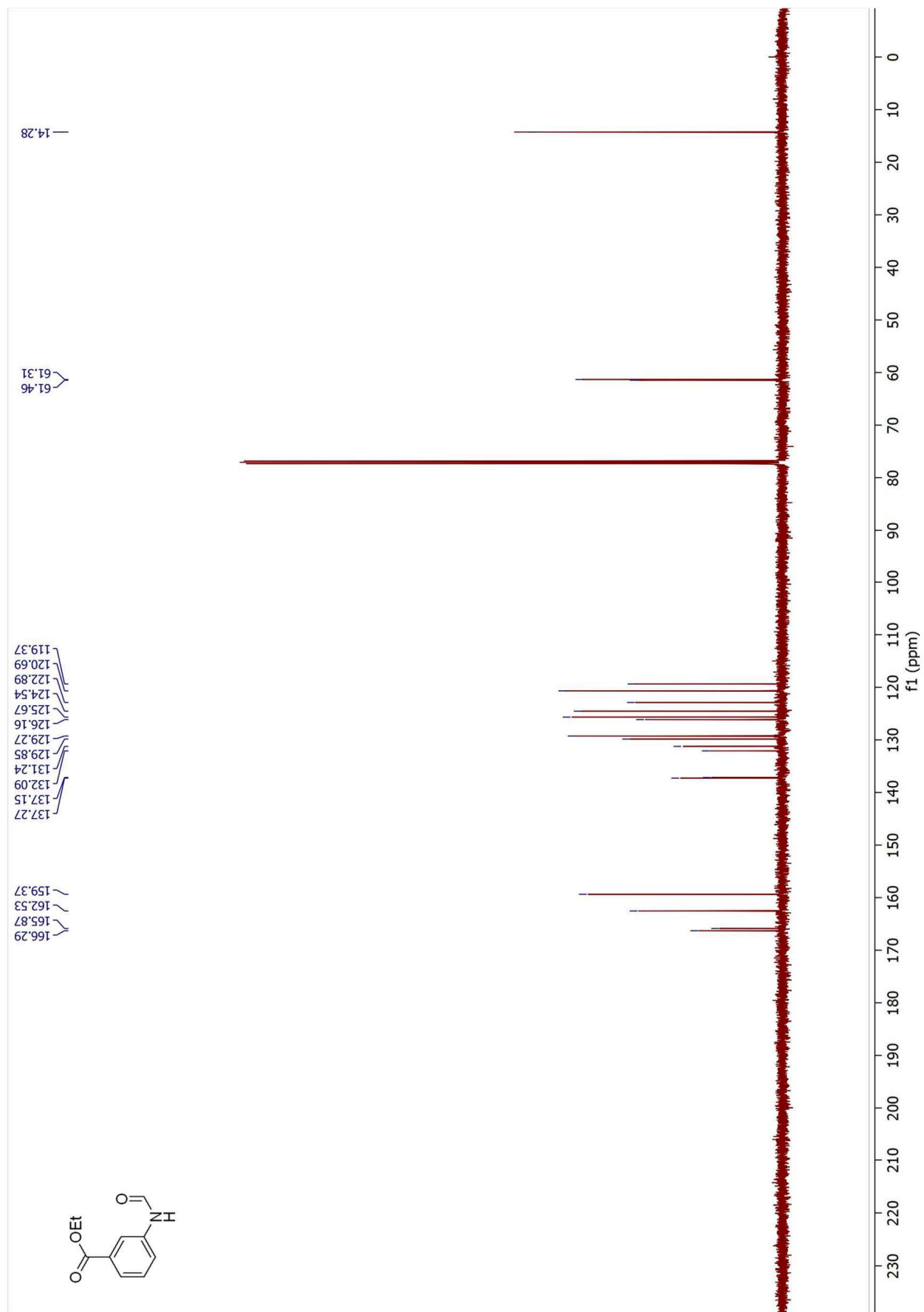


Figure 7.4 ^{13}C NMR Spectrum of **2.6** (125 MHz, CDCl_3)

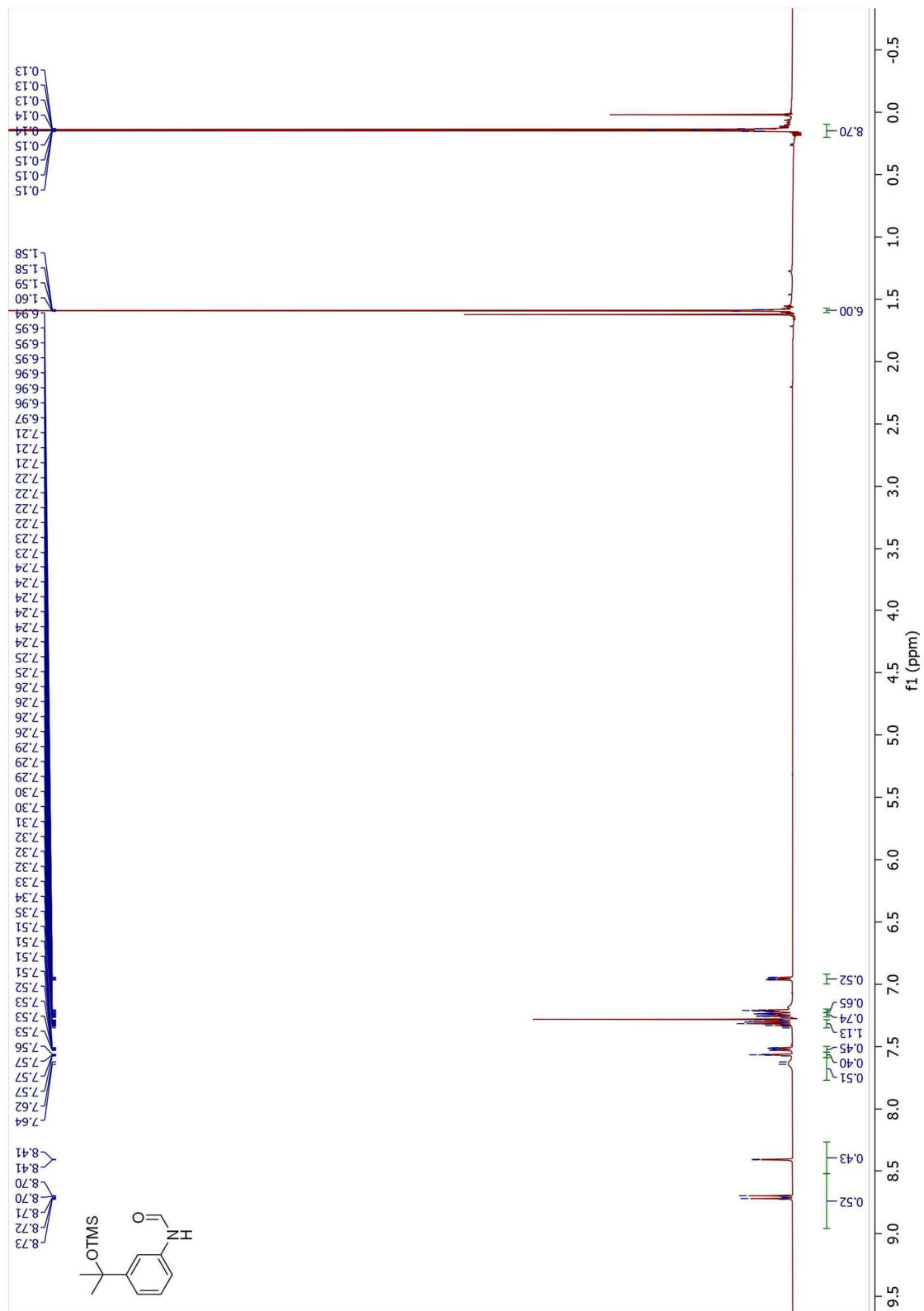


Figure 7.5 ¹H NMR Spectrum of 2.7 (500 MHz, CDCl₃)

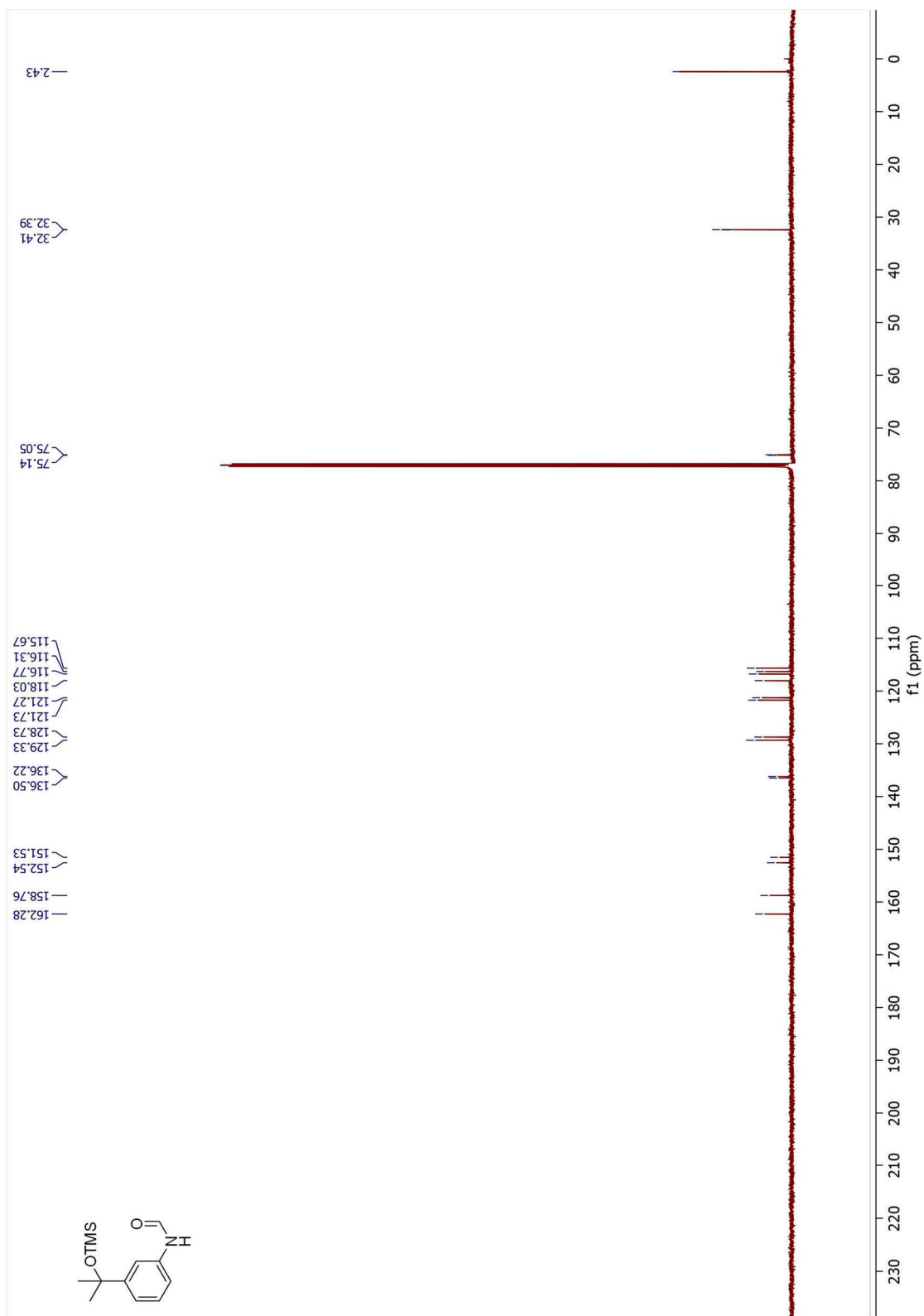


Figure 7.6 ^{13}C NMR Spectrum of 2.7 (125 MHz, CDCl_3)

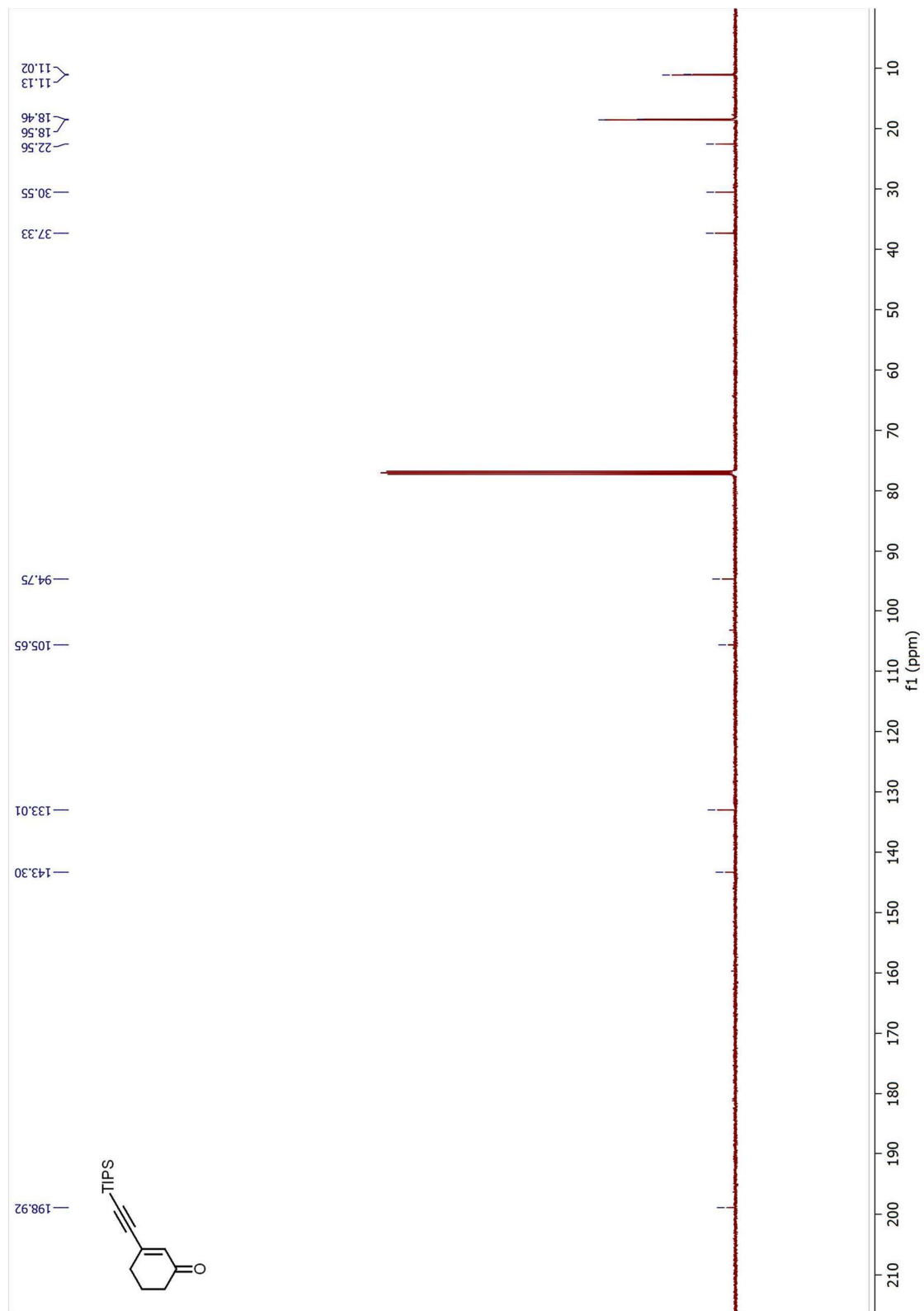


Figure 7.8 ^{13}C NMR Spectrum of **2.17** (125 MHz, CDCl_3)

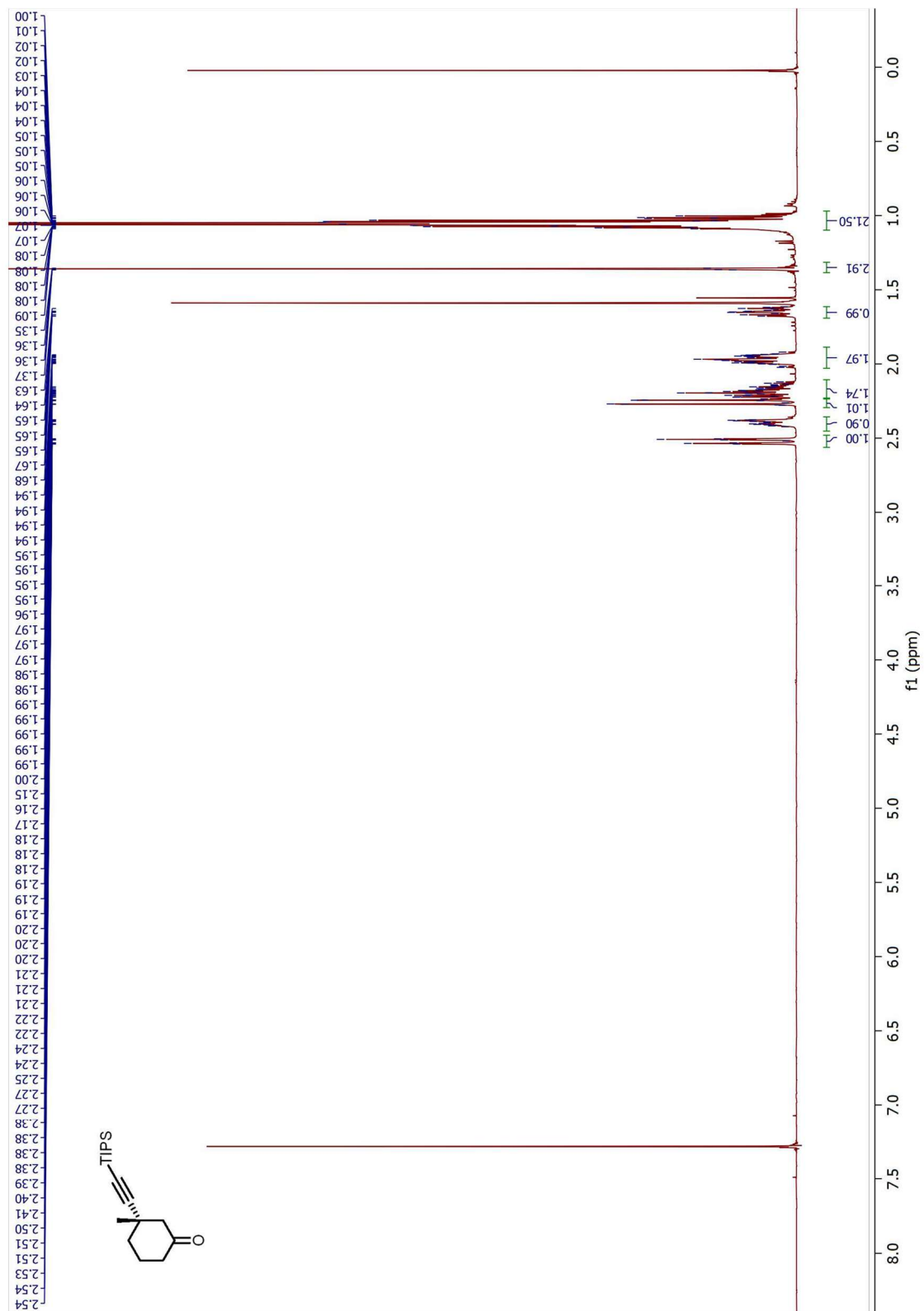


Figure 7.9 ¹H NMR Spectrum of 2.18 (500 MHz, CDCl₃)

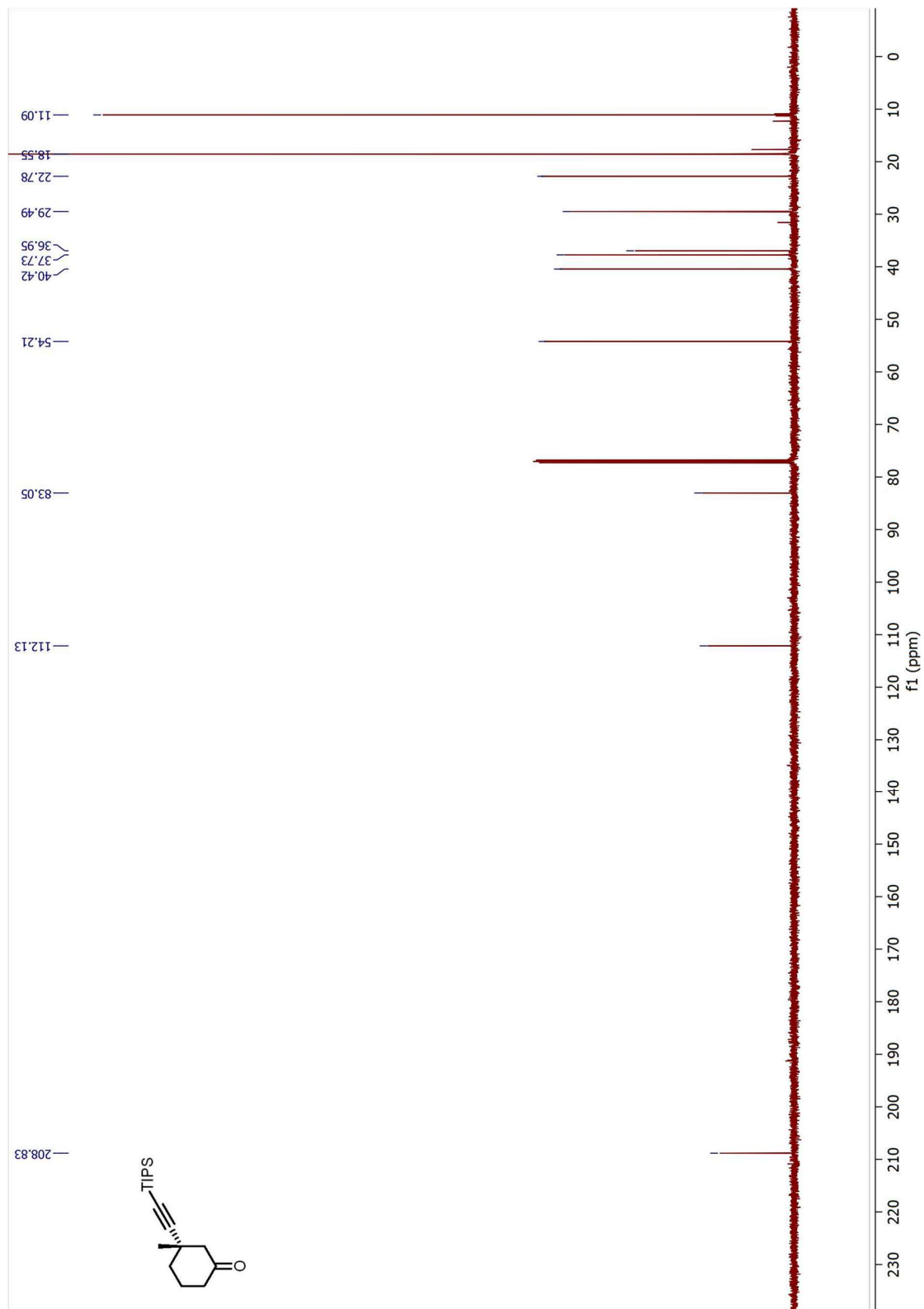


Figure 7.10 ^{13}C NMR Spectrum of **2.18** (125 MHz, CDCl_3)

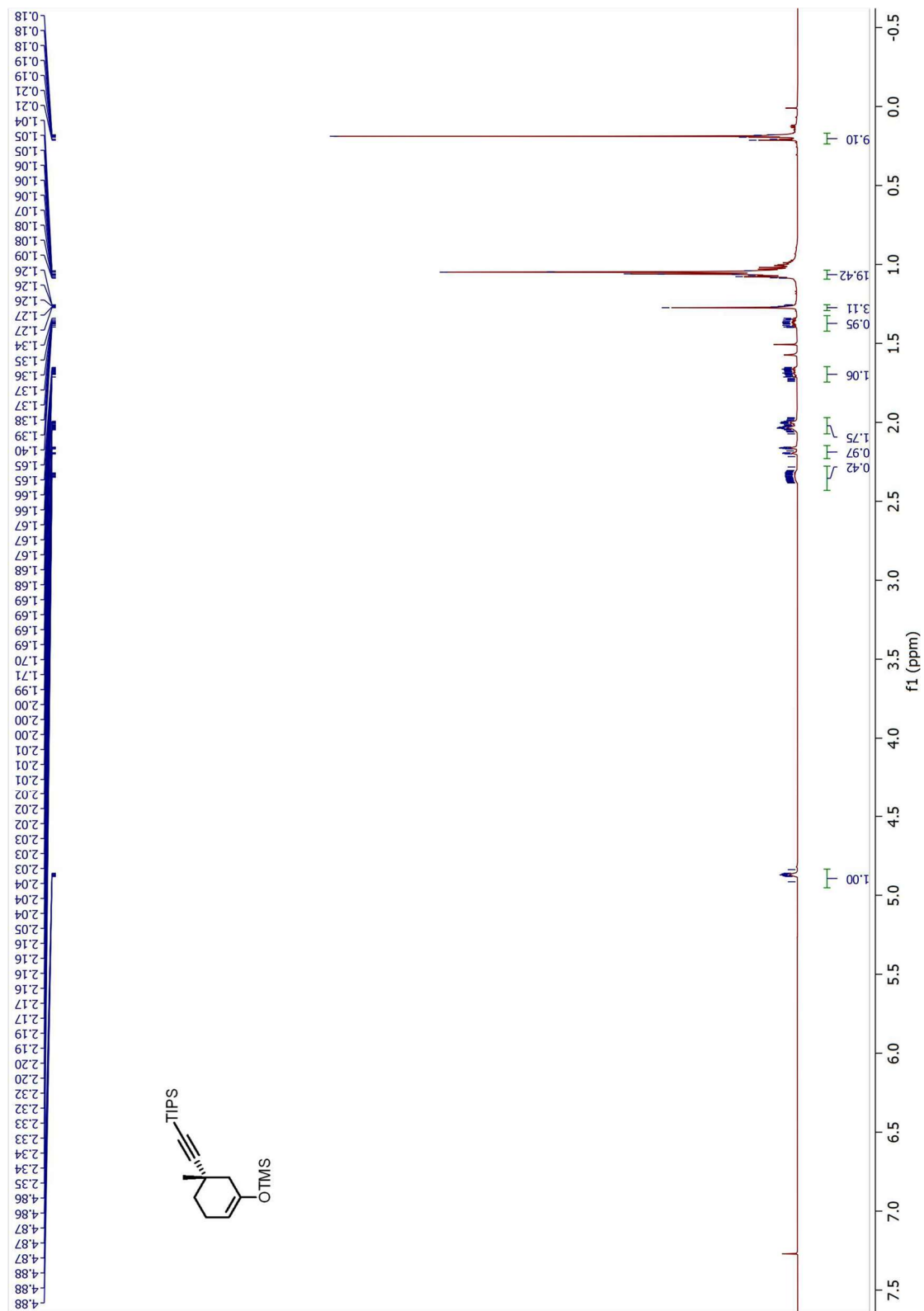


Figure 7.11 ^1H NMR Spectrum of 2.19 (500 MHz, CDCl_3)

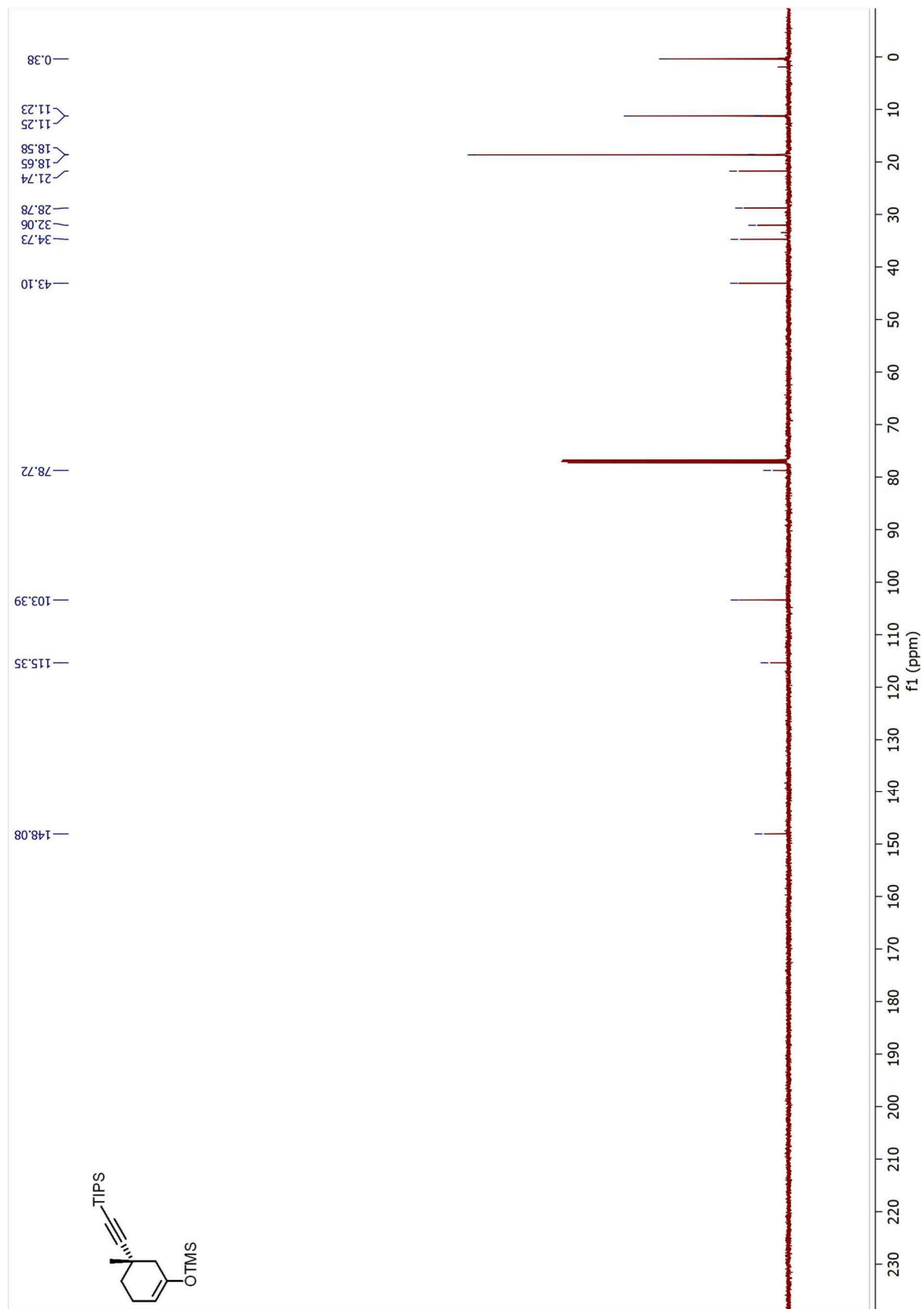


Figure 7.12 ^{13}C NMR Spectrum of **2.19** (125 MHz, CDCl_3)

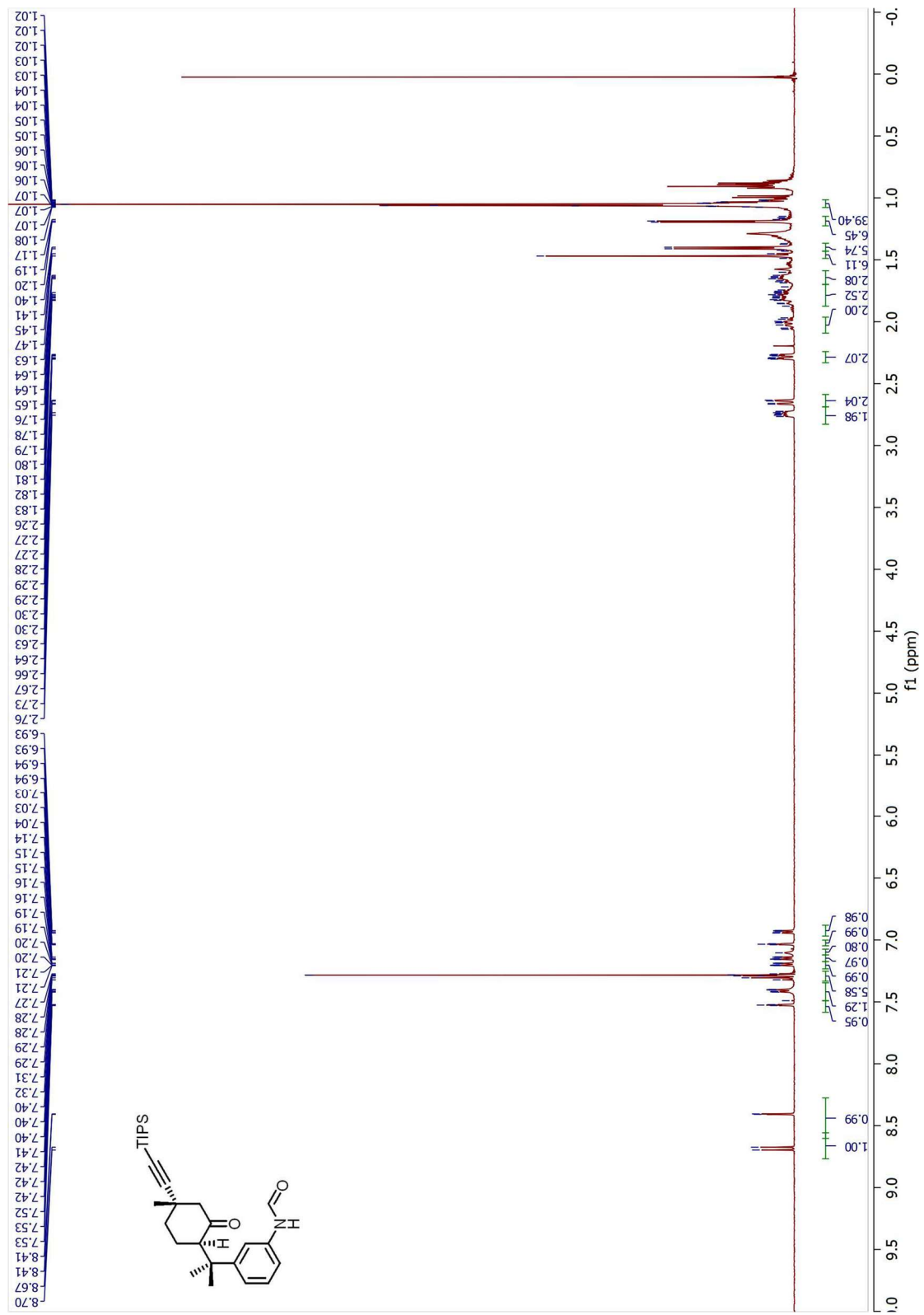


Figure 7.13 ¹H NMR Spectrum of 2.21 (500 MHz, CDCl₃)

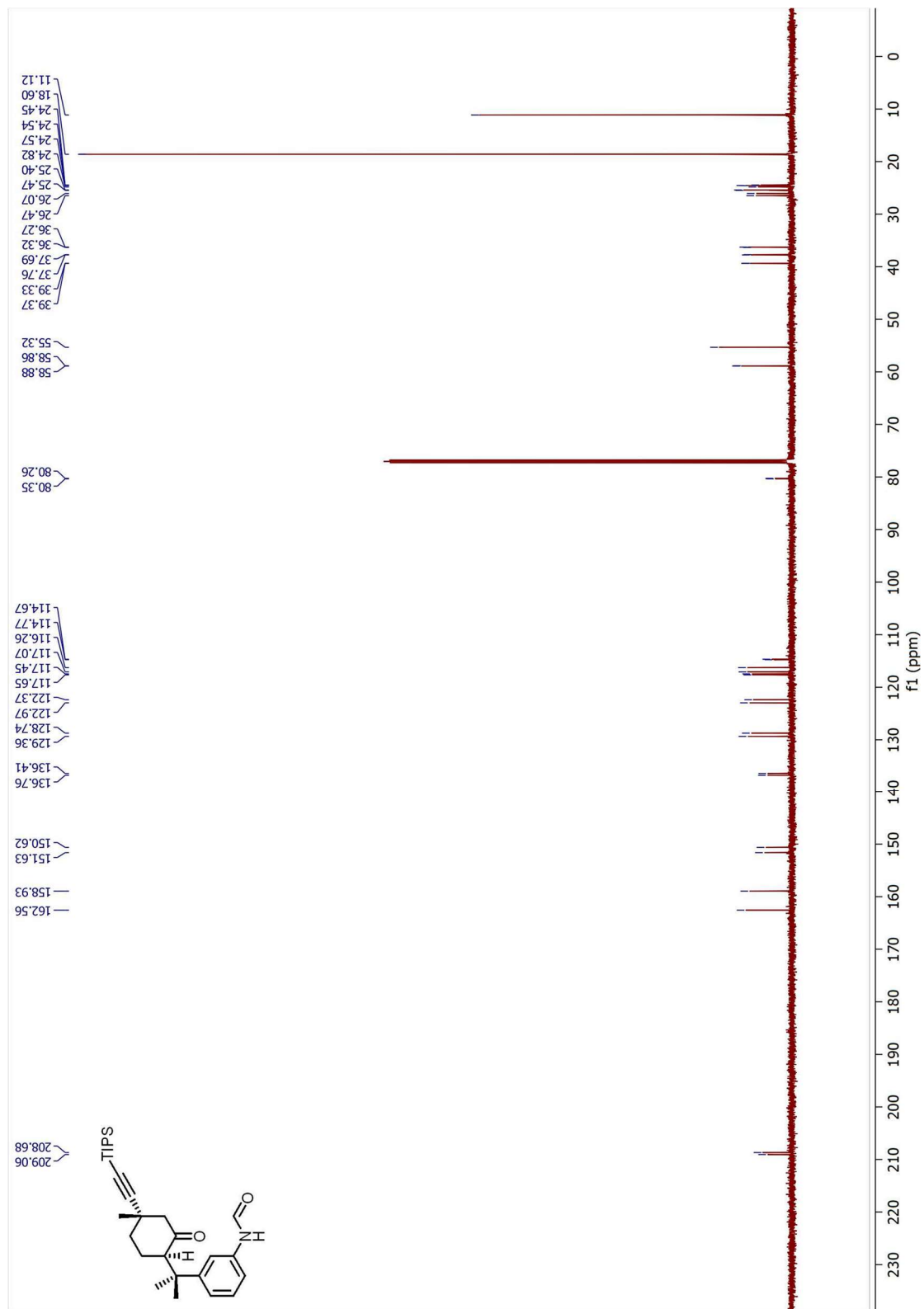


Figure 7.14 ^{13}C NMR Spectrum of 2.21 (125 MHz, CDCl_3)

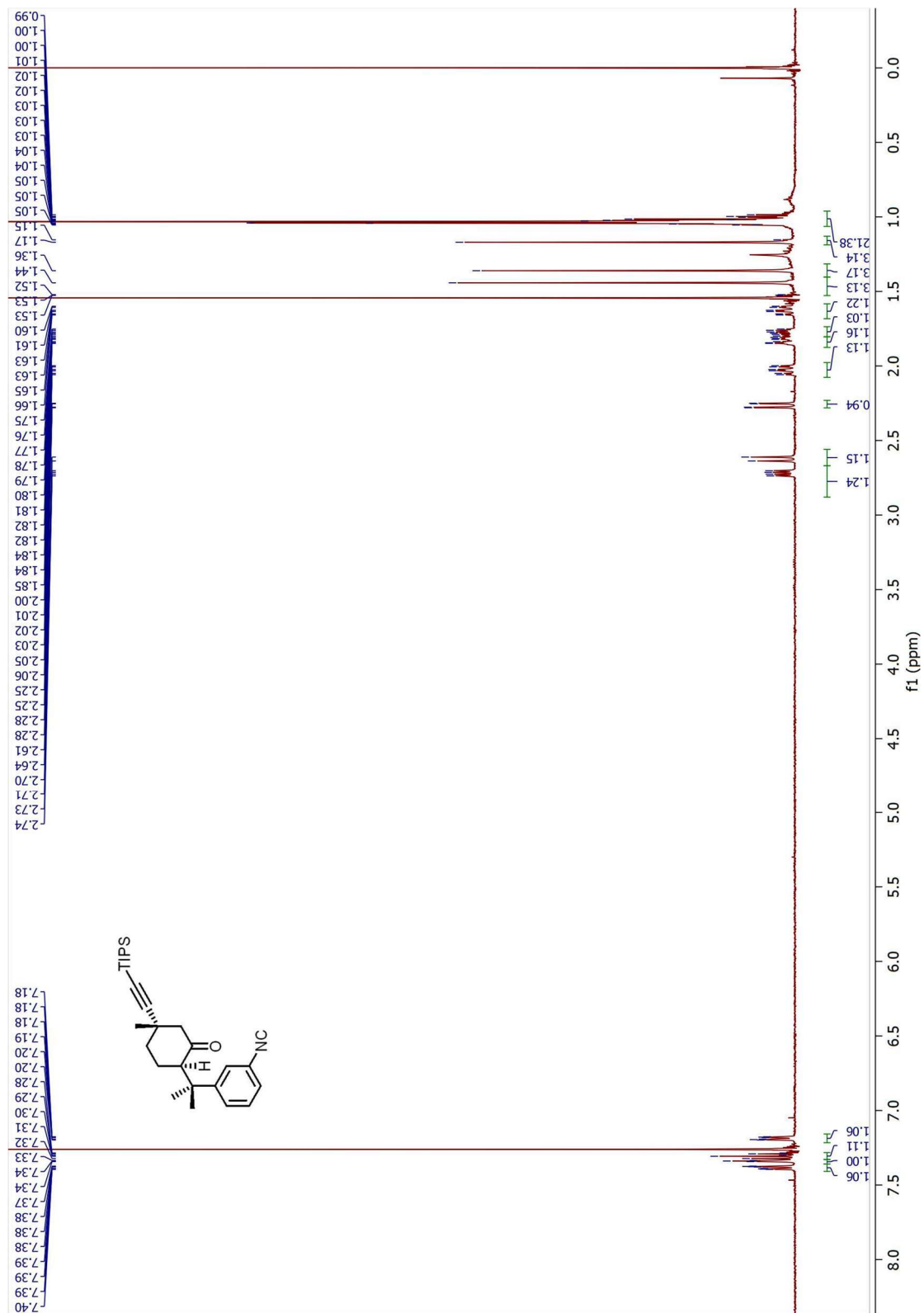


Figure 7.15 ^1H NMR Spectrum of **2.22** (500 MHz, CDCl_3)

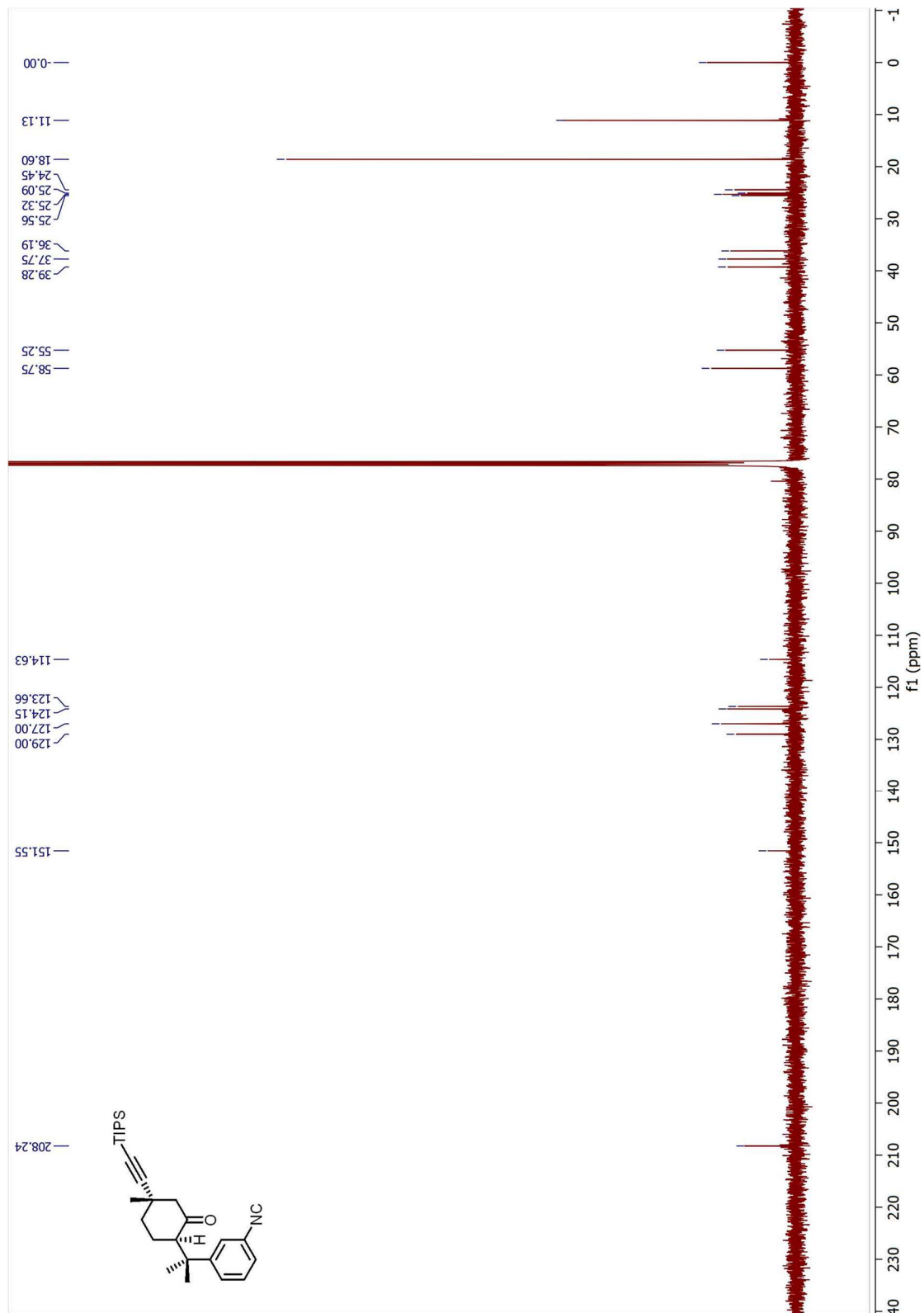


Figure 7.16 ^{13}C NMR Spectrum of **2.22** (125 MHz, CDCl_3)

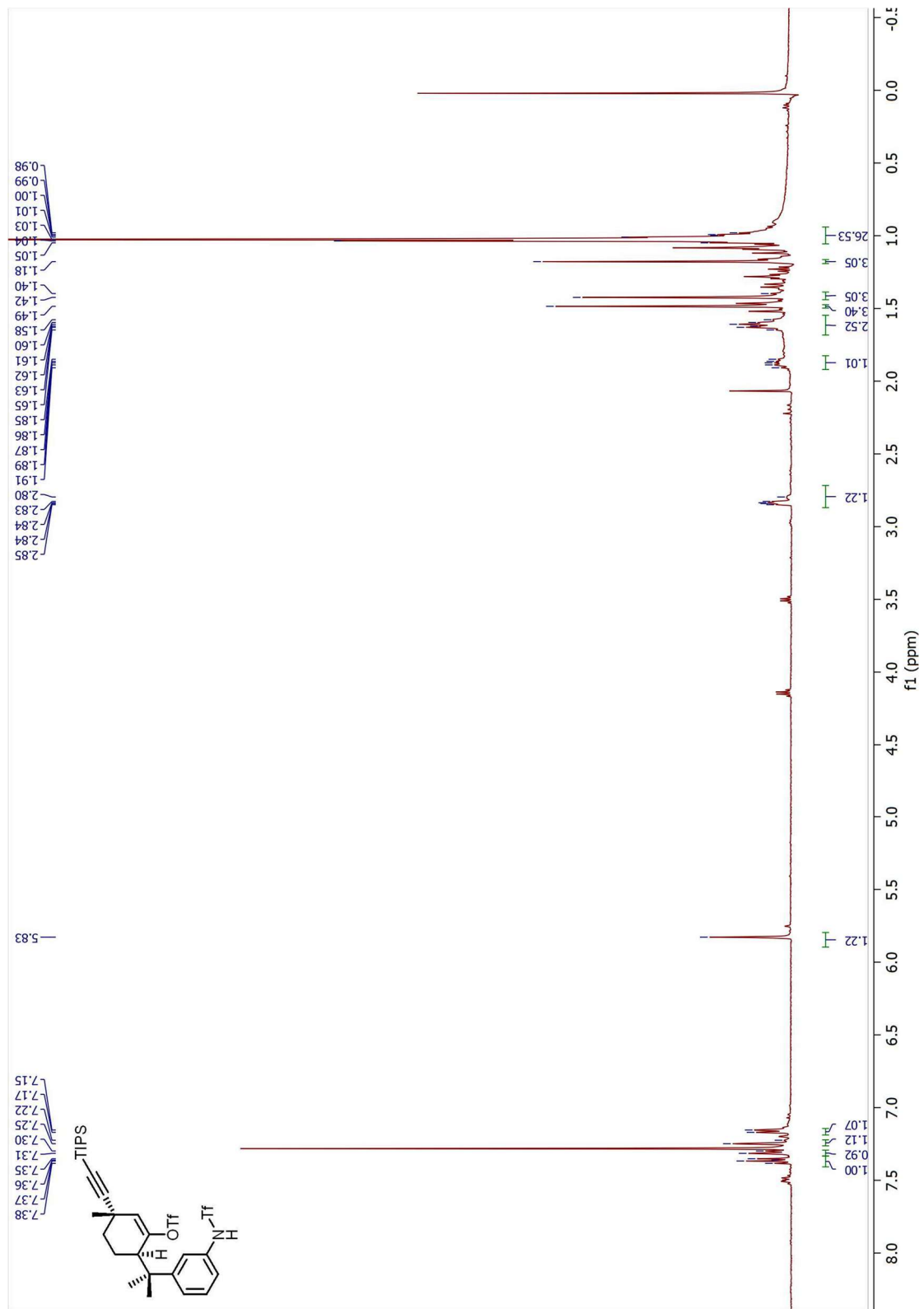


Figure 7.17 ¹H NMR Spectrum of SL.1 (500 MHz, CDCl₃)

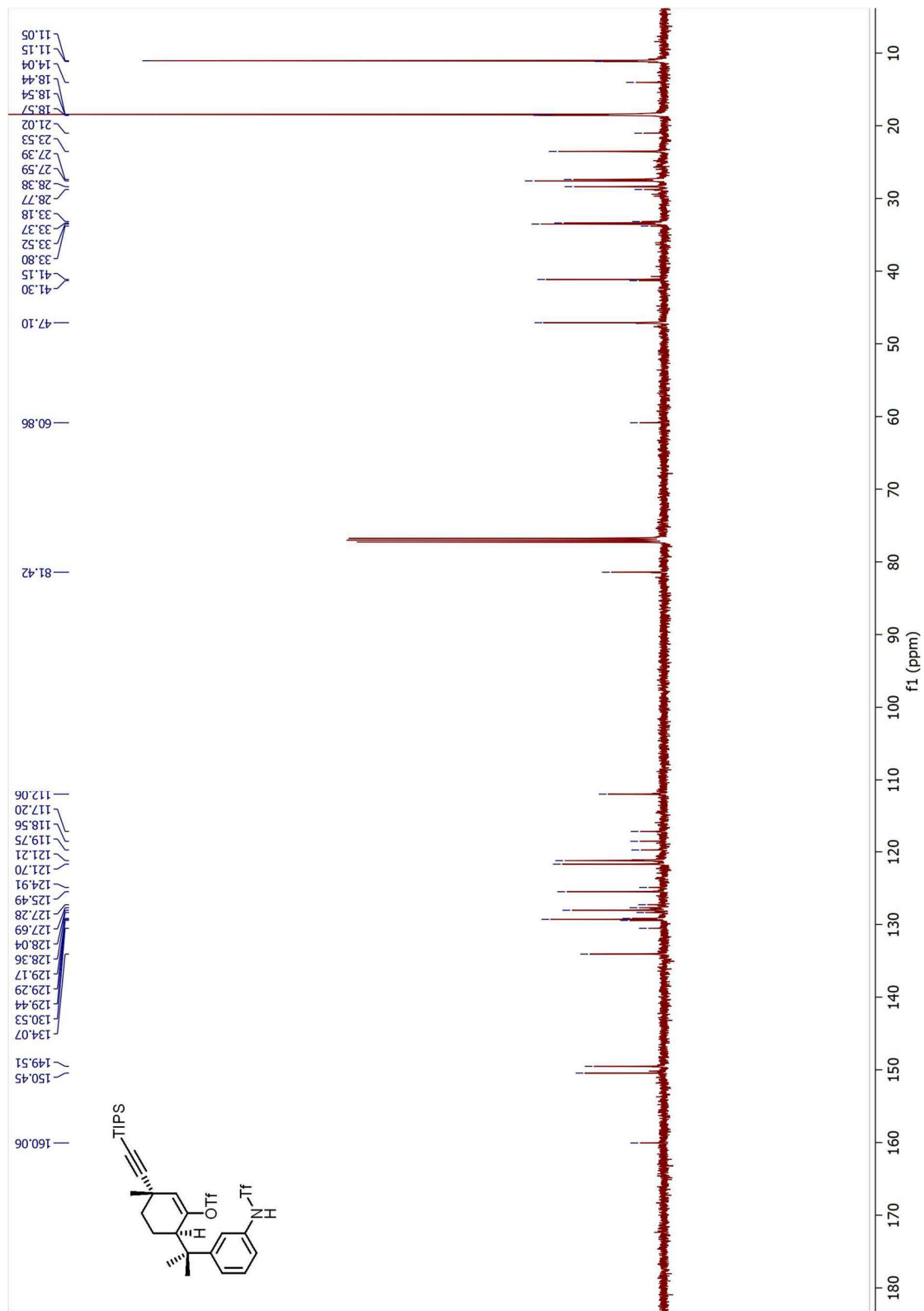


Figure 7.18 ^{13}C NMR Spectrum of **SI.1** (125 MHz, CDCl_3)

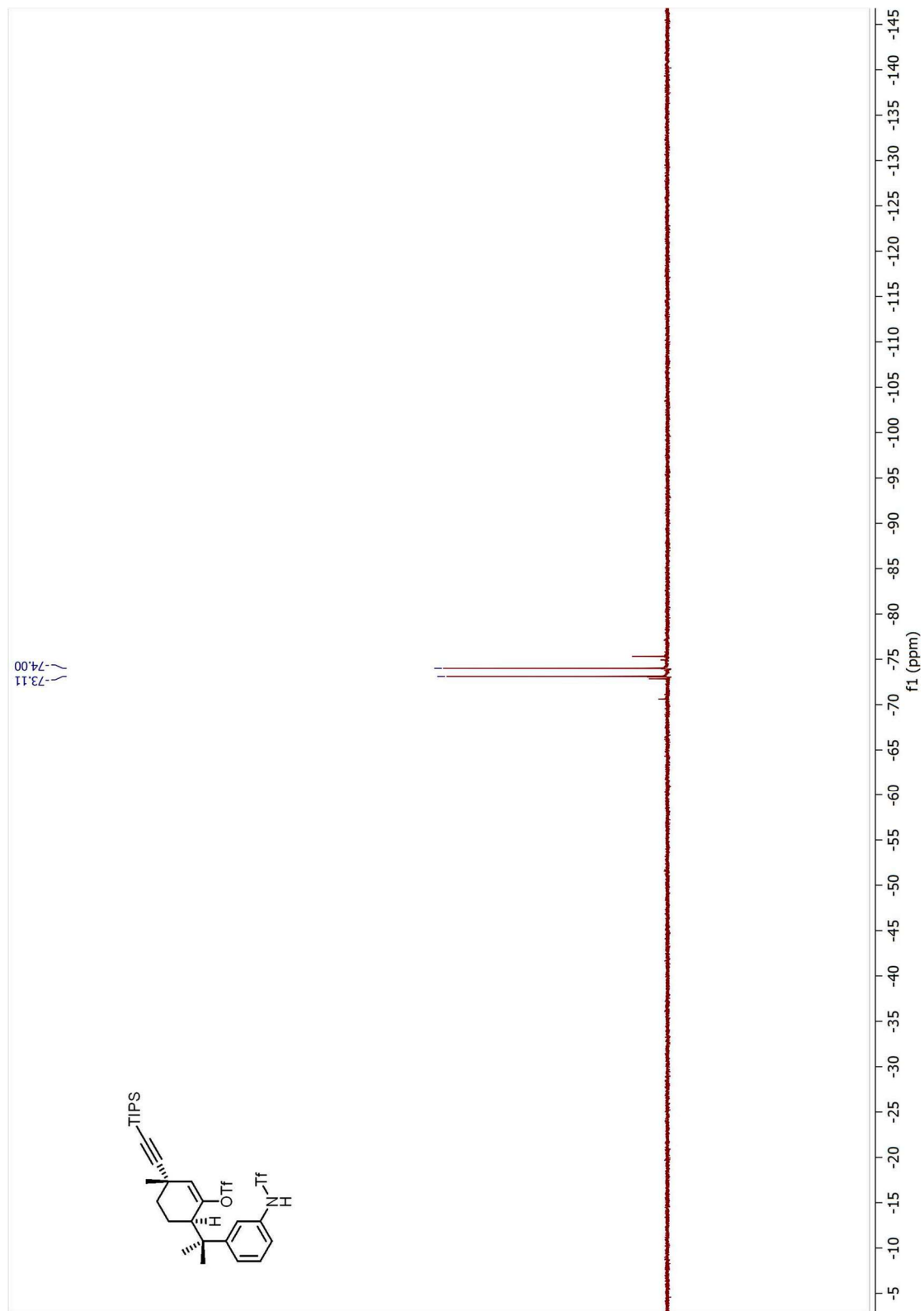


Figure 7.19 ^{19}F NMR Spectrum of **SI.1** (500 MHz, CDCl_3)

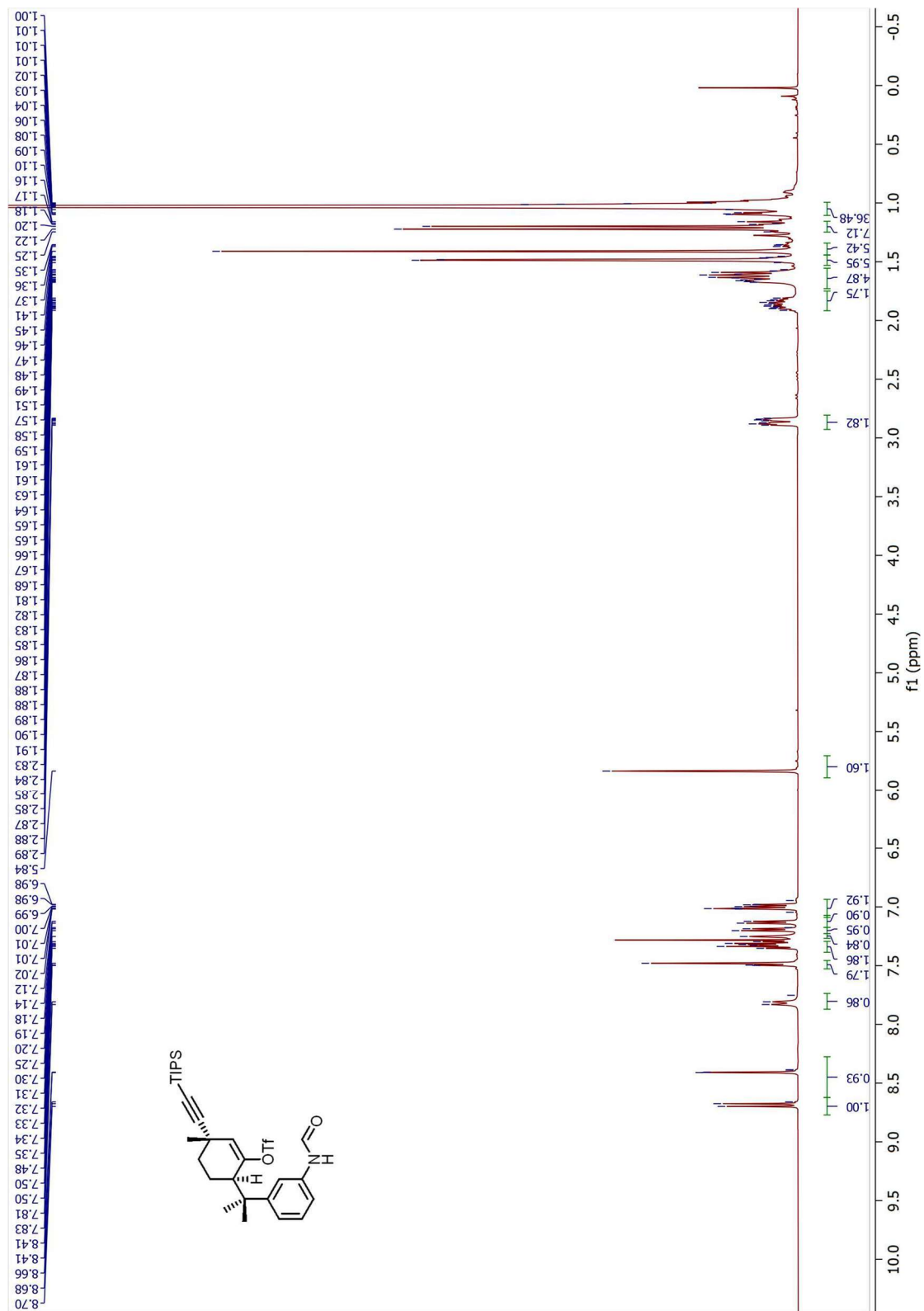


Figure 7.20 ^1H NMR Spectrum of 2.26 (500 MHz, CDCl_3)

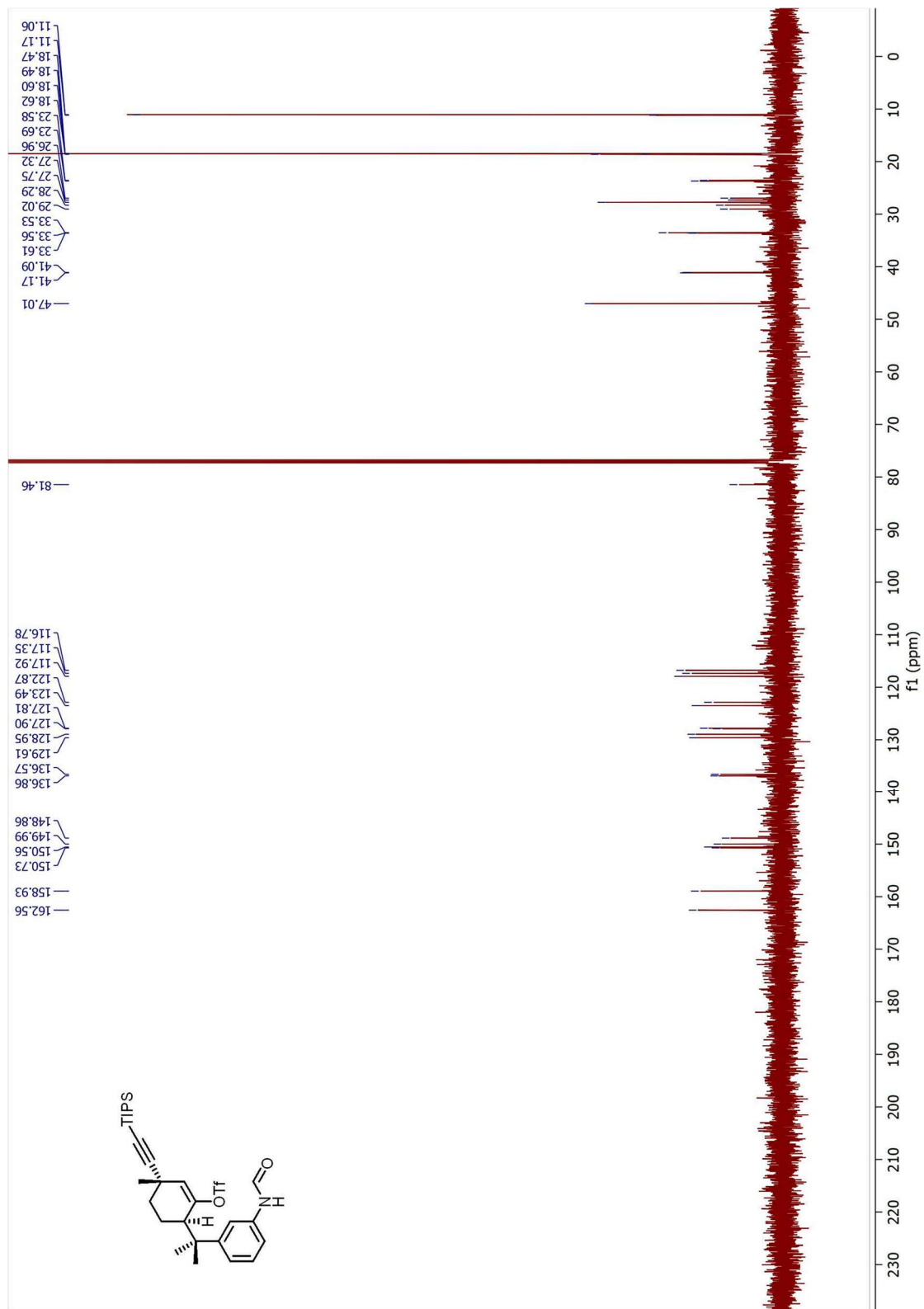


Figure 7.21 ^{13}C NMR Spectrum of 2.26 (125 MHz, CDCl_3)

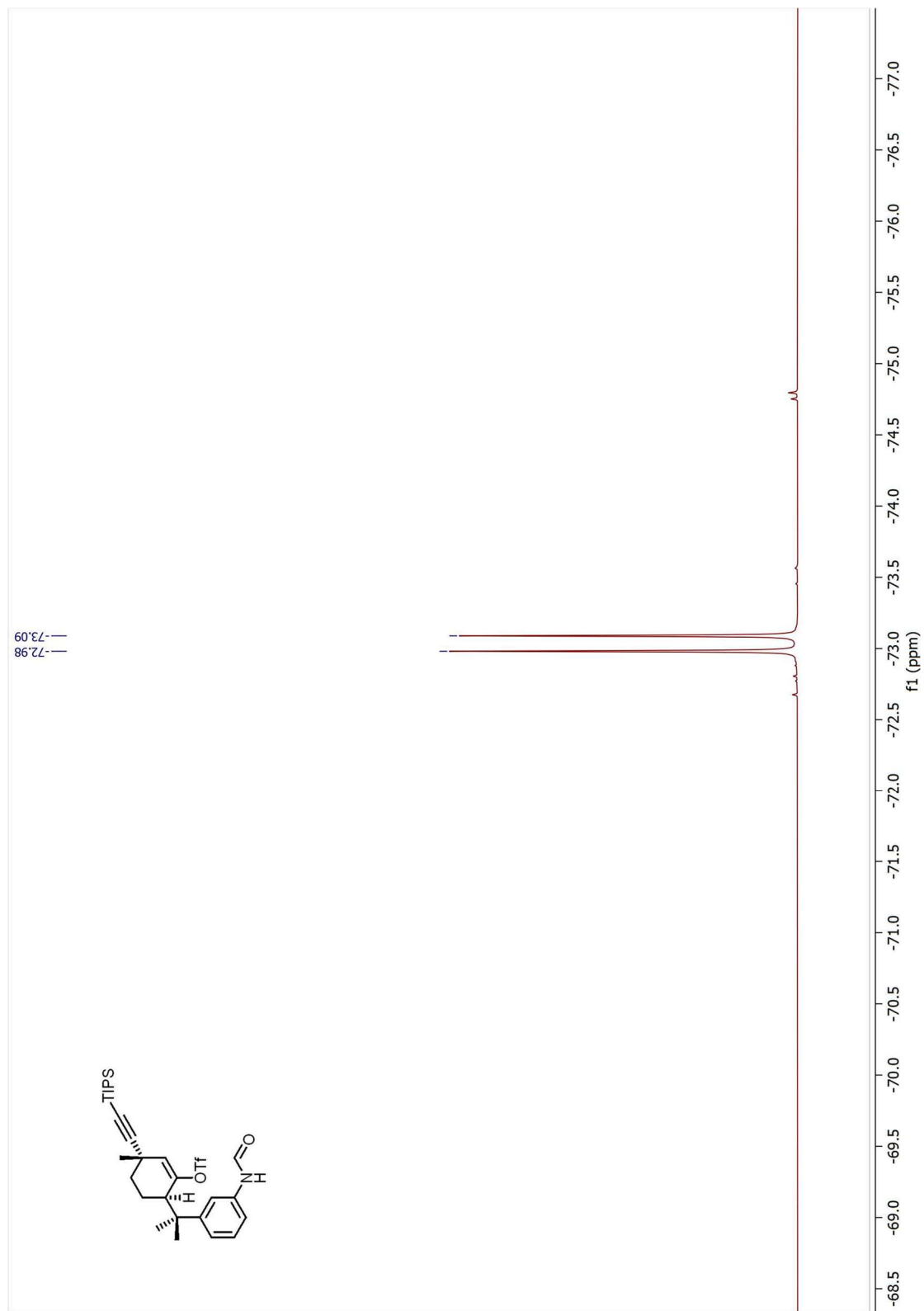


Figure 7.22 ^{19}F NMR Spectrum of **2.26** (500 MHz, CDCl_3)

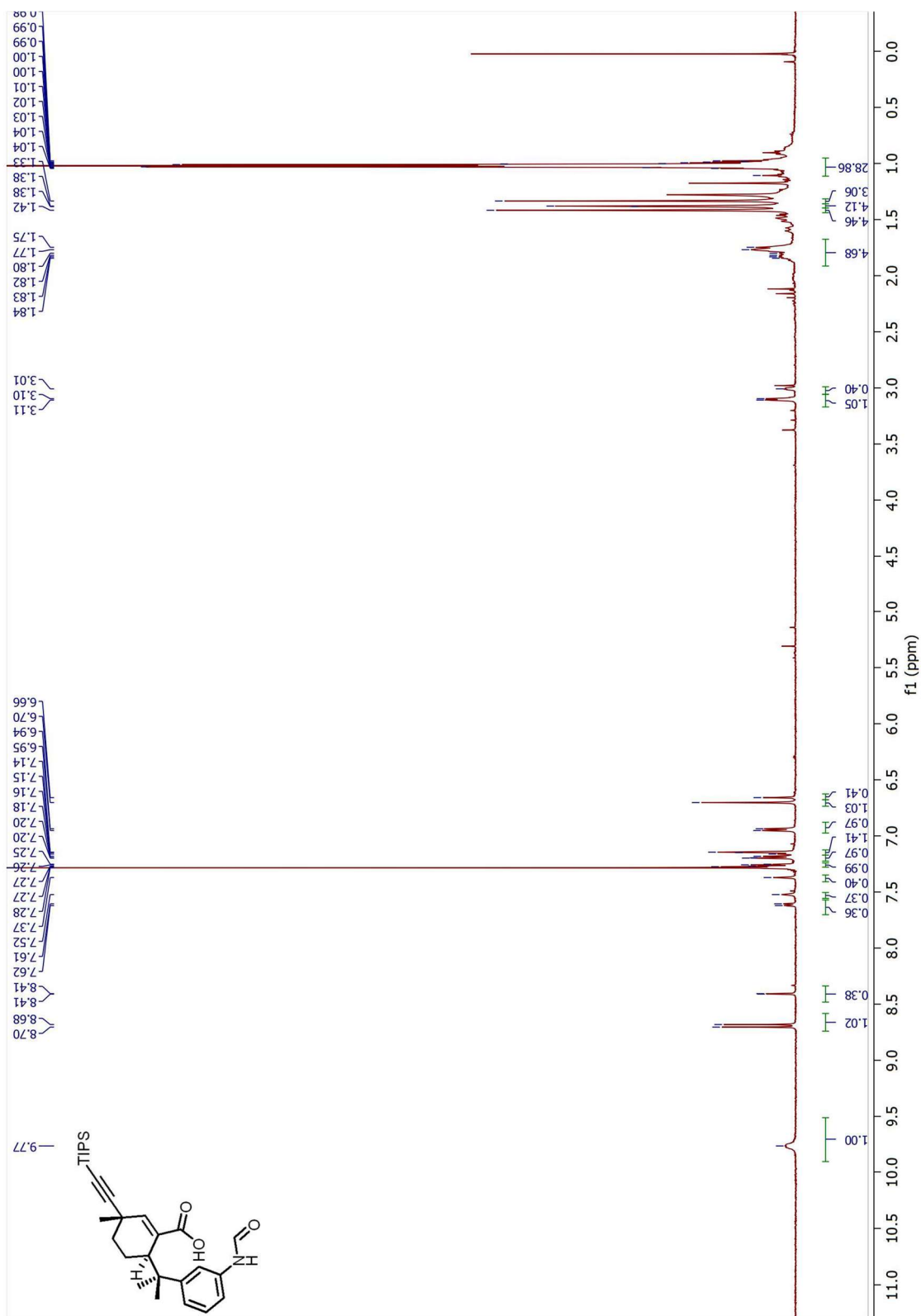


Figure 7.23 ^1H NMR Spectrum of **2.28** (500 MHz, CDCl_3)

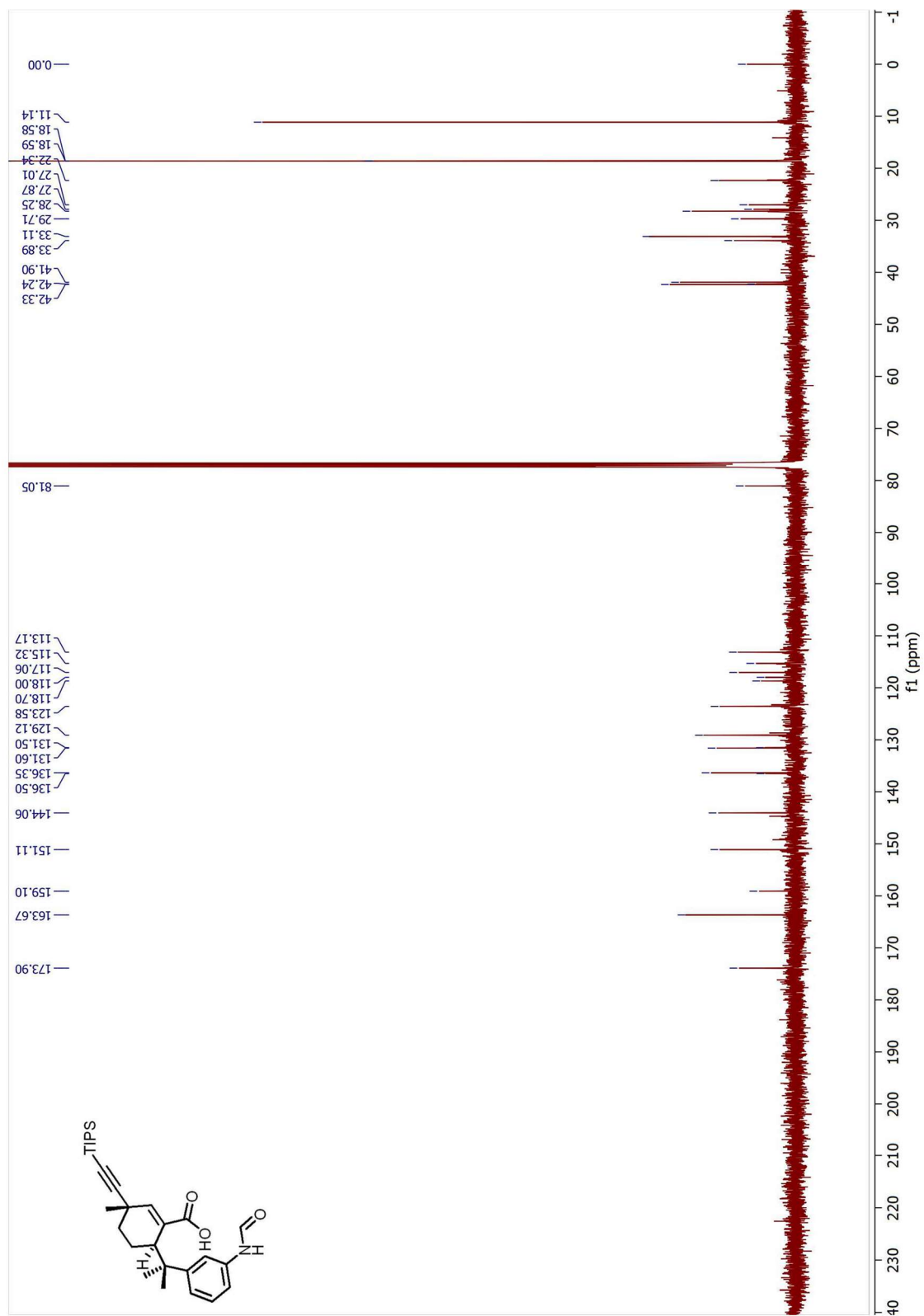


Figure 7.24 ^{13}C NMR Spectrum of **2.28** (125 MHz, CDCl_3)

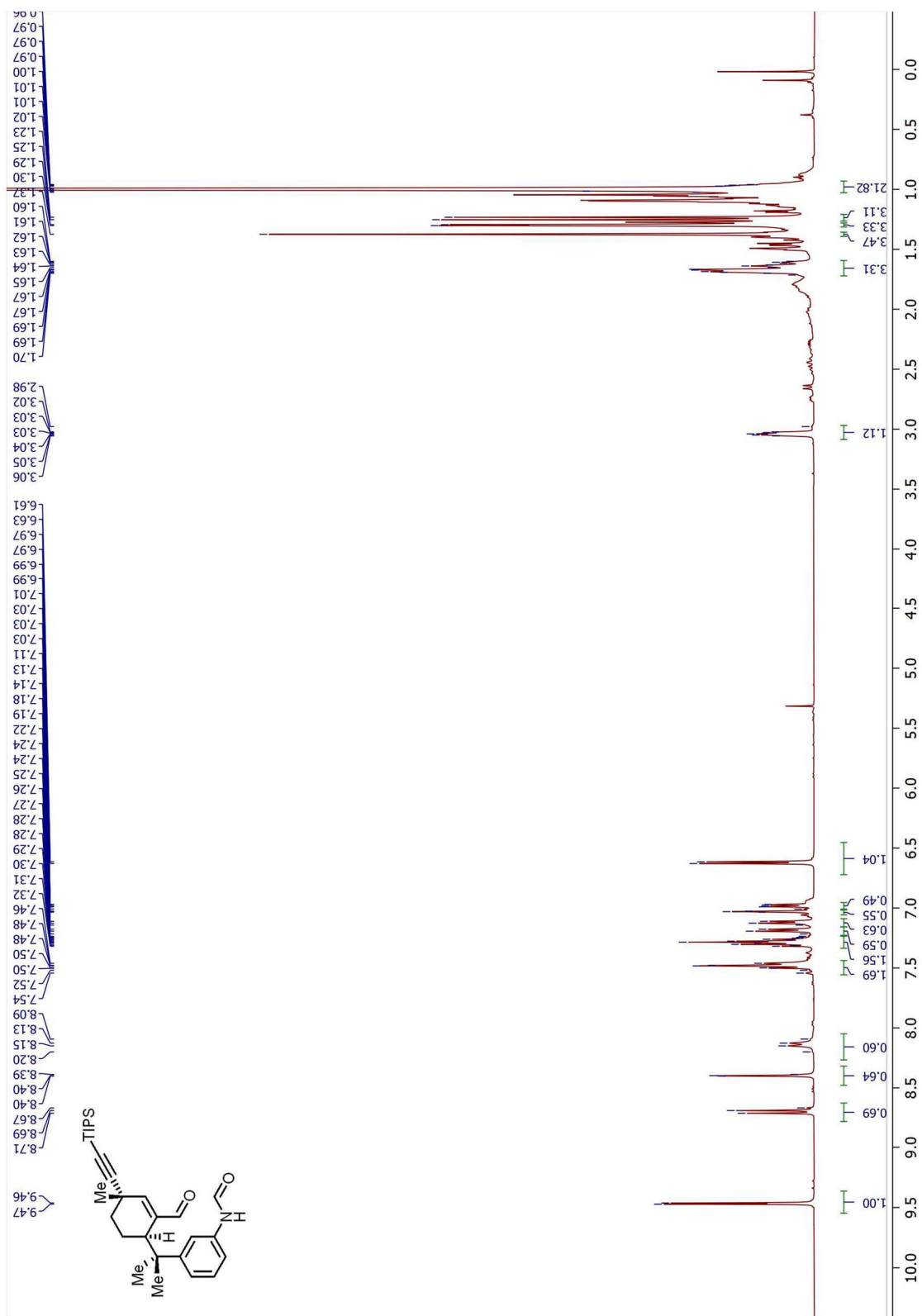


Figure 7.25 ^1H NMR Spectrum of **2.33** (500 MHz, CDCl_3)

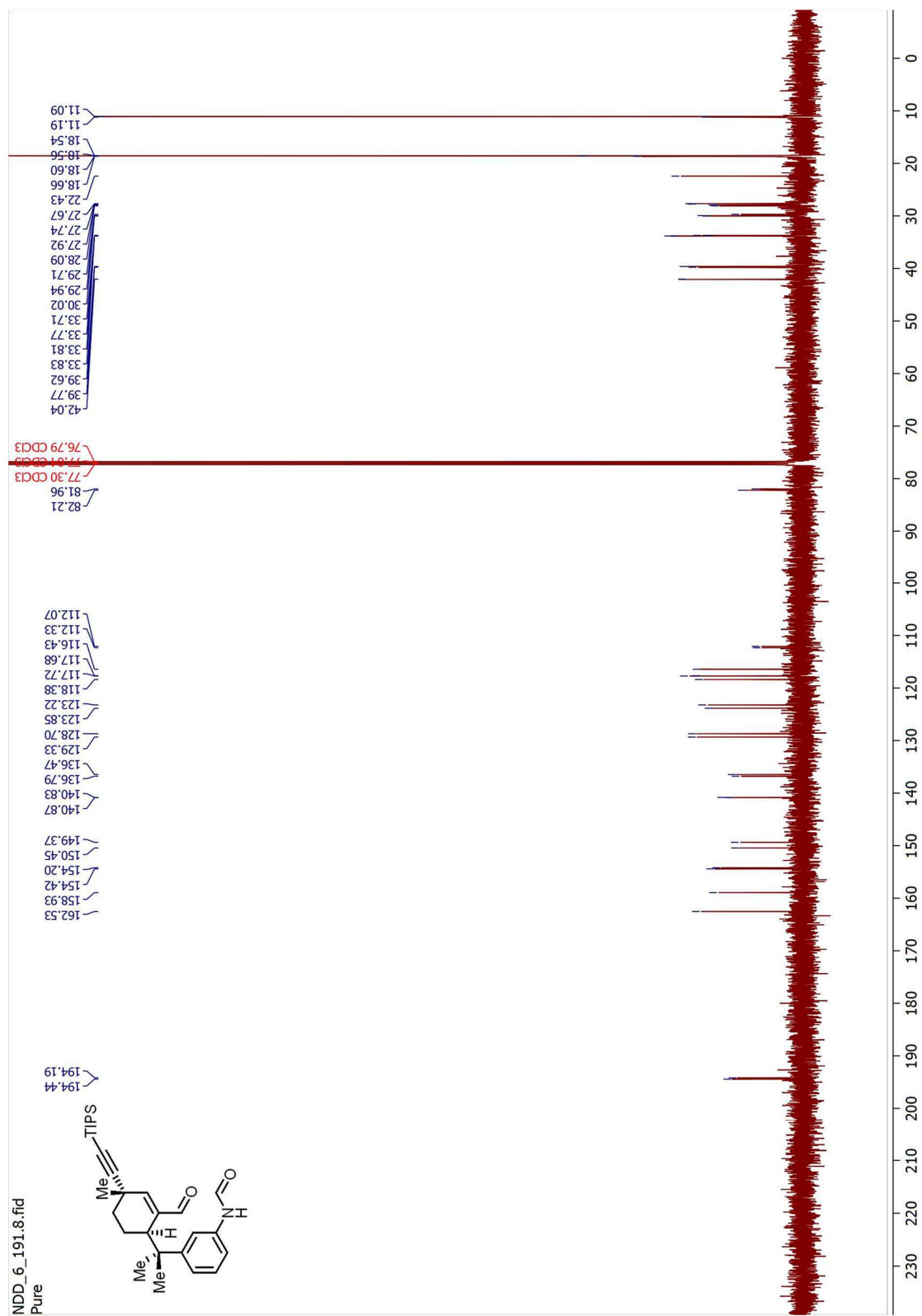


Figure 7.26 ¹³C NMR Spectrum of 2.33 (125 MHz, CDCl₃)

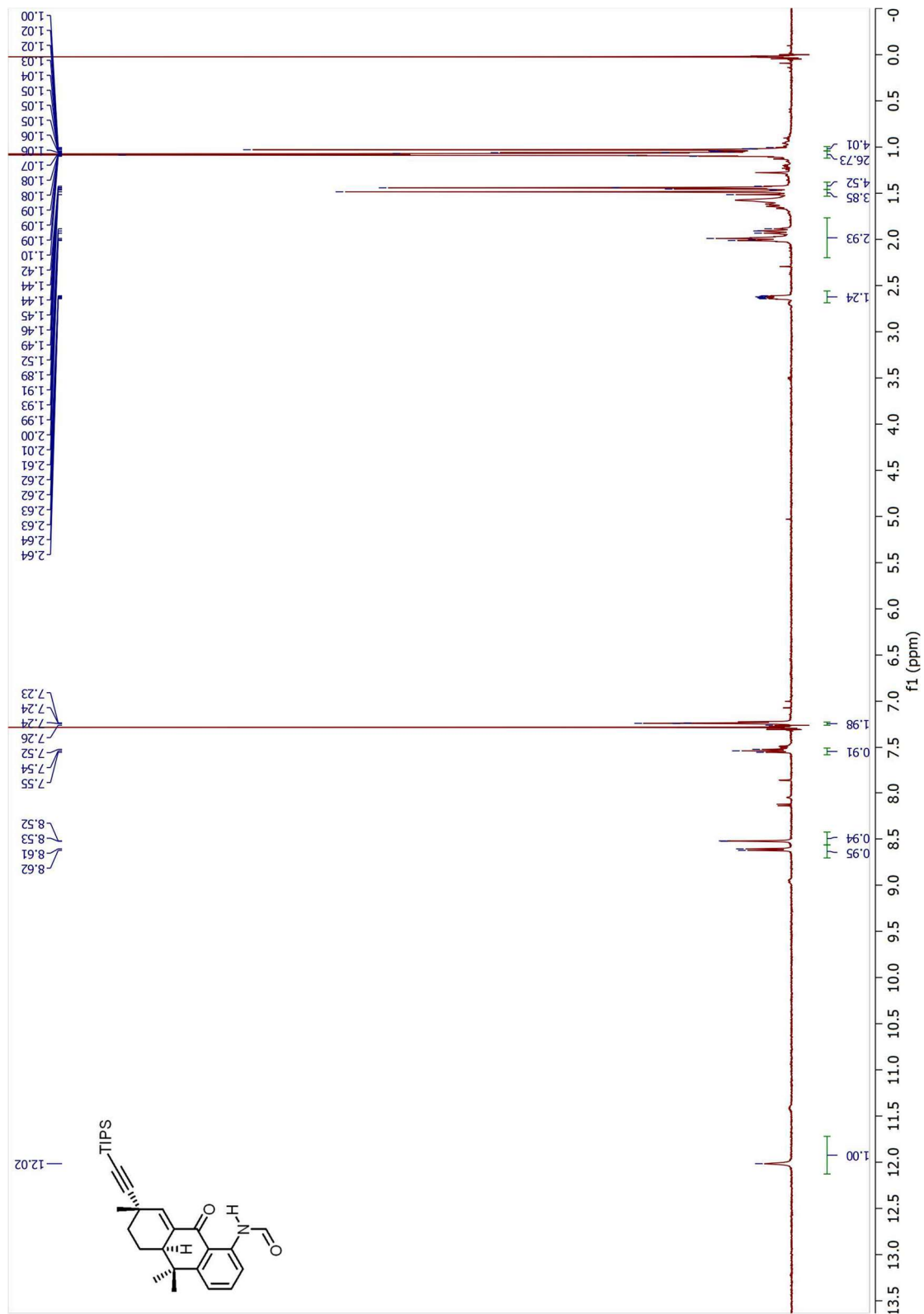


Figure 7.27 ^1H NMR Spectrum of 2.27 (500 MHz, CDCl_3)

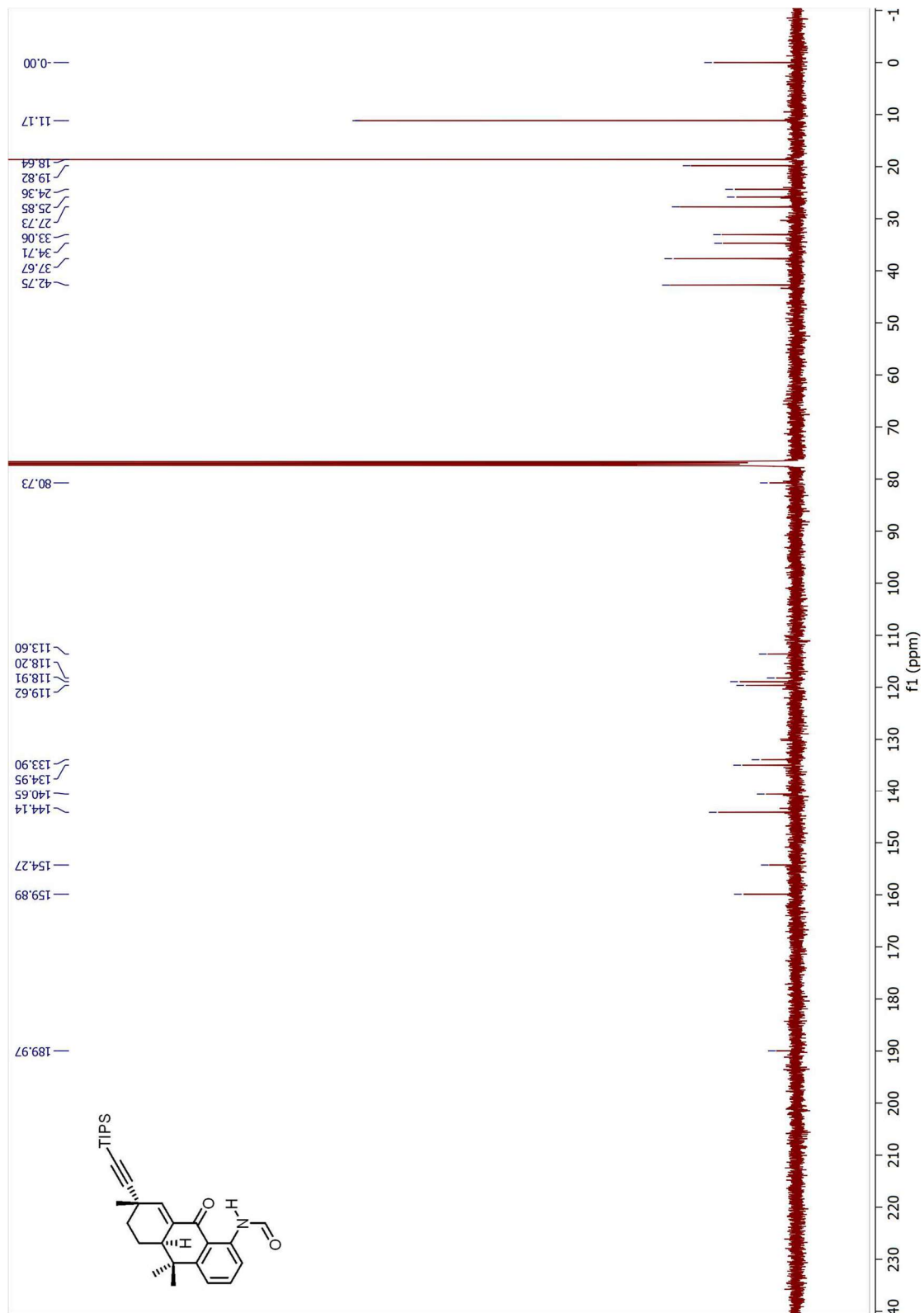


Figure 7.28 ^{13}C NMR Spectrum of **2.27** (125 MHz, CDCl_3)

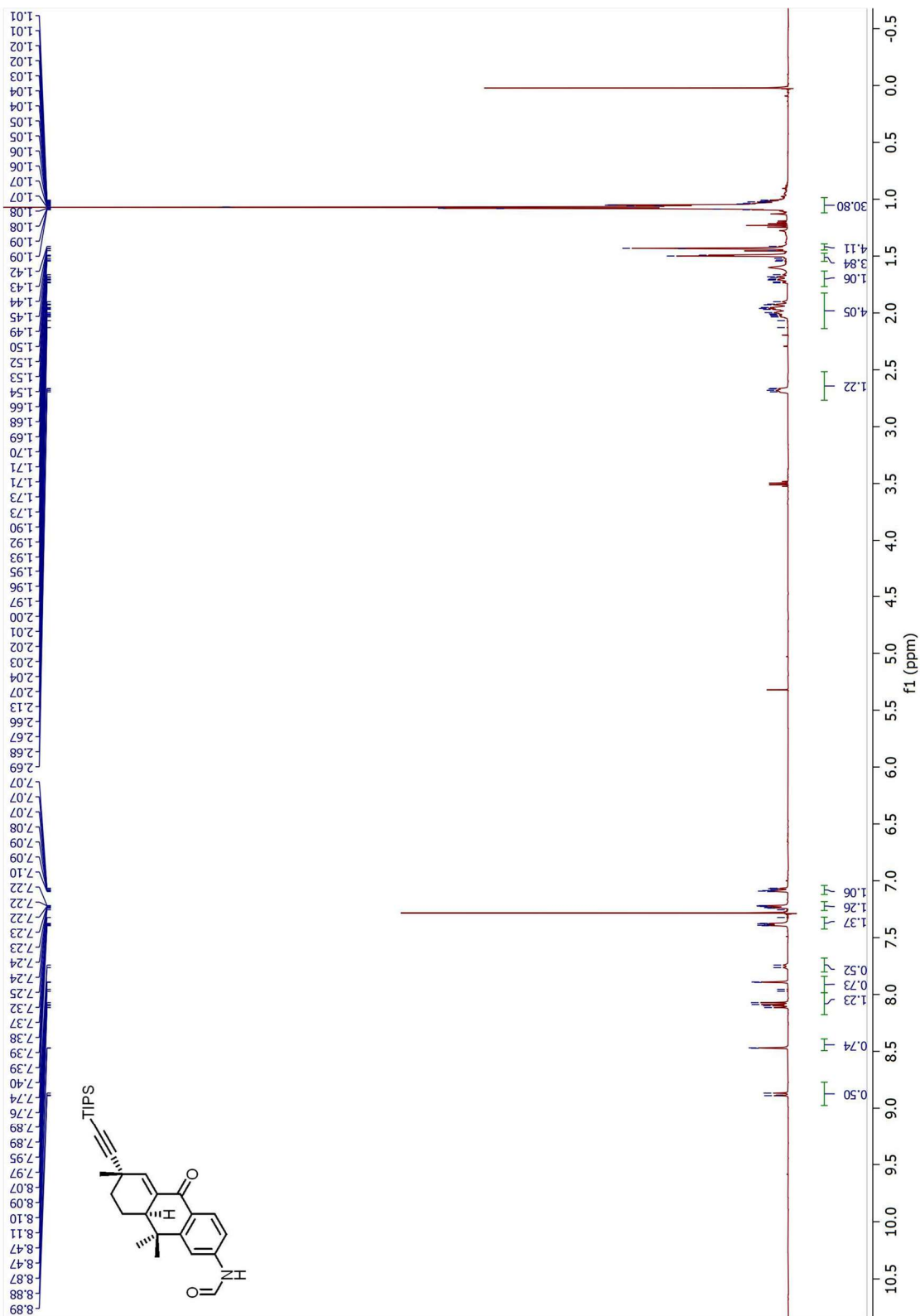


Figure 7.29 ^1H NMR Spectrum of **2.35** (500 MHz, CDCl_3)

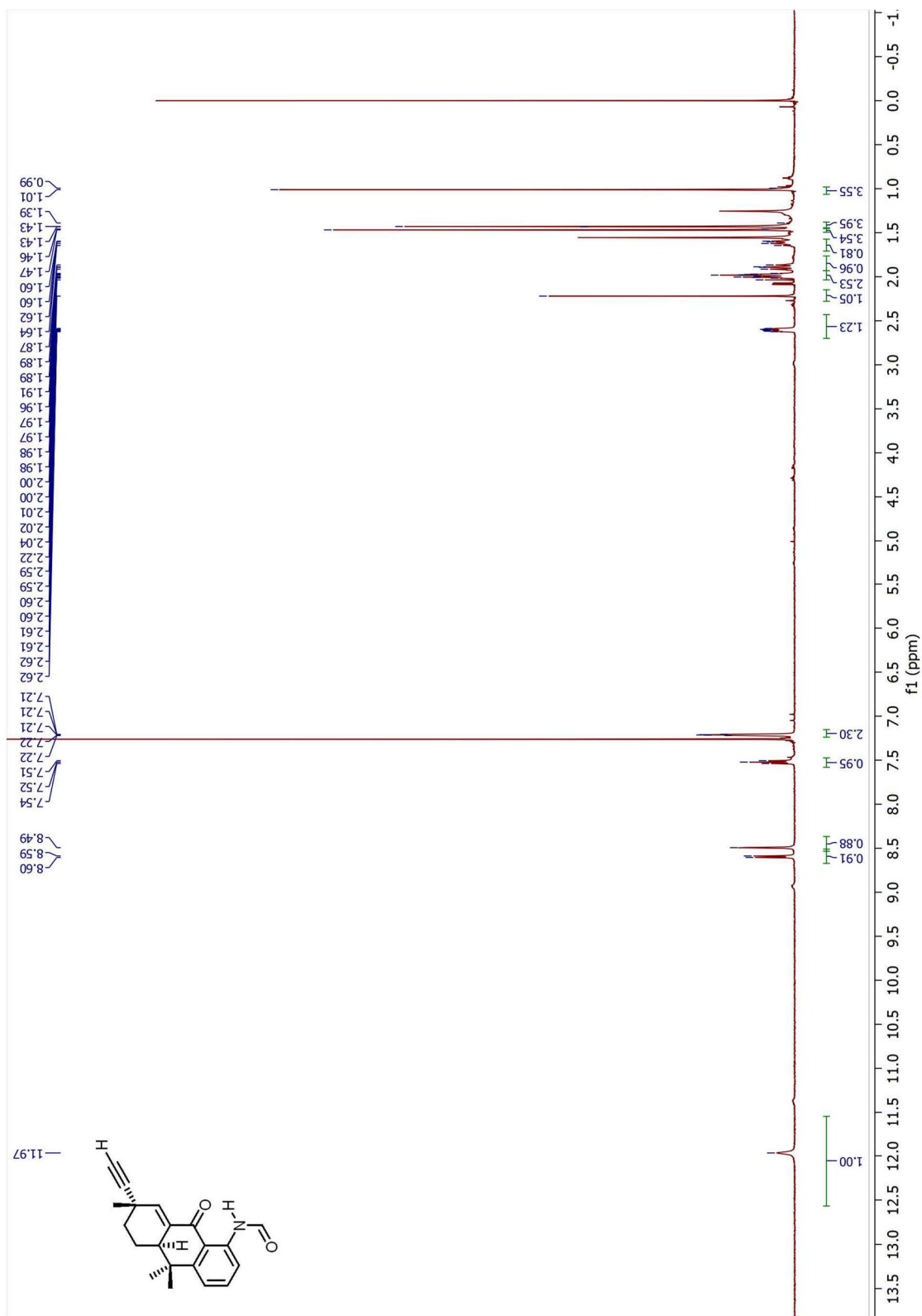


Figure 7.30 ^1H NMR Spectrum of **2.41** (500 MHz, CDCl_3)

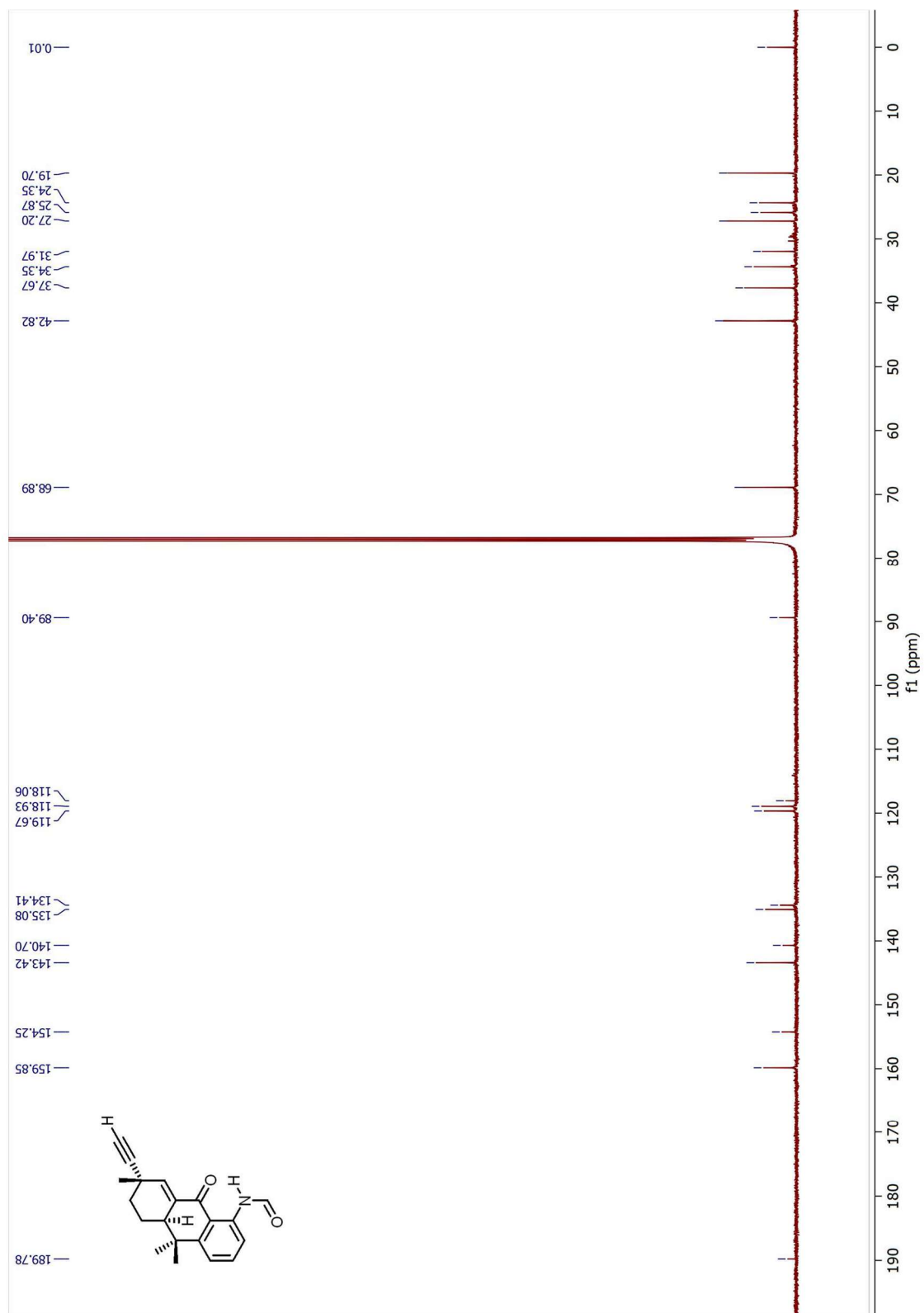


Figure 7.31 ^{13}C NMR Spectrum of **2.41** (125 MHz, CDCl_3)

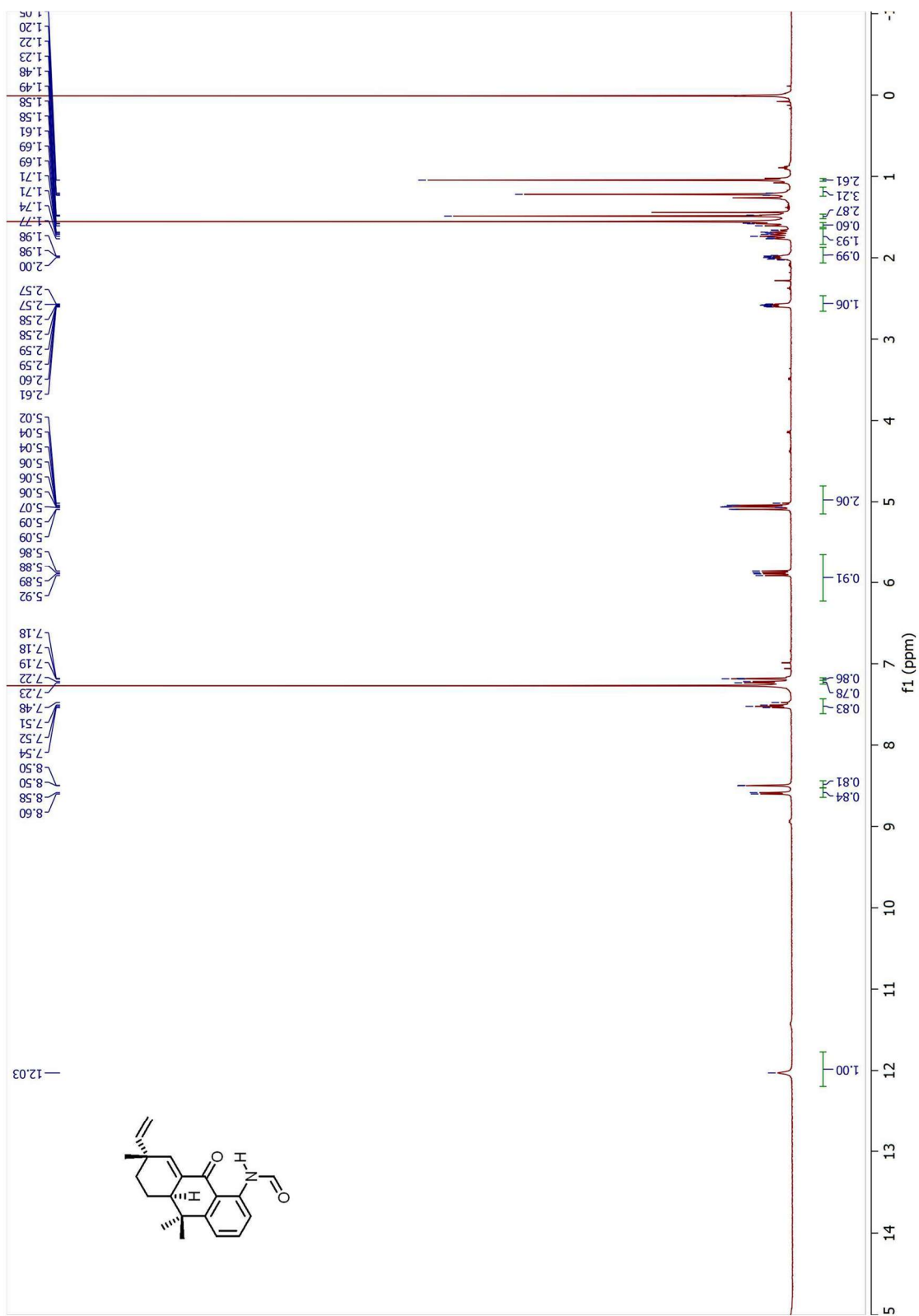


Figure 7.32 ^1H NMR Spectrum of dechlorofontonamide (500 MHz, CDCl_3)

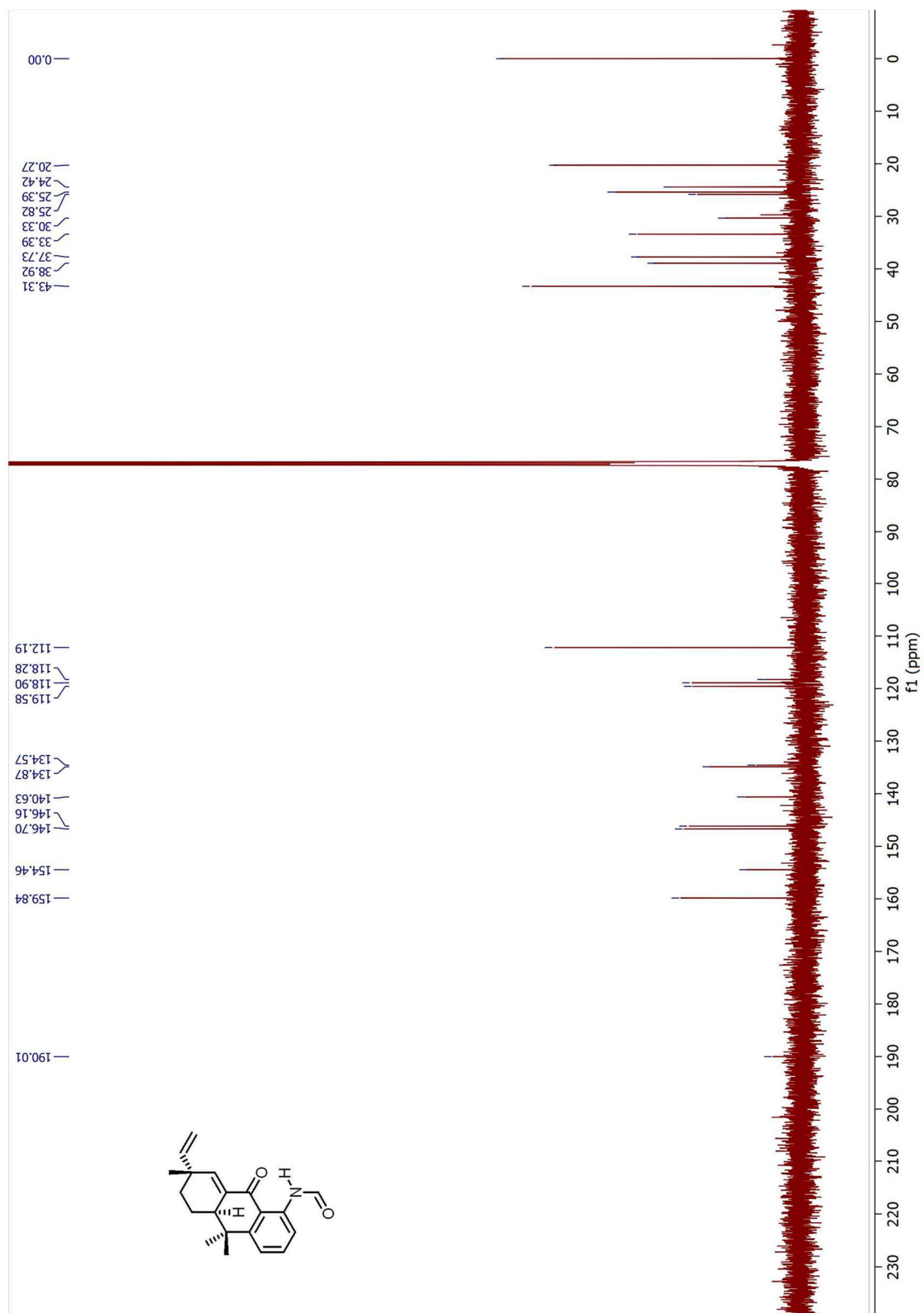


Figure 7.33 ^{13}C NMR Spectrum of dechlorofontonamide (125 MHz, CDCl_3)

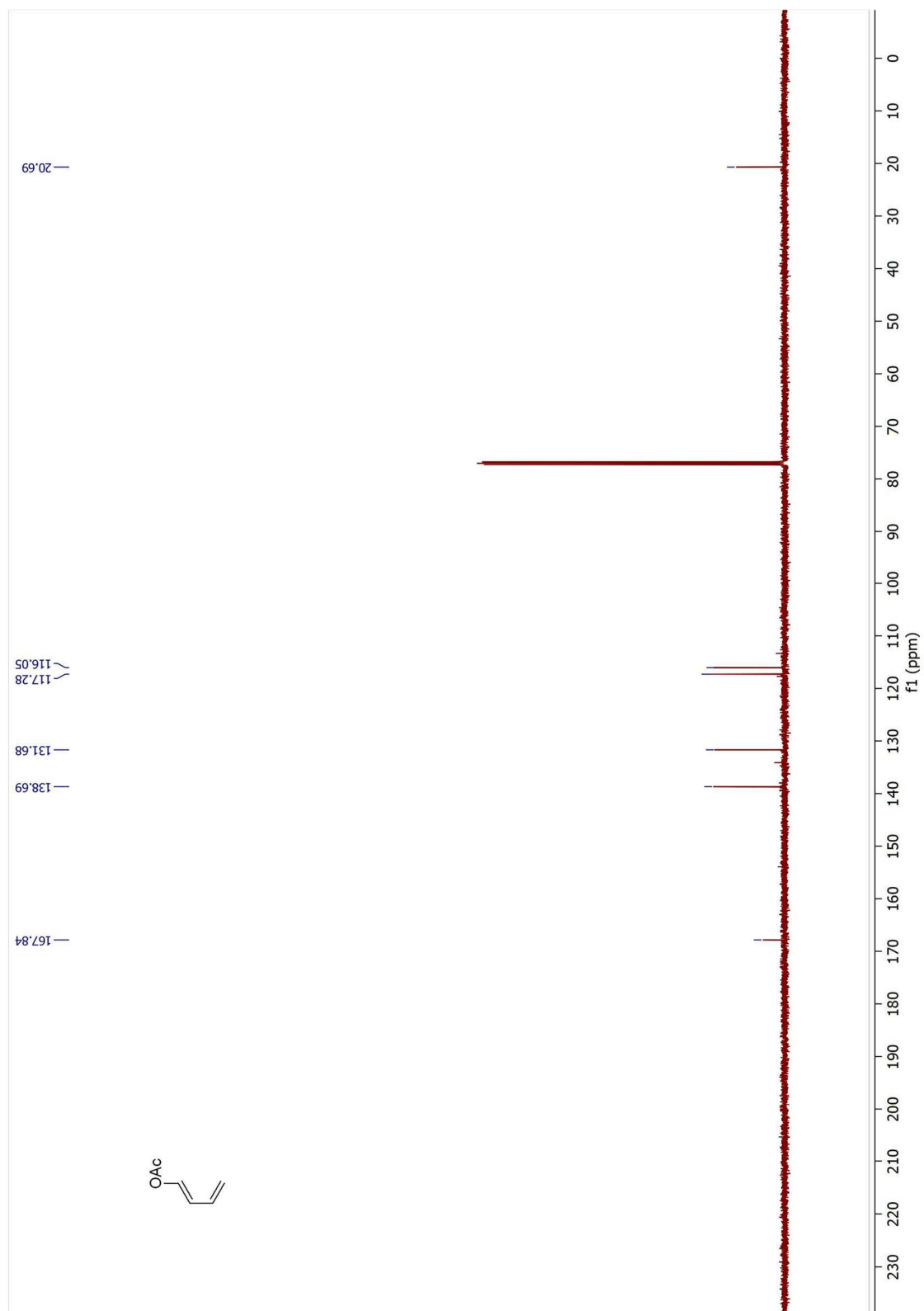


Figure 7.35 ^{13}C NMR Spectrum of **3.32** (125 MHz, CDCl_3)

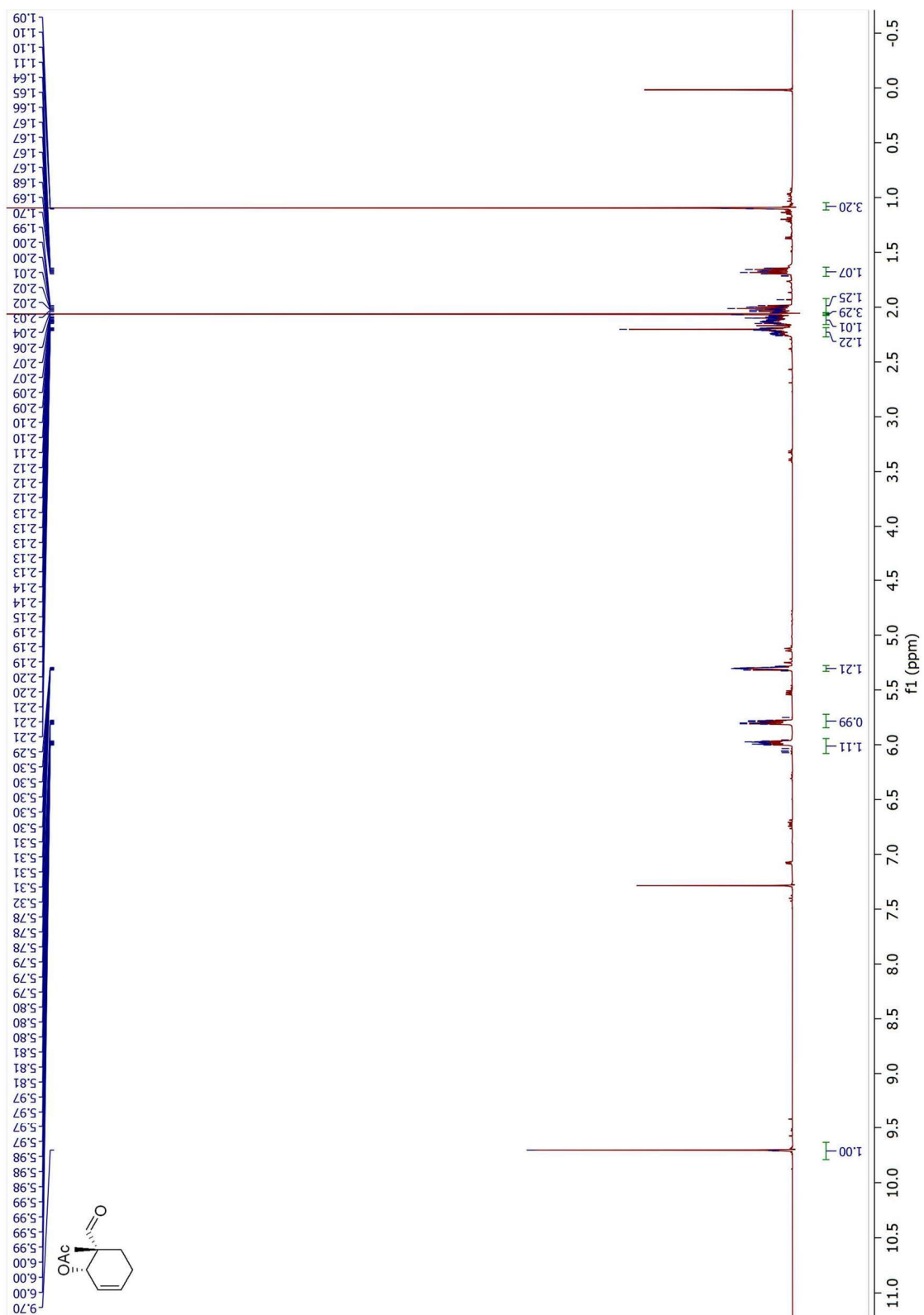


Figure 7.36 ^1H NMR Spectrum of **3.31** (500 MHz, CDCl_3)

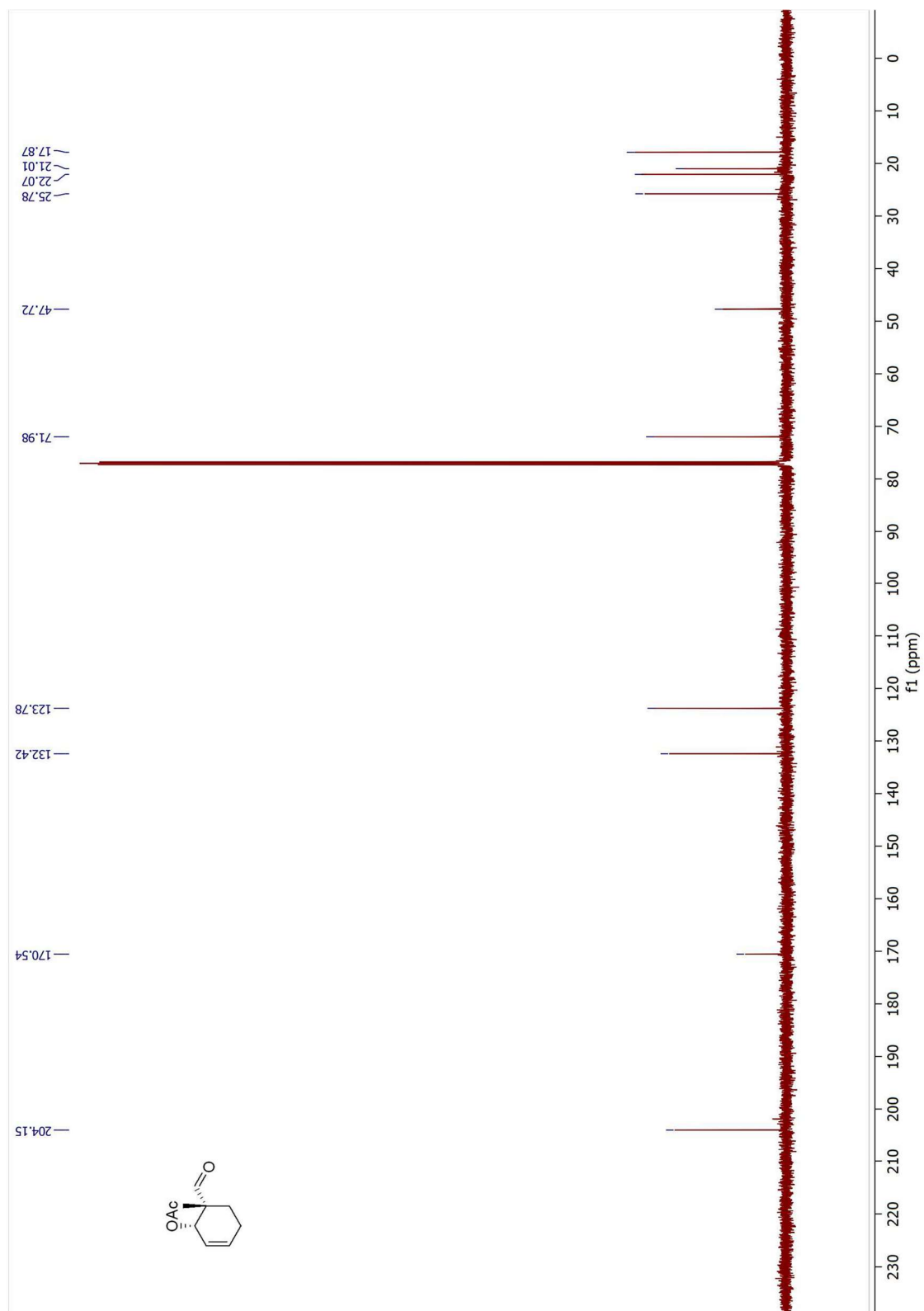


Figure 7.37 ^{13}C NMR Spectrum of **3.31** (125 MHz, CDCl_3)

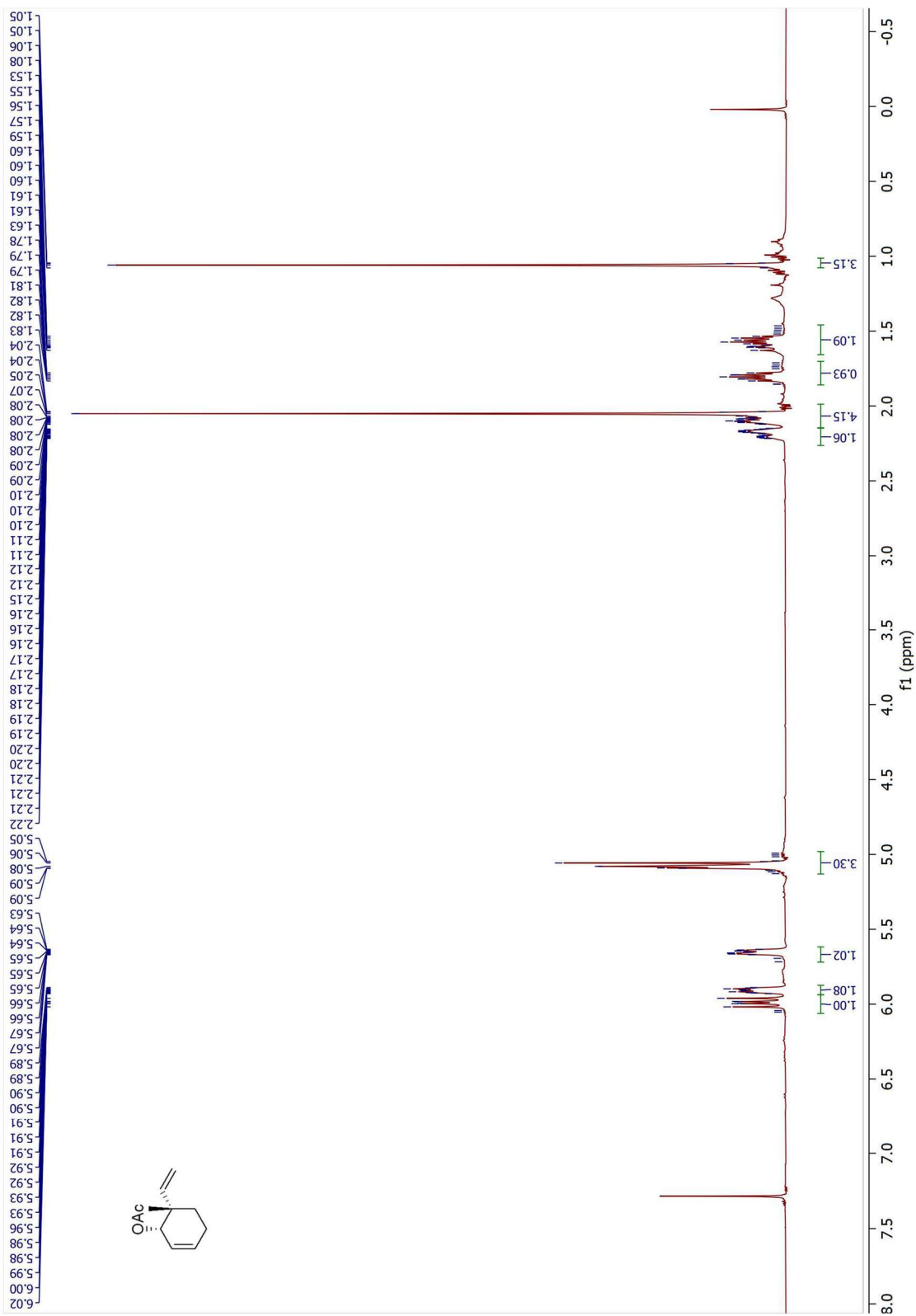


Figure 7.38 ^1H NMR Spectrum of **3.30** (500 MHz, CDCl_3)

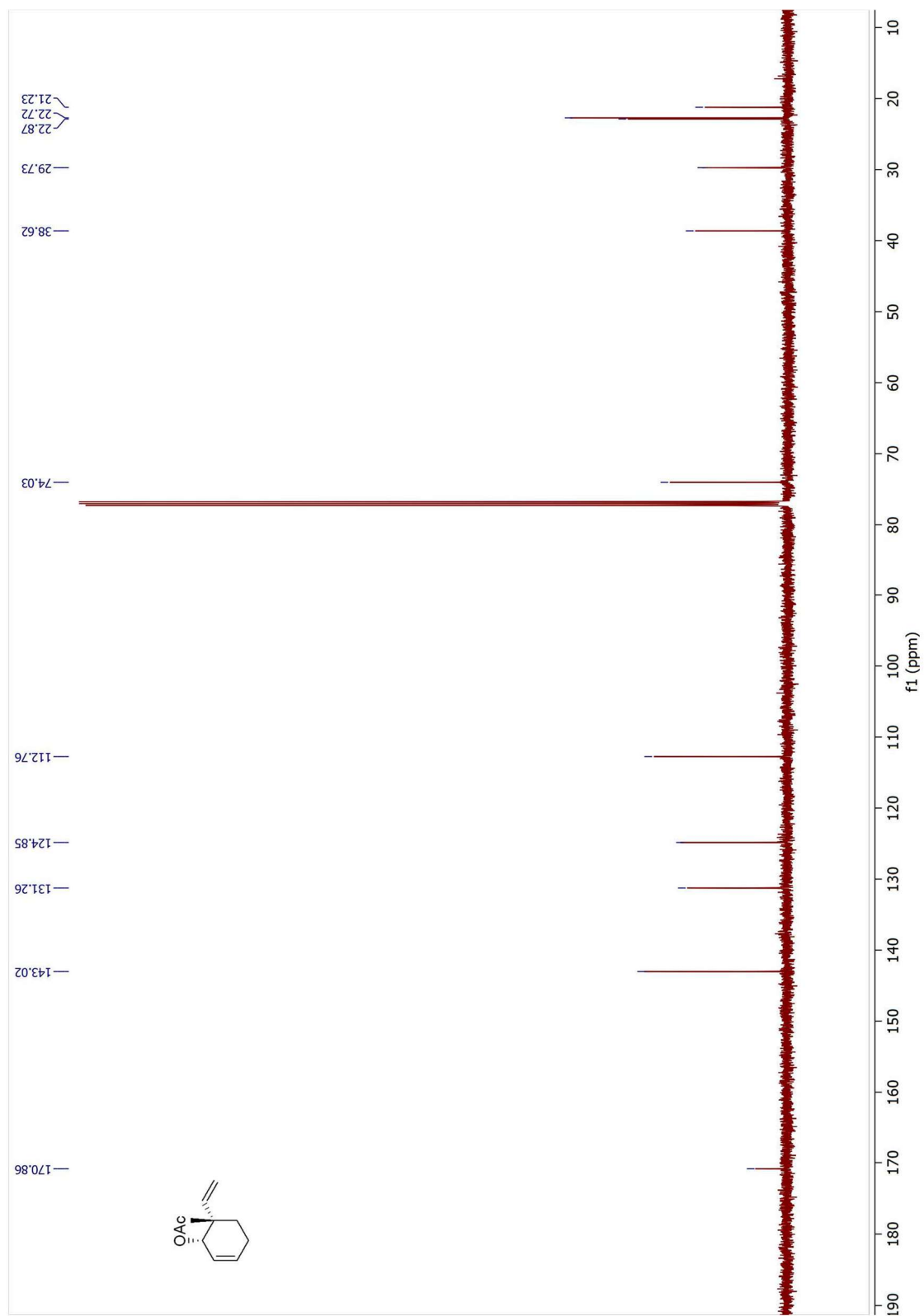


Figure 7.39 ^{13}C NMR Spectrum of **3.30** (125 MHz, CDCl_3)

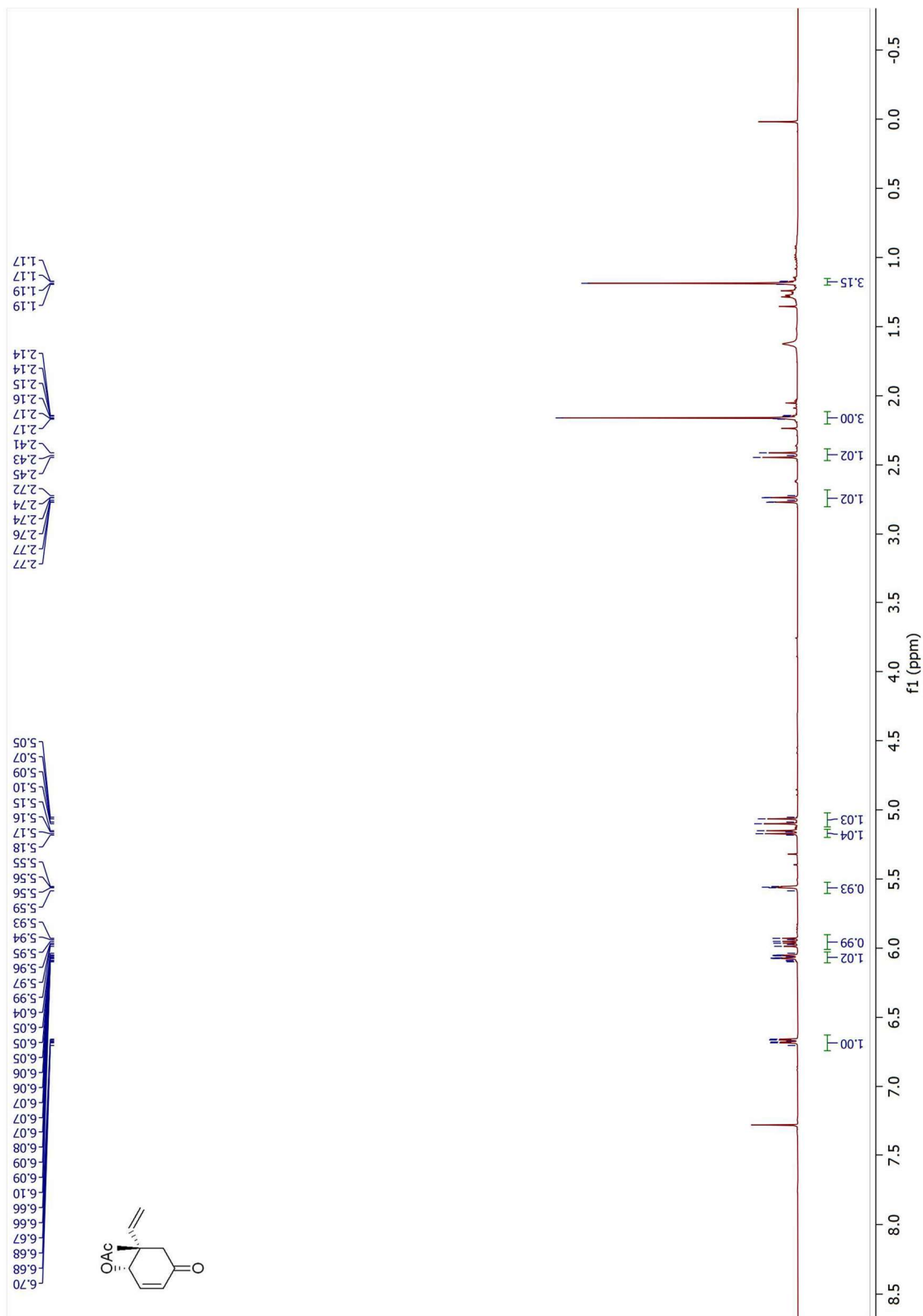


Figure 7.40 ^1H NMR Spectrum of **3.29** (500 MHz, CDCl_3)

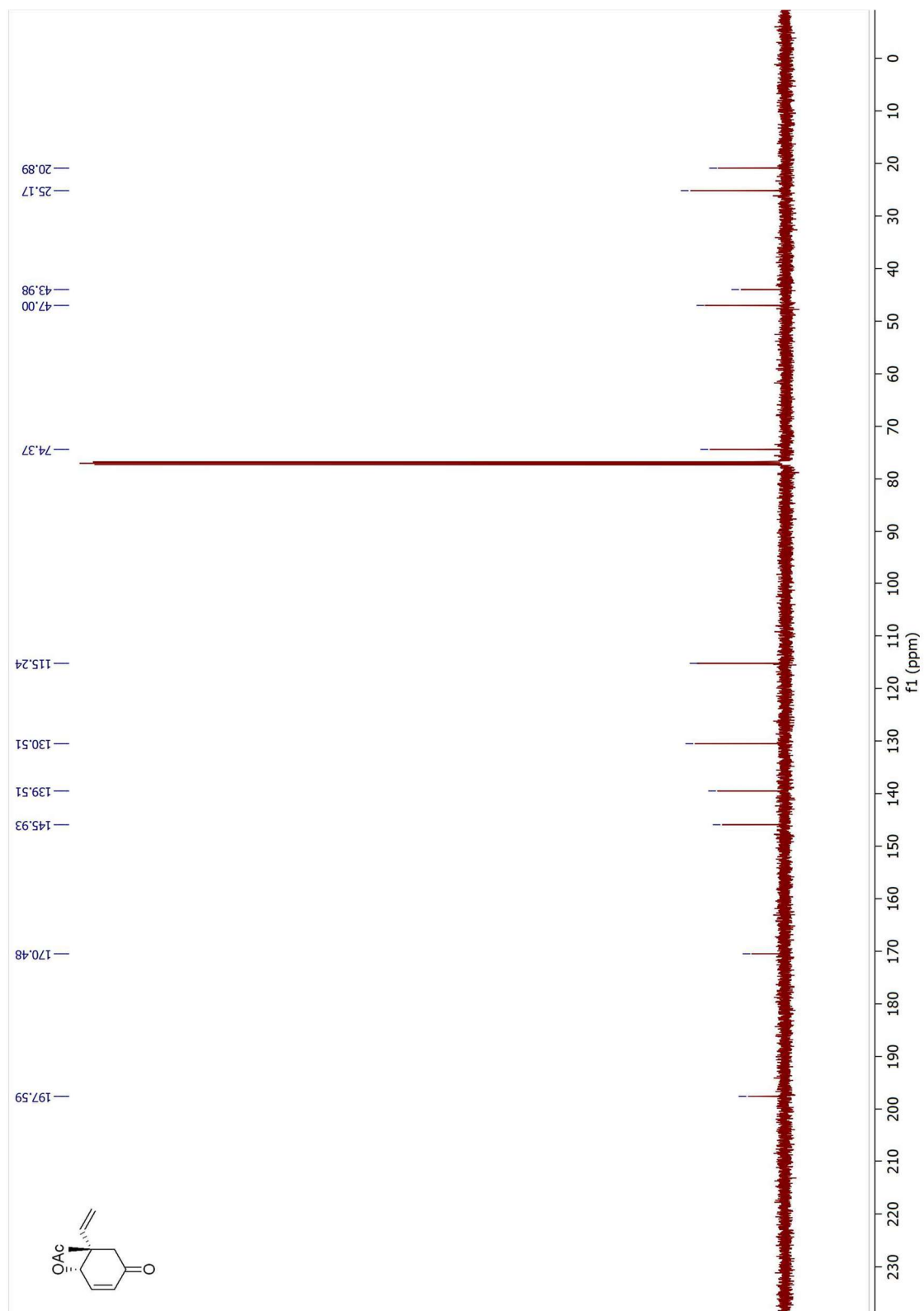


Figure 7.41 ^{13}C NMR Spectrum of **3.29** (125 MHz, CDCl_3)

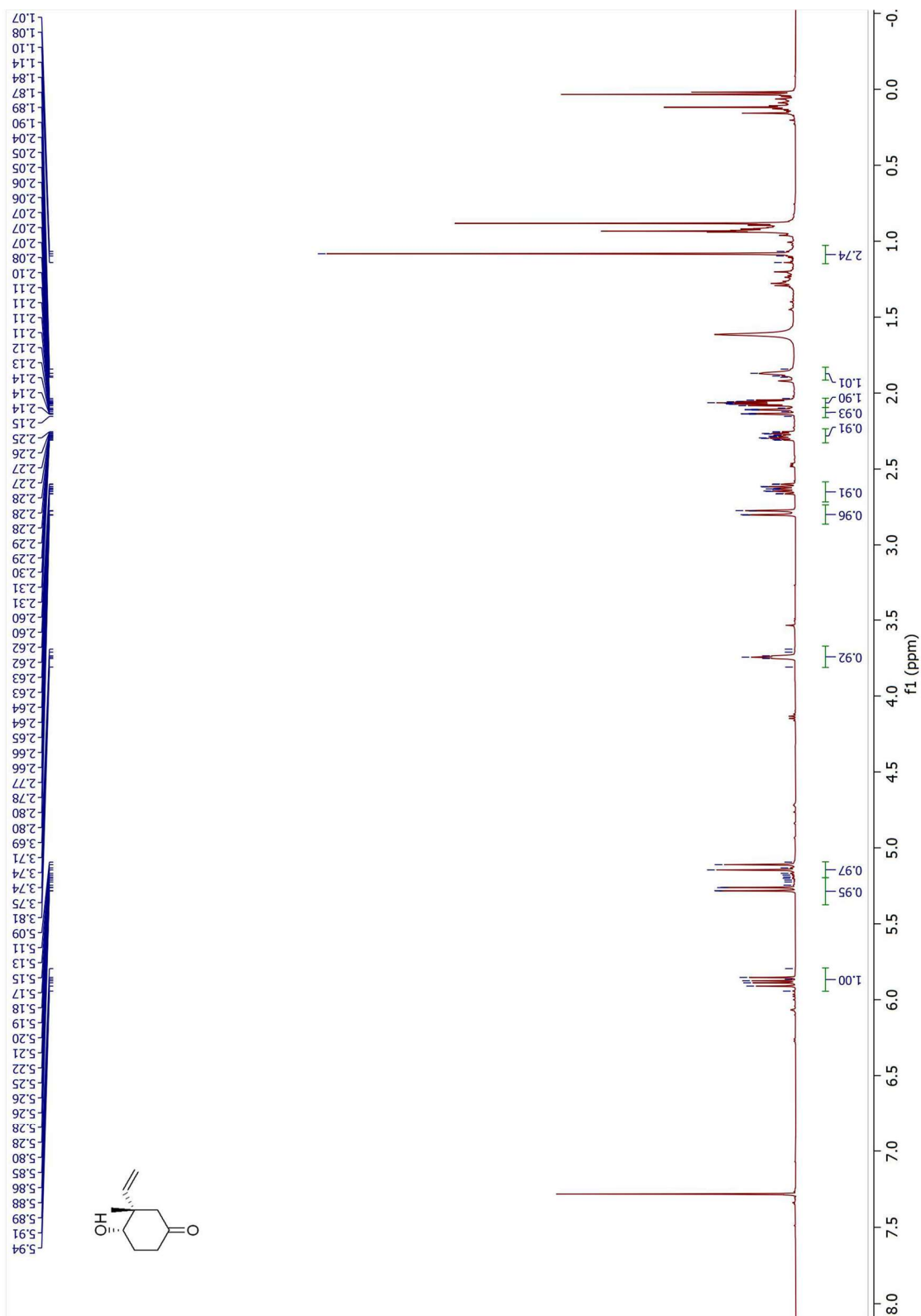


Figure 7.42 ¹H NMR Spectrum of **3.24-d** (500 MHz, CDCl₃)

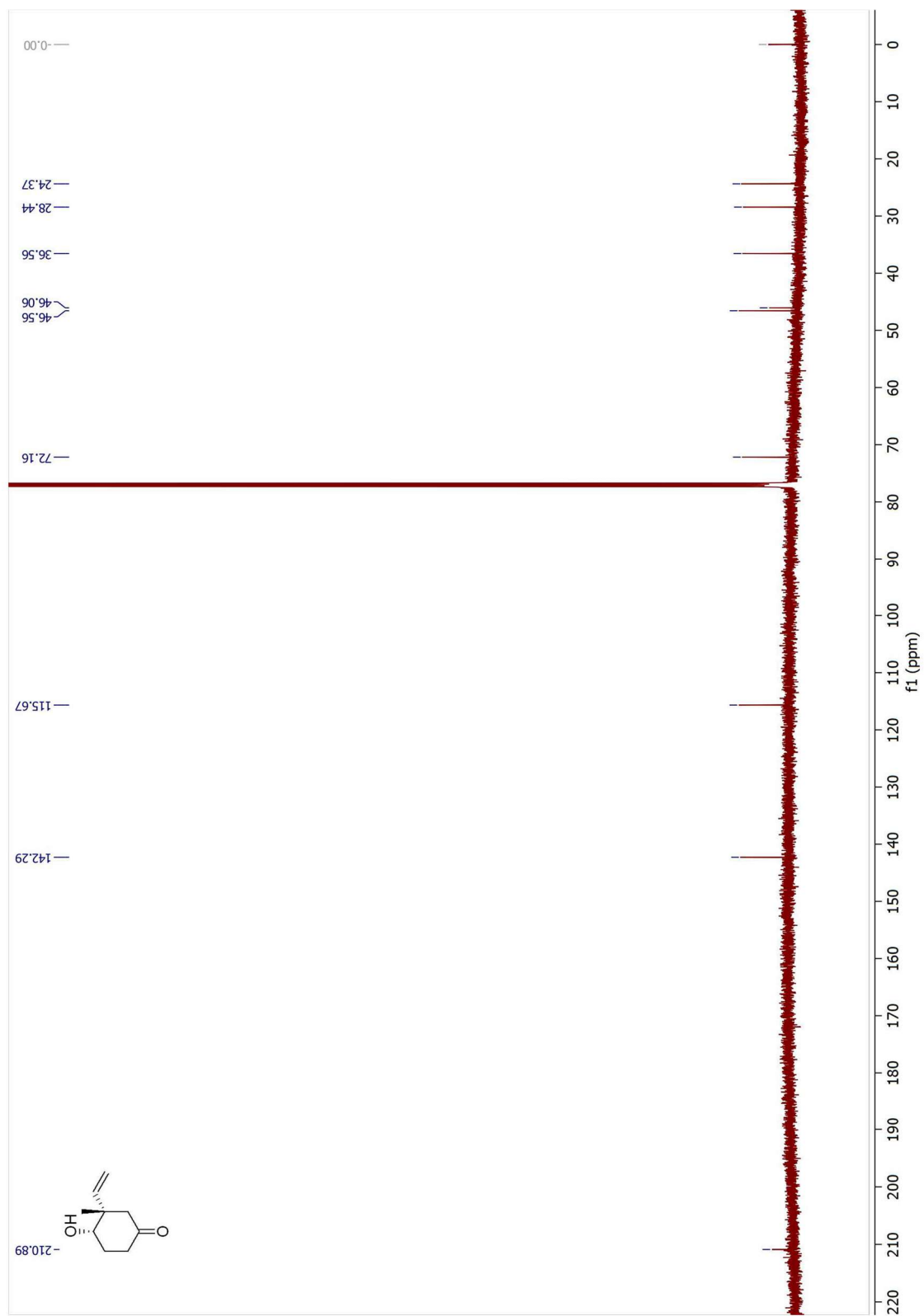


Figure 7.43 ^{13}C NMR Spectrum of **3.24-d** (125 MHz, CDCl_3)

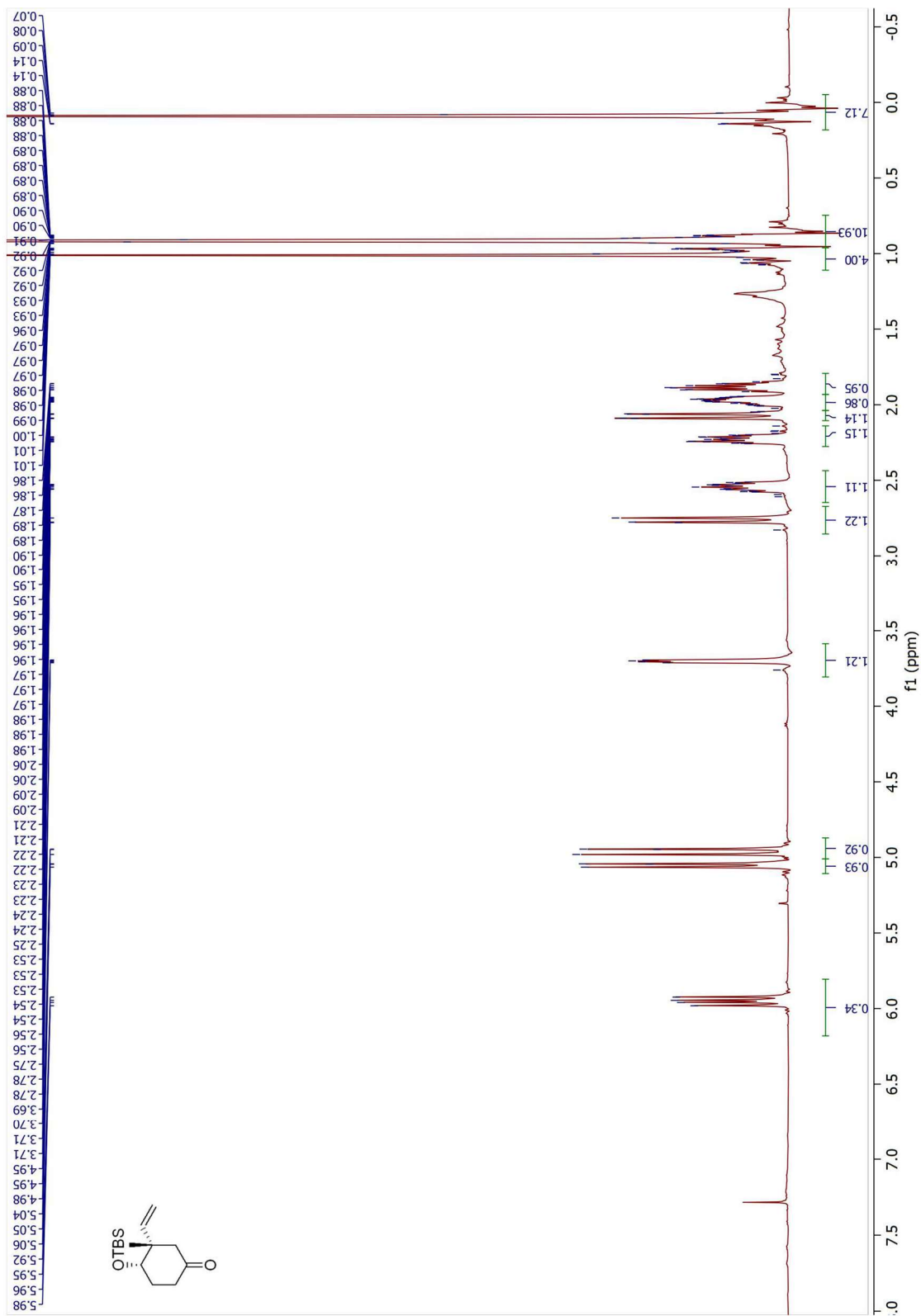


Figure 7.44 ^1H NMR Spectrum of **3.24-a** (500 MHz, CDCl_3)

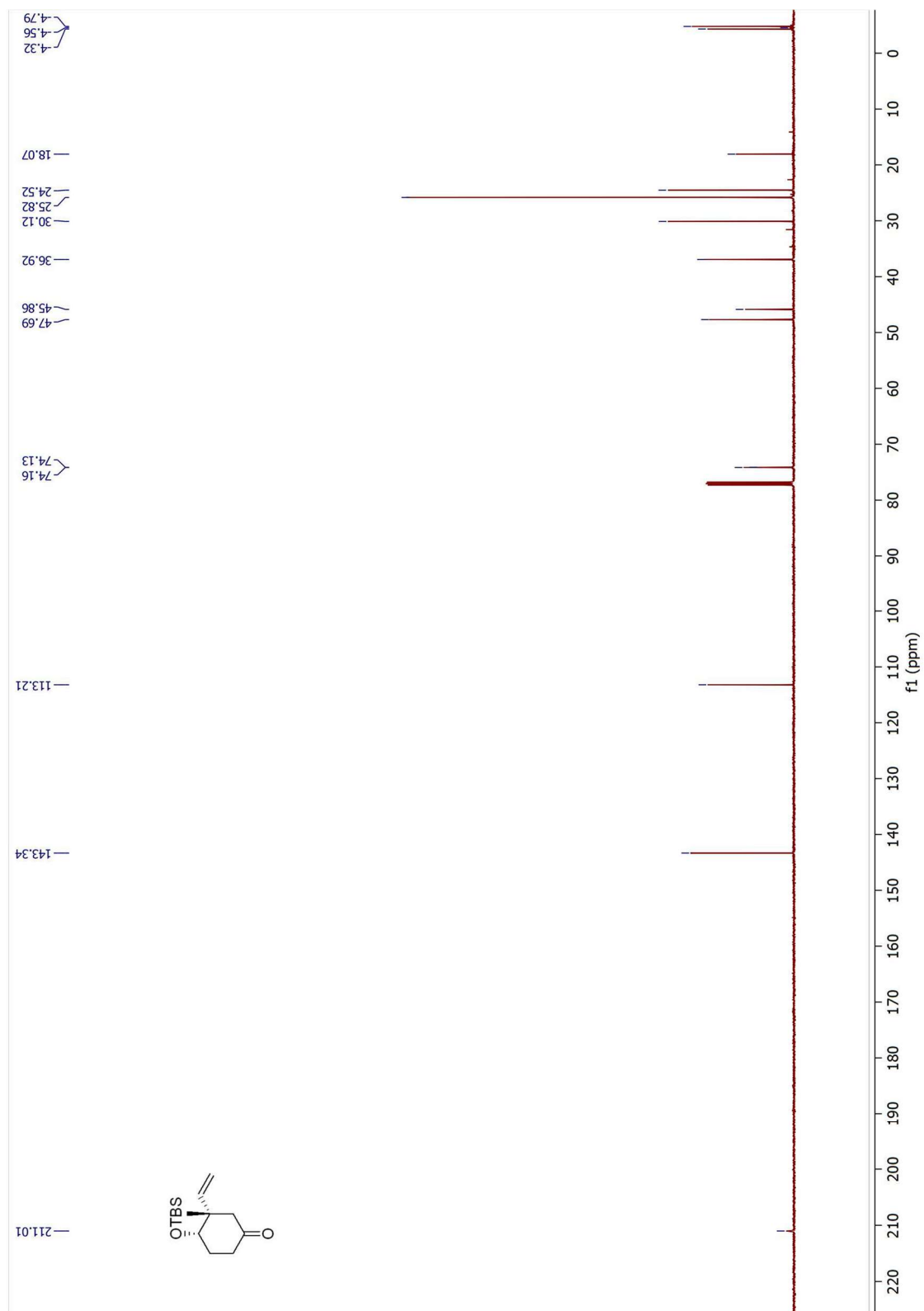


Figure 7.45 ^{13}C NMR Spectrum of **3.24-a** (125 MHz, CDCl_3)

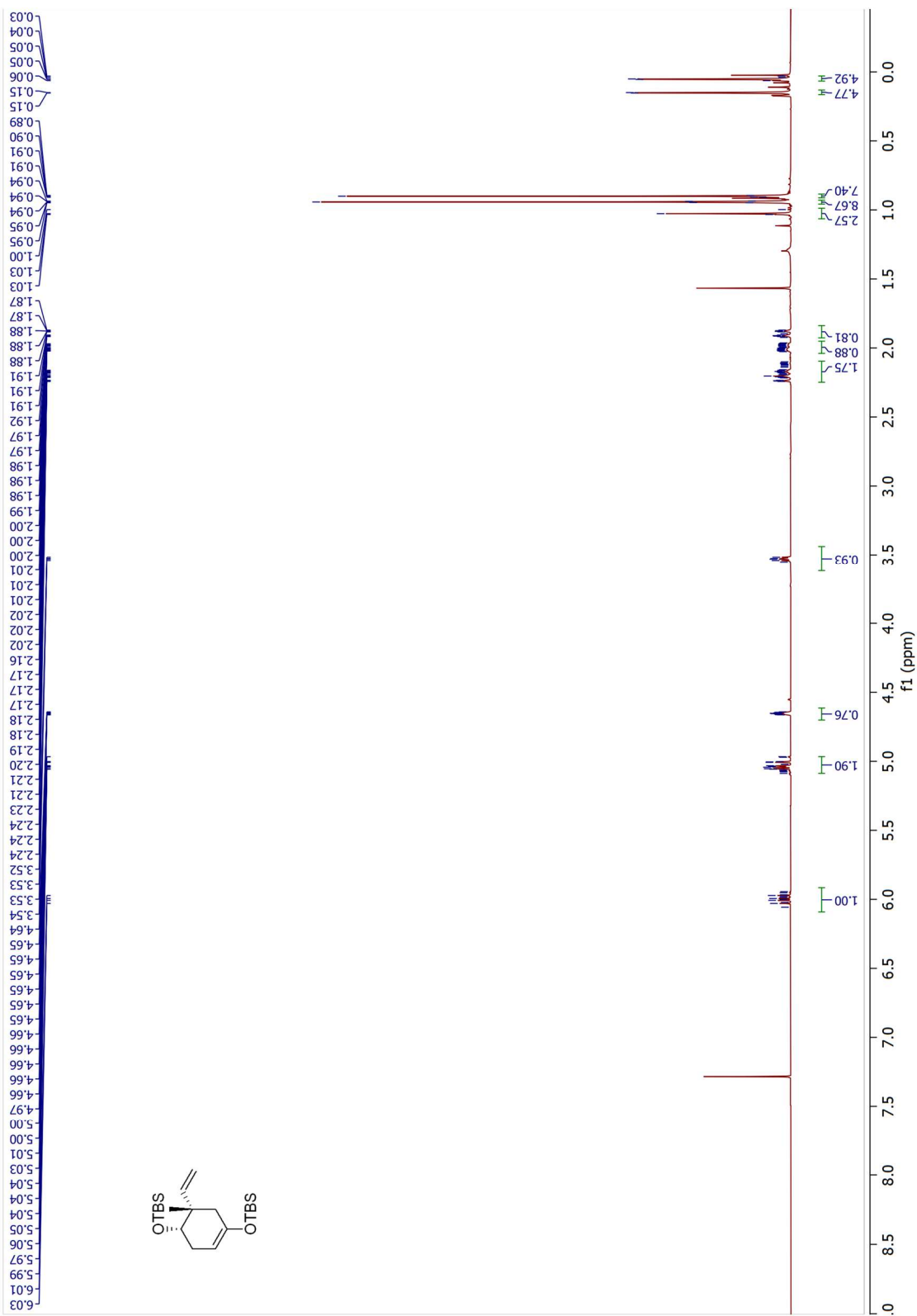


Figure 7.46 ¹H NMR Spectrum of 3.46-a (500 MHz, CDCl₃)

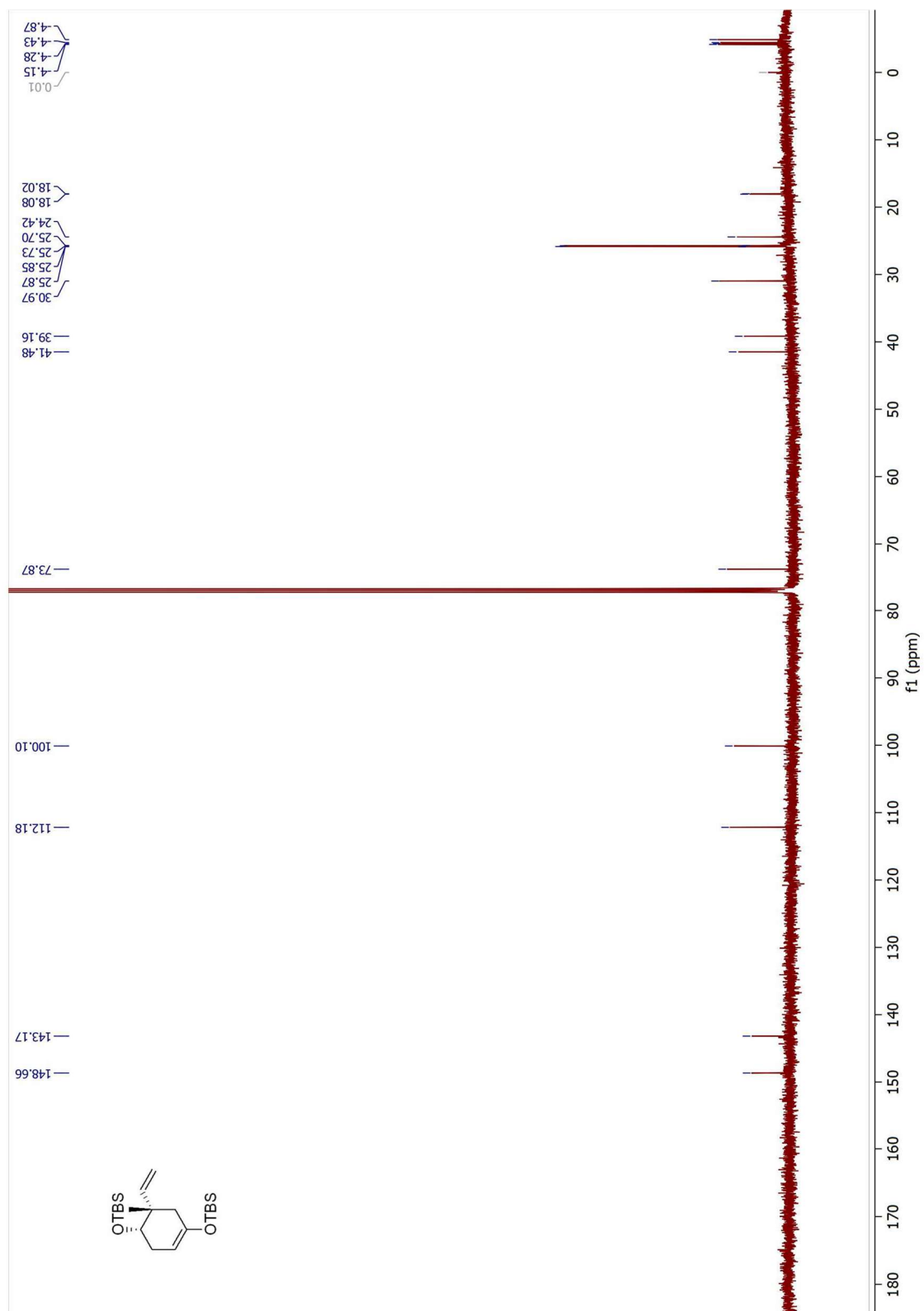


Figure 7.47 ¹³C NMR Spectrum of **3.46-a** (125 MHz, CDCl₃)

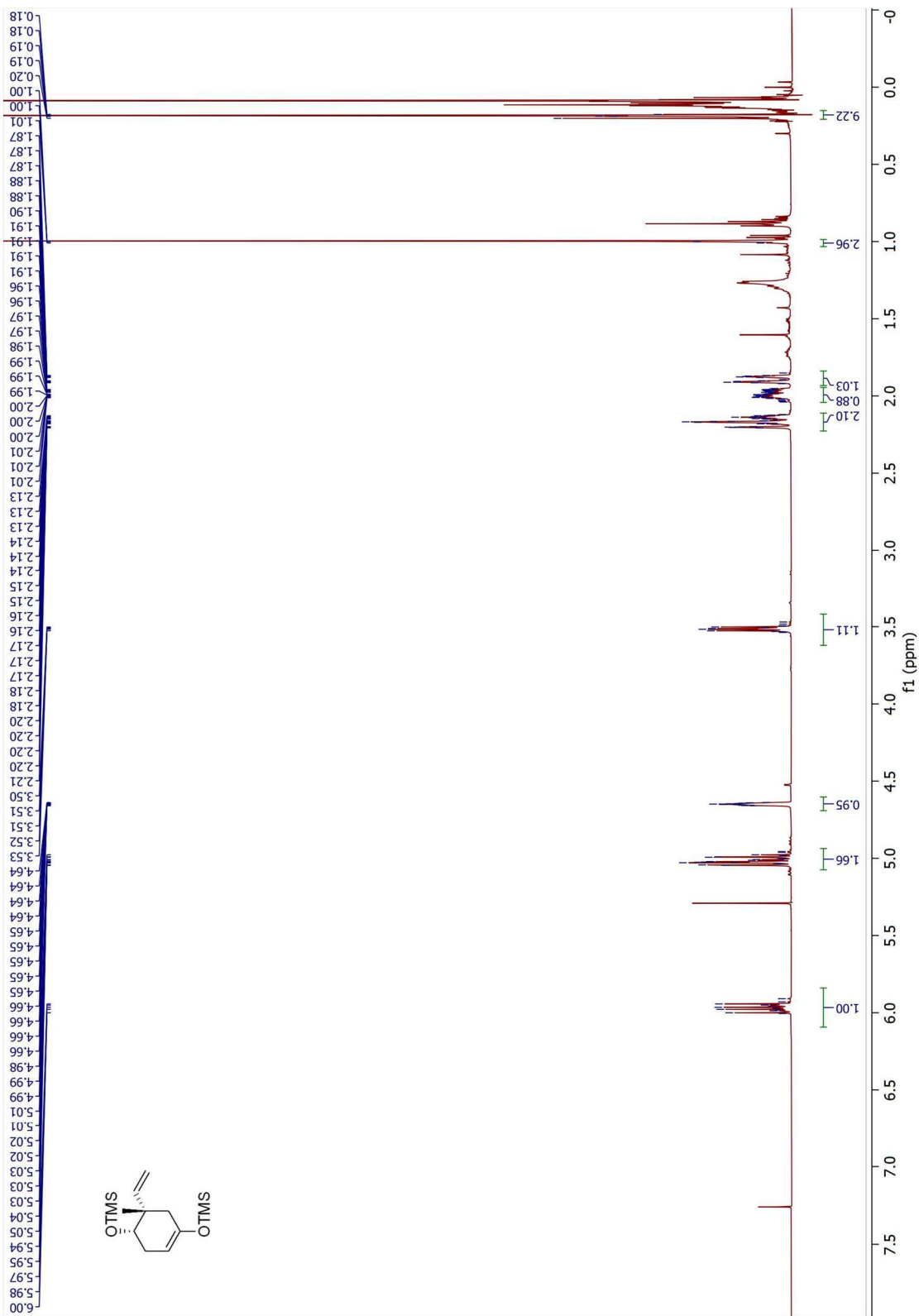


Figure 7.48 ^1H NMR Spectrum of 3.48 (500 MHz, CDCl_3)

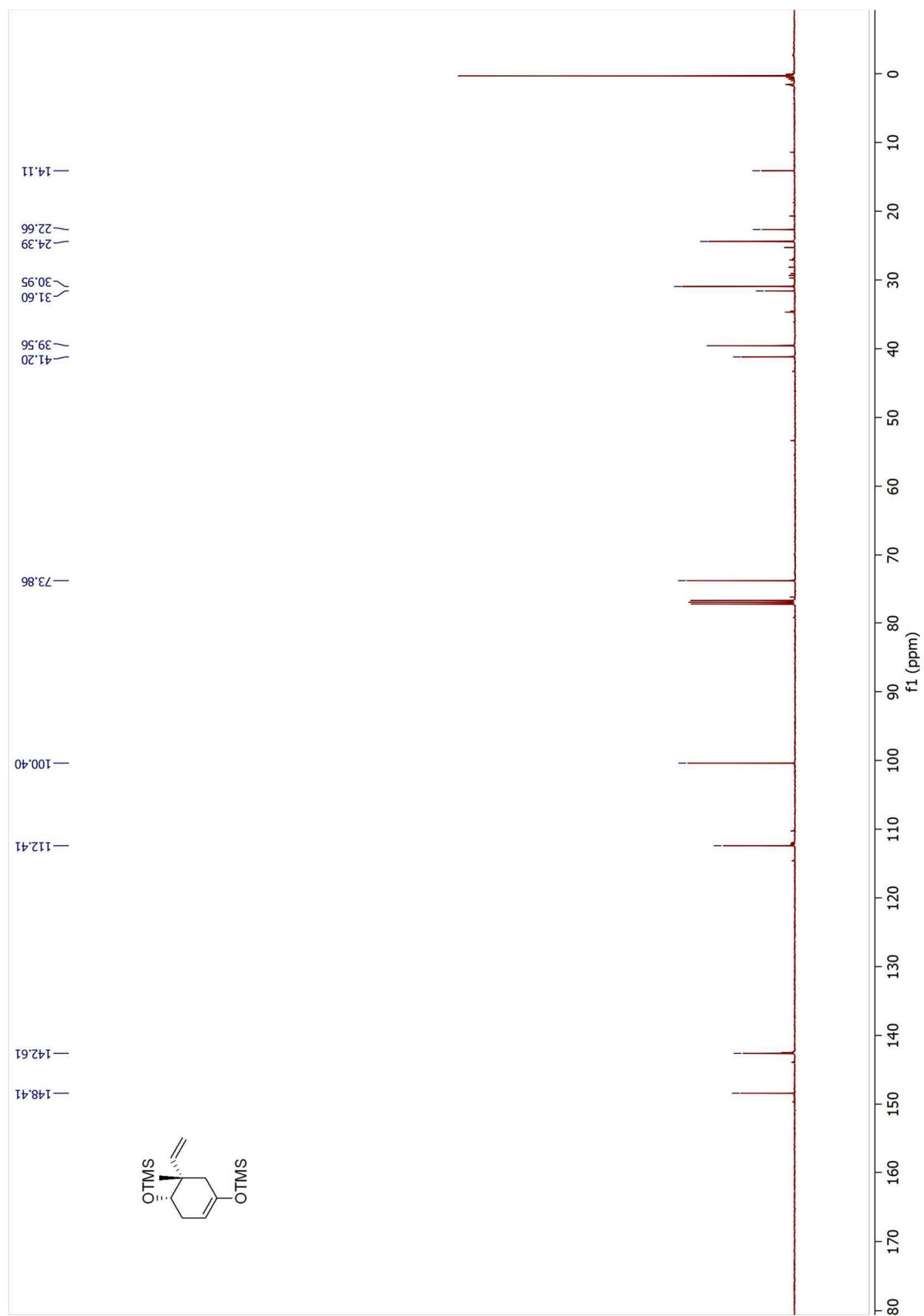


Figure 7.49 ^{13}C NMR Spectrum of **3.48** (125 MHz, CDCl_3)

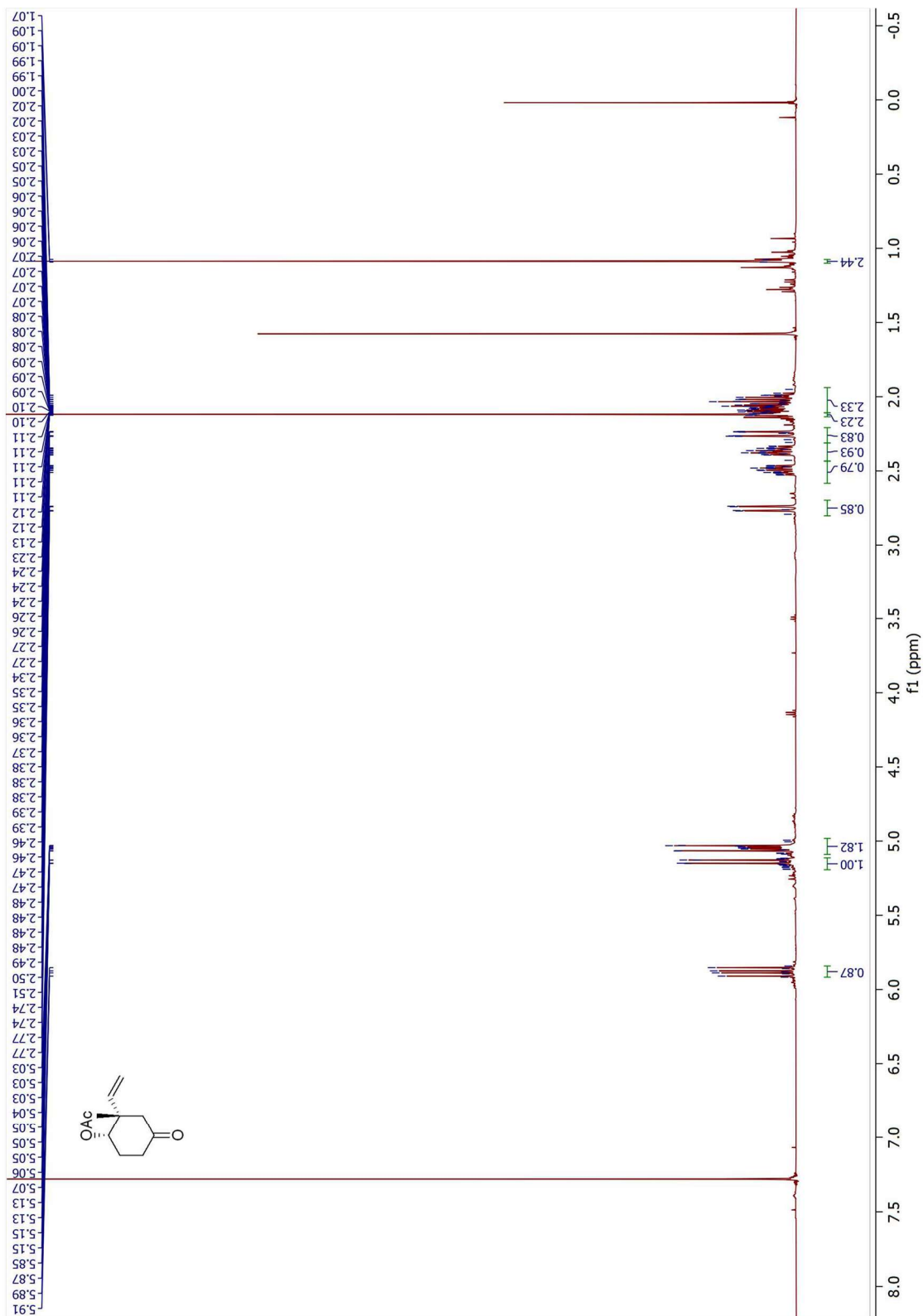


Figure 7.50 ^1H NMR Spectrum of **3.24-c** (500 MHz, CDCl_3)

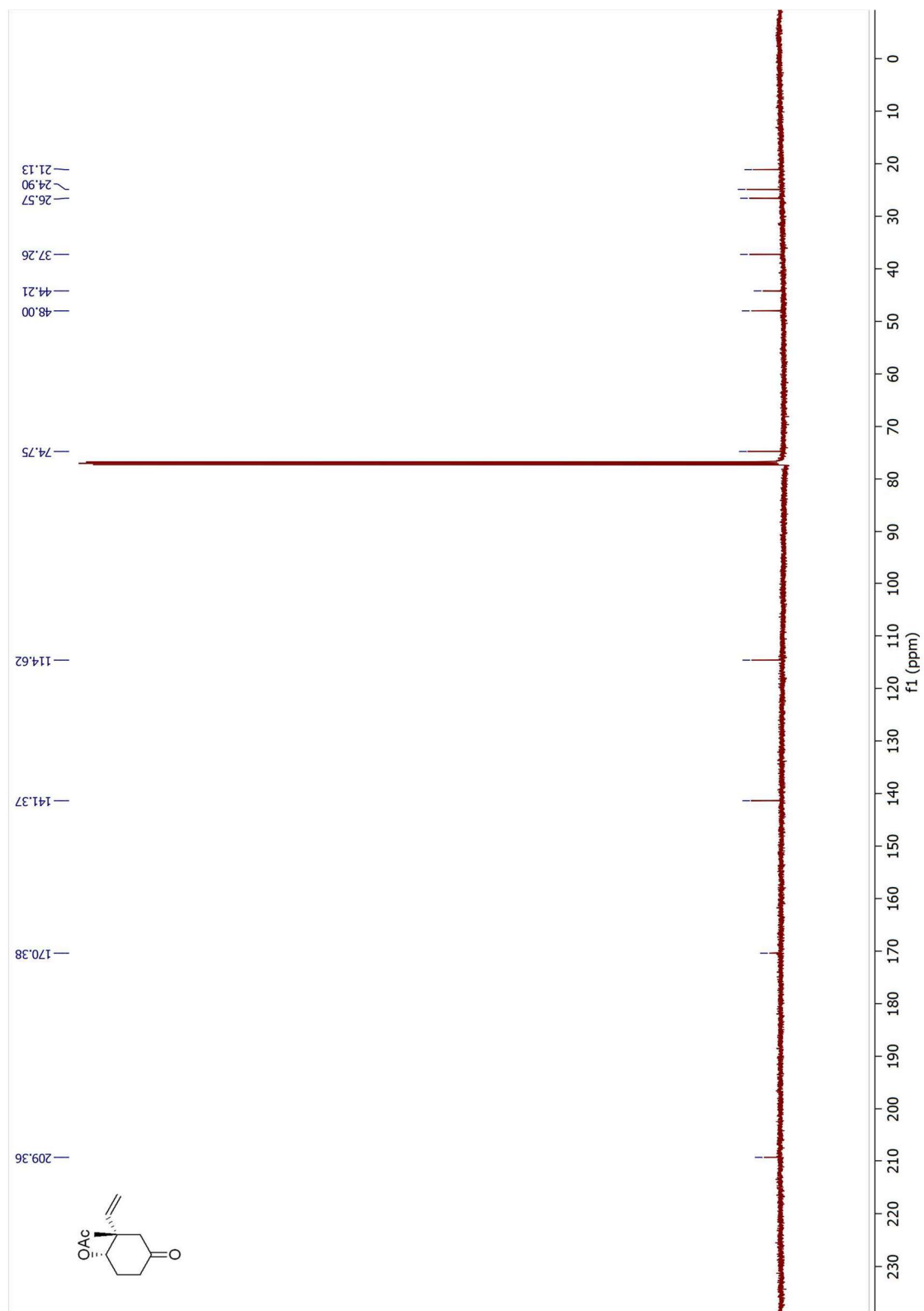


Figure 7.51 ^{13}C NMR Spectrum of **3.24-c** (125 MHz, CDCl_3)

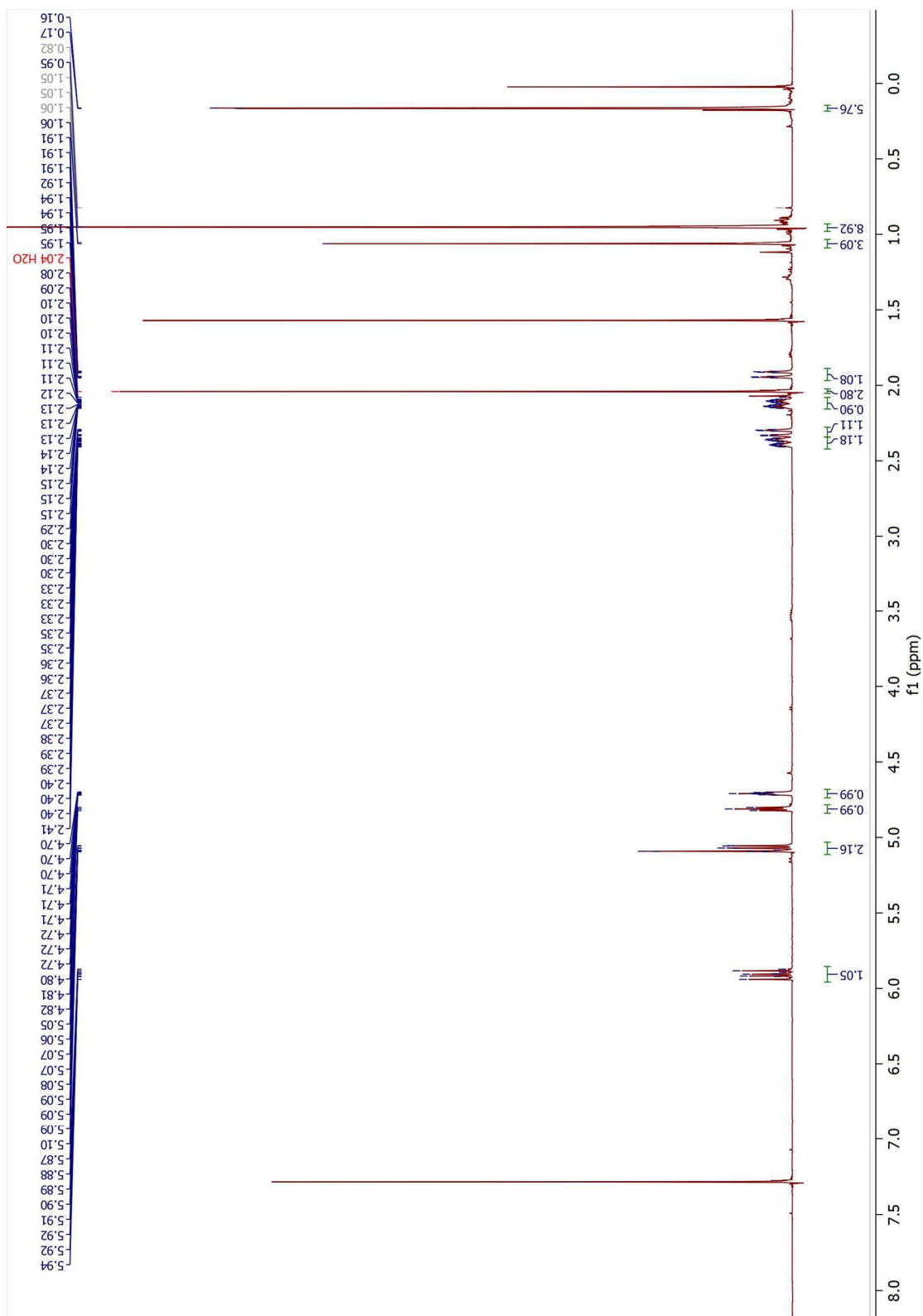


Figure 7.52 ¹H NMR Spectrum of 3.46-c (500 MHz, CDCl₃)

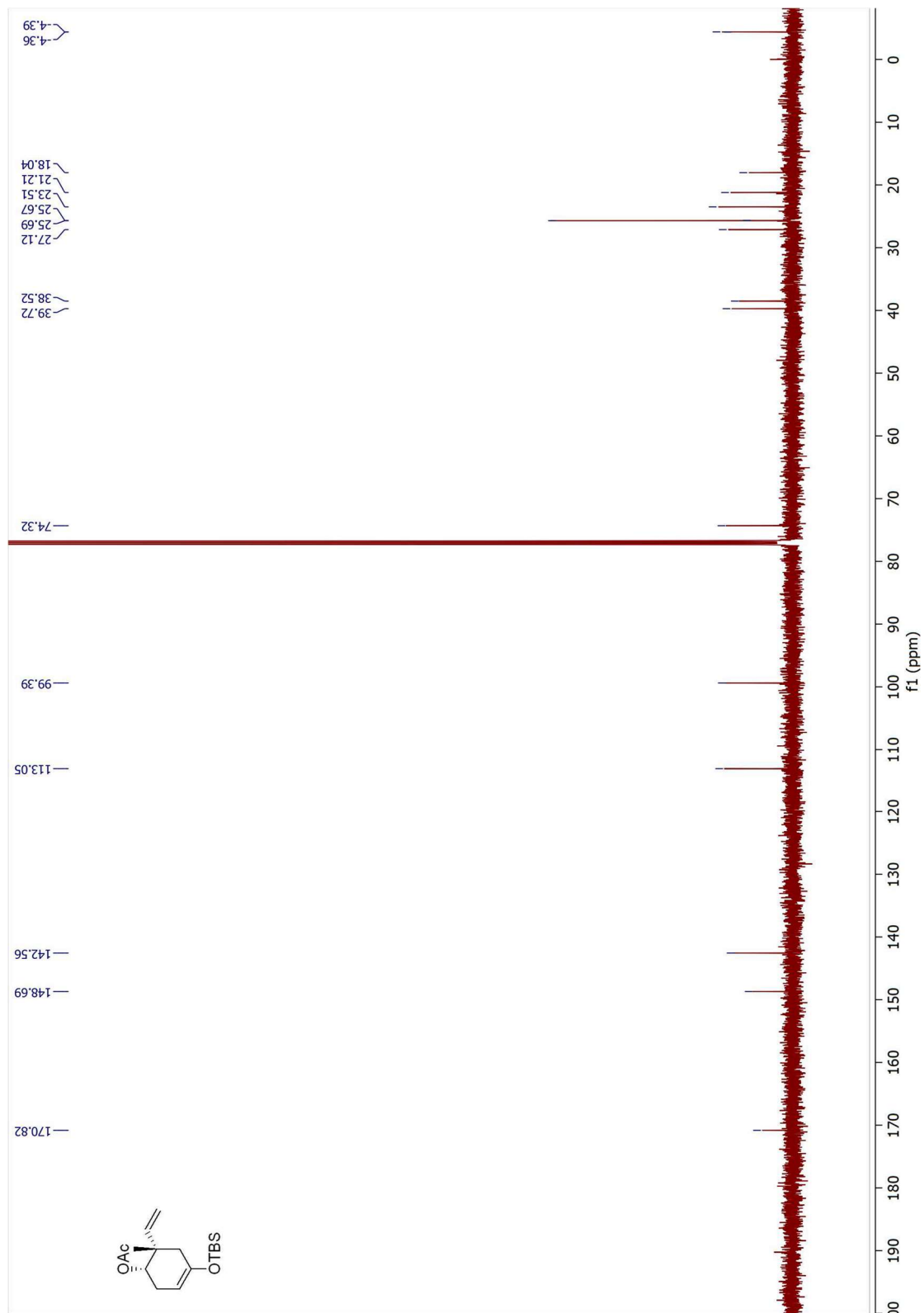


Figure 7.53 ^{13}C NMR Spectrum of **3.46-c** (125 MHz, CDCl_3)

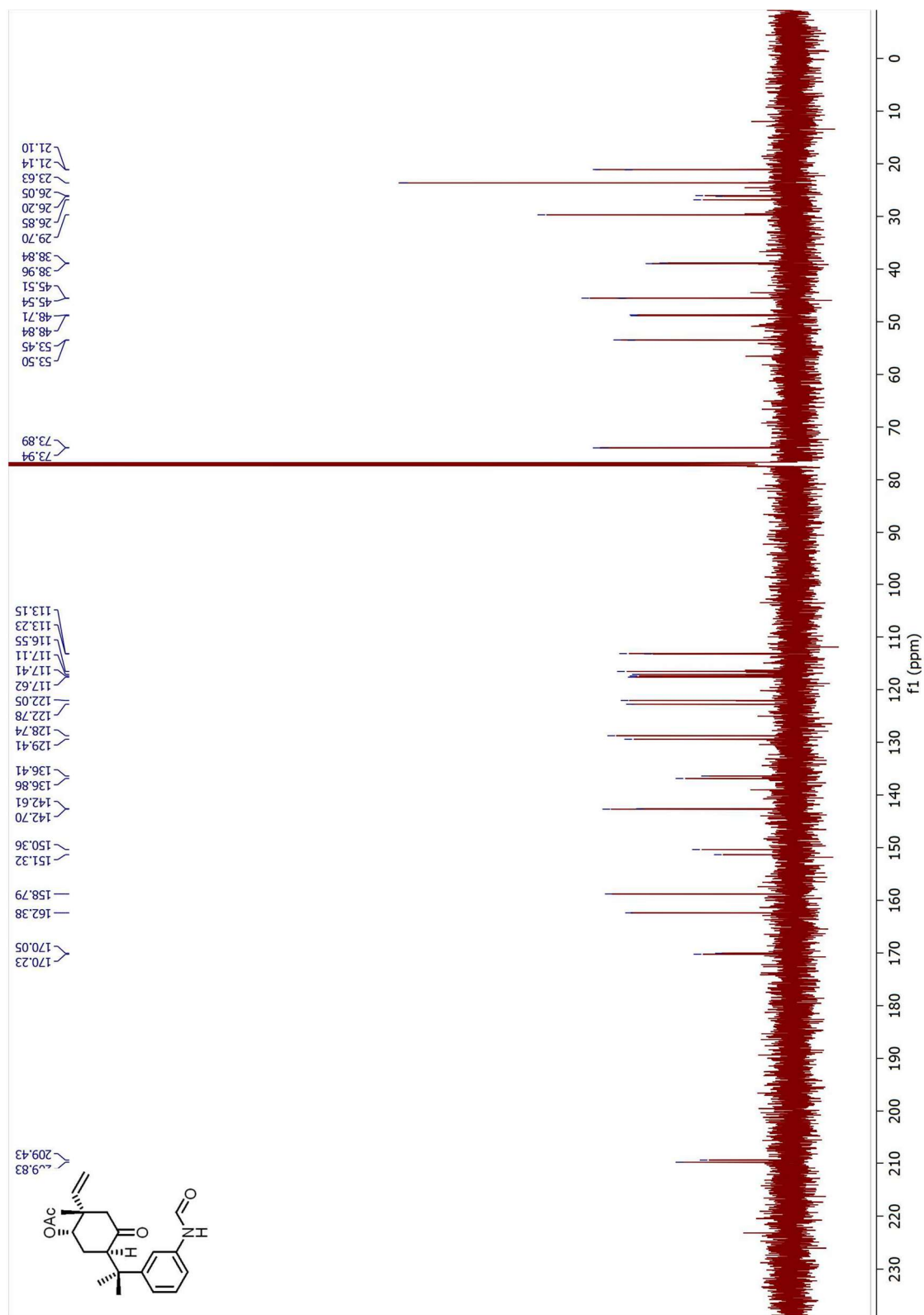


Figure 7.55 ^{13}C NMR Spectrum of 3.47-c (125 MHz, CDCl_3)

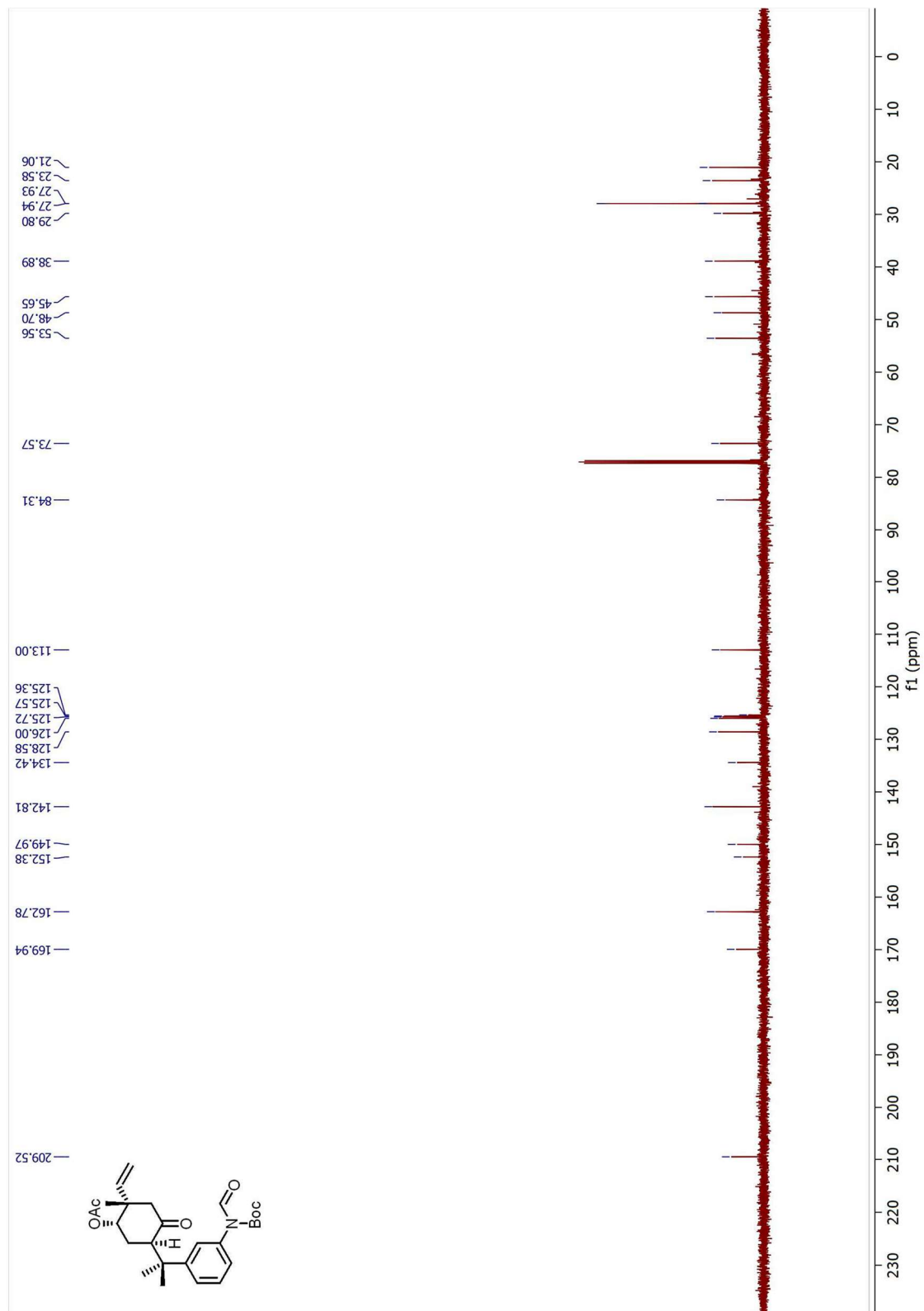
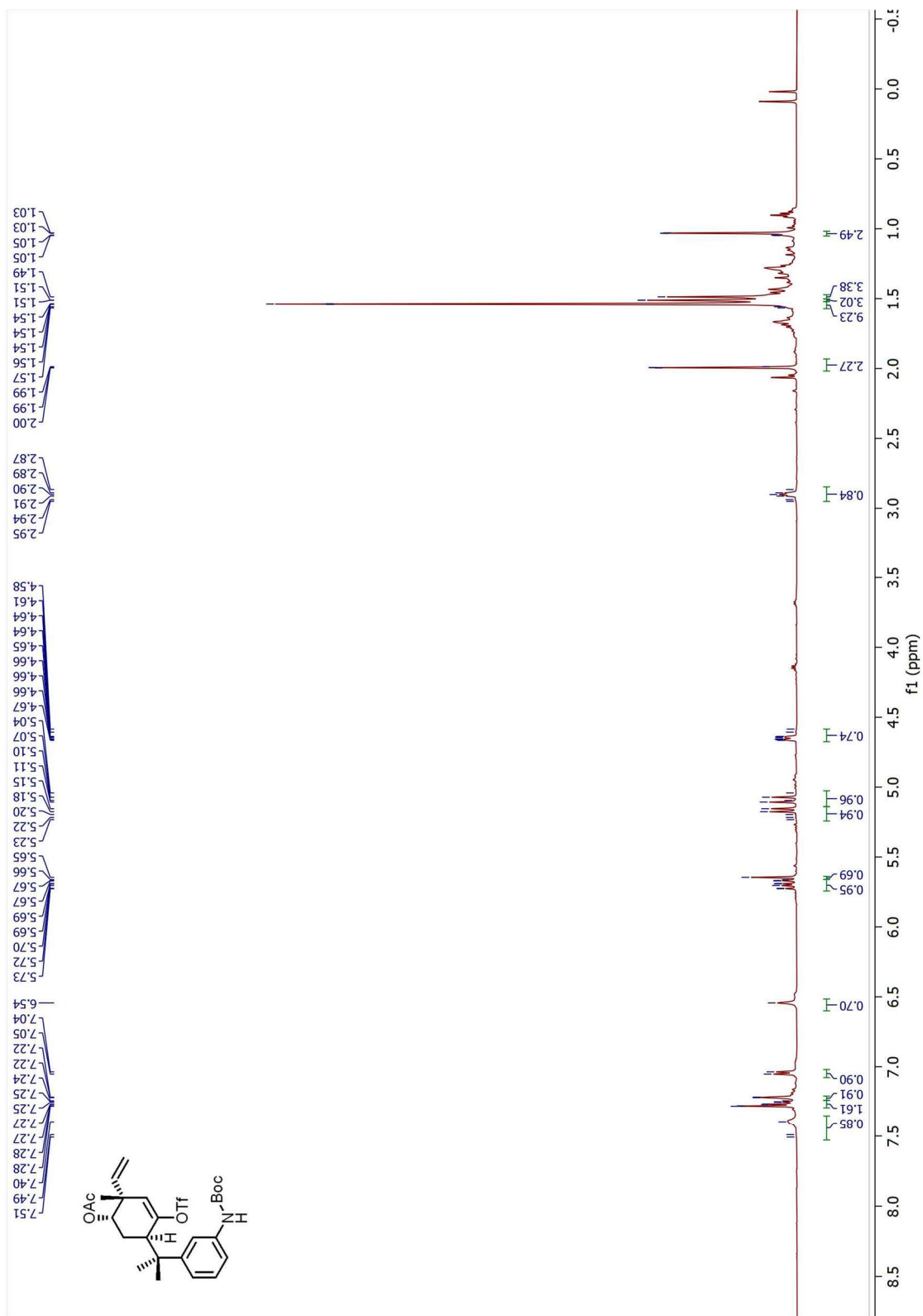


Figure 7.57 ^{13}C NMR Spectrum of **3.61** (125 MHz, CDCl_3)



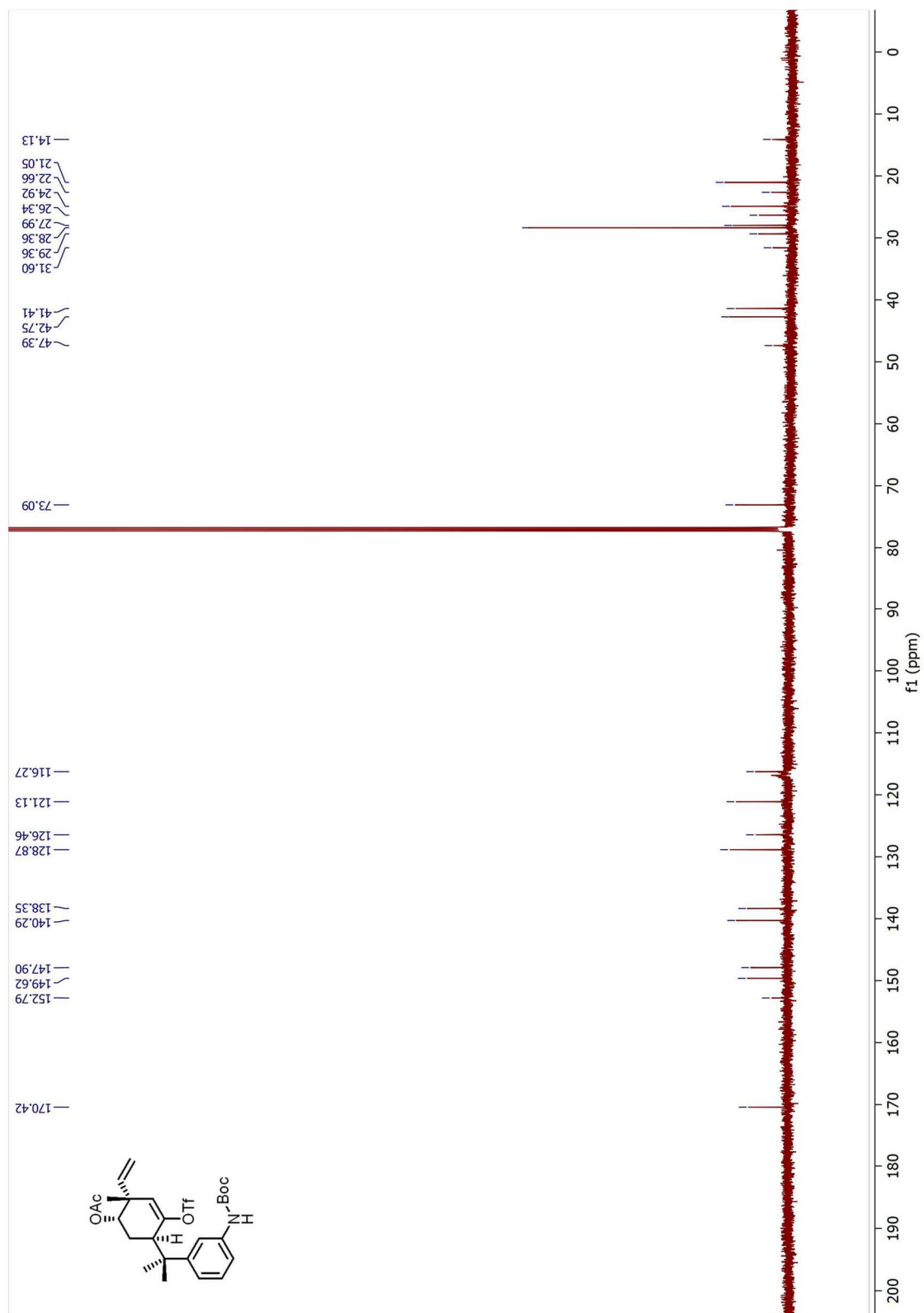


Figure 7.59 ^{13}C NMR Spectrum of **3.63** (125 MHz, CDCl_3)

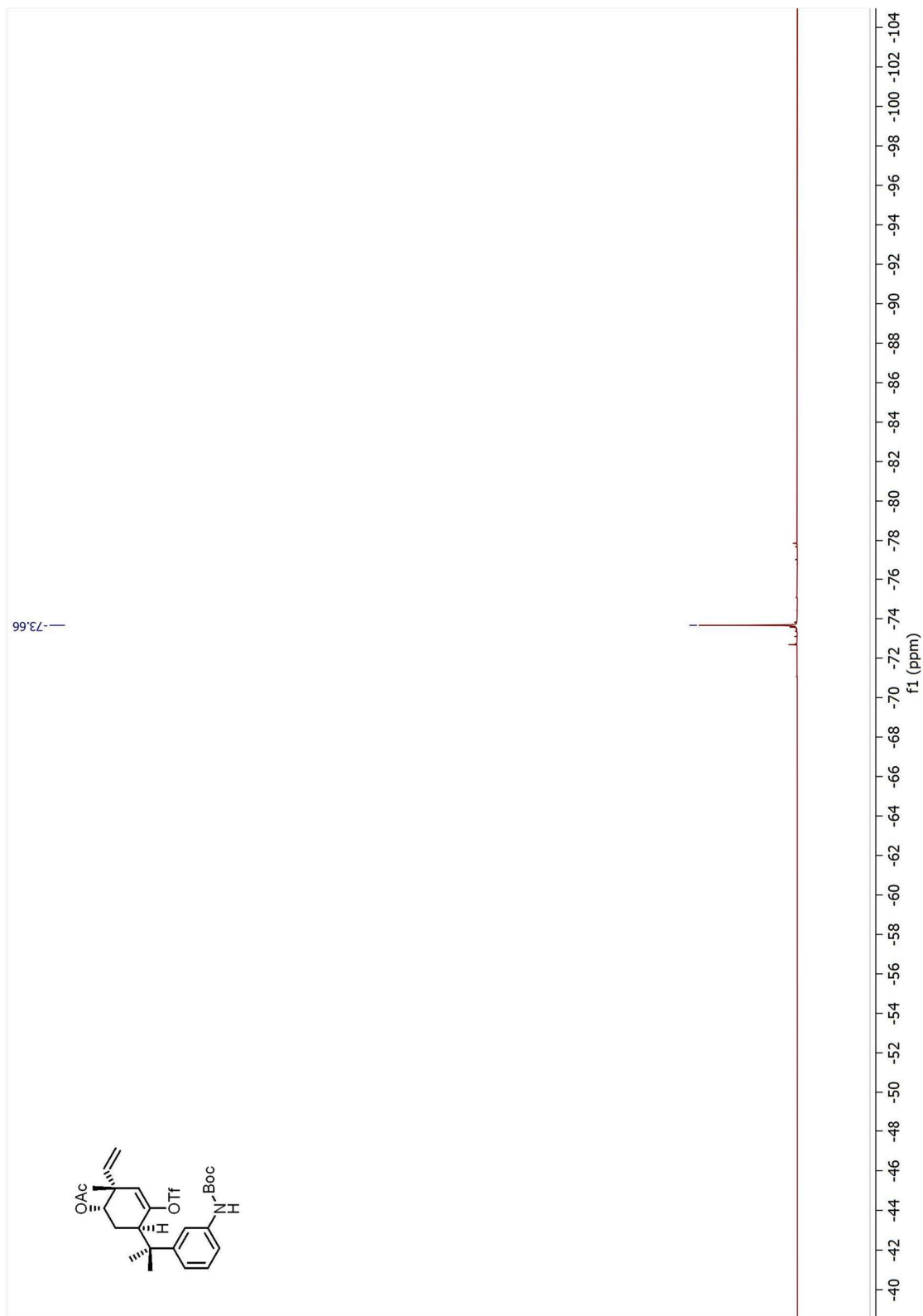


Figure 7.60 ^{19}F NMR Spectrum of **3.63** (500 MHz, CDCl_3)

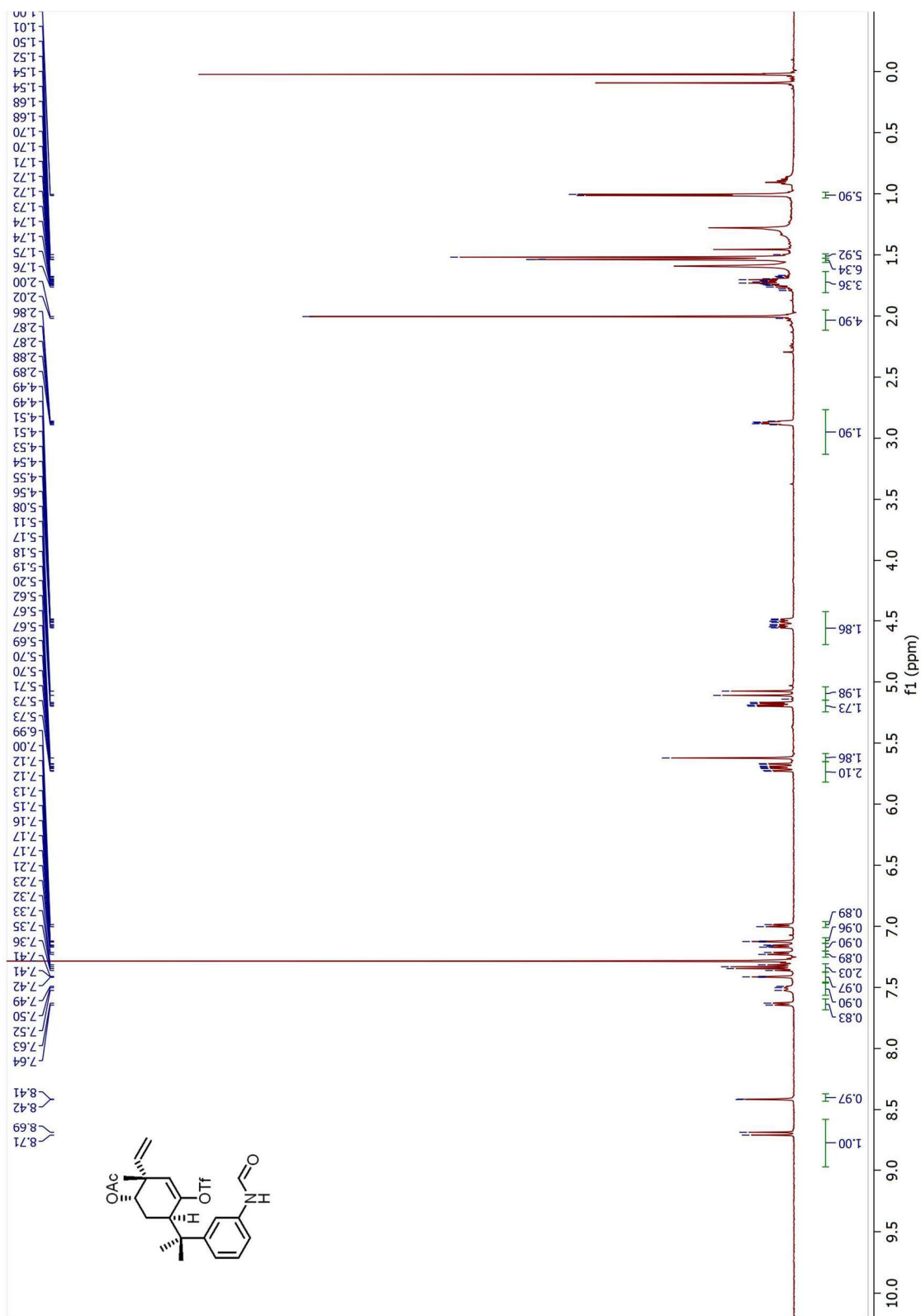


Figure 7.61 ^1H NMR Spectrum of **3.60** (500 MHz, CDCl_3)

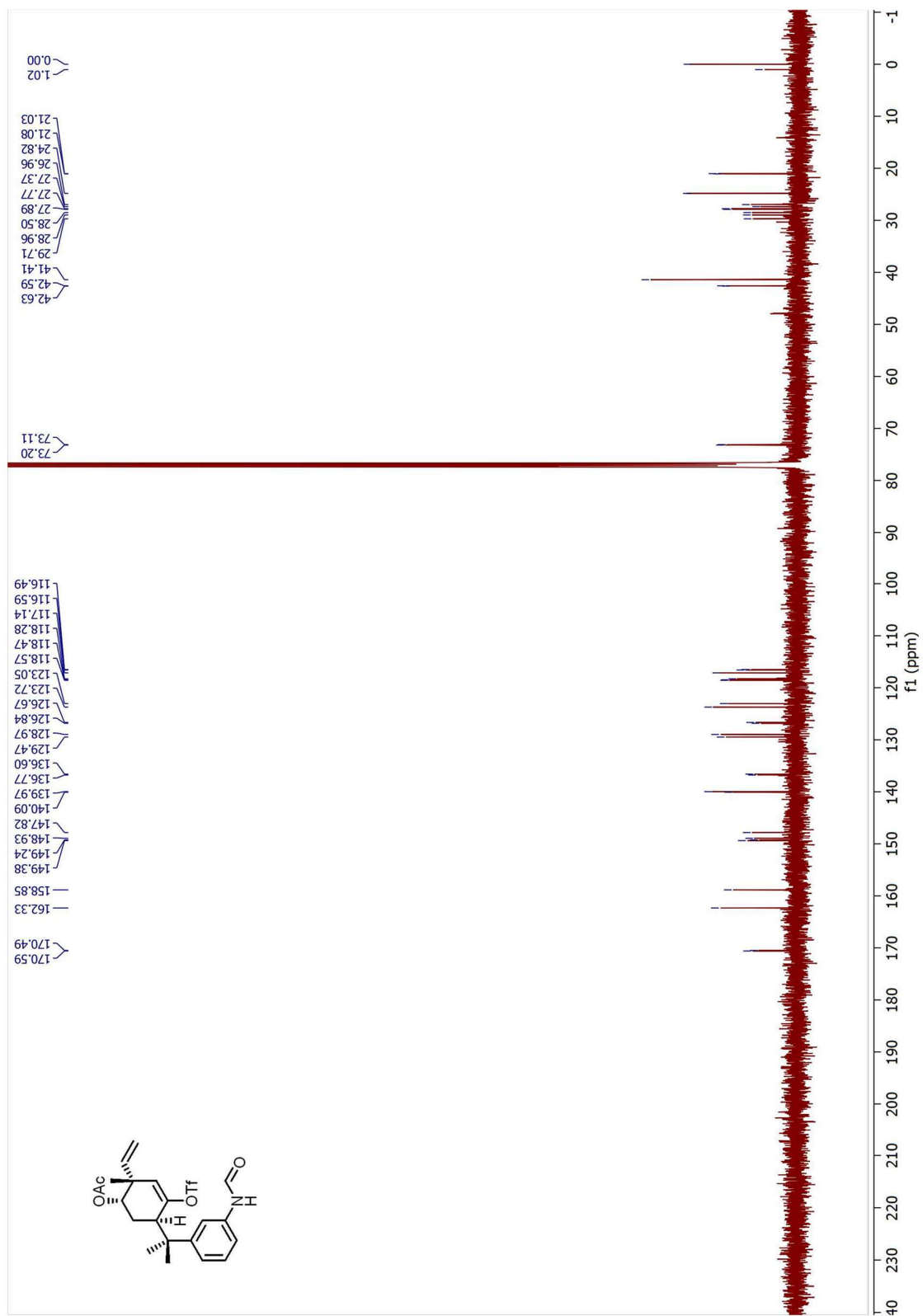


Figure 7.62 ^{13}C NMR Spectrum of **3.60** (125 MHz, CDCl_3)

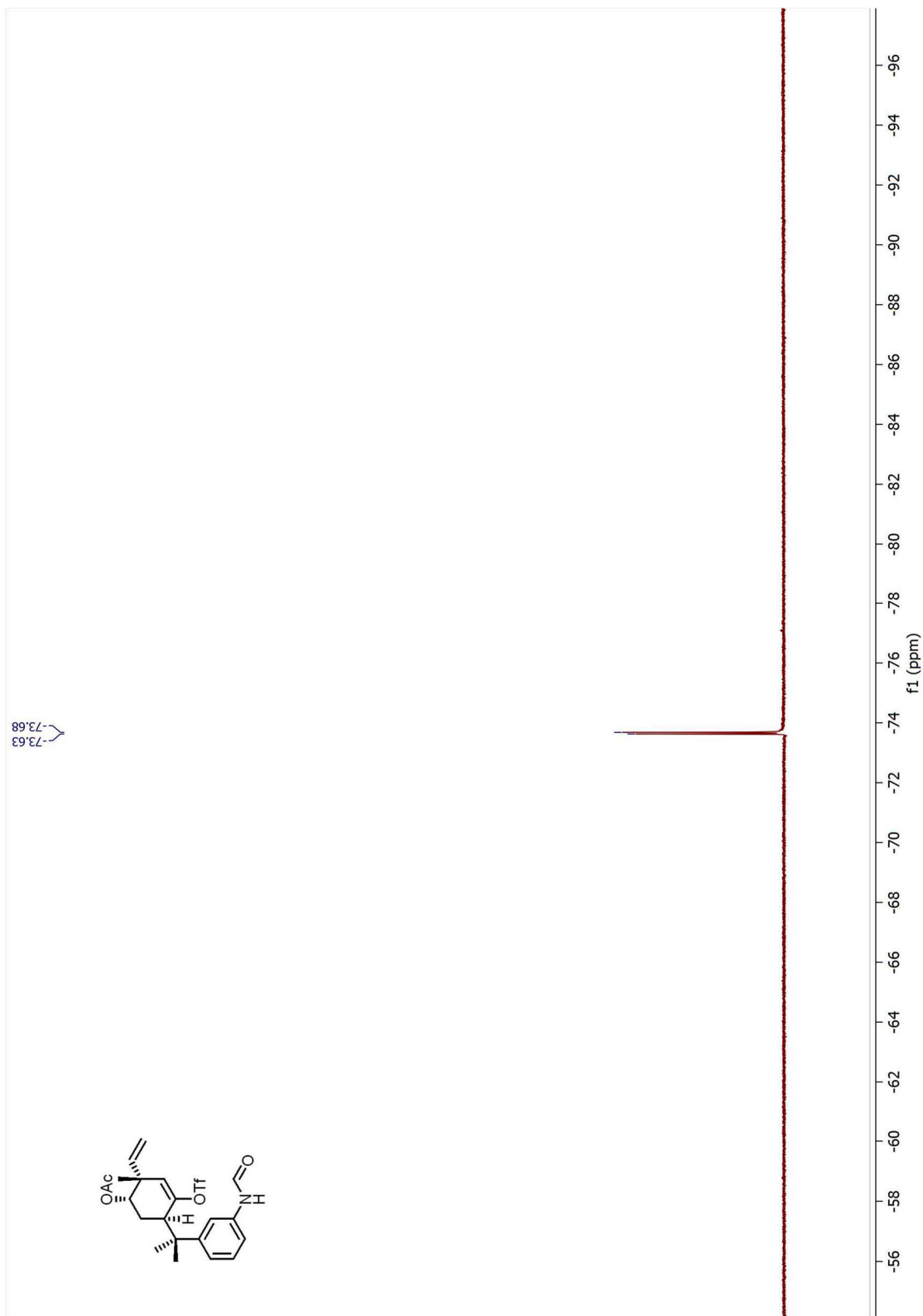


Figure 7.63 ^{19}F NMR Spectrum of **3.60** (500 MHz, CDCl_3)

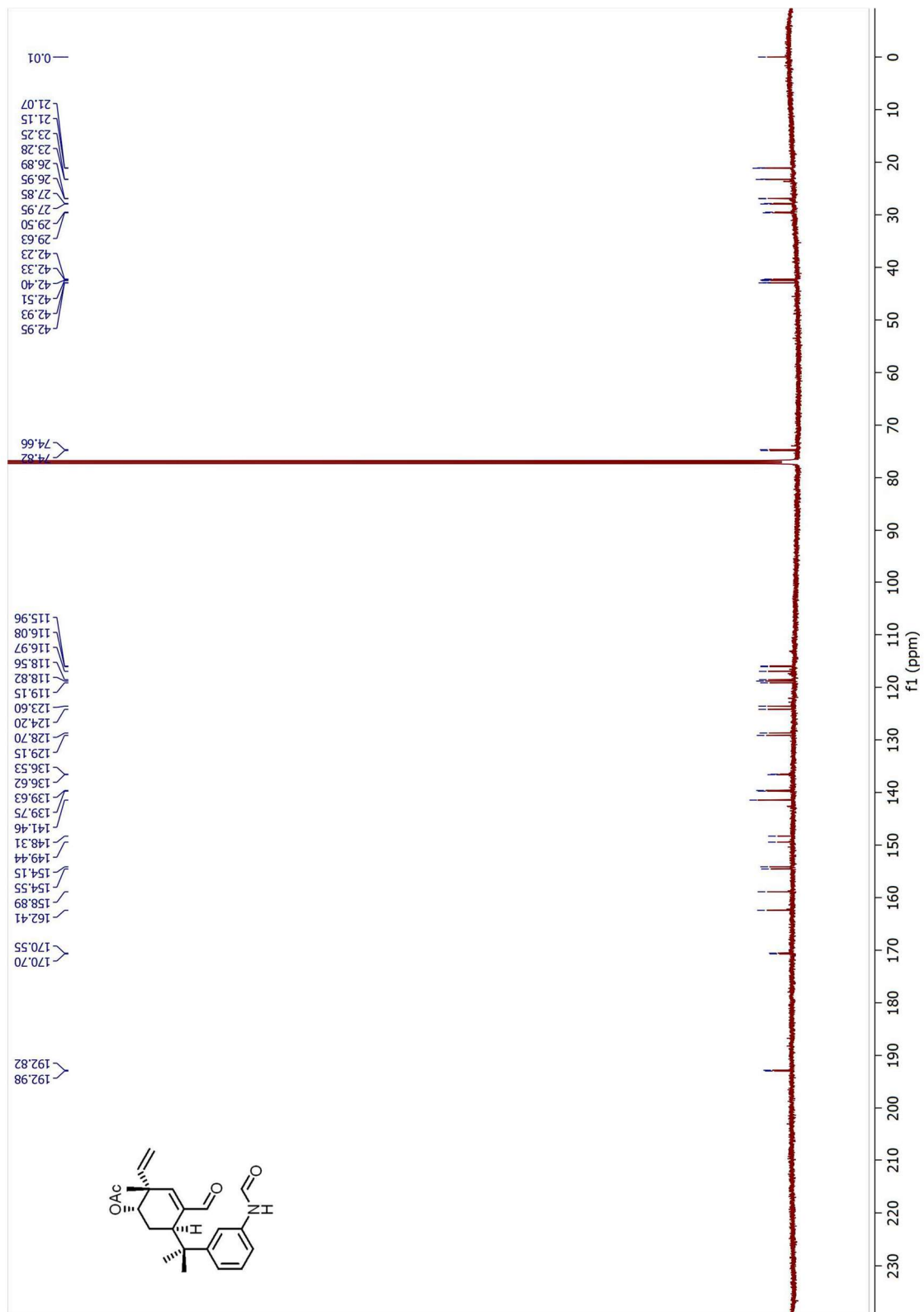


Figure 7.65 ¹³C NMR Spectrum of 3.64 (125 MHz, CDCl₃)

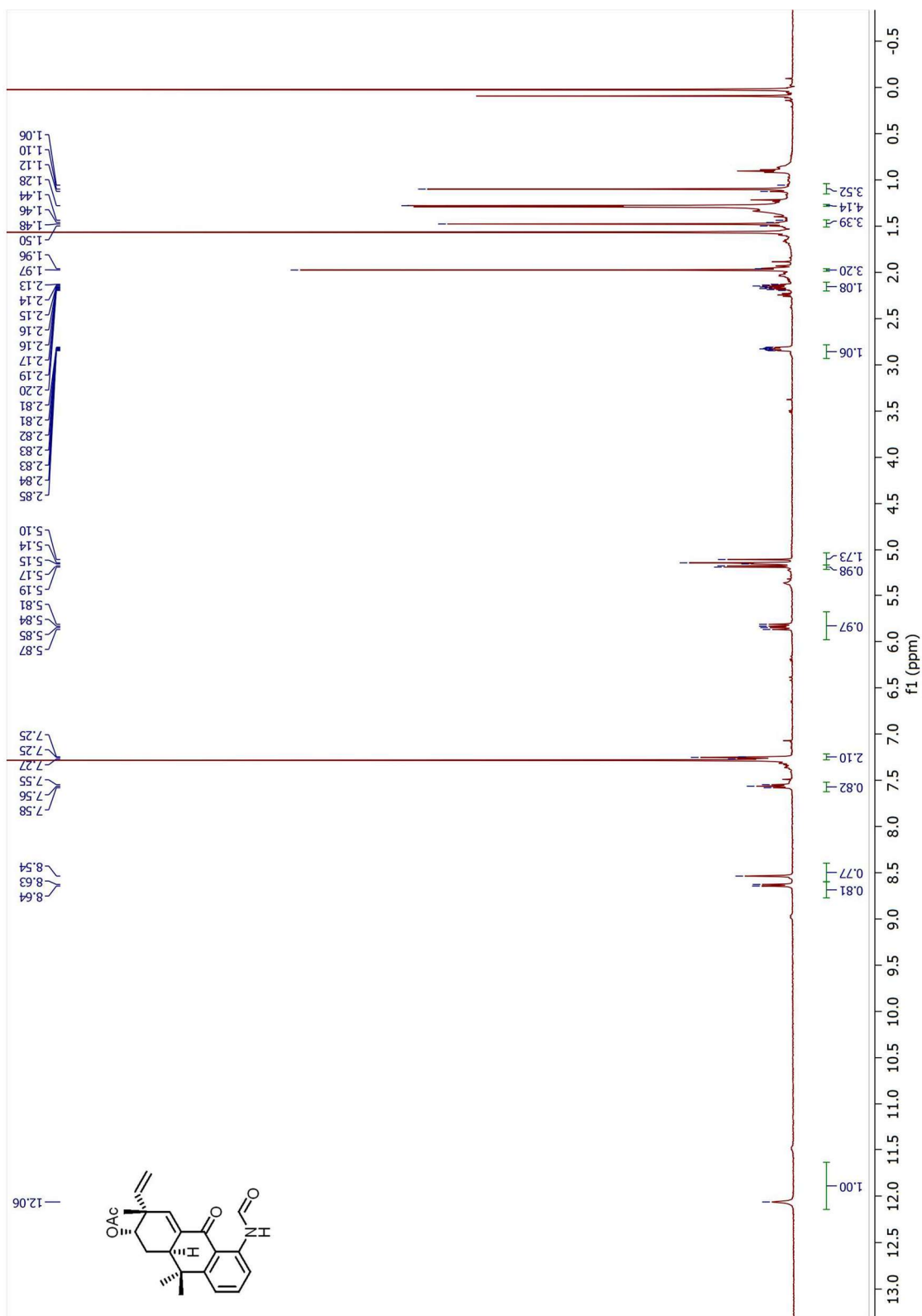


Figure 7.66 ^1H NMR Spectrum of **3.65** (500 MHz, CDCl_3)

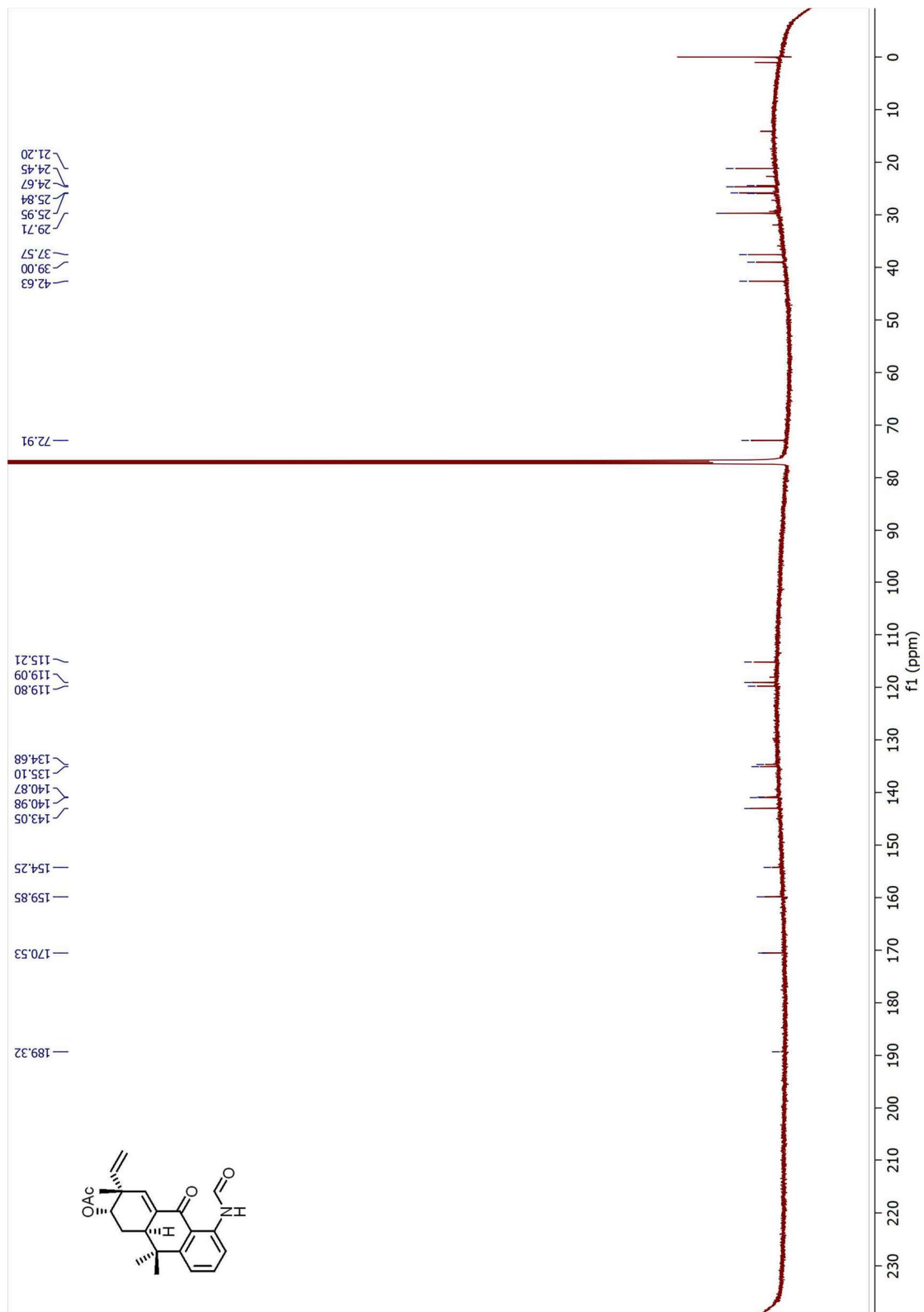


Figure 7.67 ^{13}C NMR Spectrum of 3.64 (125 MHz, CDCl_3)

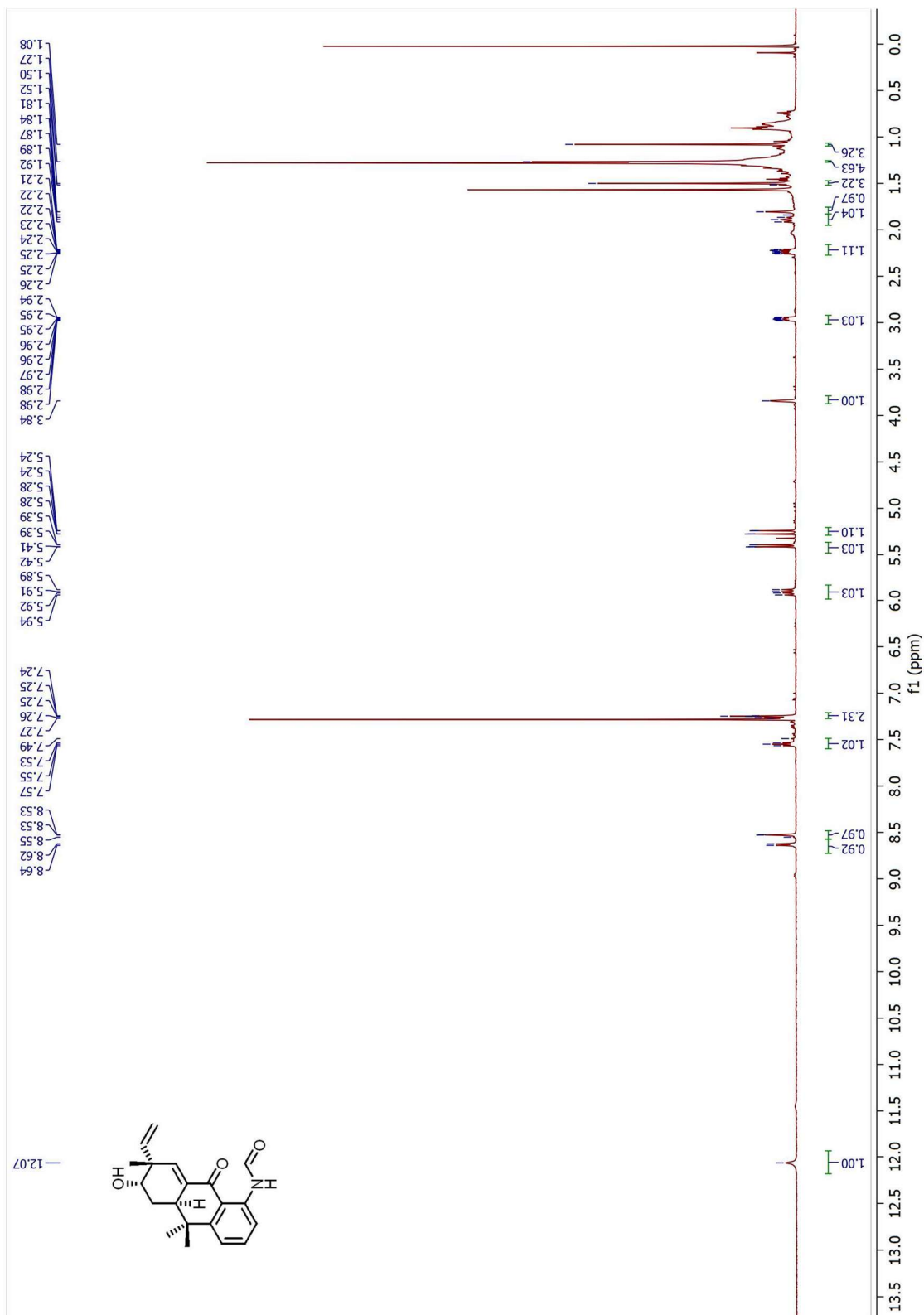


Figure 7.68 ^1H NMR Spectrum of **3.66** (500 MHz, CDCl_3)

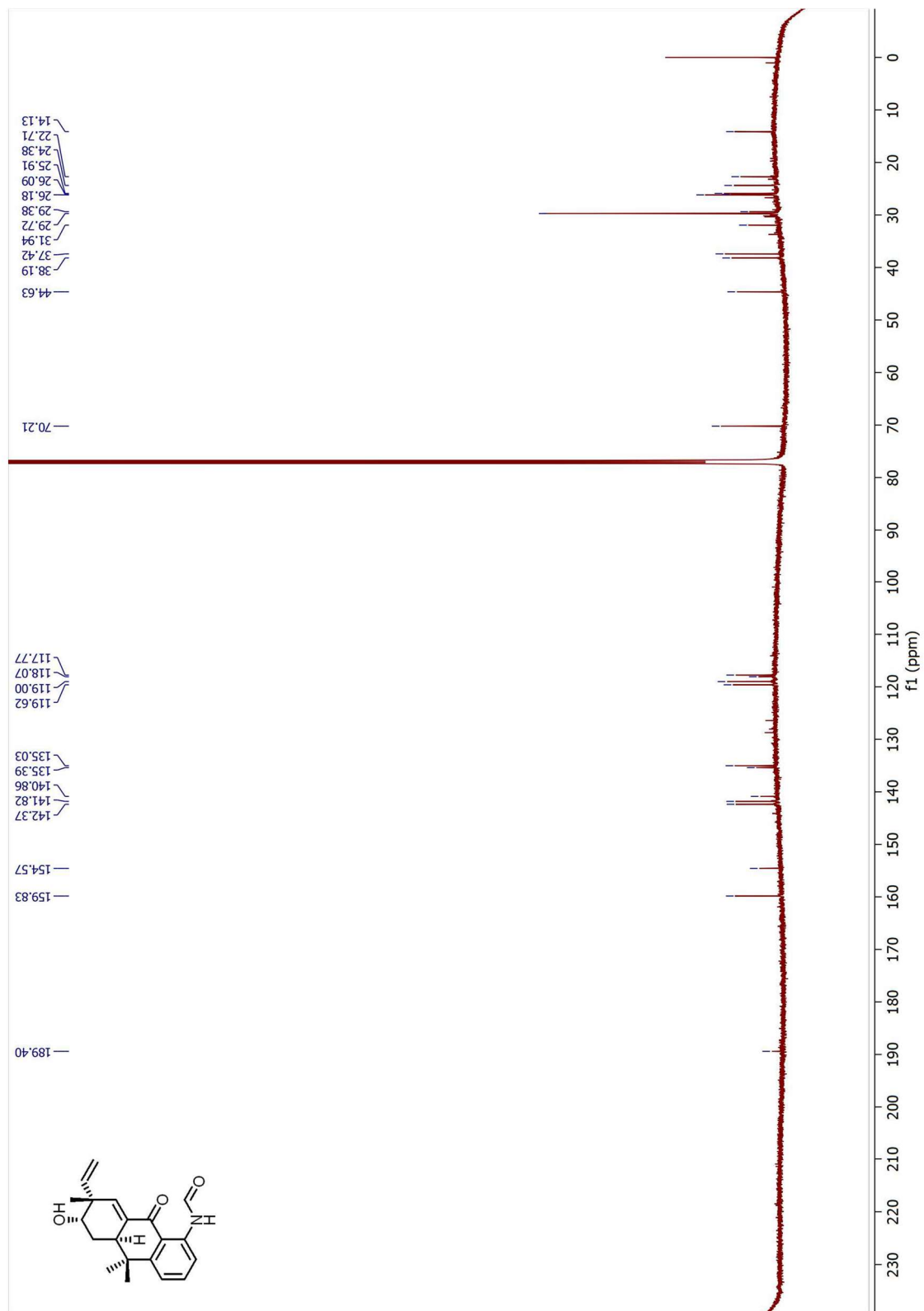


Figure 7.69 ^{13}C NMR Spectrum of **3.66** (125 MHz, CDCl_3)

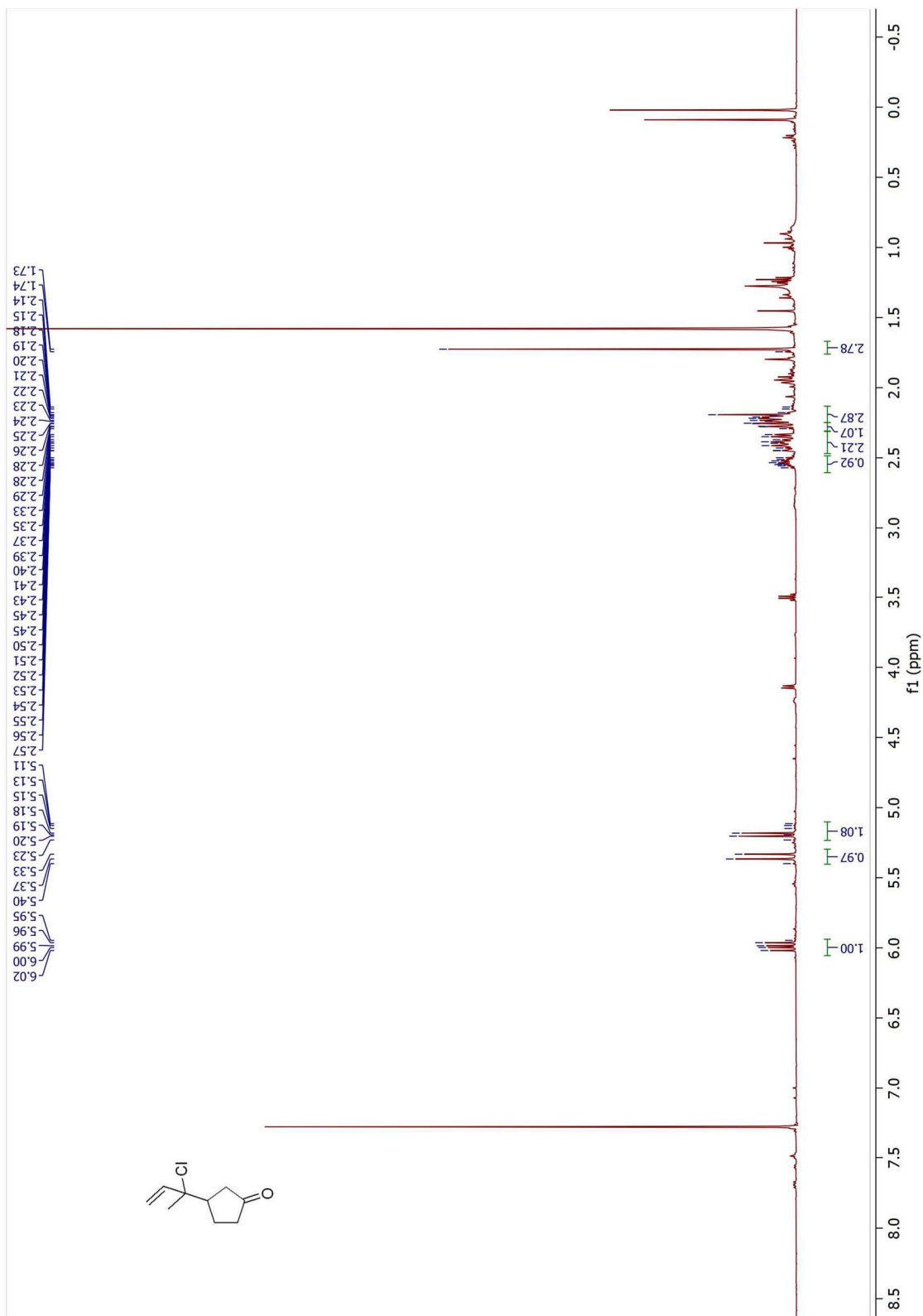


Figure 7.70 ¹H NMR Spectrum of **3.75** (500 MHz, CDCl₃)

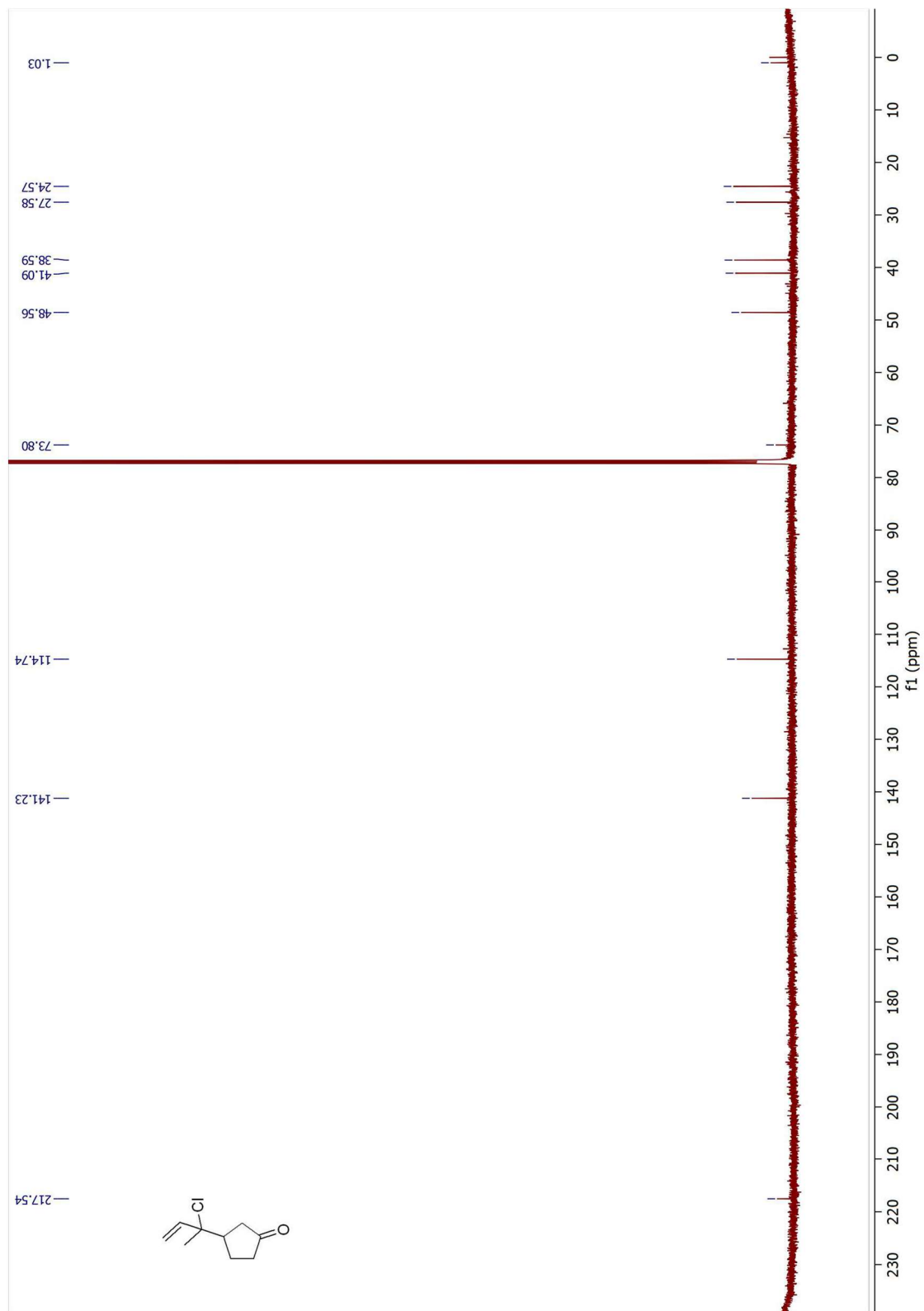


Figure 7.71 ^{13}C NMR Spectrum of **3.75** (125 MHz, CDCl_3)

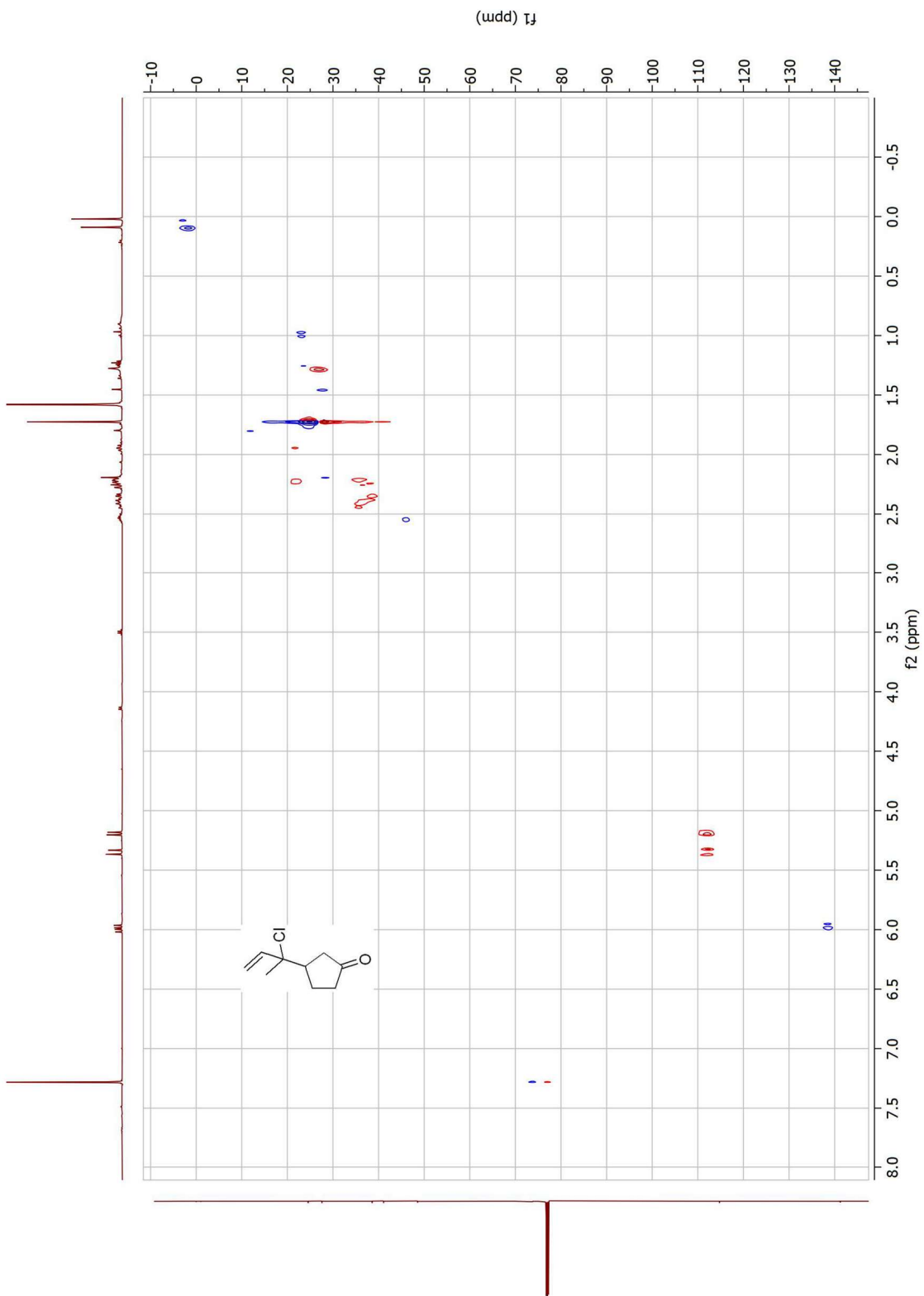


Figure 7.72 HSQC Spectrum of 3.75 (500 MHz, CDCl₃)

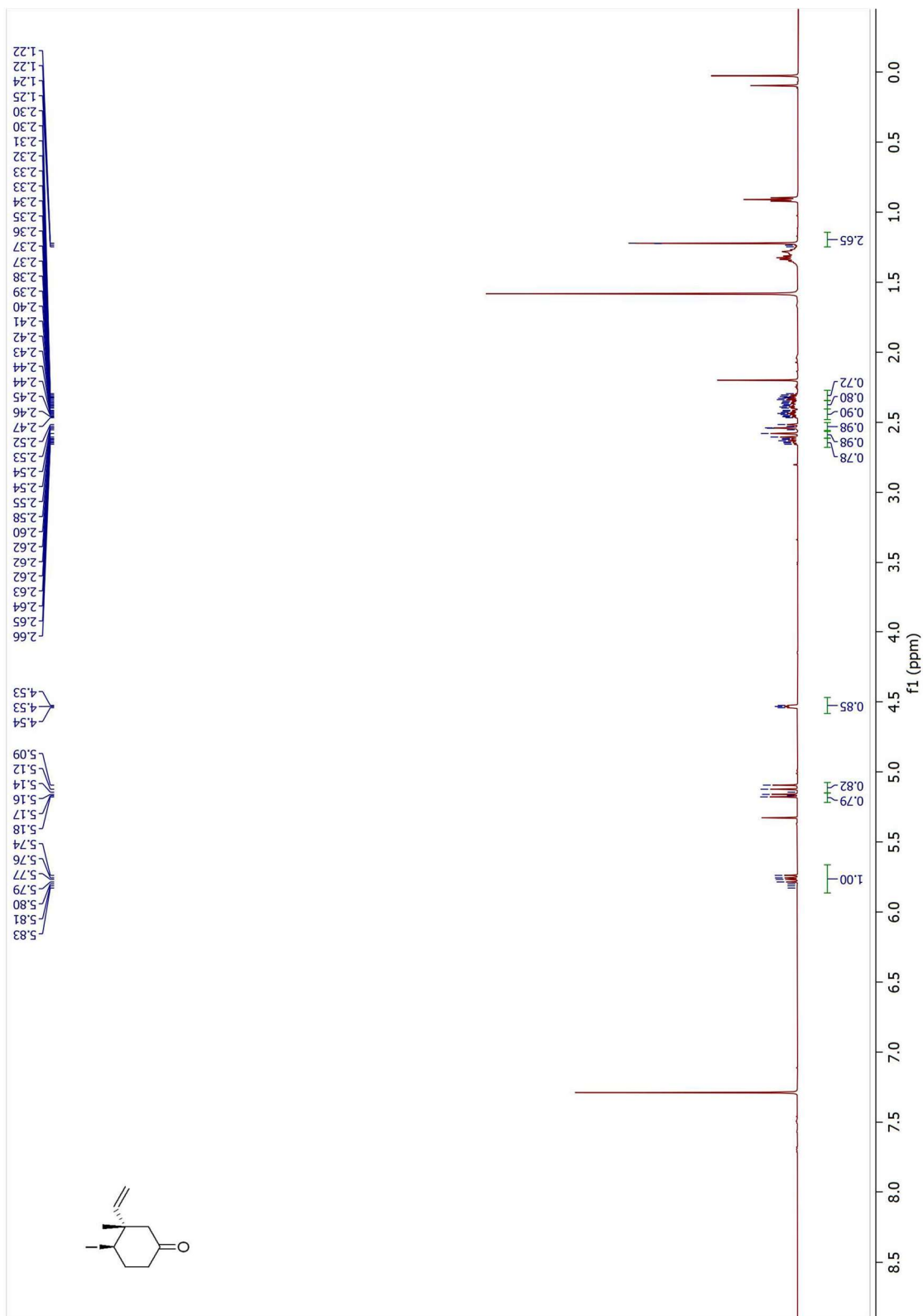


Figure 7.73 ¹H NMR Spectrum of **3.78** (500 MHz, CDCl₃)

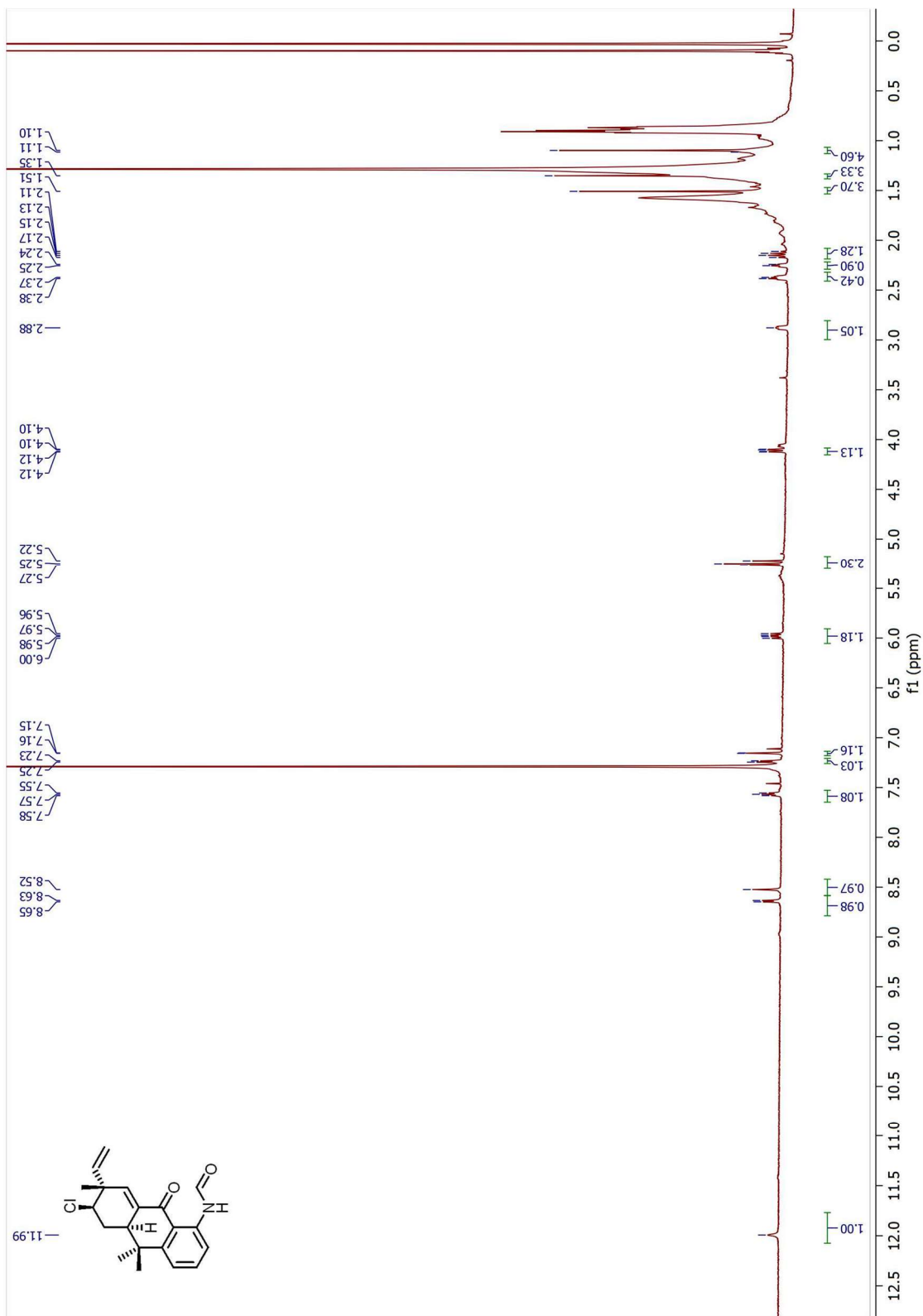


Figure 7.74 ^1H NMR Spectrum of fontonamide (500 MHz, CDCl_3)

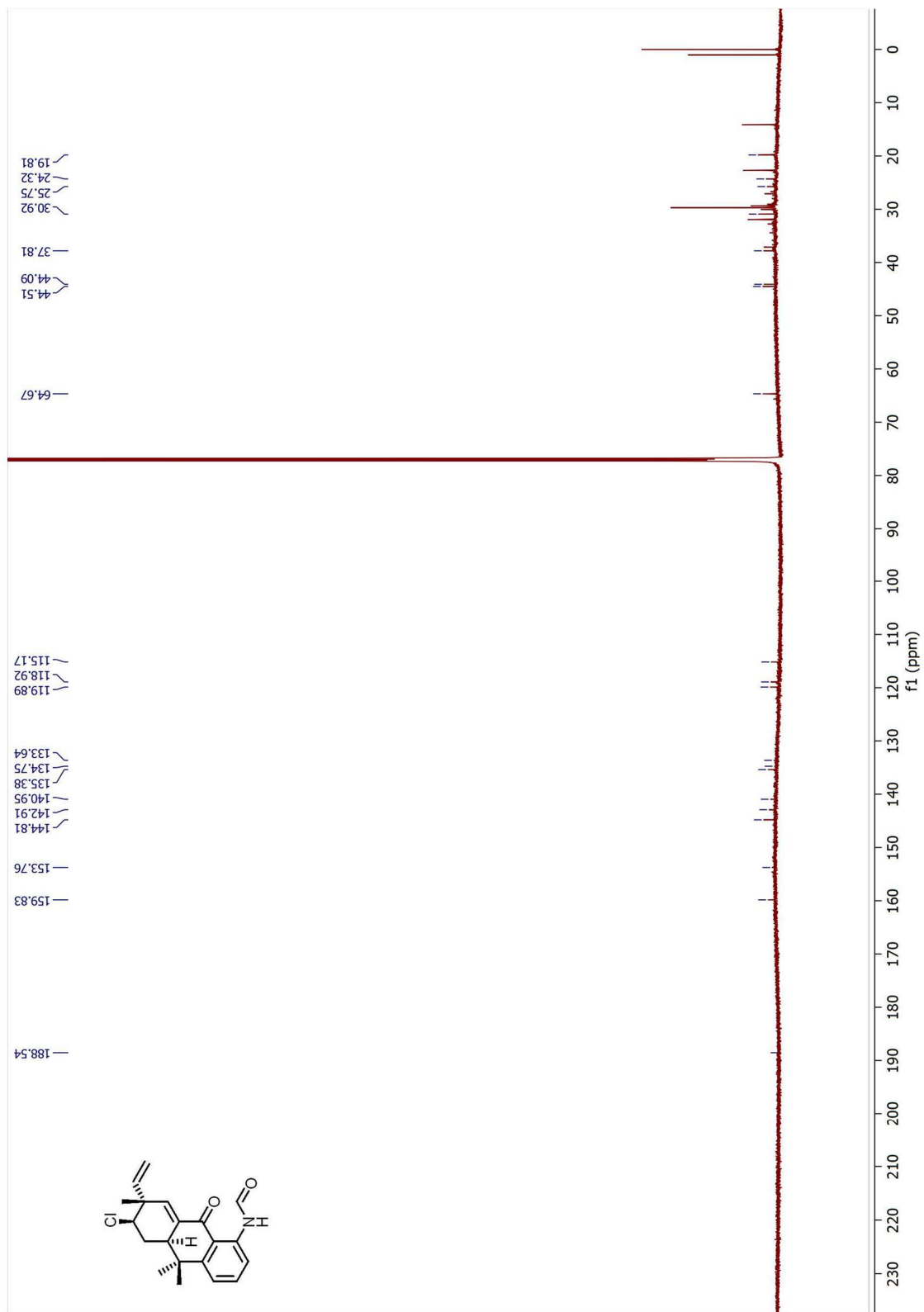


Figure 7.75 ^{13}C NMR Spectrum of **fontonamide** (125 MHz, CDCl_3)

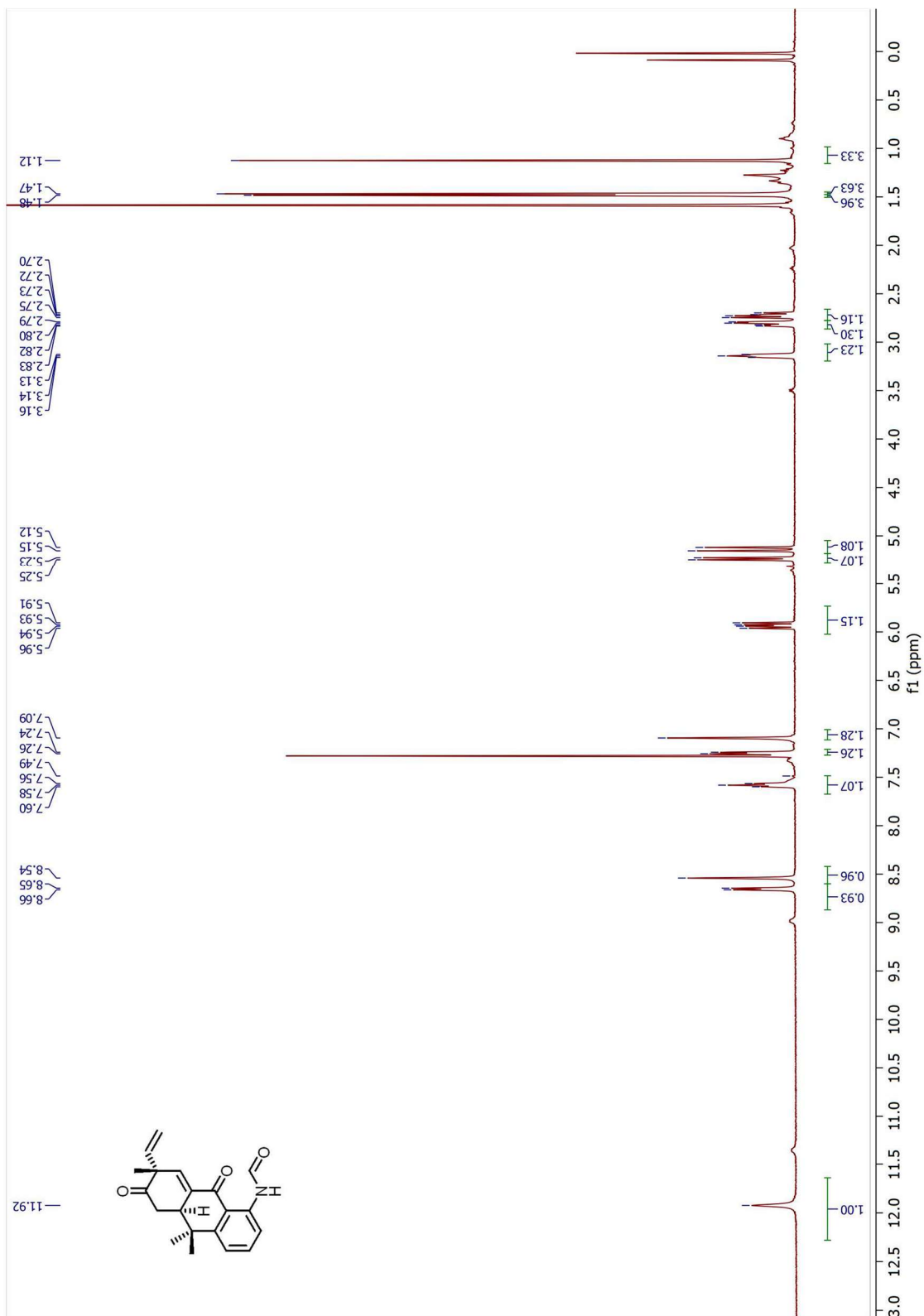


Figure 7.76 ^1H NMR Spectrum of **3.81** (500 MHz, CDCl_3)

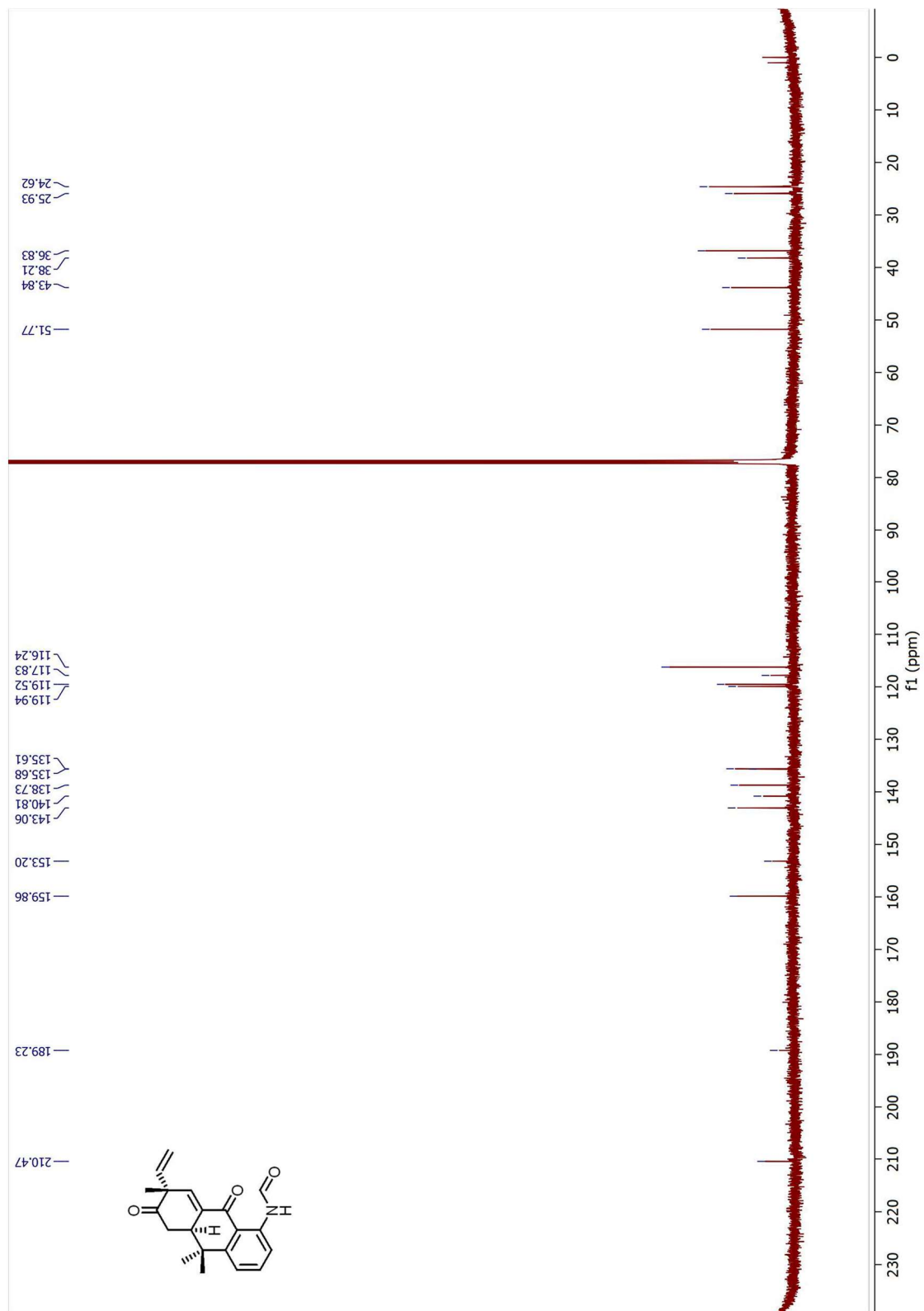


Figure 7.77 ^{13}C NMR Spectrum of **3.81** (125 MHz, CDCl_3)

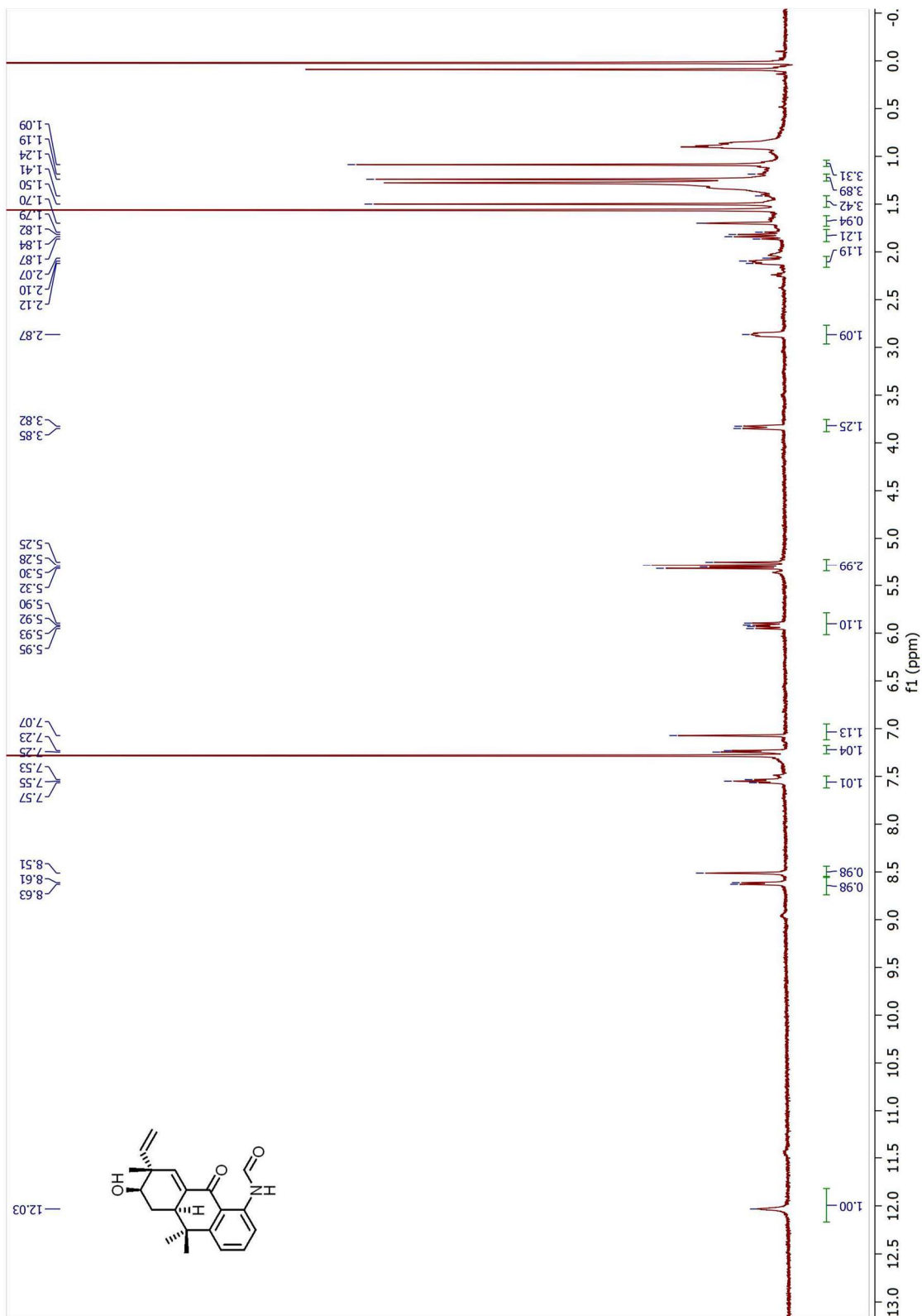


Figure 7.78 ^1H NMR Spectrum of 13-hydroxy dechlorofontonamide (500 MHz, CDCl_3)

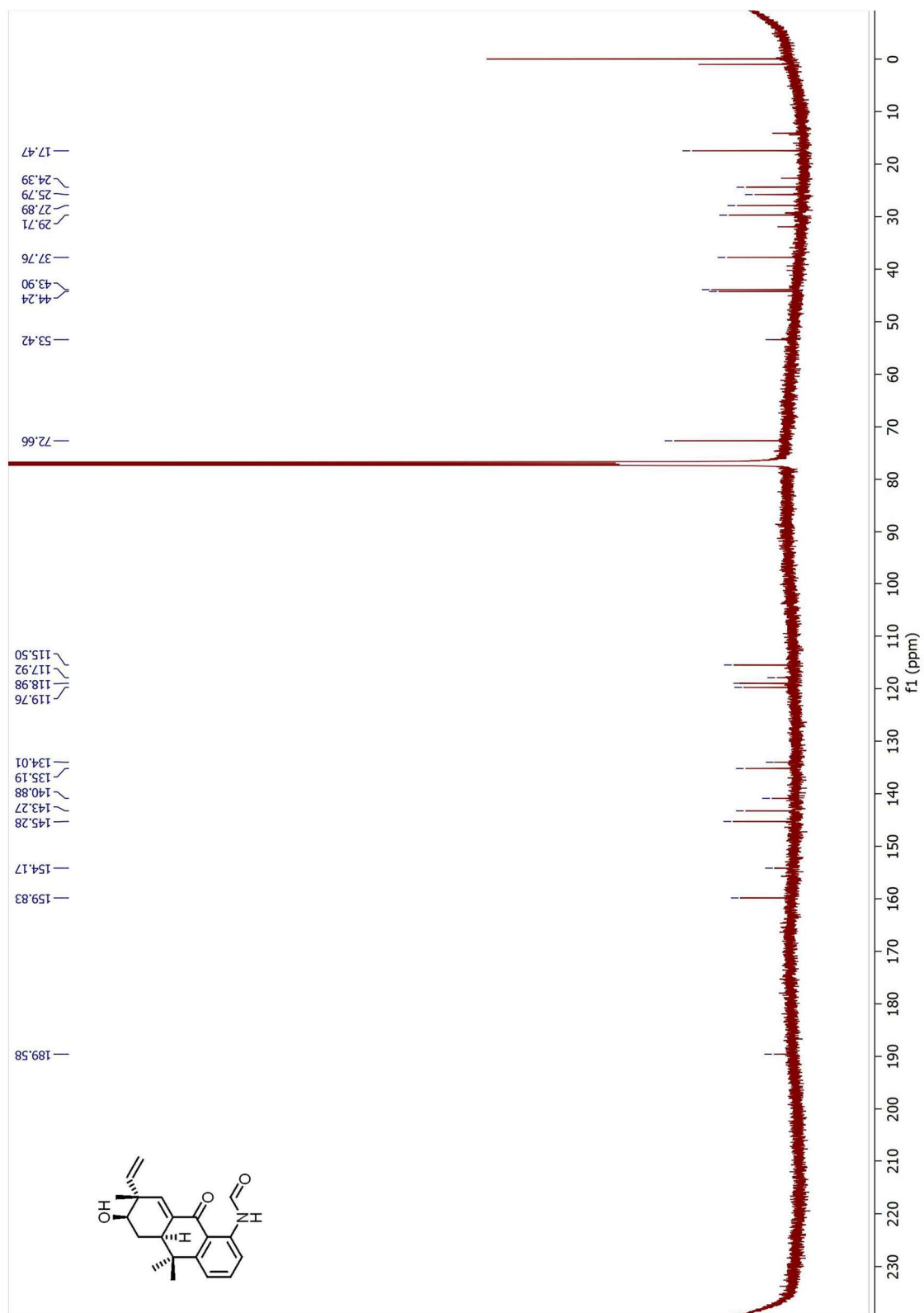


Figure 7.79 ^{13}C NMR Spectrum of 13-hydroxy dechlorofontonamide (125 MHz, CDCl_3)

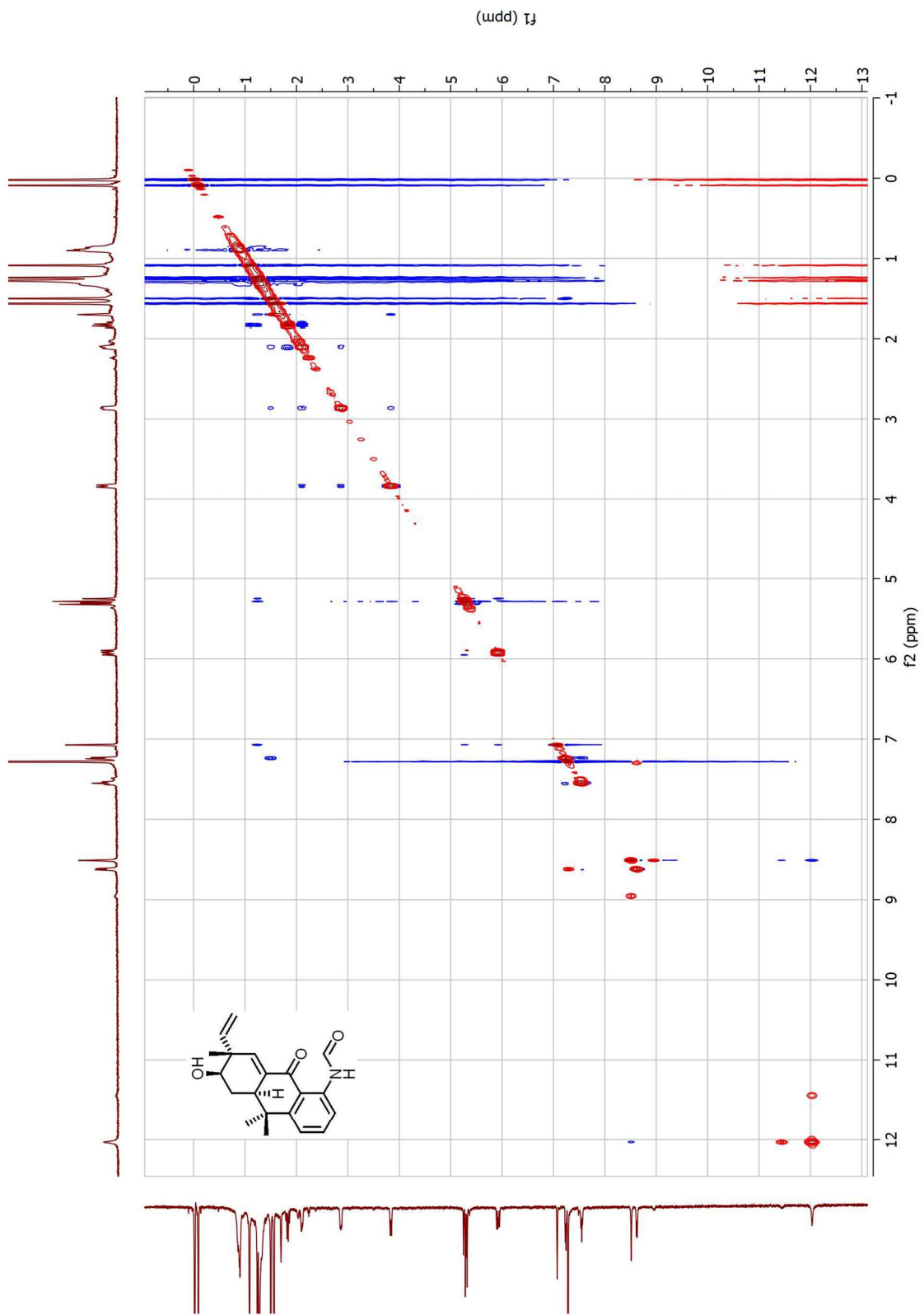


Figure 7.80 NOESY Spectrum of **13-hydroxy dechlorofontonamide** (500 MHz, CDCl₃)

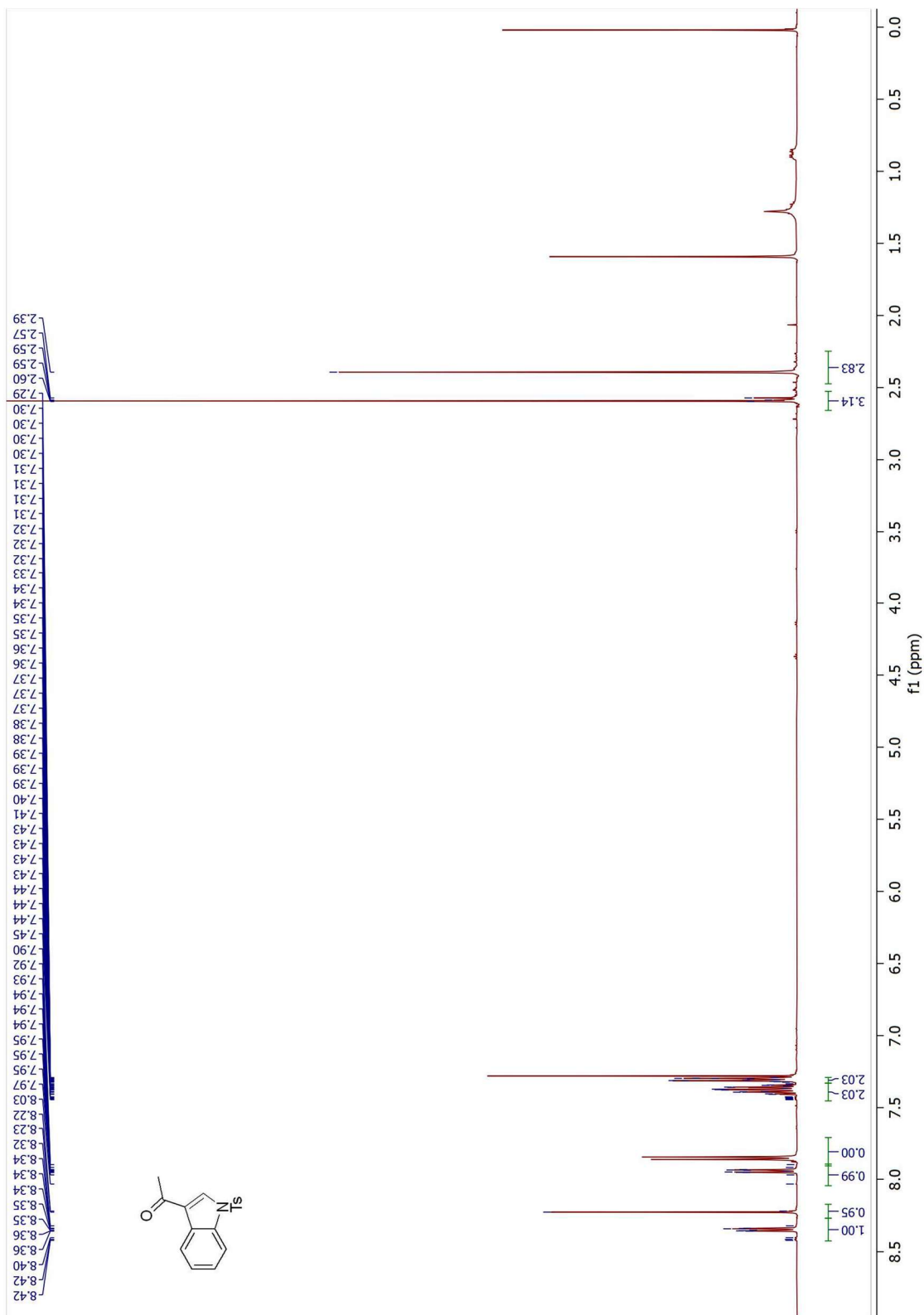


Figure 7.81 ^1H NMR Spectrum of **4.11** (500 MHz, CDCl_3)

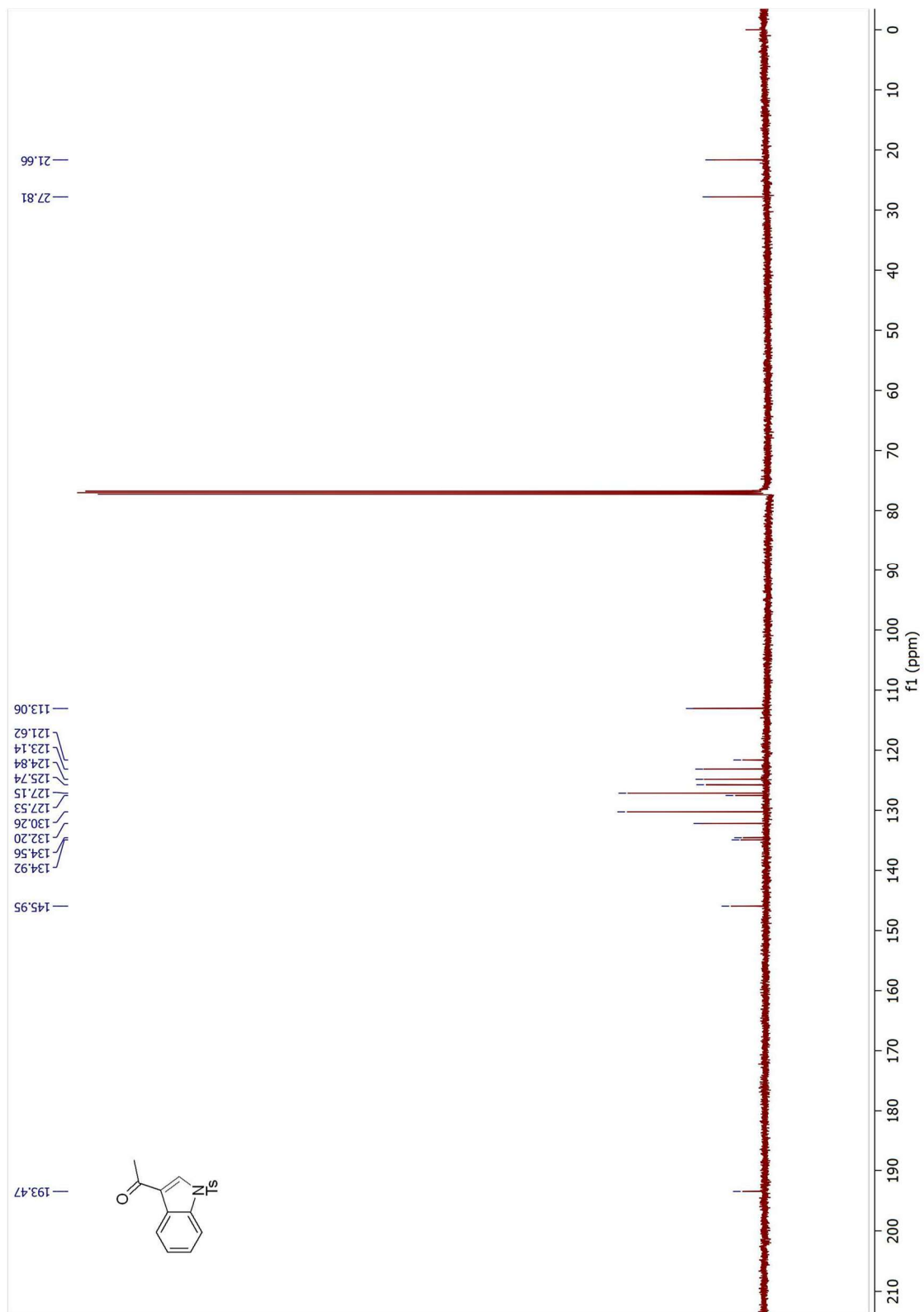


Figure 7.82 ^{13}C NMR Spectrum of **4.11** (125 MHz, CDCl_3)

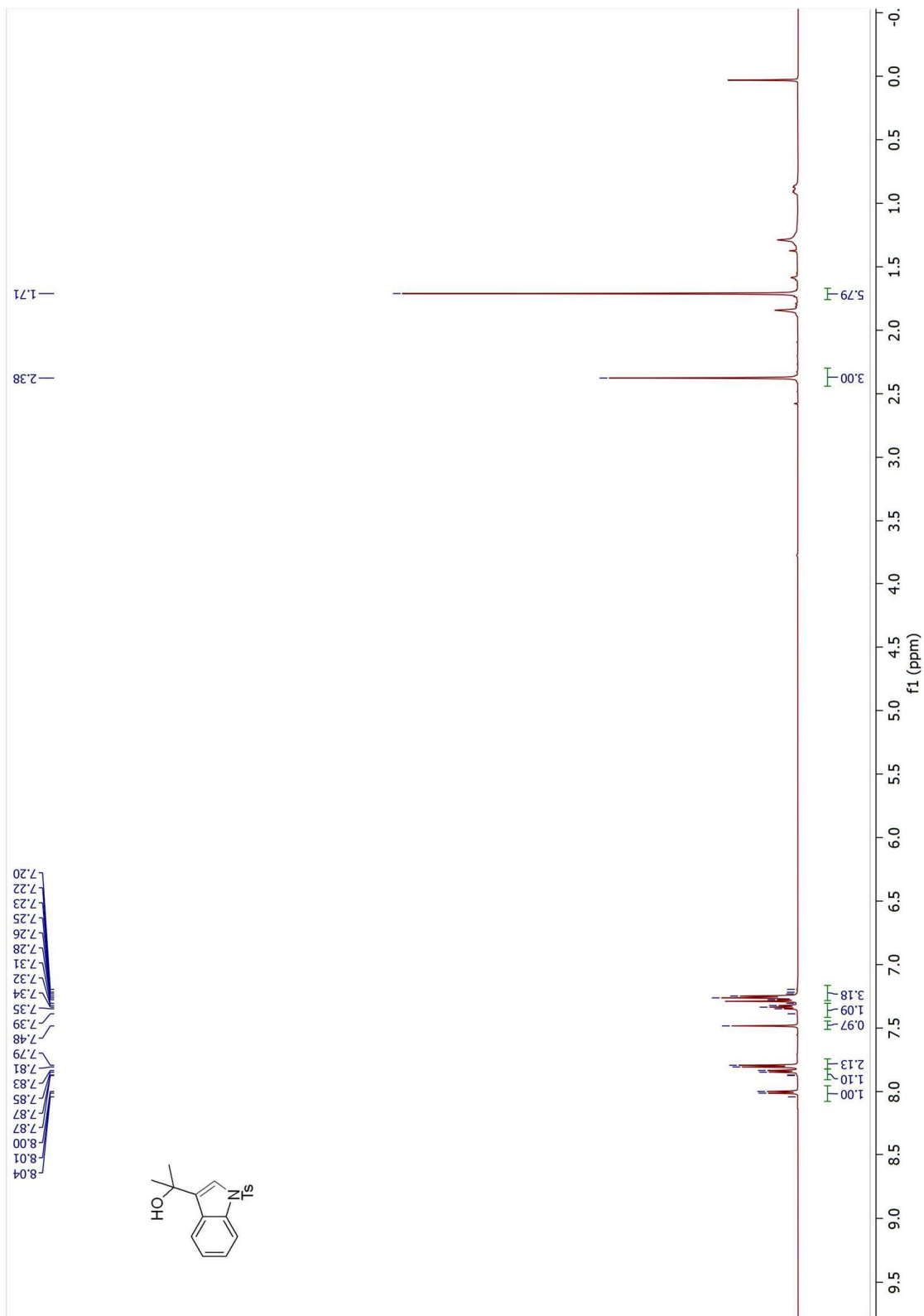


Figure 7.83 ¹H NMR Spectrum of **4.12** (500 MHz, CDCl₃)



Figure 7.84 ^{13}C NMR Spectrum of **4.12** (125 MHz, CDCl_3)

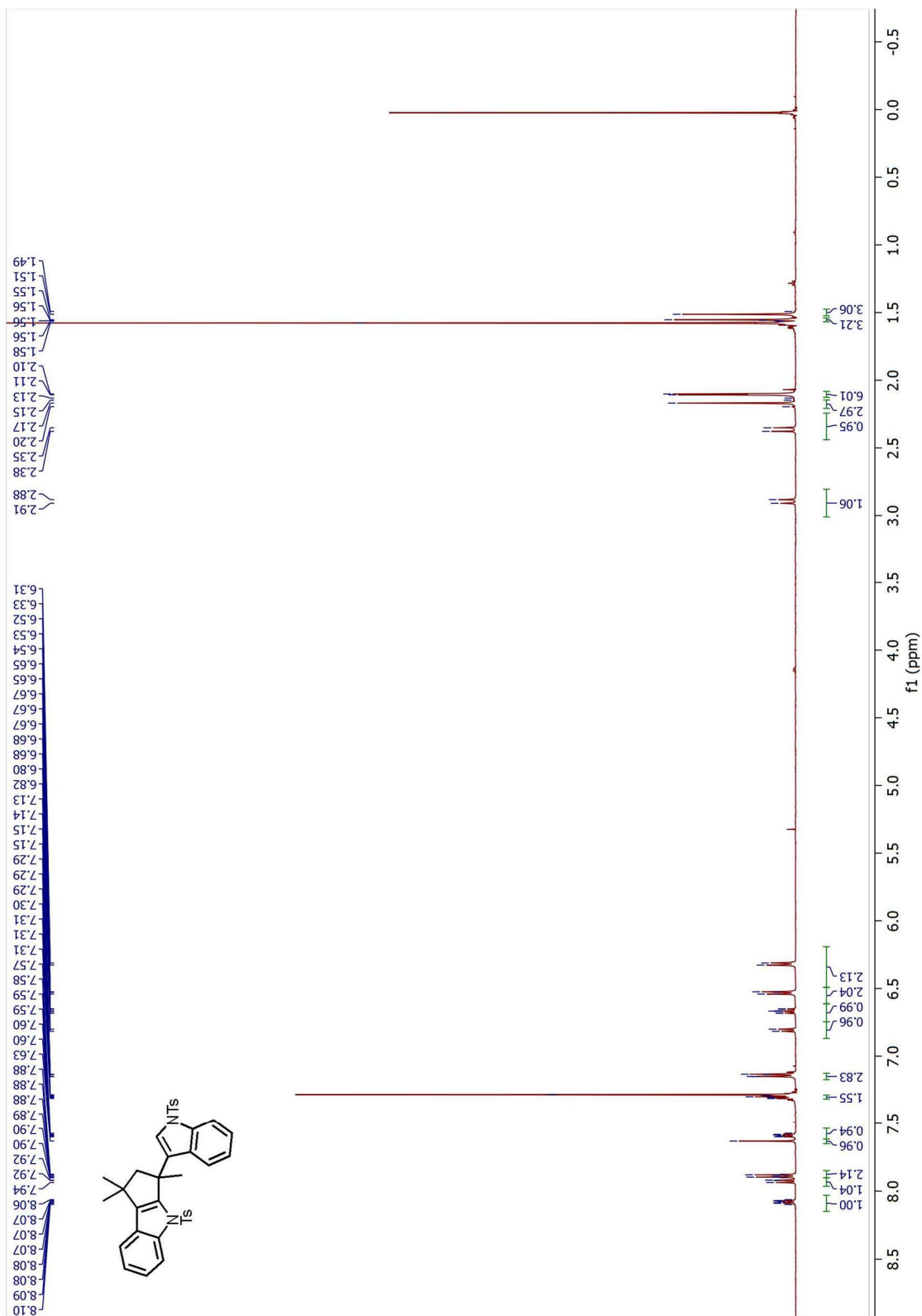


Figure 7.85 ^1H NMR Spectrum of **4.27** (500 MHz, CDCl_3)

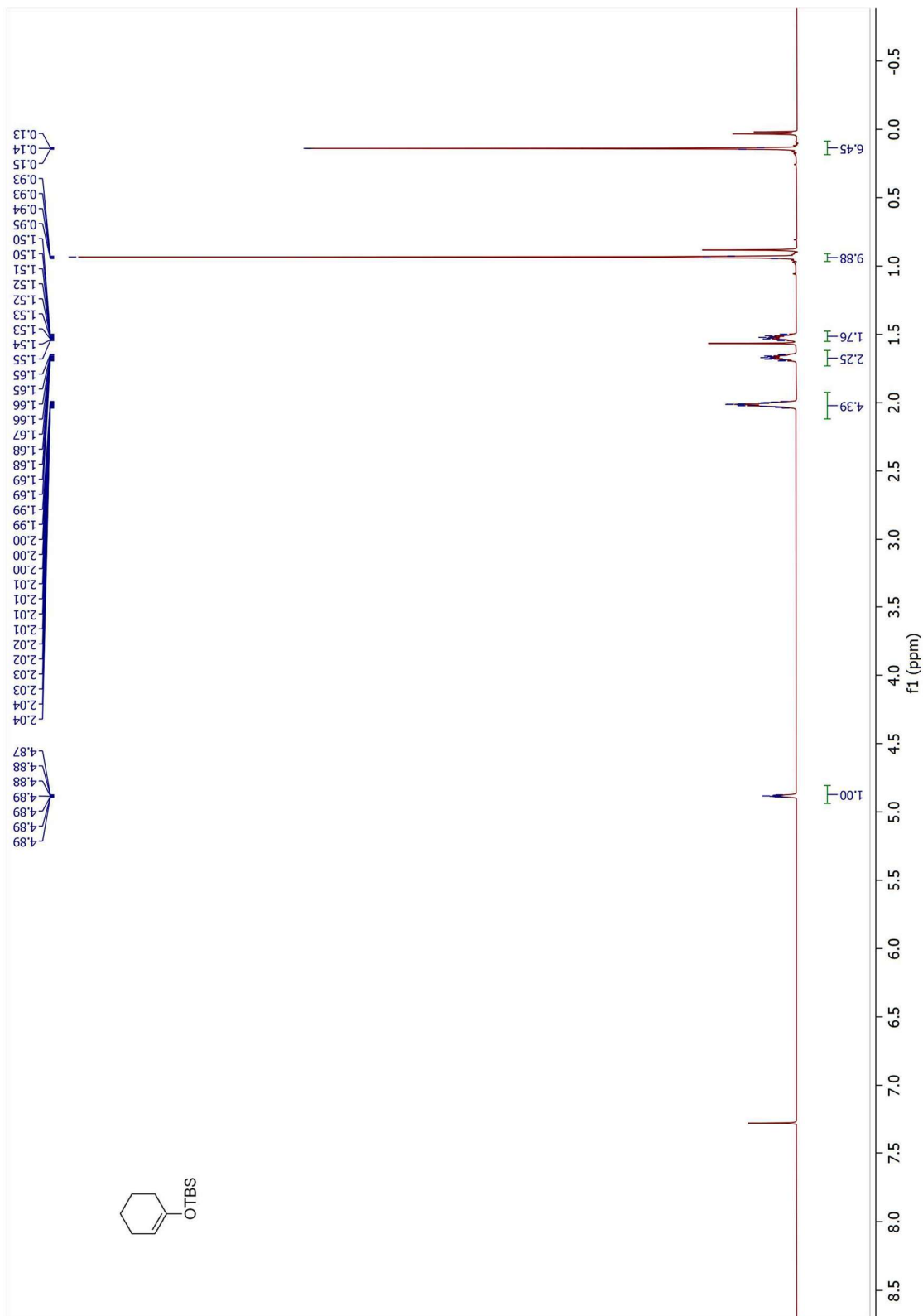


Figure 7.86 ^1H NMR Spectrum of **4.14** (500 MHz, CDCl_3)

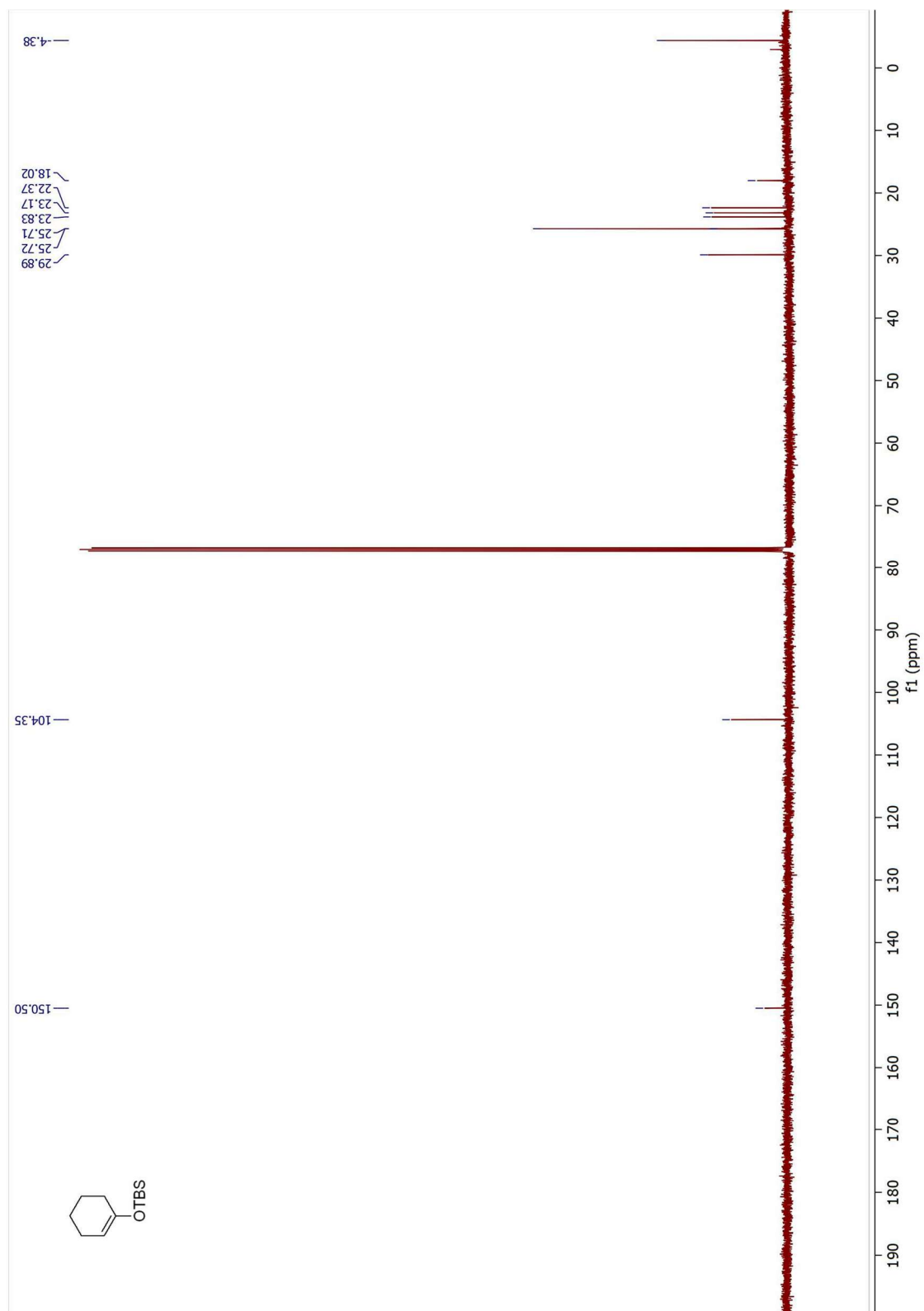


Figure 7.87 ^{13}C NMR Spectrum of **4.14** (125 MHz, CDCl_3)

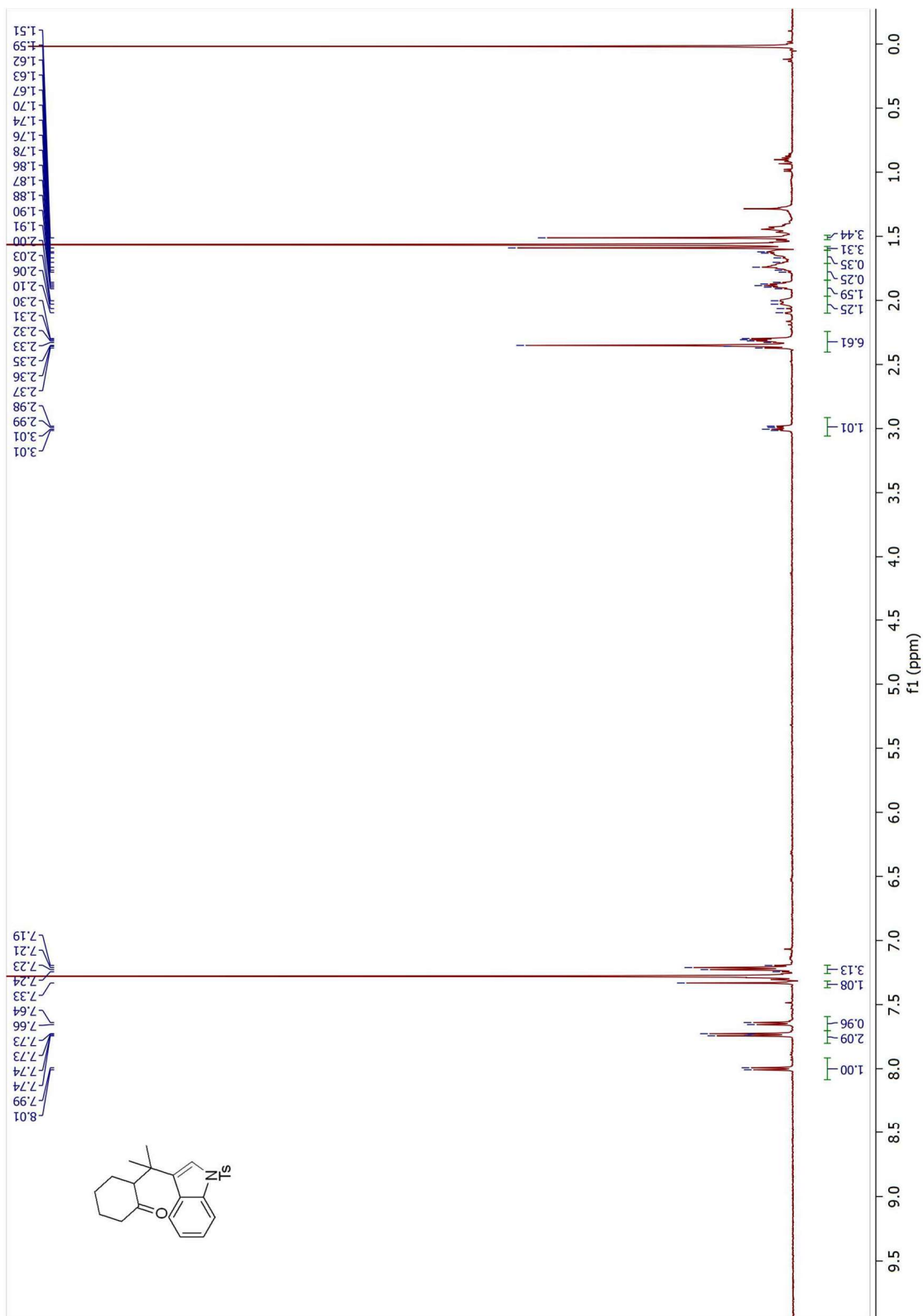


Figure 7.88 ^1H NMR Spectrum of **4.15** (500 MHz, CDCl_3)

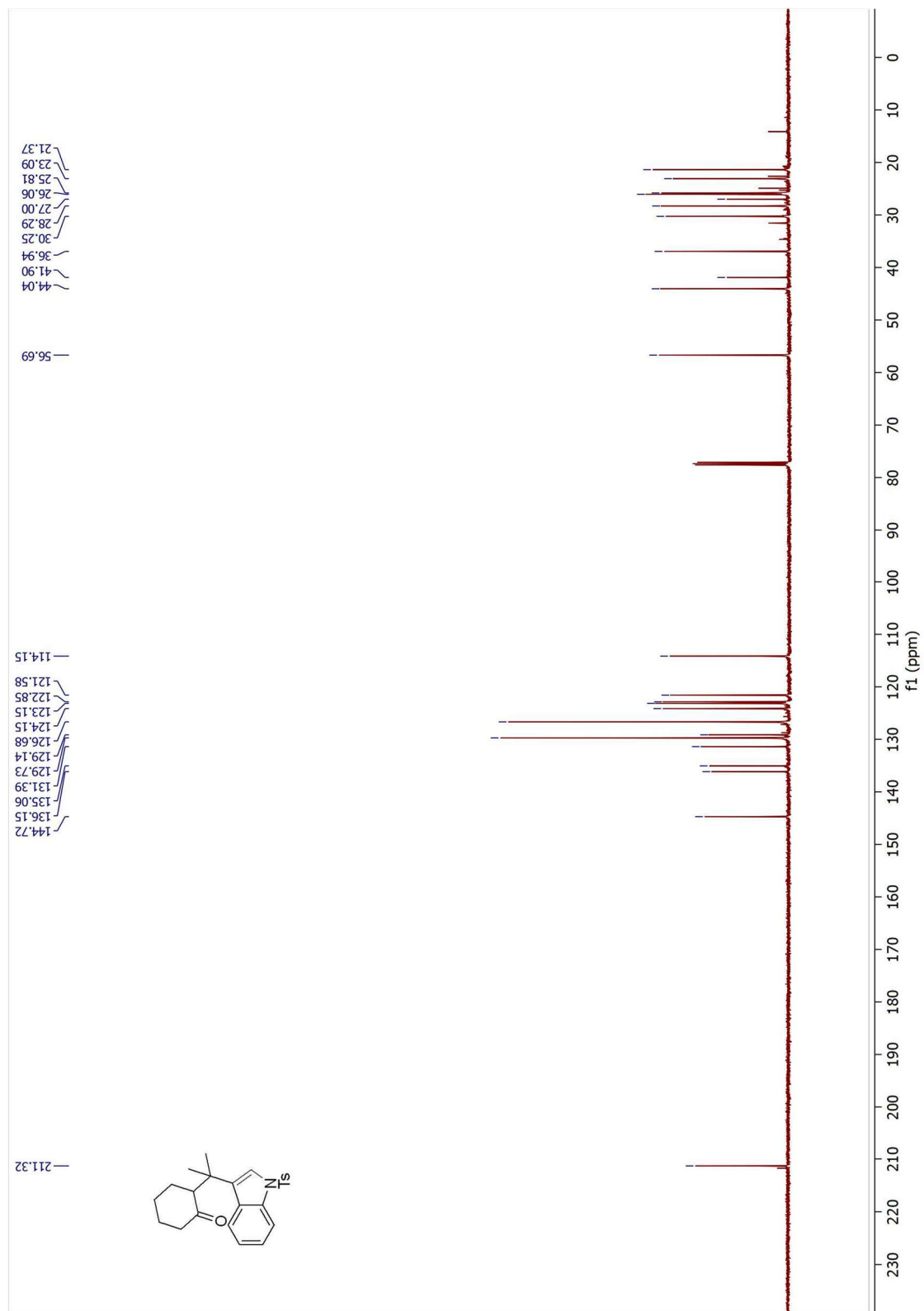


Figure 7.89 ^{13}C NMR Spectrum of **4.15** (125 MHz, CDCl_3)

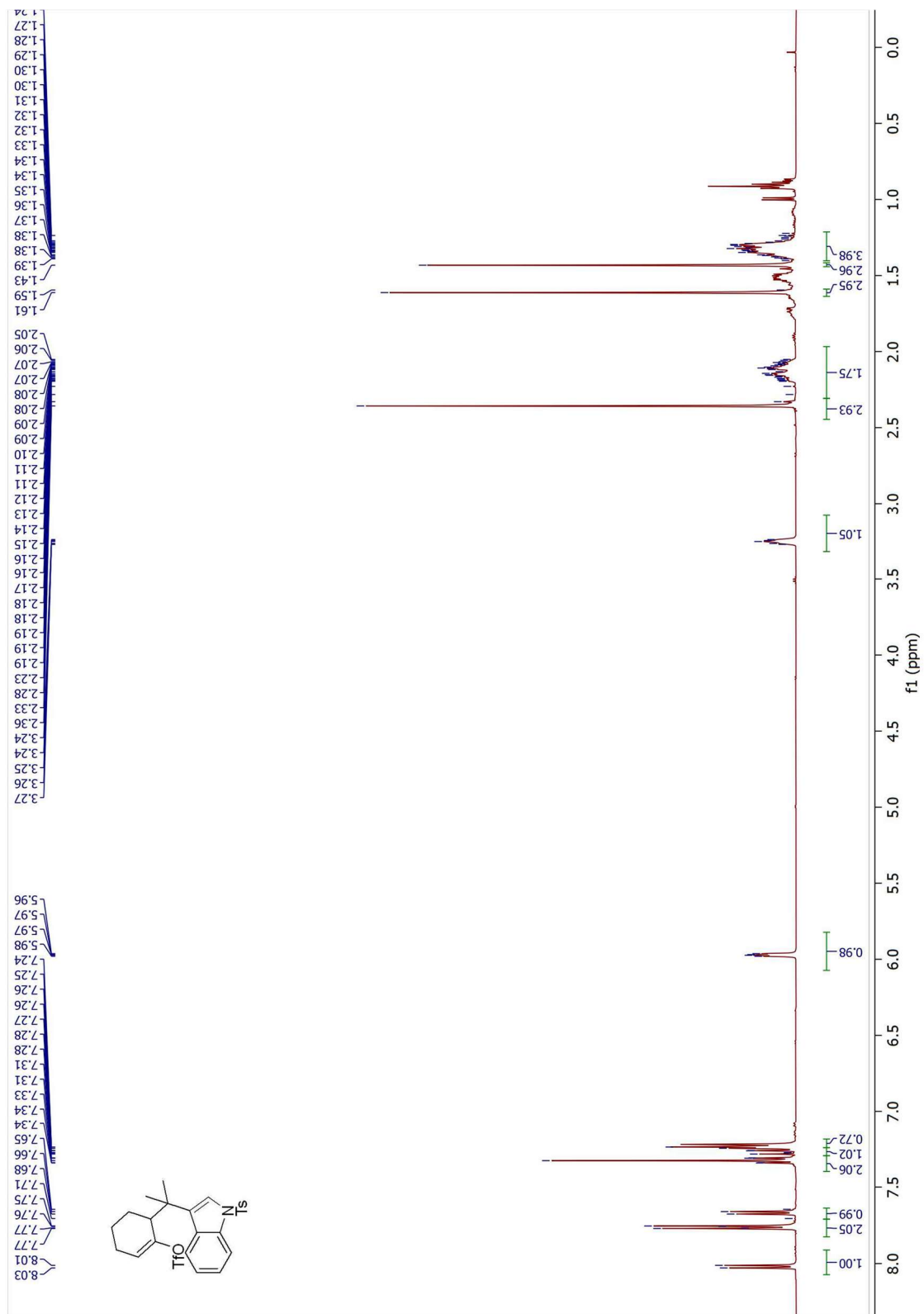


Figure 7.90 ^1H NMR Spectrum of 4.17 (500 MHz, CDCl_3)

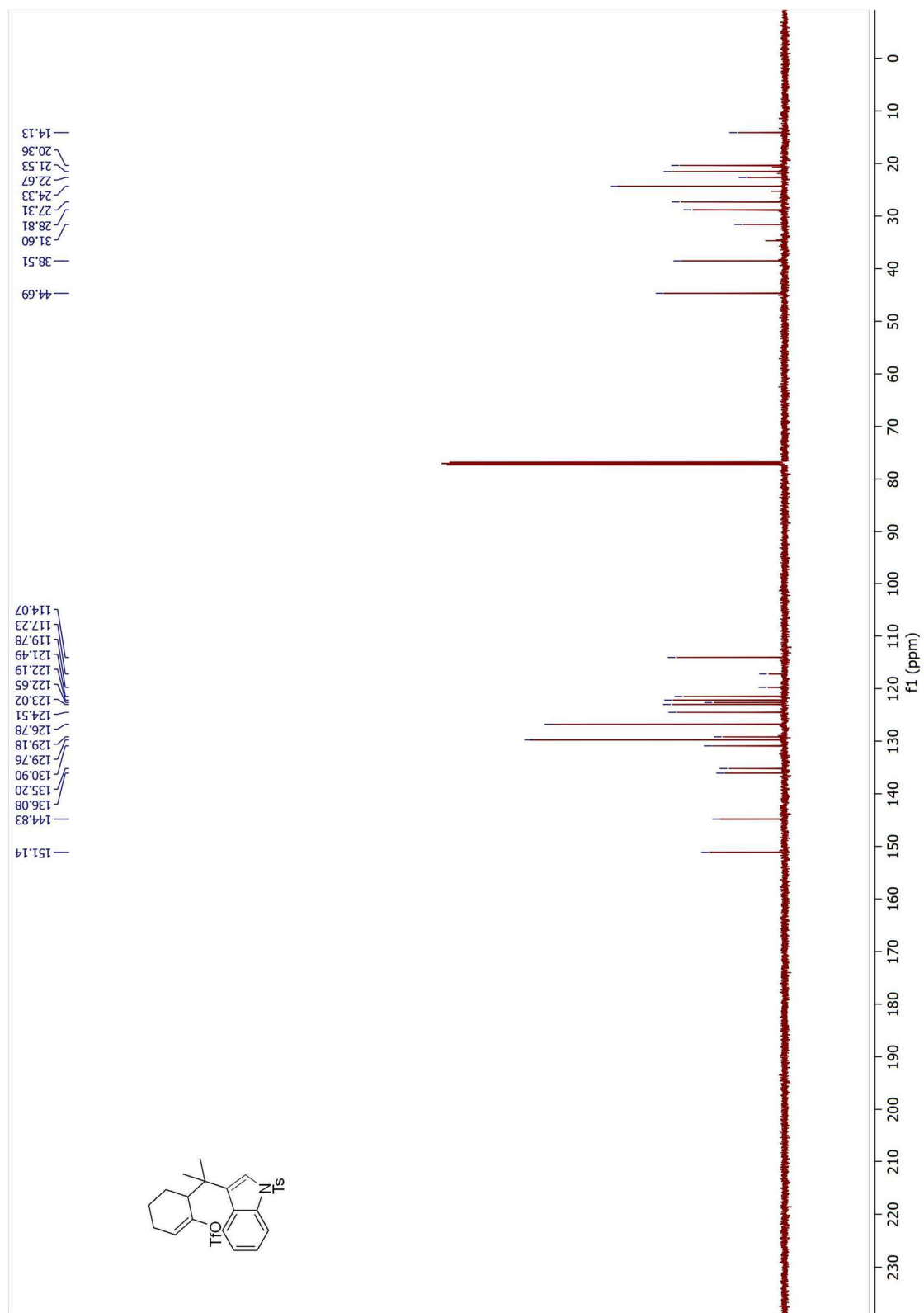


Figure 7.91 ^{13}C NMR Spectrum of 4.17 (125 MHz, CDCl_3)

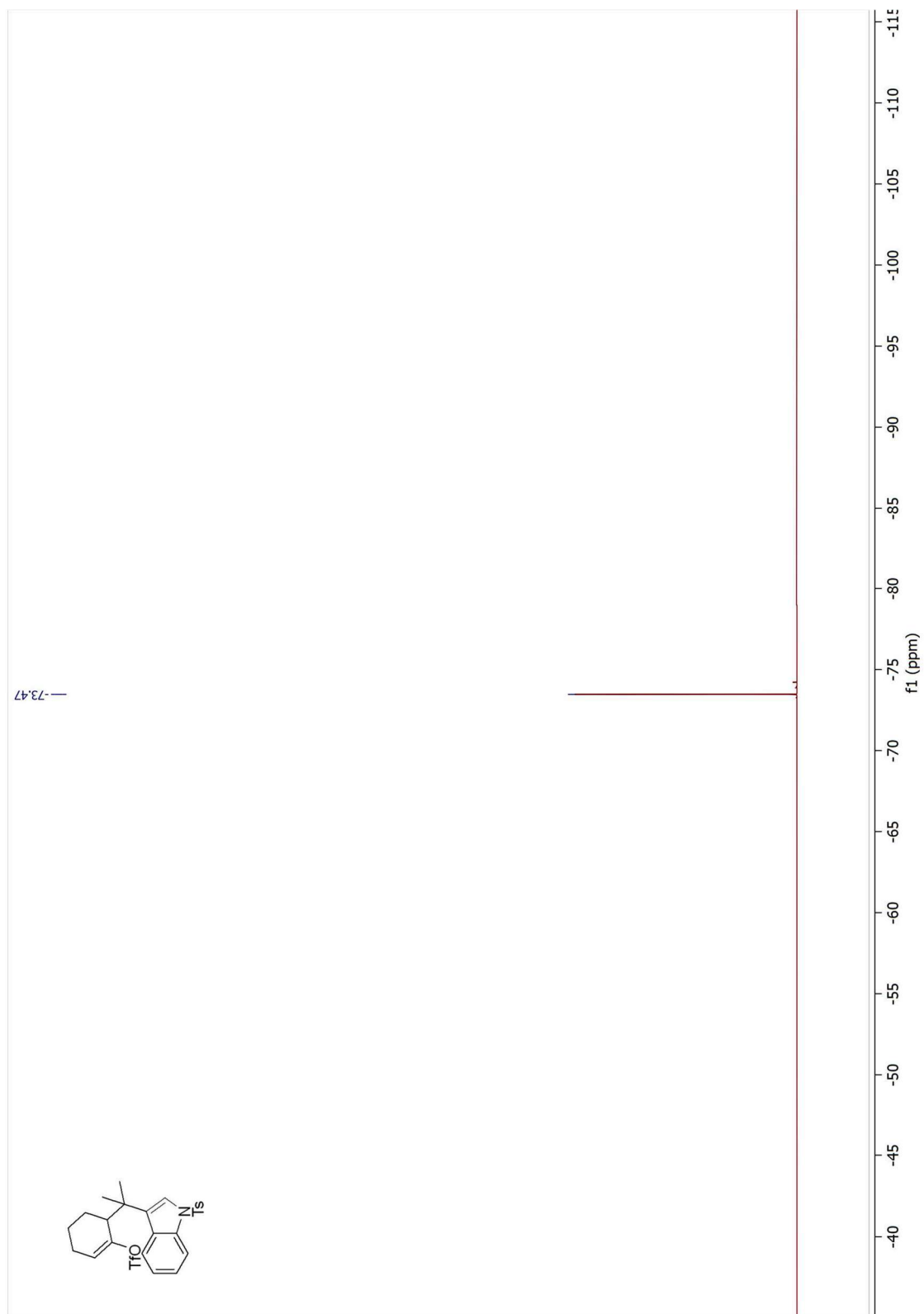


Figure 7.92 ^{19}F NMR Spectrum of **4.17** (500 MHz, CDCl_3)

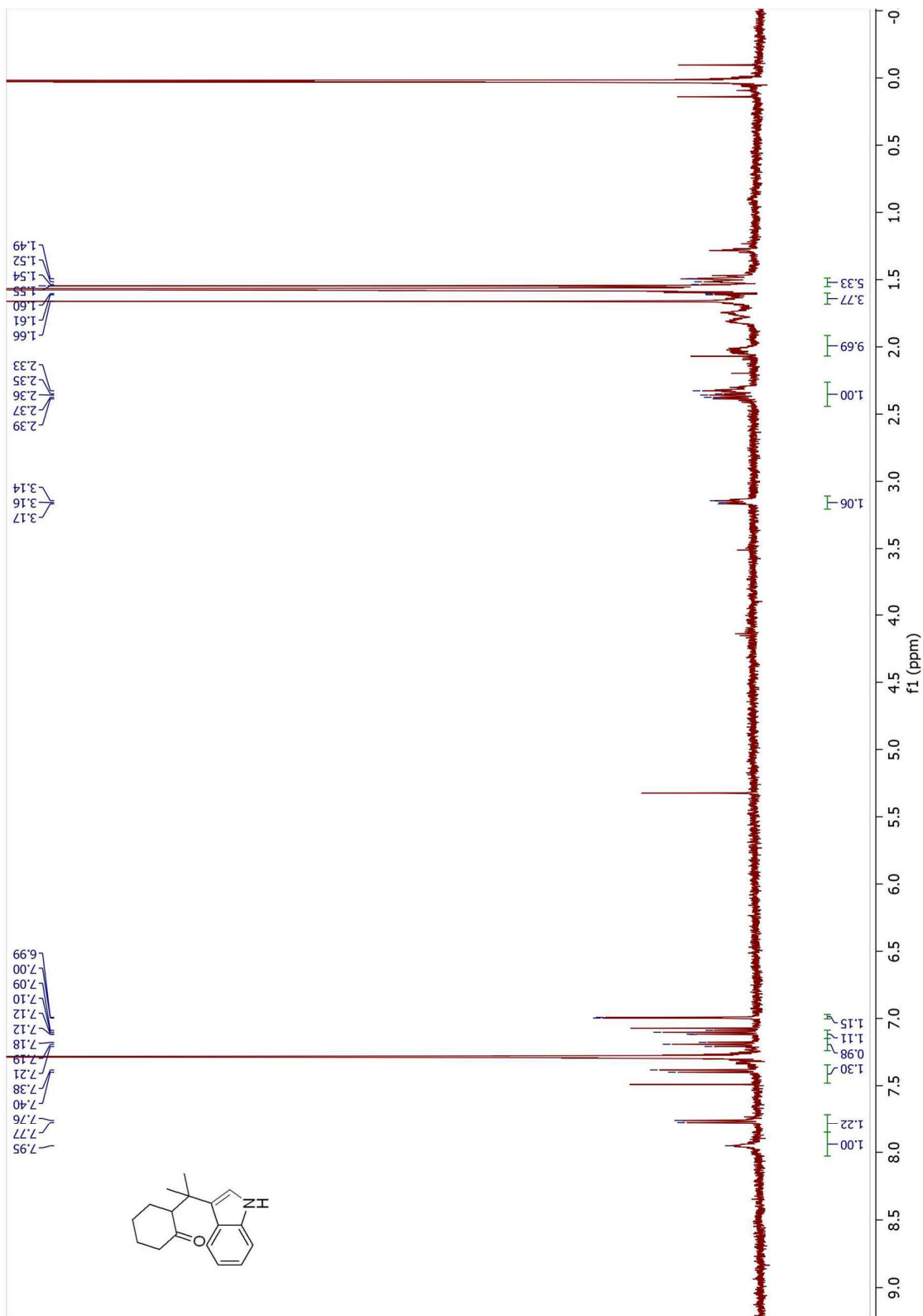


Figure 7.93 ^1H NMR Spectrum of **4.18** (500 MHz, CDCl_3)

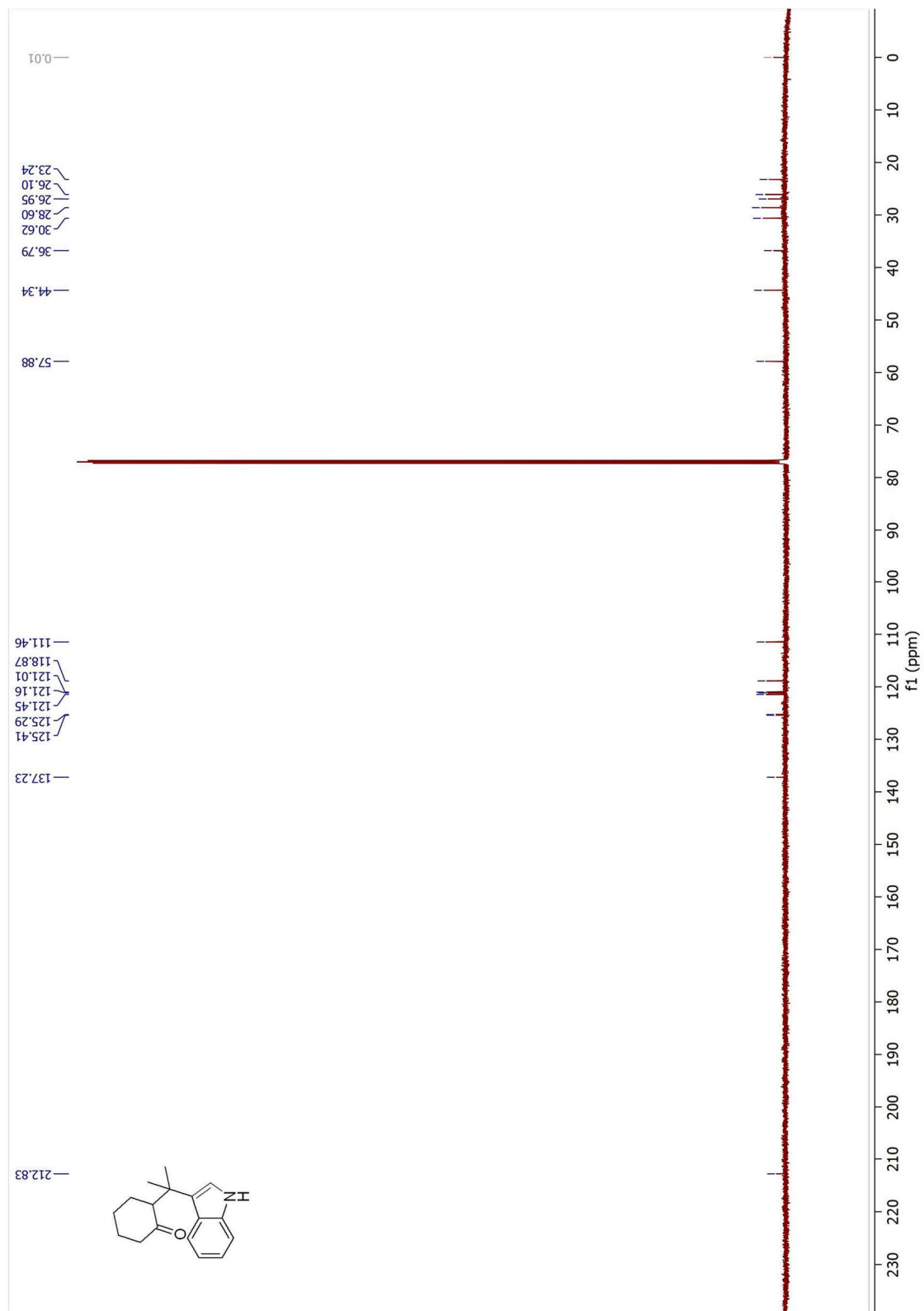


Figure 7.94 ^{13}C NMR Spectrum of **4.18** (125 MHz, CDCl_3)

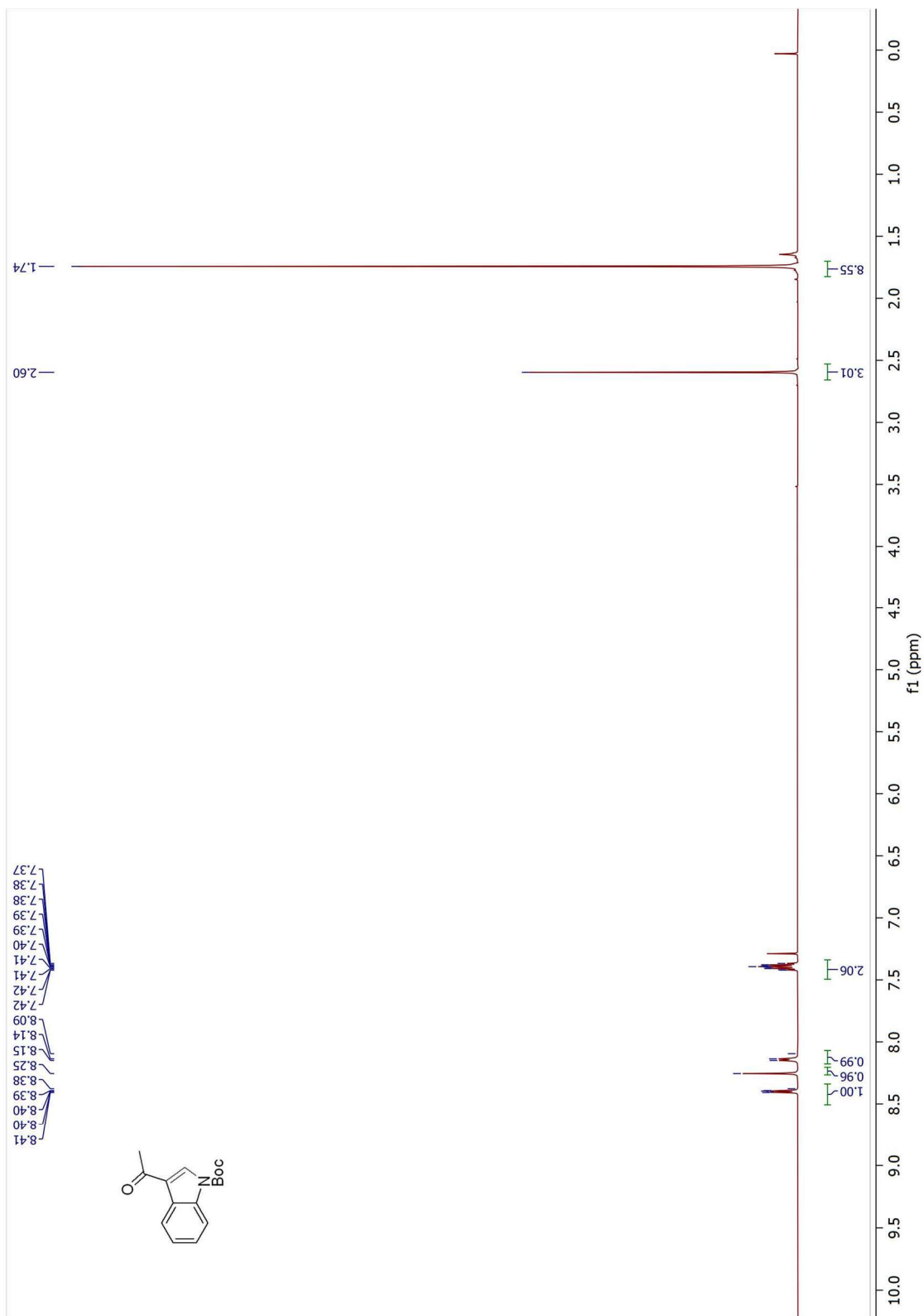


Figure 7.95 ^1H NMR Spectrum of **4.20** (500 MHz, CDCl_3)

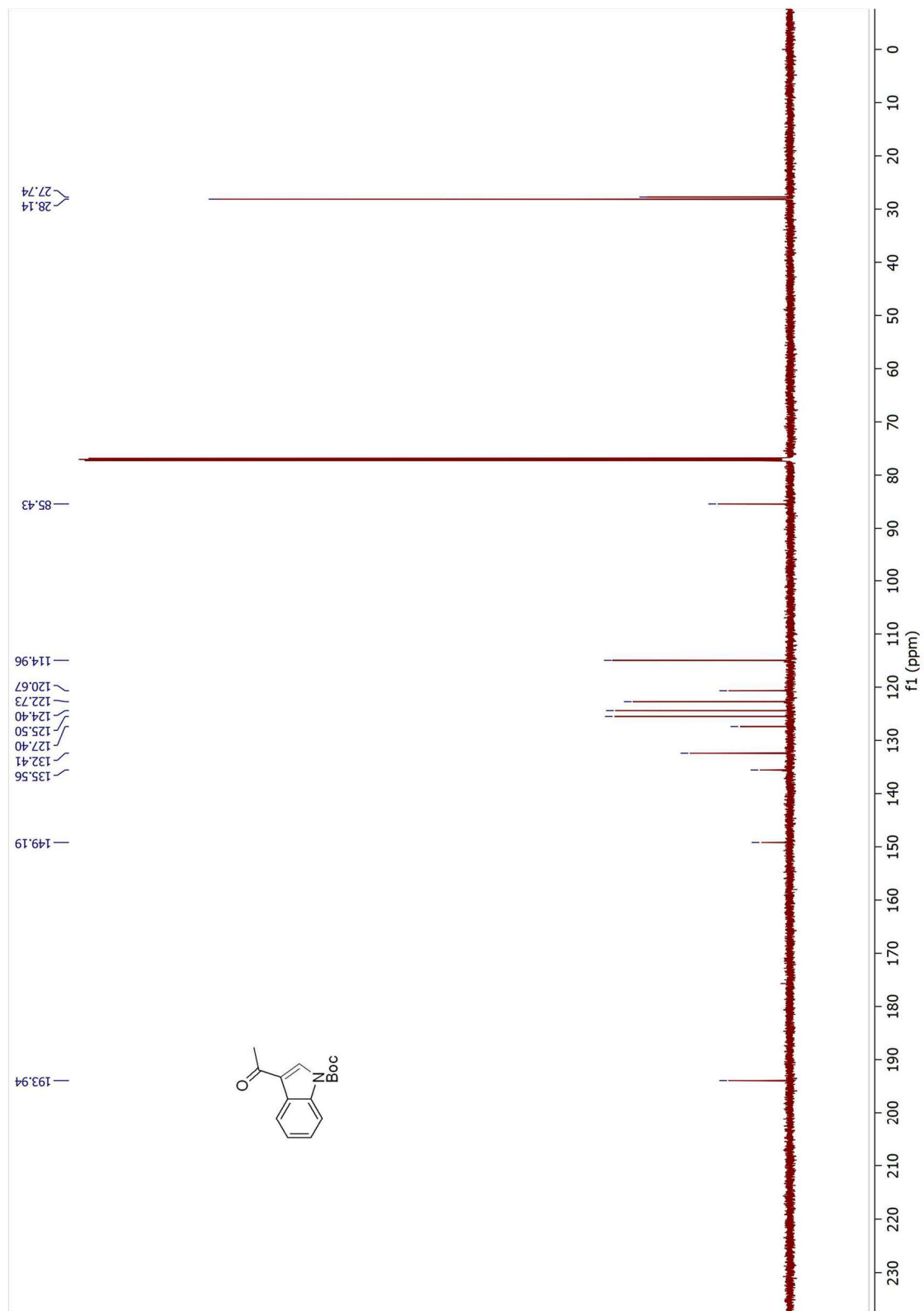


Figure 7.96 ^{13}C NMR Spectrum of **4.20** (125 MHz, CDCl_3)

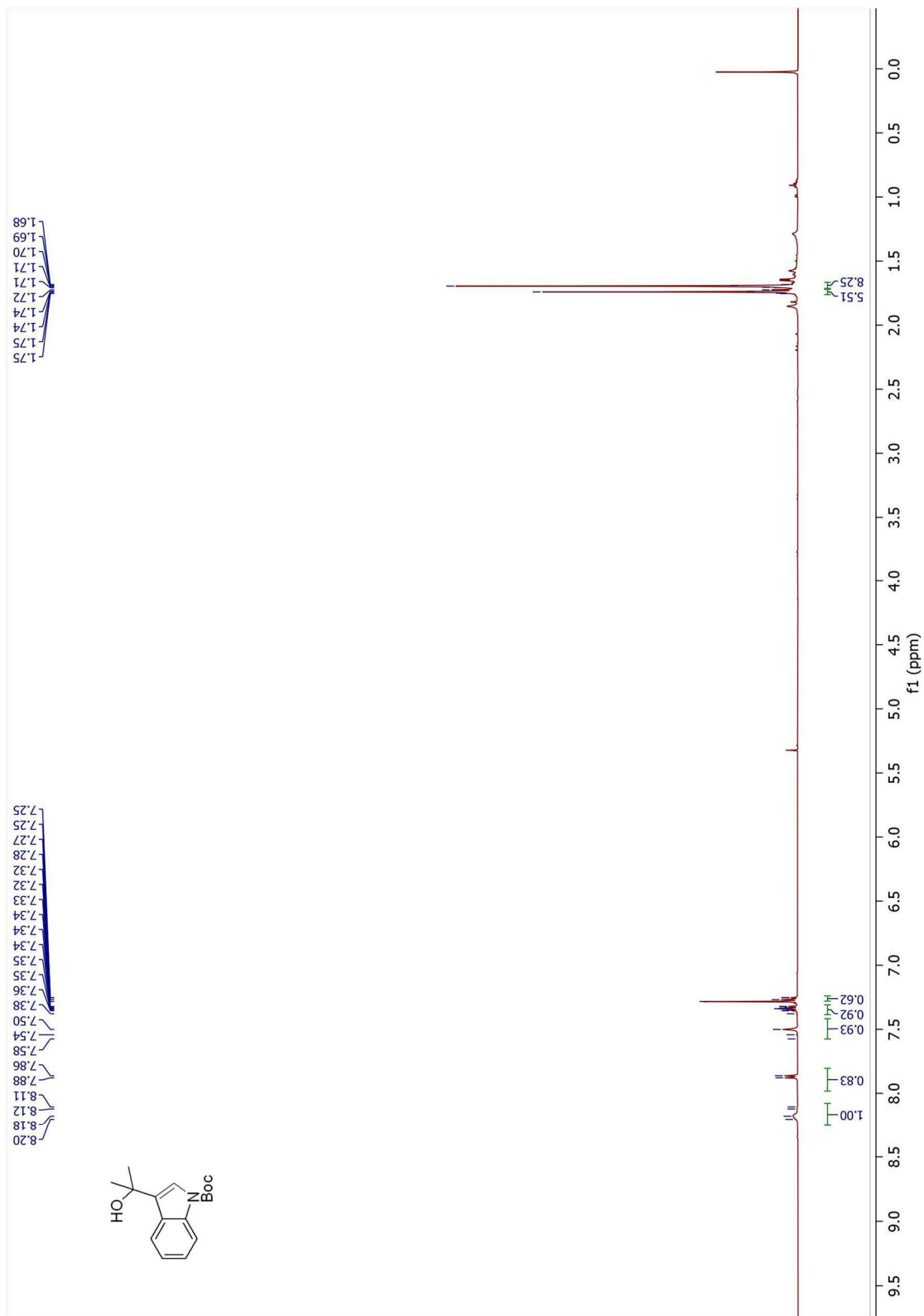


Figure 7.97 ^1H NMR Spectrum of **4.21** (500 MHz, CDCl_3)

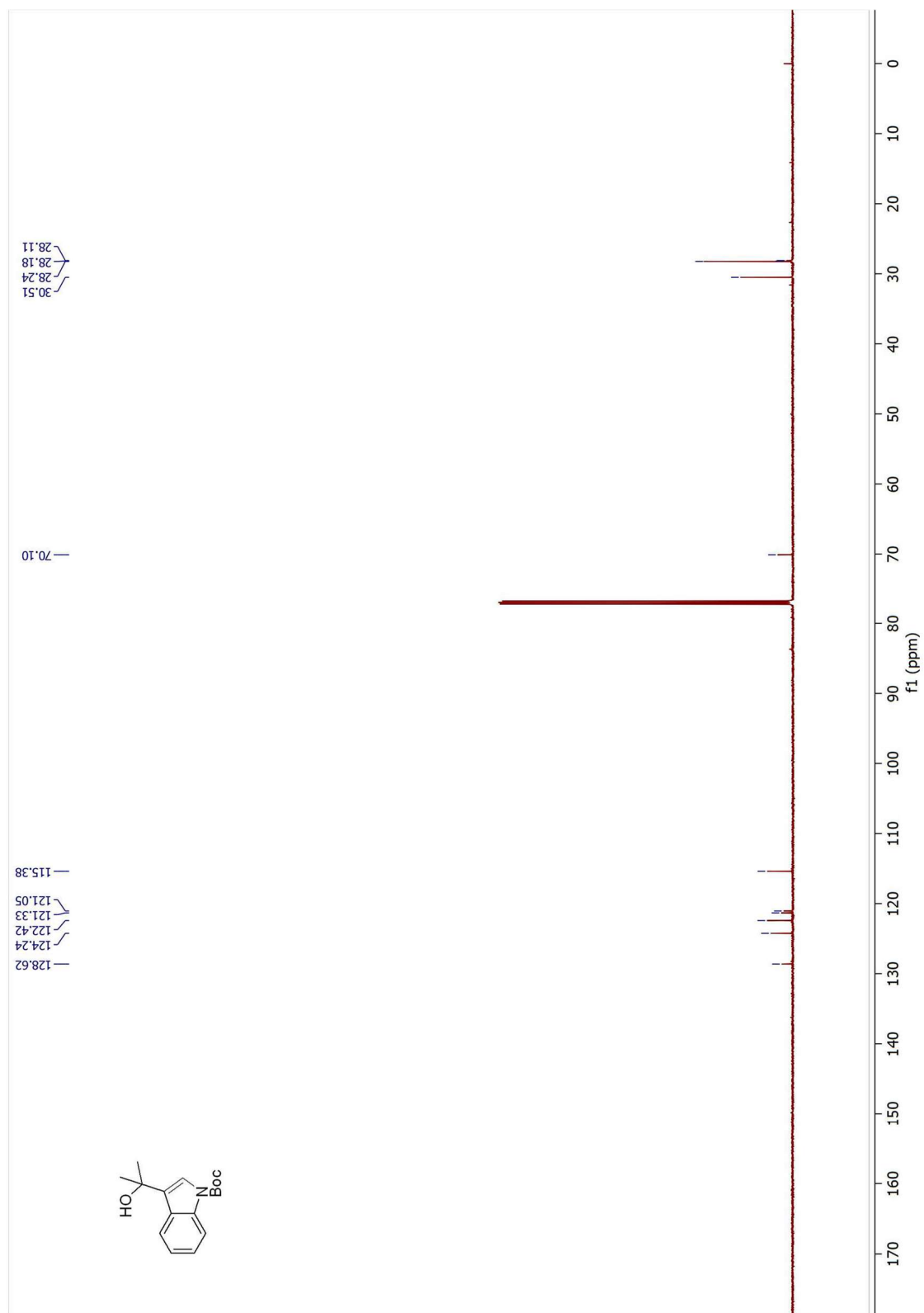


Figure 7.98 ^{13}C NMR Spectrum of **4.21** (125 MHz, CDCl_3)

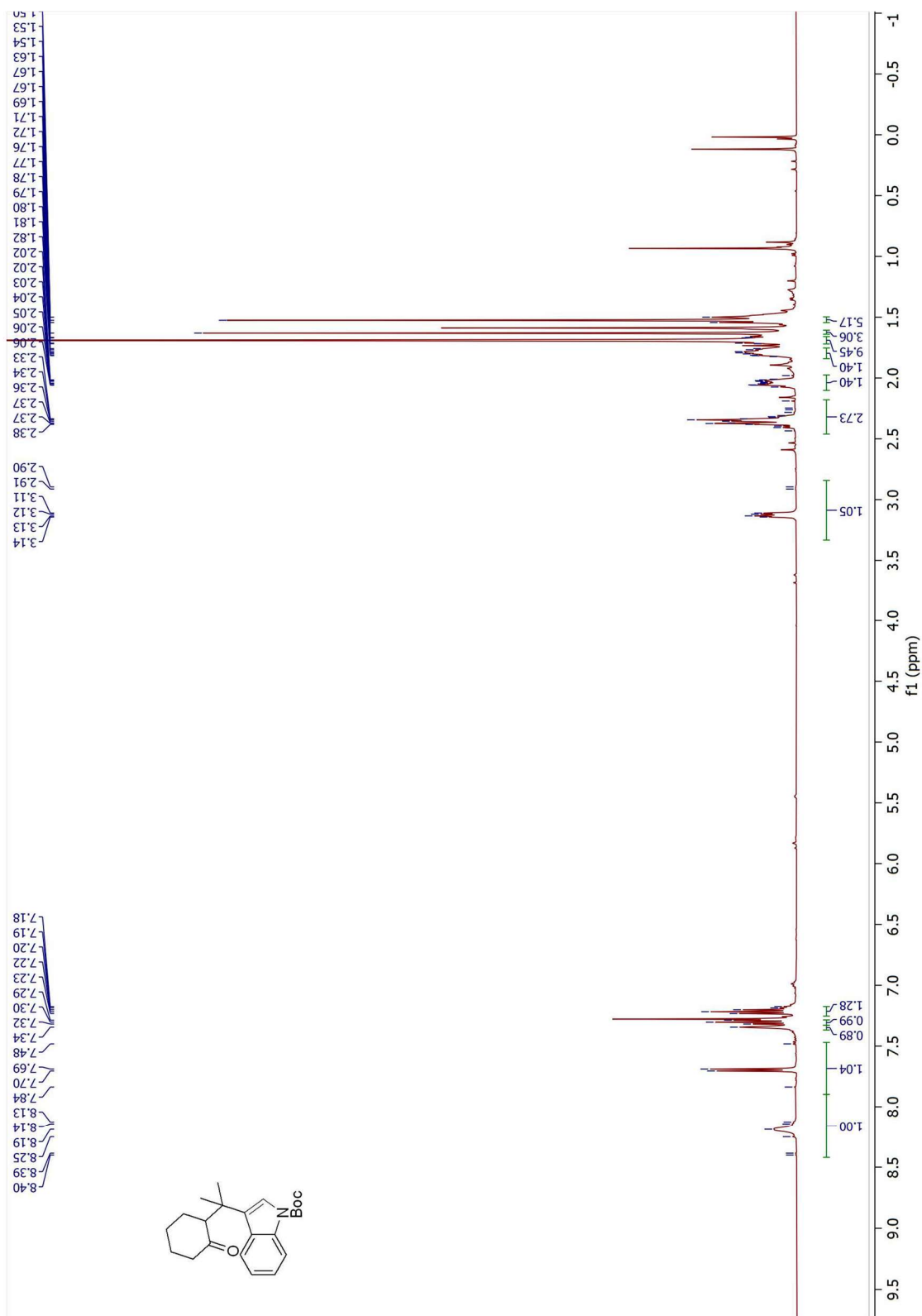


Figure 7.99 ^1H NMR Spectrum of **4.22** (500 MHz, CDCl_3)

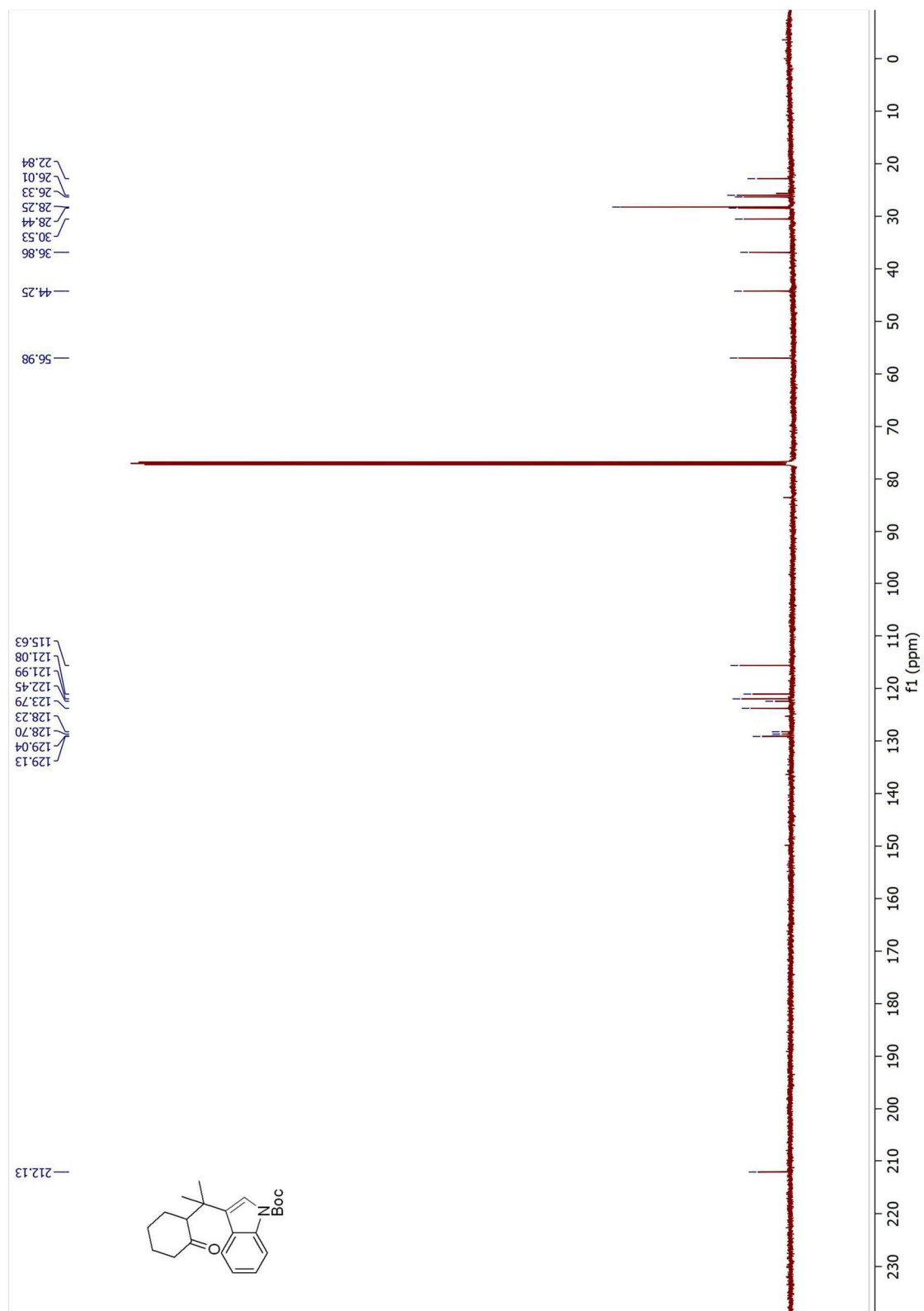


Figure 7.100 ¹³C NMR Spectrum of **4.21** (125 MHz, CDCl₃)

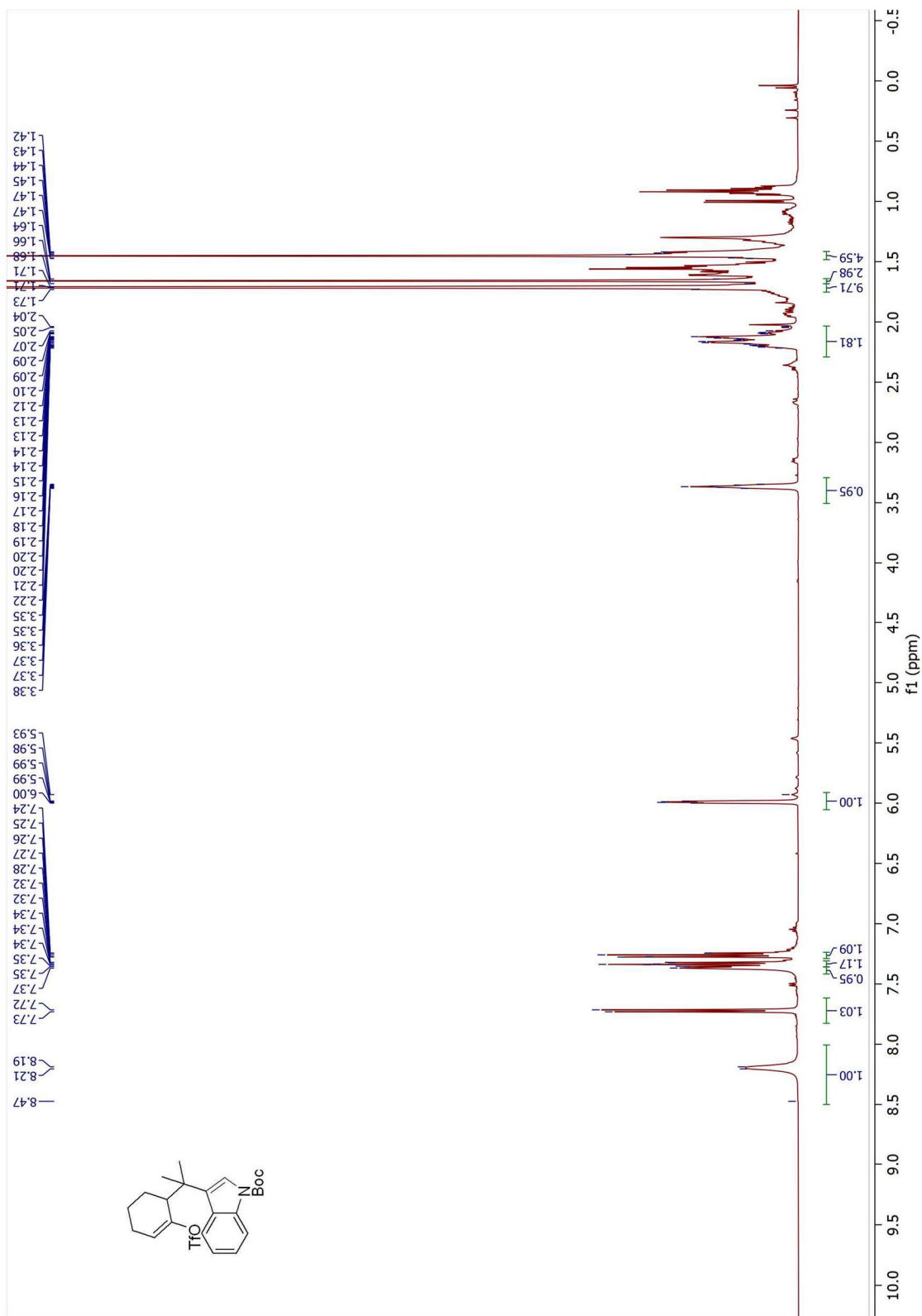


Figure 7.101 ¹H NMR Spectrum of **4.22** (500 MHz, CDCl₃)

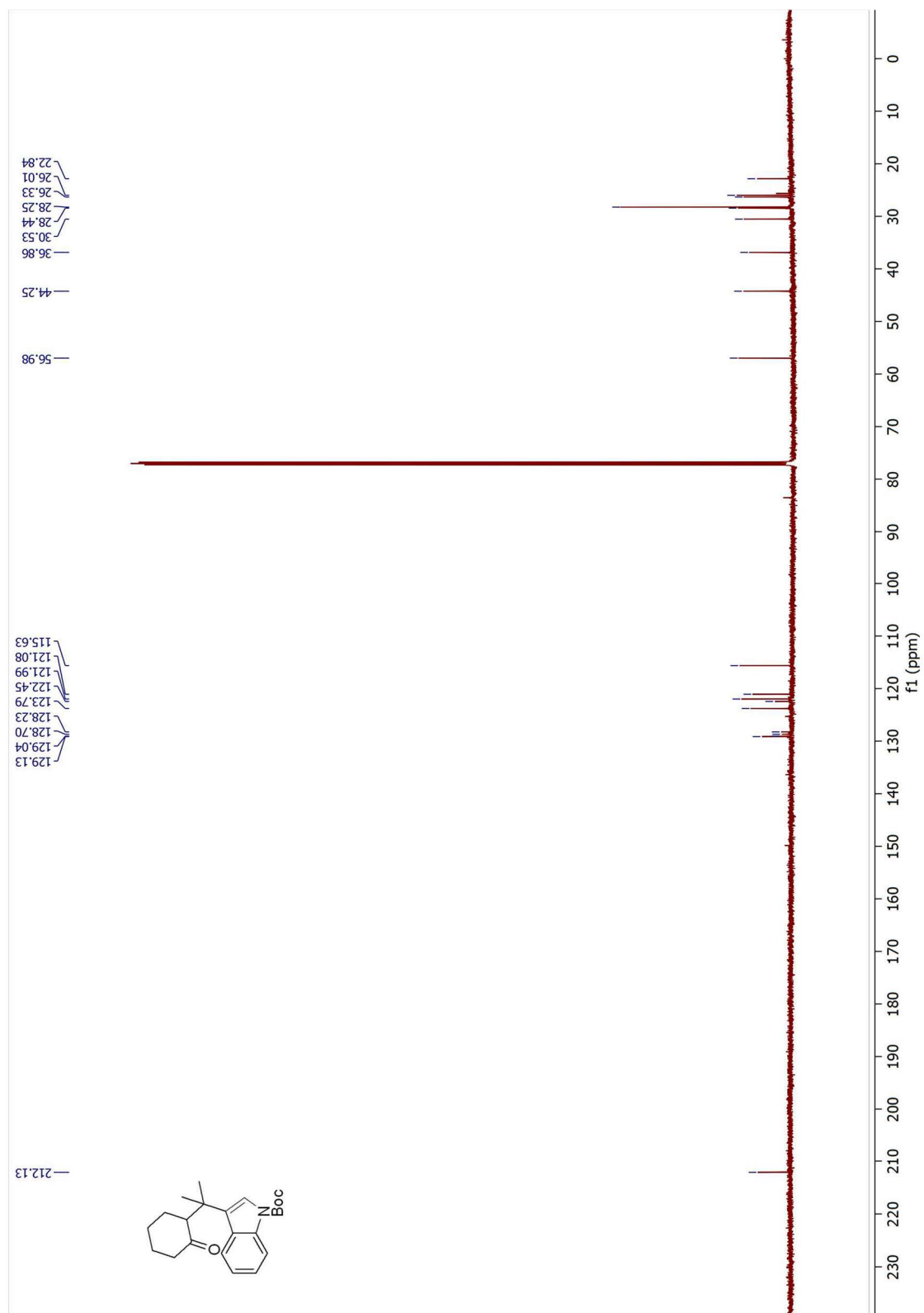


Figure 7.102 ¹³C NMR Spectrum of **4.22** (125 MHz, CDCl₃)

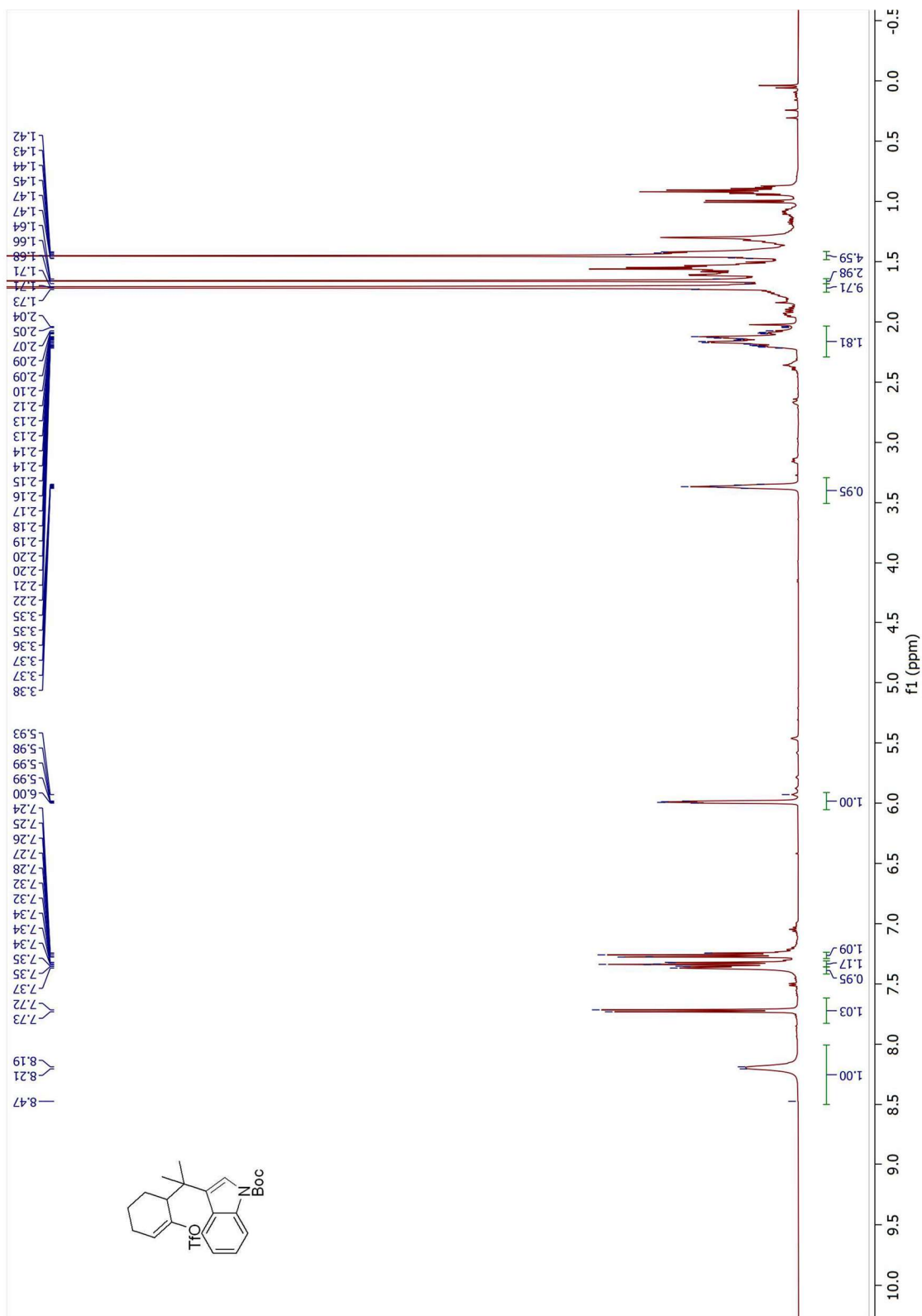


Figure 7.103 ¹H NMR Spectrum of 4.24 (500 MHz, CDCl₃)

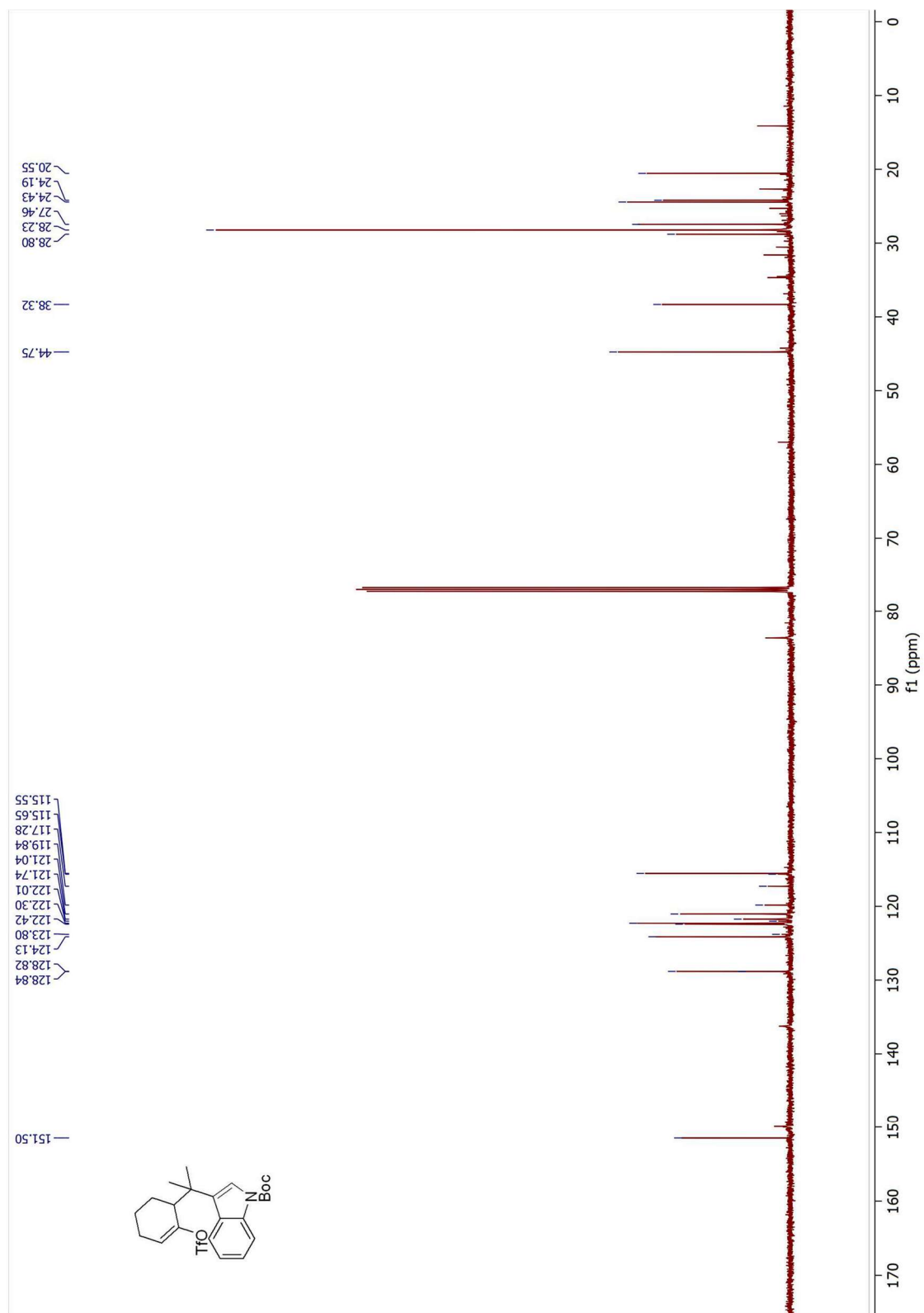


Figure 7.104 ^{13}C NMR Spectrum of **4.24** (125 MHz, CDCl_3)

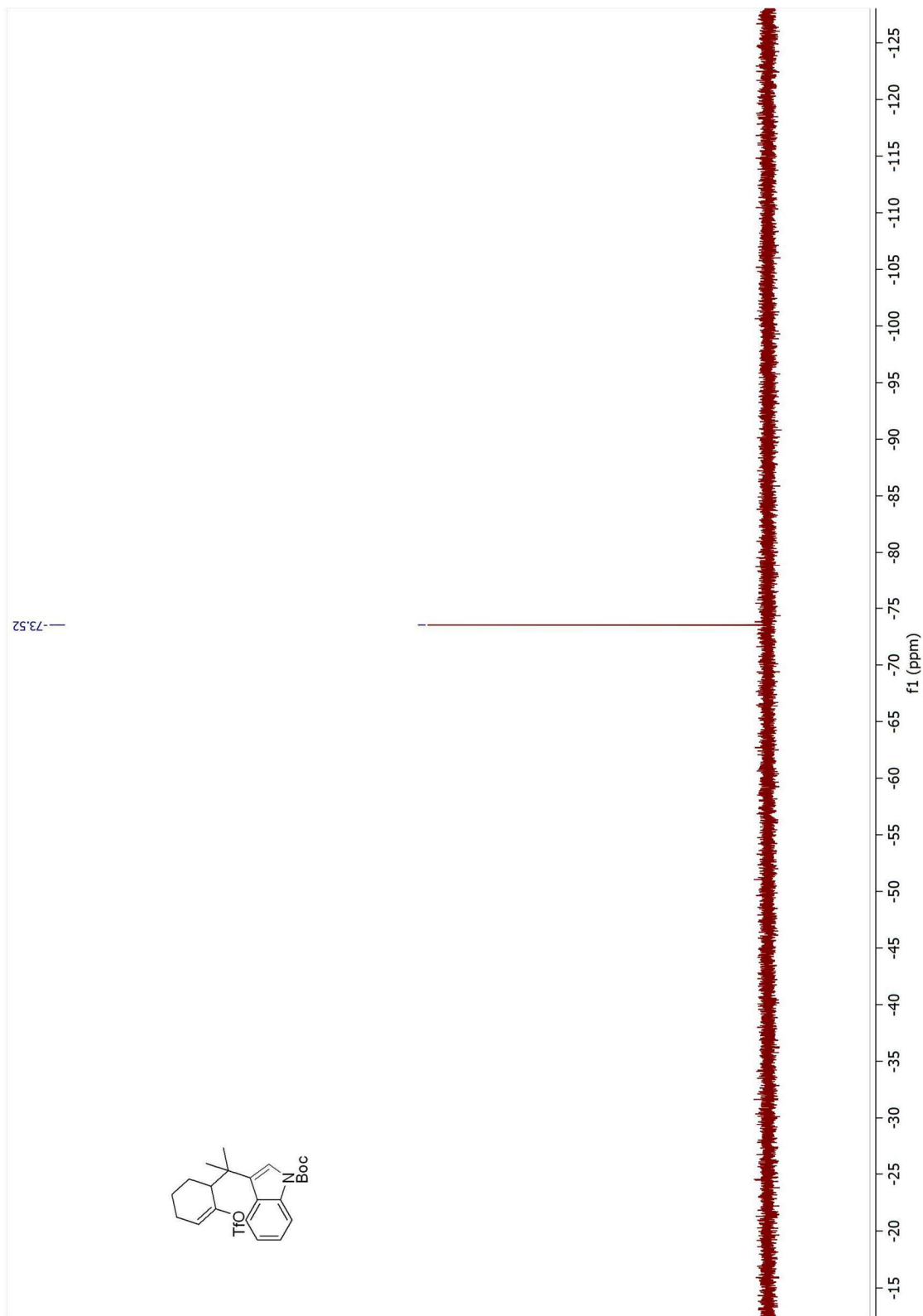


Figure 7.105 ^{19}F NMR Spectrum of **4.24** (500 MHz, CDCl_3)

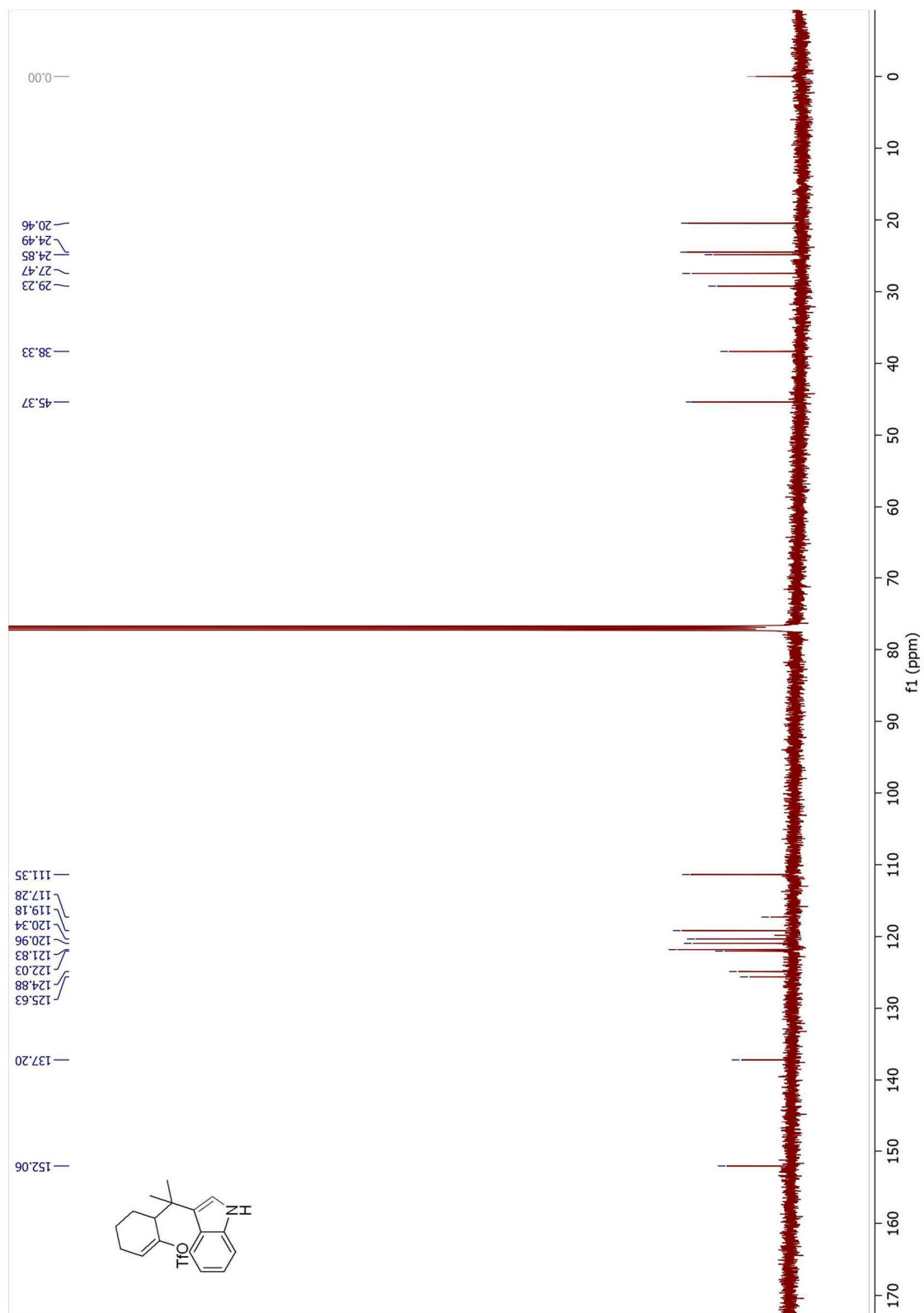


Figure 7.107 ^{13}C NMR Spectrum of **4.19** (125 MHz, CDCl_3)

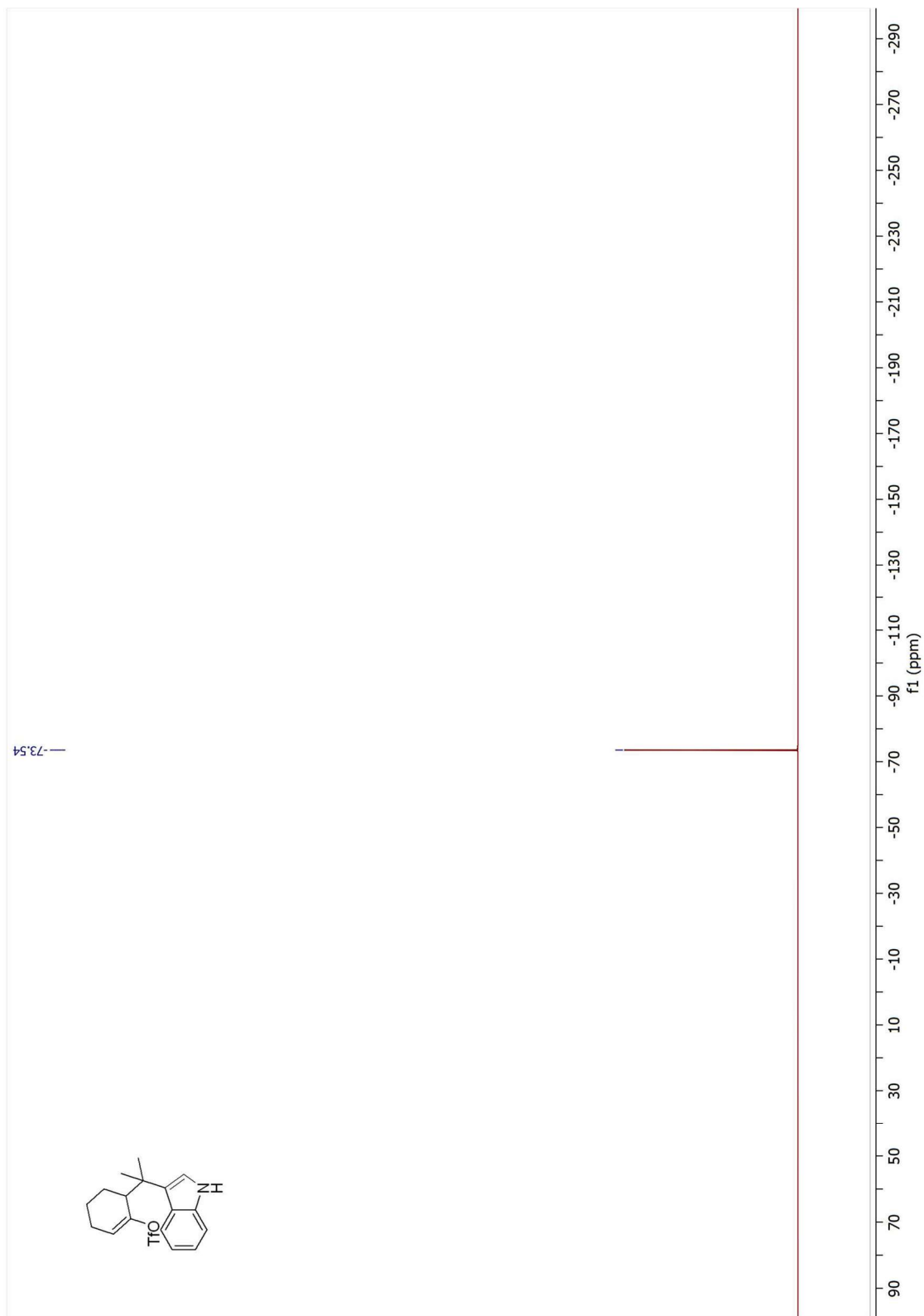


Figure 7.108 ^{19}F NMR Spectrum of **4.19** (500 MHz, CDCl_3)

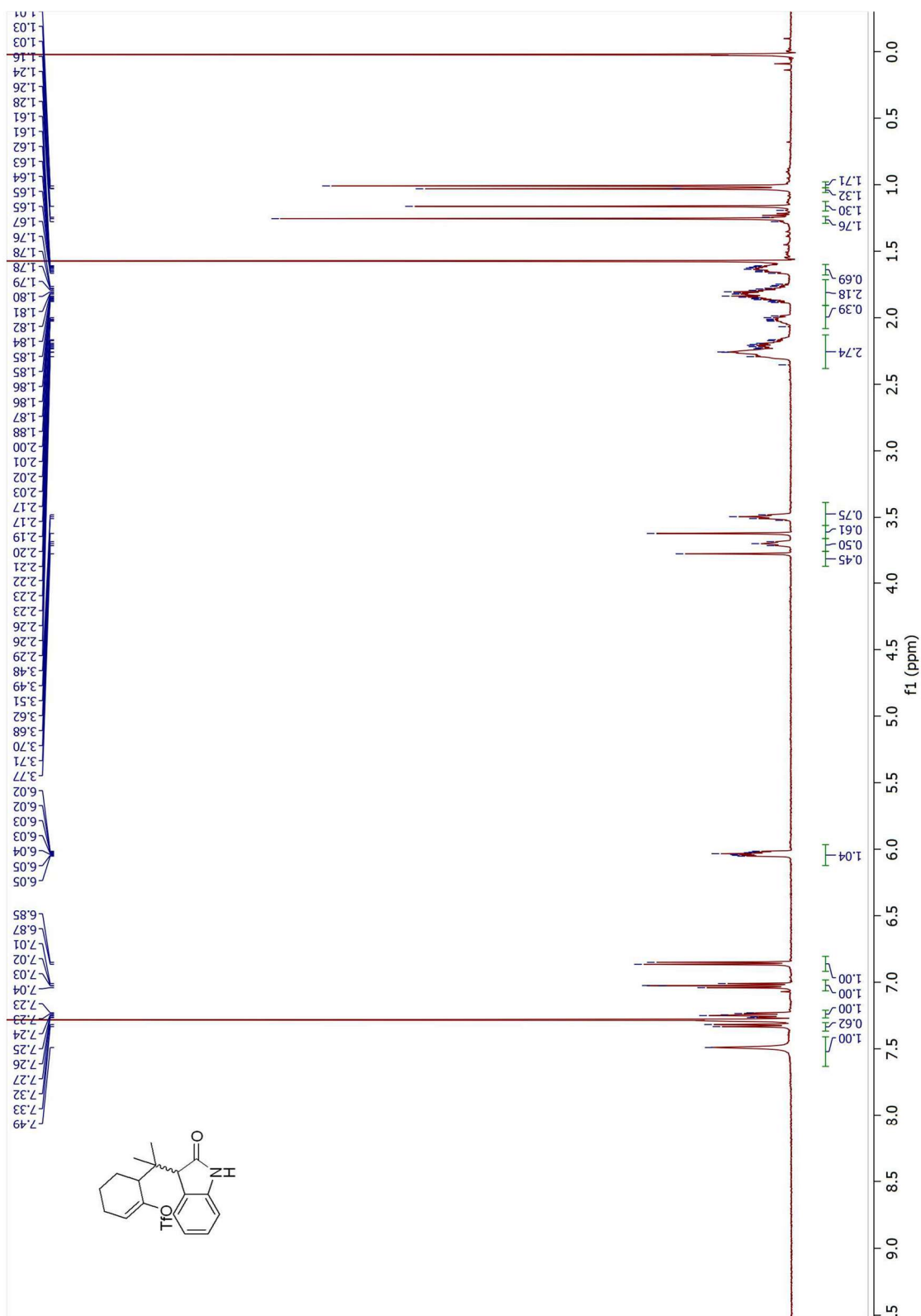


Figure 7.109 ¹H NMR Spectrum of **4.8** (500 MHz, CDCl₃)

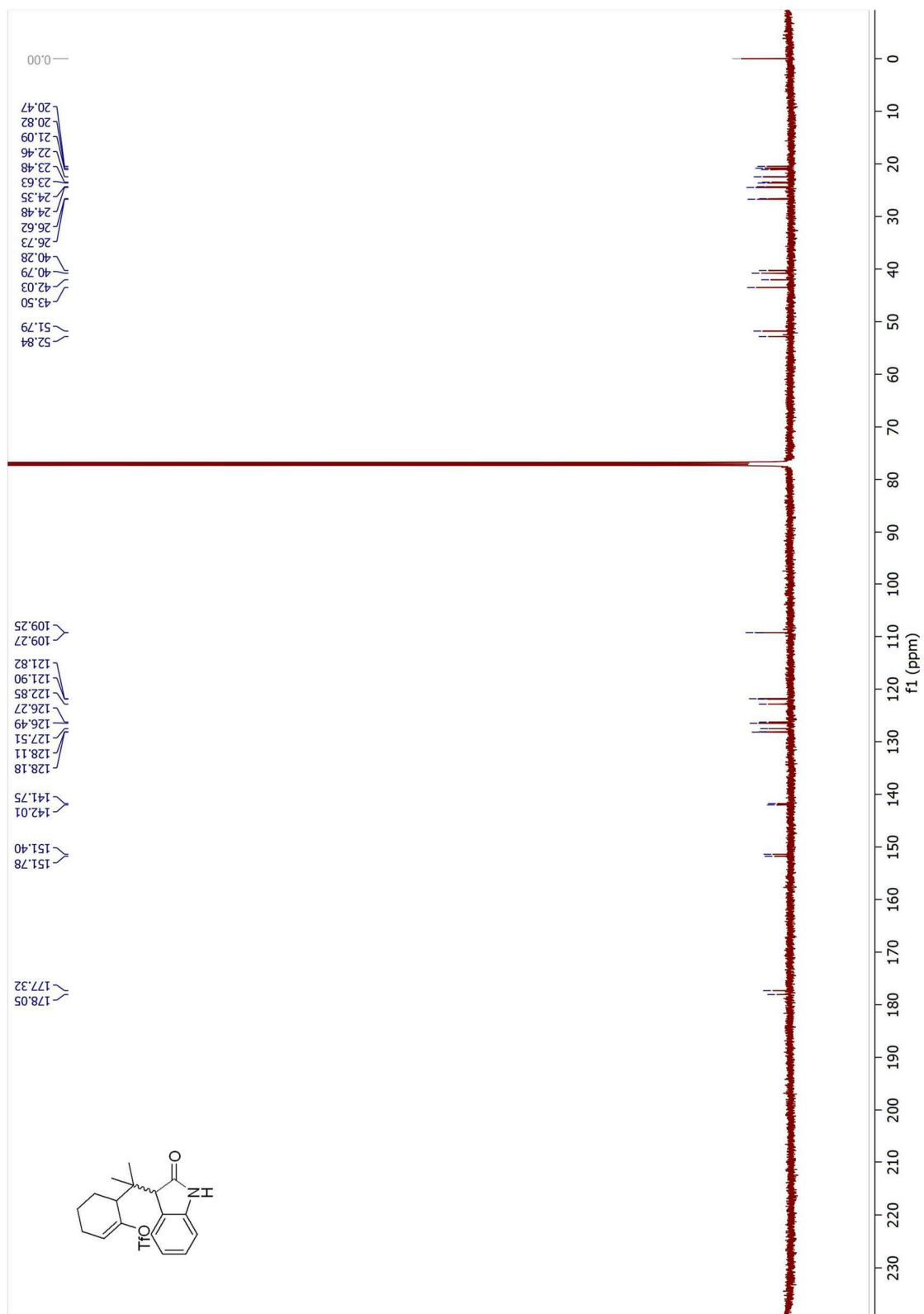


Figure 7.110 ¹³C NMR Spectrum of **4.8** (125 MHz, CDCl₃)

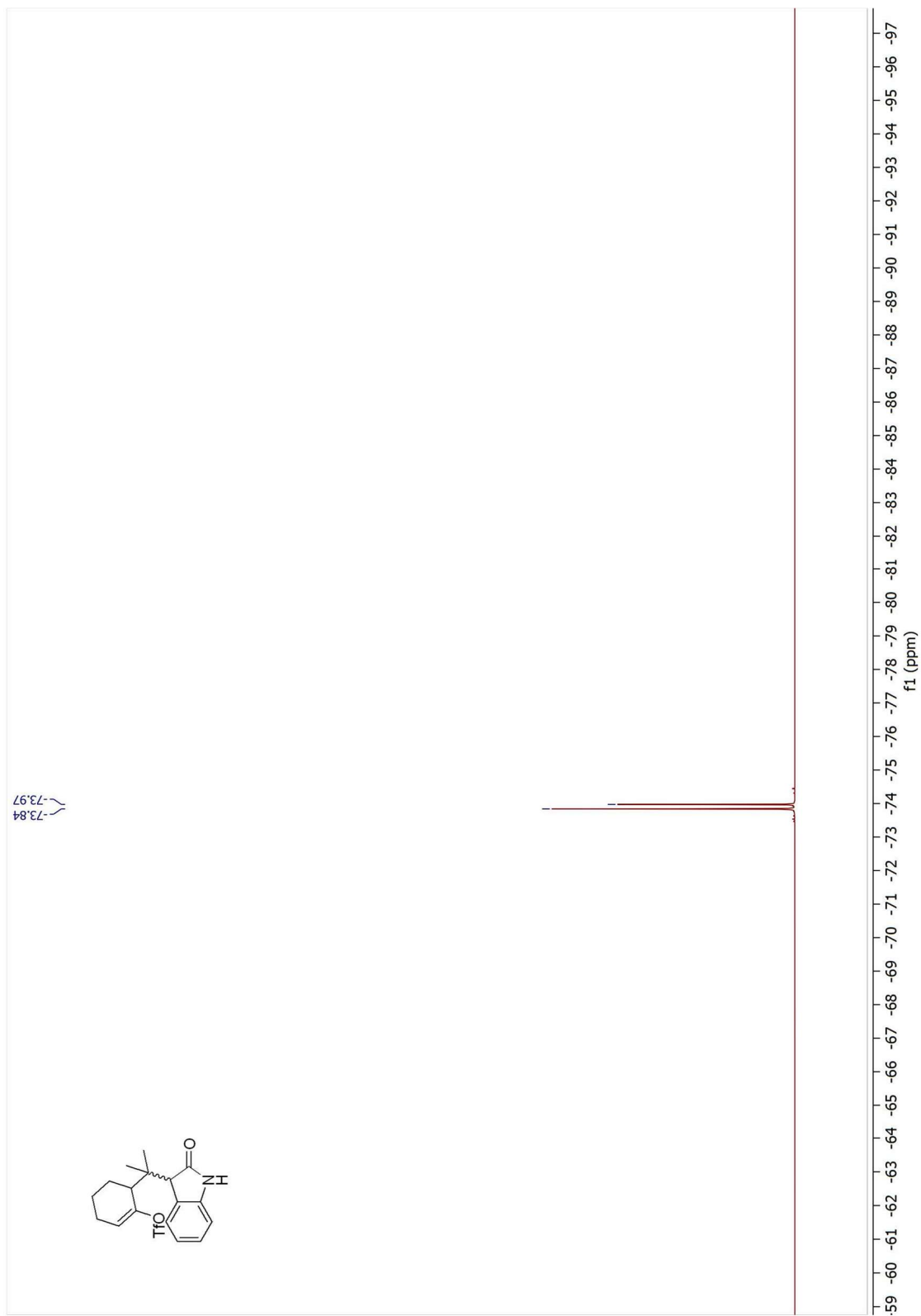


Figure 7.111 ^{19}F NMR Spectrum of **4.8** (500 MHz, CDCl_3)

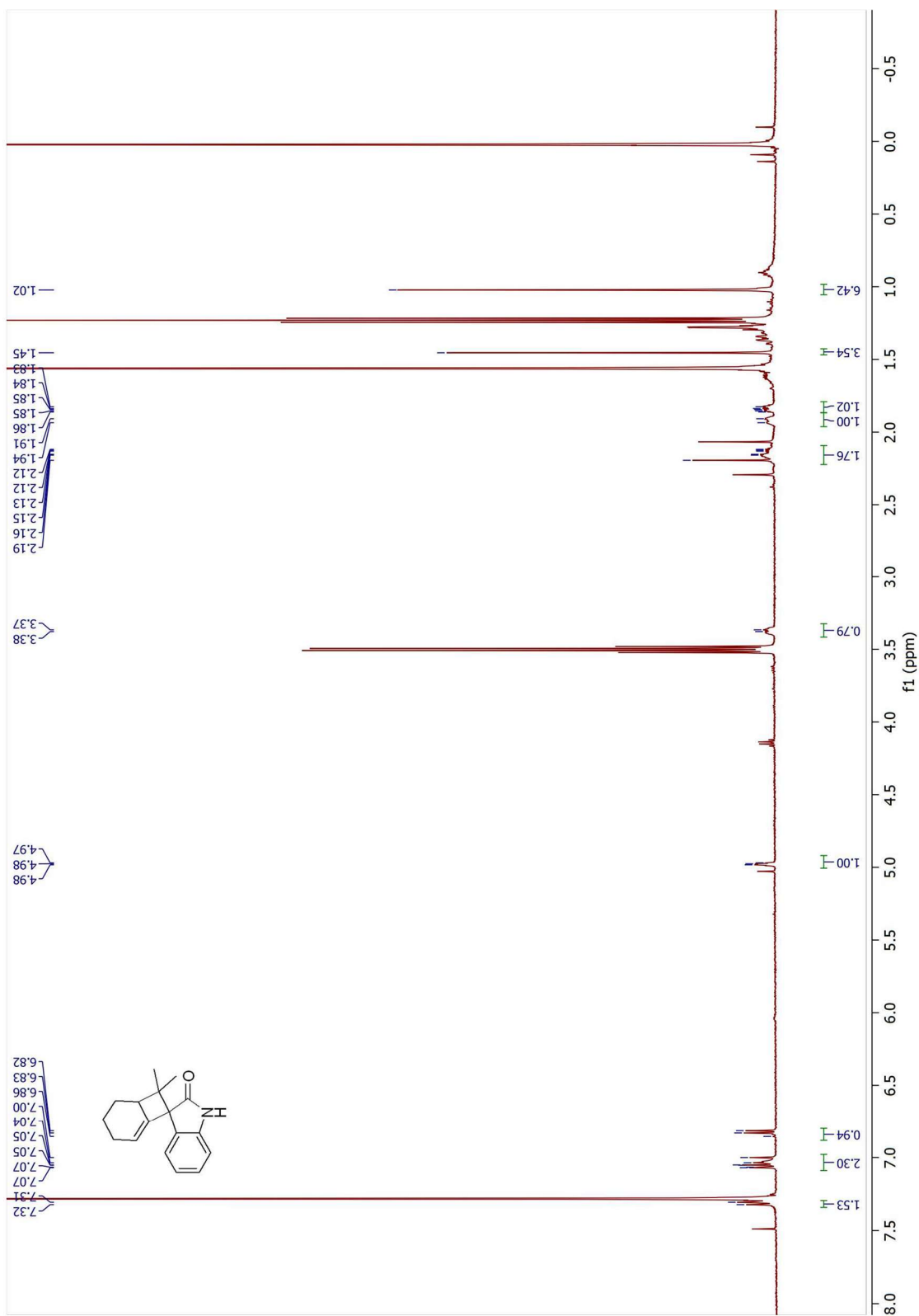


Figure 7.112 ^1H NMR Spectrum of **4.9** (500 MHz, CDCl_3)

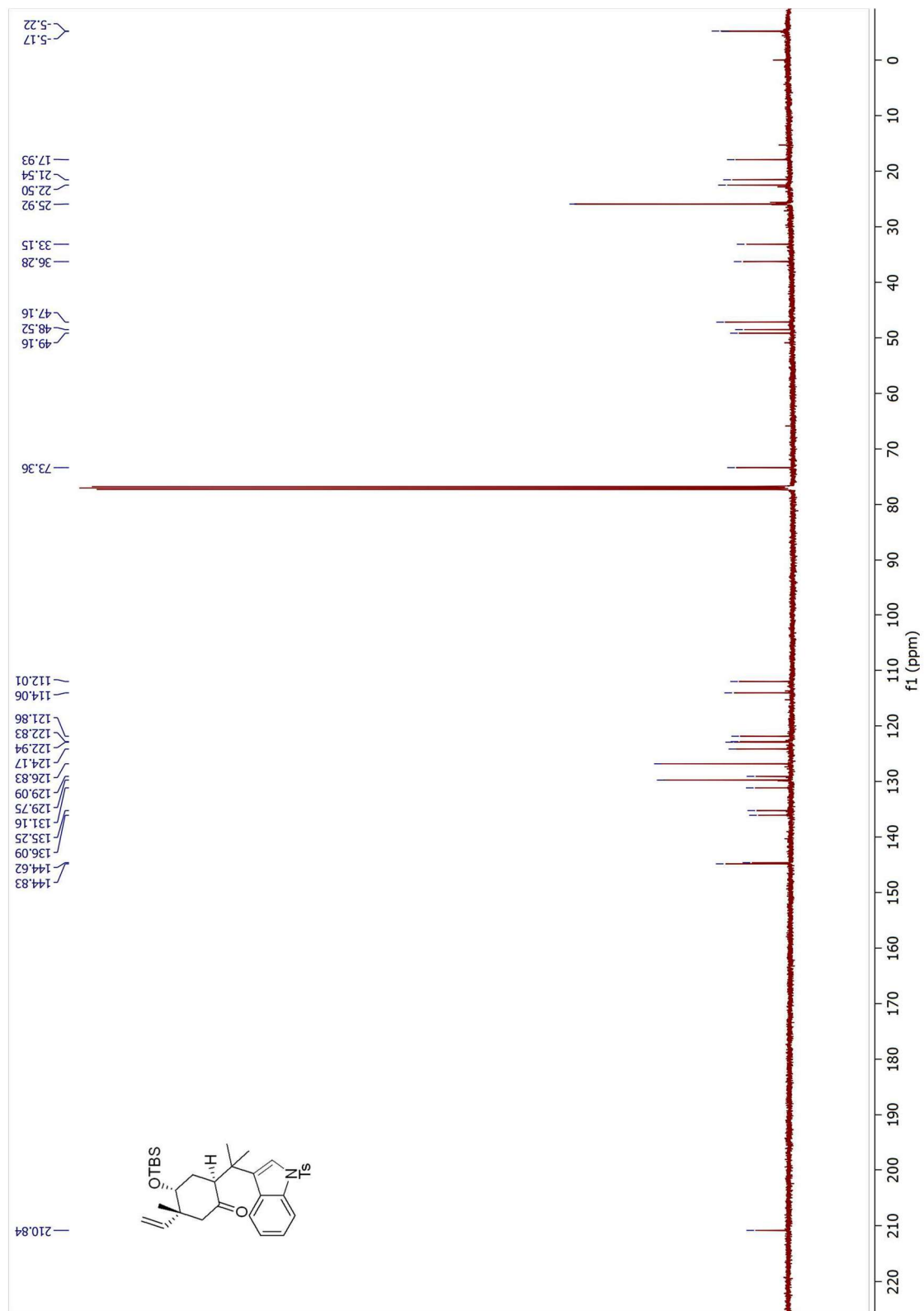


Figure 7.114 ^{13}C NMR Spectrum of 4.26 (125 MHz, CDCl_3)

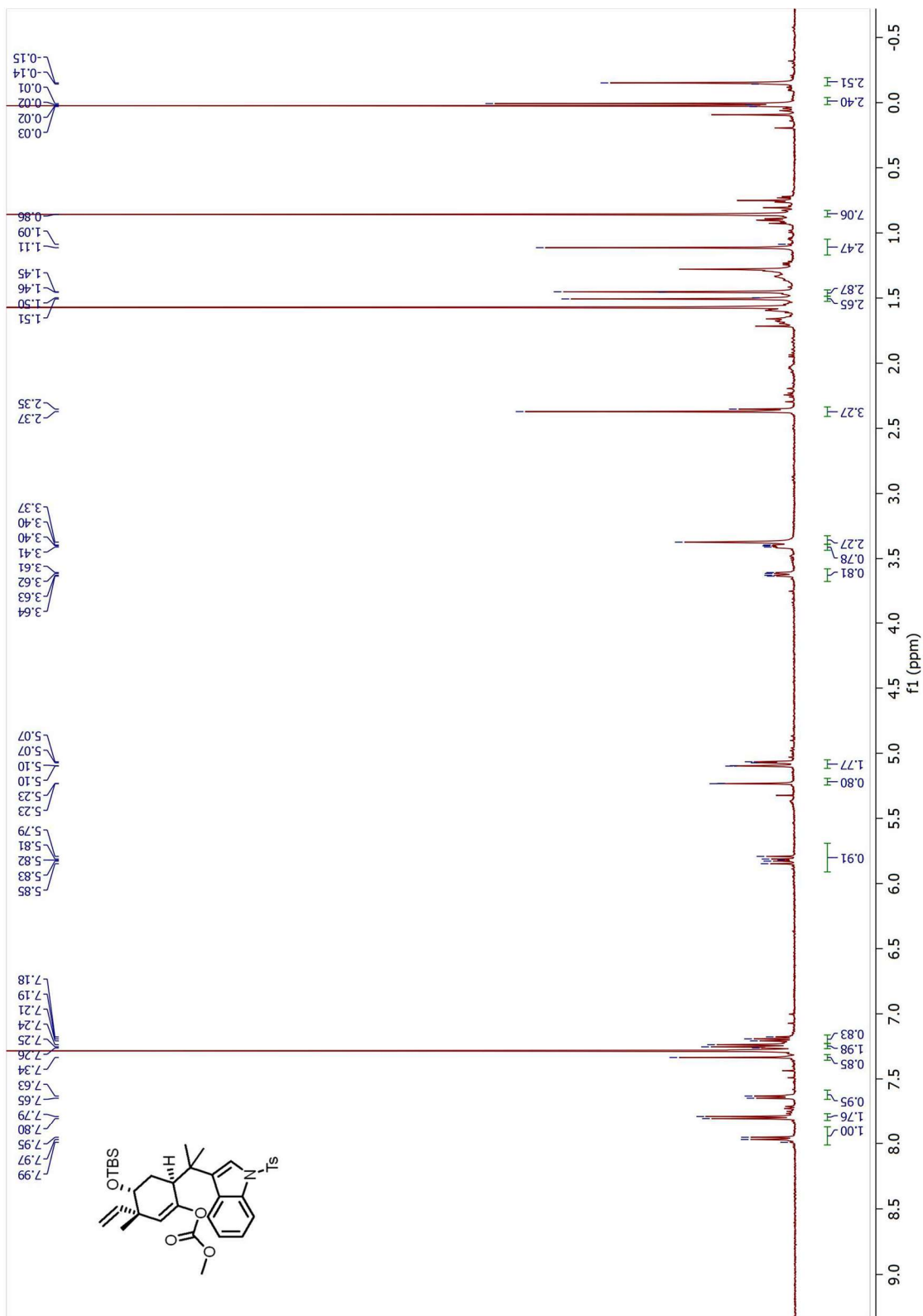


Figure 7.115 ^1H NMR Spectrum of 4.35 (500 MHz, CDCl_3)

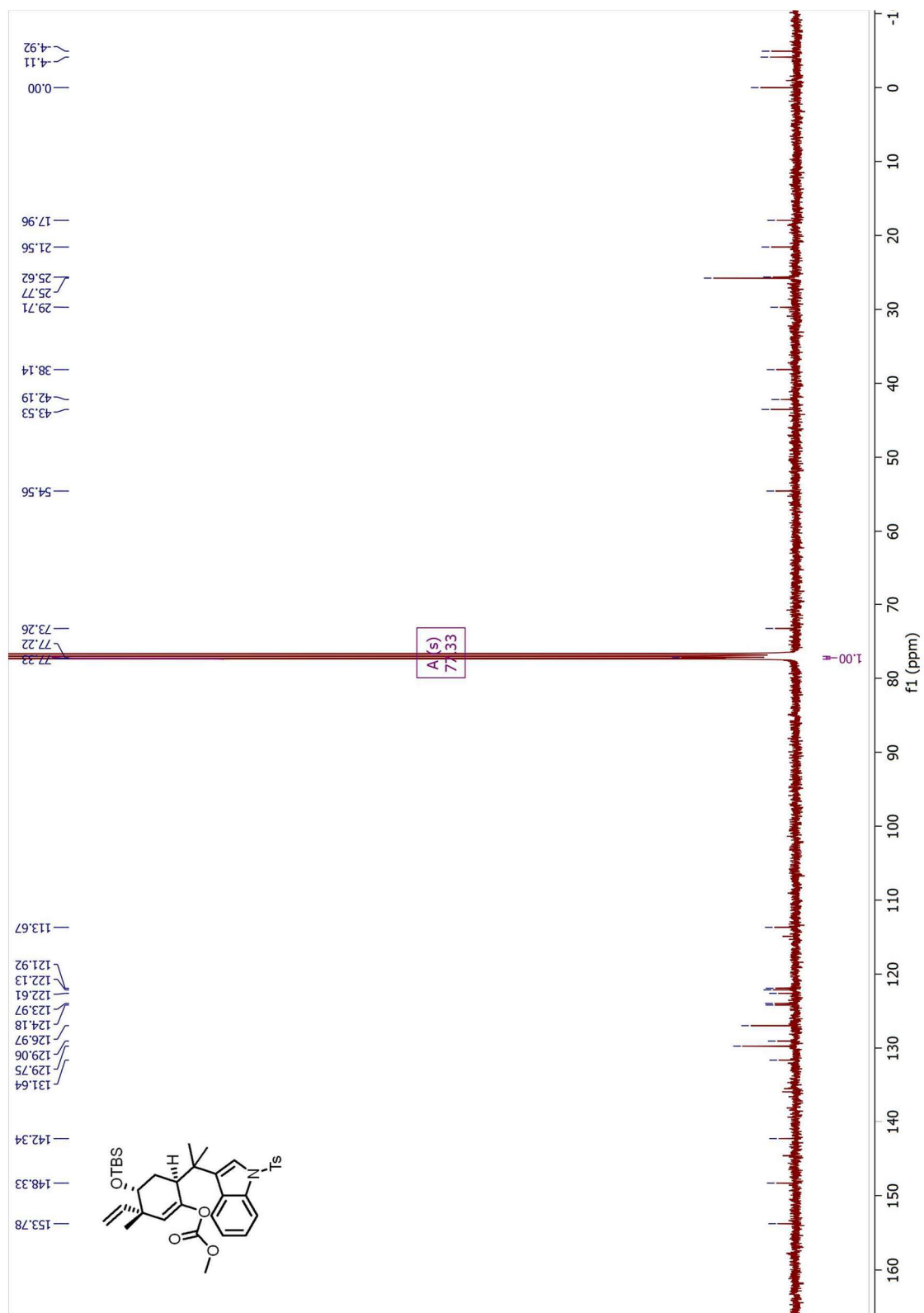


Figure 7.116 ^{13}C NMR Spectrum of **4.35** (125 MHz, CDCl_3)

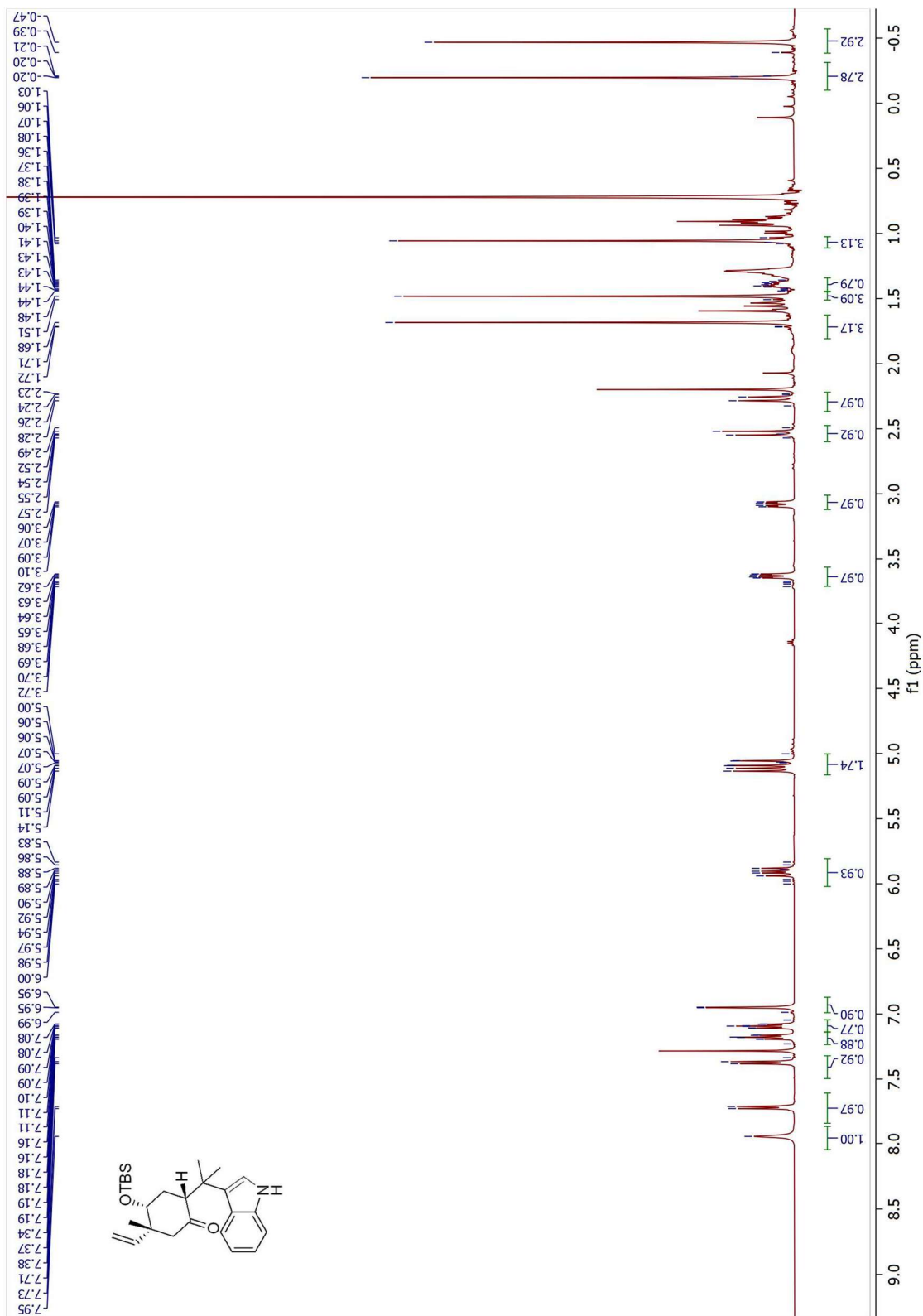


Figure 7.118 ¹H NMR Spectrum of 4.36 (500 MHz, CDCl₃)

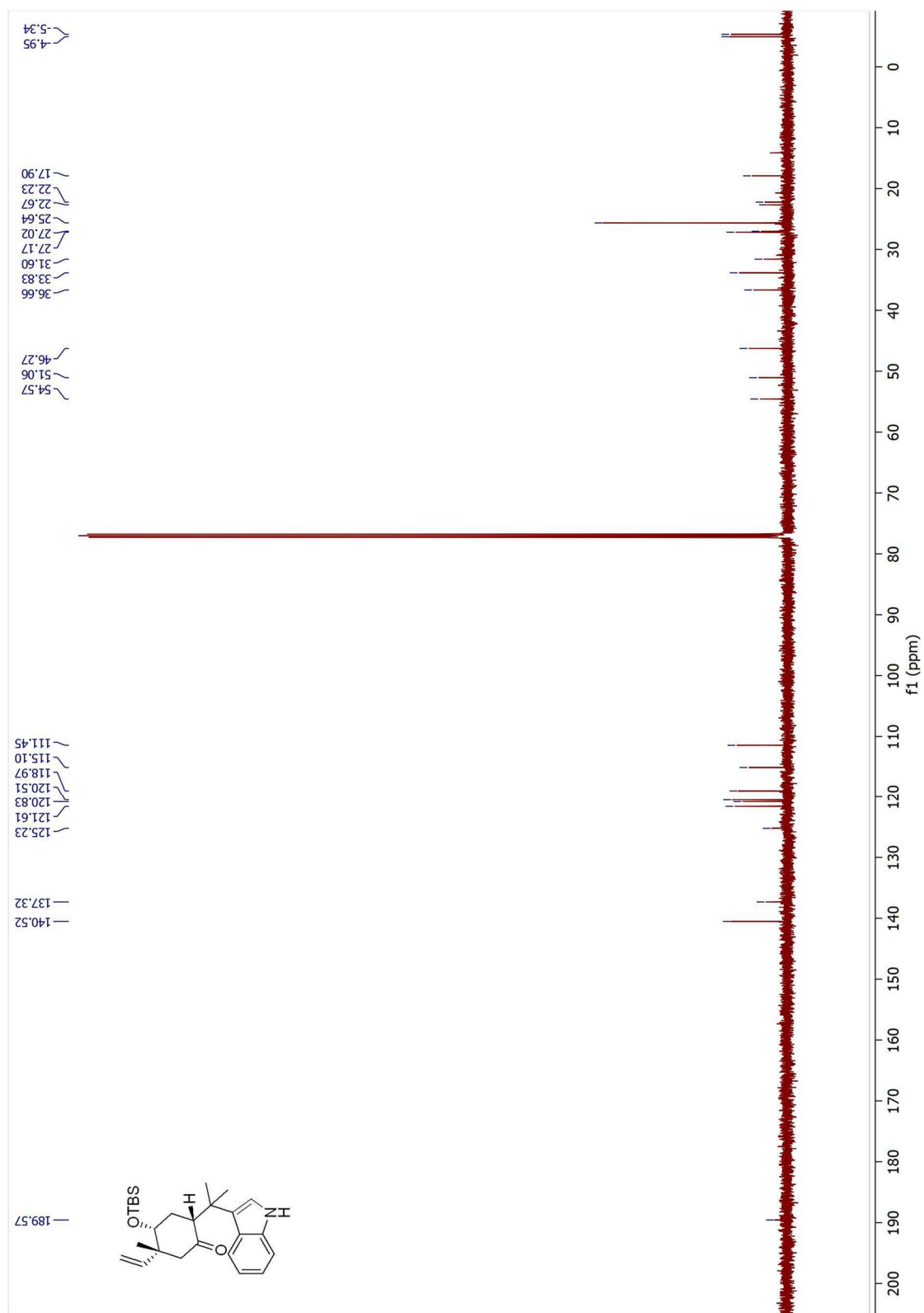


Figure 7.119 ^{13}C NMR Spectrum of 4.36 (125 MHz, CDCl_3)

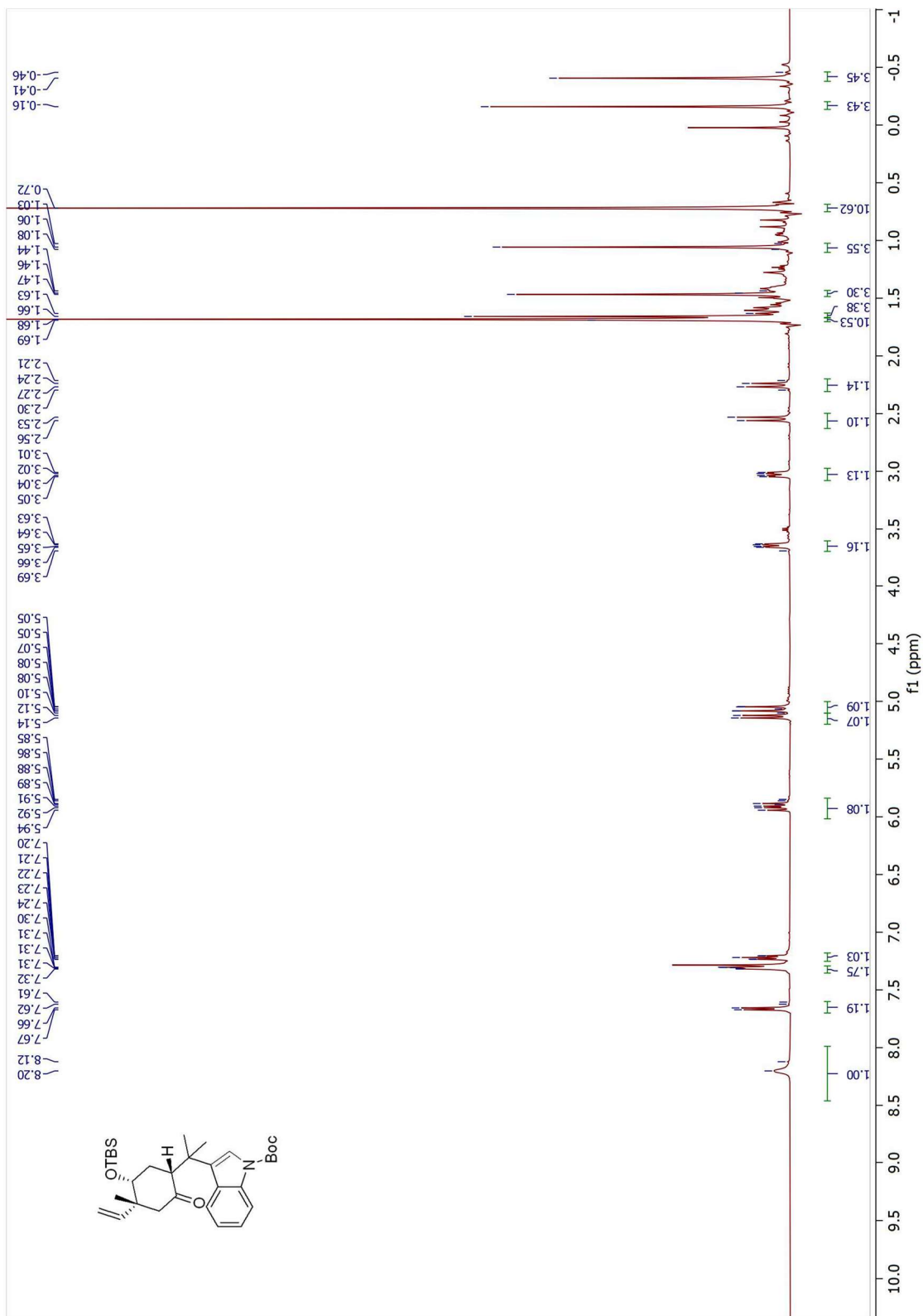


Figure 7.122 ¹H NMR Spectrum of 4.37 (500 MHz, CDCl₃)

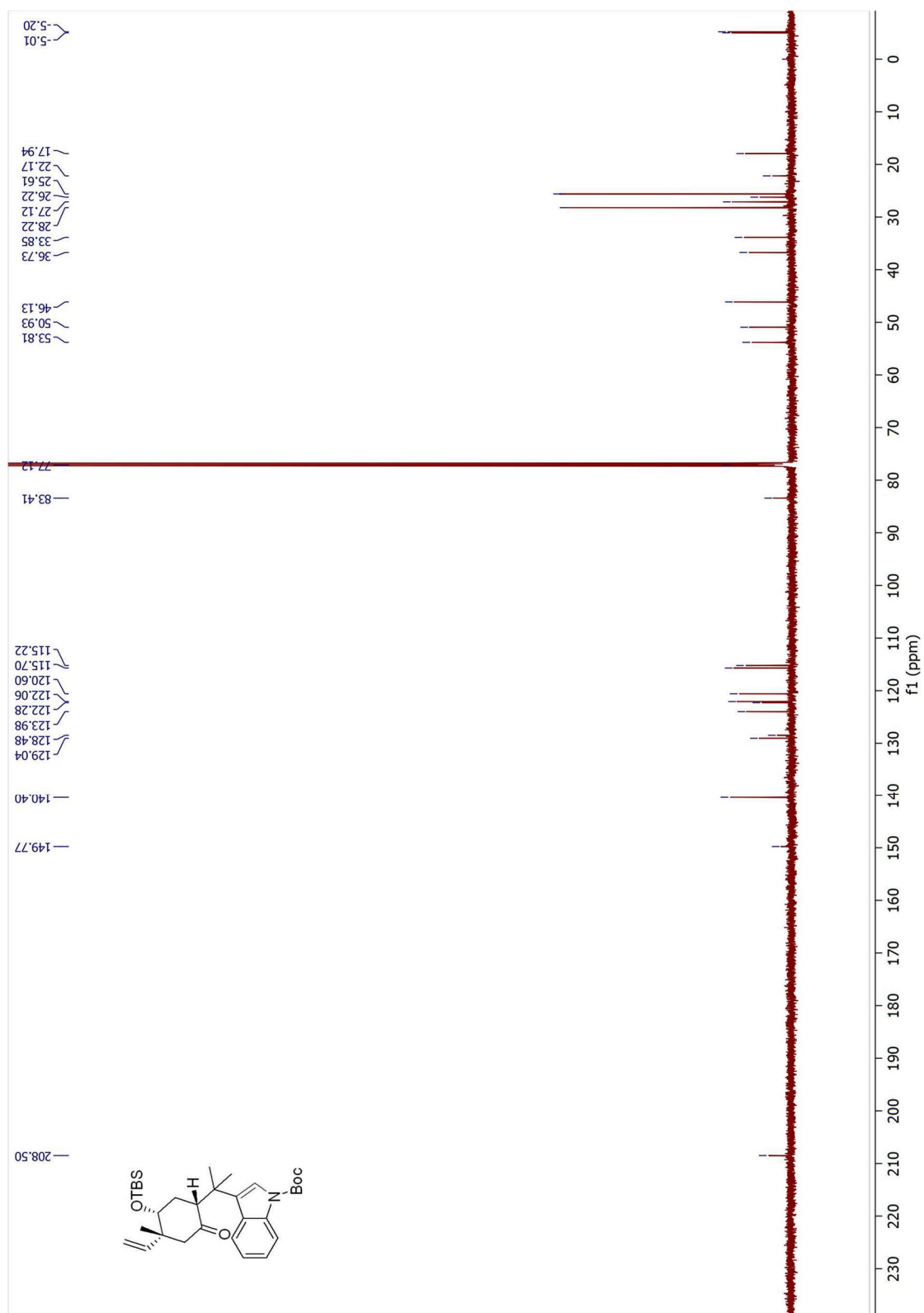


Figure 7.123 ¹³C NMR Spectrum of 4.37 (125 MHz, CDCl₃)

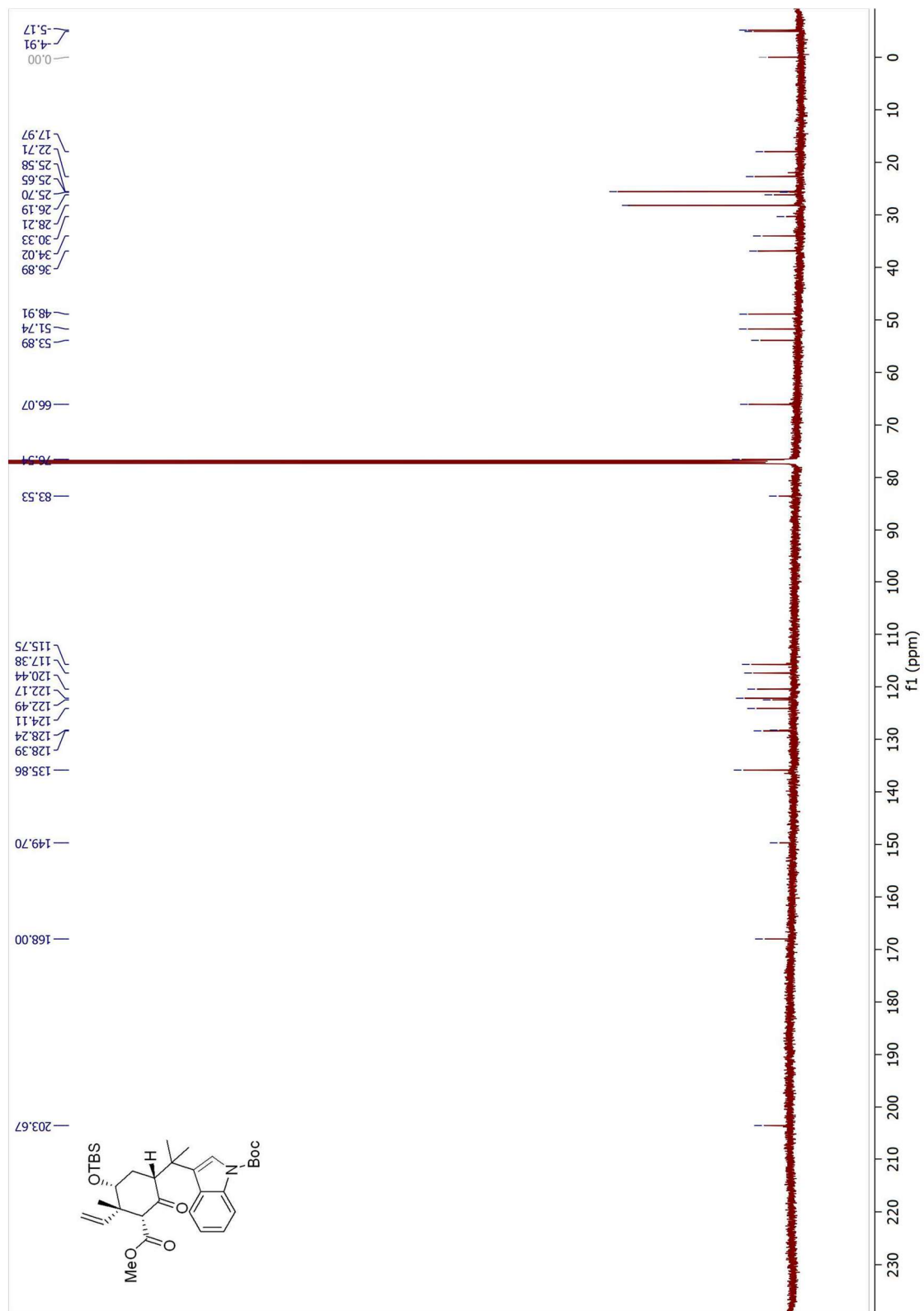


Figure 7.125 ¹³C NMR Spectrum of 4.40 (125 MHz, CDCl₃)

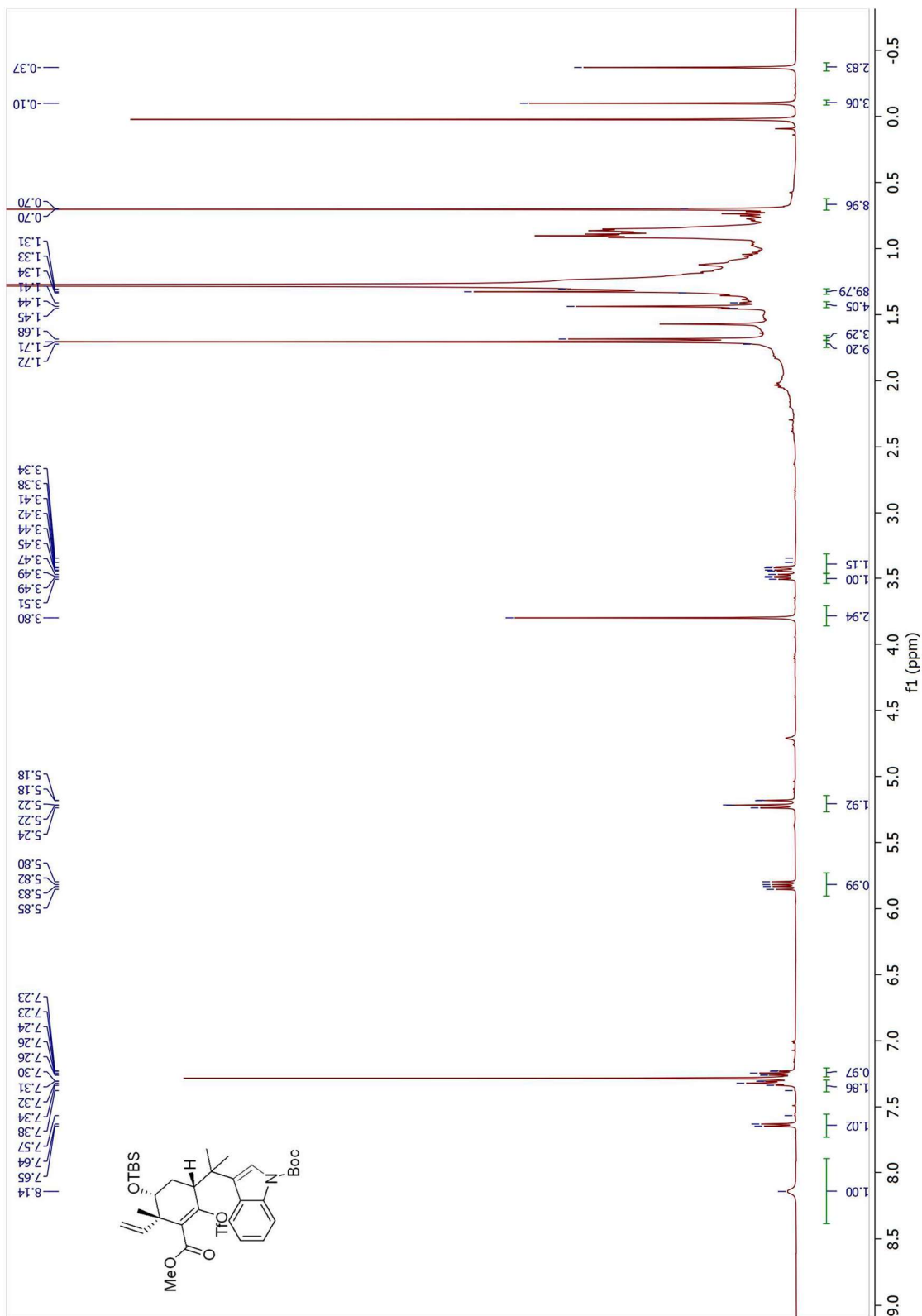


Figure 7.126 ^1H NMR Spectrum of **4.41** (500 MHz, CDCl_3)

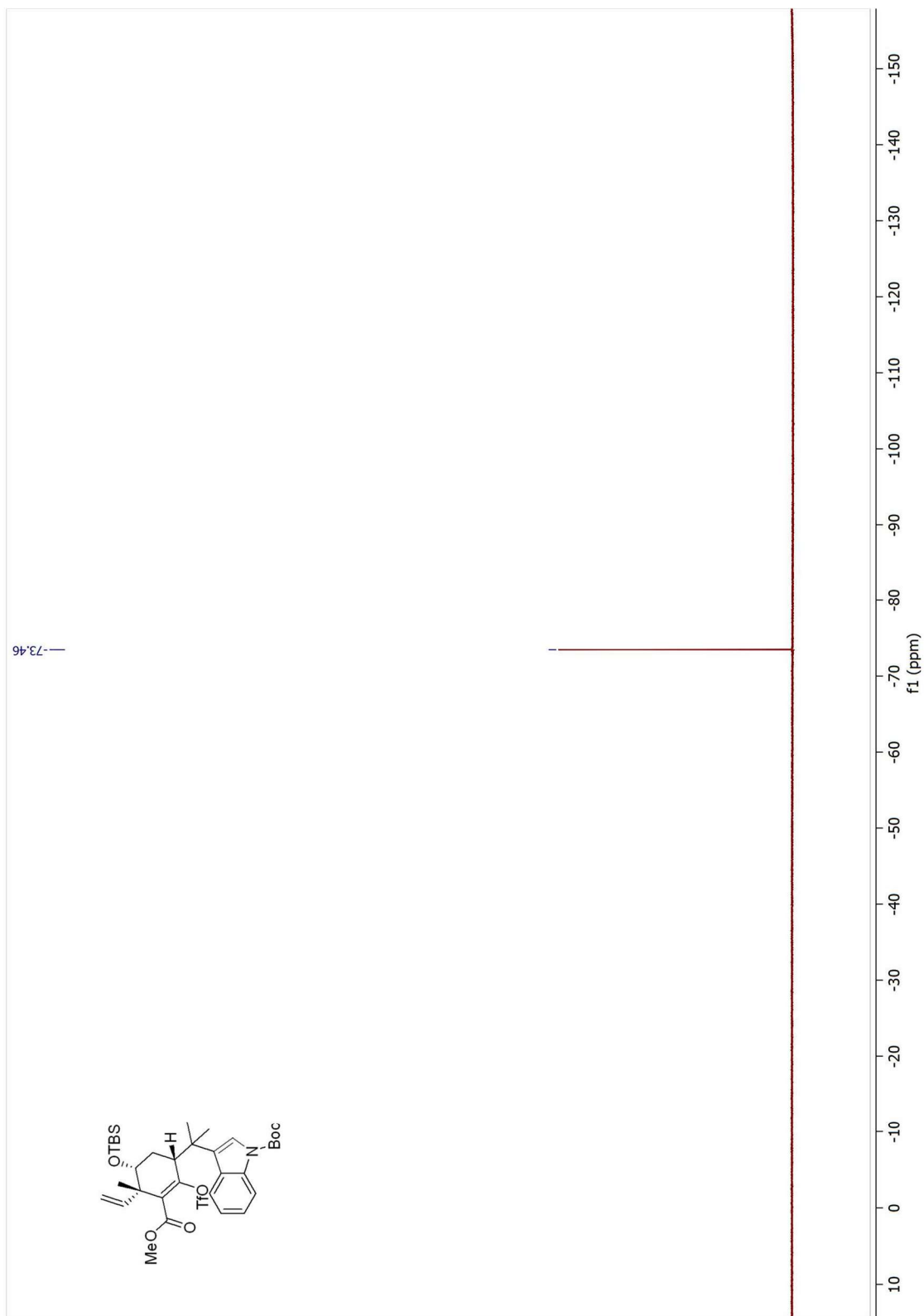


Figure 7.127 ^{19}F NMR Spectrum of **4.41** (500 MHz, CDCl_3)

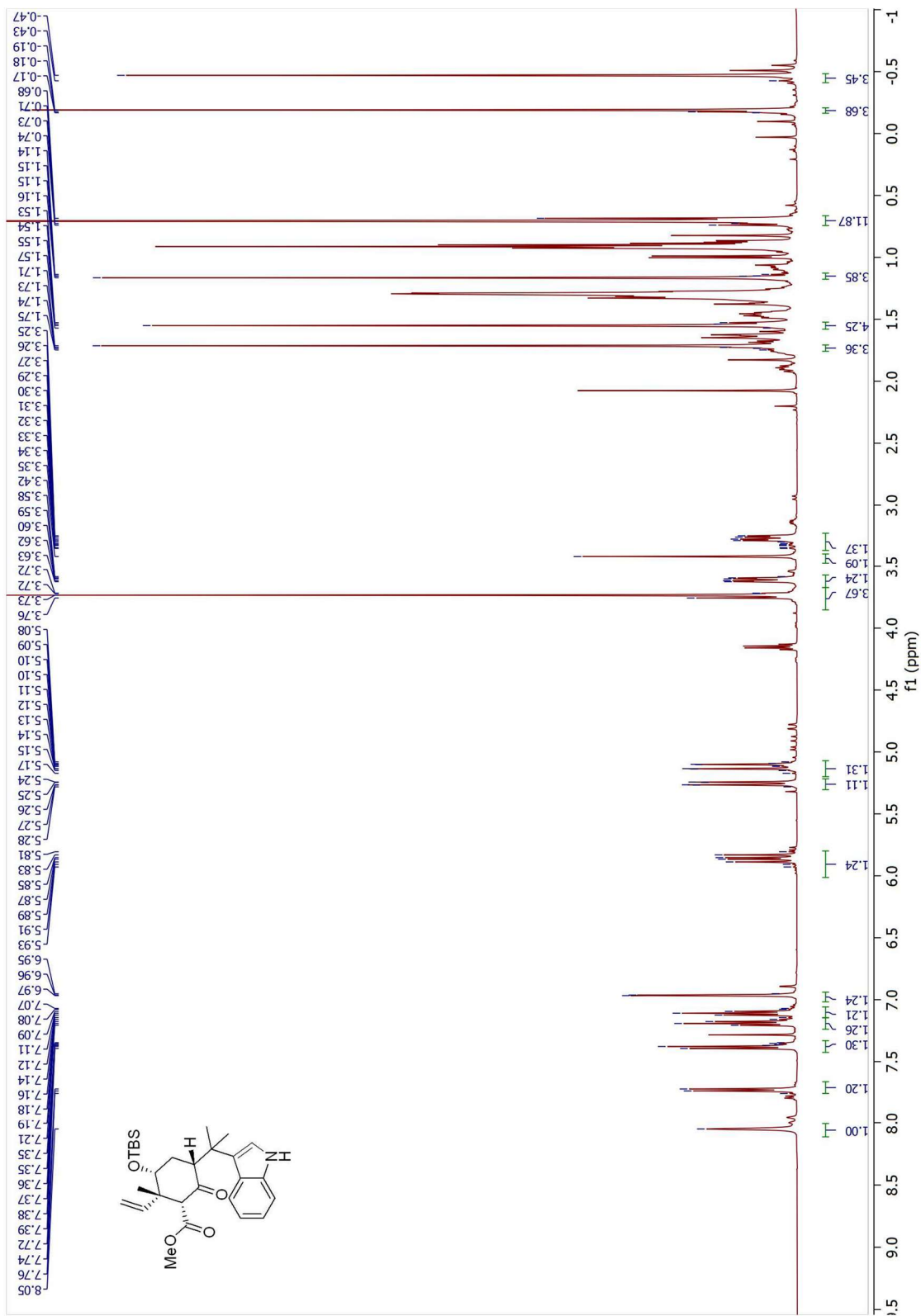


Figure 7.128 ^1H NMR Spectrum of **4.42** (500 MHz, CDCl_3)

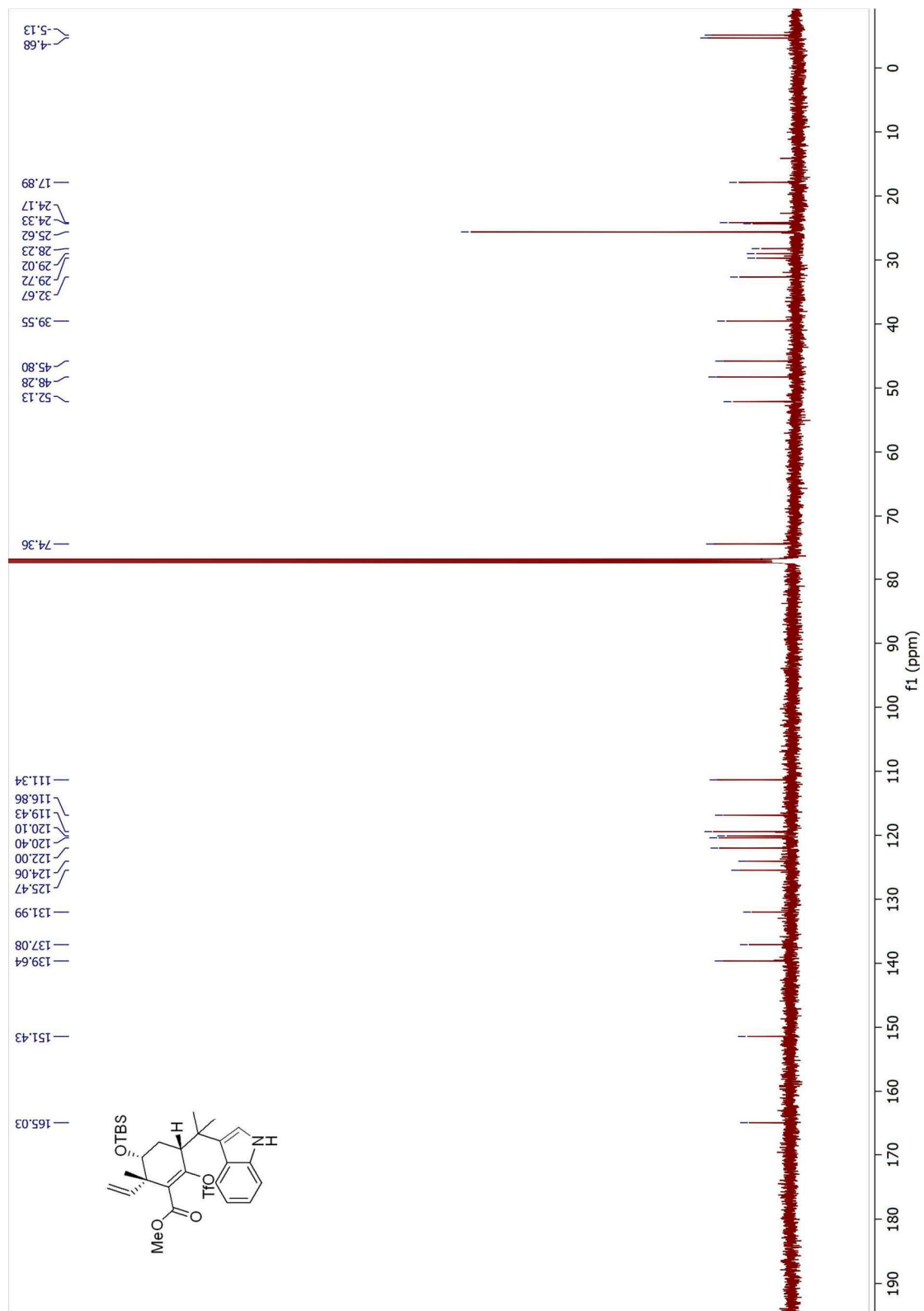


Figure 7.131 ¹³C NMR Spectrum of **4.43** (125 MHz, CDCl₃)

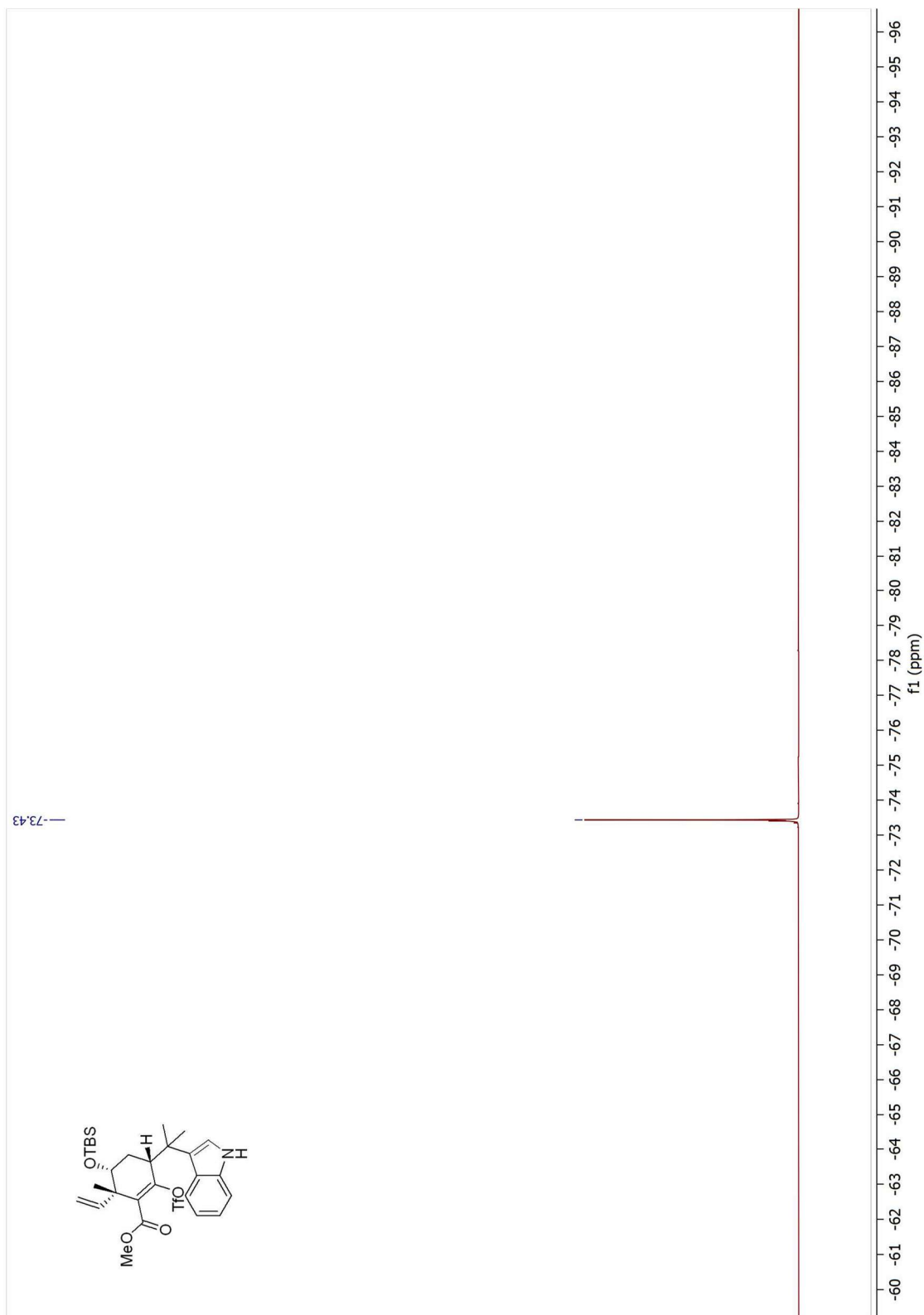


Figure 7.132 ^{19}F NMR Spectrum of **4.43** (500 MHz, CDCl_3)

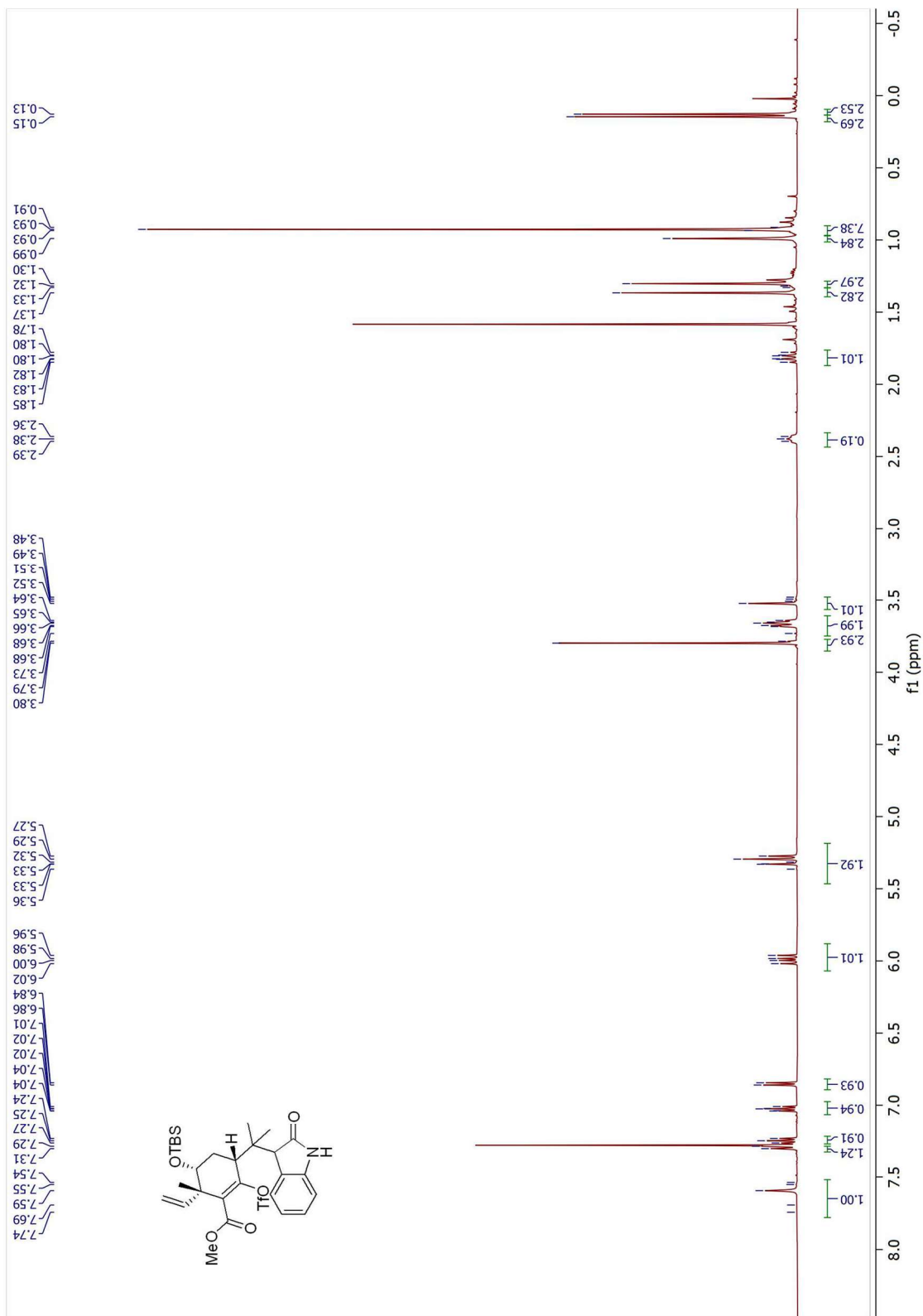


Figure 7.133 ^1H NMR Spectrum of **4.43** (500 MHz, CDCl_3)

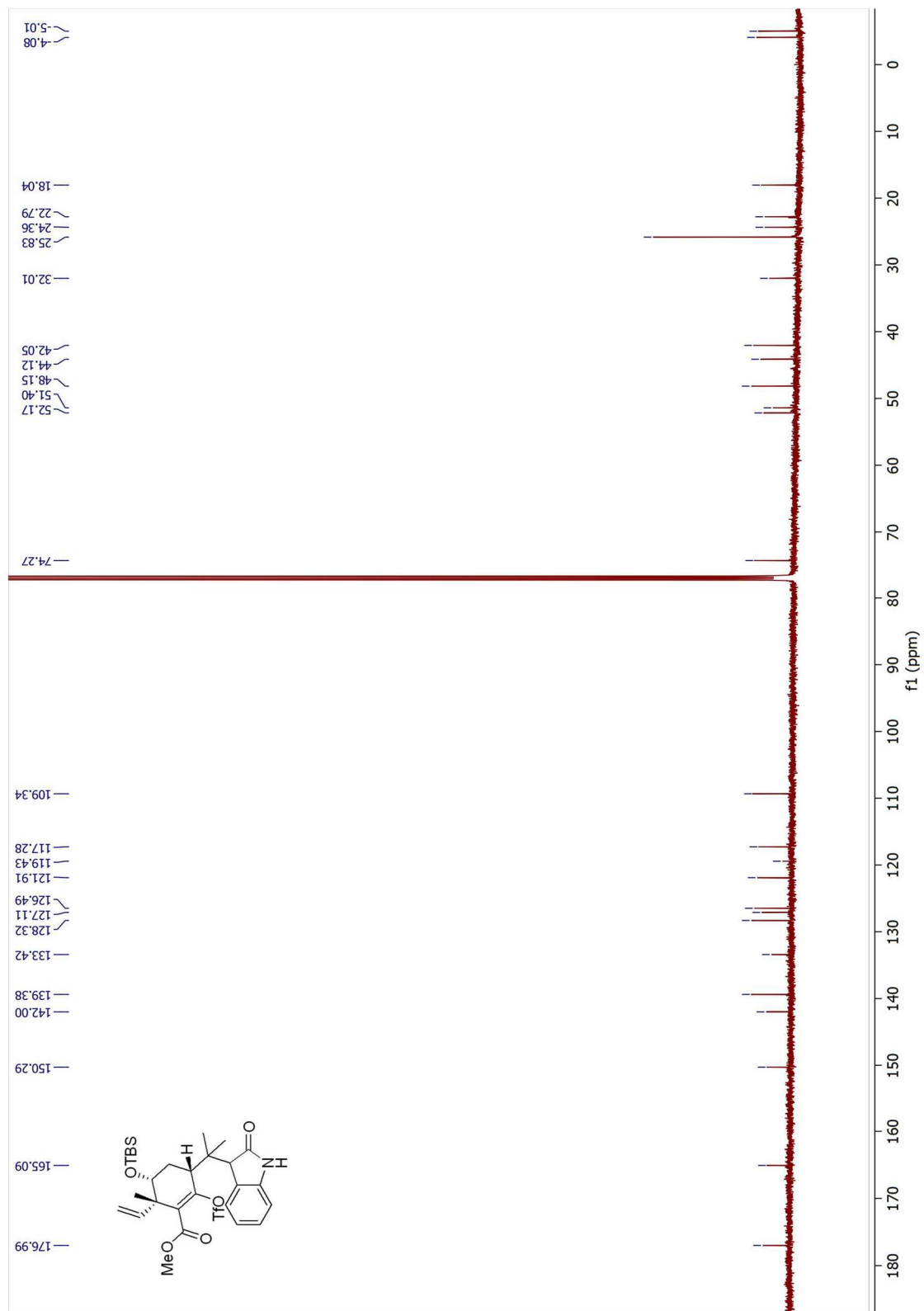


Figure 7.134 ¹³C NMR Spectrum of **4.44** (125 MHz, CDCl₃)

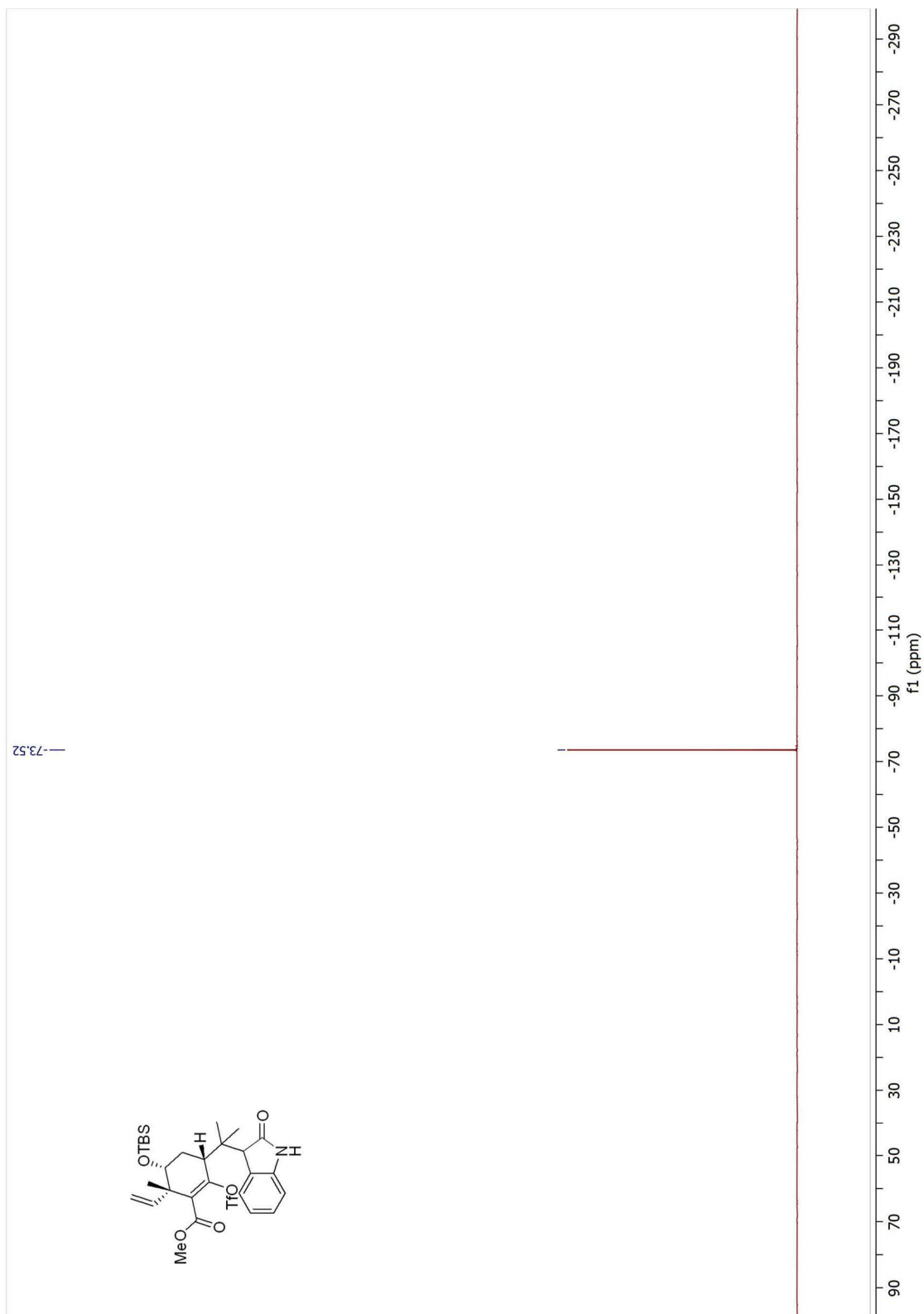


Figure 7.135 ^{19}F NMR Spectrum of **4.44** (500 MHz, CDCl_3)

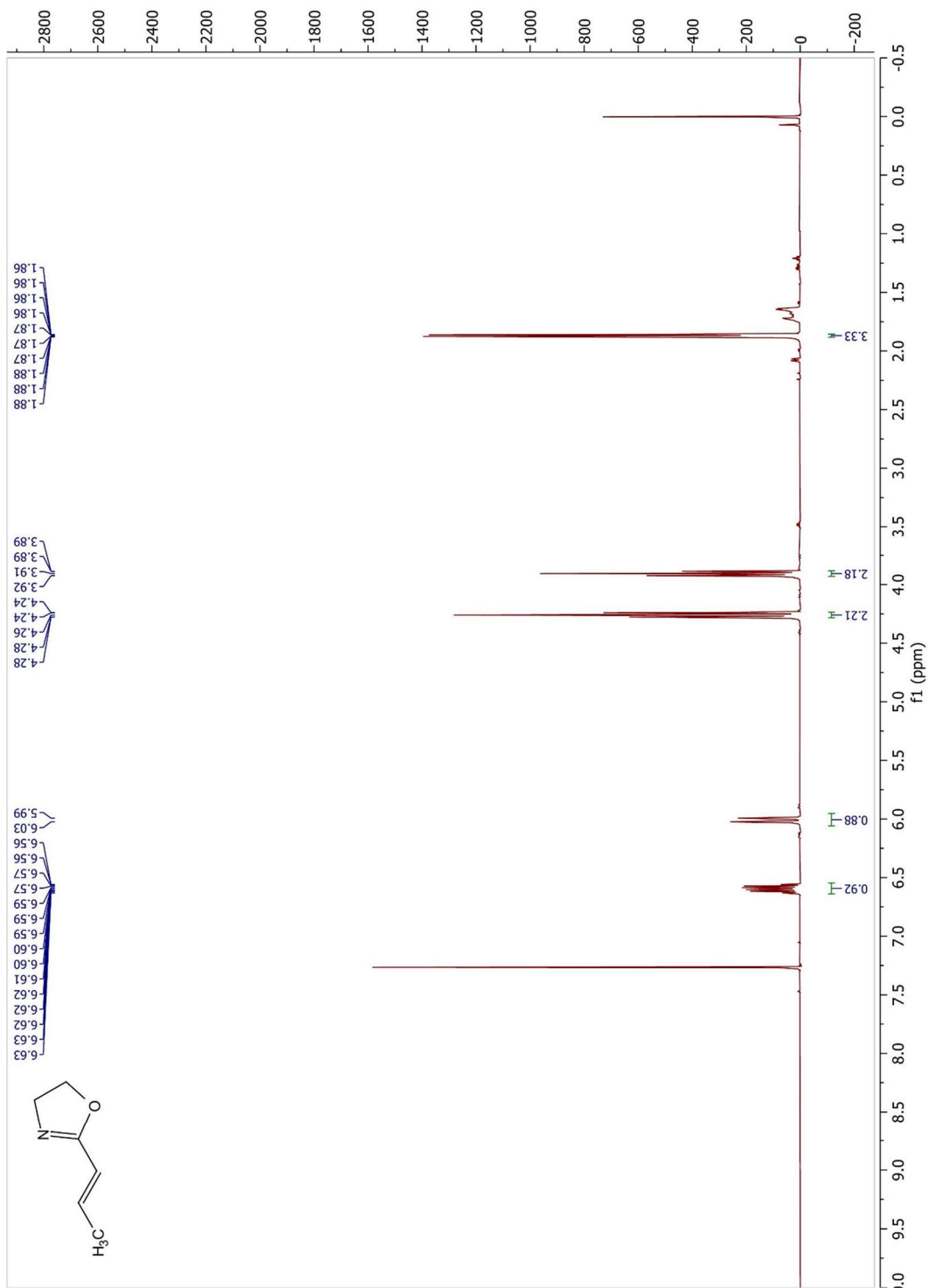


Figure 7.136 ¹H NMR Spectrum of 5.17 (500 MHz, CDCl₃)

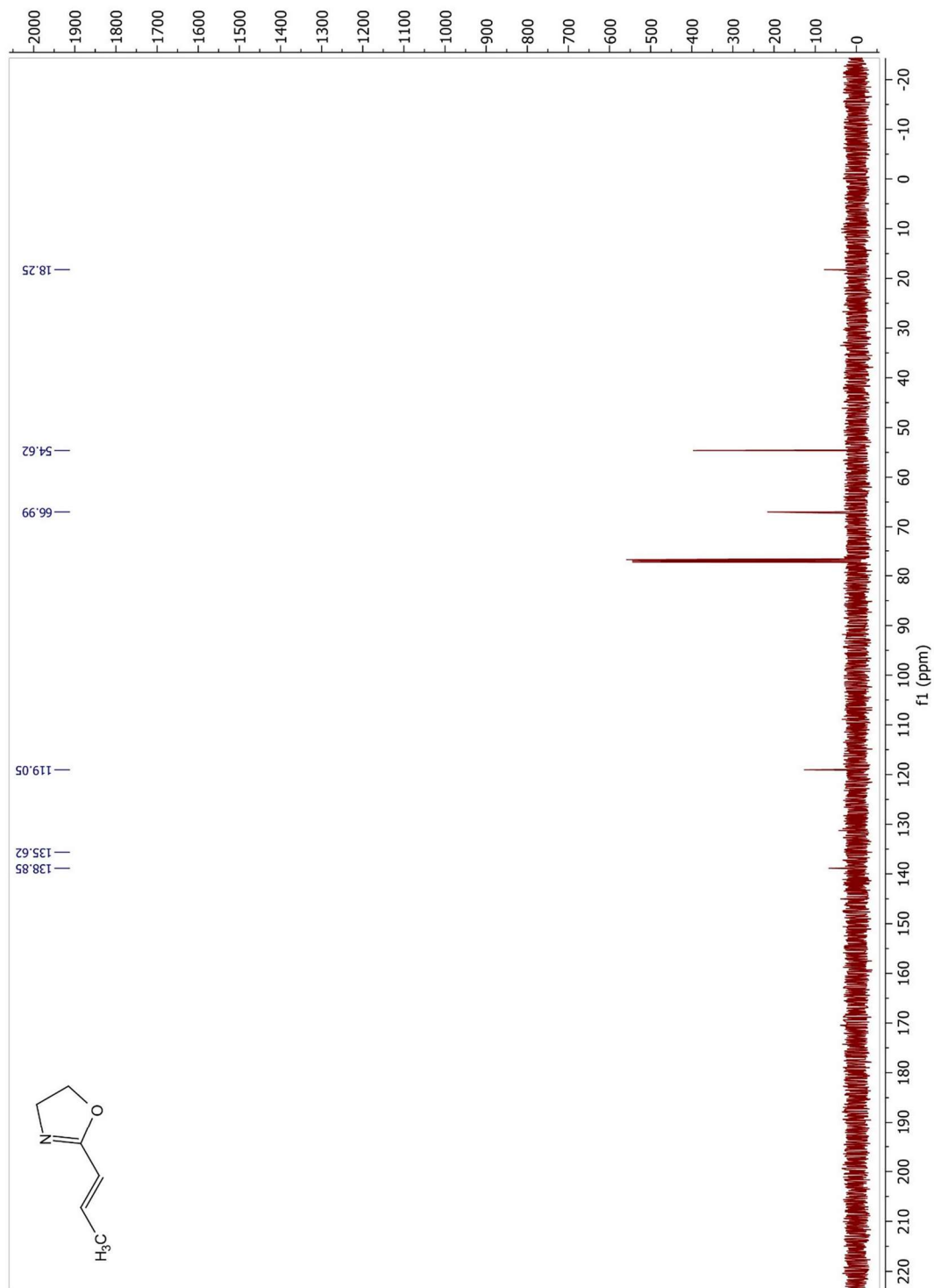


Figure 7.137 ^{13}C NMR Spectrum of **5.17** (125 MHz, CDCl_3)

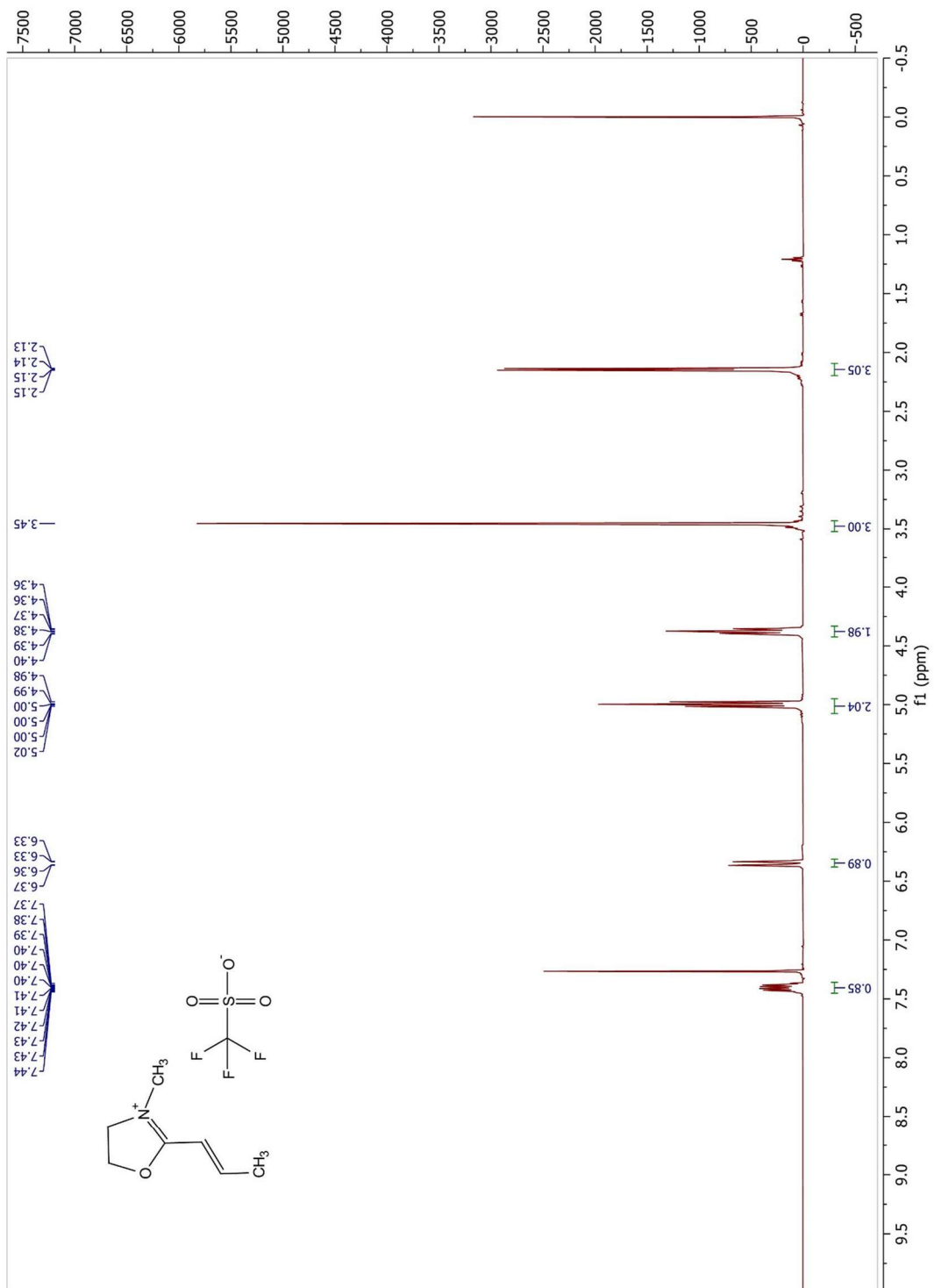


Figure 7.138 ^1H NMR Spectrum of **5.18** (500 MHz, CDCl_3)

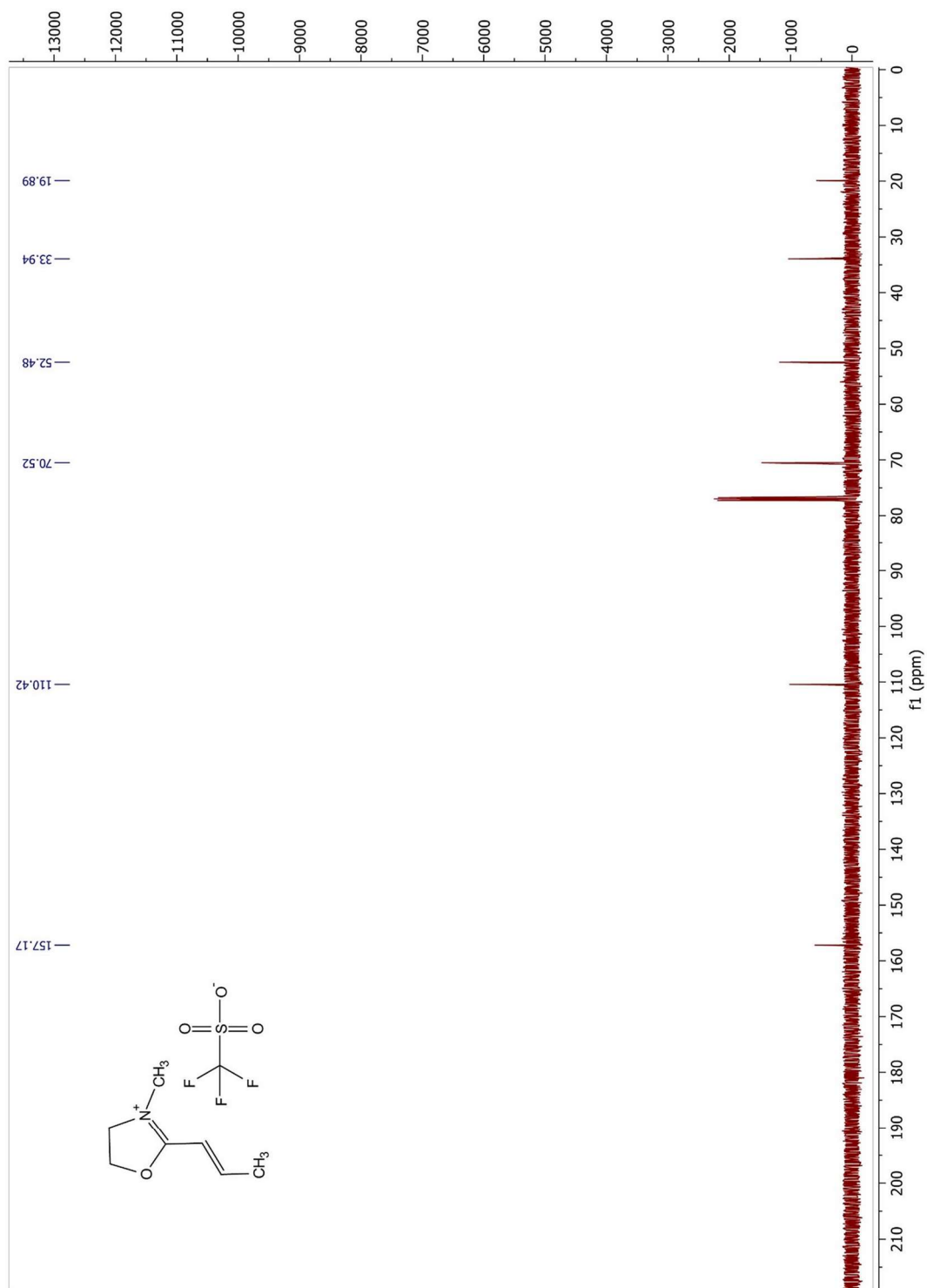


Figure 7.139 ^{13}C NMR Spectrum of 5.18 (125 MHz, CDCl_3)

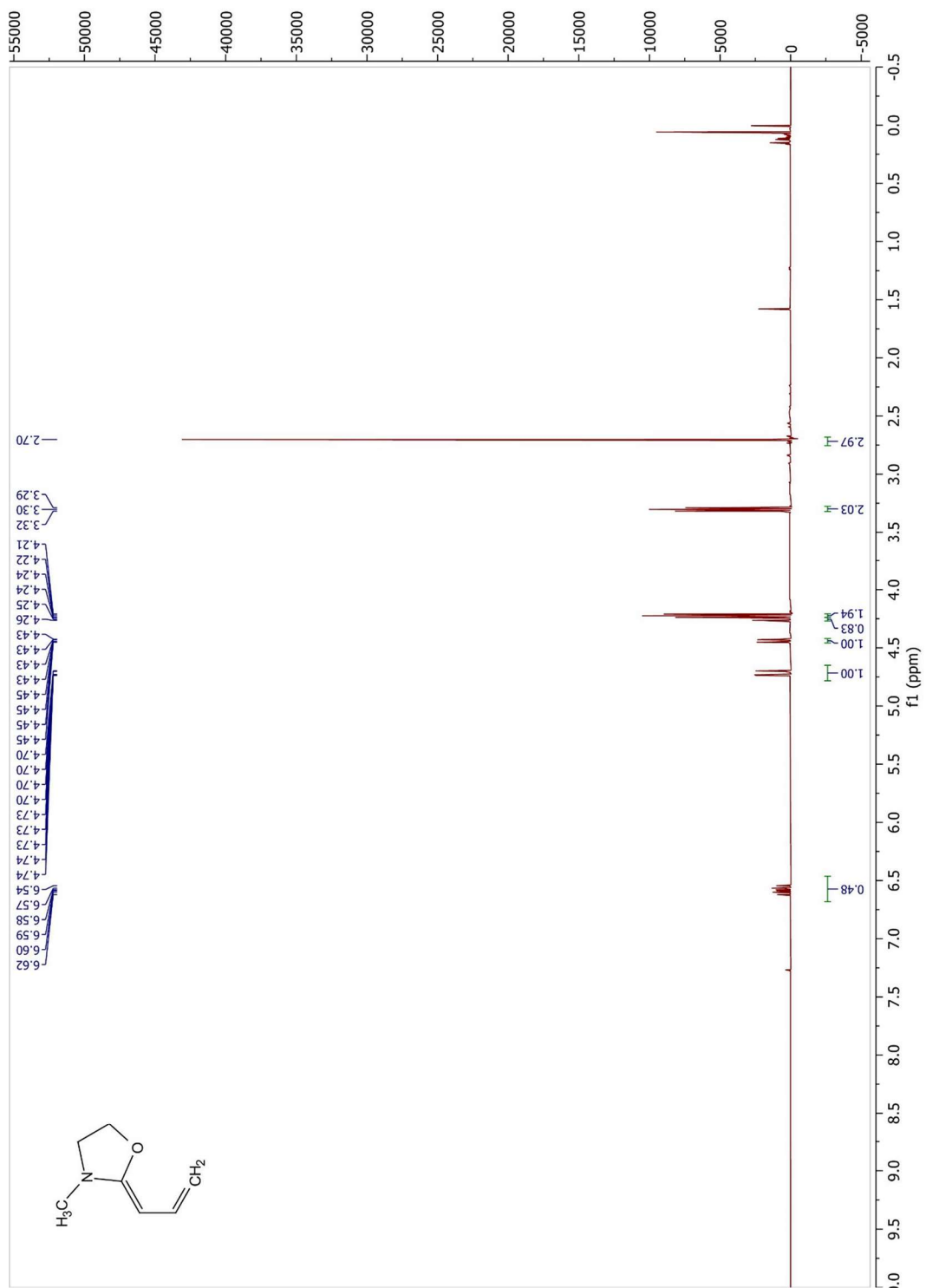


Figure 7.140 ^1H NMR Spectrum of **5.13** (500 MHz, CDCl_3)

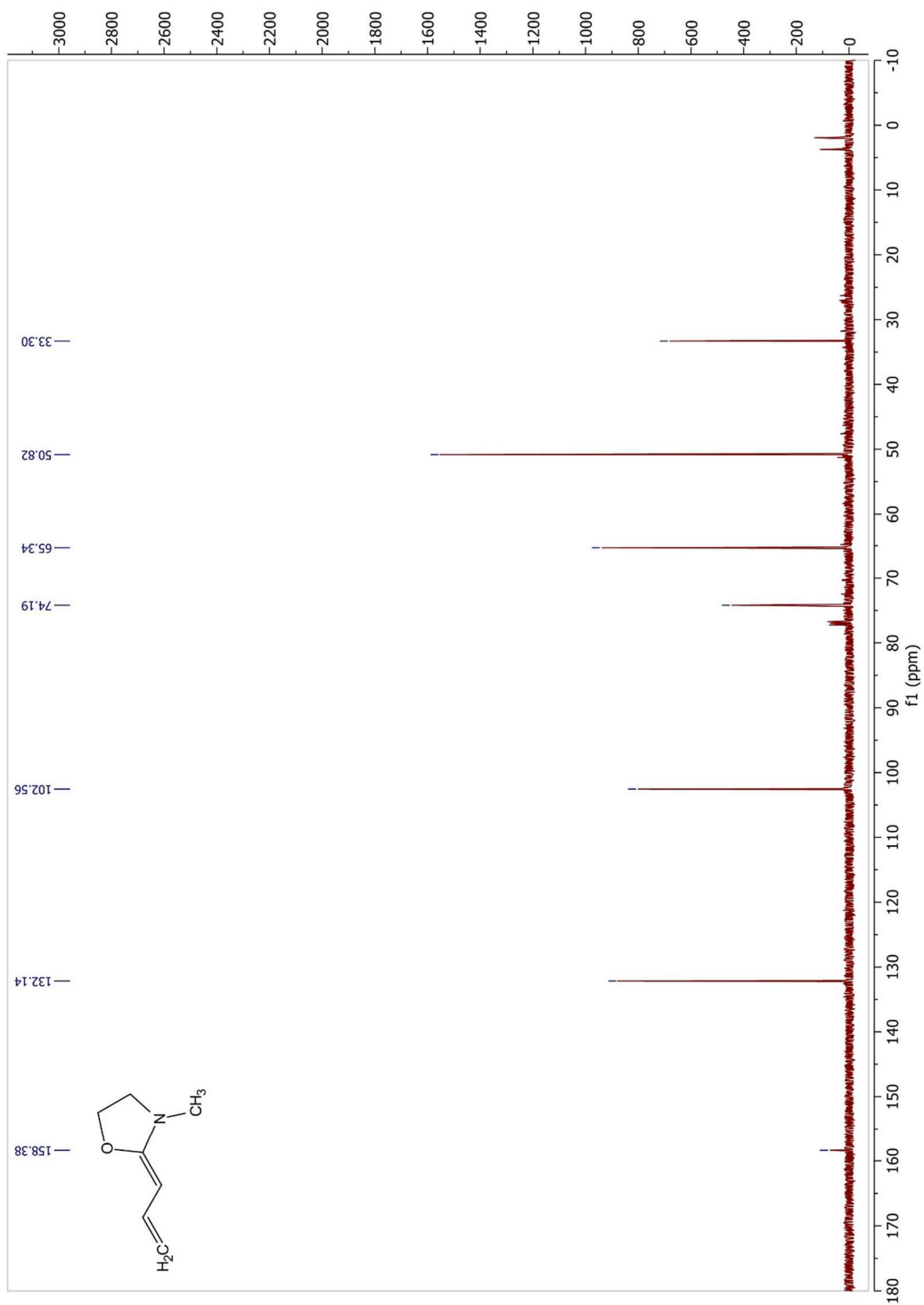


Figure 7.141 ^{13}C NMR Spectrum of **5.13** (125 MHz, CDCl_3)

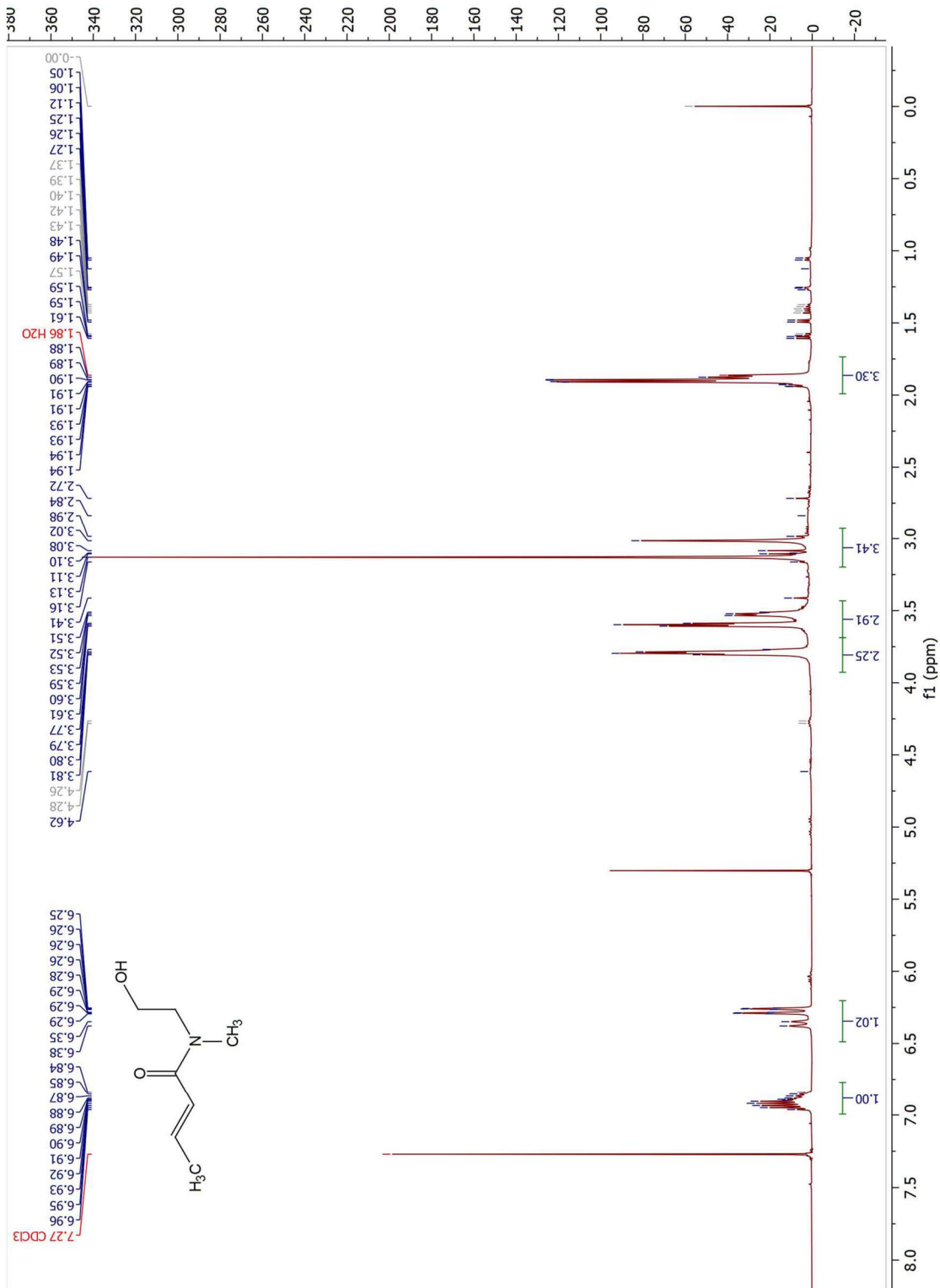


Figure 7.142 ¹H NMR Spectrum of 5.20 (500 MHz, CDCl₃)

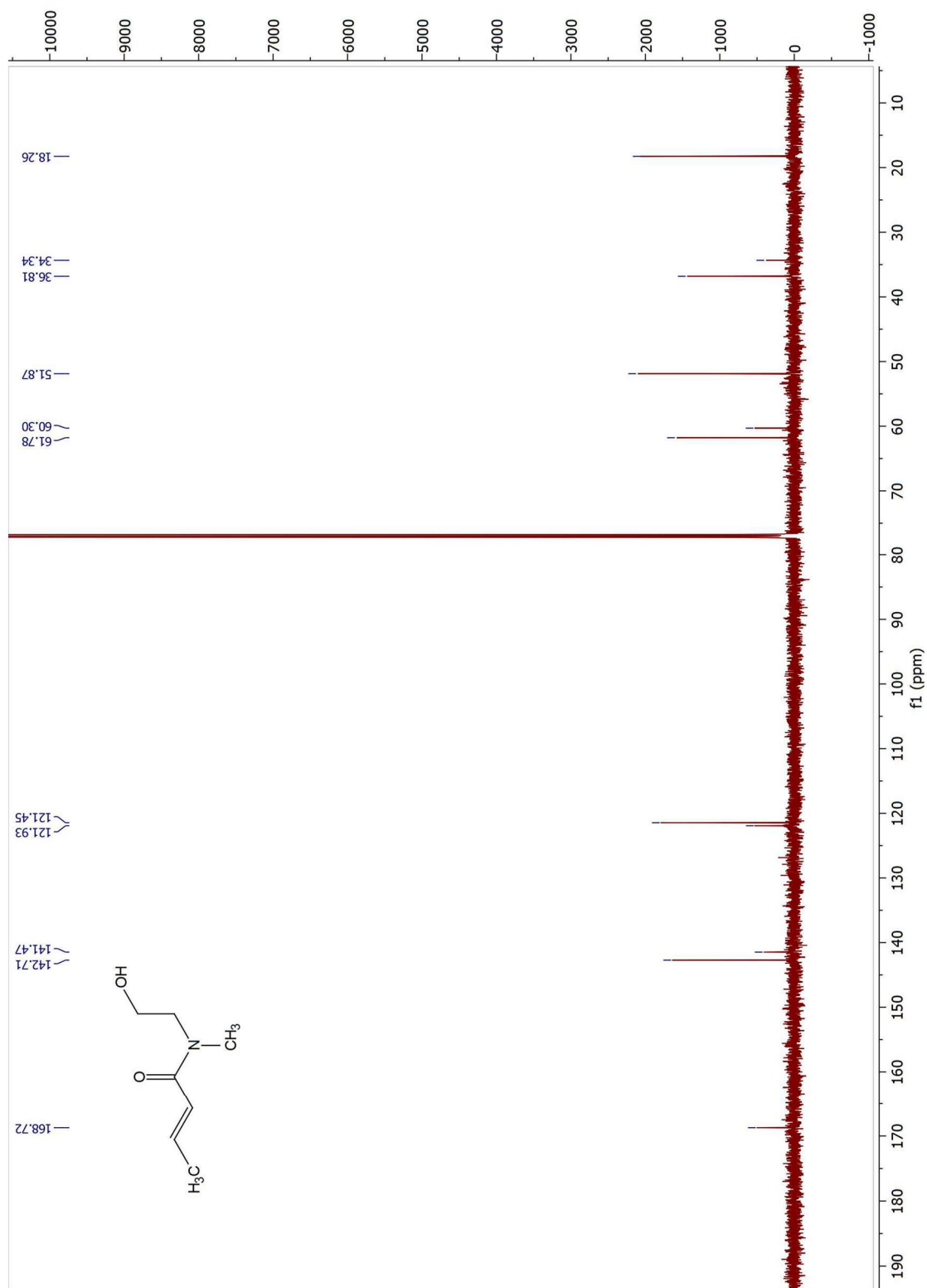


Figure 7.143 ^{13}C NMR Spectrum of **5.20** (125 MHz, CDCl_3)

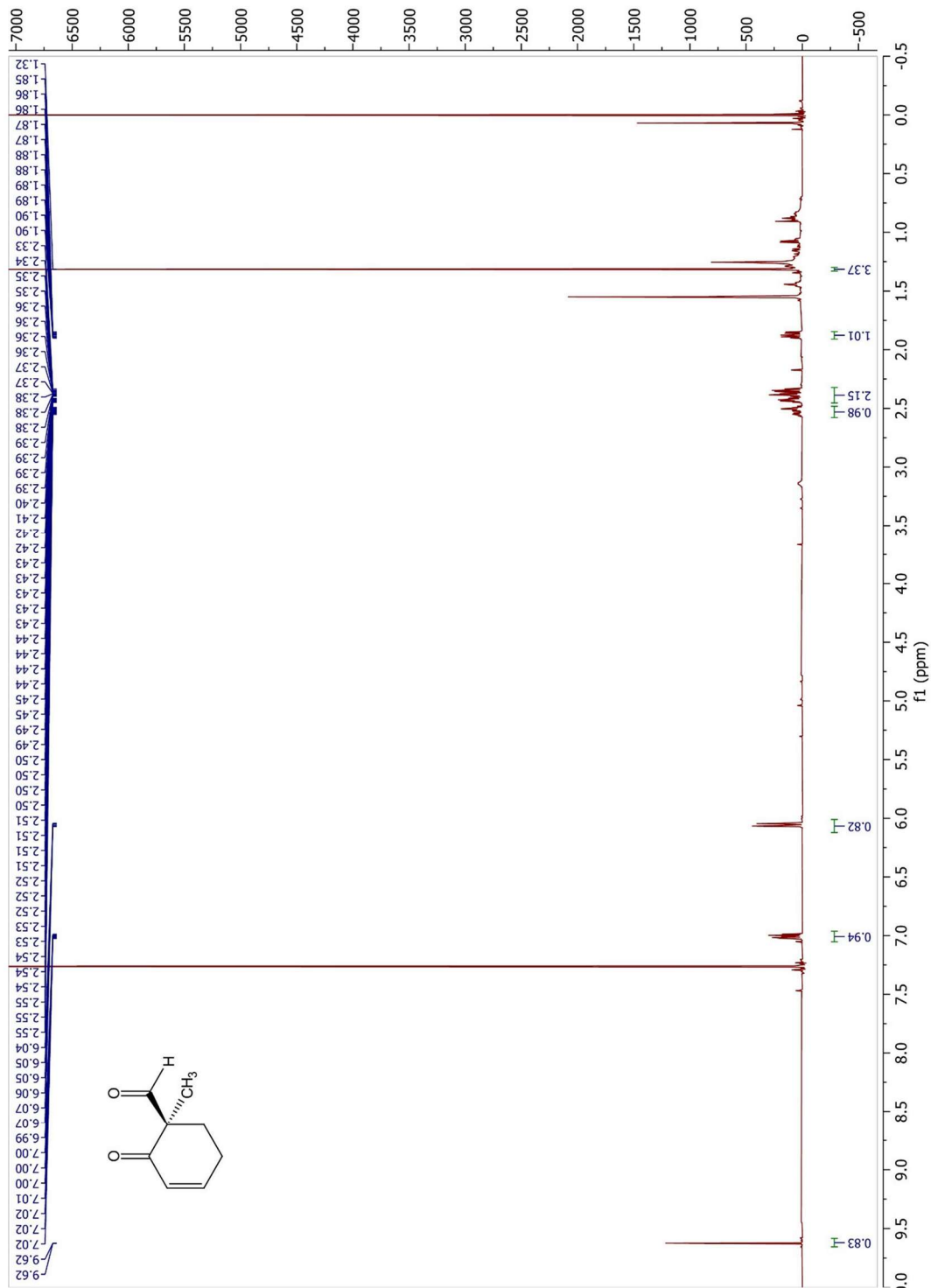


Figure 7.144 ¹H NMR Spectrum of 5.23a (500 MHz, CDCl₃)

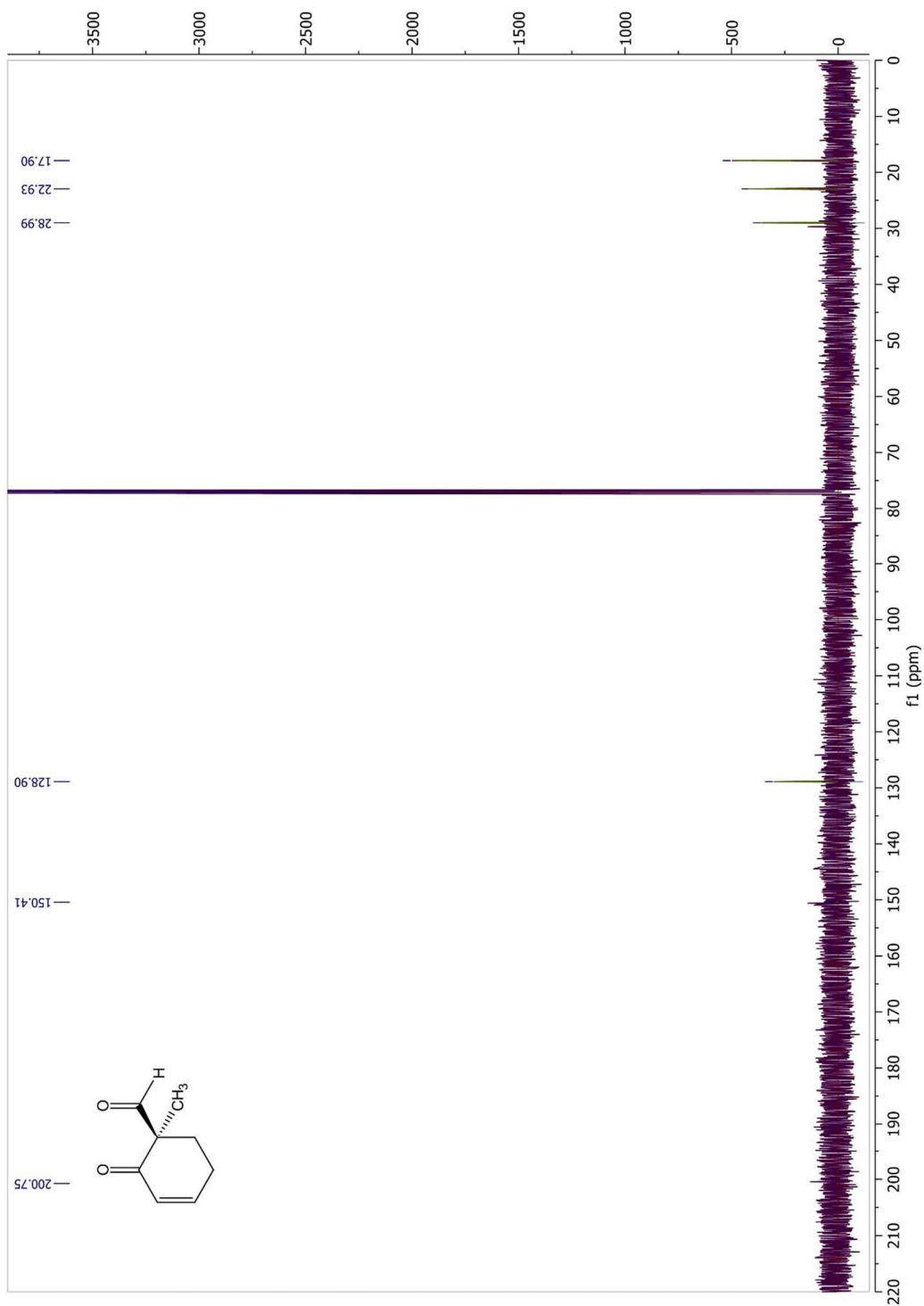


Figure 7.145 ^{13}C NMR Spectrum of **5.23a**(125 MHz, CDCl_3)

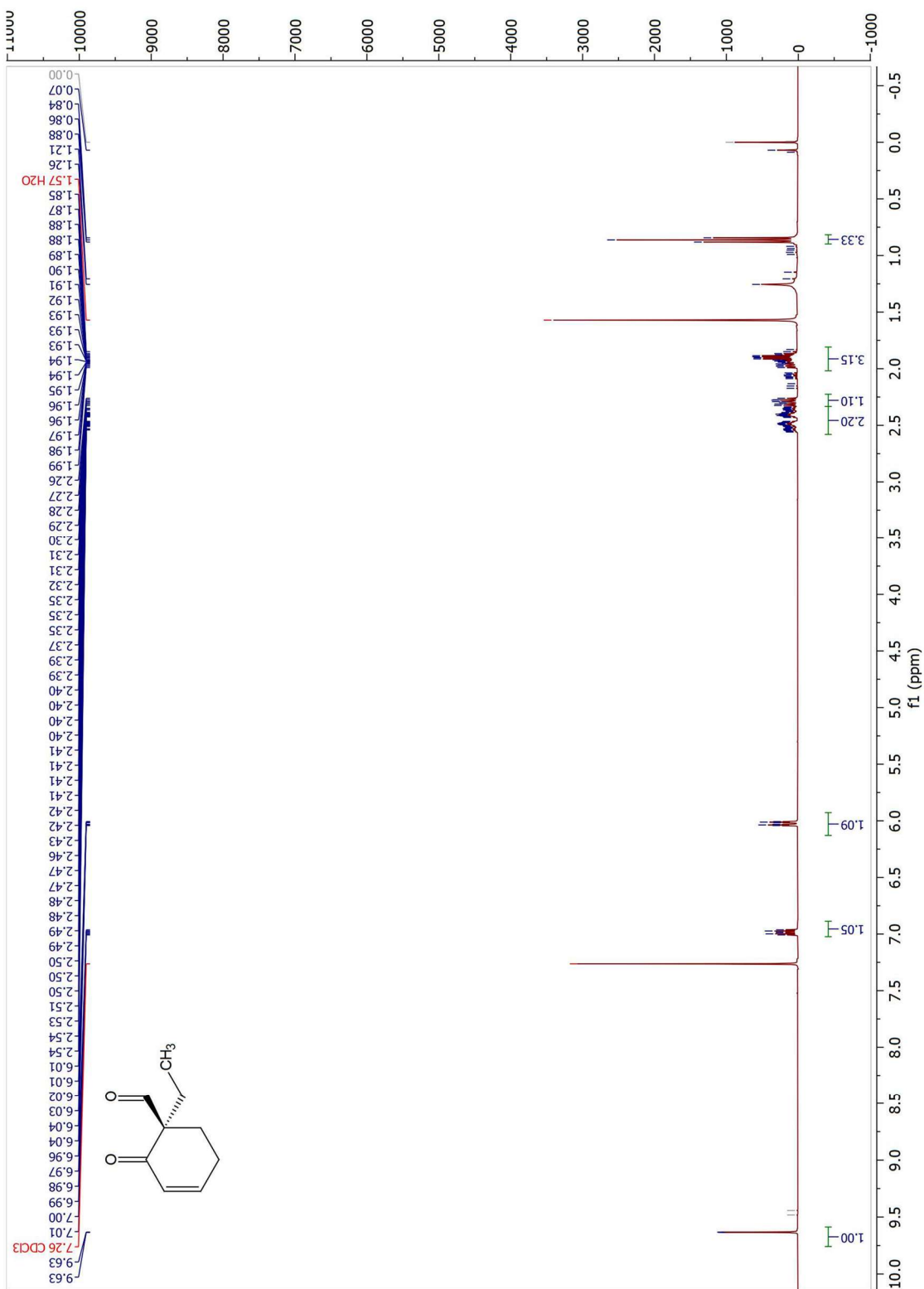


Figure 7.146 ^1H NMR Spectrum of 5.23b (500 MHz, CDCl_3)

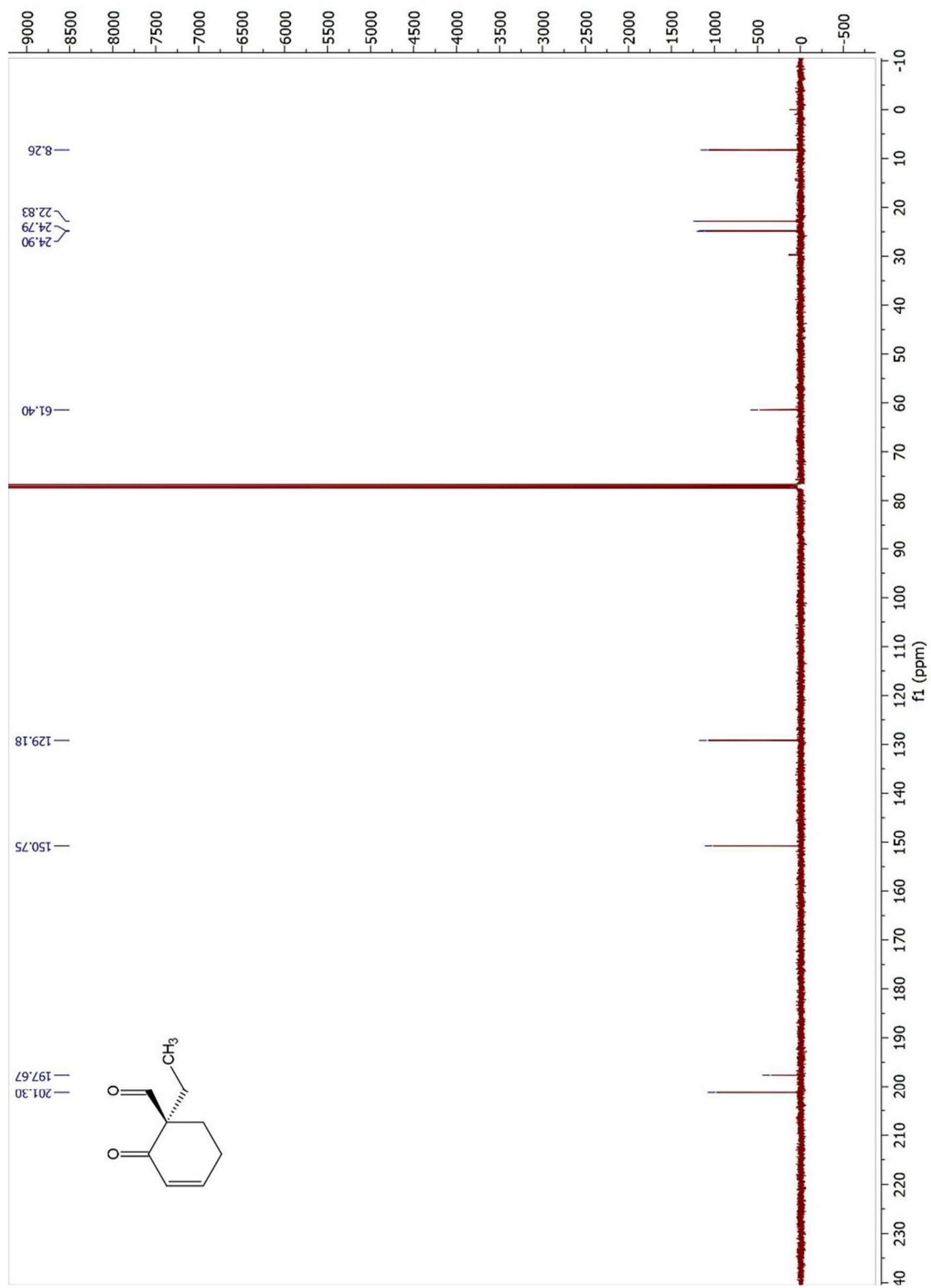


Figure 7.147 ^{13}C NMR Spectrum of **5.23b** (125 MHz, CDCl_3)

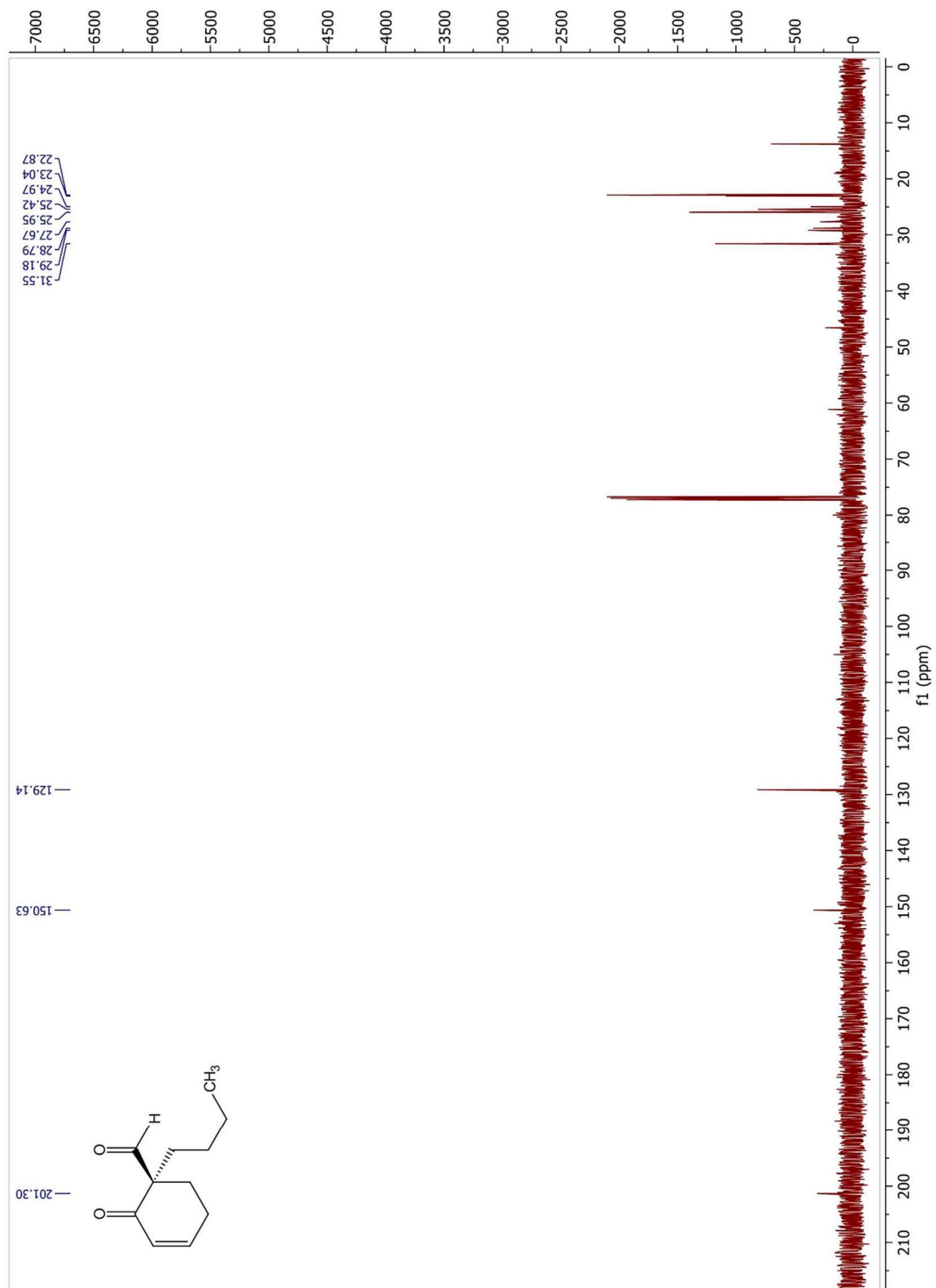


Figure 7.149 ^{13}C NMR Spectrum of **5.23c** (125 MHz, CDCl_3)

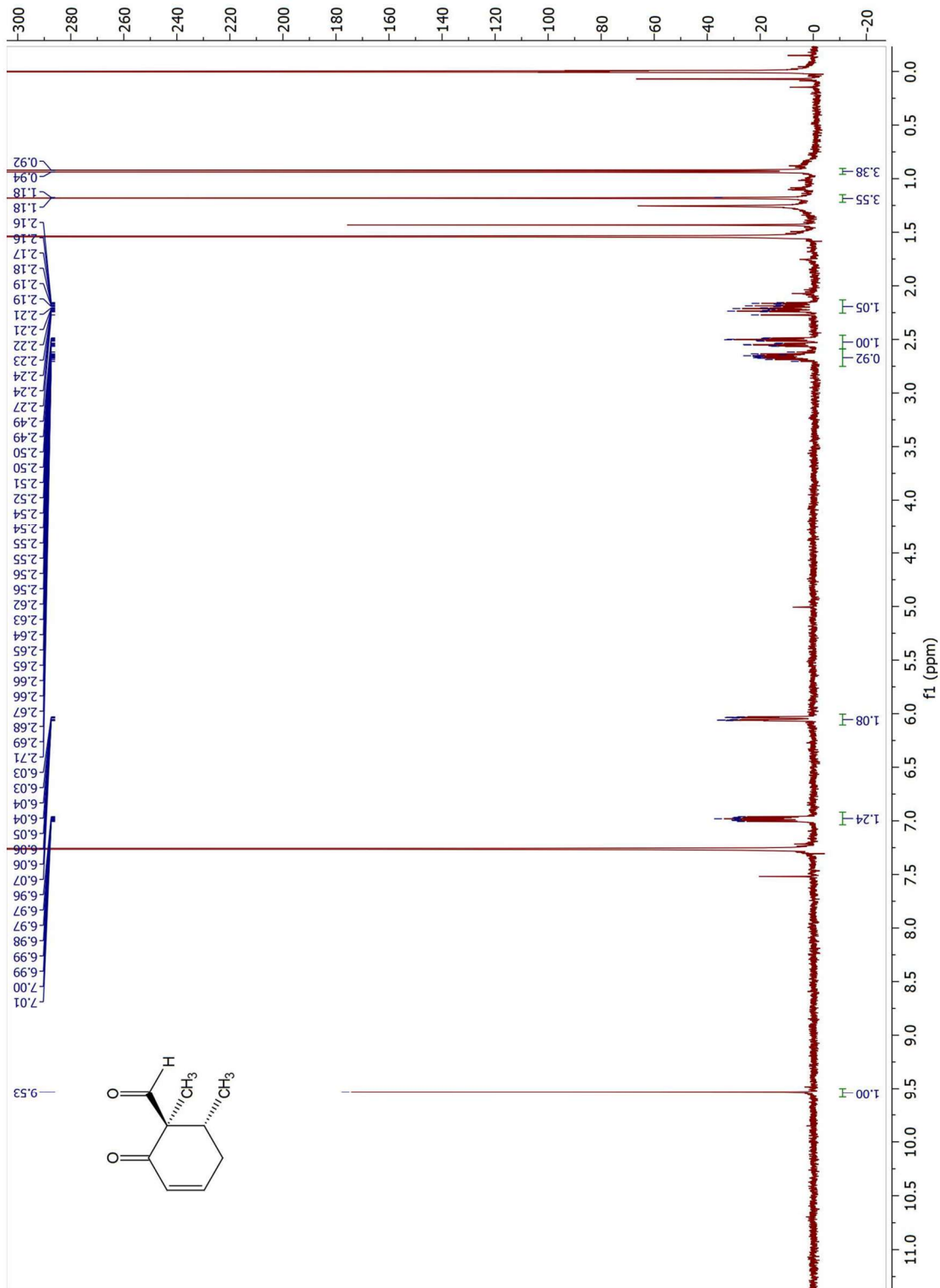


Figure 7.150 ¹H NMR Spectrum of **5.23d** (500 MHz, CDCl₃)

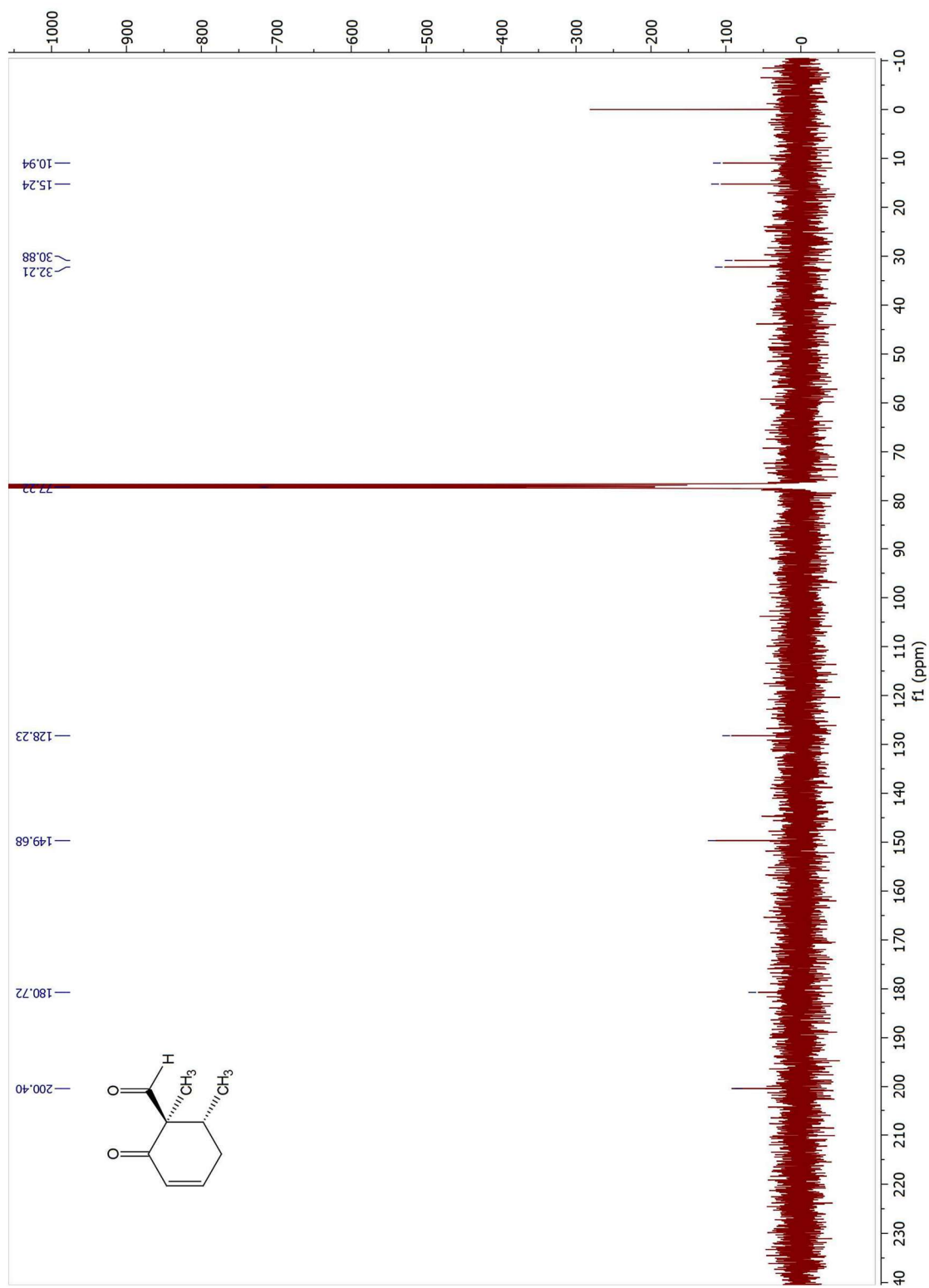


Figure 7.151 ^{13}C NMR Spectrum of **5.23d** (125 MHz, CDCl_3)

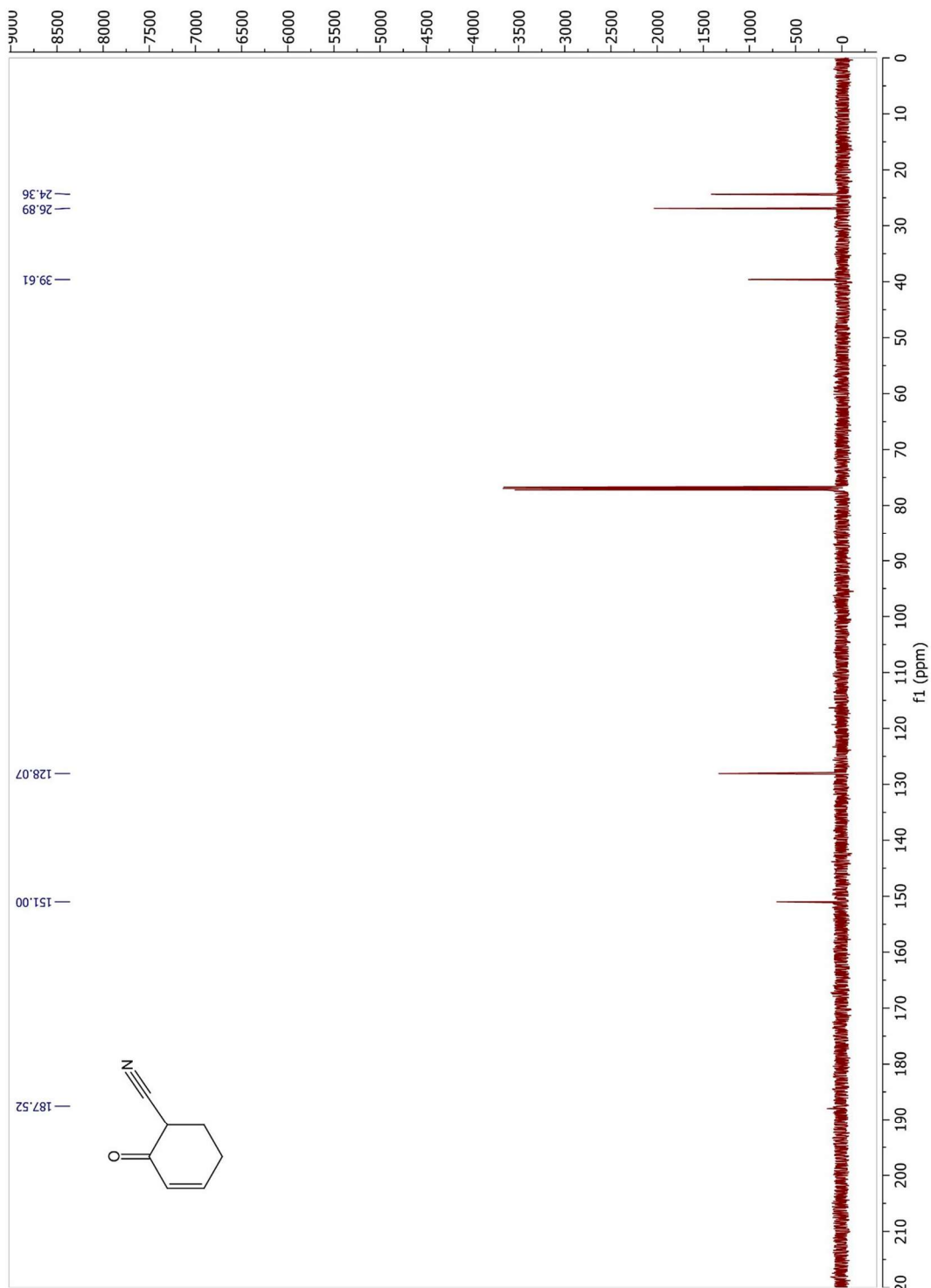


Figure 7.153 ^{13}C NMR Spectrum of **5.23f** (125 MHz, CDCl_3)

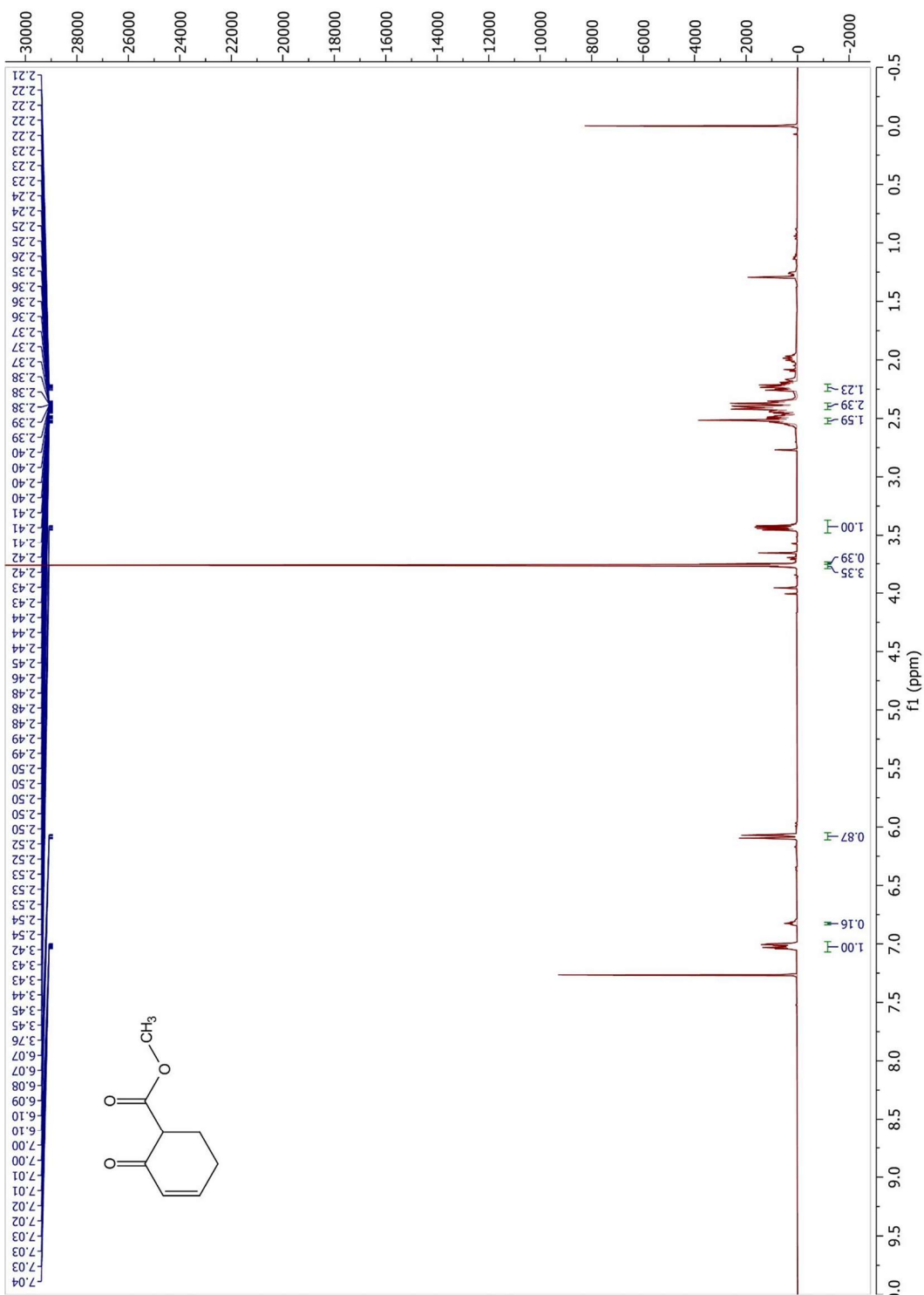


Figure 7.154 ¹H NMR Spectrum of 5.23g (500 MHz, CDCl₃)

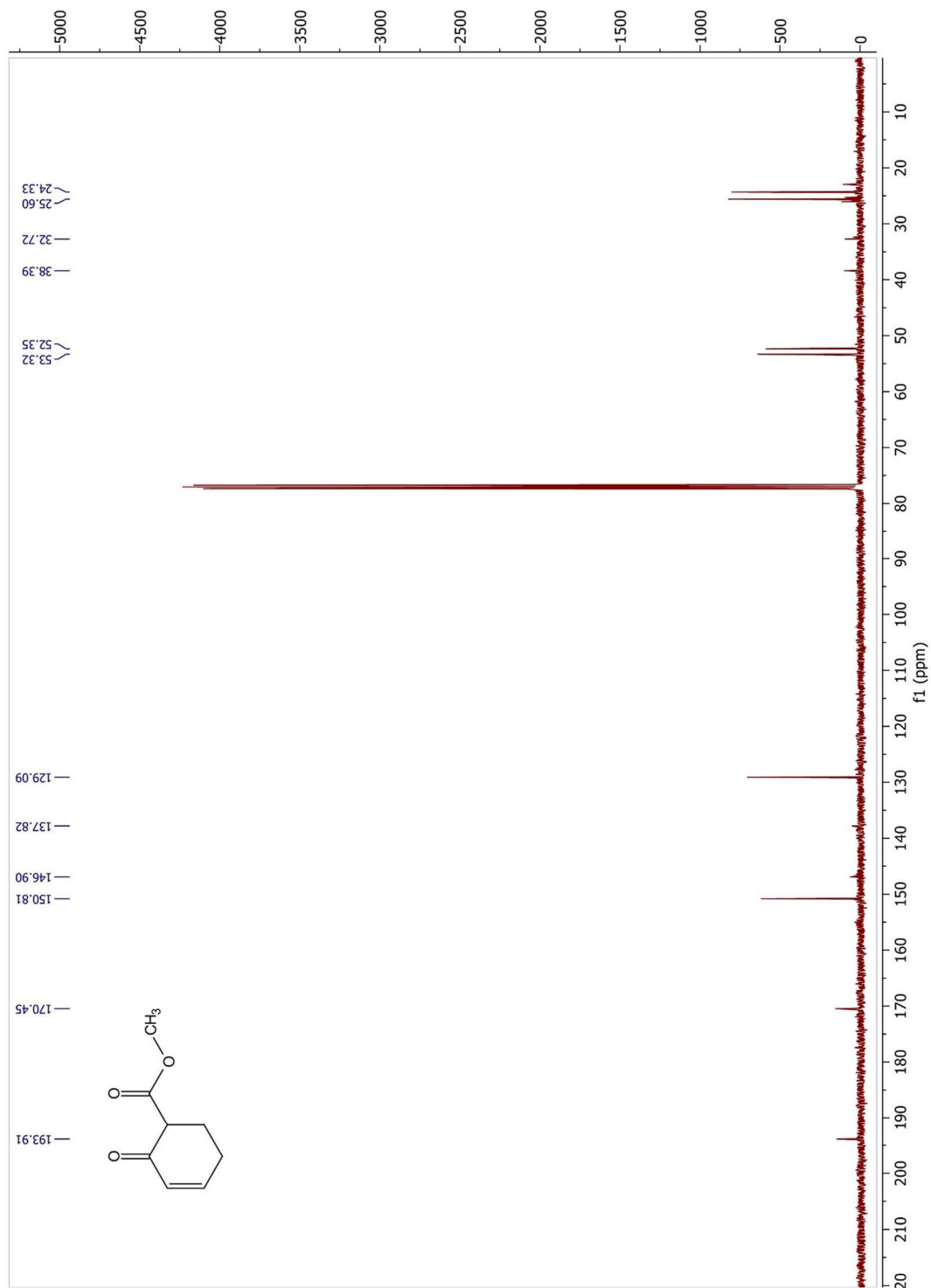


Figure 7.155 ^{13}C NMR Spectrum of 5.23g (125 MHz, CDCl_3)

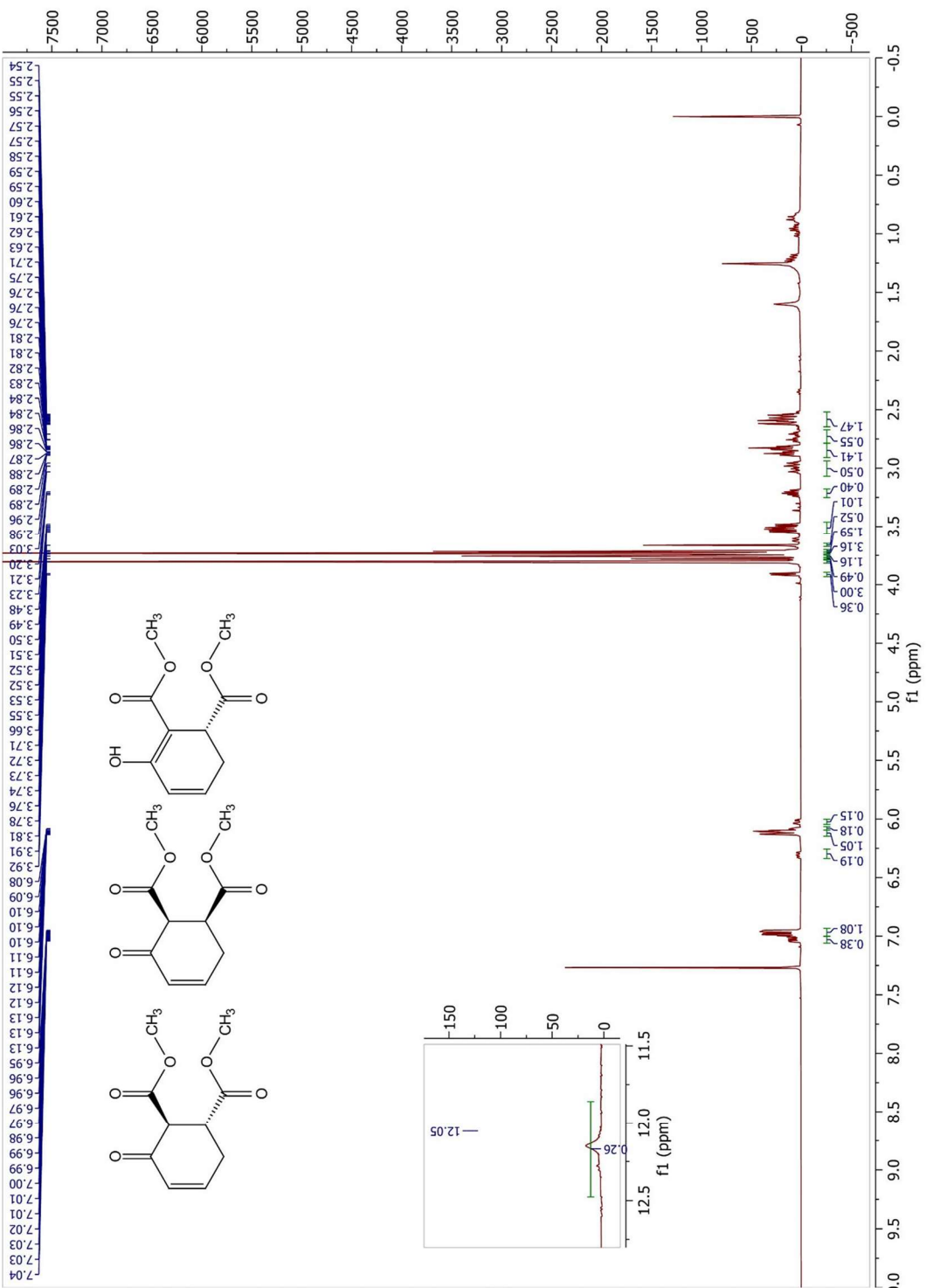


Figure 7.156 ^1H NMR Spectrum of 5.23h (500 MHz, CDCl_3)

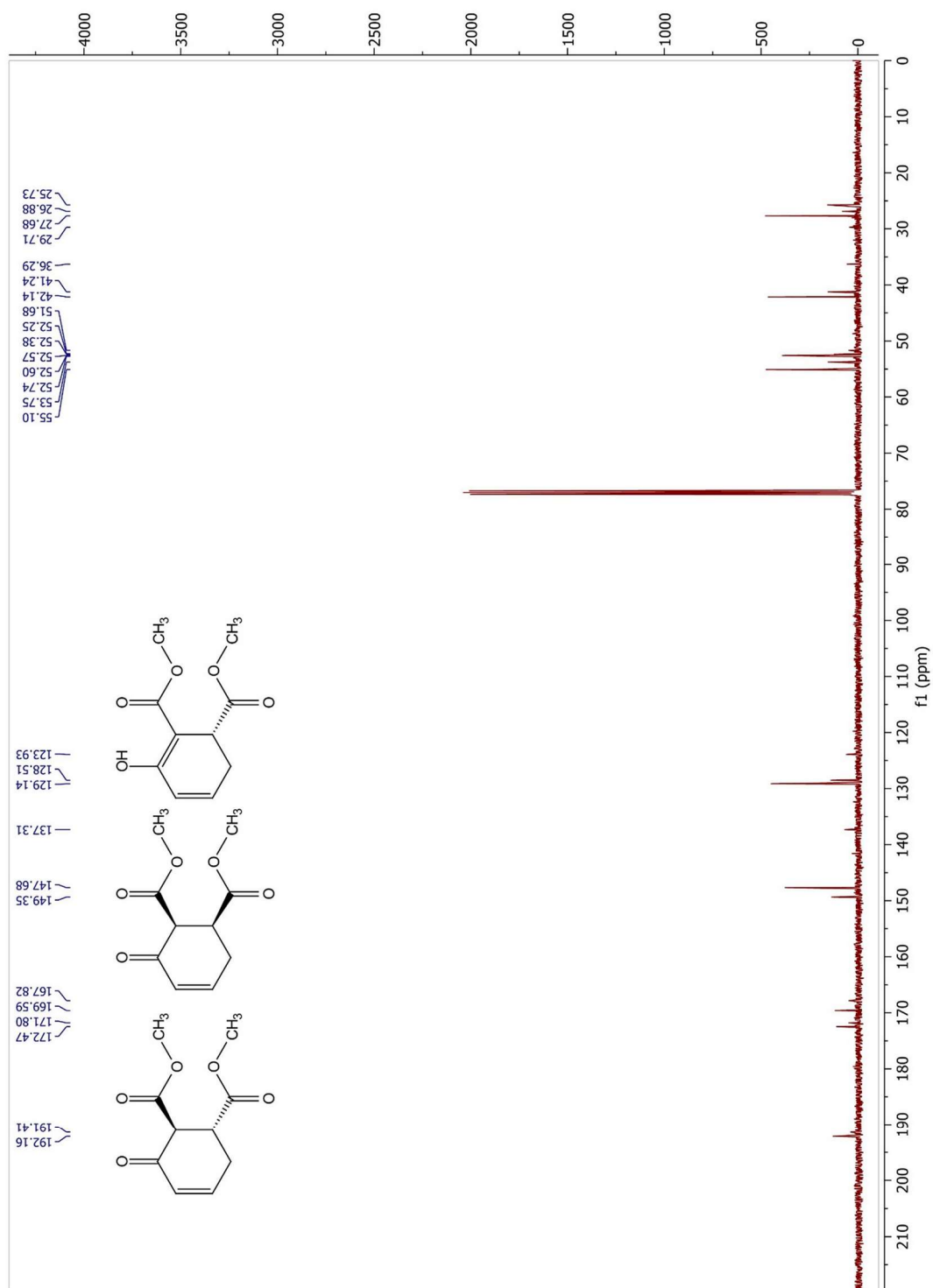


Figure 7.157 ^{13}C NMR Spectrum of **5.23h** (125 MHz, CDCl_3)

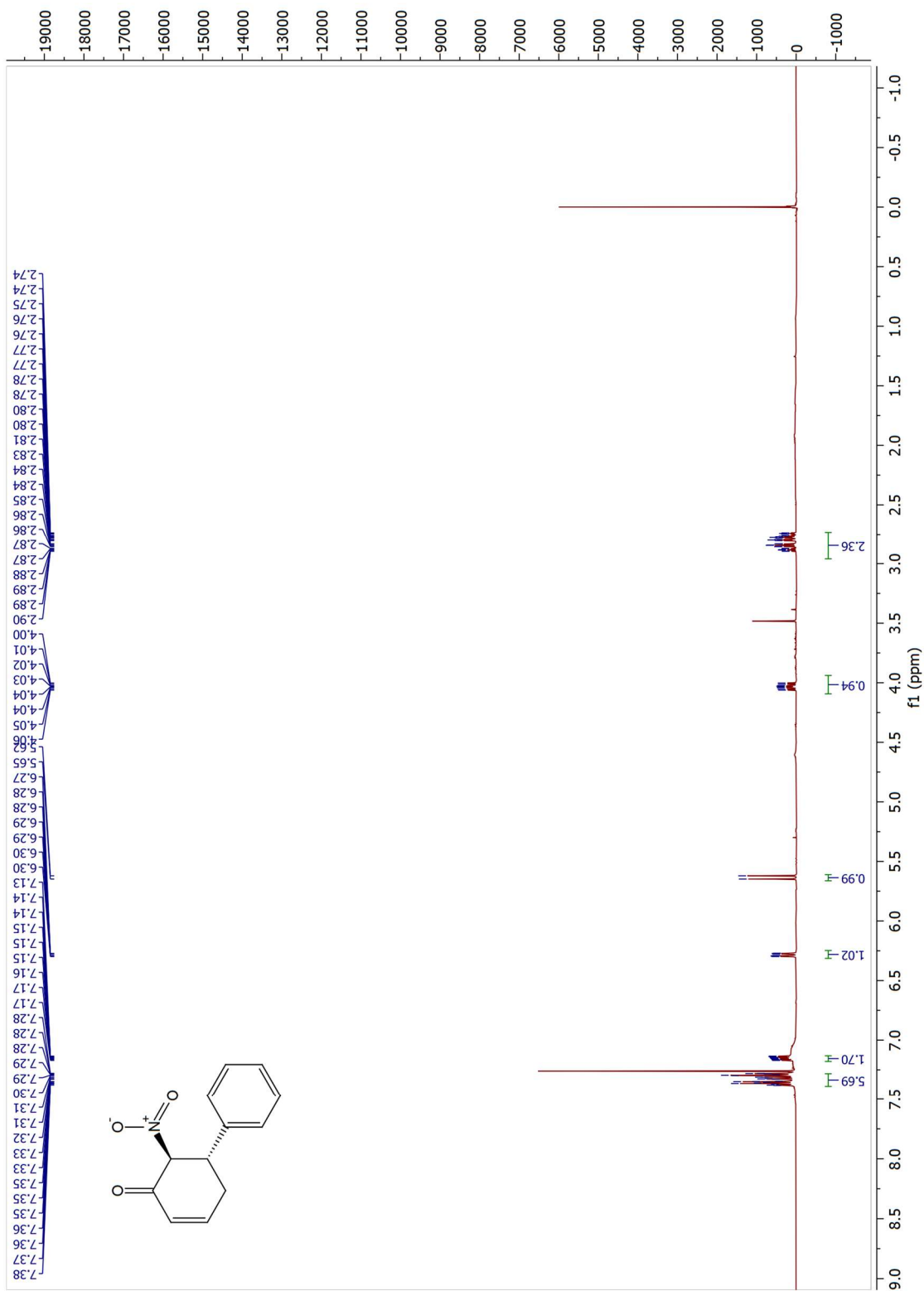


Figure 7.158 ^1H NMR Spectrum of **5.26a** (500 MHz, CDCl_3)

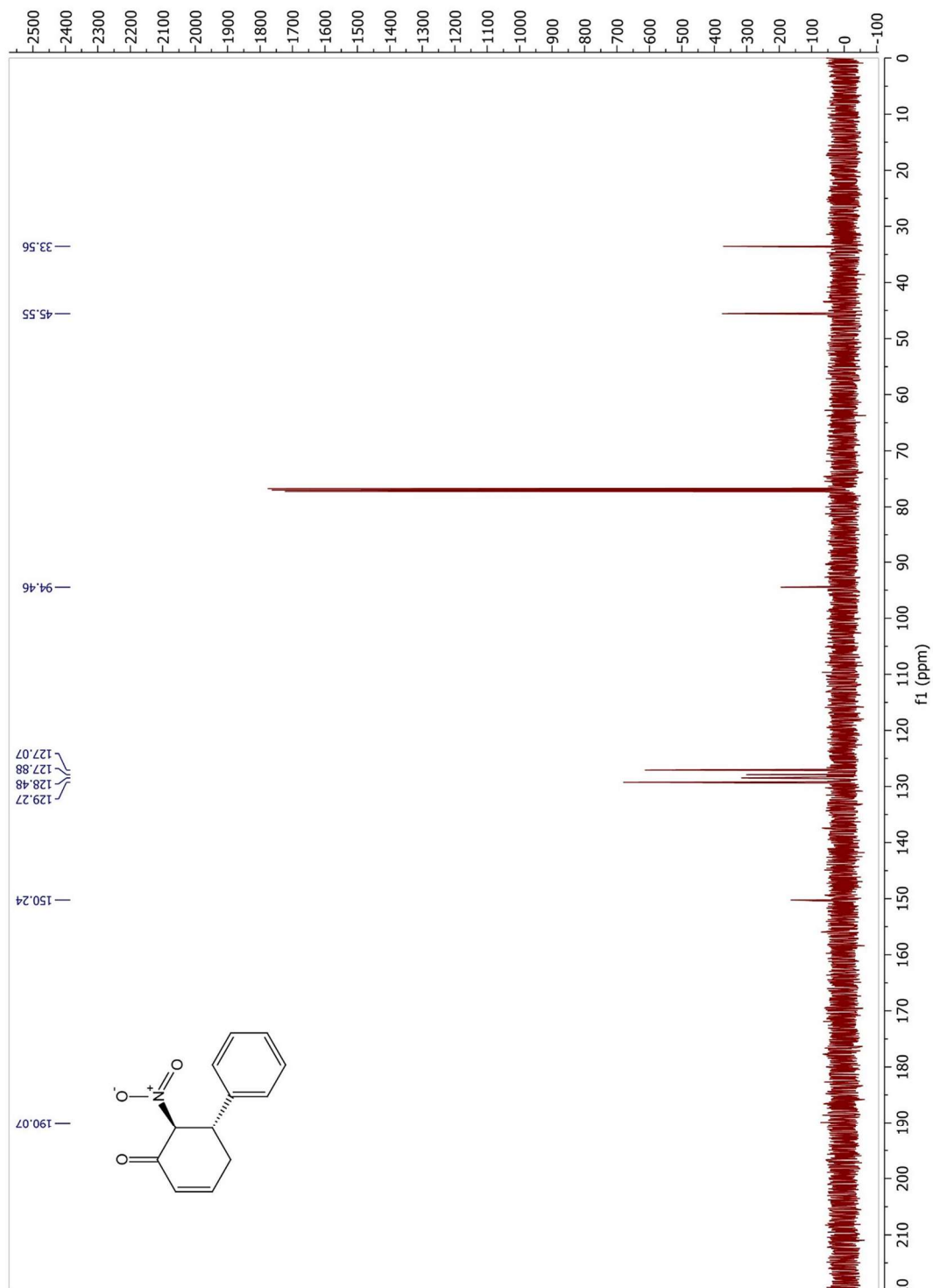


Figure 7.159 ^{13}C NMR Spectrum of **5.26a** (125 MHz, CDCl_3)

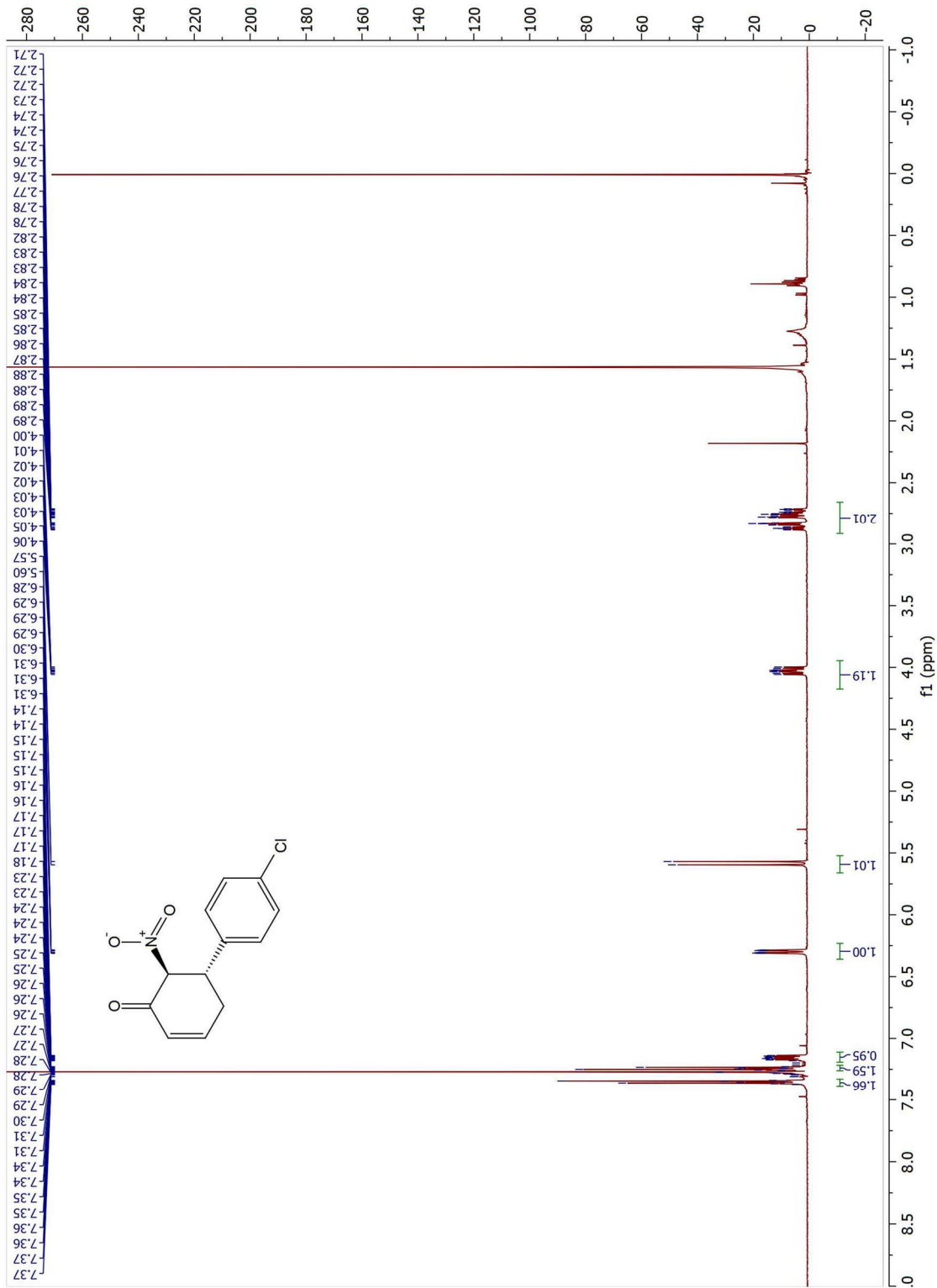


Figure 7.160 ^1H NMR Spectrum of **5.26b** (500 MHz, CDCl_3)

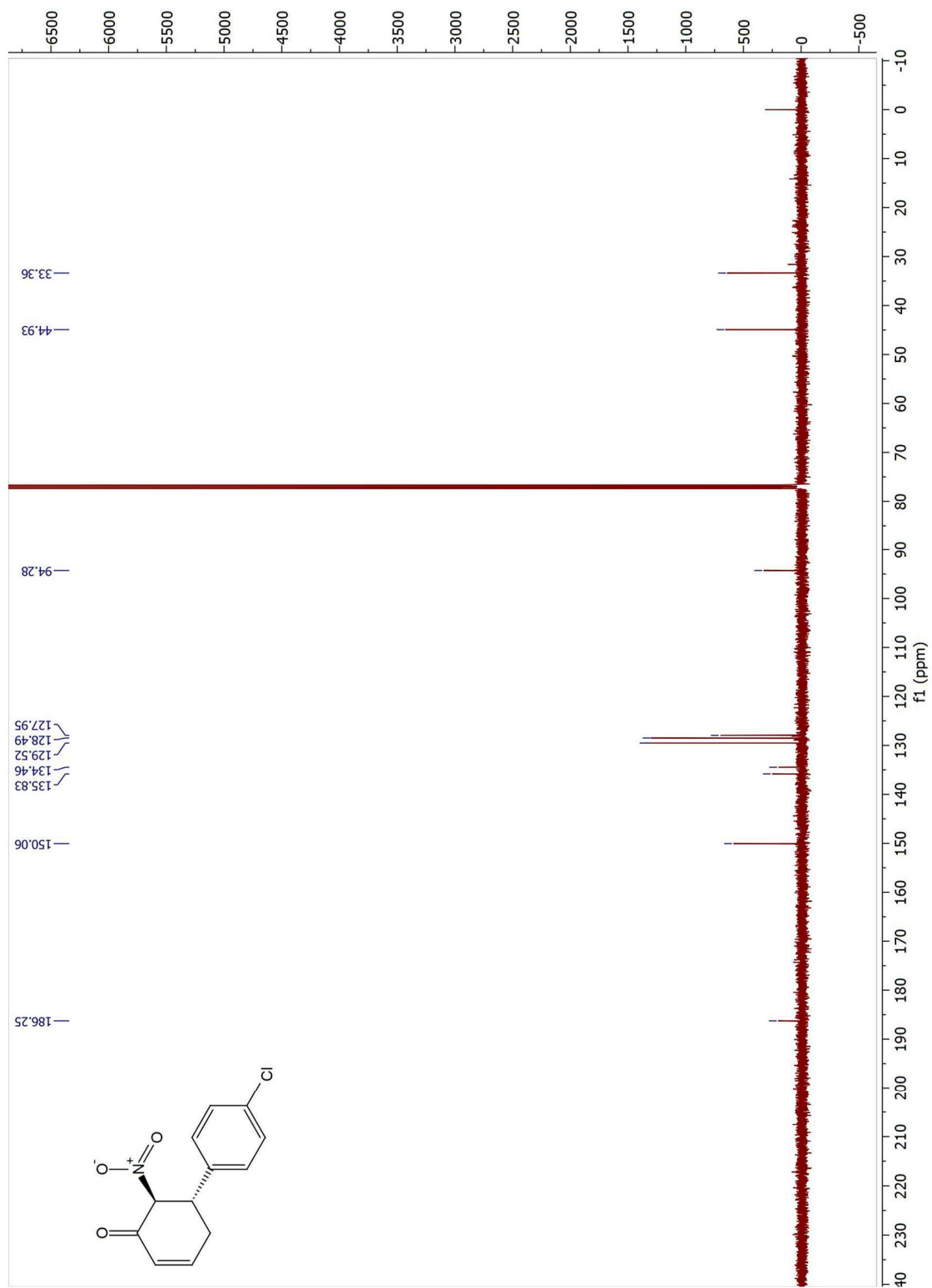


Figure 7.161 ^{13}C NMR Spectrum of **5.26b** (125 MHz, CDCl_3)

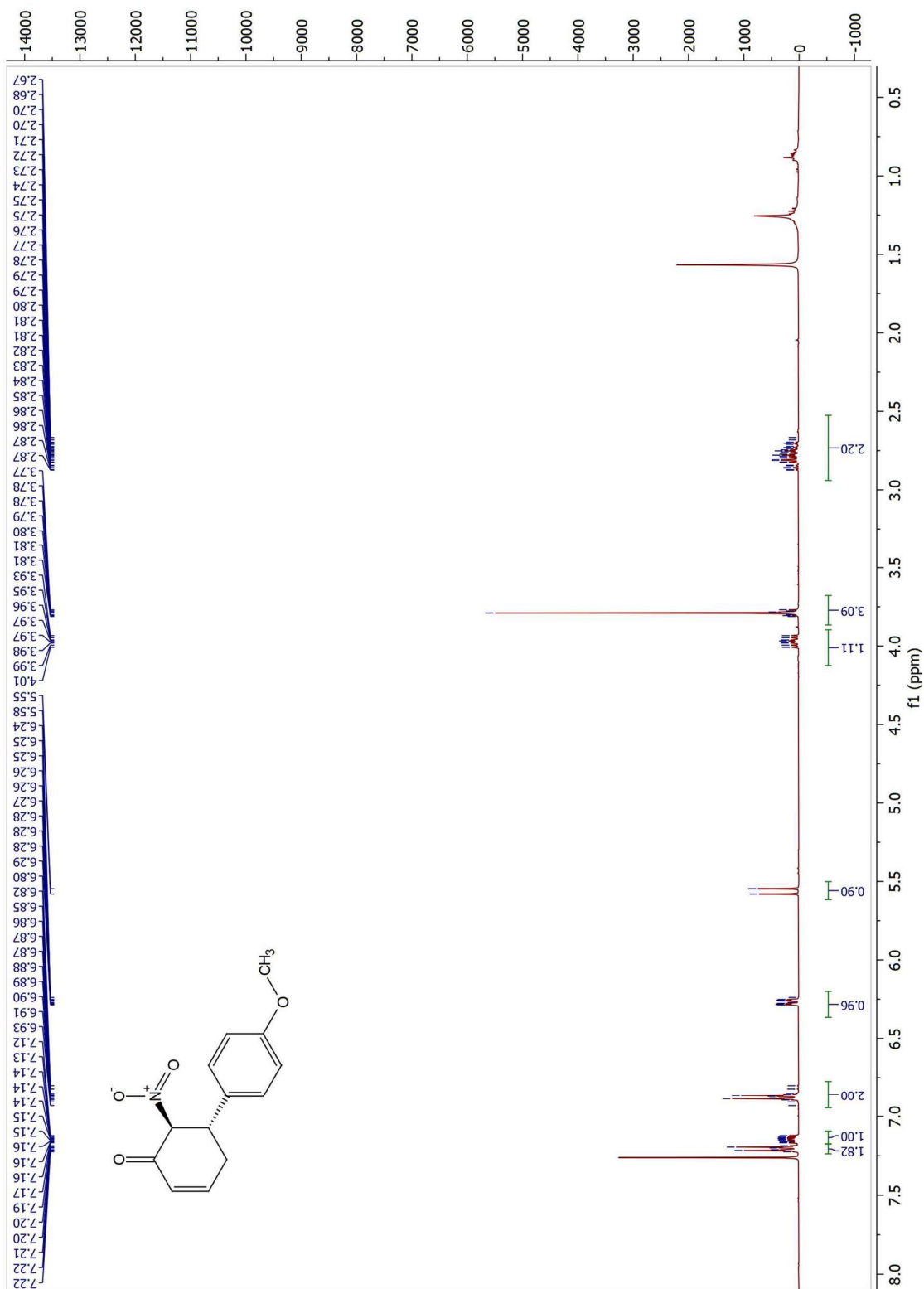


Figure 7.162 ¹H NMR Spectrum of **5.26c** (500 MHz, CDCl₃)

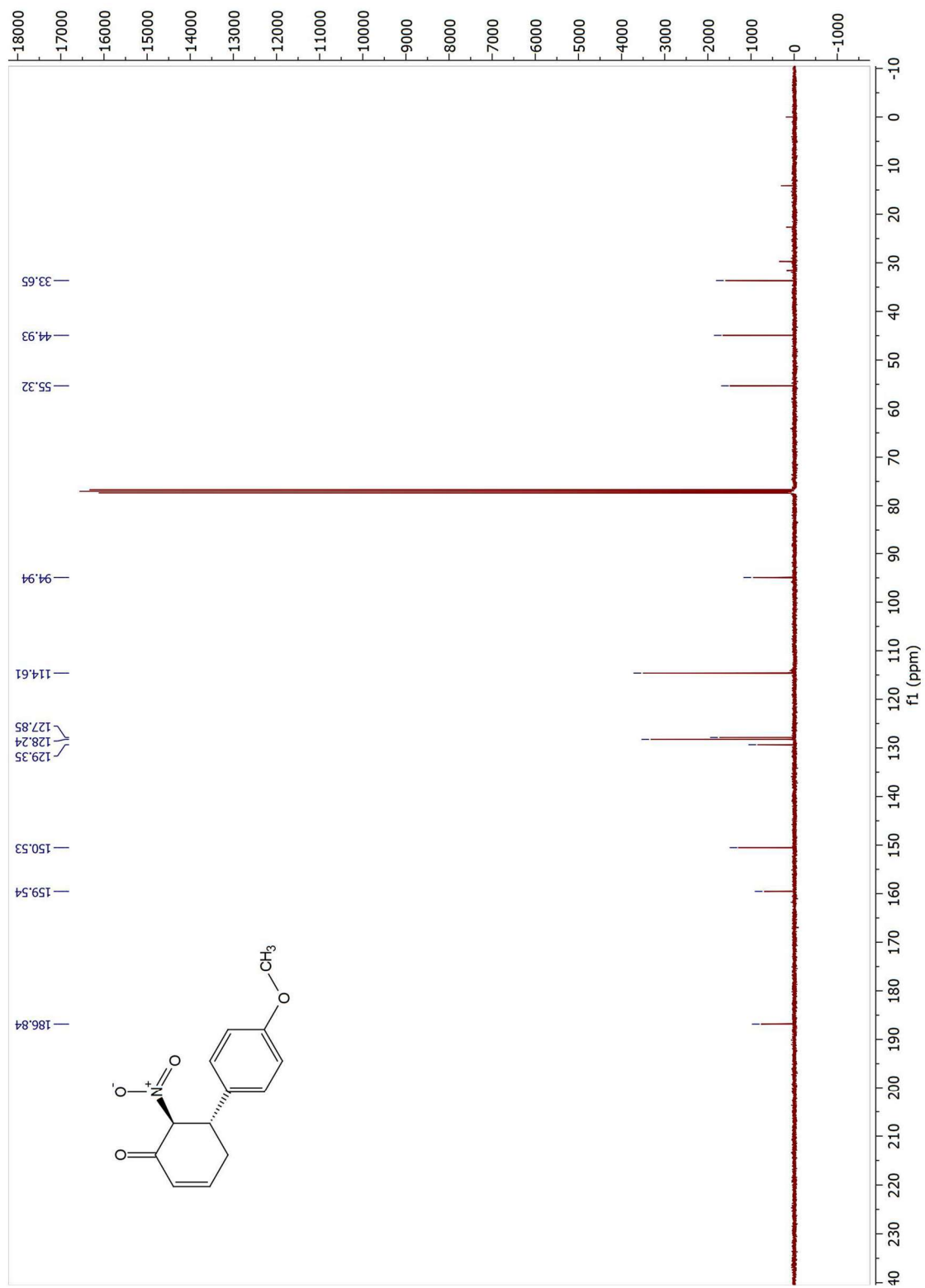


Figure 7.163 ^{13}C NMR Spectrum of **5.26c** (125 MHz, CDCl_3)

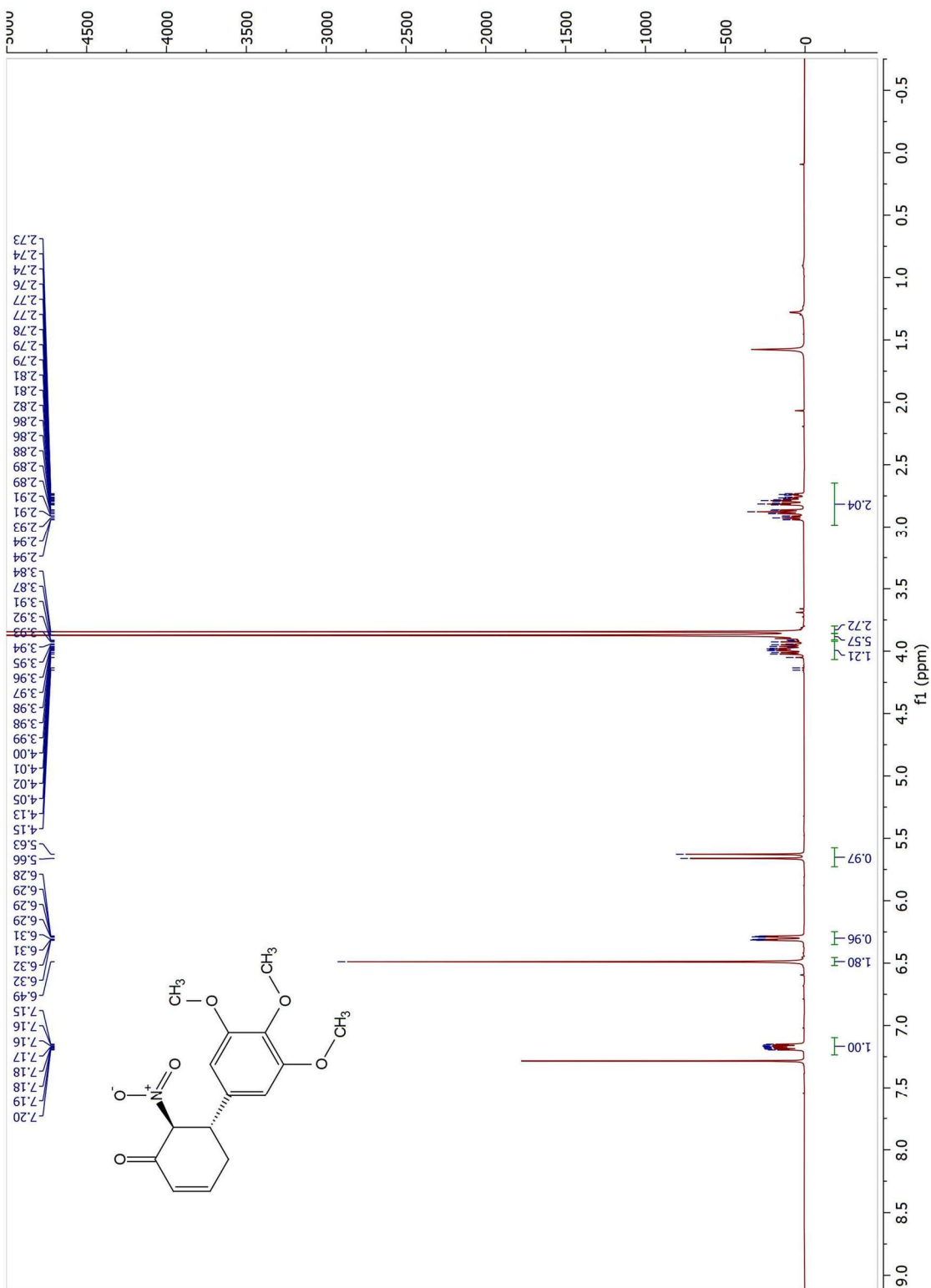


Figure 7.164 ^1H NMR Spectrum of **5.26d** (500 MHz, CDCl_3)

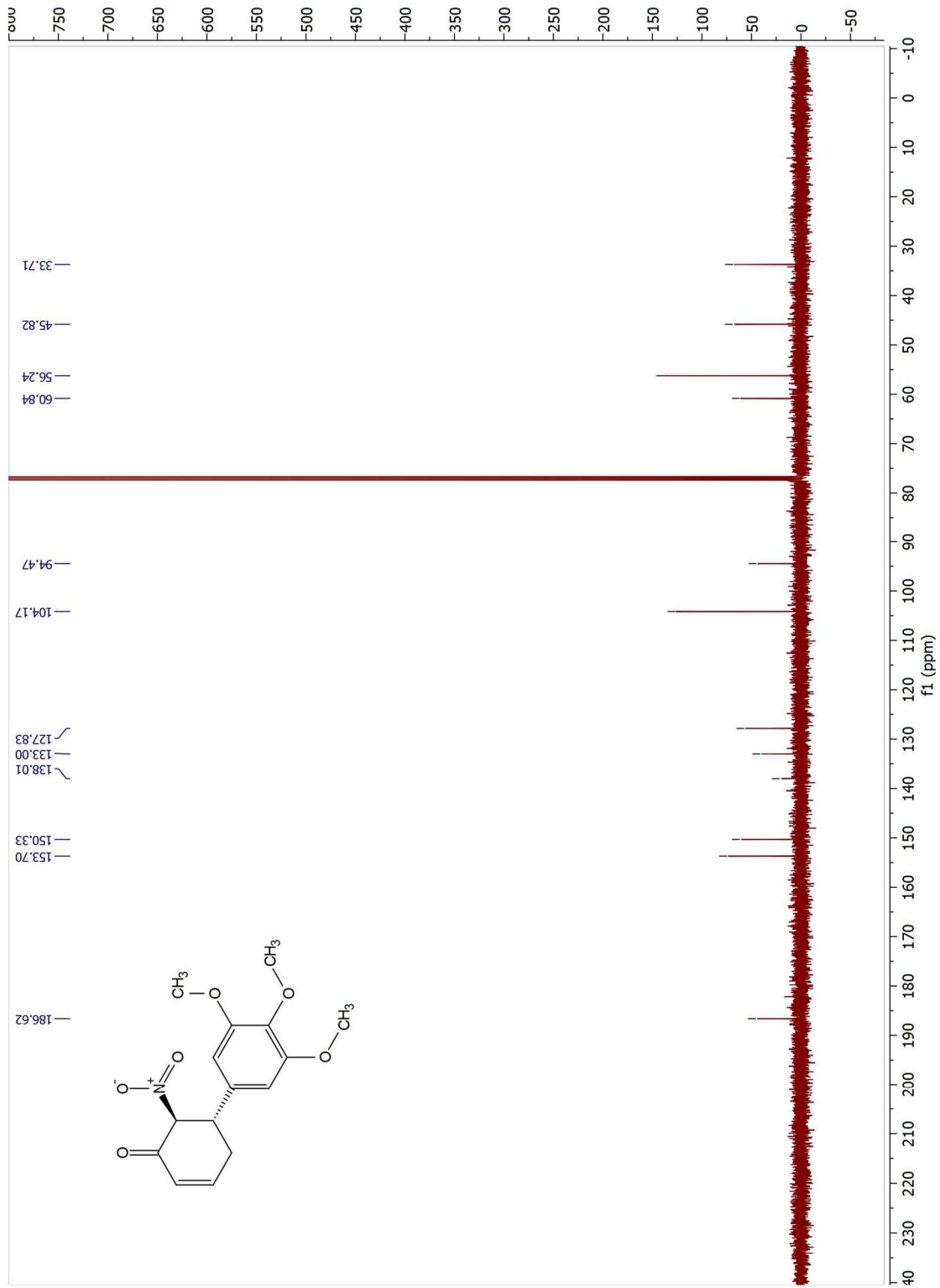


Figure 7.165 ^{13}C NMR Spectrum of **5.26d** (125 MHz, CDCl_3)

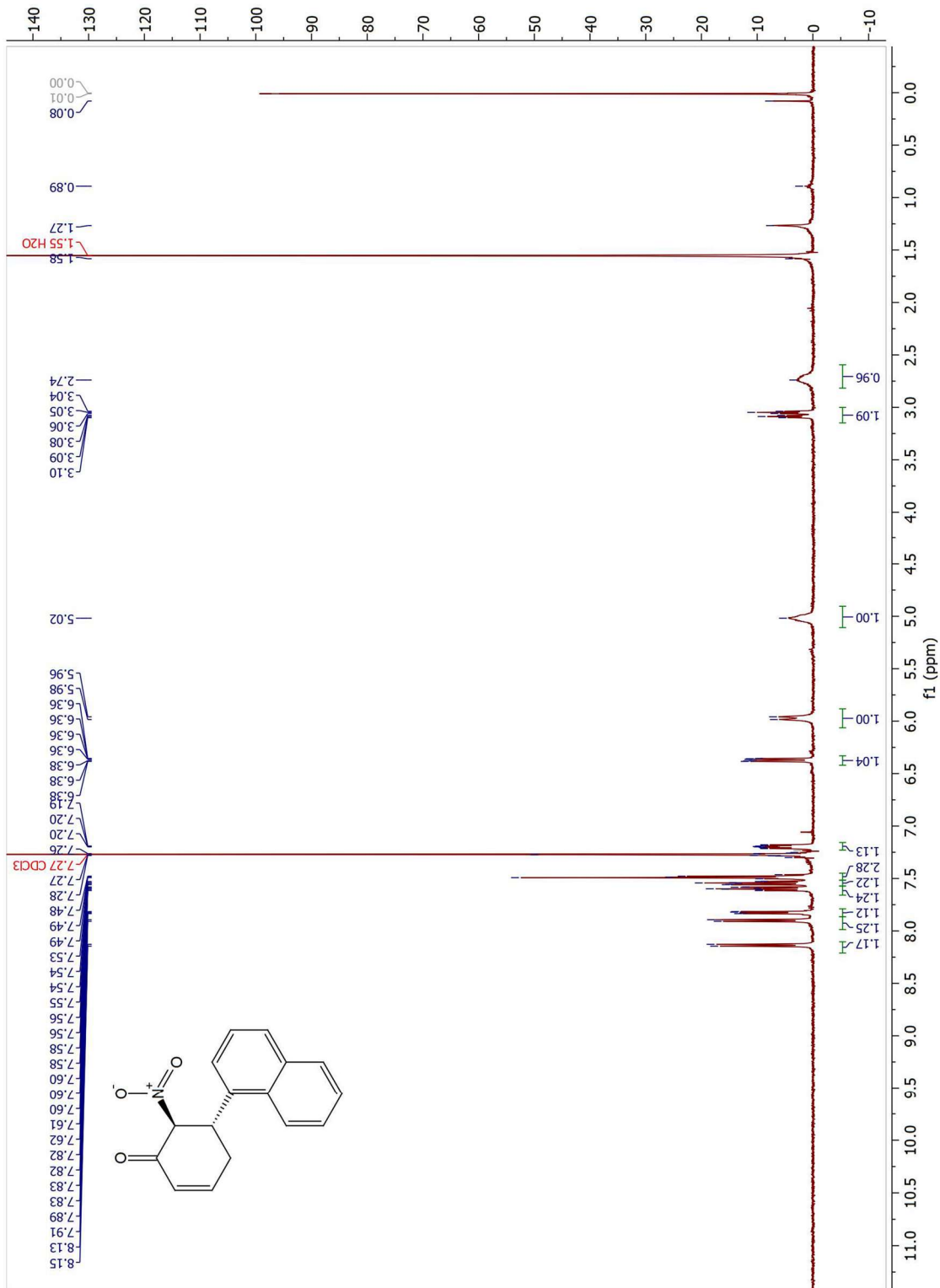


Figure 7.166 ^1H NMR Spectrum of 5.26e (500 MHz, CDCl_3)

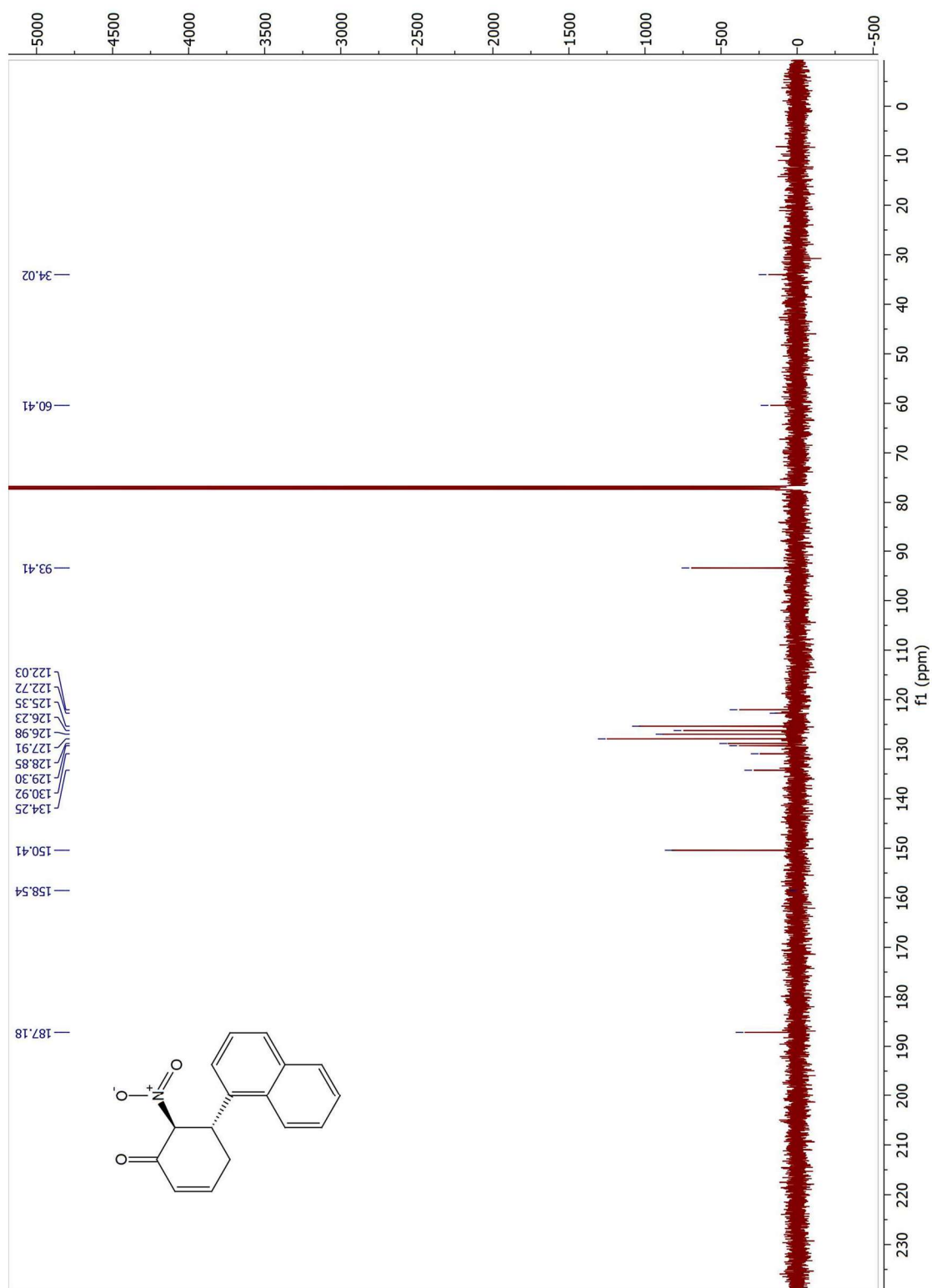


Figure 7.167 ^{13}C NMR Spectrum of **5.26e** (125 MHz, CDCl_3)

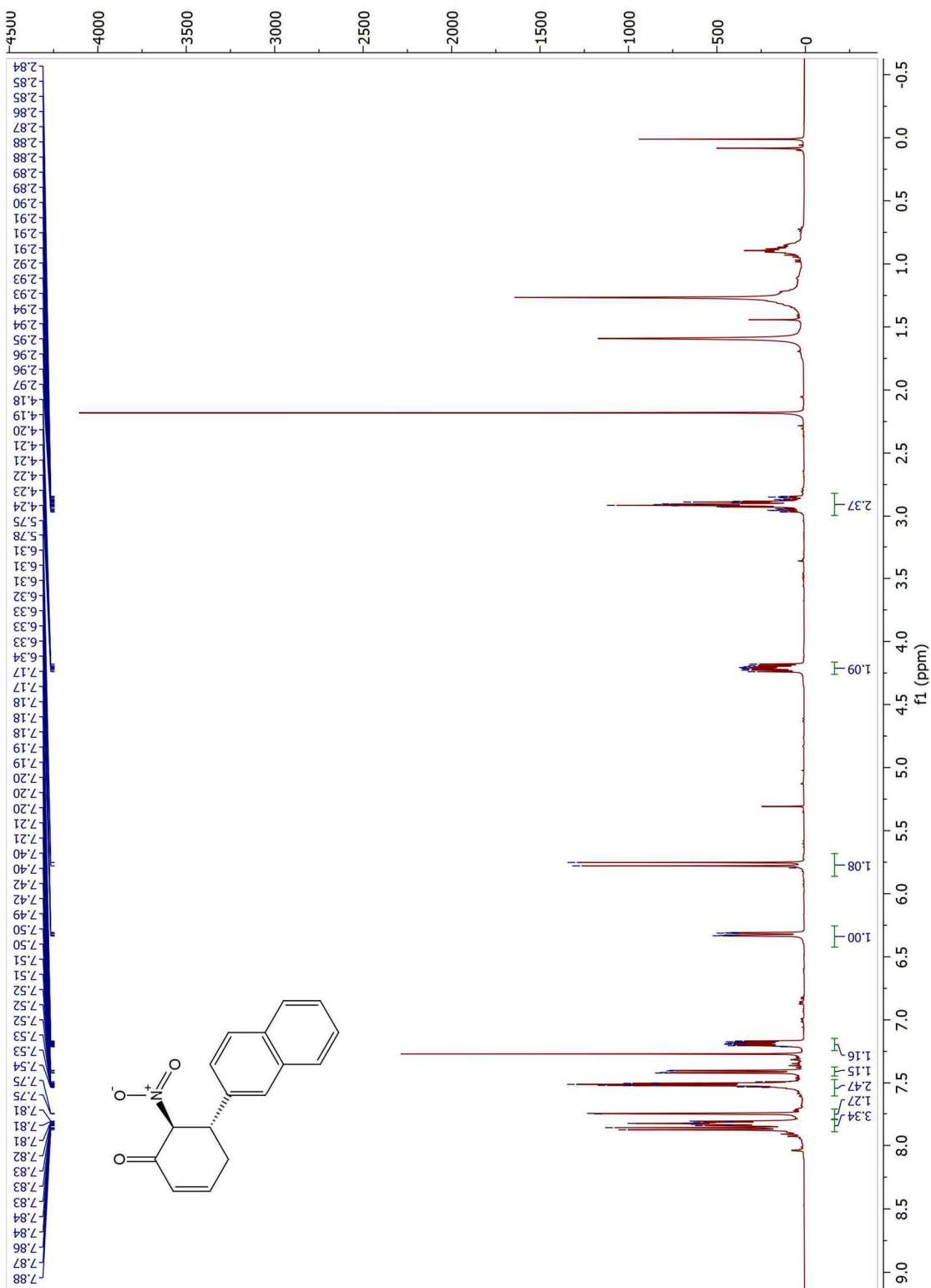


Figure 7.168 ^1H NMR Spectrum of **5.26f** (500 MHz, CDCl_3)

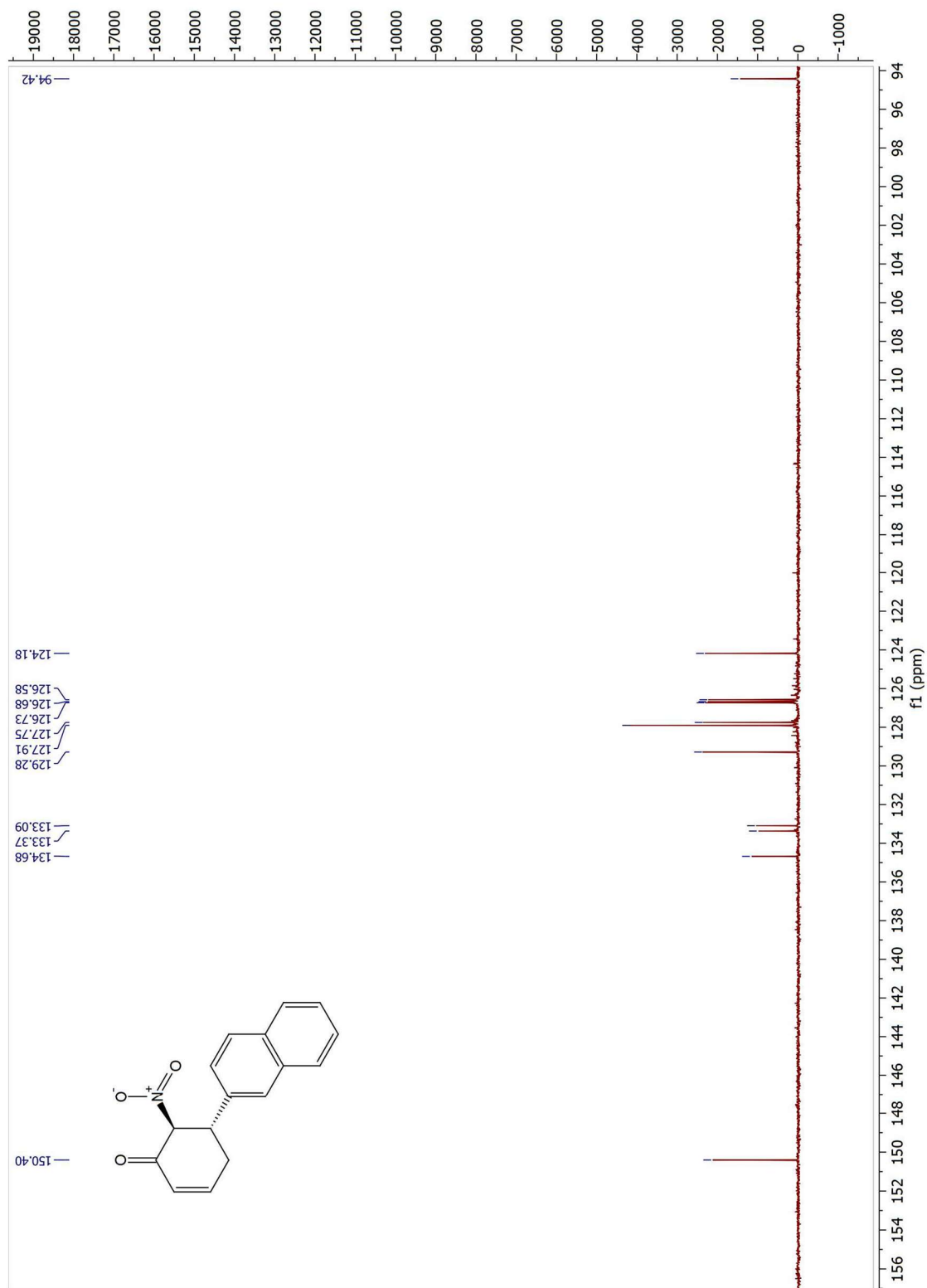
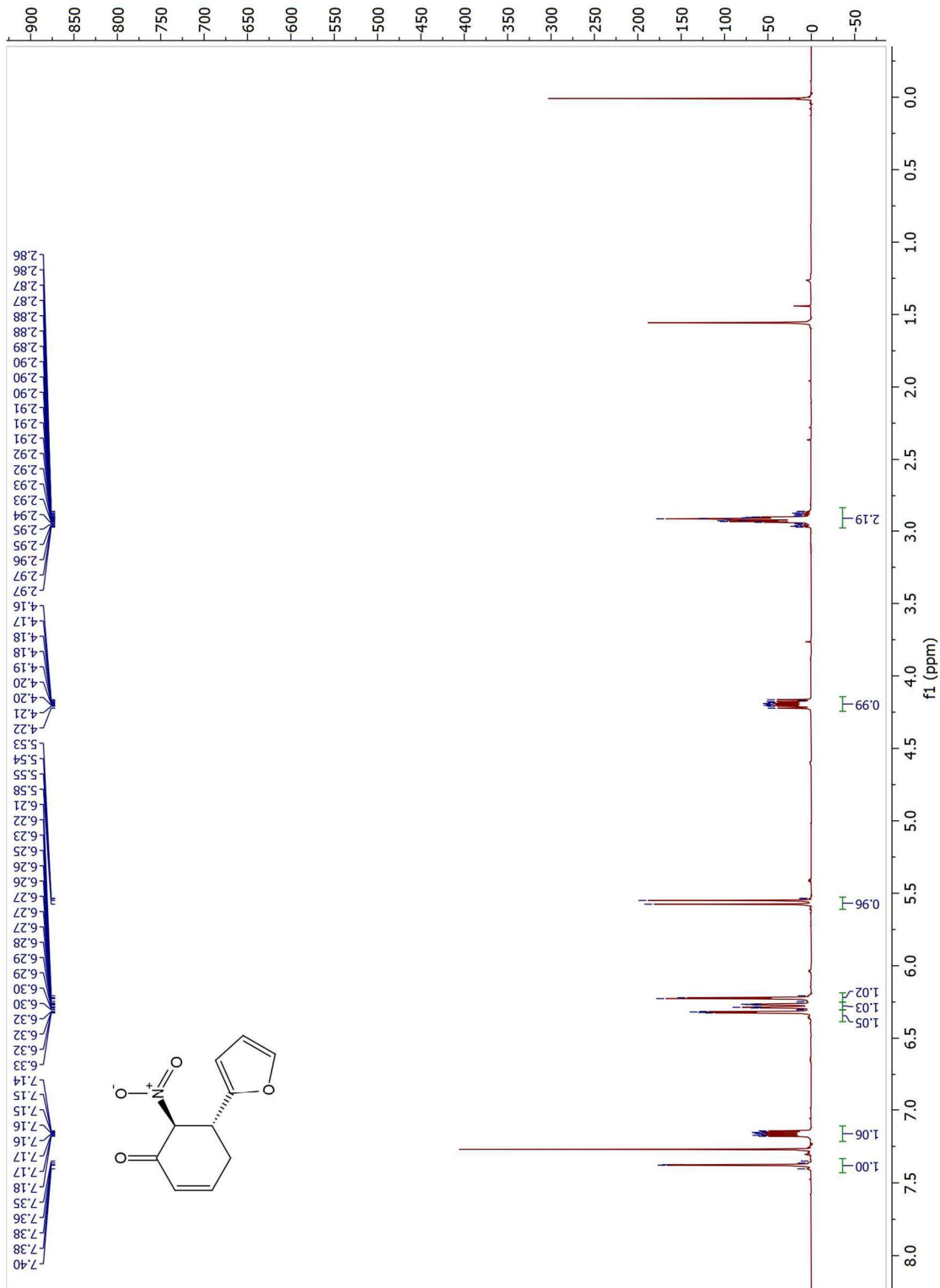


Figure 7.169 ¹³C NMR Spectrum of 5.26f (125 MHz, CDCl₃)



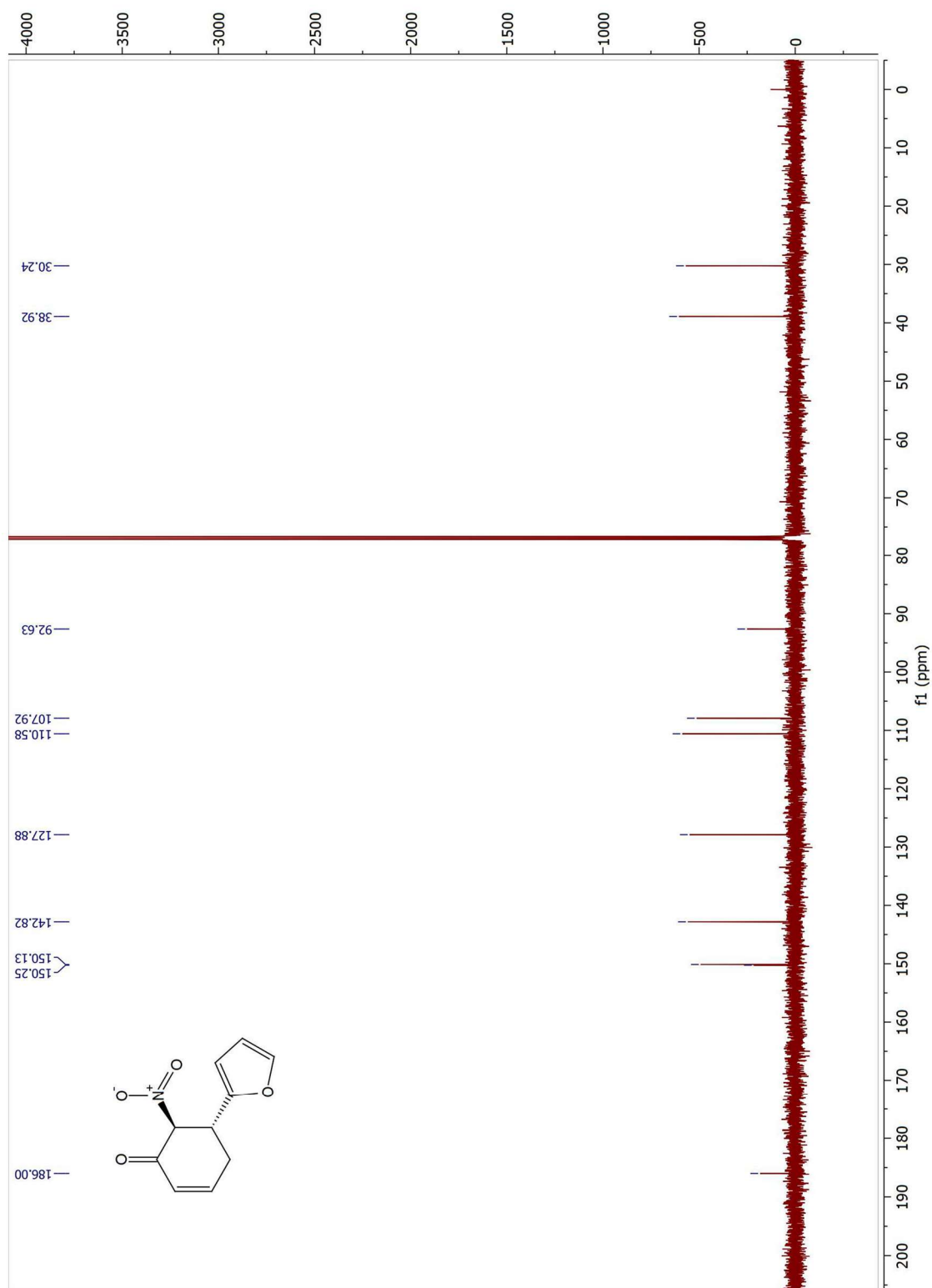


Figure 7.171 ¹³C NMR Spectrum of 5.26g (125 MHz, CDCl₃)

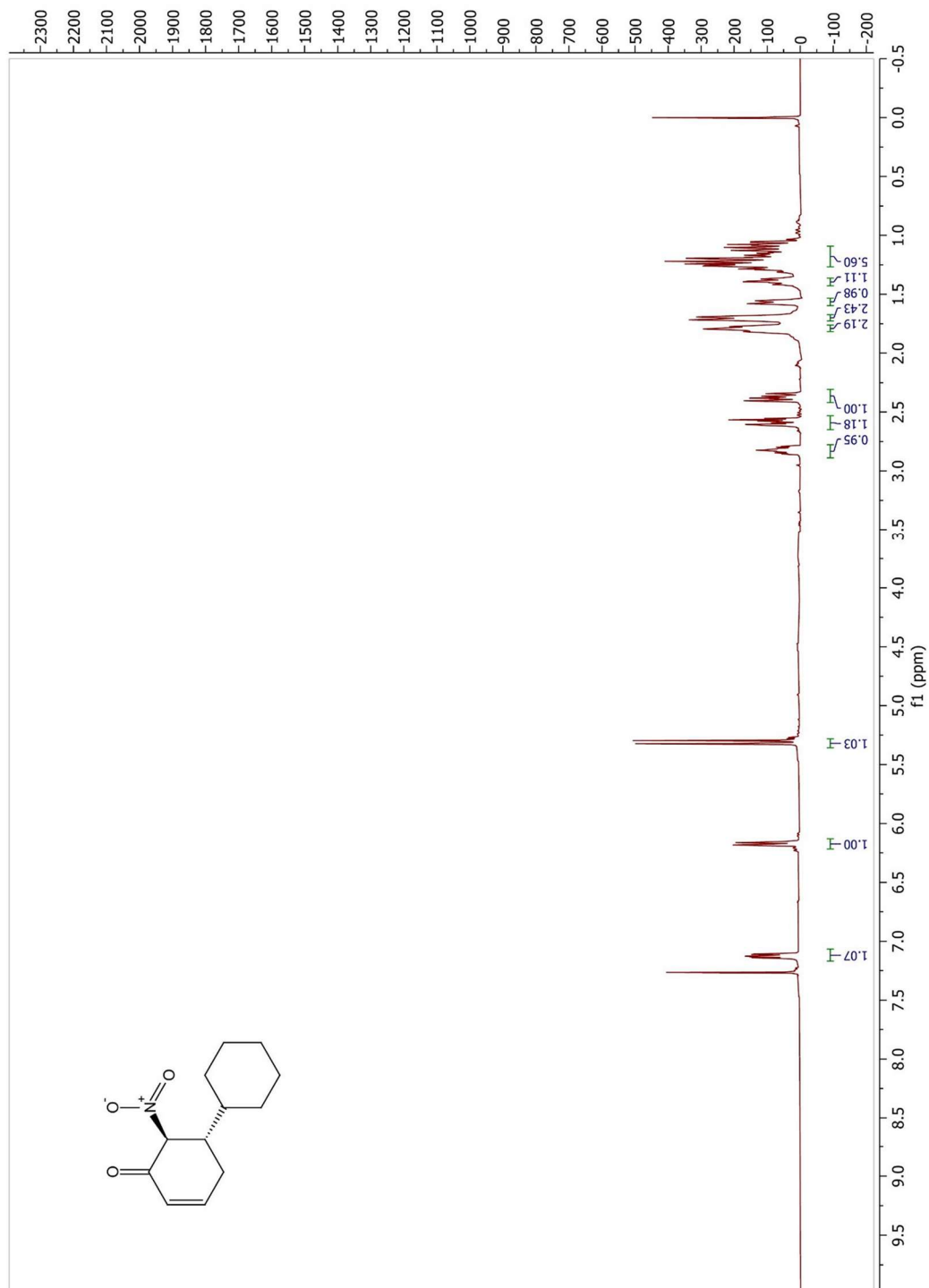


Figure 7.172 ¹H NMR Spectrum of **5.26h** (500 MHz, CDCl₃)

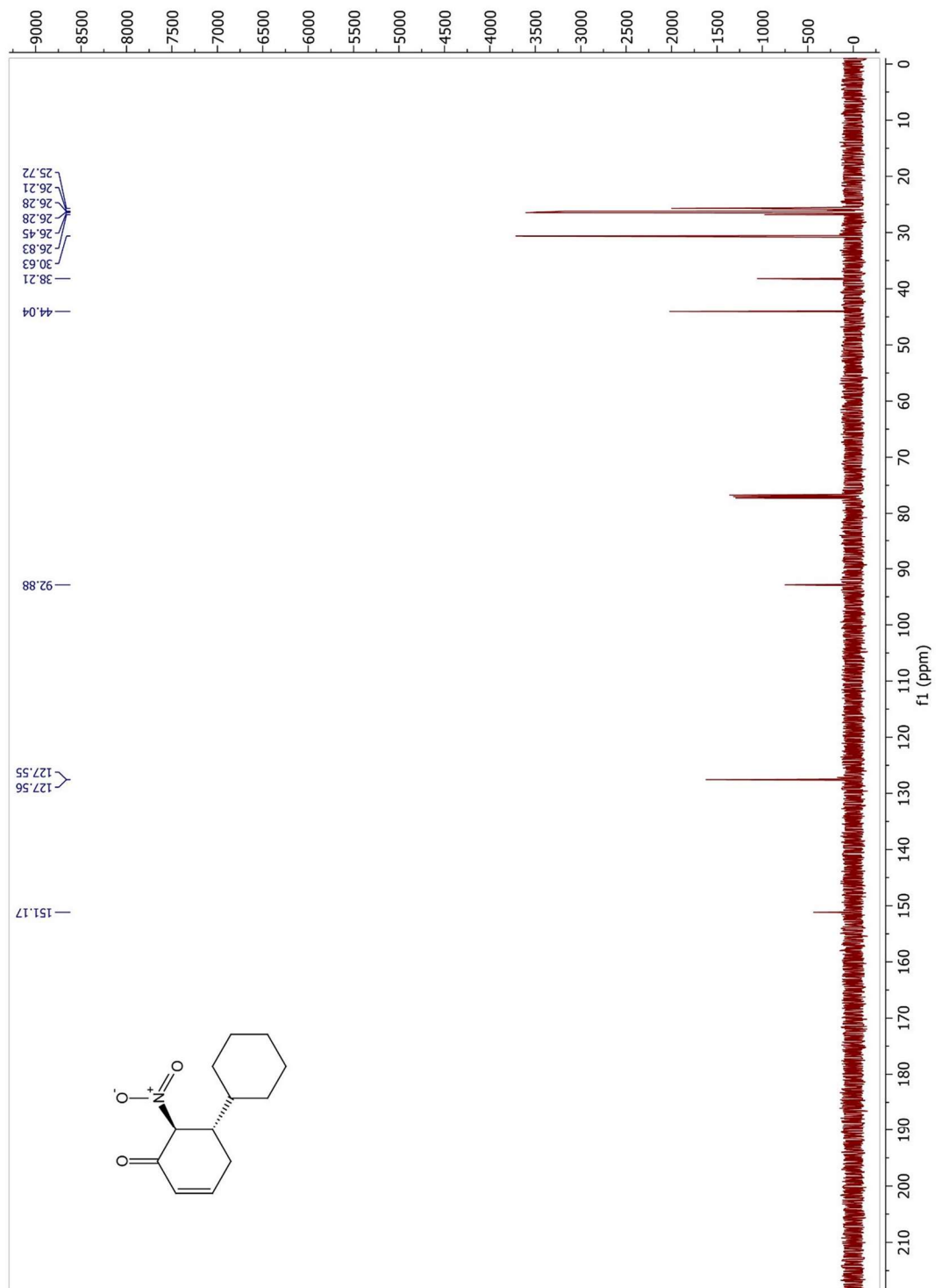


Figure 7.173 ^{13}C NMR Spectrum of **5.26h** (125 MHz, CDCl_3)

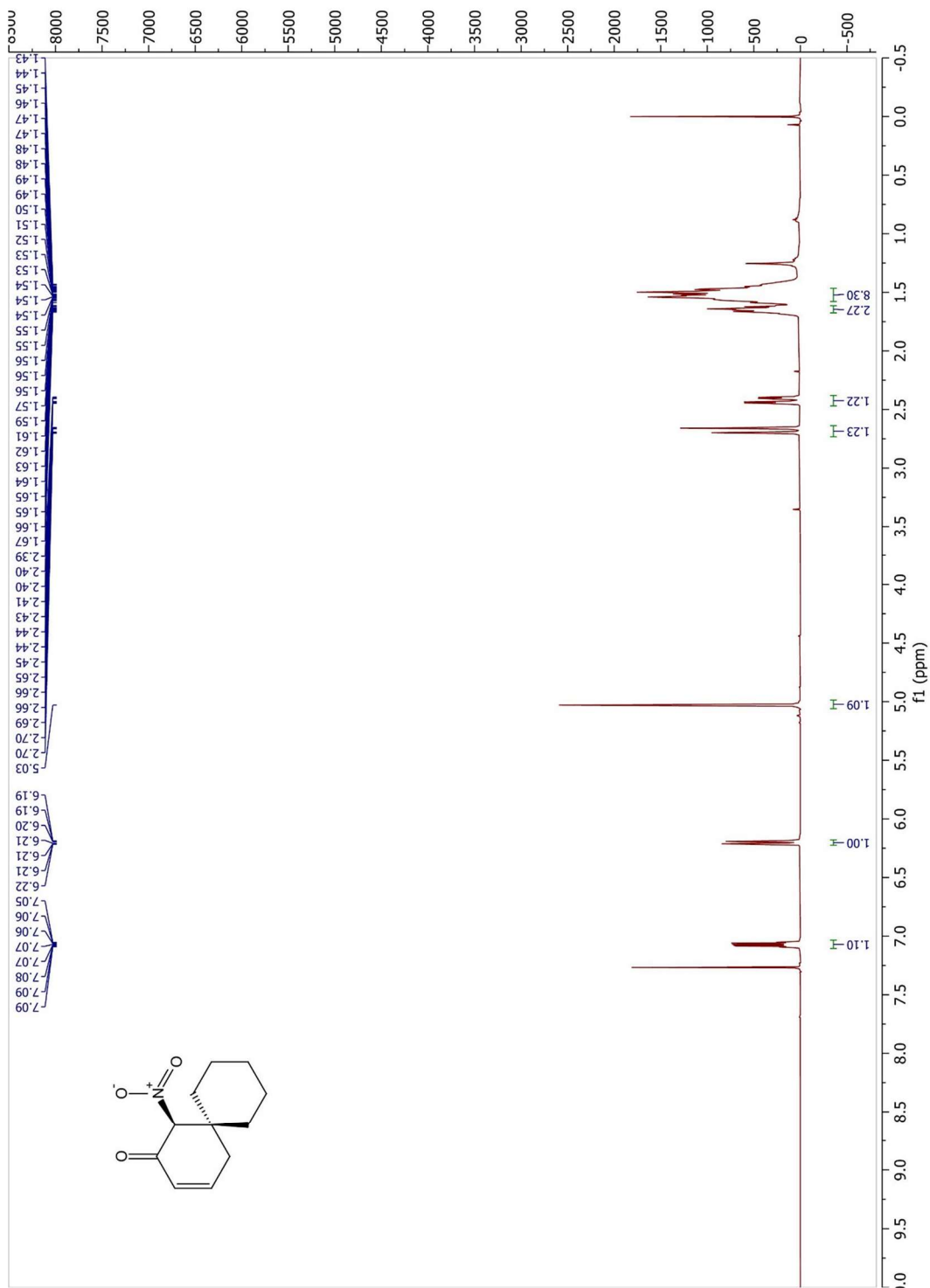


Figure 7.174 ^1H NMR Spectrum of **5.26i** (500 MHz, CDCl_3)

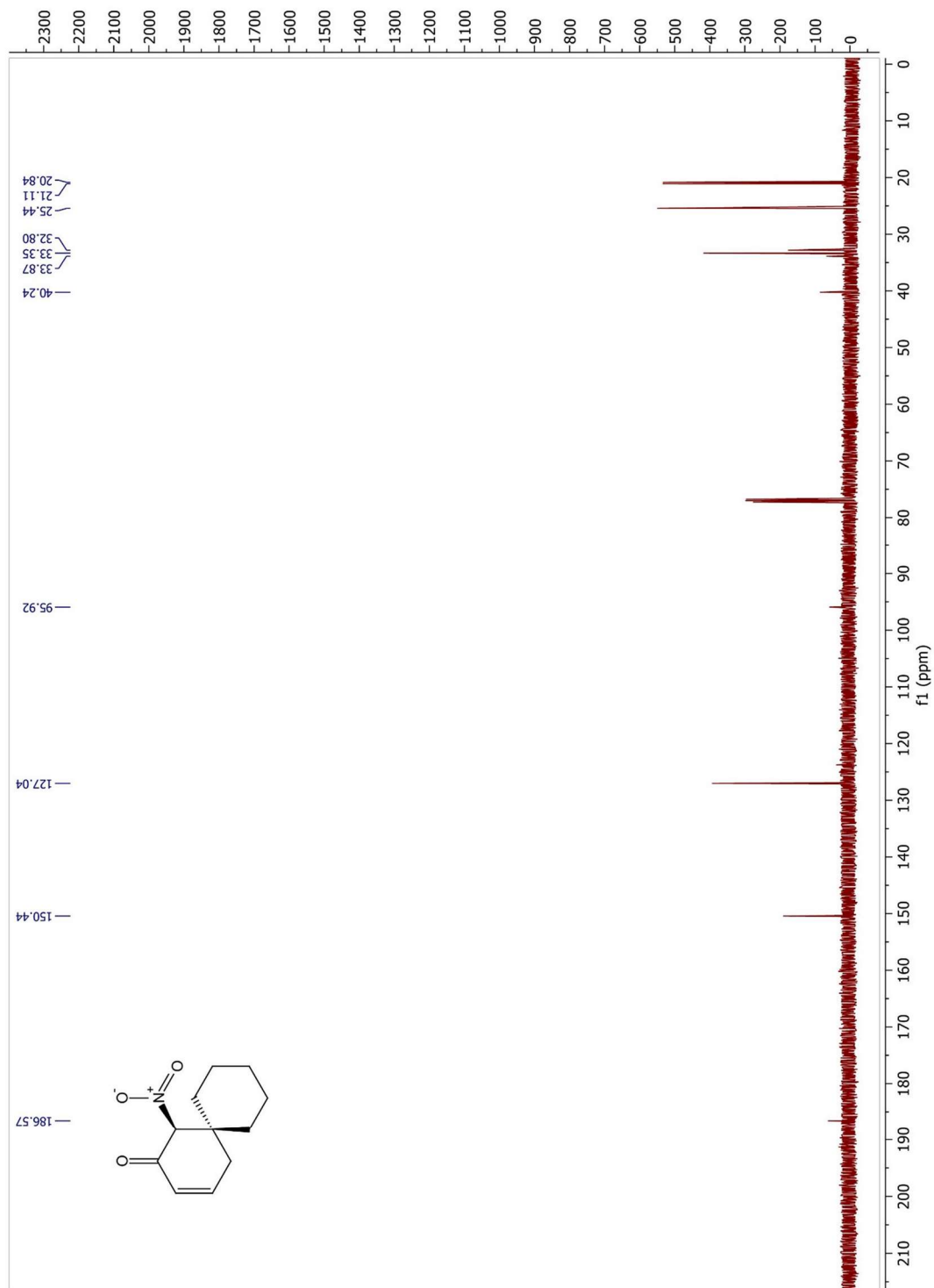


Figure 7.175 ^{13}C NMR Spectrum of 5.26i (125 MHz, CDCl_3)

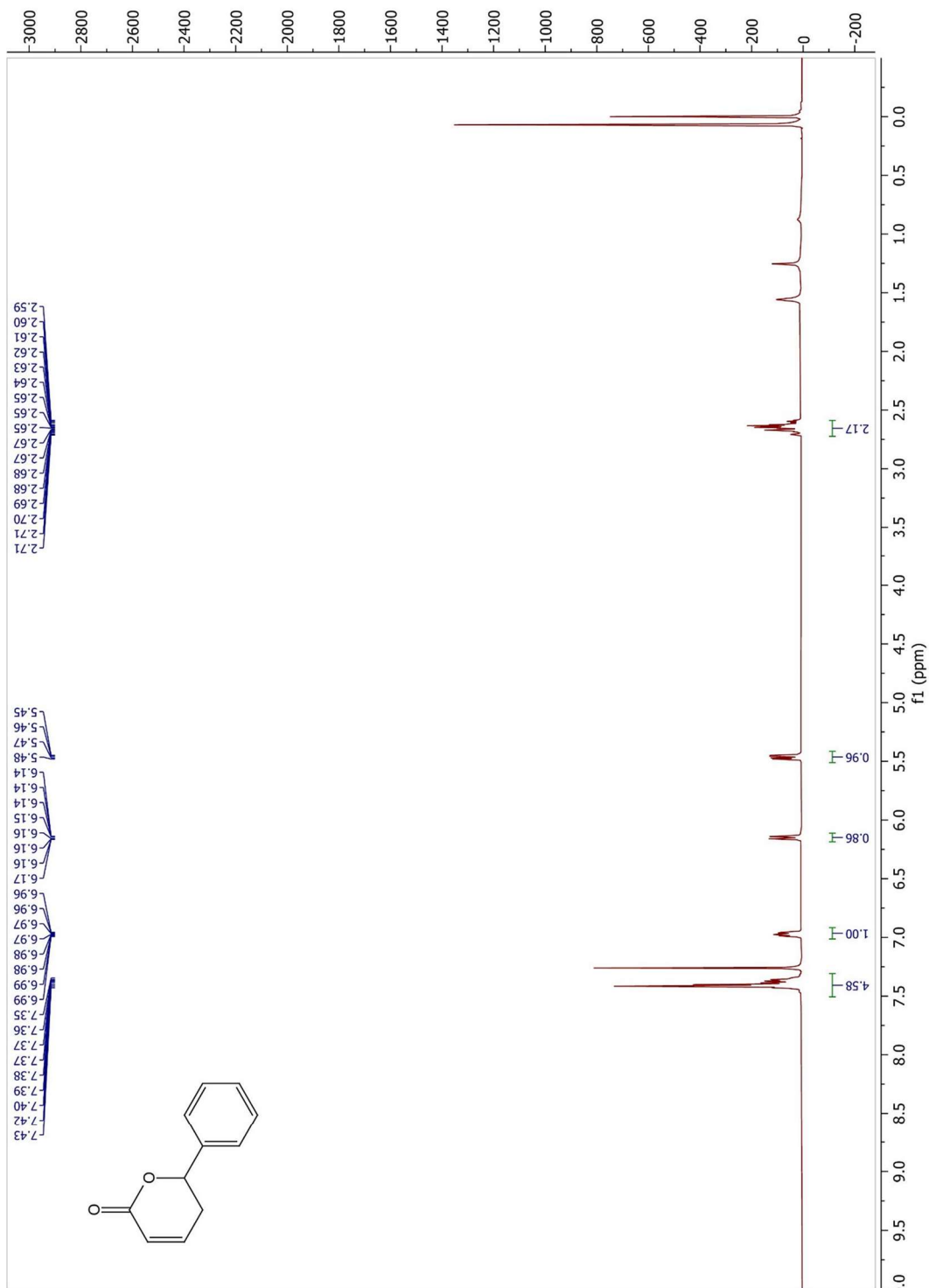


Figure 7.176 ^1H NMR Spectrum of **5.29a** (500 MHz, CDCl_3)

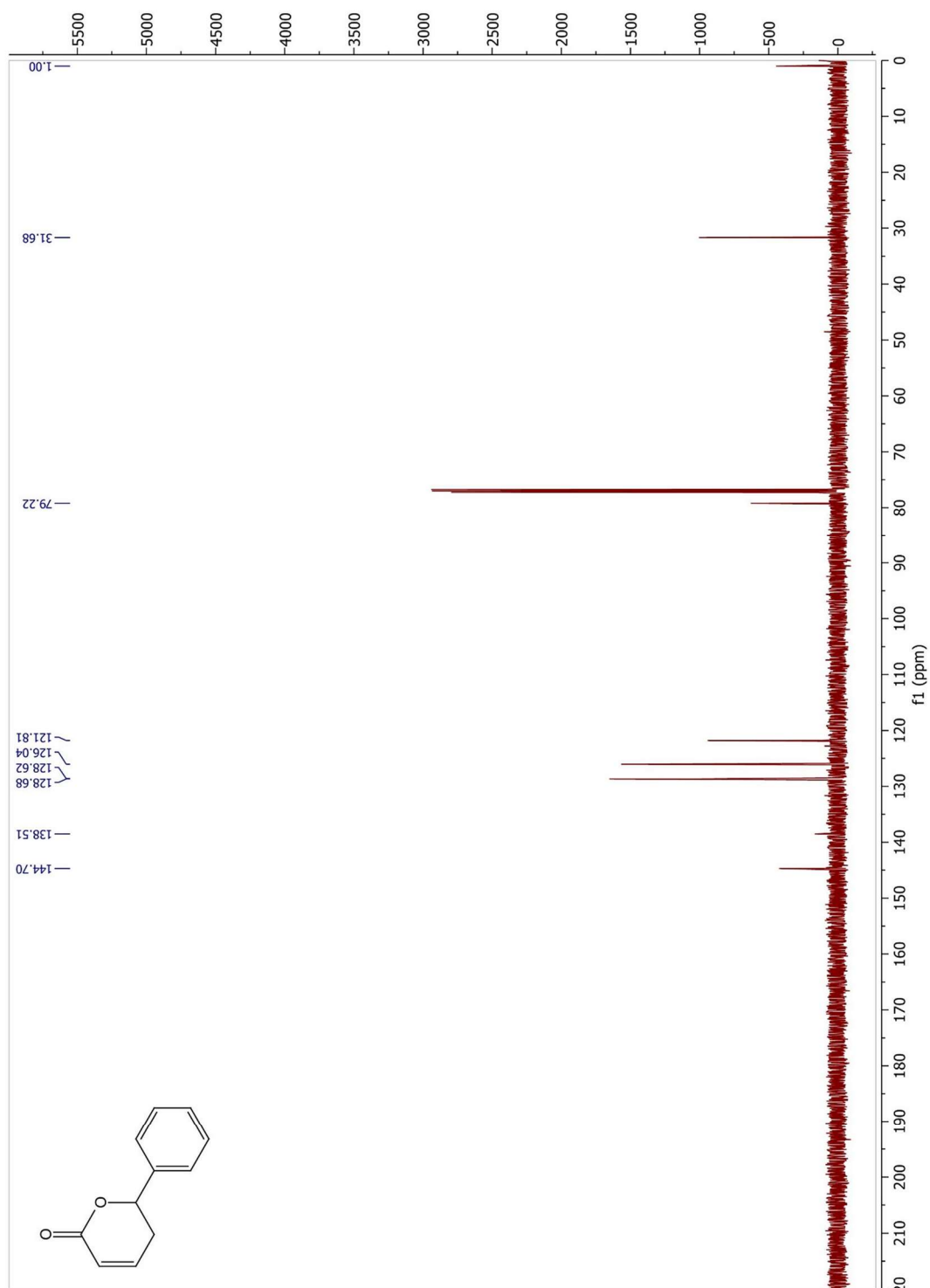


Figure 7.177 ^{13}C NMR Spectrum of **5.29a** (125 MHz, CDCl_3)

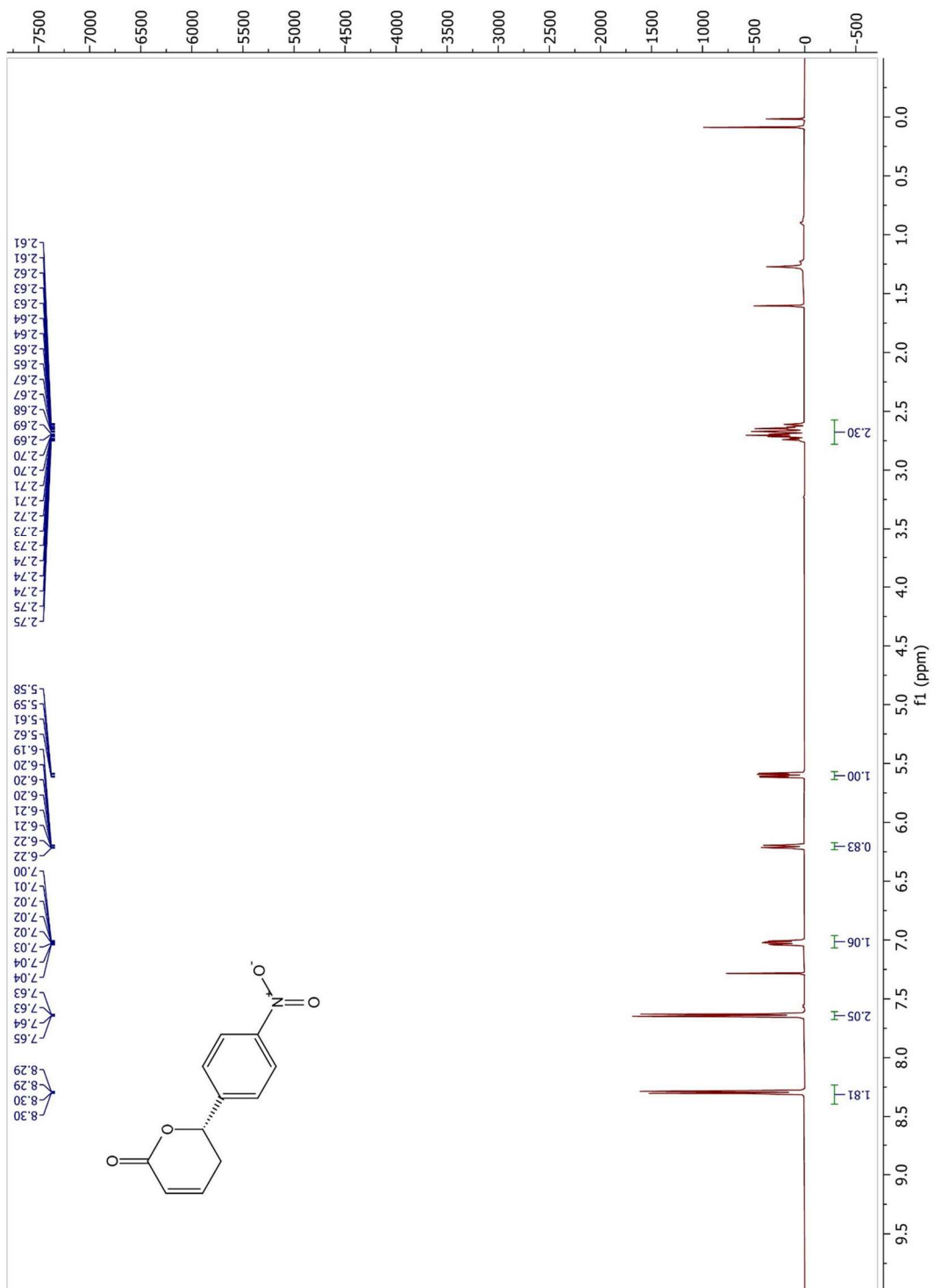


Figure 7.178 ^1H NMR Spectrum of **5.29b** (500 MHz, CDCl_3)

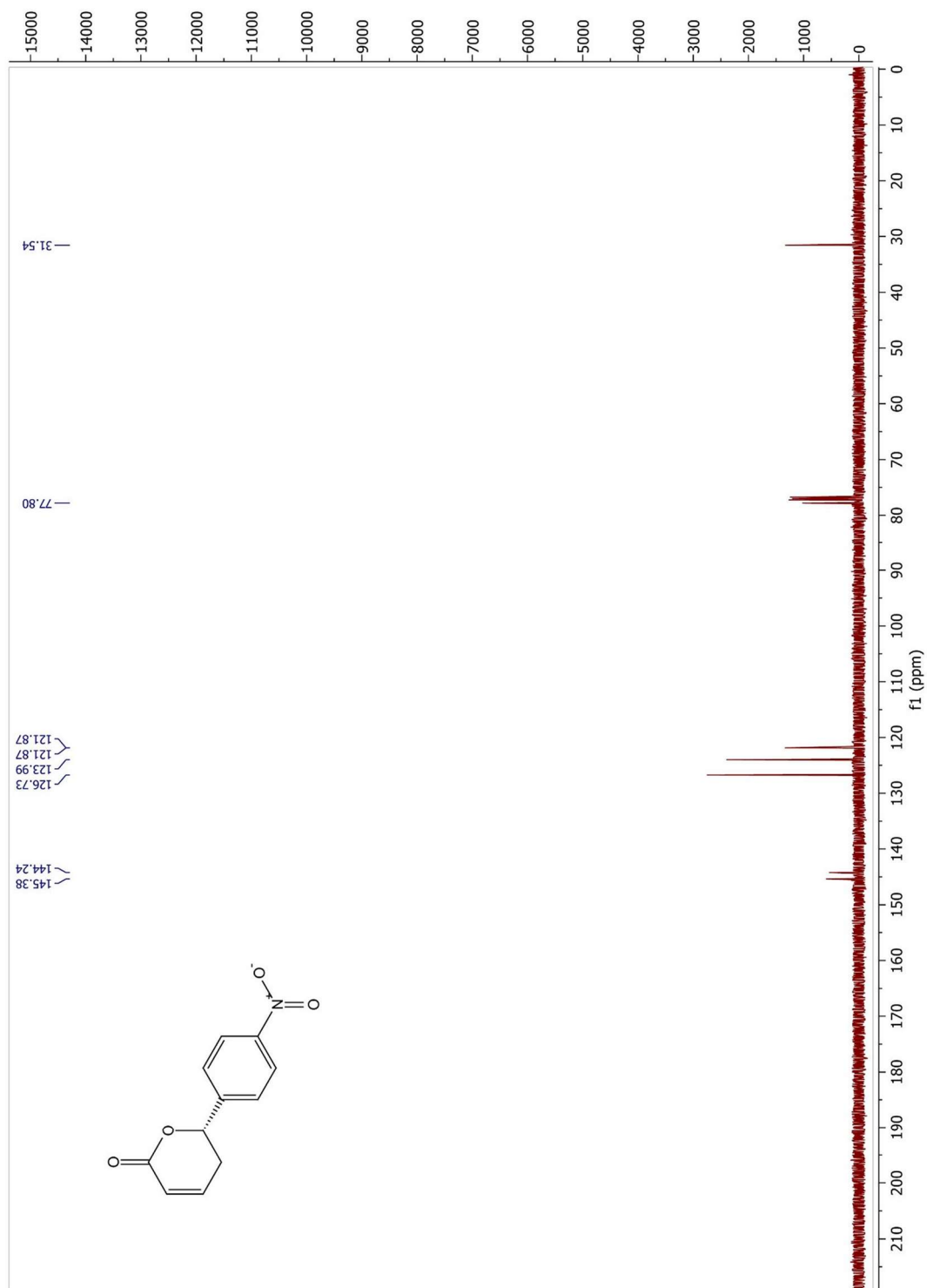


Figure 7.179 ^{13}C NMR Spectrum of **5.29b** (125 MHz, CDCl_3)

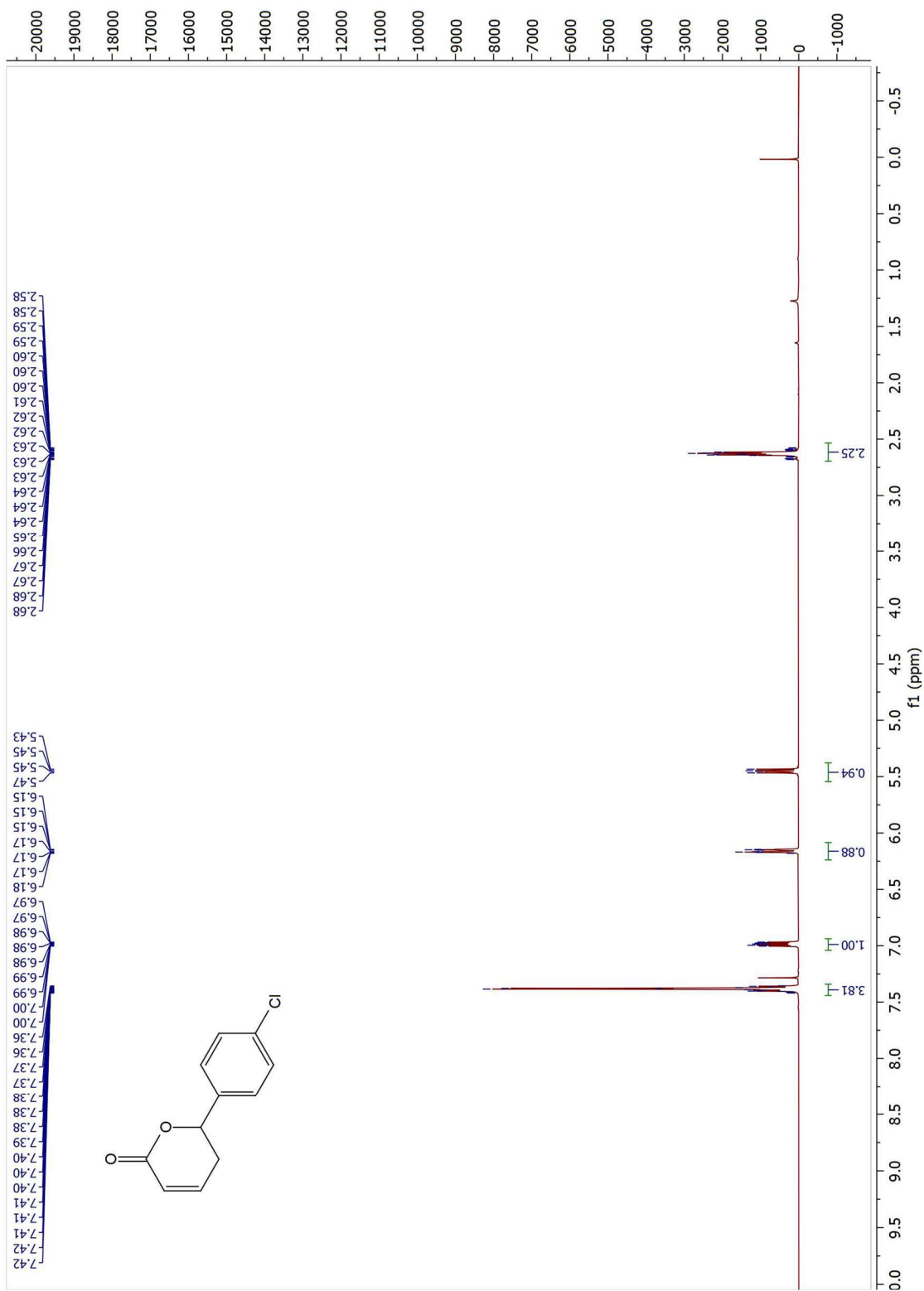


Figure 7.180 ^1H NMR Spectrum of **5.29c** (500 MHz, CDCl_3)

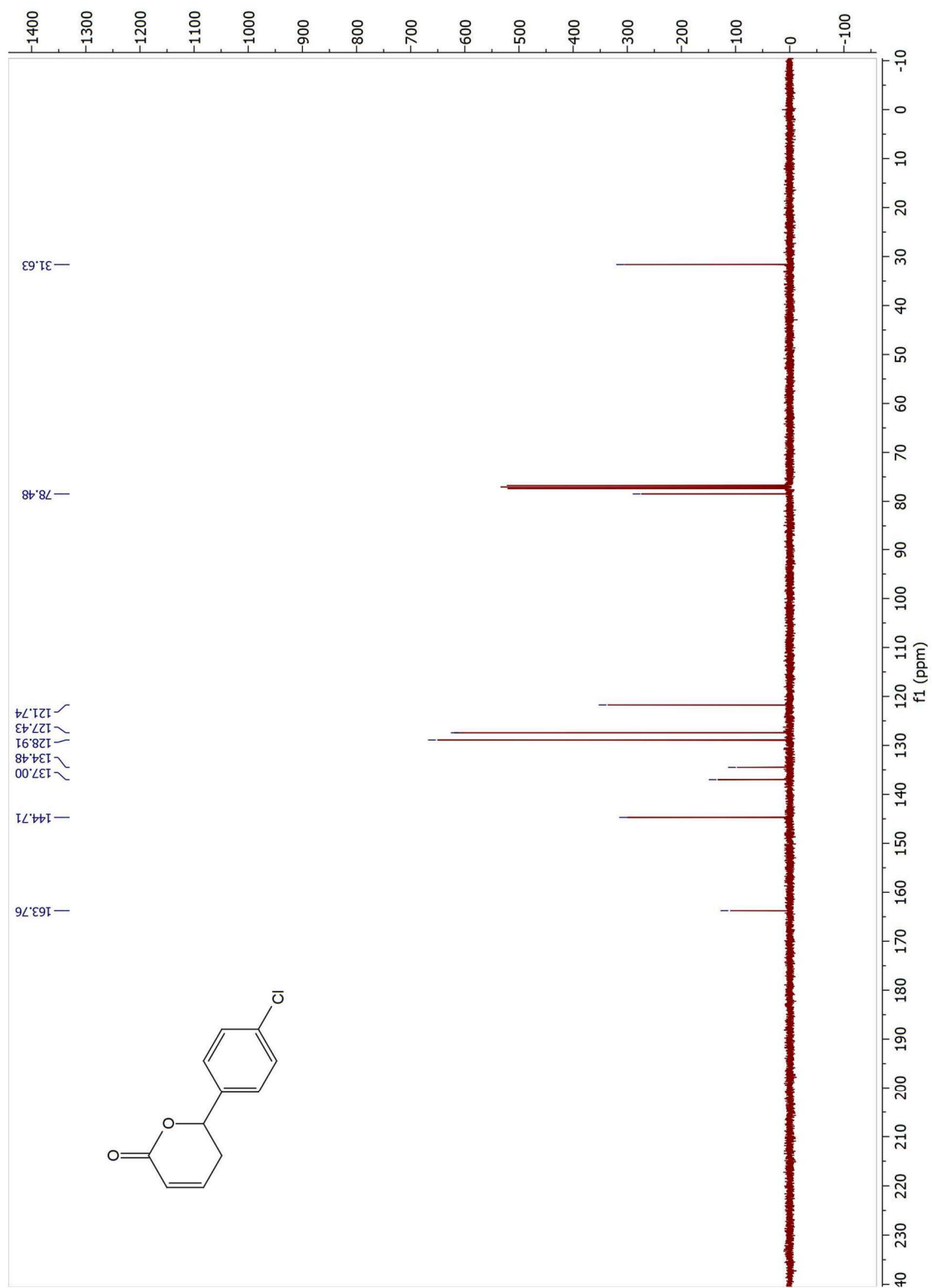


Figure 7.181 ^{13}C NMR Spectrum of **5.29c** (125 MHz, CDCl_3)

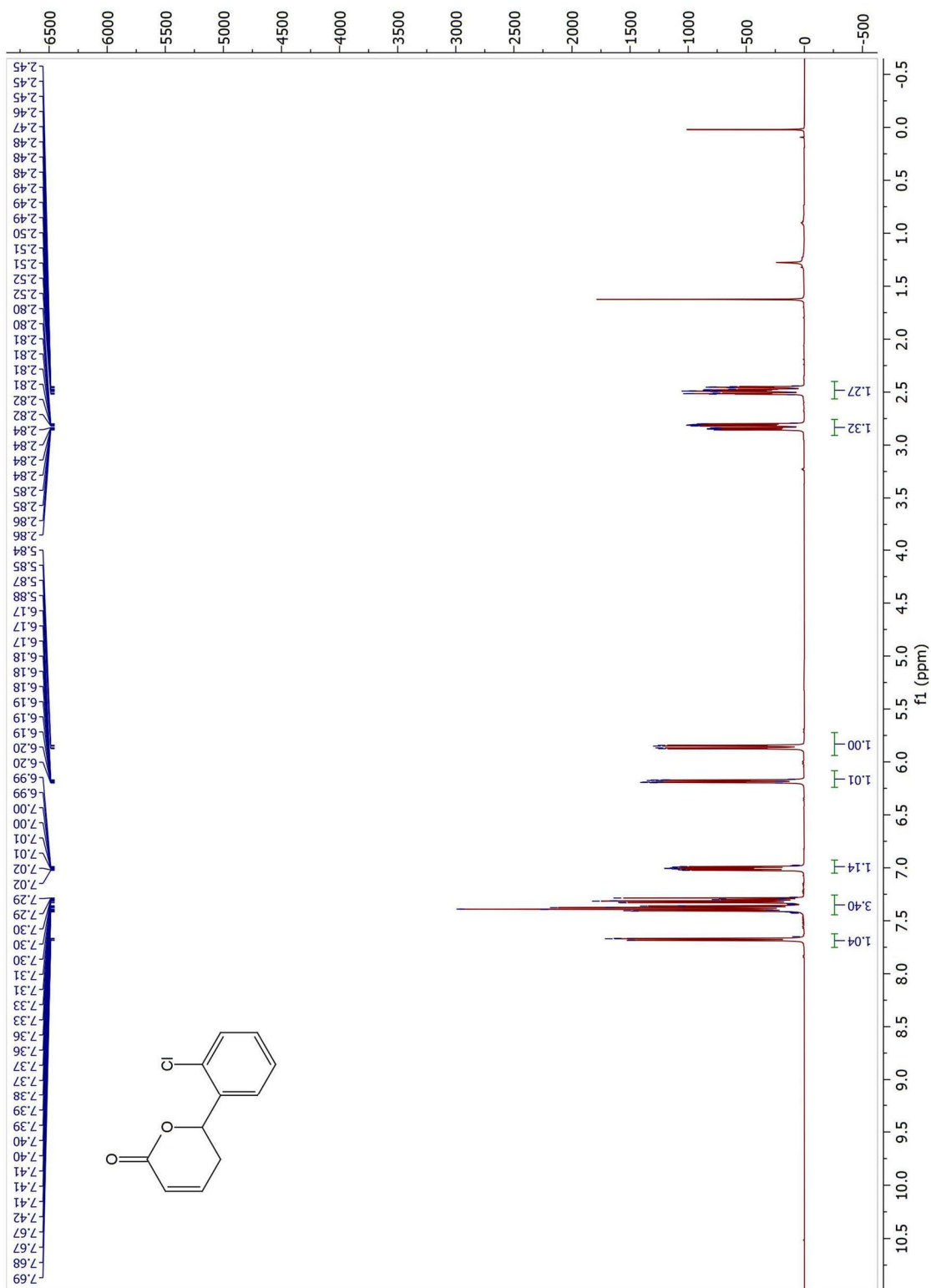


Figure 7.182 ^1H NMR Spectrum of **5.29d** (500 MHz, CDCl_3)

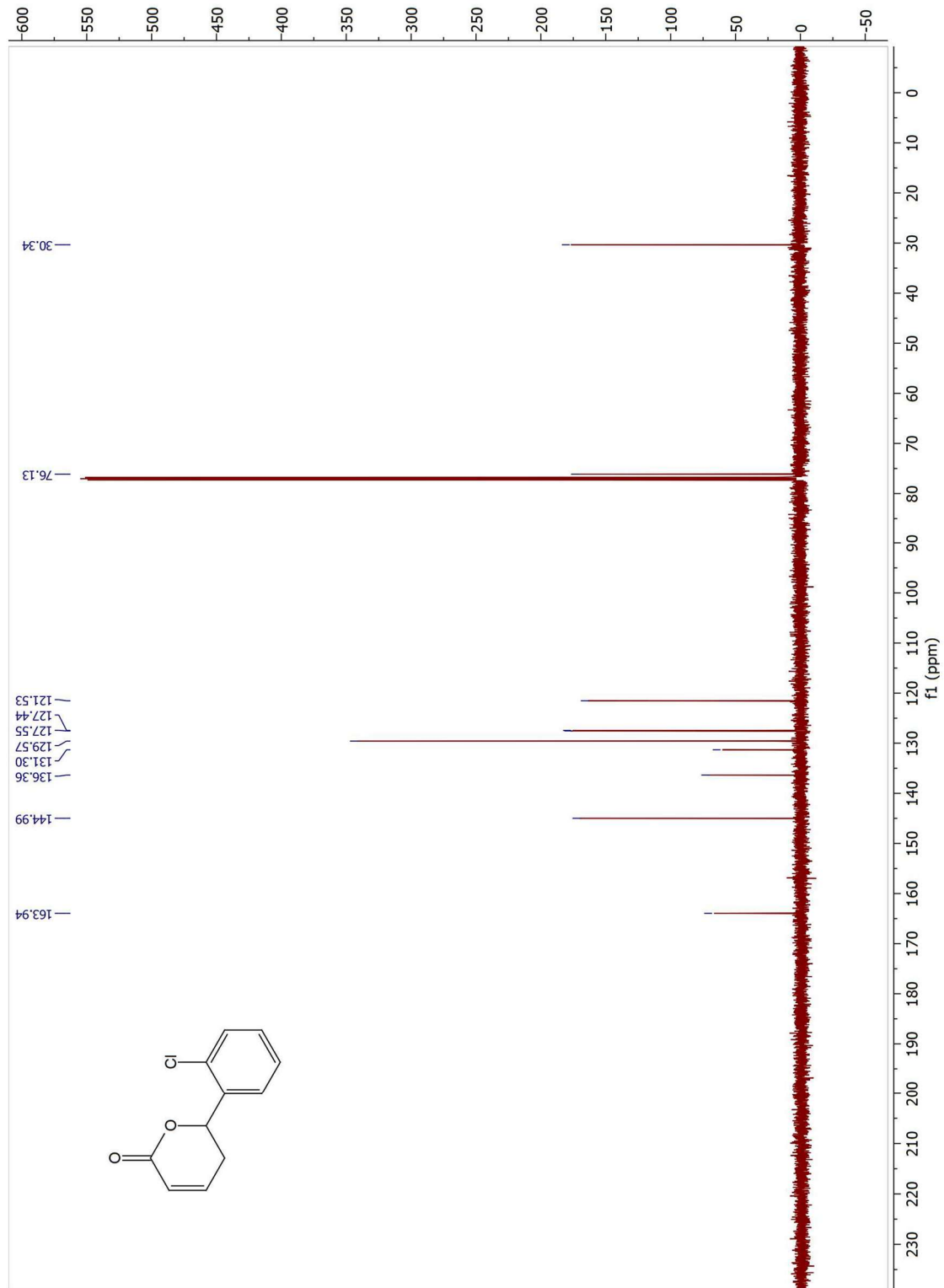


Figure 7.183 ^{13}C NMR Spectrum of **5.29d** (125 MHz, CDCl_3)

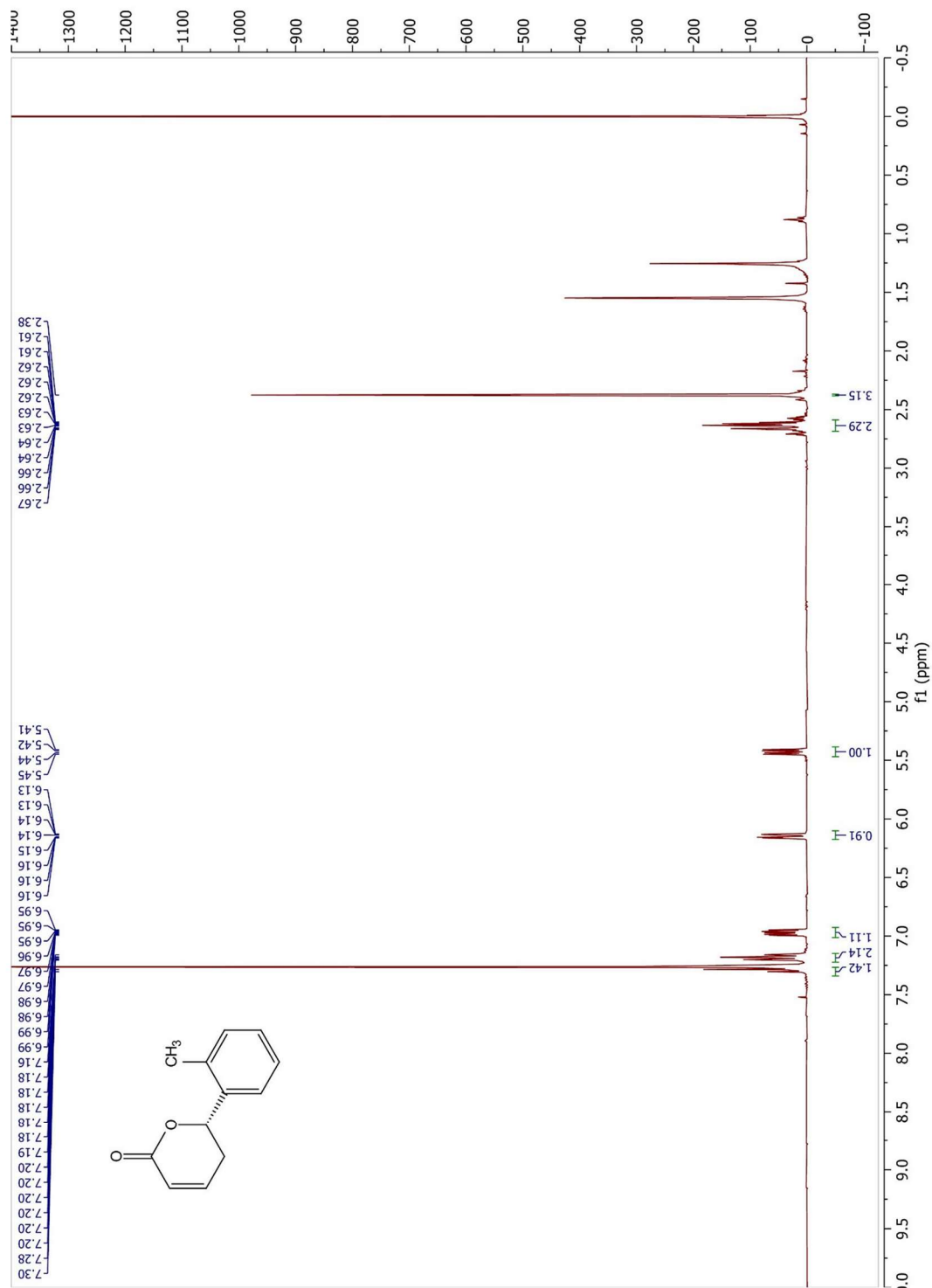


Figure 7.184 ^1H NMR Spectrum of **5.29e** (500 MHz, CDCl_3)

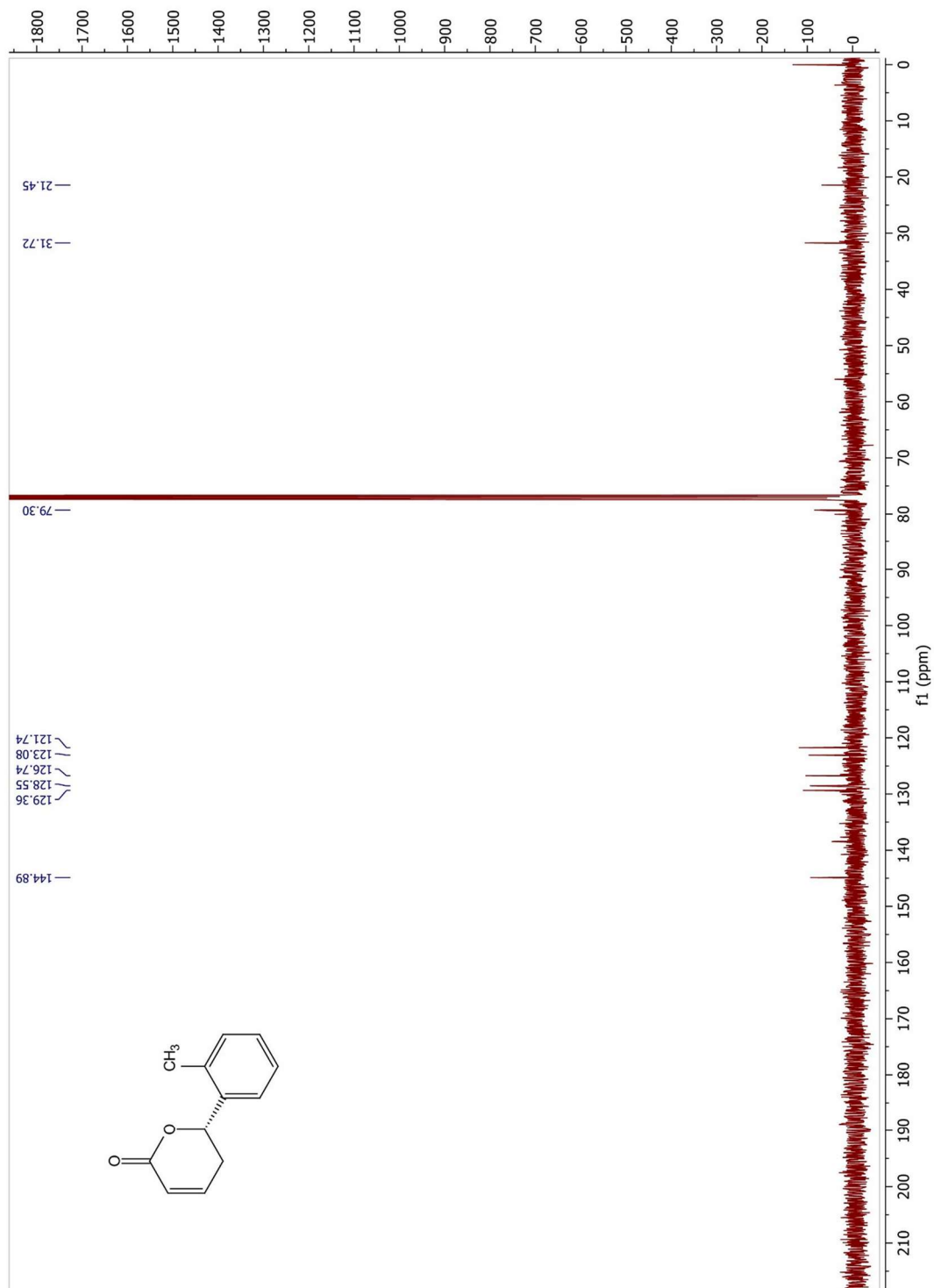


Figure 7.185 ^{13}C NMR Spectrum of **5.29e** (125 MHz, CDCl_3)

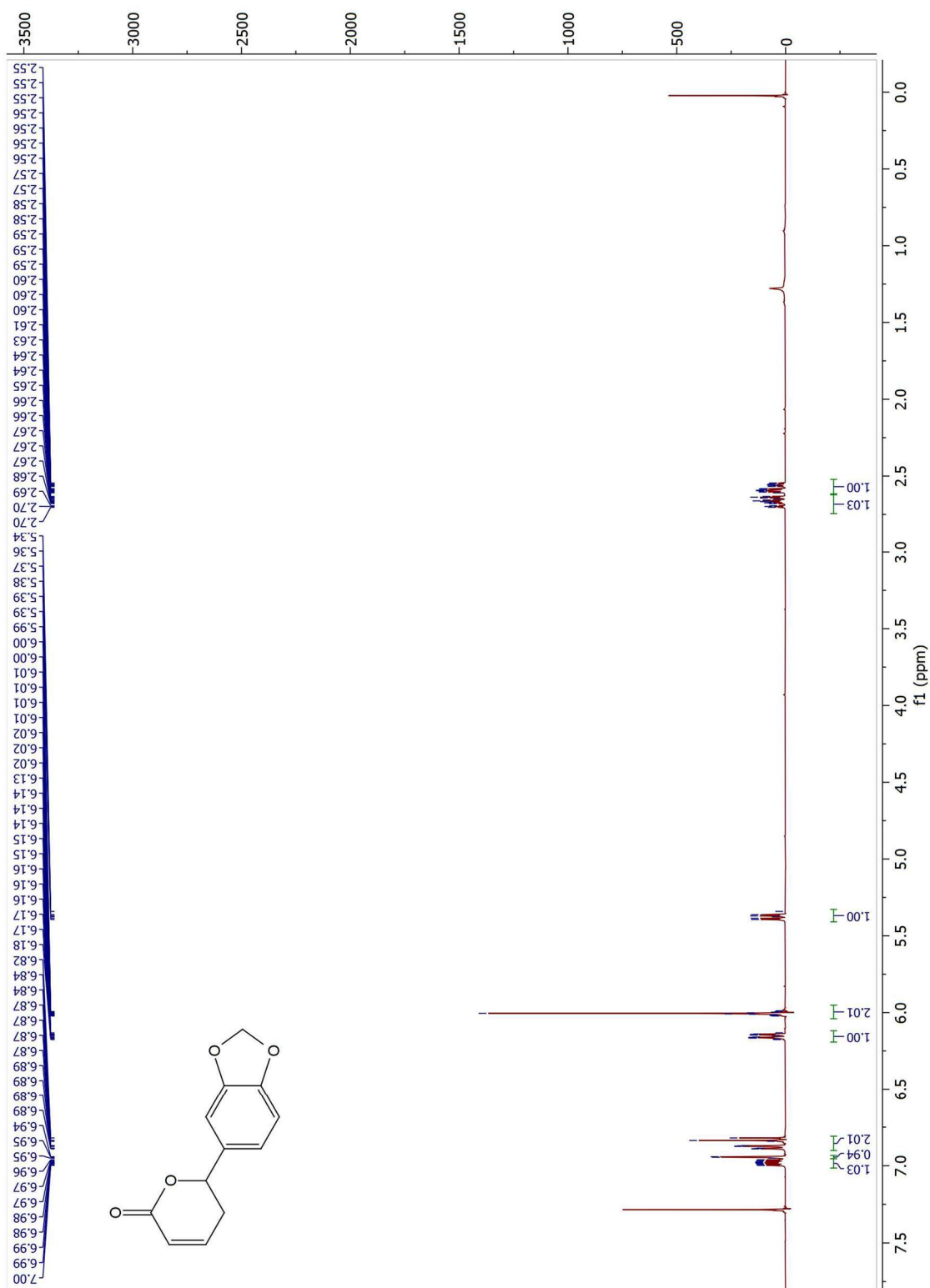


Figure 7.186 ^1H NMR Spectrum of **5.29f** (500 MHz, CDCl_3)

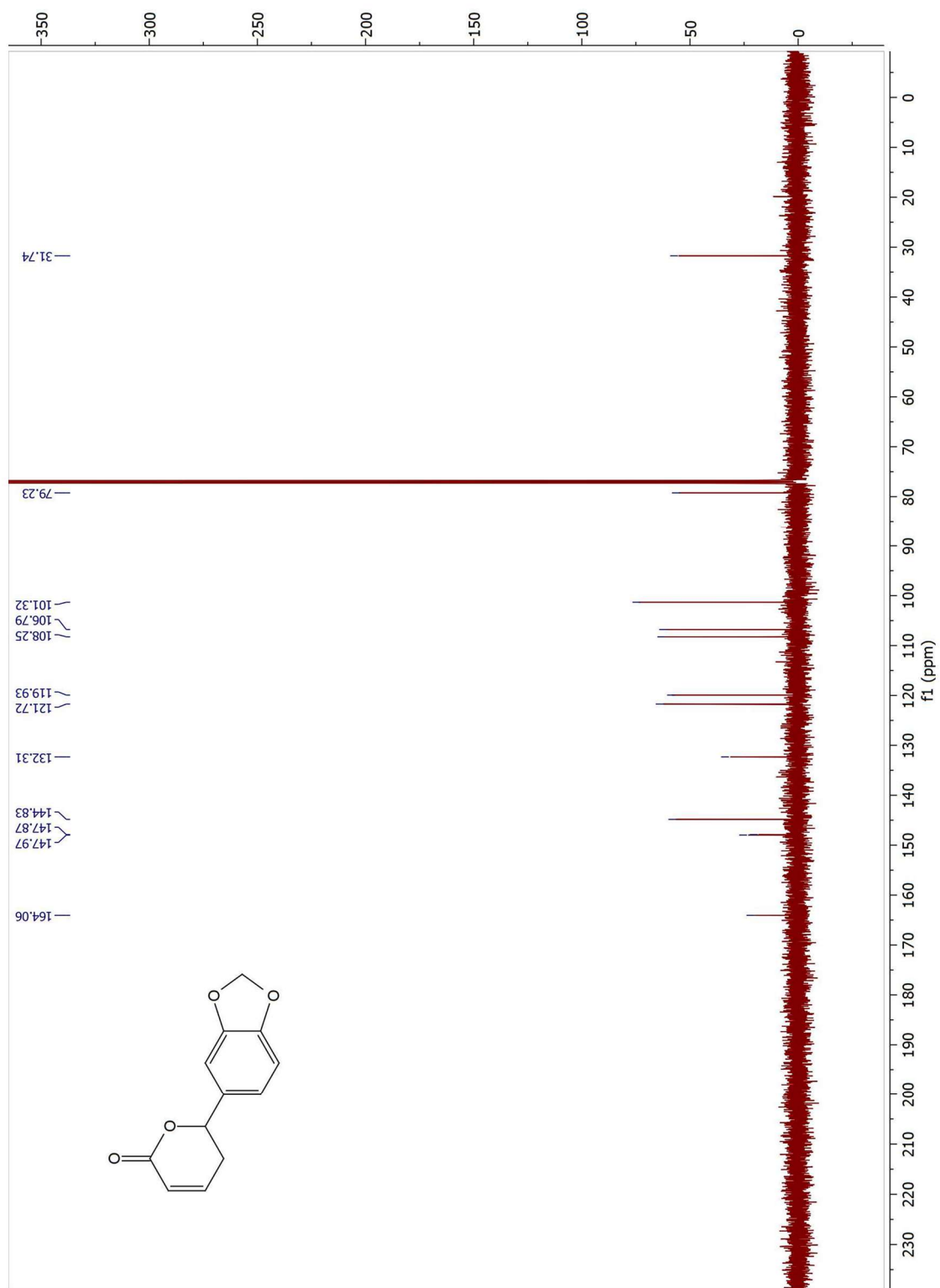


Figure 7.187 ^{13}C NMR Spectrum of **5.29f** (125 MHz, CDCl_3)